ARTICLE IN PRESS Available online http://jopr.mpob.gov.my/category/article-in-press/

Journal of Oil Palm Research

Vol. 34 (1) • March 2022

REVIEW ARTICLE

Omics Platform Technologies for Discovery and Understanding the Systems Biology of Oil Palm

eISSN 2811-4701

MPOB

JOURNAL OF OIL PALM RESEARCH (formerly known as ELAEIS)

JOURNAL OF OIL PALM RESEARCH, an international refereed journal, carries full-length original research papers, short communications and scientific review papers on various aspects of oil palm and palm oil and other palms. JOURNAL OF OIL PALM RESEARCH is published four times per year, *i.e.* March, June, September and December.

Impact Factor:
2.057
data from *2020 Journal Citation Report*® Science Edition
– A Clarivate Analytics product.

For more information on Journal of Oil Palm Research, please write to:

Editor-in-Chief
Journal of Oil Palm Research
Malaysian Palm Oil Board
6 Persiaran Institusi, Bandar Baru Bangi
43000 Kajang, Selangor, Malaysia

Tel: 603-8769 4400
E-mail: pub@mpob.gov.my
Website: jopr.mpob.gov.my

DISCLAIMER
Views of writers expressed in this publication are not necessarily endorsed by or represent the views of the Malaysian Palm Oil Board.

Published by the Malaysian Palm Oil Board

JOURNAL OF OIL PALM RESEARCH

Vol. 34 (1) March 2022

CONTENTS

Cover picture: Protein diversity in oil palm mesocarp metabolism.

EDITORIAL BOARD

(1 January 2022 – 31 December 2023)

PUBLICATION COMMITTEE

Journal of Oil Palm Research Vol. 34 (1) March 2022 p. 1-25
DOI: https://doi.org/10.21894/jopr.2020.0084

OMICS PLATFORM TECHNOLOGIES FOR DISCOVERY AND UNDERSTANDING THE SYSTEMS BIOLOGY OF OIL PALM

UMI SALAMAH RAMLI[1]*; ABRIZAH OTHMAN[1]; BENJAMIN LAU YII CHUNG[1]; HASLIZA HASSAN[1]; NUR 'AIN MOHD ISHAK[1]; ZAIN NURAZAH[1]; NURUL LIYANA ROZALI[1]; NOOR IDAYU MHD TAHIR[1]; SYAHANIM SHAHWAN[1]; SHAHIRAH BALQIS DZULKAFLI[1]; RAJINDER SINGH[1]; OMAR ABD RASID[1]; RAVIGADEVI SAMBANTHAMURTHI[1]; MOHAMAD ARIF ABD MANAF[1] and GHULAM KADIR AHMAD PARVEEZ[1]

ABSTRACT

Palm oil is the leading vegetable oil in terms of volume in the world market. Indonesia and Malaysia are the top producers and exporters of the commodity. The global production of palm oil reached 73.5 million tonnes in the period 2018/2019, up from approximately 70.5 million tonnes in 2017/2018. Oil palm is the most productive crop in the world being 10 times more productive than soybean which produces only about 0.45 t oil per hectare. Nonetheless, the industry is continuously under pressure to improve productivity and sustainability. This will require concerted innovations across the entire palm oil supply chain and fully committed research efforts including upstream technologies to expedite crop improvement. At the Malaysian Palm Oil Board (MPOB), research efforts at development of tools for improving oil palm traits by genetic modification have been augmented more recently with omics-based approaches and all of these innovations are synchronised towards improved product quality. Omics is a multi-disciplinary field encompassing genomics, epigenomics, transcriptomics, proteomics and metabolomics. Each of these fields provides an opportunity to understand and view oil palm biology from a global perspective, enabling accelerated discoveries for improved productivity and the development of new and improved varieties. An integrative omics approach promises great value in both phenotyping and diagnostic analyses. With the current technological capabilities, metabolomics is also being exploited for identifying unique chemical fingerprints to detect product contamination and adulteration in oil palm. This effort is actively being conducted in order to position the oil palm industry to meet and optimise the delivery of the highest quality oil with minimum environmental and social concerns. In this review, an overview is given on the current knowledge and progress made in oil palm research, focusing on the application of omics strategies and their integration with high-throughput technologies for oil palm crop improvement, development of geographical traceability system and ensuring that palm oil is free from residual oil contamination.

Keywords: crop improvement, metabolomics, omics research, proteomics, traceability.

Received: 17 March 2020**; Accepted:** 21 July 2020**; Published online:** 7 October 2020.

INTRODUCTION

Palm oil (from *Elaeis guineensis* Jacq.) is one of the most highly valued commodities for Malaysia and contributes significantly to the economic growth of the country (Kushairi *et al.*, 2019). In terms of yield, the oil palm is characterised as the most productive oil crop with a potential yield capacity of more than 10 t of oil per hectare per year (Murphy, 2014). However, generally, yield gaps in oil palm plantation are large, with yields typically between 4-6 t of oil per hectare for the best commercial plantations and 3-4 t oil per hectare for smallholders. Assessment

[1] Malaysian Palm Oil Board,
6 Persiaran Institusi, Bandar Baru Bangi,
43000 Kajang, Selangor, Malaysia.

* *Corresponding author e-mail: umi@mpob.gov.my*

of the underlying causes of yield gaps in oil palm production systems worldwide is still lacking (Woittiez *et al*., 2017). Palm oil is used worldwide and contributes significantly to the world's oils and fats market (Nambiappan *et al*., 2018; Parveez *et al*., 2020). There are many factors that contribute to the global demand for palm oil. These include increasing awareness of its health attributes, competitive price and versatility that allows it to be used in both food and non-food applications (Khosla, 2011; May and Nesaretnam, 2014). Malaysia is the second largest producer of palm oil in the world behind Indonesia. The overall production in Malaysia in 2019 was over 19.86 million tonnes of crude palm oil from 5.9 million hectares of planted area. India and China are the two largest palm oil export destination, with the European Union (EU) also being among the main markets for Malaysia's key commodity. In 2019, Malaysia exported a total of 16.88 million tonnes of palm oil to the world indicating a strong demand from importing countries, especially India, China and the EU as compared to 15.36 million tonnes in the previous year (Parveez *et al*., 2020).

Unstable commodity prices, labour shortage, ageing oil palm populations, and pests and diseases that seriously affect overall yield are among the key challenges faced by the oil palm industry (Alam *et al*., 2015; Murphy, 2014). A viable solution for overcoming these challenges is through the development of varieties that can increase yield per unit land, are more resilient even to climate change and produce diversified and more high value products (Murphy, 2014). Oil palm breeding programmes focussed on specific traits such as high yield, water uptake efficiency, nutrient use efficiency, disease resistance and plant architecture will be essential in the future for improving commercial yields. While conventional breeding has its limitations, application of biotechnological tools will be a viable strategy for overcoming the above challenges. Fortunately, tools are available to assist crop improvement such as genetic modification for producing high value products and developing oil palm with pest and disease tolerance. This is to keep pace with global population growth and meet the increasing demand for palm oil for both food and non-food applications (Parveez *et al*., 2015).

Tremendous progress has been made in recent years in the area of modern genetics through integration with other omics technologies (Teh *et al*., 2017). Biochemical and genetic studies have revealed that in many crops including oil palm, the majority of important agronomic traits such as yield, plant height and nutrient content are complex quantitative traits that are controlled by multiple interacting genes (Long *et al*., 2007; Ramli *et al*., 2002a; 2002b; Seng *et al*., 2016). To understand the inheritance of complex traits, the establishment of reliable screening tools and platforms that can precisely measure expression of physiological traits in realistic field environments is important. The emergence of the novel omics innovations, for example, genomics, proteomics and metabolomics has allowed scientists to identify the molecular mechanisms underpinning crop improvement (Appleton *et al*., 2014; Chaudhary *et al*., 2015; Syrenne *et al*., 2012; Tester and Langridge, 2010). In this respect, genomics and epigenomics-based technologies have successfully provided the necessary tools that will support the sustainable development of oil palm (Low *et al*., 2017; Ong-Abdullah *et al*., 2015; Singh *et al*., 2013a, 2013b; 2020). Concomitantly, remarkable progress in omics research, combining innovative and accurate technologies with the requirement for intersection with bioinformatics has resulted in the discovery of key regulators of various traits for crop improvement (Chaudhary *et al*., 2015; Fernie and Schauer, 2009; Hajduch *et al*., 2011).

The use of proteomics and metabolomics in oil palm research was initiated about 10 years ago, aimed at developing tools to accurately monitor the proteome and metabolome profiles of clonal/transgenic palms and for a variety of important biological traits, *e.g*., yield, oil quality and disease resistance (Ramli *et al*., 2016). Several technical and review reports are available on appropriate strategies for the application of molecular characterisation using proteomics and metabolomics in oil palm to improve our understanding of these complex traits, which are likely to underpin future gains in crop productivity (Dzulkafli *et al*., 2019; Hassan *et al*., 2019; Lau *et al*., 2018; Neoh *et al*., 2013; Nurazah *et al*., 2017; Rozali *et al*., 2017; Tahir *et al*., 2012; 2016; Teh *et al*., 2017; Vargas *et al*., 2014). Recent developments in high-throughput omics technologies have also accelerated the accumulation of huge amounts of omics data from multiple sources – genome, epigenome, transcriptome, proteome and metabolome, posing new challenges and opportunities for developing novel computational approaches customised for integrative analysis (Mirza *et al*., 2019). Consequently, simultaneous analysis of data obtained from different omics platforms, for the same biological specimen is expected to provide a holistic view of the complex biological interactions. The use of state-of-the-art machine learning (ML)-based approaches, which leverage prior knowledge of biological networks to integrate omics-datasets would be vital for robust biomarker modelling (Glaab, 2016; Mirza *et al*., 2019; Price *et al*., 2017; Tafti *et al*., 2017). Thus, the various omics information is not just only assisting in the establishment of deeper understanding of the complex interactions of oil palm metabolic networks and their responses to environmental and genetic changes, but also providing screening and analysis platforms to support oil

palm breeding programmes. Such information will have major implications in enhancing the future production and sustainability of the oil palm industry.

TRANSLATING GENOMICS RESEARCH TO IMPROVE OIL PALM PRODUCTIVITY

Early application of genomics-based tools in oil palm breeding was initiated in the mid-1990s, where restriction fragment length polymorphism (RFLP) markers were employed for DNA fingerprinting (Cheah *et al*., 1993; Mayes *et al*., 1996). This was followed by the use of RFLP markers for the construction of a framework genetic map (Mayes *et al*., 1997). Subsequent development of polymerase chain reaction (PCR)-based simple sequence repeat (SSR) markers led to the construction of a denser oil palm genetic map (Billotte *et al*., 2005) and made available a more robust tool for fingerprinting (Singh *et al*., 2008; Ting *et al*., 2010). Systematic study of genes in oil palm via generation of expressed sequence tags (EST) (Chan *et al*., 2010; Ho *et al*., 2007; Jouannic *et al*., 2005; Low *et al*., 2008) was an important first step in building the sequence database for oil palm, which was followed by sequencing of the hypomethylated regions of the genome (Low *et al*., 2014).

A high quality genetic blueprint of both species of oil palm, namely *E. guineensis* and *E. oleifera*, was eventually obtained using a combination of 454/Roche technology and bacterial artificial chromosome (BAC) end sequencing in 2013 (Singh *et al*., 2013a). Scaffolds from the build were successfully aligned to the 16 linkage groups of the oil palm genetic map, and sequencing of 34 transcriptomes from various tissues enhanced the annotation of the assembly. The importance of the availability of this resource was quickly realised as it proved pivotal in identifying the *Shell* and *Virescens* genes responsible for the three different fruit forms and the exocarp colour of oil palm fruits (two important monogenic traits), respectively (Singh *et al*., 2013b; 2014). The identification of these genes paved the way for the realisation of genomics guided breeding in oil palm, which was previously restricted to using molecular markers for deoxyribonucleic acid (DNA) fingerprinting and paternity testing of selected oil palm breeding lines and tissue culture clones (Singh *et al*., 2007; Thongthawee *et al*., 2010). Moving forward, and building on the experience of other crops, further refinements to the first oil palm genome assembly are necessary, especially to facilitate the identification of genes regulating complex (quantitative) traits.

Nevertheless, the availability of the *pisifera E. guineensis* genome sequence has facilitated the assembly of the *dura E. guineensis* genome apart from the resequencing of 17 other mostly advanced breeding lines (Jin *et al*., 2016). The *dura* genome as expected appeared to be similar to the *pisifera* genome in terms of the percentage of repeat sequences present (~40%), and the number of genes identified, 36 105, which was close to the number reported by Singh *et al.* (2013a). More importantly, the re-sequencing of the 17 palms revealed that the genetic diversity of palms in Southeast Asia is rather low, consistent with earlier studies using molecular markers (Maizura *et al*., 2006), which also suggested that the genetic variability of palms used for commercial cultivation in this region is low. The availability of the genome sequence had facilitated the resequencing of another 132 palms from both species and development of a high density single nucleotide polymorphism (SNP) array, consisting of 200 000 probes (Kwong *et al*., 2016). The 200 000 single nucleotide polymorphisms were selected across the genome and thus, proved useful in a Genome Wide Association Study (GWAS) that led to the identification of loci influencing oil content in selected *E. guineensis* backgrounds (Teh *et al*., 2016). A clear advantage of a fixed high density SNP array platform is that it can provide a rapid scan of the genome, with high SNP call rates and as the number of samples being genotyped increases, cost per sample gets lower (Thomson, 2014). In addition, use of a fixed array allows for a more robust comparison of fingerprints across multiple populations or accessions. However, one of the main disadvantages of the fixed array platform is that the single nucleotide polymorphisms are restricted to those found in the samples or accession used to design the array and in the case of oil palm, existing SNP platforms may not be incorporating rare single nucleotide polymorphisms found in wild germplasm samples. This can be a critical issue for oil palm breeding in Southeast Asia, where the limited diversity requires the industry to introgress desirable alleles from wild oil palm collections into advanced breeding lines (Ong-Abdullah *et al*., 2015; Singh *et al*., 2008; Zulkifli *et al*., 2012).

Developments in next generation sequencing (NGS) technologies paved the way for an alternative genotyping technique known as genotype by sequencing (GBS) (Nielsen *et al*., 2011). GBS which entails low coverage skim sequencing of samples, reduces cost substantially, nevertheless, requires a fairly good existing genome build to anchor the sequences and accurately call the SNP. The availability of the high quality oil palm genome build facilitated GBS studies in oil palm, where Pootakham *et al.* (2015), after further reducing the complexity by digesting the DNA samples with restriction enzymes, skim sequenced 108 palms from a mapping family. More than 20 000 high quality SNP were detected by mapping the GBS reads to the oil palm reference genome, which led to the construction of a genetic map, and more importantly,

identification of genomic loci associated with key agronomic traits, namely height increment and bunch weight. Using a similar GBS approach, again with the published oil palm genome sequence as reference, Bai *et al.* (2017) skim sequenced 155 palms (inclusive of both parental palms) of a F_1 family, and identified single nucleotide polymorphisms linked to oil content. The studies above clearly indicate how the availability of the genome build since 2013 has facilitated the application of the most current genomics-based technologies for marker-trait association in oil palm. Interestingly, the growing repertoire of sequences available for oil palm and research advancements in model crop systems, further facilitates the use of the candidate gene approach to uncover the molecular mechanisms influencing particular traits of interest. Exploiting this, Ong *et al.* (2018) designed SNP markers from selected candidate genes and in combination with the association mapping approach, identified a SNP marker linked to stem height in the MPOB-Angola germplasm collection - revealing an alternative but more focussed route to establish marker-trait association.

Undeniably, the genomic resources established thus far are an important foundation, that will help improve oil palm breeding efficiency (*Figure 1*). However, to capture the full complexity of a biological system like oil palm, a combined 'omics' approach is required to uncover complex traits such as disease resistance and adaption to abiotic stresses (*e.g.*, drought tolerance). Genomics efforts are in full gear currently for the oil palm and integrating with recent developments in proteomics (Lau *et al.*, 2018) and metabolomics (Ramli *et al.*, 2016; Rodrigues-Neto *et al.*, 2018) will prove important to fully understand the regulatory systems that govern complex traits. However, rapid developments in each of the 'omics' platforms is resulting in vast amounts of complex data that require high end computational analysis by competent researchers to make incisive interpretations from such multi-omics datasets (Misra *et al.*, 2019).

PROTEOMICS AND METABOLOMICS – CURRENT AND EMERGING METHODOLOGIES IN CROP IMPROVEMENT

The essential functions of living cells, *e.g.*, during cell differentiation and regulation or during disease development, are accomplished by gene products, mainly proteins. Thus, it is important to study the proteins involved in order to gain clues about their functional activity. In fact, proteomics is a tool for functional genomics and holds special promise for genetics and physiological studies towards crop improvement (Eldakak *et al.*, 2013; Fiehn *et al.*, 2001). Therefore, technologies aimed at studying proteins in a cell are a welcome complement to uncover the role of genes in cellular activities. Since proteins are involved in cellular enzymatic functions, regulatory switches and structural components, characterising the proteins expressed by a cell can give important clues to the function, organisation and responsiveness of a cell.

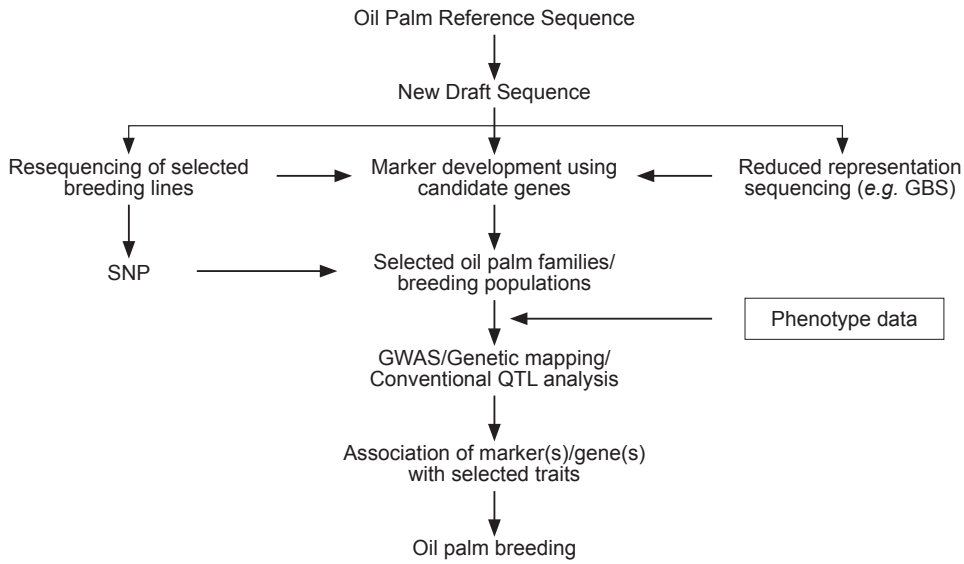

Note: GWAS - Genome Wide Association Study.
QTL - Quantitative trait loci.

Figure 1. An overview of the use of the oil palm reference genome for improving oil palm breeding efficiency. The reference genome proved useful as an anchor to establish new draft sequence, resequencing of selected lines which resulted in development of high-density single nucleotide polymorphism (SNP) array. Genotyping by sequencing (GBS) was also made possible as an alternative genotyping tool, which together with SNP arrays, assisted in establishing marker trait association. Interestingly, the availability of large repertoire of sequences also allows development of markers from candidate genes associated with traits in other crop system.

In proteomics research, all the proteins of a cell, the proteome are studied simultaneously in different physiological situations. It provides a dynamic reflection of genes and environment and offers a novel approach for gene (DNA) identification. Damerval *et al.* (1994) identified protein quantity loci (PQL) that explained some of the proteins analysed using proteomics for the purpose of implementing marker-assisted selection (MAS) to improve the traits under study. This type of research is particularly useful for breeding programmes as they provide molecular-based clues about nutritional value, yield and observed stress tolerance phenotypes and how these factors are affected by other adverse conditions (Chen and Harmon, 2006; Salekdeh and Komatsu, 2007). In addition, knowledge of key proteins that play a crucial role in the development of a plant has the potential to complement metabolomics to elucidate the biochemistry of the phenotype being expressed (Deshmukh *et al.*, 2014). There are many examples of proteomics-based studies that include the investigation of biotic and abiotic stresses, which negatively affect crop growth and productivity worldwide (Bartolini *et al.*, 1999; Hashiguchi *et al.*, 2010). Proteomics approaches are also useful to explore the molecular mechanisms underpinning plant-microbe interactions (Lodha *et al.*, 2013; Mehta *et al.*, 2008; Quirino *et al.*, 2010). Contrasting samples in respect to temporal protein accumulation during fruit development (*e.g.*, proteins expressed during early versus fruit ripening) or presence in a specific tissue (*e.g.*, proteins exclusively present in leaf, root and stem) have also been studied using proteomics (Bianco *et al.*, 2013; Nozu *et al.*, 2006).

The well-established International Rice Sequencing Protocols have delivered a substantial amount of information, where proteome studies have facilitated the detection of novel traits useful for breeding (Yu *et al.*, 2002). Accordingly, following proteome analysis, a number of previously unknown novel genes coding for enzymes in metabolic pathways were identified in a number of crops (Canovas *et al.*, 2004). Interestingly, proteome analysis of genetically modified crops has also been used to decipher substantial equivalence in comparative safety analysis to help increase the acceptance of transgenic crops and products (Barros *et al.*, 2010; Zhao *et al*., 2013).

A complete understanding of plant systems requires filling the gap between proteome and phenotype. We can study genes being expressed, and what proteins are present, but the more important question is for instance what makes certain oil palms to be higher yielding than others or why specific oil palms are more tolerant to disease. Metabolomics is perhaps the ultimate level of post-genomic analysis as it can expose changes in metabolite fluxes that are caused by only minor changes in gene expression (Allwood *et al*., 2008). Metabolomics attempts to measure the complete set of metabolites as the end products of cellular regulatory processes, and their levels can be viewed as the response of biological systems to environment or genetic manipulations (Maloney, 2004). Metabolomics distinguishes what is really occurring in a system, whereas genomics and proteomics recognise what could occur. This fact demands a different perspective and requires the measurement of transcriptional, proteomic and metabolomic data in order to obtain a complete picture of the system's response to genetic or environmental stress stimuli.

There are increasing number of examples indicating that proteome and metabolome profiling approaches are becoming more and more important to explore significant sources of variation in crops caused by genetic background, breeding methods, growing environment, genotype-environment interactions and crop cultural practices (Davies *et al*., 2010; Dixon *et al*., 2006). The combination of proteomics and metabolomics is thought of as an advanced profiling technology that broadens the spectrum of detectable compounds, which improves the efficacy of assessment strategies (Barros *et al*., 2010; Metzdorff *et al*., 2006; Zolla *et al*., 2008). Generally, the potential of applying proteomics and metabolomics in research is significant and a brief account of the various approaches in plants is given in *Table 1.* Nevertheless, proteomics and metabolomics are yet to be utilised directly on a large scale for crop improvement, and the most basic application currently is focussed on gaining an understanding of proteins and metabolites associated with complex traits such as, yield and disease resistance, both of which are major targets of crop breeding (Canovas *et al*., 2004; Kumar *et al*., 2017).

TECHNOLOGICAL PERSPECTIVES FOR PROTEOMICS AND METABOLOMICS

The advent of proteomics technologies for global detection and quantitation of proteins has generated new opportunities and challenges for scientists seeking a deeper insight into the system biology of an organism. As the proteome more accurately reflects the dynamic state of a cell, tissue or organism, it has huge potential for yielding better markers for crop improvement and monitoring of disease. However, as proteins are much more diverse physically and chemically than nucleic acids, there are several difficulties in the study of proteins that are not inherent in the study of nucleic acids. Furthermore, proteins cannot be amplified like DNA; therefore, less abundant species are more difficult to detect (Van Wijk, 2001).

More importantly, this technique demands advanced technologies focusing on improved separation, resolution and automation for the identification and characterisation of proteins including the chemical and physical properties of the target proteins. High throughput proteomics technologies coupled with advanced bioinformatics are increasingly leveraged to identify molecular signatures of economic importance based on protein pathways and signalling cascades.

TABLE 1. EXAMPLE OF INITIATIVES IN PROTEOMICS AND METABOLOMICS AS BIOTECHNOLOGICAL TOOLS FOR CROP IMPROVEMENT

Crop	Trait studied	Tools / techniques		References
Olive	Tolerance to cold *vs*. non-tolerant after cold treatments	Proteomics	Isoelectric focusing (IEF), 2-DE	Bartolini *et al*. (1999)
	Olive pulp proteins		Nano-LC/MS/MS, MALDI-TOF-MS	Capriotti *et al*. (2013) Esteve *et al*. (2011)
	Geographical characterisation	Metabolomics	NMR	Rongai *et al*. (2017)
	Olive classification		GC-QTOF/MS	Sales *et al*. (2017)
	Determination of phenolic compounds in virgin olive oil		LC coupled to fluorescence detector	Monasterio *et al*. (2016)
Maize	Unintended effects of genetic modification (GM)	Proteomics	2-DE	Barros *et al*. (2010) Zolla *et al*. (2008)
	C4 leaf development		NanoLC-LTQ-Orbitrap	Majeran *et al*. (2010)
	Ear rot infection		iTRAQ	Mohammadi *et al*. (2012)
	Seedlings		LC-MS/MS	Ning *et al*. (2016)
	Greening of leaves		LC-MS	Shen *et al*. (2009)
	Genetically modified organism (GMO)	Metabolomics	CE-TOF-MS, FT-ICR-MS	Leon *et al*. (2009)
	Salt stress tolerance		NMR	Gavaghan *et al*. (2011)
	Effect of environment and genotype		LC-MS	Baniasadi *et al*. (2014)
Rice	Etiolated shoot	Proteomics	2-DE	Komatsu *et al*. (1999)
	Unintended changes in GM rice		2-DE	Zhao *et al*. (2013)
	Rice proteome database		Shotgun proteogenomics	Helmy *et al*. (2011)
	Stress tolerance		iTRAQ	Wang *et al*. (2014)
	Chemical diversity	Metabolomics	GC-MS, LC-MS	Kusano *et al*. (2015)
	Rice quality and traceability		FT-IR, NMR	Uawisetwathana and Karoonuthaisiri (2019)
	GM-rice (insect resistance)		LC-ESI-Q/TOF MS	Chang *et al*. (2012)
	Nutritionally enhanced herbicide tolerance		GC-EI-TOF MS	Kim *et al*. (2013)
Soybean	Salt tolerance	Proteomics	MALDI-TOF/TOF	Ma *et al*. (2012)
	Wild and cultivated soybean genotypes		2-DE, MALDI, LC-MS/MS	Natarajan *et al*. (2006)
	Water and nutrient uptake		iTRAQ	Nguyen *et al*. (2012)
	Tolerance to *Phytophtora*		2-DE	Zhang *et al*. (2011)
	Drought and heat stress	Metabolomics	GC-MS/LC-MS	Das et *al*. (2017)
	Response to *Rhizoctonia* to foliar blight disease		NMR	Copley *et al*. (2017)
	Transgenic soybean		CE–TOF-MS	García-Villalba *et al*. (2008)
Oil palm	Somatic embryogenesis	Proteomics	2-DE & MALDI, TOF-MS/MS	Tan *et al*. (2016)
	Fruit development proteomics		2-DE & MALDI, TOF-MS/MS	Hassan *et al*. (2019)
	Pathogen-studies (*Ganoderma*)		LC-MS Orbitrap	Syahanim *et al*. (2019)
	Pathogen-studies (*Ganoderma*)	Metabolomics	GC-GC-TOF-MS	Rozali *et al*. (2017)
	Phytochemicals		LC-ESI-TOF-MS	Tahir *et al*. (2012)

In the area of metabolomics research, every technique employed has specific advantages and limitations. Thus, clearly there is no single method that is ideal for all research purposes. Analytical techniques that are most often used for metabolite profiling include nuclear magnetic resonance (NMR) (Nicholson *et al*., 1999), gas chromatography-mass spectrometry (GC-MS) (Roessner *et al*., 2000), liquid chromatography-mass spectrometry (LC-MS) (Fraser *et al*., 2000; Huhman and Sumner, 2002; Tolstikov *et al*., 2003) and capillary electrophoresis-mass spectrometry (CE-MS) (Sato *et al*., 2004). Generally, NMR instrument is arguably the most powerful technique for an organic chemist to determine structure in metabolomics research. MS excels at selective identification of a molecular entity, while NMR excels at identification of all proton containing species in a sample. Specifically, interfacing liquid chromatography with parallel MS or NMR (LC-NMR-MS) has been shown to give comprehensive structural data on metabolites of novel drugs in development. Although MS and NMR are the most common tools used for large scale analysis of metabolites whether targeted or non-targeted, metabolomics is not limited to these techniques. Other techniques such as thin layer chromatography (TLC), high performance liquid chromatography (HPLC) with ultraviolet (UV)/visible absorbance, photodiode array (PDA) or electrochemical detectors, Fourier transform-infrared (FT-IR) and variety of other enzymatic assays have also been widely used to improve metabolite coverage and increase quantification limits (Gamache *et al*., 2004; Kristal and Matson, 2002; Shulaev, 2006). Generally, specific platforms are not a prerequisite for metabolomics investigations, so in theory, any technique capable of generating comprehensive metabolite measurements can be used for metabolomics.

As seen today, metabolomics employs multiple complementary analytical devices starting from sample preparation to determining the measurement details of all analytical platforms, and finally to corresponding specific steps of data analysis (*Table 1*). The choice of technique primarily depends on the research strategies and the nature of the samples. Three basic strategies can be used in metabolomics: (i) targeted analysis, (ii) metabolite profiling, and (iii) metabolic fingerprinting (Fiehn, 2002; Halket *et al*., 2004). These techniques are commonly used to reveal the phenotype of silent mutations (Raamsdonk *et al*., 2001), studying responses to environmental stress (Huntingford *et al*., 2005; Rosenblum *et al*., 2005), assessing global effects of genetic manipulation (Catchpole *et al*., 2005), comparing different growth/fruit development (Hurtado-Fernández *et al*., 2015), nutrition (German *et al*., 2002) and natural product discovery (Fiehn *et al*., 2001). Specifically, the major analytical technologies driving metabolomics such as LC-MS have enormous potential for metabolite profiling and for analysing selected metabolites as a complement to GC-MS. In addition, NMR spectroscopy has high discriminatory power at the level of metabolic fingerprints. However, NMR fingerprints provide limited information on individual metabolites and therefore purification of the metabolites is required for accurate identification (Jorge *et al*., 2016; Weckwerth, 2003).

Like other functional genomics research, the future of proteomics and metabolomics lies in the combination of different techniques for identification and quantification of proteins and metabolites to achieve a complete view; no single technique alone can cope with the diversity and structural complexity of the proteome and metabolome. We believe that protein and metabolite analyses are much more powerful when used in combination than individually. Furthermore, the combination of the data generated from proteomics and metabolomics requires specific bioinformatics support in the form of databases, visualisation and data integration to provide a meaningful assessment of the research. A review by Weckwerth (2008) provides the strategy for data integration, which combines high throughput profiling methods with exploratory multivariate data mining. In fact, a combination of computer-aided metabolic modelling and multivariate data mining will enable a systematic comparison for identifying key steps involved in metabolism using extensive and multi-dimensional datasets from proteomics, transcriptomics and metabolomics studies (Mehrotra and Mendes, 2006; Morgenthal *et al*., 2006).

Along with the establishment of a database platform, the streamlined workflow is now available to facilitate research in oil palm proteomics and metabolomics (*Figure 2*). This includes a combination of approaches, either gel-based or liquid chromatography (gel-free), with tandem mass spectrometry to optimally extract proteins by modifying existing methods described in literature. At present, proteomics technologies are being applied to identify potential biomarkers associated with oil production, fruit ripening, embryogenic lines and disease resistance (Al-Obaidi *et al*., 2017; Hassan *et al*., 2019; Lau *et al*., 2018; Syahanim *et al*., 2013; Tan *et al*., 2016). Looking beyond the proteome, advanced metabolomics technologies also include key elements, starting from sample extraction to profiling of targeted and non-targeted metabolites using multiple technologies, mainly LC and GC coupled to tandem mass spectrometry (Nurazah *et al*., 2017; Rozali *et al*., 2017; Tahir *et al*., 2012; 2016). We foresee that proteomics and metabolomics technologies will play a more significant role in the near future to address diverse issues related to the oil palm in the effort to assist on-going breeding activities to further improve the oil crop.

An important point to consider is that the large multi-dimensional datasets that result from proteomics and metabolomics require complex and high throughput statistical analysis to render the data meaningful and make rational conclusions in the study. Thus, bioinformatics tools are essential for the efficient processing of huge datasets. Proteomics data also have to be linked to the existing gene, transcripts and ribonucleic acid sequencing (RNAseq) datasets to develop tissue specific expression atlases and proteome maps. Integration of transcriptomics, proteomics as well as metabolomics with genotyping and phenotyping data and establishment of appropriate databases, with the corresponding bioinformatic infrastructure will lead to a functional understanding and improved prediction accuracy of yield and quality parameters for developing sophisticated strategies such as genome-wide MAS to improve breeding efficiency. Although the interpretation of the different 'omics' datasets is not straightforward, the combined information is an important step towards uncovering correlation(s) between the expressed genetic information and the phenotypic response of the oil palm crop.

Charting Proteome-based Knowledge for Improving Oil Palm Yield and Quality

Increasing oil production of a key crop such as oil palm is essential for a more sustainable and greener future. A better understanding of how plants regulate oil biosynthesis will assist in efforts towards breeding palms that produce more oil, with specific fatty acid compositions which relate to quality (Lau *et al.*, 2018; Ramli *et al.*, 2002a; 2002b). This provides a more sustainable way to produce more of the desired natural oils from existing hectarage instead of simply increasing the area of land used for agriculture. In this respect, several key enzymes and genes involved in the regulation of fatty acid biosynthesis of the oil palm have been characterised and purified, mainly for utilisation in the genetic modification programme (Masura *et al.*, 2017; Parveez *et al.*, 2010; Ramli *et al.*, 2012; Sambanthamurthi *et al.*, 2000). The information is also useful for genomics-based improvement of the crop. In fact, combining transcriptome and proteome analyses is essential for developing a comprehensive understanding of the molecular mechanisms regulating fruit development and fatty acid metabolism. Several studies which employed gel-based comparative proteomics, provided an overview of proteins that are abundant during oil palm fruit development, as well as insights into proteins that play a key role during fruit maturation. There has been much progress in technologies and chemometrics application that have revealed changes in proteins that accumulate during oil palm mesocarp development (Hassan *et al.*, 2019).

In its early stages, the oil palm fruit consists of storage and structural carbohydrates and

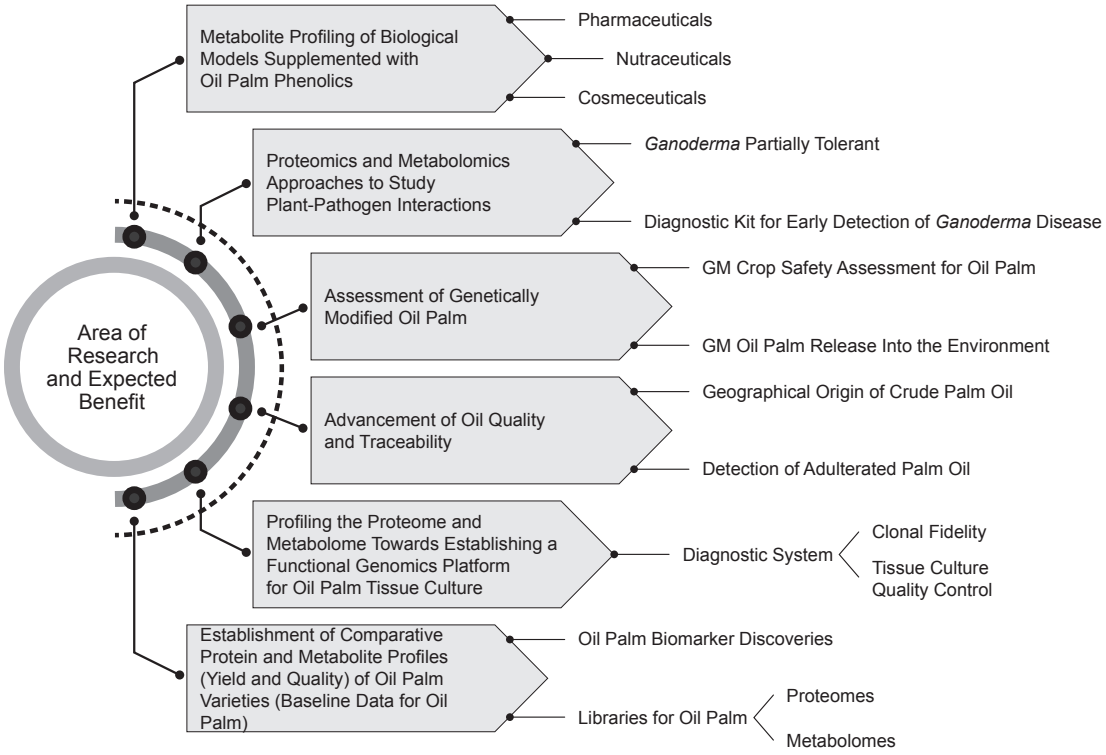

Figure 2. Priority research areas in oil palm proteomics and metabolomics.

membrane lipids but very little oil. As it approaches maturity, the formation of oil increases rapidly in the mesocarp tissue and the ripeness of the fruit bunch is marked by huge changes in the exocarp tissues. Several targeted and untargeted proteomics and metabolomics studies have been carried out to gain a holistic understanding of molecular mechanisms regulating fruit maturation to complement available genomic information. The metabolomics platform of MS in particular, which results in huge amounts of data has proven useful in the analysis of molecular fractions at specific time points during oil palm fruit development (Teh *et al.*, 2013). Hassan *et al.* (2019) developed proteomics protocol to study major metabolism including those involved in lipid production, energy, secondary metabolites and amino acid, which were found to be significantly altered during fruit development (*Figure 3*). Independent research which focused on the analysis of proteins and metabolites from high yielding oil palm and storage oil production (Loei *et al.*, 2013; Neoh *et al.*, 2013; Ooi *et al.*, 2015) has mostly complemented the earlier findings on the different proteins accumulated during fruit development. To further build capacity, more than 4000 proteins have been identified from oil palm fruit mesocarp (Hassan *et al.*, 2014; Lau *et al.*, 2018; 2020) can be catalogued in a database to facilitate future research. In another interesting research, Lau *et al.* (2015) studying high-oleate palms, described advanced proteomic techniques to isolate, detect and identify chromoplast-based proteins associated with the fatty acid biosynthesis pathway. It was revealed that control of oleic acid production is not restricted to enzymes associated with fatty acid biosynthesis, supporting previous biochemical studies that the flux of fatty acids into most plant oils is controlled in large part by the relative activity of more than one pathway (Ramli *et al.*, 2002b). Lau *et al.* (2016) also reported the plausibility of phosphorylation involvement in the regulation mechanism.

Using the integrated omics approach, Appleton *et al*. (2014) discovered that subtle changes in carbon flux can lead to increased oil synthesis in oil palm. They reported that although genetic markers are important for oil palm crop improvement, marker accuracy varies across population backgrounds depending on genetic distance of markers from controlling genes and population diversity. Furthermore, development of accurate marker selection tools is especially challenging for highly polygenic traits like yields that are largely influenced by the environment. There is a recognition that biochemical omics techniques could act as a link between controlling genes and associated genetic markers by determining genes and biochemical pathways that are more directly associated with the final trait. Along this line, the team investigated the differences in biochemical regulation of high yielding individuals compared to average performers within a group of siblings planted in

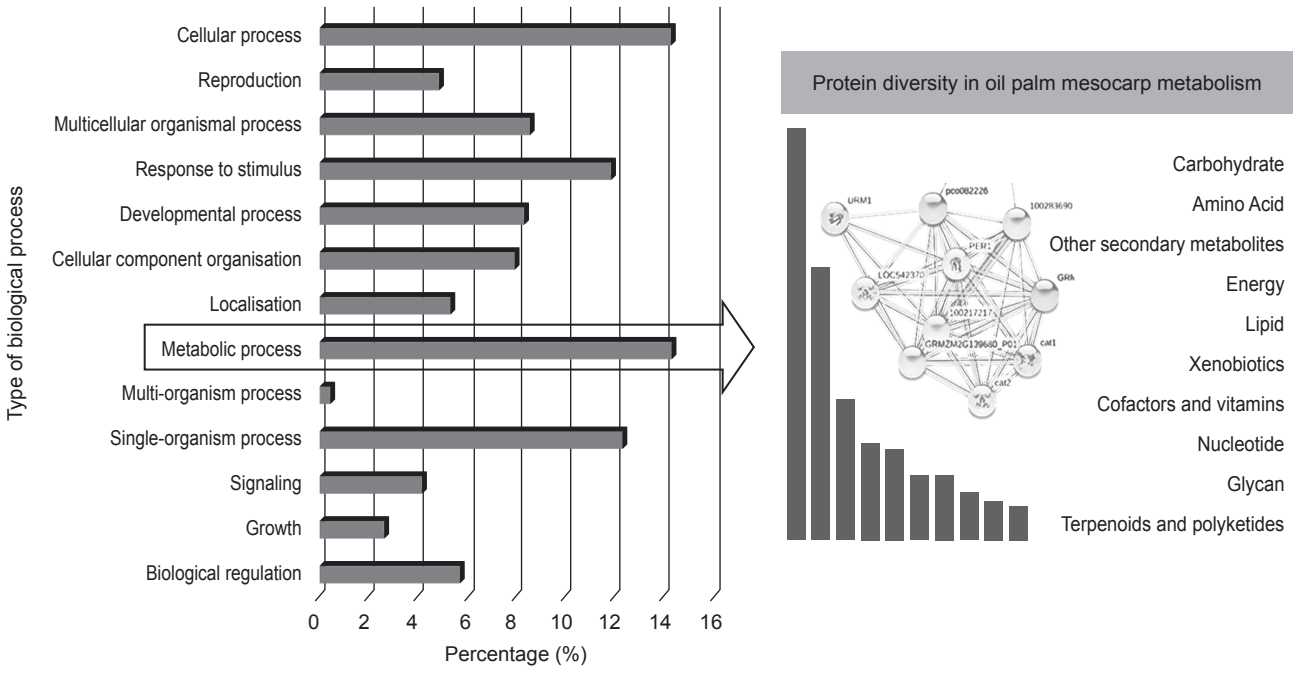

Figure 3. Functional classification of identified proteins from oil palm mesocarp tissue using gel-based proteomics approach (adapted from Hassan et al.*, 2019).*

the same location. Transcriptomics, proteomics and metabolomics were used to compare biochemical changes before, during and after oil biosynthesis in the mesocarp to obtain further understanding of regulation of oil biosynthesis in the oil palm. Genome polymorphisms associated with the genes identified were subsequently prioritised when conducting genome-wide association studies on larger sets of more diverse populations.

Teh *et al*. (2014) investigated changes in expression of polyamines, hormones and cell-wall-related genes, and metabolites in the oil palm mesocarp at different stages of fruit development and described the relationship between the structural and biochemical metabolism during ripening. A distinct reduction in auxin-responsive gene expression was observed from 18 to 22 weeks after anthesis. Fruit enlargement during lipid accumulation and later stage of fruit maturation coincided with high polyamine concentrations. Actin, expansin and polygalacturonase gene expressions were also observed to increase during fruit maturation. The combined omics approach provided a more detailed understanding of the coordinated process involved in fruit ripening and oil accumulation and could potentially lead to the identification of the master regulators of these important processes.

Oil palm and date palm exhibit an extreme difference in carbon partitioning, with oil palm accumulating high amount of oil in its mesocarp, and the closely related date palm accumulating almost exclusively sugars. Bourgis *et al.* (2011) compared the transcriptome and metabolite content of oil palm and date palm and discovered that despite more than a 100-fold difference in flux to lipids, most enzymes of triacylglycerol assembly were expressed at similar levels in oil palm and date palm. Oil palm had much higher transcript levels for all fatty acid synthesis enzymes, and transcripts of an orthologue of the WRI1 transcription factor were 57-fold higher in oil palm compared to date palm. The combination of transcriptomics and metabolomics confirmed earlier flux studies by Ramli *et al*. (2002a; 2002b; 2009) that fatty acid synthesis plays a more predominant role than triacylglycerol assembly in the regulation of lipid synthesis in oil palm.

Deciphering the Molecular Interactions in Oil Palm Disease Using Proteomics and Metabolomics

The most important oil palm diseases are basal stem rot (BSR) (*Ganoderma* spp.), *Fusarium* vascular wilt (*Fusarium oxysporum* f.sp. *elaeidis*), red ring (*Rhadinaphelenchus cocophilus*), *Phytoplasma* sudden wilt (*Phytomonas staheli*), *Phyhthoptora* bud rot (*Phyhthoptora palmivora*), Marchitez/lethal wilt (*Phytoplasma* sp.), *Cercospora* leaf spot (*Cercospora elaeidis*) and *chlorotic* ring (*Potyvirus*) (Ariffin *et al*., 2000; Chinchilla, 1988; Di Lucca *et al*., 2013; Flood, 2006; Morales *et al*., 2002; Torres *et al*., 2010; Weir, 1968). In Malaysia and other oil palm producing countries in Southeast Asia, *Ganoderma boninense* is the dominant fungal pathogen responsible for BSR disease in *Elaeis guineensis* (Idris *et al*., 2011; Susanto *et al*., 2005; Turner and Gillbanks, 2003). Statistical data revealed that in Malaysia, losses due to *Ganoderma* disease can reach up to RM1.5 million a year (Arif *et al*., 2011) and it was estimated that the total area affected by *Ganoderma* disease in 2020 would be around 443 430 ha or 65.6 million of oil palms (Roslan and Idris, 2012). As yet no effective remedial method to prevent spread of the disease to healthy stands has been reported (Idris *et al*., 2016).

As palm oil represents the largest share of the world's vegetable oil market, 80% of which is used by the food industry, BSR may have a serious effect on global food security. Continuous efforts have been made to select tolerant oil palm progenies (Durand-Gasselin *et al*., 2005; Idris *et al*., 2004) or to develop best management practices to control the spread of the disease (Susanto *et al*., 2005). Metabolomics tools have been used to explore metabolite profiles in highly tolerant and susceptible genetic backgrounds to improve our current understanding of its biology. Although it is still preliminary, the developed method provides a basic tool as a standard protocol for future efforts aimed at selective breeding of oil palm via metabolomics-assisted breeding techniques (Rozali *et al*., 2017). The Deli palms (in Malaysia and Indonesia) are more susceptible to *Ganoderma* than those from the African germplasm (Cameroon) (Idris *et al*., 2004). The elucidation of potential metabolite markers, *i.e*., shikimic acid, glucose and malic acid that were responsible for separately clustering Deli and MPOB-Cameroon *dura*s as highlighted by Nurazah *et al.* (2017) provides an initial clue into what may distinguish susceptible and tolerant planting materials. The results suggest that the employed methodology is a powerful approach to profile and portray leaf metabolome with different susceptibility to *G. boninense*. In the future, we envision additional studies that incorporate metabolomics as well as other different omics platforms for screening larger populations of truly resistant and susceptible palms, to obtain a holistic view of oil palm's response to *Ganoderma*, with a view to conduct detailed pathway analysis.

The use of omics technologies to better understand incidences of BSR in oil palm has been reported recently (Othman *et al*., 2019a). The assignment of fatty acid composition in oil palm leaves in relation to severity of *Ganoderma* infection, and protein analysis of *G. boninense* using gel- and LC-based approaches are examples of how

proteomics and metabolomics studies are contributing to improve our current understanding of BSR (Dzulkafli *et al*., 2019; Nurazah *et al*., 2013; Othman *et al*., 2017). Due to its great potential, proteomics specifically has been used to better understand the pathogen, *Ganoderma* spp. itself (Dzulkafli *et al*., 2016; Syahanim *et al*., 2019). The identification of differential proteins in two *Ganoderma* spp., namely *G. boninense* (pathogenic) and *G. tornatum* (non-pathogenic) will prove invaluable in understanding virulence and pathogenicity (Al-Obaidi *et al*., 2016). This will also help in long-term efforts at elucidating the mechanisms of how the fungus infects oil palm. Protein identification depends not only on analytical technologies but also on the existence of complete genome sequence databases for comparison. The genome sequence information for this phytopathogen was recently published by a joint group of researchers from France and Malaysia who assembled a total of 63 Mb using Illumina and 454 platforms to identify microsatellite markers for genetic diversity studies (Mercière *et al*., 2015). More recently, additional information on the sequence and number of reads generated for *G. boninense* and *G. tornatum* samples were also reported (Nagappan *et al*., 2018).

Omics – A Tool to Assist in the Generation and Assessment of Transgenic Oil Palm

The identification of genes regulating specific traits will play a key role towards the improvement of the oil palm, with potential application in modifying oil content and fatty acid composition by genetic engineering (Othman *et al*., 2000; Parveez *et al*., 2015; Ramli *et al*., 2012) and managing the *Ganoderma* disease (Lim *et al*., 2017; Mohamad Arif *et al*., 2017; Rasid *et al*., 2014; Safiza *et al*., 2015). Despite its economic importance, authorisation and commercialisation of genetically modified organism (GMO) has always been controversial within the scientific and public communities. The advancements in omics technologies are tremendously useful both to facilitate the generation and safety assessment of transgenic crops. First and foremost, omics platforms, especially the transcriptome data, are highly valuable for establishing the basic genetic resources required in the genetic engineering efforts. Identification and isolation of key genes, proteins or promoters are very much simplified. This is illustrated by several recent publications. On promoter isolation, Siti Suriawati *et al.* (2019) reported the identification of a gene that was highly expressed in mesocarp tissue through *in silico* analysis of oil palm transcriptome datasets. The expression specificity of the gene in the tissue was confirmed by real-time quantitative polymerase chain reaction (qPCR) analysis. Using a similar approach, potential root specific genes were also identified (Masura *et al*., 2019a). Identification of these tissue-specific sequences is crucial for the isolation of their promoter sequences and ultimately for directing the expression of transgenes into the desired tissues.

The application of transcriptome data has also led to the identification and isolation of a number of constitutive promoters from oil palm (Masura *et al*., 2011; 2019b). In addition, omics data have also led to the identification of several indicative sequences and metabolites that are associated with several traits of interest (Masura *et al*., 2017). All of these findings could potentially be used in the genetic engineering of oil palm. Oil palm is known to be recalcitrant to genetic transformation, and as such, the development of genotype-independent transformation technology is crucial for this crop. This could help improve oil palm transformation efficiency, which currently is quite low. One approach is through the use of *Baby boom* (*Bbm*) and *Wuschel2* (*Wus2*) genes, which can help establish a biological context to improve transformation efficiency.

The availability of oil palm omics data, especially transcriptome analysis of various tissues and development stages has facilitated the identification and isolation of key genes, which are being selectively applied in research related to genetic modification of oil palm (Masani *et al*., 2018). The existing omics information also has huge potential for utilisation in the exciting area of genome editing. Genome editing offers several advantages over the conventional genetic engineering protocols. First, the technique results in a more predictable and precise gene modification. Since the technique does not add any external or foreign sequence to the recipient cells, it is also more readily acceptable to consumers as well as regulatory authorities. Research on the application of this in oil palm has already been initiated (Bahariah *et al*., 2019), and will likely open up opportunities for genome editing-based improvement. The availability of omics data would facilitate the efforts in two primary ways. First, the omics data would allow more accurate prediction of the target locations. This would minimise the possibilities of off targets in the resultant modified plants. Besides, the data are also useful for the identification of the target or key genes. Increasing oleic acid content has been the main objective of oil palm genetic engineering research at MPOB. Extensive studies to identify the target genes and important regulatory controls over the biosynthesis pathway have been carried out and reviewed (Parveez *et al*., 2015). This has resulted in the formulation of a comprehensive strategy to produce high oleic oil palms through conventional genetic engineering. However, the immense omics

data will allow even more comprehensive analysis of the fatty acid biosynthesis or other pathways.

The analysis will not only allow for the identification of target sequences of the pathway and discrimination of different isoforms but could also determine the crucial elements that are not directly involved in the pathway, such as transcription factors. For example, Dussert *et al.* (2013) identified paralogues of the *WRINKLED1* transcription factors that were highly expressed during oil deposition in the oil palm mesocarp and endosperm. Manipulation of these regulatory elements has proven to be effective in a number of recent studies. For example, overexpression of transcription factors *GmDof4* and *GmDof11* was shown to increase the oleic acid content of *Brassica napus* seeds (Sun *et al.*, 2018). Similarly, oil content of peanut seeds was significantly increased through overexpression of the transcription factor *AtLEC1* (Tang *et al.*, 2018). In tomato, lycopene content was increased up to 5.1-fold through CRISPR/Cas9 multiplex genome editing. It was further illustrated that the regulator protein *SGR1* has a greater control over the lycopene accumulation compared to a number of enzymes in the carotenoid biosynthesis pathway (Li *et al.*, 2018).

Gene editing is also relevant in the field of pests and diseases. A number of recent reports have demonstrated the feasibility of manipulating regulatory sequences to create disease or pest resistant or tolerant plants. For example, genetic manipulation of the disease susceptibility gene *CsLOB1* through CRISPR/Cas9 technique produced plants that are resistant to citrus canker. The *CsLOB1* is a member of the Lateral Organ Boundaries Domain (LBD) gene family of plant transcription factors that can be recognised and induced by the pathogen transcription activator-like (TAL) effectors (Jia *et al.*, 2017). Another example is demonstrated by the increased tolerance to rice blast using transcription factor *OsSRF922*. Mutation of the gene through CRISPR/Cas9 has resulted in significant decrease in pathogen infection in all mutant lines tested (Wang *et al.*, 2016). Initial development in this area has also started to take place in oil palm. Studies to unravel the interaction between oil palm and its most serious pathogen *G. boninense* have been carried out and reported using transcriptomic, proteomic and metabolomic analyses (Al-Obaidi *et al.*, 2016; Ho *et al.*, 2016; Nusaibah *et al.*, 2016; Syahanim *et al.*, 2013). The findings from these studies will eventually contribute towards creating *Ganoderma* tolerant oil palm.

As the research for developing genetically modified (GM) oil palm pushes forward, omics platforms will be essential to confirm that only the intended genomic alterations have occurred. Analysis of the genome, proteome and metabolome will increase the chances of detecting unintended effects, if any (Gong and Wang, 2013). As an example, the proteomics-based analysis of the GM round-up ready soybean revealed no significant alteration in the expression of allergens following genetic modification. Similarly, Gong *et al.* (2012) showed that genetic modification did not alter the protein profile of rice compared to those produced via conventional breeding. However, other studies have shown differences between GM products and non-GM controls (Luo *et al.*, 2009). Metabolomics analysis showed significant difference in selected metabolites between the conventional and GM insect resistant maize (Levandi *et al.*, 2008). The differences observed are likely due to exogenous gene(s) being inserted and the site(s) where the insertion occurs among other factors (Gong and Wang, 2013). This demonstrates the important role of omics-based platforms in evaluating GM oil palm in the near future.

Integrative Omics for Understanding Oil Palm Seed Germination

Despite the critical importance of germination of oil palm seeds, our knowledge on the physiology of the process is limited. Most metabolic studies were carried out in the 1980s and there has been little advancement in our knowledge of molecular players and metabolic controls involved in germination. Oil palm seeds have a low germination rate because of a long dormancy attributed to restrictions of embryo growth because of the hard endocarp which results in mechanical constraints and resistance to oxygen absorption. The germination of oil palm seeds can take years, under natural conditions. Elevated temperature and appropriate levels of seed moisture are necessary for rapid and optimal germination. For commercial seed production, oil palm seeds are heat treated under controlled conditions to break dormancy. However, the effect of heat treatment on phytohormone-related genes/proteins/metabolites and possible relationship with dormancy release is not well understood. Wang *et al.* (2019) carried out integrative omics analysis on the phytohormones involved in oil palm seed germination under conditions used for commercial production to discover the mechanisms involved in oil palm seed germination. Differentially expressed genes and proteins (DEG and DEP) related to seed germination were identified using RNA-seq and isobaric tags for relative and absolute quantitation (iTRAQ) and the results validated with qPCR and western blot. LC-MS/MS was used to determine endogenous phytohormones while exogenous phytohormones were also applied to validate their effects on seed germination. The authors confirmed the important role of phytohormones in oil palm seed germination with abscisic acid (ABA) acting as an inhibitor. Heat treatment breaks dormancy at

least partly by eliminating endogenous ABA. The results emphasised how the omics platforms of transcriptomics, proteomics and metabolomics in combination led to an improved understanding of oil palm seed germination.

Although key metabolic pathways such as β-oxidation are common in germination of all oleaginous seeds including oil palm, palm seeds have unique attributes such as the involvement of the haustorium that digests the endosperm and eventually invades the seed (Cui *et al*., 2020). This involves important metabolic processes such as fatty acid transport and coenzyme A cycling. Despite the importance of these aspects, advances in germination metabolism have been scarce. It is increasingly obvious that integrated omics approaches will be key in resolving the complex processes underpinning germination. Functional genomics will identify gene functions and interactions relevant to seed germination. Proteomics analyses will be of importance to find key transporters, confirm the localisation of enzymes involved in mobilisation of reserves including but not limited only to lipids, and identify proteins associated with kernel oil bodies. Metabolomics may help unravel the spatial and temporal profile of metabolites in the various tissues of the germinating seed. This was recently achieved for maize (Feenstra *et al*., 2017). Such information will be useful for identifying molecular markers associated with superior germination performance which will be advantageous for oil palm breeding.

Geographical and Authentication Tracing of Palm Oil Using Omics-based Technologies

Ensuring food safety requires the monitoring of its source of production and distribution throughout the supply chain. This will enable a sound certification system and also prevent the introduction of adulterants or contaminants during the production and processing stage (Goggin and Murphy, 2018). The ability to distinguish palm oil from different regions or sources requires the development of a geographical traceability system by using robust and precise methods that allow the palm oil consignment to be traced back to its origin at every phase of production. The attempt to differentiate palm oil according to its geographical source has been explored using a wide range of omics tools. These tools include advanced analytical techniques such as GC-flame ionisation detector (GC-FID), proton transfer reaction-MS (PTR-MS), UV-visible spectroscopy, elemental analyser coupled to an isotope ratio mass spectrometer (EA-IRMS), HPLC and GC-ion mobility spectrometry (GC-IMS) combined to cheminformatics of principle component analysis (PCA), partial least squares-discriminant analysis (PLS-DA), orthogonal partial least squares-discriminant analysis (OPLS-DA), hierarchical cluster analysis (HCA) and soft independent modelling of class analogy (SIMCA) (Ramli *et al*., 2020). Promising markers that can facilitate geographical differentiation of palm oil include fatty acid profiles, triacylglycerols, volatile organic compounds, isotopic composition, phytosterols and carotenoid content, in combination with chemometrics (Goggin and Murphy, 2018; Muhammad *et al*., 2018; Tres *et al*., 2013). The possibility of utilising genomics-based DNA fingerprints of palm oil is also being explored due to its success in differentiating other vegetable oils (Costa *et al*., 2012). However, the ability of DNA markers to track palm oil samples across the supply chain to their geographical origin is going to be challenging, as genotypes with different genetic backgrounds are usually planted, even in a single block of a large plantation (Ooi *et al*., 2006; Ramli *et al*., 2020). Nevertheless, the work is important to detect and nail down fraudulent and unsafe milling and processing activities, if any. With the current technological capabilities, metabolomics is also being exploited for identifying unique chemical fingerprints to detect product contamination and adulteration. This effort is actively being conducted in order to position the oil palm industry to meet and optimise the delivery of the highest quality oil with minimum environmental and social concerns. Efforts are being directed to specifically look into the potential of technologies to ensure that palm oil, especially crude palm oil (CPO) and refined palm oil meet international standards including those related to 3-monochloropropane-1,2-diol (3-MCPD) (Tarmizi *et al*., 2019). Adherence to the practice of not adding sludge palm oil (SPO) or other residual oils, such as palm fibre oil (PFO) back to the CPO, will help maintain the Malaysian palm oil industry at the forefront of the vegetable oils and fats industry. Omics-based technologies can be applied to ensure that CPO is free from such residual oils. This was demonstrated in a recent study, where GC-IMS was used for rapid and cost-effective screening of CPO for detection of PFO and SPO based on their characteristic volatile organic compound (VOC) fingerprints. The study demonstrated that the identification of contaminants, adulterations and/or off flavours at very low concentrations is possible in CPO samples (Othman *et al*., 2019b). This paves the way for this technology to be used for quality assurance and eventually for product traceability.

CONCLUSION

Genomic platforms represent a key resource towards achieving the target of producing superior oil palm. However, understanding the cellular biology and biochemistry underlying the specific traits is no substitute for studying proteins and

metabolites, since these are directly responsible for cellular activity. Therefore, to complete the view offered by genomics and transcriptomic-based analysis, proteomics and metabolomics offer a new comprehensive perspective to better understand regulatory mechanisms that govern complex phenotypes, especially those under environmental influence. As such, an integrated omics approach is essential to uncover the complexities and diverse physiological processes that govern complex traits in the oil palm (*e.g.*, yield, quality and disease resistance), which can lead to biomarkers that can more accurately predict these traits. Undeniably, proteomics and metabolomics research on oil palm is still at its infancy and there is a need for further development of relevant methods and techniques for comprehensive analysis of proteins and metabolites towards understanding complex traits in oil palm. Although challenges are aplenty, on-going technical improvements will facilitate application of integrated omics technologies in developing new and improved oil palm varieties. The pressure of upholding sustainability in a situation where resources are limited warrants a shift in paradigm for the oil palm industry. At this juncture, strict regulations including risk assessment of transgenic oil palm, and making sure CPO is free of adulterants require established analytical tools that can be adopted by the industry. Thus, new technological advances which can provide fast and robust detection for quality and eventually traceability purposes, cannot be over-emphasised. The application of these techniques to agricultural systems is a step forward towards the implementation of translational proteomics and metabolomics in crop breeding. The integration of multi-layered omics data will allow for reconstruction of regulatory networks and provide a stereoscopic view of dynamic molecular processes and interacting networks of genes in the oil palm. This will lead to deeper insights into target traits and facilitate precision breeding of the oil palm.

ACKNOWLEDGEMENT

The authors wish to thank members of the Proteomics and Metabolomics Unit, Advanced Biotechnology and Breeding Centre, MPOB for their technical assistance.

REFERENCES

Al-Obaidi, J R; Hussin, S N I S; Saidi, N B; Rahmad, N and Idris, A S (2017). Comparative proteomic analysis of *Ganoderma* species during *in vitro* interaction with oil palm root. *Physiol. Mol. Plant Pathol., 99*: 16-24.

Al-Obaidi, J R; Saidi, N B; Usuldin, S R A; Rahmad, N; Zean, N B and Idris, A S (2016). Differential proteomic study of oil palm leaves in response to *in vitro* inoculation with pathogenic and non-pathogenic *Ganoderma* spp. *J. Plant Pathol., 98(2)*: 235-244.

Alam, A F; Er, A C and Begum, H (2015). Malaysian oil palm industry: Prospect and problem. *J. Food Agric. Environ., 13*(2): 143-148.

Allwood, J W; Ellis, D I and Goodacre, R (2008). Metabolomic technologies and their application to the study of plants and plant-host interactions. *Physiol. Plant., 132(2)*: 117-135.

Appleton, D R; Teh, H F; Neoh, B K; Ooi, E K; Wong, Y C and Kulaveerasingam, H (2014). Omics reveals subtle changes in carbon flux that lead to increased oil biosynthesis in oil palm. *Inform Magazine AOCS May 2014*. https://www.aocs.org/stay-informed/inform-magazine/featured-articles/omics-reveals-subtle-changes-in-carbon-flux-that-lead-to-increased-oil-biosynthesis-in-oil-palm.

Arif, M S; Roslan, A and Idris, A S (2011). Economics of oil palm pests and *Ganoderma* disease and yield losses. *Proc. of the Third MPOB-IOPRI International Seminar: Integrated Oil Palm Pests and Diseases Management*. 14 November 2011. Kuala Lumpur Convention Centre.

Ariffin, D; Idris, A S and Singh, G (2000). Status of *Ganoderma* in oil palm. *Ganoderma Diseases of Perennial Crops* (Flood, J; Bridge, P D and Holderness, M eds.). CABI Bioscience, Egham, UK. p. 49-68.

Azmil Haizam Ahmad Tarmizi; Raznim Arni Abd Razak; Abdul Niefaizal; Abdul Hammid and Ainie Kuntom (2019). Effect of anti-clouding agent on the fate of 3-monochloropropane-1, 2-diol esters and glycidyl esters in palm olein during repeated frying. *Molecules*, *24(12)*: 2332.

Bahariah, B; Masani, M Y A; Rasid, O A; Parveez; G K A; Tang, Y; Ji, Z; Wei, Z; Wang, C and Zhao, K (2019). CRISPR/Cas9-mediated genome editing of FAD2 gene in rice: A monocotyledonous model plant for oil palm. *Proc. of the PIPOC 2019 International Palm Oil Congress*. MPOB, Bangi. p. 30-34.

Bai, B; Wang, L; Lee, M; Zhang, Y; Alfiko, Y; Ye, B Q; Wan, Z Y; Lim, C H; Suwanto, A; Chua, N-H and Yue, G H (2017). Genome-wide identification of markers for selecting higher oil content in oil palm. *BMC Plant Biol., 17(1)*: 93.

Baniasadi, H; Vlahakis, C; Hazebroek, J; Zhong, C and Asiago, V (2014). Effect of environment and

genotype on commercial maize hybrids using LC/MS-based metabolomics. *J. Agr. Food Chem., 62(6)*: 1412-1422.

Barros, E; Lezar, S; Anttonen, M J; Van Dijk, J P; Röhlig, R M; Kok, E J and Engel, K H (2010). Comparison of two GM maize varieties with a near-isogenic non-GM variety using transcriptomics, proteomics and metabolomics. *Plant Biotechnol. J., 8(4)*: 436-451.

Bartolini, G; Di Monte, G; Rea, E and Toponi, M A (1999). Protein patterns in response to cold stress on clones of *Olea europaea* L., cv Leccino. *Acta Hortic., 474*: 481-484.

Bianco, L; Alagna, F; Baldoni, L; Finnie, C; Svensson, B and Perrotta, G (2013). Proteome regulation during *Olea europaea* fruit development. *PLoS ONE, 8(1)*: e53563.

Billotte, N; Marseillac, N; Risterucci, A M; Adon, B; Brottier, P; Baurens, F C; Singh, R; Herran, A; Asmady, H; Billot, C and Amblard, P (2005). Microsatellite-based high density linkage map in oil palm (*Elaeis guineensis* Jacq.). *Theor. Appl. Genet., 110(4)*: 754-765.

Bourgis, F; Kilaru, A; Cao, X; Ngando-Ebongue, G-F; Drira, N; Ohlrogge, J B and Vincent Arondel, V (2011). Comparative transcriptome and metabolite analysis of oil palm and date palm mesocarp that differ dramatically in carbon partitioning. *Proc. Natl. Acad. Sci. USA, 108(30)*: 12527-12532.

Canovas, F M; Dumas-Gaudot, E; Recorbet, G; Jorrin, J; Mock, H P and Rossignol, M (2004). Plant proteome analysis. *Proteomics, 4(2)*: 285-298.

Capriotti, A L; Cavaliere, C; Foglia, P; Piovesana, S; Samperi, R; Stampachiacchiere, S and Laganà, A (2013). Proteomic platform for the identification of proteins in olive (*Olea europaea*) pulp. *Anal. Chim. Acta, 800*: 36-42.

Catchpole, G S; Beckmann, M; Enot, D P; Mondhe, M; Zywicki, B; Taylor, J; Hardy, N; Smith, A; King, R D; Kell, D B; Fiehn, O and Draper, J (2005). Hierarchical metabolomics demonstrates substantial compositional similarity between genetically modified and conventional potato crops. *Proc. Natl. Acad. Sci. USA, 102(40)*: 14458-14462.

Chan, P L; Ma, L S; Low, E T L; Shariff, E M; Ooi, L C L; Cheah, S C and Singh, R (2010). Normalized embryoid cDNA library of oil palm (*Elaeis guineensis*). *Electron. J. Biotechnol., 13(1)*: 10-11.

Chang, Y; Zhao, C; Zhu, Z; Wu, Z; Zhou, J; Zhao, Y; Lu, X and Xu, G (2012). Metabolic profiling based on LC/MS to evaluate unintended effects of transgenic rice with cry1Ac and sck genes. *Plant Mol. Biol., 78*: 477-487.

Chaudhary, J; Patil, G B; Sonah, H; Deshmukh, R K; Vuong, T D; Valliyodan, B and Nguyen, H T (2015). Expanding omics resources for improvement of soybean seed composition traits. *Front. Plant Sci., 6*: 1021-1037.

Cheah, S C; Maria, M; Ooi, L C; Rahimah, A R and Siti Nor Akmar, A (1993). Detection of DNA variability in the oil palm using RFLP probes. *Proc. of the PIPOC 1993 International Palm Oil Congress*. 9-14 September 1993, Kuala Lumpur, Malaysia.

Chen, S and Harmon, A C (2006). Advances in plant proteomics. *Proteomics, 6(20)*: 5504-5516.

Chinchilla, C M (1988). The red ring-little leaf syndrome in oil palm and coconut. *Bol. Tec Opo-CB, 2(4)*: 113-136.

Copley, T R; Aliferis, K A; Kliebenstein, D J and Jabaji, S H (2017). An integrated RNAseq-1 H NMR metabolomics approach to understand soybean primary metabolism regulation in response to *Rhizoctonia* foliar blight disease. *BMC Plant Biol., 17(1)*: 84.

Costa, J; Mafra I and Oliveira, M B P P (2012). Advances in vegetable oil authentication by DNA-based markers. *Trends Food Sci. Technol., 26(1)*: 43-55.

Cui, J; Lamade, E and Tcherkez, G (2020). Seed germination in oil palm (*Elaeis guineensis* Jacq.): A review of metabolic pathways and control mechanisms. *Int. J. Mol. Sci., 21(12)*: 4227.

Damerval, C; Maurice, A; Josse, J M and De Vienne, D (1994). Quantitative trait loci underlying gene product variation: A novel perspective for analyzing regulation of genome expression. *Genetics, 137(1)*: 289-301.

Das, A; Rushton, P and Rohila, J (2017). Metabolomic profiling of soybeans (*Glycine max* L.) reveals the importance of sugar and nitrogen metabolism under drought and heat stress. *Plants, 6(2)*: 21.

Davies, H V; Shepherd, L V; Stewart, D; Frank, T; Röhlig, R M and Engel, K H (2010). Metabolome variability in crop plant species – When, where, how much and so what? *Regul. Toxicol. Pharmacol., 58(3)*: S54-S61.

Deshmukh, R; Sonah, H; Patil, G; Chen, W; Prince, S; Mutava, R; Vuong, T; Valliyodan, B and Nguyen, H T (2014). Integrating omic approaches for abiotic stress tolerance in soybean. *Front. Plant Sci., 3(5)*: 244. DOI: 10.3389/fpls.2014.00244.

Di Lucca, A G T; Trinidad Chipana, E F; Talledo Albújar, M J; Dávila Peralta, W; Montoya Piedra, Y C and Arévalo Zelada, J L (2013). Slow wilt: Another form of Marchitez in oil palm associated with trypanosomatids in Peru. *Trop. Plant Pathol., 38*(*6*): 522-533.

Dixon, R A; Gang, D R; Charlton, A J; Fiehn, O; Kuiper, H A; Reynolds, T L; Tjeerdema, R S; Jeffery, E H; German, J B; Ridley, W P and Seiber, J N (2006). Applications of metabolomics in agriculture. *J. Agric. Food Chem., 54(24)*: 8984-8994.

Durand-Gasselin, T; Asmady, H; Flori, A; Jacquemard, J C; Hayun, Z; Breton, F and De Franqueville, H (2005). Possible sources of genetic resistance in oil palm (*Elaeis guineensis* Jacq.) to basal stem rot caused by *Ganoderma boninense* - Prospects for future breeding. *Mycopathologia, 159(1)*: 93-100.

Dussert, S; Guerin, C; Andersson, M; Joët, T; Tranbarger, T J; Pizot, M; Sarah, G; Omore, A; Durand-Gasselin, T and Morcillo, F (2013). Comparative transcriptome analysis of three oil palm fruit and seed tissues that differ in oil content and fatty acid composition. *Plant Physiol., 162(3)*: 1337-1358.

Dzulkafli, S B; Othman, A; Shahwan, S; Nurazah, Z; Manaf, M A A; Idris, A S; Amiruddin, M D; Tahir, N I and Ramli, U S (2019). Identification of chelidonic acid and asparagine in *Ganoderma boninense*-inoculated oil palm seedlings. *J. Oil Palm Res., 31(1)*: 53-66.

Dzulkafli, S B; Othman, A; Lau, B Y C; Shahwan, S; Idris, A S and Ramli, U S (2016). Optimization of protein extraction from *Ganoderma boninense* for sodium dodecyl sulfate-polyacrylamide gel electrophoresis (SDS-PAGE) analysis. *Transactions of Persatuan Genetik Malaysia.* p. 193-197.

Eldakak, M; Milad, S I M; Nawar, A I and Rohila, J S (2013). Proteomics: A biotechnology tool for crop improvement. *Front. Plant Sci., 4(35)*: 1-12.

Esteve, C; Cañas, B; Moreno-Gordaliza, E; Del Río, C; García, M C and Marina, M L (2011). Identification of olive (*Olea europaea*) pulp proteins by matrix-assisted laser desorption/ionization time-of-flight mass spectrometry and nano-liquid chromatography tandem mass spectrometry. *J. Agric. Food Chem., 59(22)*: 12093-12101.

Feenstra, A D; Alexander, L E; Song, Z; Korte, A R; Yandeau-Nelson, M D; Nikolau, B J and Lee, Y J (2017). Spatial mapping and profiling of metabolite distributions during germination. *Plant Physiol., 174:* 2532-2548.

Fernie, A R and Schauer, N (2009). Metabolomics-assisted breeding: A viable option for crop improvement? *Trends Genet., 25(1)*: 39-48.

Fiehn, O (2002). Metabolomics - The link between genotypes and phenotypes. *Plant Mol. Biol., 48*: 155-171.

Fiehn, O; Kloska, S and Altmann, T (2001). Integrated studies on plant biology using multiparallel techniques. *Curr. Opin. Biotechnol., 12*(*1*): 82-86.

Flood, J (2006). A review of *Fusarium* wilt of oil palm caused by *Fusarium oxysporum* f. sp. *elaeidis*. *Phytopathology, 96(6)*: 660-662.

Fraser, P D; Pinto, M E S; Holloway, D E and Bramley, P M (2000). Application of high-performance liquid chromatography with photodiode array detection to the metabolic profiling of plant isoprenoids. *Plant J., 24(4)*: 551-558.

Gamache, P H; Meyer, D F; Granger, M C and Acworth, I N (2004). Metabolomic applications of electrochemistry/mass spectrometry. *J. Am. Soc. Mass Spectrom., 15(12)*: 1717-1726.

García-Villalba, R; León, C; Dinelli, G; Segura-Carretero, A; Fernández-Gutiérrez, A; Garcia-Cañas, V and Cifuentes, A (2008). Comparative metabolomic study of transgenic versus conventional soybean using capillary electrophoresis-time-of-flight mass spectrometry. *J. Chromatogr. A, 1195*: 164-173.

Gavaghan, C L; Li, J V; Hadfield, S T; Hole, S; Nicholson, J K; Wilson, I D; Howe, P W A; Stanley, P D and Holmes, E (2011). Application of NMR-based metabolomics to the investigation of salt stress in maize (*Zea mays*). *Phytochem. Anal., 22(3)*: 214-224.

German, J B; Roberts, M A; Fay, L and Watkins, S M (2002). Metabolomics and individual metabolic assessment: The next great challenge for nutrition. *J. Nutr., 132(9)*: 2486-2487.

Glaab, E (2016). Using prior knowledge from cellular pathways and molecular networks for diagnostic specimen classification. *Brief. Bioinform., 17(3)*: 440-452.

Goggin, K A and Murphy, D J (2018). Monitoring the traceability, safety and authenticity of imported palm oils in Europe. *OCL*, *25*: A603.

Gong, C Y; Li, Q; Yu, H T; Wang, Z and Wang, T (2012). Proteomics insight into the biological safety of transgenic modification of rice as compared with conventional genetic breeding and spontaneous genotypic variation. *J. Proteome Res.*, *11(5)*: 3019-3029.

Gong, C Y and Wang, T (2013). Proteomic evaluation of genetically modified crops: Current status and challenges. *Front. Plant Sci.*, *4*: 41.

Hajduch, M; Matusova, R; Houston, N L and Thelen, J J (2011). Comparative proteomics of seed maturation in oilseeds reveals differences in intermediary metabolism. *Proteomics, 11(9)*: 1619-1629.

Halket, J M; Waterman, D; Przyborowska, A M; Patel, R K P; Fraser, P D and Bramley, P M (2004). Chemical derivatization and mass spectral libraries in metabolic profiling by GC/MS and LC/MS/MS. *J. Exp. Bot.*, *56(410)*: 219-243.

Hashiguchi, A; Ahsan, N and Komatsu, S (2010). Proteomics application of crops in the context of climatic changes. *Food Res. Int., 43(7)*: 1803-1813.

Hassan, H; Amiruddin, M D; Weckwerth, W and Ramli, U S (2019). Deciphering key proteins of oil palm (*Elaeis guineensis* Jacq.) fruit mesocarp development by proteomics and chemometrics. *Electrophoresis, 40(2)*: 254-265.

Hassan, H; Lau, B Y C and Ramli, U S (2014). Extraction methods for analysis of oil palm leaf and root proteins by two-dimensional gel electrophoresis. *J. Oil Palm Res., 26(1)*: 54-61.

Helmy, M; Tomita, M and Ishihama, Y (2011). OryzaPG-DB: Rice proteome database based on shotgun proteogenomics. *BMC Plant Biol., 11(1)*: 63.

Ho, C L; Kwan, Y Y; Choi, M C; Tee, S S; Ng, W H; Lim, K A; Lee, Y P; Ooi, S E; Lee, W W; Tee, J M and Tan, S H (2007). Analysis and functional annotation of expressed sequence tags (ESTs) from multiple tissues of oil palm (*Elaeis guineensis* Jacq.). *BMC Genomics*, *8(1)*: 381.

Ho, C L; Tan, Y C; Yeoh, K A; Ghazali, A K; Yee, W Y and Hoh, C C (2016). *De novo* transcriptome analyses of host-fungal interactions in oil palm (*Elaeis guineensis* Jacq.). *BMC Genomics, 17(1)*: 66.

Huhman, D V and Sumner, L W (2002). Metabolic profiling of saponins in *Medicago sativa* and *Medicago truncatula* using HPLC coupled to an electrospray ion-trap mass spectrometer. *Phytochemistry, 59(3)*: 347-360.

Huntingford, C; Hugo Lambert, F; Gash, J H C; Taylor, C M and Challinor, A J (2005). Aspects of climate change prediction relevant to crop productivity. *Philos. Trans. R. Soc. Lond. B Biol. Sc., 360(1463)*: 1999-2009.

Hurtado-Fernández, E; Pacchiarotta, T; Mayboroda, O A; Fernández-Gutiérrez, A and Carrasco-Pancorbo, A (2015). Metabolomic analysis of avocado fruits by GC-APCI-TOF MS: Effects of ripening degrees and fruit varieties. *Anal. Bioanal. Chem., 407(2)*: 547-555.

Idris, A S; Nurrashyeda, R; Mohd Hefni, R; Shamala, S and Norman, K (2016). *Standard Operating Procedures (SOP) Guidelines for Managing* Ganoderma *Disease in Oil Palm*. MPOB, Bangi. p. 41.

Idris, A S; Mior, M H A Z; Maizatul, S M and Kushairi, A (2011). Survey on status of *Ganoderma* disease of oil palm. *Proc. of the PIPOC 2011 International Palm Oil Congress*. MPOB, Bangi. p. 235-238.

Idris, A; Kushairi, A; Ismail, S and Ariffin, D (2004). Selection for partial resistance in oil palm progenies to *Ganoderma* basal stem rot. *J. Oil Palm Res., 16(2)*: 12-18.

Jia, H; Zhang, Y; Orbović, V; Xu, J; White, F F; Jones, J B and Wang, N (2017). Genome editing of the disease susceptibility gene CsLOB1 in citrus confers resistance to citrus canker. *Plant Biotechnol. J., 15(7)*: 817-823.

Jin, J; Lee, M; Bai, B; Sun, Y; Qu, J; Rahmadsyah; Alfiko, Y; Lim, C H; Suwanto, A; Sugiharti, M; Wong, L; Ye, J; Chua, N-H and Yue, G H (2016). Draft genome sequence of an elite *Dura* palm and whole-genome patterns of DNA variation in oil palm. *DNA Res., 23(6)*: 527-533.

Jorge, T F; Mata, A T and António, C (2016). Mass spectrometry as a quantitative tool in plant metabolomics. *Phil. Trans. R. Soc. A, 374(2079)*: 20150370. DOI: 10.1098/rsta.2015.0370.

Jouannic, S; Argout, X; Lechauve, F; Fizames, C; Borgel, A; Morcillo, F; Aberlenc-Bertossi, F; Duval, Y and Tregear, J (2005). Analysis of expressed sequence tags from oil palm (*Elaeis guineensis*). *FEBS Lett.*, *579(12)*: 2709-2714.

Khosla, P (2011). Nutritional characteristics of palm oil. *Reducing Saturated Fats in Foods*. Woodhead Publishing. p. 112-127.

Kim, J K; Park, S-Y; Lee, S M; Lim, S-H; Kim, H J; Oh, S-D; Yeo, Y; Cho, H S and Ha, S-H (2013). Unintended polar metabolite profiling of carotenoid-biofortified transgenic rice reveals substantial equivalence to its non-transgenic counterpart. *Plant Biotechnol. Rep., 7(1)*: 121-128.

Komatsu, S; Muhammad, A and Rakwal, R (1999). Separation and characterization of proteins from green and etiolated shoots of rice (*Oryza sativa* L.): Towards a rice proteome. *Electrophoresis, 20(3)*: 630-636.

Kristal, B S and Matson, W R (2002). Simultaneous analysis of multiple redox-active metabolites from biological matrices. *Oxidative Stress Biomarkers and Antioxidant Protocols*. Humana Press. p. 185-194.

Kumar, R; Bohra, A; Pandey, A K; Pandey, M K and Kumar, A (2017). Metabolomics for plant improvement: Status and prospects. *Front. Plant Sci.*, *8*: 1302.

Kusano, M; Yang, Z; Okazaki, Y; Nakabayashi, R; Fukushima, A and Saito, K (2015). Using metabolomic approaches to explore chemical diversity in rice. *Mol. Plant., 8*(*1*): 58-67.

Kushairi, A; Ong-Abdullah, M; Nambiappan, B; Hishamuddin, E; Bidin, M N I Z; Ghazali, R; Subramaniam, V; Sundram, S and Parveez, G K A (2019). Oil palm economic performance in Malaysia and R&D progress in 2018. *J. Oil Palm Res., 31(2)*: 165-194.

Kwong, Q B; Teh, C K; Ong, A L; Heng, H Y; Lee, H L; Mohamed, M; Low, J Z-B; Apparow, S; Chew, F T; Mayes, S; Kulaveerasingam, H; Tammi, M and Appleton, D R (2016). Development and validation of a high-density SNP genotyping array for African oil palm. *Mol. Plant., 9(8)*: 1132-1141.

Lau, B Y C; Othman, A and Ramli, U S (2018). Application of proteomics technologies in oil palm research. *Protein J., 37(6)*: 473-499.

Lau, B Y C; Deb-Choudhury, S; Morton, J D; Clerens, S; Dyer, J M and Ramli, U S (2015). Method developments to extract proteins from oil palm chromoplast for proteomic analysis. *SpringerPlus, 4(1)*: 791.

Lau, B Y C; Clerens, S; Morton, J D; Dyer, J M; Deb-Choudhury, S and Ramli, U S (2016). Application of a mass spectrometric approach to detect the presence of fatty acid biosynthetic phosphopeptides. *Protein J., 35(2)*: 163-170.

Lau, B Y C; Amiruddin, M D and Othman, A (2020). Proteomics analysis on lipid metabolism in *Elaeis guineensis* and *Elaeis oleifera*. *Data Brief., 31*: 105714.

Leon, C; Rodriguez-Meizoso, I; Lucio, M; Garcia-Cañas, V; Ibañez, E; Schmitt-Kopplin, P and Cifuentes, A (2009). Metabolomics of transgenic maize combining Fourier transform-ion cyclotron resonance-mass spectrometry, capillary electrophoresis-mass spectrometry and pressurized liquid extraction. *J. Chromatogr. A, 1216(43)*: 7314-7323.

Levandi, T; Leon, C; Kaljurand, M; Garcia-Cañas, V and Cifuentes, A (2008). Capillary electrophoresis time-of-flight mass spectrometry for comparative metabolomics of transgenic versus conventional maize. *Anal. Chem., 80(16)*: 6329-6335.

Li, Y; Fang, T; Zhu, S; Huang, F; Chen, Z and Wang, Y (2018). Detection of olive oil adulteration with waste cooking oil via Raman spectroscopy combined with iPLS and SiPLS. *Spectrochim. Acta A. Mol. Biomol. Spectrosc., 189*: 37-43.

Lim, F H; Fakhrana, I N; Rasid, O A; Idris, A S; Ho, C L; Shaharuddin, N A and Parveez, G K A (2017). Molecular cloning and expression analysis of *Ganoderma boninense* cyclophilins at different growth and infection stages. *Physiol. Mol. Plant P., 99*: 31-40.

Lodha, T D; Hembram, P and Nitile Tep, J B (2013). Proteomics: A successful approach to understand the molecular mechanism of plant-pathogen interaction. *Am. J. Plant Sci., 4(06)*: 1212.

Loei, H; Lim, J; Tan, M; Lim, T K; Lin, Q S; Chew, F T; Kulaveerasingam, H and Chung, M C M (2013). Proteomic analysis of the oil palm fruit mesocarp reveals elevated oxidative phosphorylation activity is critical for increased storage oil production. *J. Proteome Res., 12(11)*: 5096-5109.

Long, Y; Shi, J; Qiu, D; Li, R; Zhang, C; Wang, J; Hou, J; Zhao, J; Shi, L and Park, B S (2007). Flowering time quantitative trait loci analysis of oilseed *Brassica* in multiple environments and genomewide alignment with *Arabidopsis*. *Genetics, 177(4)*: 2433-2444.

Low, E T L; Alias, H; Boon, S H; Shariff, E M; Tan, C Y A; Ooi, L C; Cheah, S C; Raha, A R; Wan, K L and Singh, R (2008). Oil palm (*Elaeis guineensis* Jacq.) tissue culture ESTs: Identifying genes associated

with callogenesis and embryogenesis. *BMC Plant Biol., 8(1)*: 62.

Low, E T L; Rosli, R; Jayanthi, N; Azizi, N; Chan, K L; Maqbool, N J; Maclean, P; Brauning, R; McCulloch, A; Moraga, R and Ong-Abdullah, M (2014). Analyses of hypomethylated oil palm gene space. *PLoS ONE, 9(1)*: e86728.

Low, E T L; Jayanthi, N; Chan, K L; Mohd, N S N; Angel, L; Ong-Abdullah, M; Singh, R; Manaf, M A A; Sambanthamurthi, R and Parveez, G K A (2017). The oil palm genome revolution. *J. Oil Palm Res., 29(4)*: 456-468.

Luo, J; Ning, T; Sun, Y; Zhu, J; Zhu, Y; Lin, Q and Yang, D (2009). Proteomic analysis of rice endosperm cells in response to expression of hGM-CSF. *J. Proteome Res., 8(2)*: 829-837.

Ma, H; Song, L; Shu, Y; Wang, S; Niu, J; Wang, Z; Yu, T; Gu, W and Ma, H (2012). Comparative proteomic analysis of seedling leaves of different salt tolerant soybean genotypes. *J. Proteomics, 75(5)*: 1529-1546.

Maizura, I; Rajanaidu, N; Zakri, A H and Cheah, S C (2006). Assessment of genetic diversity in oil palm (*Elaeis guineensis* Jacq.) using Restriction Fragment Length Polymorphism (RFLP). *Genet. Resour. Crop Evol., 53(1)*: 187-195.

Majeran, W; Friso, G; Ponnala, L; Connolly, B; Huang, M; Reidel, E; Zhang, C; Asakura, Y; Bhuiyan, N H; Sun, Q; Turgeon, R and Van Wijk, K J (2010). Structural and metabolic transitions of C4 leaf development and differentiation defined by microscopy and quantitative proteomics in maize. *Plant Cell, 22(11)*: 3509-3542.

Maloney, V (2004). Plant metabolomics. *BioTeach. J., 2*: 92-99.

Masani, M Y A; Izawati, A M D; Rasid, O A and Parveez, G K A (2018). Biotechnology of oil palm: Current status of oil palm genetic transformation. *Biocatal. Agric. Biotechnol., 15*: 335-347.

Masura, S S; Parveez, G K A and Low, E T L (2011). Isolation and characterization of an oil palm constitutive promoter derived from a translationally control tumor protein (TCTP) gene. *Plant Physiol. Biochem., 49(7)*: 701-708.

Masura, S S; Rasid, O A; Noor Azmi, S; Masani, M Y A; Mohd Puad, A; Azzreena, M A and Parveez, G K A (2019a). Mining of transcriptome data for root-specific promoters from oil palm. *Proc. of the PIPOC 2019 International Palm Oil Congress*. MPOB, Bangi. p. 495-499.

Masura, S S; Parveez, G K A and Rasid, O A (2019b). Isolation of an oil palm constitutive promoter derived from ubiquitin extension protein (UEP2) gene. *J. Oil Palm Res., 31(1)*: 28-41.

Masura, S S; Tahir, N I; Rasid, O A; Ramli, U S; Othman, A; Masani, M Y A; Parveez, G K A and Kushairi, A (2017). Post-genomic technologies for the advancement of oil palm research. *J. Oil Palm Res., 29(4)*: 469-486.

May, C Y and Nesaretnam, K (2014). Research advancements in palm oil nutrition. *Eur. J. Lipid Sci. Technol., 116(10)*: 1301-1315.

Mayes, S; Jack, P L; Corley, R H V and Marshall, D F (1997). Construction of a RFLP genetic linkage map for oil palm (*Elaeis guineensis* Jacq.). *Genome, 40(1)*: 116-122.

Mayes, S; James, C M; Horner, S F; Jack, P L and Corley, R H V (1996). The application of restriction fragment length polymorphism for the genetic fingerprinting of oil palm (*Elaeis guineensis* Jacq.). *Mol. Breeding, 2(2)*: 175-180.

Mehrotra, B and Mendes, P (2006). Bioinformatics approaches to integrate metabolomics and other systems biology data. *Plant Metabolomics* (Saito, K; Dixon, R A and Willmitzer, L eds.). Springer Berlin, Heidelberg, Germany. p. 105-115.

Mehta, A; Brasileiro, A C M; Souza, D S L; Romano, E; Campos, M A; Grossi-De-Sá, M F; Silva, M S; Franco, O L; Fragoso, R R and Bevitori, R (2008). Plant-pathogen interactions: What is proteomics telling us? *FEBS J., 275(15)*: 3731-3746.

Mercière, M; Laybats, A; Carasco-Lacombe, C; Tan, J S; Klopp, C; Durand-Gasselin, T; Alwee, S S R S; Camus-Kulandaivelu, L and Breton, F (2015). Identification and development of new polymorphic microsatellite markers using genome assembly for *Ganoderma boninense*, causal agent of oil palm basal stem rot disease. *Mycol. Progress, 14(11)*: 103.

Metzdorff, S B; Kok, E J; Knuthsen, P and Pedersen, J (2006). Evaluation of a non-targeted 'omic' approach in the safety assessment of genetically modified plants. *Plant Biol., 8(05)*: 662-672.

Mirza, B; Wang, W; Wang, J; Choi, H; Chung, N C and Ping, P (2019). Machine learning and integrative analysis of biomedical big data. *Genes, 10(2)*: 87.

Misra, B B; Langefeld, C; Olivier, M and Cox, L A (2019). Integrated omics: Tools, advances and future approaches. *J. Mol. Endocrinol., 62*(*1*): R21-R45.

Mohamad Arif, A M; Izawati, A M D; Zubaidah, R; Masani, A M Y; Safiza, M; Lim, F H; Nurniwalis, A W; Rasid, O A and Parveez, G K A (2017). Biotechnology for diversification and improved resilience of the oil palm. *The Planter, 93(1093)*: 237-249.

Mohammadi, H; Soltani, A; Sadeghipour, H R and Zeinali, E (2012). Effects of seed aging on subsequent seed reserve utilization and seedling growth in soybean. *Int. J. Plant Prod., 5(1)*: 65-70.

Monasterio, R; Olmo-García, L; Bajoub, A; Fernández-Gutiérrez, A and Carrasco-Pancorbo, A (2016). Potential of LC coupled to fluorescence detection in food metabolomics: Determination of phenolic compounds in virgin olive oil. *Int. J. Mol. Sci., 17(10)*: 1627.

Morales, F J; Lozano, I; Sedano, R; Castaño, M and Arroyave, J (2002). Partial characterization of a potyvirus infecting African oil palm in South America. *J. Phytopathol., 150(4-5)*: 297-301.

Morgenthal, K; Weckwerth, W and Steuer, R (2006). Metabolomic networks in plants: Transitions from pattern recognition to biological interpretation. *Biosystems, 83(2-3)*: 108-117.

Muhammad, S A; Seow, E K; Omar, A M; Rodhi, A M; Hassan, H M; Lalung, J; Lee, S C and Ibrahim, B (2018). Variation of δ2H, δ18O & δ13C in crude palm oil from different regions in Malaysia: Potential of stable isotope signatures as a key traceability parameter. *Sci. Justice, 58*: 59-66.

Murphy, D (2014). The future of oil palm as a major global crop: Opportunities and challenges. *J. Oil Palm Res., 26(1)*: 1-24.

Nagappan, J; Chin, C F; Angel, L P L; Cooper, R M; May, S T and Low, E T L (2018). Improved nucleic acid extraction protocols for *Ganoderma boninense*, *G. miniatocinctum* and *G. tornatum*. *Biotechnol. Lett., 40(11-12)*: 1541-1550.

Nambiappan, B; Ismail, A; Hashim, N; Ismail, N; Nazrima, S; Idris, N A N; Omar, N; Saleh, K; Hassan, N A M and Kushairi, A (2018). Malaysia: 100 years of resilient palm oil economic performance. *J. Oil Palm Res., 30(1)*: 13-25.

Natarajan, S S; Xu, C; Bae, H; Caperna, T J and Garrett, W M (2006). Characterization of storage proteins in wild (*Glycine soja*) and cultivated (*Glycine max*) soybean seeds using proteomic analysis. *J. Agric. Food Chem., 54(8)*: 3114-3120.

Neoh, B K; Teh, H F; Ng, T L M; Tiong, S H; Thang, Y M; Ersad, M A; Mohamed, M; Chew, F T; Kulaveerasingam, H and Appleton, D R (2013). Profiling of metabolites in oil palm mesocarp at different stages of oil biosynthesis. *J. Agric. Food Chem., 61(8)*: 1920-1927.

Nguyen, T H N; Brechenmacher, L; Aldrich, J T; Clauss, T R; Gritsenko, M A; Hixson, K K; Libault, M; Tanaka, K; Yang, F; Yao, Q; Pas a-Tolic, L; Xu, D; Nguyen, H T and Stacey, G (2012). Quantitative phosphoproteomic analysis of soybean root hairs inoculated with *Bradyrhizobium japonicum*. *Mol. Cell Proteomics, 11(11)*: 1140-1155.

Nicholson, J K; Lindon, J C and Holmes, E (1999). 'Metabonomics': Understanding the metabolic responses of living systems to pathophysiological stimuli via multivariate statistical analysis of biological NMR spectroscopic data. *Xenobiotica, 29(11)*: 1181-1189.

Nielsen, R; Paul, J S; Albrechtsen, A and Song, Y S (2011). Genotype and SNP calling from next-generation sequencing data. *Nat. Rev. Genet., 12(6)*: 443-451.

Ning, D-L; Liu, K-H; Liu, C-C; Liu, J-W; Qian, C-R; Yu, Y; Wang, Y-F; Wang, Y-C and Wang, B-C (2016). Large-scale comparative phosphoprotein analysis of maize seedling leaves during greening. *Planta, 243(2)*: 501-517.

Nozu, Y; Tsugita, A and Kamijo, K (2006). Proteomic analysis of rice leaf, stem and root tissues during growth course. *Proteomics, 6(12)*: 3665-3670.

Nurazah, Z; Idris, A S; Kushairi, A; Amiruddin, M D; Othman, A and Ramli, U S (2017). Metabolomics unravel differences between Cameroon *Dura* and Deli *Dura* oil palm (*Elaeis guineensis* Jacq.) genetic backgrounds against basal stem rot. *J. Oil Palm Res., 29(2)*: 227-241.

Nurazah, Z; Idris, A S; Kushairi, A and Ramli, U S (2013). Metabolite profiling of oil palm towards understanding basal stem rot (BSR) disease. *J. Oil Palm Res., 25(1)*: 58-71.

Nusaibah, S A; Siti Nor Akmar, A; Idris, A S; Sariah, M and Mohamad Pauzi, Z (2016). Involvement of metabolites in early defense mechanism of oil palm (*Elaeis guineensis* Jacq.) against *Ganoderma* disease. *Plant Physiol. Biochem., 109*: 156-165.

Ong-Abdullah, M; Ordway, J M; Jiang, N; Ooi, S E; Kok, S Y; Sarpan, N; Azimi, N; Hashim, A T; Ishak, Z; Rosli, S K; Malike, F A; Abu Bakar, N A;

Marjuni, M; Abdullah, N; Yaakub, Z; Mohd Din, A; Nookiah, R; Singh, R; Low, E T L; Chan, K L; Azizi, N; Smith, S W; Bacher, B; Budiman, M A; Van Brunt, A; Wischmeyer, C; Beil, M; Hogan, M; Lakey, N; Lim, C C; Arulandoo, X; Wong, C K; Choo, C N; Wong, W C; Kwan, Y Y; Syed Alwee, S S R; Sambanthamurthi, R and Martienssen, R A (2015). Loss of karma transposon methylation underlies the mantled somaclonal variant of oil palm. *Nature*, *525*: 533-537.

Ong, P W; Maizura, I; Marhalil, M; Rajanaidu, N; Abdullah, N A P; Rafii, M Y; Ooi, L C L; Low, E T L and Singh, R (2018). Association of SNP markers with height increment in MPOB-Angolan natural oil palm populations. *J. Oil Palm Res., 30(1)*: 61-70.

Ooi, T E K; Yeap, W C; Daim, L D J; Ng, B Z; Lee, F C; Othman, A M; Appleton, D R; Chew, F T and Kulaveerasingam, H (2015). Differential abundance analysis of mesocarp protein from high- and low-yielding oil palms associates non-oil biosynthetic enzymes to lipid biosynthesis. *Proteome Sci., 13(1)*: 28.

Ooi, L C L; Singh, R and Cheah, S C (2006). *Detection of DNA in Crude Palm Oil*. Project Completion (Viva) Report. MPOB, Bangi.

Othman, A; Lazarus, C; Fraser, T and Stobart, K (2000). Cloning of a palmitoyl-acyl carrier protein thioesterase from oil palm. *Biochem. Soc. Trans., 28(6)*: 619-622.

Othman, A; Bohari, B; Nurazah, Z; Syahanim, S; Mohamad Arif, A M; Idris, A S; Marjuni, M; Amiruddin, M D and Ramli, U S (2017). Fatty acid composition levels in oil palm leaves in relation to severity of *Ganoderma* infection. *Proc. of the PIPOC 2017 International Palm Oil Congress.* MPOB, Bangi. p. 94-96.

Othman, A; Goggin, K A; Tahir, N I; Brodrick, E; Singh, R; Sambanthamurthi, R; Parveez, G K A; Davies, A N; Murad, A J; Muhammad, N H and Ramli, U S (2019a). Use of headspace-gas chromatography-ion mobility spectrometry to detect volatile fingerprints of palm fibre oil and sludge palm oil in samples of crude palm oil. *BMC Res. Notes*, *12(1)*: 229. DOI: 10.1186/s13104-019-4263-7.

Othman, A; Rasid, O A; Nagappan, J; Low, E T L; Lim, F H; Nurazah, Z; Shahwan, S; Dzulkafli, S B; Rozali, N L; Bohari, B; Angel, L P L; Tahir, N I; Idris, A S; Marjuni, M; Shamala, S; Amiruddin M D; Ramli, U S and Mohamad Arif, A M (2019b). Molecular characterisation of oil palm responses to *Ganoderma* infection. *International Seminar on Breeding for* Ganoderma *Tolerance in Oil Palm*. p. 137-146.

Parveez, G K A; Ong-Abdullah, M; Hasan, Z A A; Hishamuddin, E; Loh, S K; Zanal Bidin, M N I; Salleh, K M; Sundram, S and Idris, Z (2020). Oil palm economic performance in Malaysia and R&D progress in 2019. *J. Oil Palm Res., 32(2)*: 159-191. DOI: 10.21894/jopr.2020.0032.

Parveez, G K A; Rasid, O A; Masani, M Y A and Sambanthamurthi, R (2015). Biotechnology of oil palm: Strategies towards manipulation of lipid content and composition. *Plant Cell Rep., 34(4)*: 533-543.

Parveez, G K A; Othman, A; Nurhafizah, R and Bahariah, B (2010). Functional analysis of oil palm palmitoyl-ACP thioesterase (FatB) gene via down-regulation in a model plant: *Arabidopsis thaliana*. *J. Oil Palm Res., 22*: 803-813.

Pootakham, W; Jomchai, N; Ruang-Areerate, P; Shearman, J R; Sonthirod, C; Sangsrakru, D; Tragoonrung, S and Tangphatsornruang, S (2015). Genome-wide SNP discovery and identification of QTL associated with agronomic traits in oil palm using genotyping-by-sequencing (GBS). *Genomics, 105*(*5*): 288-295.

Price, N D; Magis, A T; Earls, J C; Glusman, G; Levy, R; Lausted, C; McDonald, D T; Kusebauch, U; Moss, C L; Zhou, Y and Qin, S (2017). A wellness study of 108 individuals using personal, dense, dynamic data clouds. *Nat. Biotechnol., 35(8)*: 747.

Quirino, B F; Candido, E S; Campos, P F; Franco, O L and Krüger, R H (2010). Proteomic approaches to study plant-pathogen interactions. *Phytochem., 71(4)*: 351-362.

Raamsdonk, L M; Teusink, B; Broadhurst, D; Zhang, N; Hayes, A; Walsh, M C; Berden, J A; Brindle, K M; Kell, D B and Rowland, J J (2001). A functional genomics strategy that uses metabolome data to reveal the phenotype of silent mutations. *Nat. Biotechnol., 19(1)*: 45-50.

Ramli, U S; Tahir, N I; Rozali, N L; Othman, A; Muhammad, N H; Muhammad, S A; Tarmizi, A H A; Hashim, N; Sambanthamurthi, R; Singh, R; Manaf, M A A and Parveez, G K A (2020). Sustainable palm oil - The role of screening and advanced analytical techniques for geographical traceability and authenticity verification. *Molecules*, *25*: 2927.

Ramli, U S; Lau, B Y C; Tahir, N; Shahwan, S; Hassan, H; Nurazah, Z; Rozali, N L; Dzulkafli, S;

Ishak, N A and Othman, A (2016). Proteomics and metabolomics: Spearheading oil palm improvement and sustainability. *The Planter, 92(1087)*: 727-737.

Ramli, U S; Sambanthamurthi, R; Rasid, O A; Parveez G K A; Mohamad Arif A M; Othman, A; Yunus, A M; Choo, C S; Alwee, S S R S and Abdullah, S N A (2012). The isolation and characterisation of oil palm (*Elaeis guineensis* Jacq.) β-ketoacyl-acyl carrier protein (ACP) synthase (KAS) II cDNA. *J. Oil Palm Res., 24*: 1480-1491.

Ramli, U S; Baker, D S; Quant, P A and Harwood, J L (2002a). Control mechanisms operating for lipid biosynthesis differ in oil palm (*Elaeis guineensis* Jacq.) and olive (*Olea europaea* L.) callus cultures. *Biochem. J., 364(2)*: 385-391.

Ramli, U S; Baker, D S; Patti, A and Harwood, J L (2002b). Control analysis of lipid biosynthesis in tissue cultures from oil crops shows that flux control is shared between fatty acid synthesis and lipid assembly. *Biochem. J., 364(2)*: 393-401.

Ramli, U S; Salas, J J; Quant, P A and Harwood, J L (2009). Use of metabolic control analysis to give quantitative information on control of lipid biosynthesis in the important oil crop, *Elaeis guineensis* (oil palm). *New Phytologist., 184(2)*: 330-339.

Rasid, O A; Lim, F-H; Noor Azmi, S; Fakhrana, I N; Idris, A S and Parveez, G K A (2014). Isolation of a partial cDNA clone coding for *Ganoderma boninense* pde. *J. Oil Palm Res., 26:* 265-269.

Rodrigues-Neto, J C; Correia, M V; Souto, A L; Ribeiro, J A D A; Vieira, L R; Souza, M T; Rodrigues, C M and Abdelnur, P V (2018). Metabolic fingerprinting analysis of oil palm reveals a set of differentially expressed metabolites in fatal yellowing symptomatic and non-symptomatic plants. *Metabolomics, 14(10)*: 142.

Roessner, U; Wagner, C; Kopka, J; Trethewey, R N and Willmitzer, L (2000). Simultaneous analysis of metabolites in potato tuber by gas chromatography–mass spectrometry. *Plant J., 23(1)*: 131-142.

Rongai, D; Sabatini, N; Del Coco, L; Perri, E; Del Re, P; Simone, N; Marchegiani, D and Fanizzi, F P (2017). ^{1}H NMR and multivariate analysis for geographic characterization of commercial extra virgin olive oil: A possible correlation with climate data. *Foods, 6(11)*: 96.

Rosenblum, E S; Viant, M R; Braid, B M; Moore, J D; Friedman, C S and Tjeerdema, R S (2005). Characterizing the metabolic actions of natural stresses in the California red abalone, *Haliotis rufescens* using ^{1}HNMR metabolomics. *Metabolomics, 1(2)*: 199-209.

Roslan, A and Idris, A S (2012). Economic impact of *Ganoderma* incidence on Malaysian oil palm plantation - A case study in Johor. *Oil Palm Industry Economic J., 12(1)*: 24-30.

Rozali, N L; Yarmo, M A; Idris, A S; Kushairi, A and Ramli, U S (2017). Metabolomics differentiation of oil palm (*Elaeis guineensis* Jacq.) spear leaf with contrasting susceptibility to *Ganoderma boninense*. *Plant Omics, 10(2)*: 45-52.

Safiza, M; Anita, J; Manaf, M A A and Fazliza, M A (2015). Differentially expressed genes in *G. boninense* naturally-infected palms. *Proc. of the PIPOC 2015 International Palm Oil Congress.* MPOB, Bangi. p. 617-621.

Salekdeh, G H and Komatsu, S (2007). Crop proteomics: Aim at sustainable agriculture of tomorrow. *Proteomics, 7(16)*: 2976-2996.

Sales, C; Cervera, M I; Gil, R; Portolés, T; Pitarch, E and Beltran, J (2017). Quality classification of Spanish olive oils by untargeted gas chromatography coupled to hybrid quadrupole-time of flight mass spectrometry with atmospheric pressure chemical ionization and metabolomics-based statistical approach. *Food Chem., 216*: 365-373.

Sambanthamurthi, R; Sundram, K and Tan, Y A (2000). Chemistry and biochemistry of palm oil. *Prog. Lipid Res., 39(6)*: 507-558.

Sato, S; Soga, T; Nishioka, T and Tomita, M (2004). Simultaneous determination of the main metabolites in rice leaves using capillary electrophoresis mass spectrometry and capillary electrophoresis diode array detection. *Plant J., 40(1)*: 151-163.

Seng, T-Y; Ritter, E; Saad, S H M; Leao, L-J; Singh, R; Zaman, F Q; Tan, S-G; Alwee, S S R S and Rao, V (2016). QTLs for oil yield components in an elite oil palm (*Elaeis guineensis*) cross. *Euphytica, 212(3)*: 399-425.

Shen, Z; Li, P; Ni, R-J; Ritchie, M; Yang, C-P; Liu, G-F; Ma, W; Liu, G-J; Ma, L; Li, S-J and Wei, Z G (2009). Label-free quantitative proteomics analysis of etiolated maize seedling leaves during greening. *Mol. Cell. Proteom., 8(11)*: 2443-2460.

Shulaev, V (2006). Metabolomics technology and bioinformatics. *Brief Bioinform., 7(2)*: 128-139.

Singh, R; Zaki, N M; Ting, N C; Rosli, R; Tan, S G; Low, E T L; Ithnin, M and Cheah, S C (2008). Exploiting

an oil palm EST database for the development of gene-derived SSR markers and their exploitation for assessment of genetic diversity. *Biologia, 63(2)*: 227-235.

Singh, R; Low, E T L; Ooi, L C L; Ong-Abdullah, M; Nookiah, R; Ting, N C; Marjuni, M; Chan, P L; Ithnin, M; Mohamad Arif A M; Nagappan, J; Chan, K L; Rosli, R; Halim, M A; Azizi, N; Budiman, M A; Lakey, N; Bacher, B; Van Brunt, A; Wang, C; Hogan, M; He, D; Macdonald, J D; Smith, S W; Ordway, J M; Martienssen, R A and Sambanthamurthi, R (2014). The oil palm *Virescens* gene controls fruit colour and encodes a R2R3-MYB. *Nat. Commun., 5*: 4106. DOI: 10.1038/ncomms5106.

Singh, R; Ong-Abdullah, M; Low, E T L; Mohamad Arif, A M; Rosli, R; Nookiah, R; Ooi, L C L; Ooi, S E; Chan, K L; Halim, M A A; Azizi, N; Nagappan, J; Bacher, B; Lakey, N; Smith, S W; He, D; Hogan, M; Budiman, M A; Lee, E K; DeSalle, R; Kudrna, D; Goicoechea, J L; Wing, R A; Wilson, R K; Fulton, R S; Ordway, J M; Martienssen, R A and Sambanthamurthi, R (2013a). Oil palm genome sequence reveals divergence of interfertile species in Old and New worlds. *Nature, 500*: 335-339.

Singh, R; Low, E T L; Ooi, C L L; Ong-Abdullah, M; Ting, N C; Nagappan, J; Nookiah, R; Mohd Din, A; Rosli, R; Mohamad Arif, A M; Chan, K L; Mohd Amin, H; Azizi, N; Lakey, N; Smith, S W; Budiman, M A; Hogan, M; Bacher, B; Van Brunt, A; Wang, C; Ordway, J M; Sambanthamurthi, R and Martienssen, R A (2013b). The oil palm SHELL gene controls oil yield and encodes a homologue of SEEDSTICK. *Nature*, *500:* 340-344.

Singh, R; Nagappan, J; Tan, S-G; Panandam, J M and Cheah, S C (2007). Development of simple sequence repeat (SSR) markers for oil palm and their application in genetic mapping and fingerprinting of tissue culture clones. *Asia Pac. J. Mol. Biol Biotech., 15(3)*: 121-131.

Singh, R; Low, E T L; Ooi, L C L; Ong-Abdullah, M; Ting, N C; Nookiah, R; Ithnin, M; Marjuni, M; Mustaffa, S; Yaakub, Z; Amiruddin, M D; Manaf, M A A; Chan, K L; Halim, M A A; Sanusi, N S N M; Lakey, N; Sachdeva, M; Bacher, B; Garner, P A; MacDonald, J D; Smith, S W; Wischmeyer, C; Budiman, M A; Beil, M; Stroff, C; Reed, J; Van Brunt, A; Berg, H; Ordway, J M and Sambanthamurthi, R (2020). Variation for heterodimerization and nuclear localization among known and novel oil palm SHELL alleles. *New Phytol., 226(2)*: 426-440.

Siti Suriawati, B; Chan, K L; Chan, P L; Parveez, G K A and Rasid, O A (2019). Identification of genes preferentially expressed in mesocarp tissue of oil palm using *in silico* analysis of transcripts. *J. Oil Palm Res., 31(4)*: 540-549.

Sun, Q; Xue, J; Lin, L; Liu, D; Wu, J; Jiang, J and Wang, Y (2018). Overexpression of soybean transcription factors GmDof4 and GmDof11 significantly increase the oleic acid content in seed of *Brassica napus* L. *Agronomy, 8(10)*: 222. DOI: 10.3390/agronomy8100222.

Susanto, A; Sudharto, P S and Purba, R Y (2005). Enhancing biological control of basal stem rot disease (*Ganoderma boninense*) in oil palm plantations. *Mycopathologia, 159(1)*: 153-157.

Syahanim, S; Othman, A; Manaf, M A A; Idris, A S and Amiruddin, M D (2013). Identification of differentially expressed proteins in oil palm seedlings artificially infected with *Ganoderma*: A proteomics approach. *J. Oil Palm Res., 25(3)*: 298-304.

Syahanim, S; Othman, A; Dzulkafli, S B; Hassan, H; Idris, A S; Amiruddin, M D and Ramli, U S (2019). Quantitative proteomics analysis of oil palm root during early stages of *Ganoderma* inoculation. *BMC Proc., 13(8)*: 10.

Syrenne, R D; Shi, W; Stewart, C N and Yuan, J S (2012). Omics platforms: Importance of twenty-first century genome-enabled technologies in seed developmental research for improved seed quality and crop yield. *Seed Development: OMICS Technologies toward Improvement of Seed Quality and Crop Yield.* Springer, Dordrecht. p. 43-57.

Tafti, A P; LaRose, E; Badger, J C; Kleiman, R and Peissig, P (2017). Machine learning-as-a-service and its application to medical informatics. *International Conference on Machine Learning and Data Mining in Pattern Recognition*. Springer, Cham., USA. p. 206-219.

Tahir, N; Abas, F; Ghulam Kadir, A P; Ishak, Z and Ramli, U S (2012). Characterization of apigenin and luteolin derivatives from oil palm (*Elaeis guineensis* Jacq.) leaf using LC-ESI-MS/MS. *J. Agric. Food Chem., 60*: 11201-11210.

Tahir, N I; Shaari, K; Abas, F; Ishak, Z; Ahmad Tarmizi, H; Amiruddin, M D; Parveez, G K A and Ramli, U S (2016). Metabolome analysis of oil palm clone P325 of different planting trials. *J. Oil Palm Res., 28(4)*: 431-441.

Tan, H S; Liddell, S; Abdullah, M O; Wong, W C and Chin, C F (2016). Differential proteomic analysis of embryogenic lines in oil palm (*Elaeis guineensis* Jacq.). *J. Proteomics, 143*: 334-345.

Tang, G; Xu, P; Ma, W; Wang, F; Liu, Z; Wan, S and Shan, L (2018). Seed-specific expression of AtLEC1 increased oil content and altered fatty acid composition in seeds of peanut (*Arachis hypogaea* L.). *Front. Plant Sci., 9*: 260.

Teh, H F; Neoh, B K; Ithnin, N; Daim, L D J; Ooi, T E K and Appleton, D R (2017). Omics and strategic yield improvement in oil crops. *J. Amer. Oil Chem. Soc., 94(10)*: 1225-1244.

Teh, H F; Neoh, B K; Wong, Y C; Kwong, Q B; Ooi, T E K; Ng, T L M; Tiong, S H; Low, J Y S; Danial, A D; Ersad, M A; Kulaveerasingam, H and Appleton, D R (2014). Hormones, polyamines, and cell wall metabolism during oil palm fruit mesocarp development and ripening. *J. Agric. Food Chem., 62(32)*: 8143-8152.

Teh, C K; Ong, A L; Kwong, Q B; Apparow, S; Chew, F T; Mayes, S; Mohamed, M; Appleton, D and Kulaveerasingam, H (2016). Genome-wide association study identifies three key loci for high mesocarp oil content in perennial crop oil palm. *Sci. Rep., 6(1)*: 19075.

Teh, H F; Neoh, B K; Hong, M P L; Low, J Y S; Ng, T L M; Ithnin, N; Thang, Y M; Mohamed, M; Chew, F T and Yusof, H M (2013). Differential metabolite profiles during fruit development in high-yielding oil palm mesocarp. *PLoS ONE, 8(4)*: e61344.

Tester, M and Langridge, P (2010). Breeding technologies to increase crop production in a changing world. *Science, 327(5967)*: 818-822.

Thomson, M J (2014). High-throughput SNP genotyping to accelerate crop improvement. *Plant Breed. Biotechnol., 2*(3): 195-212.

Thongthawee, S; Tittinutchanon, P and Volkaert, H (2010). Microsatellites for parentage analysis in an oil palm breeding population. *Thai J. Genet., 3(2)*: 172-181.

Ting, N C; Zaki, N M; Rosli, R; Low, E T L; Ithnin, M; Cheah, S C; Tan, S G and Singh, R (2010). SSR mining in oil palm EST database: Application in oil palm germplasm diversity studies. *J. Genetics, 89(2)*: 135-145.

Tolstikov, V V; Lommen, A; Nakanishi, K; Tanaka, N and Fiehn, O (2003). Monolithic silica-based capillary reversed-phase liquid chromatography/ electrospray mass spectrometry for plant metabolomics. *Anal. Chem., 75(23)*: 6737-6740.

Torres, G A; Sarria, G A; Varon, F; Coffey, M D; Elliott, M L and Martinez, G (2010). First report of bud rot caused by *Phytophthora palmivora* on African oil palm in Colombia. *Plant Disease, 94(9)*: 1163-1163.

Tres, A; Ruiz-Samblás, C; Van Der Veer, G and Van Ruth, S M (2013). Geographical provenance of palm oil by fatty acid and volatile compound fingerprinting techniques. *Food Chem., 137*: 142-150.

Turner, P D and Gillbanks, R A (2003). *Oil Palm Cultivation and Management*. Incorporated Society of Planters. Kuala Lumpur, Malaysia. 672 pp.

Uawisetwathana, U and Karoonuthaisiri, N (2019). Metabolomics for rice quality and traceability: Feasibility and future aspects. *Curr. Opin. Food Sci., 28*: 58-66.

Van Wijk, K J (2001). Challenges and prospects of plant proteomics. *Plant Physiol., 126(2)*: 501-508.

Vargas, L H; Ribeiro, J A; Sifuentes, D N; Júnior, M T; Rodrigues, C M and Abdelnur, P V (2014). An analytical platform based on untargeted metabolomics for leaves of oil palm. *Pesquisa e Inovação da, 70770*. 112 pp.

Wang, F; Wang, C; Liu, P; Lei, C; Hao, W; Gao, Y; Liu, Y G and Zhao, K (2016). Enhanced rice blast resistance by CRISPR/Cas9-targeted mutagenesis of the ERF transcription factor gene OsERF922. *PLoS ONE, 11(4):* e0154027.

Wang, Z Q; Xu, X Y; Gong, Q Q; Xie, C; Fan, W; Yang, J L; Lin, Q S and Zheng, S J (2014). Root proteome of rice studied by iTRAQ provides integrated insight into aluminum stress tolerance mechanisms in plants. *J. Proteomics, 98*: 189-205.

Wang, Y; Htwe, Y M; Li, J; Shi, P; Zhang, D; Zhao, Z and Ihase, L O (2019). Integrative omics analysis on phytohormones involved in oil palm seed germination. *BMC Plant Biol., 19*: 363.

Weckwerth, W (2003). Metabolomics in systems biology. *Annu. Rev. Plant Biol., 54(1)*: 669-689.

Weckwerth, W (2008). Integration of metabolomics and proteomics in molecular plant physiology-coping with the complexity by data-dimensionality reduction. *Physiol. Plantarum, 132(2)*: 176-189.

Weir, G M (1968). Leaf spot of the oil palm caused by *Cercospora elaeidis*, Stey. Aspects of atmospheric humidity and temperature. *J. Nigerian Institute Oil Palm Res., 5(17)*: 41-55.

Woittiez, L S; Van Wijk, M T; Slingerland, M; Van Noordwijk, M and Giller, K E (2017). Yield gaps

in oil palm: A quantitative review of contributing factors. *Eur. J. Agron.*, *83*: 57-77.

Yu, J; Hu, S; Wang, J; Wong, G KS; Li, S; Liu, B; Deng, Y; Dai, L; Zhou, Y; Zhang, X and Cao, M (2002). A draft sequence of the rice genome (*Oryza sativa* L. ssp. indica). *Science, 296(5565)*: 79-92.

Zhang, Y; Zhao, J; Xiang, Y; Bian, X; Zuo, Q; Shen, Q; Gai, J and Xing, H (2011). Proteomics study of changes in soybean lines resistant and sensitive to *Phytophthora sojae*. *Proteome Sci., 9*(*1*): 52.

Zhao, X X; Tang, Tan, G; Liu, F X; Lu, C L; Hu, X L; Ji, L L and Liu, Q Q (2013). Unintended changes in genetically modified rice expressing the lysine-rich fusion protein gene revealed by a proteomics approach. *J. Integr. Agric., 12(11)*: 2013-2021.

Zolla, L; Rinalducci, S; Antonioli, P and Righetti, P G (2008). Proteomics as a complementary tool for identifying unintended side effects occurring in transgenic maize seeds as a result of genetic modifications. *J. Proteome Res., 7(5)*: 1850-1861.

Zulkifli, Y; Maizura, I and Rajinder, S (2012). Evaluation of MPOB oil palm germplasm (*Elaeis guineensis*) populations using EST-SSR. *J. Oil Palm Res., 24*: 1368-1377.

Journal of Oil Palm Research Vol. 34 (1) March 2022 p. 26-34
DOI: https://doi.org/10.21894/jopr.2021.0018

MORPHO-PHYSIOLOGICAL ASSESSMENT OF OIL PALM (*Elaeis guineensis* Jacq.) SEEDLINGS EXPOSED TO SIMULATED DROUGHT CONDITIONS

IKHAJIAGBE, B[1]; AITUAE, W[2] and OGWU, M C[3]*

ABSTRACT

Elaeis guineensis *Jacq. (oil palm) production is threatened by drought due to climate change and anthropogenic deforestation. This study aims to understand how drought conditions contribute to changes in foliar nitrate-nitrogen concentration as well as the effects on the growth and development of oil palm seedlings. Seventy oil palm seedlings were maintained in a screen house and subjected to simulated drought conditions. There was a significant reduction in the number of leaves with increased drought exposure from 10 to four per plant. Oil palm leaves exposed to higher drought levels had less broad leaves, with leaf area ranging from 133.25-172.22 cm^2 compared to the control (383.73 cm^2). The foliar yield per plant was low in plants exposed to extreme drought condition (2.27 g), compared to 71.98 g in the control. Moreover, total drought-exposed oil palm seedlings had the highest concentration of nitrate-nitrogen.* E. guineensis *exposed to no-drought conditions had more roots (18 roots) than those exposed to total or partial drought (6-10 roots per plant). Overall, there was a decrease in height, leaf area and the number of leaves for most of the seedlings exposed to drought condition, which might be detrimental to their photosynthetic ability and growth.*

Keywords: climate change effects, drought, foliar nitrogen, oil palm (*Elaeis guineensis*).

Received: 13 May 2020**; Accepted:** 17 February 2021**; Published online:** 4 May 2021.

INTRODUCTION

Oil palm (*Elaeis guineensis* Jacq.), is a monocotyledonous tropical palm tree, which belongs to the family Arecaceae and is believed to have originated in West Africa (Poku, 2002). It is the major source of edible and industrial oil in west, east and central parts of Africa and Madagascar. *Elaeis guineensis* is also domesticated in Sri Lanka, Indonesia, Malaysia, Madagascar, Central America, along with many other island states in the Indian and Pacific Oceans. It is a close relative of the American oil palm [*Elaeis oleifera* (Kunth.) Cortes] and a distant relative of maripa palm [*Attalea maripa* (Aubl.) Mart.] found in the Caribbean (Hormaza *et al*., 2012). Human use of oil palms dates as far back as 5000 years in West Africa. Three cultivars of oil palm are common in Nigeria; namely *Dura, Pisifera* and *Tenera* (FAO, 2002; Okolo *et al*., 2019). The preferred variety among oil palm farmers in Nigeria is the hybrid cultivar, *Tenera*; which is a crossbreed of *Dura* (female) and *Pisifera* (male). *Tenera* seedlings are produced by the Nigeria Institute for Oil Palm Research (NIFOR) and largely used in extension works to promote oil palm cultivation (Iankova *et al*., 2016). In terms of comparison, the fruit of the *Tenera* contains 25% oil (by weight), whereas it is 18% in *Dura*. Oil palm is common in Edo State, Nigeria where climate change events are becoming more frequent (Ogwu *et al.*, 2014; Ogwu, 2019).

[1] Department of Plant Biology and Biotechnology, Faculty of Life Sciences, University of Benin, Ugbowo, Benin City PMB 1154, Nigeria.

[2] Physiology Division, Nigeria Institute for Oil Palm Research, Benin City, Nigeria.

[3] School of Biosciences and Veterinary Medicine, University of Camerino – Center for Floristic Research of the Apennine, Gran Sasso and Monti Della Laga National Park, San Colombo, 67021 Barisciano, L'Aquila, Italy.

* *Corresponding author e-mail: matthew.ogwu@uniben.edu*

Uptake of nutrients is low during the first year in oil palm but increases steeply between year one and three (when harvesting commences) and stabilises around year five to six (Woittiez *et al*., 2017). Early applications of fertiliser, better planting material and more rigid culling have led to a dramatic increase in early yields in the third to sixth year after planting. Nitrogen, which mostly enters the plant as soluble nitrate ion, is a building block for tissue growth. Nitrogen is an integral part of most essential components including in chlorophyll and nucleic acids. Without nitrogen, there might be limited to no growth and yield. Nitrogen deficiency first shows up as discolouration of young oil palm fronds, which lose their healthy dark green colour and turn yellow (chlorosis). Nitrogen deficiency is caused by some factors including poor drainage and waterlogged soil; inherently infertile soils exhausted by previous agricultural activities, excessive competition from weeds (Hartley, 1988; Lai *et al*., 2019). In regions without a significant drop in rainfall, yields of over 25 t of fresh fruit bunches (FFB) per hectare have been achieved in the second year of harvesting. On the other hand, drought stress results when water loss from the plant exceeds the ability of roots to absorb water and when the plant's water content is reduced enough to interfere with normal plant processes. Water is a universal solvent needed by plants to grow and is a major constituent of plant cells, without which, photosynthesis and consequently, growth processes may be hampered (Carr, 2011; Safitri *et al*., 2019).

This study aims to understand how drought conditions contribute to changes in foliar nitrate-nitrogen concentration as well as the effects on the growth and development of oil palm. The combined use of morphology and other traits to characterise plant germplasm is increasingly commonplace (Osawaru *et al*., 2013; 2014a; 2014b). Drought stress may take time to become visible in plants and depends on the water holding capacity (WHC) of the soil, environmental conditions, stage of plant growth and plant species. Moreover, poorly established plants are more susceptible to drought stress because of the limited root system (low root-shoot ratio). During drought conditions, there is a shortage of water for plant use. Hence, given the obvious challenges posed by recent trends in climate change, it is pertinent to assess drought stress in oil palm seedlings.

MATERIALS AND METHODS

Plant Materials and Growth Conditions

Seventy palm samples, all of which were six months old where selected randomly from a pool of oil palm nursery at NIFOR, Benin City, Nigeria. The oil palm seedlings were held in black polyethene nursery bags and maintained in a screen house to shield the palms from rainfall. It is in the screen house that different water treatments were applied to the oil palm seedlings. The experiment was initiated in July 2018, but the application of treatments started in August 2018, which was enough time for the oil palm seedlings to get acclimatised to the screen house. Measurements of experimental parameters took place six months after sowing.

Collection of Topsoil Used in the Study

Topsoil (0-15 cm) was collected from NIFOR and pooled to obtain composite samples. The soil was sun-dried to constant weight. Thereafter 7.50 kg was measured each into perforated nursery bags. A total of 70 bags were arranged in the screen house for the experiment.

Water Holding Capacity (WHC) of the Soil

The experiment relied on the restricted application of water and the WHC of the soil was determined before commencing the experimental procedures. About 1.00 kg of sun-dried soil was placed in a funnel initially lined with Whatman's filter paper (A). Water was poured unto it to completely saturate the soil. This was left overnight in a darkroom. The next morning, the weight of the saturated soil was taken (B) and the difference (B-A) was expressed in mL per kg. The WHC of the soil was determined to be 480 mL kg^{-1}. This amounted to 3600 mL per nursery bag.

Simulation of Drought

The drought conditions for the experiment was a factor of the WHC. There were six levels comprising of control, total drought, 0.05% WHC, 0.10% WHC, 0.50% WHC, 1.00% WHC and 5.00% WHC (*Table 1*).

Application of Treatment

Initially, the entire nursery bags received 3600 mL of water, which represented the WHC of the entire 7.50 kg soil. Thereafter, the oil palm seedlings were transplanted and left in the screen house for two weeks. Subsequently, the seedlings were divided into seven groups, comprising 10 per group and randomised within the experimental block. Each group received the designated amount of water as presented in *Table 1.*

Determination of Plant Growth Characteristics

Some plant growth characteristics including the number of leaves as well as dry weight of the total number of leaves (hereafter referred to as

foliar yield). Number of roots were also physically counted. In the experiment, the prominent roots were defined as those roots that were significantly larger and longer than the other roots. The lengths of these prominent roots were determined. Similar to foliar yield, root yield per plant was calculated as dry weight of all physically removed roots.

Determination of Nitrate-Nitrogen

This was carried out according to Smith (1974) and summarised here - test plant was oven-dried at 65ºC for 24 hr and then ground to 40-mesh sized powder. The ground sample was re-dried in an oven at 70ºC. A measure of 100 mg of ground sample was suspended in deionised water and incubated at 45ºC for 1 hr. The incubated suspension was then mixed and centrifuged at 5000 xg for 15 min to sediment tissue residues. The supernatant was decanted and kept for analysis.

Preparation of Stock Nitrate Solution

Potassium trinitrate (V) (KNO_3) was oven dried for 24 hr at 105ºC and then 1.63 g of the dried salt was weighed into 250 mL flask and dissolved with distilled water. The solution was transferred into 1-L flask made to the mark with distilled water to obtain 1000 ppm of stock KNO_3 solution.

Preparation of Standard Nitrate Solution

Using a 100 mL measuring cylinder, 50 mL of the stock solution was measured into 500 mL flask and made to the mark with water. This was carefully swirled to mix to obtain 100 mg L^{-1} of the stock. From the 100 mg L^{-1} standards concentrations of 80-10 mg L^{-1} was prepared by serial dilution.

Preparation of 2N Solution of Sodium hydroxide (NaOH)

Exactly 40 g of NaOH pellets were introduced into a 250 mL beaker and dissolved with distilled water. The solution obtained was transferred into a 500 mL flask and made up to the mark.

Preparation of Salicylic Acid Solution

Five grams of salicylic acid was dissolved in concentrated sulphuric acid (H_2SO_4) and diluted to 100 mL with the same acid. The solution obtained was stored in amber bottles.

Calibration and Estimation of Nitrate-N in Plant Tissue

Aliquots (0.1 mL) of working standards solution in 30.0 mL tube were mixed thoroughly with 0.4 mL salicylic acid solution. After 20 min at room temperature, 9.5 mL 2N sodium hydroxide (NaOH) solution was slowly added to obtain 0.1-1.0 mg L^{-1} NO_3-N solutions. The plant extract was analysed for Nitrate-N by mixing 5 g plant extract, 0.8 mL concentrated H_2SO_4, 19.0 mL of NaOH and 0.4 mL of salicylic acid solution. A similar mixture of the plant extract (without salicylic acid) was used as blank. The nitrosalicylic acid complex formed was read at maximum absorption of 412 nm using a spectrophotometer.

For this determination, seven different water rates were applied to oil palm seedlings; control, total drought, 0.05% WHC, 0.1% WHC, 0.5% WHC, 1% WHC and 5% WHC. Each treatment was replicated 10 times namely; A, B, C, D, E, F, G, H, I, J, culminating in 70 experimental units. The experimental units were then laid out in the completely randomised design in the NIFOR screen house.

Statistical Analysis

Data obtained from the study were analysed using statistical package for social sciences (SPSS) statistical software version 21. Results were presented as the mean of 10 replicates and separated at 95% confidence interval.

TABLE 1. EXPERIMENTAL TREATMENTS TO SIMULATE DROUGHT CONDITIONS

Treatments	Treatment factor per 7.5 kg soil	Quantity of water applied to soil (7.5 kg) per week
Control	Soil was watered normally	Frequent soil wetting as soon as soil moisture was reduced
Total drought	No water applied at all	0.36 mL applied to soil weekly
0.05% WHC	0.005 x 3600 = 1.8 mL	1.8 mL applied to soil on a weekly basis
0.1% WHC	0.0001 x 3600 = 3.6 mL	23.6 mL applied to soil on a weekly basis
0.5% WHC	0.0001 x 3600 = 18.0 mL	18.0 mL applied to soil on a weekly basis
1% WHC	0.0001 x 3600 = 36.0 mL	36.0 mL applied to soil on a weekly basis
5% WHC	0.0001 x 3600 = 180.0 mL	180.0 mL applied to soil on a weekly basis

Note: WHC - water holding capacity.

RESULTS AND DISCUSSION

The present study explored the assimilation of nitrogen in oil palm seedlings exposed to drought stress. Some morphological parameters of the palm seedlings at six months after sowing are presented in *Table 2*. Results showed a significant reduction in the number of leaves with increased drought exposure from 10 to four per plant. Similarly, leaves that were exposed to higher drought levels had less broad leaves, with leaf area ranging from 133.25-172.22 cm^2, compared to the control with a leaf area of 383.73 cm^2. The foliar yield per plant was significantly low in the plant with the total drought treatment (2.27 g), compared to 71.98 g in the control. Altogether, these results suggest the importance of water supply in oil palm production as earlier suggested by Carr (2011). Moreover, this also supports the findings of Caliman and Southworth (1998), which highlighted the effects *El Nino*-induced droughts in oil palm cultivation region of Southeast Asia.

There was a general decrease in the height of most of the seedlings exposed to drought condition. It was observed that the height of oil palm seedlings at Week 4 was 31.10 cm and 36.40 cm at Week 16 in T1, which showed less than 15% increase in height compared to the control group. Height of seedling increased from 27.5 cm at Week 4 to 57.1 cm in control, which showed over 50% increase with respect height of seedlings. The difference is clearly because the control oil palm seedlings were not subjected to physiological (and other) stress and therefore performed normal metabolic functions needed for its growth and development. In the same way, Gupta *et al*. (2001) also observed a slow progression in height of their test plants, which they attributed to low water potential elicited by drought condition. Further, this may have raised the osmotic potential in the test plant, thus, prompting the expression of genes that code for traits essential for survival without a significant increase in height (Delperee *et al*., 2003; Zgallai *et al*., 2006). Neilson *et al*. (2015) used advanced high-throughput screening platforms equipped with an automated irrigation system to measure a wide range of morpho-physiological variables in a large number of genotypes of cereal crops to support their view that plants have the capacity to down-regulate genes for certain metabolic activities under drought stress. The age of the oil palm seedlings and the duration of the drought period are important factors in the present study. However, plants can respond properly to drought stress with enhanced growth-promoting hormones like auxin (Mshelmbula *et al*., 2015; Ogwu, 2018; Ogwu *et al*., 2015).

The number of necrotic leaves on oil palm seedlings at six months after planting are presented in *Table 3*. The effects of drought was noticed in all the test plants as leaf necrosis began to appear after four weeks and progressed over time. There were 4.80 necrotic leaves at Week 4 in the total drought-exposed oil palm seedlings and increased to 5.08 by Week 14. In oil palm seedlings exposed to soils with 0.1% WHC, the number of necrotic leaves were 4.85 at Week 4 and 5.03 at Week 14, whereas the number of necrotic leaves in the control group remains significantly negligible compared to the test plants subjected to drought stress. Observably, although oil palm seedlings exposed to soils with 0.5% WHC showed similar evidence of drought stress with evidence of necrosis like other test plants, the number of necrotic leaves in the plant had remained fairly the same throughout the study. The work of Ikhajiagbe and Anoliefo (2011) suggest that plant tolerance to drought can be enhanced by using soil amendments.

TABLE 2. MORPHOLOGICAL ASSESSMENT OF DROUGHT-EXPOSED OIL PALM SEEDLINGS AT SIX MONTHS AFTER SOWING

Treatments	Plant height (cm)	*No. of leaves	Leaf area (cm^2)	Foliar yield/ plant (g)	Percentage senescence (%)	Stem girth (cm)
Total drought	35.8 ± 2.3^{a}	5 ± 2^{a}	166.27 ± 45.32^{a}	2.27 ± 1.08^{a}	25.36 ± 9.02^{ab}	4.40 ± 0.92^{a}
0.05% WHC	33.4 ± 3.4^{a}	6 ± 2^{a}	133.25 ± 52.14^{a}	4.37 ± 1.65^{a}	43.39 ± 11.37^{b}	4.58 ± 1.01^{a}
0.1% WHC	36.4 ± 2.7^{a}	6 ± 2^{a}	142.76 ± 27.22^{a}	5.46 ± 2.01^{a}	22.21 ± 9.11^{ab}	4.75 ± 0.65^{a}
0.5% WHC	36.5 ± 3.2^{a}	4 ± 2^{a}	160.76 ± 75.06^{a}	4.77 ± 1.88^{a}	33.37 ± 8.02^{b}	4.03 ± 0.42^{a}
1% WHC	34.4 ± 4.1^{a}	5 ± 3^{a}	152.42 ± 66.93^{a}	5.88 ± 2.66^{a}	37.52 ± 9.02^{b}	4.20 ± 0.73^{a}
5% WHC	43.2 ± 2.9^{b}	7 ± 2^{ab}	172.22 ± 55.11^{a}	20.13 ± 8.42^{b}	11.10 ± 7.14^{a}	5.63 ± 1.12^{a}
Control	49.7 ± 2.3^{c}	10 ± 3^{b}	383.73 ± 85.73^{b}	71.98 ± 19.02^{c}	0.00^{c}	9.30 ± 1.82^{b}
p-value	<0.001	0.034	<0.001	<0.001	<0.001	<0.001

Note: *Means and standard error have been provided to the nearest whole number. The concentrations of water applied to soil were based on soil's initial water holding capacity. Values on same column with similar alphabetic superscripts are not significantly different from one another ($p>0.05$). FL/Plant = No. of foraged leaves/plant; PFC - percentage foliar chlorosis; WHC - water holding capacity.

Leaf area is affected during drought stress conditions in plants, as plants tend to reduce the possibility of losing more water in addition to the prevalent condition. There were general increases in the leaf areas in all the experimental plants irrespective of the treatment. Nonetheless, the increase in leaf area was lower in all the oil palm seedlings subjected to drought conditions compared to that of control group. This could probably be due to the restrained metabolic processes necessary to promote leaf enlargement in the plant and also reduce evapotranspiration, which could hasten the death of drought-stressed plant through acute dehydration (Parker and Pallardy, 1985; Puértolas *et al*., 2017). As the stress condition intensified, the plant may resort to drastic steps to increase its chances of survival under the prevailing unsupportive environment and this may be effective by the production of metabolites that cause leaf senescence resulting from stress and not from age. This explains the reduction in the number of leaves observed in oil palm seedlings after exposure to drought stress in the present study (*Table 3*). This view is in line with the outcome of previous investigations including those of Kabiri (2010); Kafi and Mahdavi-Damghani (1999); Kavar *et al*. (2007).

Nitrate concentration was assayed in oil palm seedlings during the present study and results showed that total drought-exposed oil palm seedlings had the highest concentration of nitrate-nitrogen (*Table 4*). Nitrate concentration was 3.17 mg kg^{-1} dry weight (DW) of oil palm seedling in the total drought-exposed oil palm seedlings whereas it was 0.88 mg kg^{-1} DW in the oil palm seedlings exposed to 0.5% WHC, and it was 1.64 k kg^{-1} DW and 1.62 mg kg^{-1} DW in oil palm seedlings exposed to 0.1% WHC and 1% WHC respectively. Symptoms of drought in oil palm include general paling and stiffening of the pinnae, which lose their glossy lustre. The report of Al-Amin *et al*. (2011) suggests that drought lower the yield of FFB in oil palm up to 26.30%. The decline of oil palm yield is a direct effect of inhibition of the photosynthetic rate of oil palm (Jafaar and Ibrahim, 2012; Russell *et al*., 2017). Increasing nitrogen utilisation in the face of environmental stress can also improve plant performance (Ikhajiagbe *et al.,* 2020).

TABLE 3. NUMBER OF LEAVES WITH NECROTIC LESIONS OF DROUGHT-EXPOSED OIL PALM SEEDLINGS AT SIX MONTHS AFTER SOWING

	Weeks after transplanting						
Treatments	**4**	**6**	**8**	**10**	**12**	**14**	**16**
Total drought	4.8 ± 0.44^{ab}	5.45 ± 0.98^{a}	5.75 ± 0.83^{a}	5.70 ± 0.93^{c}	4.6 ± 0.52^{a}	5.08 ± 0.83^{a}	4.40 ± 0.52^{a}
0.05% WHC	4.47 ± 0.65^{a}	4.72 ± 1.01^{a}	4.88 ± 0.73^{a}	4.9 ± 0.74^{bc}	4.1 ± 0.99^{a}	4.75 ± 1.22^{a}	4.58 ± 0.73^{a}
0.1% WHC	4.85 ± 0.83^{ab}	5.25 ± 0.93^{a}	5.58 ± 1.06^{a}	5.23 ± 0.41^{bc}	4.8 ± 0.73^{a}	5.03 ± 0.734^{a}	4.75 ± 1.01^{a}
0.5% WHC	4.8 ± 0.81^{ab}	4.40 ± 1.01^{a}	5.18 ± 0.99^{a}	4.35 ± 0.44^{b}	5.6 ± 1.04^{a}	4.60 ± 1.42^{a}	4.03 ± 0.55^{a}
1% WHC	5.5 ± 0.38^{b}	4.67 ± 0.85^{a}	5.28 ± 0.75^{a}	4.68 ± 0.39^{b}	5.1 ± 0.79^{a}	5.18 ± 2.02^{a}	4.20 ± 0.92^{a}
5% WHC	5.2 ± 0.42^{ab}	5.12 ± 0.73^{a}	4.58 ± 1.03^{a}	$4.8^{b} \pm 0.31^{c}$	5.9 ± 1.15^{a}	5.70 ± 1.55^{a}	5.63 ± 1.15^{a}
Control	1.1 ± 0.33^{c}	1.23 ± 0.18^{c}	1.32 ± 0.78^{c}	1.24 ± 0.66^{a}	1.2 ± 0.78^{b}	1.18 ± 0.64^{b}	1.30 ± 0.56^{b}
***p*-value**	0.323	0.415	0.776	0.004	0.004	0	0
F-value	1.248	1.062	0.535	4.531	4.495	11.97	32.906

Note: The concentrations of water applied to soil were based on soil's initial water holding capacity (WHC). Values on the same column with similar alphabetic superscripts do not differ from one another (p>0.05).

TABLE 4. CONCENTRATION OF NITRATE IN THE LEAVES OF DROUGHT-EXPOSED OIL PALM SEEDLINGS AT SIX MONTHS AFTER SOWING

Treatments	**Foliar nitrate concentration (mg kg^{-1} DW)**
Total drought	3.17 ± 1.04^{b}
0.05% WHC	1.36 ± 0.78^{ab}
0.1% WHC	1.64 ± 0.65^{ab}
0.5% WHC	1.26 ± 0.82^{ab}
1% WHC	1.62 ± 0.79^{ab}
5% WHC	0.88 ± 0.23^{a}
Control	1.07 ± 0.64^{a}
F-value	1.73×10^{6}
***p*-value**	1.84×10^{6}

Note: The concentrations of water applied to soil were based on soil's initial water holding capacity (WHC). Values on the same column with similar alphabetic superscripts are not significantly different from one another (p>0.05).

Below ground parameters of the test plants showed that plants exposed to non-drought conditions had significantly more roots (18 roots) than those exposed to total or partial drought (6-10 roots per plant) (*Table 5*). There were between two and four prominent roots across the experiment, irrespective of drought conditions. However, root yield per plant, which was determined in the study as the dried weight of entire roots obtained per plant, was higher in the control (11.46 g) than in the drought-exposed plants (3.50-6.53 g). The low stomatal conductance decreases the rate of carbon dioxide (CO_2) diffusion so that the photosynthetic activity of oil palm is inhibited (Henson and Harun, 2007). Other factors that inhibit the rate of photosynthesis in drought conditions are the relatively low water content (Fahramand *et al*., 2014; Zain *et al*., 2014), low chlorophyll *a*/*b*, and reduced nitrogen and phosphorus contents in leaf tissue of plants (Ashraf and Harris, 2013; Zlatev and Lindon, 2012).

Morphological description of drought-exposed oil palm seedlings at six months after sowing are presented in *Table 6*. Results showed that plants that were exposed to total drought showed dried-out leaves and most of them folded upwards. Leaves of the control plants were green, with no signs of chlorotic or necrosis; only two leaves showed signs of foliar scorching. During periods of drought, nutrient deficiency and changes in metabolism are common in oil palm (Silva *et al*., 2018). Our results support the recent findings by Corley *et al*. (2018) that the future of the oil palm industry will depend on the successful breeding of drought-resistant species.

CONCLUSION

In conclusion, drought stress leads to poor growth and development in oil palm seedlings, which may lower production in oil palm. Drought causes stomatal conductance of oil palm leaves to decline rapidly as more stomata close, which may also be detrimental to the photosynthetic ability and growth of the plant. Oil palm is very sensitive to drought and countries where products are greatest are highly vulnerable to this climate change effect. Therefore, if current trends are left unchecked, in a few decades climate change-induced drought might significantly affect the global output of oil palm. Agronomic approaches can be taken to reduce the sensitivity of oil palm to drought including planting drought-resistant varieties and adopting

TABLE 5. NUMBER OF ROOTS AND LENGTH OF PROMINENT ROOT OF DROUGHT-EXPOSED OIL PALM SEEDLINGS AT SIX MONTHS AFTER TRANSPLANTING

Treatments	No of roots	*No. of prominent roots	Length of prominent roots	Total root weight (g DW)
Total drought	10 ± 3^{b}	2 ± 1^{a}	23.4 ± 8.3^{c}	3.504 ± 1.032^{a}
0.05% WHC	7 ± 3^{b}	4 ± 2^{a}	27.1 ± 7.1^{c}	3.195 ± 1.109^{a}
0.1% WHC	10 ± 2^{b}	3 ± 1^{a}	27.7 ± 6.8^{c}	3.054 ± 1.047^{a}
0.5% WHC	6 ± 3^{b}	2 ± 1^{a}	35.5 ± 7.4^{bc}	4.832 ± 0.092^{a}
1% WHC	7 ± 3^{b}	3 ± 1^{a}	24.4 ± 9.3^{c}	4.194 ± 0.432^{a}
5% WHC	9 ± 3^{b}	2 ± 1^{a}	70.5 ± 11.1^{a}	6.532 ± 0.509^{b}
Control	18 ± 4^{a}	3 ± 1^{a}	57.5 ± 9.4^{ab}	11.458 ± 2.093^{c}
p-value	0.002	0.643	0.015	<0.001

Note: *Means and standard error have been provided to the nearest whole number. The concentrations of water applied to soil were based on soil's initial water holding capacity (WHC). Values on the same column with similar alphabetic superscripts are not significantly different from one another (p>0.05).

TABLE 6. MORPHOLOGICAL DESCRIPTION OF DROUGHT-EXPOSED OIL PALM SEEDLINGS AT SIX MONTHS AFTER SOWING

Treatments	Morphological description
Total drought	Leaves were totally dry and most of them were folded upwards
0.05% WHC	All of its leaves had dried up and two out of the five leaves where folded
0.1% WHC	Leaves were necrotic (dried up)
0.5% WHC	Leaves were brown and the whole seedling was dry
1% WHC	Leaves were necrotic with one out of its five leaves twisted
5% WHC	Signs of foliar necrosis. An additional leaf showed partial necrosis
Control	Leaves were fresh and green, only two leaves showed signs of foliar scorching

Note: WHC – water holding capacity.

sustainable irrigation practices. The findings from this study suggest that drought produces variable growth and developmental response in *E. guineensis* seedlings such as a decrease in height, leaf area, number of leaves and roots for most of the seedlings exposed to drought condition. An important caveat to the findings reported here is a potential birch effect resulting from the drying of experimental soil. However, many oil palm cultivation regions around the world are currently having prolonged dry seasons without rain.

ACKNOWLEDGEMENT

The authors would like to thank the Director-General of MPOB for permission to publish this article.

REFERENCES

Al-Amin, A Q; Filho, W L; De la Trinxeria, J M; Jaafar, A H and Ghani, Z A (2011). Assessing the impacts of climate change in the Malaysian agriculture sector and its influences in investment decision. *Middle-East J. Sci. Res., 7(2)*: 225-234.

Ashraf, M and Harris, P J C (2013). Photosynthesis under stressful environments: An overview. *Photosynthetica, 51(20*): 163-190.

Caliman, J P and Southworth, A (1998). Effect of drought and haze on the performance of oil palm. *1998 International Oil Palm Conference – Commodity of the Past, Today and the Future. Indonesia Oil Palm Research Institute (IOPRI) and Indonesia Palm Oil Producers Association (GAPKI)*. 23-25 September 1998. Bali, Indonesia. p. 40.

Carr, M K V (2011). The water relations and irrigation requirements of oil palm (*Elaeis guineensis*): A review. *Exp. Agric., 47(4)*: 629-652.

Corley, R H V; Rao, V; Palat, T and Praiwan, T (2018). Breeding for drought tolerance in oil palm. *J. Oil Palm Res., 30(1)*: 26-35.

Delperee, C; Kinet, J M and Lutts, S (2003). Low irradiance modifies the effect of water stress on survival and growth-related parameters during the early developmental stages of buckwheat (*Fagopyrum esculentum*). *Physiol. Plant., 119(20)*: 211-220.

Fahramand, M; Mahmoody, M; Keykha, A; Noori, M and Rigi, K (2014). Influence of abiotic stress on proline, photosynthetic enzymes and growth. *Int. Res. J. Appl. Basic Sci., 8*: 257-265.

FAO (2002). Small-scale palm oil processing in Africa. *Agricultural Services Bulletin.* Food and Agriculture Organisation of the United Nations (FAO). http://www.fao.org/3/y4355e/y4355e03.htm

Gupta, N K; Gupta, S and Kumar, A (2001). Effect of water stress on physiological attributes and their relationship with growth and yield of wheat cultivars at different stages. *J. Agron. Crop Sci., 186(1)*: 55-62.

Hartley, C W S (1988). *The Oil Palm*: (*Elaeis guineensis* Jacq.). Tropical Agriculture Series. Longman. 59 pp.

Henson, I E and Harun, M H (2007). Short-term responses of oil palm to an interrupted dry season in North Kedah, Malaysia. *J. Oil Palm Res., 19:* 364-372.

Hormaza, P; Fuquen, E M and Romero, H M (2012). Phenology of oil palm interspecific hybrid *Elaeis oleifera* x *Elaeis guineensis. Sci. Agric.*, *69(4)*: DOI: 10.1590/S0103-90162012000400007.

Iankova, K; Hassan, A and L'Abbe, R (2016*). Indigenous People and Economic Development: An International Perspective.* 1st edition. Routleedge. 344 pp.

Ikhajiagbe, B and Anoliefo, G O (2011). Impact of substrate amendment on the polyaromatic hydrocarbon contents of a five month old waste engine oil polluted soil. *Afr. J. Environ. Sci. Technol., 5(10)*: 769-777.

Ikhajiagbe, B; Anoliefo, G O; Olise, F O; Rackelmann, F; Sommer, M and Adekunle, I J (2020). Major phosphorus in soils is unavailable, yet critical for plant development. *Not. Sci. Biol., 12(3)*: 500-535.

Jafaar, H Z E and Ibrahim, M H (2012). Photosynthesis and quantum yield of oil palm seedlings to elevated carbon dioxide. *Advances in Photosynthesis – Fundamental Aspects* (Najafpour, M ed.). IntechOpen, United Kingdom. p. 321-334.

Kabiri, R (2010). *Effect of salicylic acid to reduce the oxidative stress caused by drought in the hydroponic cultivation of Nigella sativa (Nigella sativa).* Masters thesis. Shahid Bahonar University of Kerman, Iran. 132 pp.

Kafi, M and Mahdavi-Damghany, M A (1999). Mechanisms of resistance of plants to environmental stresses (Translation). University of Mashhad, Iran. 84 pp.

Kavar, T; Maras, M; Kidric, M; Sustar-Vozlic, J and Meglic, V (2007). Identification of genes involved in the response of leaves of *Phaseolus vulgaris* to drought stress. *Mol. Breeding, 21(5)*: 159-172.

Lai, C H; Settinayake, A R H; Yeo, W S; Lau, S W and Jong, T K (2019). Crop nutrients review and the impact of fertilizer on the plantation in Malaysia: A mini review. *Commun. Soil Sci. Plant Anal., 50(17)*: 2089-2105.

Mshelmbula, B P; Okooboh, G; Mensah, J K; Ikhajiagbe, B and Zakariya, R (2015). The effects of indole-3-acetic acid (IAA) on the growth and yield of sesame (*Sesamum indicum* L.) under drought conditions. *Int. J. Sci. Knowl., 4(1)*: 60-65.

Neilson, E H; Edwards, A M; Blomstedt, C K; Berger, B; Møller, B L and Gleadow, R M (2015). Utilization of a high-throughput shoot imaging system to examine the dynamic phenotypic responses of a C4 cereal crop plant to nitrogen and water deficiency over time. *J. Exp. Bot., 66(41)*: 1817-1832.

Okolo, C C; Okolo, E C; Nnadi, A I; Obikwelu, F E; Obalum, S E and Igwe, C A (2019). The oil palm (*Elaeis guineensis* Jacq.): Nature's ecological endowment to eastern Nigeria. *Agro-Sci., 18(3)*: 48-57.

Ogwu, M C (2018). Effects of Indole-3-Acetic Acid on growth parameters of *Citrullus lanatus* (Thunberg) Matsum and Nakai. *Momona Ethiop. J. Sci., 10(1)*: 109-125. DOI: 10.4314/mejs.v10i1.8.

Ogwu, M C (2019). Towards sustainable development in Africa: The challenge of urbanization and climate change adaptation. *The Geography of Climate Change Adaptation in Urban Africa* (Cobbinah, P B and Addaney, M eds.). Springer Nature, Switzerland. p. 29-55. DOI: 10.1007/978-3-030-04873-0_2.

Ogwu, M C; Aiwansoba, R O and Osawaru, M E (2015). Effects of indole-3-acetic acid on germination in lead polluted petri dish of *Citrullus lanatus* (Thunberg) Matsumura and Nakai, Cucurbitaceae. *Aceh Int. J. Sci. Technol., 4(3)*: 107-113. DOI: 10.13170/aijst.4.3.3021.

Ogwu, M C; Osawaru, M E and Chime, A O (2014). Comparative assessment of plant diversity and utilization patterns of tropical home gardens in Edo State, Nigeria. *Scientia Africana, 13(2)*: 146-162.

Osawaru, M E; Ogwu, M C and Ahana, C M (2014a). Study of the distinctiveness of two genera of Cocoyam [*Colocasia* (Schott) and *Xanthosoma* (Schott)] using SDS – PAGE. *Nigerian Soc. Exp. Biol. J., 14(3)*: 168-179.

Osawaru, M E; Ogwu, M C and Omologbe, J (2014b). Characterization of three Okra [*Abelmoschus* (L.)] Accessions using morphology and SDS-PAGE for the basis of conservation. *Egyptian Acad. J. Biol. Sci., 5(1)*: 55-65.

Osawaru, M E; Ogwu, M C; Ogbeifun, N S and Chime, A O (2013). Microflora diversity of the phylloplane of wild Okra (*Corchorus olitorius* L. Jute). *Bayero J. Pure Appl. Sci., 6(2)*: 136-142.

Parker, W C and Pallardy, S G (1985). Genotypic variation in tissue water relations of leaves and roots of black walnut (*Juglans nigra*) seedlings. *Physiol. Plant. J., 64(1)*: 105-110.

Poku, K (2002). Oil palm. *FAO Agricultural Services Bulletin No. 148*. Food and Agriculture Organization of the United Nations (FAO). Rome, Italy.

Puértolas, J; Larsen, E K; Davies, W J and Dodd, I C (2017). Applying 'drought' to potted plants by maintaining suboptimal soil moisture improves plant water relations. *J. Exp. Bot., 68(9)*: 2413-2424.

Russell, R; Peterson, M and Lima, N (2017). Climate change affecting oil palm agronomy and oil palm cultivation increasing climate change, require amelioration. *Ecol. Evol., 8(1)*: 452-461.

Safitri, L; Hermantoro, H; Purboseno, S; Kautsar, V; Saptomo, S K and Kurniawan, A (2019). Water footprint and crop usage of oil palm (*Elaeis guineensis*) in central Kalimantan: Environmental sustainability indicators for different crop age and soil conditions. *Water, 11*: 35. DOI: 10.3390/w11010035.

Silva, P A; Cosme, V S; Rodrigues, K C B; Detmann, K S C; Leao, F M; Cunha, R L; Buselli, R A F; da Matta, F M and Pinheiro, H A (2018). Drought tolerance in two oil palm hybrids as related to adjustments in carbon metabolism and vegetative growth. *Acta Physiol. Plant., 39*: 58. DOI 10.1007/s11738-017-2354-4.

Smith, G R (1974). Rapid determination of nitrate-nitrogen in soil and plants with the nitrate electrode. *Electrochemistry, 8(7)*: 503-508.

Woittiez, L S; van Wijk, M T; Slingerland, M; van Noordwijk, M and Giller, K E (2017). Yield gap in oil palm: A quantitative review of contributing factors. *Eur. J. Agron., 83*: 57-77.

Zain, N A M; Ismail, M R; Mahmood, M; Puteh, A and Ibrahim, M H (2014). Alleviation of water stress effects on MR220 rice by application of periodical water stress and potassium fertilization. *Molecules, 19*: 1795-1819.

Zgallai, H; Steppe, K and Lemeur, R (2006). Effects of different levels of water stress on leaf water potential, stomata resistance, protein and chlorophyll content and certain anti-oxidative enzymes in tomato plants. *J. Integ. Plant Biol., 48(22)*: 679-685.

Zlatev, Z and Lindon, F C (2012). An overview on drought induced changes in plant growth, water relations and photosynthesis. *Emir. J. Food Agric., 24(1)*: 57-72.

Journal of Oil Palm Research Vol. 34 (1) March 2022 p. 35-45
DOI: https://doi.org/10.21894/jopr.2021.0021

HISTONE MODIFICATION MARKS IMPROVE IDENTIFICATION OF OIL PALM TRANSCRIPTION START SITES

SARPAN, N[1]; TATARINOVA, T V[2]; LOW, E-T L[1]; ONG-ABDULLAH, M[1]; SAPIAN, I S[3] and OOI, S-E[1]*

ABSTRACT

Epigenetic regulation involves modifications of chromatin components such as post-translational modifications of histone proteins, methylation of cytosines in deoxyribonucleic acid (DNA), the involvement of small RNA and chromatin remodeling. Numerous methods have been established to understand the epigenetic control of agronomically important traits. Chromatin immunoprecipitation with sequencing (ChIP-Seq) is widely used to identify the binding sites of transcription factors or modified histones on a genome-wide scale. Here, ChIP-Seq targeting H3K4me3 and H3K27me3 marks in oil palm spears were conducted to examine genomic regions enriched with these histone modifications. Due to low DNA amounts from ChIP experiments, the data analysis workflow was optimised based on ChIP-Seq workflows on other plants. Mapping to specific target regions revealed that the histone mark peak positions were located close to predicted transcription start sites (TSS). This agrees with H3K4me3 and H3K27me3 profiles in other plants where H3K4me3 marks are generally associated with active genes and promoter regions while H3K27me3 marks are linked to repressed genes. Gene-wide mapping for low coverage ChIP-Seq data showed that H3K4me3 and H3K27me3 profiles on the oil palm genome corresponded to consensus histone profiles in other plants. This is the first ChIP-Seq analysis workflow reported for oil palm spears, which can be used to develop future oil palm ChIP-Seq studies.

Keywords: ChIP-Seq, *Elaeis guineensis*, epigenetics, H3K4me3, H3K27me3.

Received: 19 October 2020**; Accepted:** 2 February 2021**; Published online:** 19 May 2021.

INTRODUCTION

Epigenetics mechanisms lead to spatial-temporal gene expression changes that are not mediated by changes in the underlying deoxyribonucleic acid (DNA) sequence (Wollmann and Berger, 2012). Unlike the genome, the epigenome is dynamically altered by environmental factors (Baulcombe and Dean, 2014). In oil palm, crop improvement programmes involve numerous breeding trials, which are then selected for massive multiplication through tissue culture (Zulkifli *et al.*, 2017). However, the production of elite clonal materials has yet to be maximised due to the occurrence of mantled fruits that causes oil and yield losses. Through epigenome-wide association studies, the loss of DNA methylation at the E*gDEF1*'s *Karma* epi-allele in tissue culture regenerants was associated with the mantling phenotype (Ong-Abdullah *et al.*, 2015). Subsequently, an epi-fingerprinting assay for *in vitro* cultured palms was developed to discriminate true-to-types from off-types (Ong-Abdullah *et al.*, 2016). This step serves as quality control (QC) to improve the efficiency of the tissue culture process and thus, marks the beginning of applied epigenetics for the

[1] Malaysian Palm Oil Board,
6 Persiaran Institusi, Bandar Baru Bangi,
43000 Kajang, Selangor, Malaysia.

[2] Department of Biology, University of La Verne,
La Verne CA, USA.

[3] Malaysian Genome Institute,
National Institute of Biotechnology Malaysia,
Jalan Bangi, 43000 Kajang, Selangor, Malaysia.

* *Corresponding author e-mail: oseng@mpob.gov.my*

oil palm industry through the identification of low-risk planting materials.

Chromatin, which is built by a nucleosome array containing 147 bp of DNA and pairs of histones H2A, H2B, H3 and H4, acts as a target for epigenetic modifiers comprising methylation of cytosines in the DNA, modifications at the N-terminal tails of histone proteins and small non-coding ribonucleic acid (RNA) molecules (Lu *et al.*, 2020). These mechanisms affect the packaging of chromatin and accessibility of the transcriptional machinery, thus, influencing gene expression. The pattern of modifications on histone tails, known as the histone code, contribute to shaping chromatin structure into either condensed heterochromatin or open euchromatin (Prakash and Fournier, 2018). H3K4me3 and H3K27me3 are two widely investigated histone marks in plants. The wide distribution of H3K4me3 marks in promoter regions is associated with active transcription, while H3K27me3 marks are usually associated with the Polycomb Repressive Complex involved in gene silencing (Gan *et al.*, 2015; Zhang *et al.*, 2009). In plants, histone modification signatures are seen for several developmental processes, including response to stress (Zeng *et al.*, 2019), flower morphogenesis (Engelhorn *et al.*, 2017) and embryogenesis (Berenguer *et al.*, 2017). Studies on histone modifications often involve locating their binding sites through a method called chromatin immunoprecipitation with sequencing (ChIP-Seq) (Liu *et al.*, 2010). In ChIP-Seq, genomic DNA is first fragmented, followed by the capturing of histone-bound fragments. The non-histone fractions are then discarded, leaving only the enriched fraction that will be sequenced. Subsequent bioinformatics analysis of ChIP-Seq datasets generally includes QC checks of sequencing reads, aligning reads to the reference genome and finding peaks corresponding to ChIP-enriched regions. Reported ChIP-Seq data usually involves at least 20 million mapped reads (Zhang *et al.*, 2015; Zong *et al.*, 2013), but the chromatin immunoprecipitation step generally provides low yields in the nanogram range (Ranawaka *et al.*, 2020). Thus, reads duplication is more apparent when insufficient DNA from inefficient immunoprecipitation is used in constructing sequencing library and becomes more abundant when the library is deeply sequenced (Landt *et al.*, 2012).

In this study, the histone modifications H3K4me3 and H3K27me3 in oil palm leaf spear tissue were investigated using ChIP-Seq. These two histone modifications were selected based on their influence on transcriptional regulation, whereby the H3K4me3 is associated with active transcription while the H3K27me3 is linked to repressed transcription at gene-rich regions. The DNA bound to histones enriched with these two histone modifications was immunoprecipitated and sequenced. The low DNA yields obtained through ChIP led to low coverage ChIP-Seq data. To circumvent this limitation and still gain preliminary insights on these histone marks in oil palm, a gene-wide mapping approach was able to demonstrate that H3K4me3 and H3K27me3 profiles in oil palm are in concordance with their consensus distribution patterns on gene regions in other plants. To our knowledge, this is the first report of a ChIP-Seq workflow described for the oil palm.

MATERIALS AND METHODS

Plant Material

Spear leaf tissues of 10 clonal palms at the MPOB Bagan Datuk Research Station, Perak, Malaysia were sampled, frozen in liquid nitrogen and stored at -80°C until further use. The palms, labeled from A to J (*Table 1*), originated from the same tissue used in *in vitro* cloning and are thus, grouped as biological replicates.

Chromatin Immunoprecipitation and Sequencing

Chromatin was isolated following a protocol described by Kaufmann *et al.* (2010), with modifications, as described by Sarpan *et al.* (2018). Briefly, the spears were ground in liquid nitrogen, added with lysis buffer and cold-incubated. The mixture was filtered and centrifuged to collect the pellet. The pellet underwent a few series of washing steps prior to shearing. Chromatin was sheared using a Covaris M220 (Covaris, USA) for 25 min in a screw-cap microtube at 4°C with the following settings: 5% duty factor and 200 cycles/burst. ChIP-validated antibodies, anti-H3K4me3 (ab12209) and anti-H3K27me3 (ab6002, Abcam, United Kingdom), as used by Sarpan *et al.* (2018) and EpiSeeker ChIP Kit-Plants (Abcam, United Kingdom) were used for immunoprecipitation in this study. Sequencing libraries were prepared from ChIP DNA using the TruSeq® ChIP library preparation kit (Illumina, USA). The amount of input DNA (non-immunoprecipitated) used was 10 ng, while ChIP DNA starting amounts were varied between 1 and 5 ng. A total of 10 H3K27me3 ChIP-Seq libraries were prepared but only nine H3K4me3 ChIP-Seq libraries were generated as library preparation failed for one of the samples. Libraries were sequenced paired-end at a read-length of 125 bp on a HiSeq2500 Illumina platform with a depth of at least 20 million reads.

ChIP-Seq Analysis

The quality of sequencing reads was assessed using FastQC v0.11.3 software (Babraham Bioinformatics). Raw reads were trimmed using Flexbar v3.4.0 (Dodt *et al.*, 2012) to filter out

TABLE 1. ChIP-SEQ DATASETS MAPPED TO GENOME-WIDE

Histone modification	Library type	Biological replicate	Raw reads	[a]Trimmed reads	[b]Mapped reads	[c]Non-duplicate reads	[d]Total bases (all positions)	Bases with 0 read	Bases with ≥1 reads	[e]Genome coverage (%)	[f]Read coverage per base
H3K4me3	control	A	35 984 910	35 669 154	35 435 466	27 736 510	1 533 938 362	724 607 480	809 330 882	52.76	4.15
		B	52 050 286	51 645 526	51 260 135	44 625 812	1 534 342 085	586 712 882	947 629 203	61.76	5.71
		C	44 381 902	43 997 588	43 663 651	29 644 138	1 534 144 289	683 468 435	850 675 854	55.45	4.22
		D	51 083 054	50 730 270	50 409 026	26 731 614	1 533 860 846	813 524 274	720 336 572	46.96	4.46
		E	42 168 806	41 837 986	41 552 394	29 891 260	1 534 001 008	712 662 441	821 338 567	53.54	4.40
		G	31 800 882	31 520 392	31 273 417	22 813 368	1 534 001 840	745 401 962	788 599 878	51.41	3.51
		H	43 756 708	43 306 396	42 991 826	41 011 330	1 534 132 957	580 113 958	954 018 999	62.19	5.23
		I	45 063 152	44 692 636	44 387 622	33 418 384	1 533 094 523	839 258 804	693 835 719	45.26	5.81
		J	36 742 346	36 400 994	36 126 280	34 781 924	1 534 176 063	624 238 482	909 937 581	59.31	4.65
H3K4me3	ChIP	A	75 862 582	74 810 274	74 233 306	12 315 882	1 533 453 476	974 321 640	559 131 836	36.46	2.66
		B	197 624 588	195 934 548	194 325 596	30 171 318	1 534 277 620	707 660 415	826 617 205	53.88	4.39
		C	31 412 106	31 142 214	30 666 435	5 612 798	1 530 823 722	1 205 596 031	325 227 691	21.25	2.08
		D	41 919 552	41 336 506	40 039 231	1 144 332	1 500 495 388	1 424 719 833	75 775 555	5.05	1.77
		E	37 965 452	37 673 322	37 148 105	4 575 718	1 529 556 467	1 265 983 936	263 572 531	17.23	2.08
		G	30 519 894	30 095 468	29 652 732	888 572	1 492 505 662	1 427 678 548	64 827 114	4.34	1.61
		H	39 010 174	38 420 070	37 793 093	1 972 456	1 514 677 266	1 382 847 468	131 829 798	8.70	1.77
		I	41 431 160	41 078 370	40 688 442	12 273 908	1 533 401 893	945 981 023	587 420 870	38.31	2.53
		J	31 687 056	31 418 340	29 694 600	2 759 248	1 522 564 714	1 346 184 740	176 379 974	11.58	1.87
H3K27me3	control	A	42 210 292	41 827 008	41 538 453	39 473 908	1 534 224 788	614 003 122	920 221 666	59.98	5.22
		B	46 295 636	45 851 060	45 506 248	43 114 494	1 534 212 412	578 584 051	955 628 361	62.29	5.49
		C	45 928 412	45 554 732	45 207 704	42 536 726	1 534 283 404	581 509 659	952 773 745	62.10	5.43
		D	38 714 154	38 364 604	38 108 722	36 248 822	1 534 182 116	635 612 490	898 569 626	58.57	4.91
		E	43 061 204	42 605 744	42 319 874	39 330 794	1 534 193 919	604 591 944	929 601 975	60.59	5.14
		F	43 003 696	42 602 988	42 314 438	36 935 124	1 534 202 778	613 186 747	921 016 031	60.03	4.88
		G	44 338 502	43 910 016	43 597 559	41 560 574	1 534 240 271	589 113 789	945 126 482	61.60	5.35
		H	42 273 554	42 001 334	41 707 342	31 618 422	1 534 196 992	655 137 242	879 059 750	57.30	4.37
		I	38 556 918	38 204 874	37 945 426	35 059 998	1 534 159 267	629 116 433	905 042 834	58.99	4.72
		J	43 319 140	42 897 120	42 608 417	38 481 480	1 534 100 471	591 154 107	942 946 364	61.47	4.96

TABLE 1. ChIP-SEQ DATASETS MAPPED TO GENOME-WIDE (continued)

Histone modification	Library type	Biological replicate	Raw reads	[a]Trimmed reads	[b]Mapped reads	[c]Non-duplicate reads	[d]Total bases (all positions)	Bases with 0 read	Bases with ≥1 reads	[e]Genome coverage (%)	[f]Read coverage per base
H3K27me3	ChIP	A	39 351 328	38 796 698	35 957 556	1 238 748	1 502 697 938	1 418 341 444	84 356 494	5.61	1.72
		B	34 223 168	33 686 222	32 394 786	3 189 744	1 524 866 923	1 318 306 613	206 560 310	13.55	1.85
		C	32 242 982	31 992 096	31 521 609	6 887 100	1 531 912 824	1 133 843 209	398 069 615	25.99	2.09
		D	40 658 292	40 110 788	35 257 532	6 727 856	1 532 091 408	1 166 333 508	365 757 900	23.87	2.22
		E	47 270 818	46 593 894	44 711 067	1 394 144	1 505 655 829	1 413 482 364	92 173 465	6.12	1.79
		F	46 424 912	45 977 946	45 627 608	35 221 778	1 534 212 270	608 918 890	925 293 380	60.31	4.63
		G	21 385 898	21 071 740	20 673 777	917 326	1 495 112 267	1 425 848 085	69 264 182	4.63	1.57
		H	34 458 854	34 167 082	33 471 587	5 316 020	1 530 673 976	1 207 494 470	323 179 506	21.11	1.98
		I	36 855 828	36 572 002	36 136 392	6 325 896	1 531 558 077	1 193 266 507	338 291 570	22.09	2.26
		J	35 552 140	35 069 174	34 490 720	3 386 116	1 525 684 917	1 309 144 878	216 540 039	14.19	1.88

Note: [a]Total reads after trimming using Flexbar.
[b]Total reads after mapping using Bowtie2.
[c]Total reads after duplicates removal using samtools markdup function in SAMtools package.
[d]Total bases (positions) identified using samtools depth function in SAMtools package.
[e]Percentage of genome covered with ChIP-Seq reads.
[f]Average number of reads at any position in the genome.

contaminated adapter sequences and low-quality reads. The trimmed reads were aligned to (1) *Elaeis guineensis* P5-build reference genome (NCBI BioProject accessions PRJNA192219, accessions ASJS00000000) (Singh *et al.*, 2013) and, (2) gene models (Sanusi *et al.*, 2018) ±1 kb flanking regions (define as 'gene-wide'), using Bowtie2 v2.2.5 (Langmead and Salzberg, 2012) with --very-sensitive-local settings. Removal of duplicate reads and read coverage assessments were performed using SAMtools v1.9 (Li *et al.*, 2009). Mean coverage was calculated in R. Histone-bound regions were identified using MACS2 v2.1.1.20160309 (Zhang *et al.*, 2008) with options *-q* 0.05 specified for H3K4me3, while *--broad --broad-cutoff* 0.05 was conducted for H3K27me3. Gene-wide distribution patterns of pooled H3K4me3 and H3K27me3 peaks was plotted based on the average pileup reads of the peaks calculated for a 2 kb window around gene translation start positions and visualised using R. Average pileup is calculated by adding the pileup for individual genes at all positions of the detected peak and then dividing by the number of peaks. Prediction of TSS was made using SoftBerry tools. ChIP-Seq data can be accessed under GEO Accession No. GSE159142.

RESULTS

Raw sequencing reads in *fastq* format was analysed with FastQC, which provides a quality assessment of the raw sequencing data. For all datasets, quality scores per base were generally good with a slight decrease towards the end of the reads. Approximately 1%-2% of the sequence reads were eventually discarded during the read trimming process due to the presence of adapter sequences and low-quality calls (*Table 1*).

Low ChIP Recovery for ChIP-Seq Lead to Low Sequence Coverage and High Duplication

In standard bioinformatics pipelines, sequencing reads are made informative by mapping to a reference genome using an aligner software. In this study, the trimmed reads were initially aligned to the P5-build of the *E. guineensis* reference genome (Singh *et al.*, 2013). This step generated an alignment result in the Sequence Alignment/Map (SAM) format, which assigns specific genomic locations to each read. H3K4me3 and H3K27me3 ChIP-Seq sets in this study comprised the ChIP and their respective non-immunoprecipitated (denoted hereafter as control) sequencing data. While biological replicates A-J in the control group showed a consistent mapping percentage of more than 99%, mapping efficiencies of the immunoprecipitated biological replicates A-J were lower, ranging from 95%-99% for H3K4me3 and 88%-99% for H3K27me3 (*Table 2*). The

overall read mapping performance was acceptable (*Figure 1*), but duplication was high in each ChIP data compared to their corresponding control (*Figure 2* and *Table 2*). The high amount of duplicates was probably due to the low amounts of ChIP DNA used to prepare the ChIP-Seq libraries. Duplicates also reflect the redundant reads resulting from polymerase chain reaction (PCR) overamplification, leading to an over-representation of ChIP-Seq reads at some genomic regions (Loh *et al.*, 2017). The duplicates are technically identified as read pairs with their 5′ ends mapped to the same genomic coordinates. Removal of duplicates was deemed necessary in this study due to the high duplication observed; otherwise peak calling or statistical analyses would be affected by the high duplication. Removal of duplicates thus, led to significant losses in reads, leaving only <20% of data for further analysis (*Figure 2*). The number of remaining reads after duplicates removal did not correlate with the amounts of starting material used to prepare the ChIP-Seq libraries (*Tables 1* and *2*). While control data mapped to 45%-62% of the genome, only 4%-60% of the genome was covered by ChIP reads (*Table 1*). On average, about 4-6 mapped reads per base were observed in control data, but only 2-4 and 2-5 read coverage was observed for H3K4me3- and H3K27me3-ChIP data respectively (*Table 1*). Overall, the immunoprecipitated ChIP-Seq data had high duplication rates and reduced coverage, which was most likely due to the low starting DNA input for library preparation, and is therefore not suitable for genome-wide analysis. However, it may still be useful for a targeted working hypothesis limited to selective regions, *e.g.*, genes, repeats and intergenic regions, as reported in the following section.

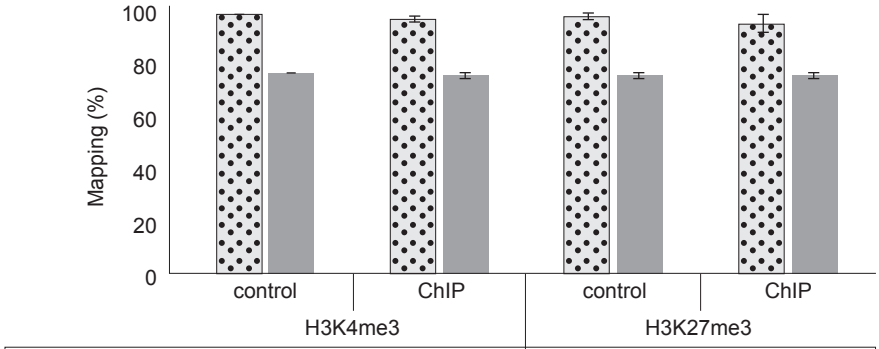

genome-wide	99.29	98.09	99.30	96.37
gene-wide	76.47	75.84	75.80	74.49

Figure 1. Average mapping percentages of ChIP-Seq data aligned to genome-wide and gene-wide E. guineensis pisifera *reference databases. Error bars indicate standard deviation (H3K4me3; n=9 and H3K27me3; n=10). Values below indicate the mapping percentage of each bar.*

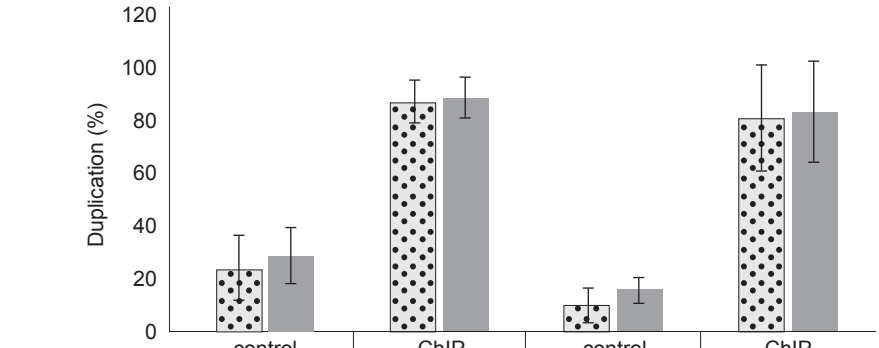

genome-wide	22.99	87.61	9.30	82.26
gene-wide	27.30	89.17	14.89	83.81

Figure 2. Presence of sequence duplicates in ChIP-Seq data aligned to genome-wide or gene-wide E. guineensis pisifera *reference databases. Error bars indicate standard deviation (H3K4me3; n=9 and H3K27me3; n=10). Values below indicate the percentage of duplication for each bar.*

TABLE 2. SUMMARY OF ChIP-SEQ DATASETS

Histone modification	Library type	Biological replicate	[a]Library starting material	[b]Mapping (%)		[c]Duplication (%)	
				Genome-wide	Gene-wide	Genome-wide	Gene-wide
H3K4me3	control	A	10	99.34	76.49	22.24	25.68
		B	10	99.25	75.76	13.59	18.30
		C	10	99.24	76.09	32.62	35.55
		D	10	99.37	77.03	47.31	50.59
		E	10	99.32	76.51	28.55	31.80
		G	10	99.22	76.21	27.62	30.39
		H	10	99.27	76.07	5.30	11.09
		I	10	99.32	78.40	25.23	32.84
		J	10	99.25	75.64	4.45	9.50
H3K4me3	ChIP	A	5.79	99.23	76.43	83.54	85.58
		B	2.10	99.18	77.12	84.60	87.28
		C	1.43	98.47	76.30	81.98	83.85
		D	3.81	96.86	74.65	97.23	97.79
		E	5.38	98.61	75.96	87.85	89.57
		G	4.01	98.53	76.21	97.05	97.70
		H	2.23	98.37	76.59	94.87	95.84
		I	7.29	99.05	76.50	70.12	72.60
		J	6.21	94.51	72.84	91.22	92.31
H3K27me3	control	A	10	99.31	75.48	5.63	12.00
		B	10	99.25	75.72	5.97	12.73
		C	10	99.24	75.70	6.63	12.14
		D	10	99.33	75.63	5.51	11.73
		E	10	99.33	75.93	7.69	12.94
		F	10	99.32	75.96	13.30	18.51
		G	10	99.29	75.78	5.35	11.77
		H	10	99.30	76.12	24.72	28.78
		I	10	99.32	75.75	8.23	13.25
		J	10	99.33	75.96	10.29	15.08
H3K27me3	ChIP	A	2.38	92.68	71.76	96.81	97.25
		B	2.68	96.17	74.07	90.53	91.74
		C	3.70	98.53	75.95	78.47	80.47
		D	2.71	87.90	67.79	83.23	83.25
		E	4.74	95.96	73.88	97.01	97.65
		F	10.10	99.24	76.32	23.39	28.48
		G	2.95	98.11	76.41	95.65	96.40
		H	1.12	97.96	75.93	84.44	86.19
		I	4.35	98.81	76.51	82.70	84.90
		J	3.81	98.35	76.25	90.34	91.79

Note: [a]DNA recovered from immunoprecipitation reactions used to prepare ChIP-Seq library.
[b]Percentage of reads mapped to the reference databases using Bowtie2.
[c]Duplicates presence in the mapped reads.

Gene-wide as an Alternative to Genome-wide Alignment

Read mapping on a genome-wide scale is a common practice in next-generation sequencing analysis and is widely acknowledged as a reliable approach when biases and limitations are minimal. With the limited number of unique ChIP reads, an alternative is to map onto a targeted region. In this study, a gene-wide database was built from genic areas consisting of gene models from their translation start to stop ±1 kb of their flanking upstream and downstream regions. The upstream 1 kb region would contain part of the promoter regions important for gene regulation, including the transcription start sites located around 50-200 bp upstream of the start codon (Shahmuradov *et al.*, 2017). These genic, upstream and downstream regulatory regions are usually covered by H3K4me3 and H3K27me3 modifications in other plants such as *Arabidopsis*, peach and potato (de la Fuente *et al.*, 2015; Yang *et al.*, 2018; Zeng *et al.*, 2019). This database generated for the oil palm was ~236 Mb, comprising 24 927 genes with their upstream and downstream regions. Predicted TSS are available for 13 016 genes. As a small portion of genes have multiple predicted TSS, a total of 14 353 TSS and 16 405 transcription termination sites (TTS) positions were identified. Gene-wide mapping rates were only slightly lower compared to genome-wide (*Figure 1*), with the majority of reads in ChIP and control datasets (~75%) mapping to genic regions (*Table 2*). The remaining 25%, therefore, most likely mapped to intergenic regions. This observation also suggested that most H3K4me3 and H3K27me3 marks are focused on or near genic regions. These observations are in agreement with the properties of H3K4me3 and H3K27me3 marks reported for plants such as *Arabidopsis*, peach and potato (de la Fuente *et al.*, 2015; Yang *et al.*, 2018; Zeng *et al.*, 2019), *i.e.*, both marks are highly associated with regulatory elements of genes and transcription. These results also suggested that the low coverage ChIP-Seq data could provide preliminary insights into H3K4me3 and H3K27me3 profiles on targeted oil palm genic regions. The current version of the oil palm genome assembly is a preliminary one (Chan *et al.*, 2017); there are 40 360 genomic scaffolds, ranging in length from 1992 to 22 100 610 nt. By focusing on the relevant regions (genic and regulatory) of well-annotated genes, we avoid 'dilution' of the signal from spurious mapping of reads to incorrectly assembled regions. This approach has improved the mapping precision of ChIP-Seq reads on target genic regions. However, the ChIP method on oil palm spears will require further optimisation to increase the DNA yield recovery, most likely by pooling an increased number of immunoprecipitation reactions.

Histone Marks Highly Associate with Predicted TSS of Genes

After mapping analysis, genomic regions with ChIP enrichment over background noise were detected as peaks using the Model-based Analysis of ChIP-Seq (MACS2) peak-calling software. These 'called peaks' represent biologically relevant histone modification sites. Peak detection parameters were optimised based on the binding properties of the specific histone modification, *i.e.*, a 'sharp' feature for H3K4me3 and a 'broad' feature for H3K27me3 at 0.05 false discovery rate (FDR) cut-off. Using the MACS2 peak caller, 300 to 4000 peaks associating with H3K4me3 and H3K27me3 were identified, albeit inconsistently among the biological replicates, likely due to their low coverage (*Table 3*). The H3K4me3 and H3K27me3 peak distribution profiles indicated that their abundance was predominant near the predicted TSS of genes (*Figure 3*). The oil palm H3K4me3 profile showed a narrow distribution with its peak centered at the predicted TSS (located on average 100 bp upstream of translation start positions) (*Figure 3a*), while H3K27me3 peak profile was much broader and was distributed over the gene region from the TSS (*Figure 3b*). These profiles were generally consistent with H3K4me3 and H3K27me3 patterns in other plants (de la Fuente *et al.*, 2015; Yang *et al.*, 2018; Zeng *et al.*, 2019). These profiles suggest that low coverage ChIP-Seq data could still reveal prominent characteristics of these histone modification profiles in oil palm.

TABLE 3. NUMBER OF ChIP-SEQ PEAKS IDENTIFIED USING MACS2 PACKAGE

Histone modification	Biological replicate	No. of ChIP-Seq peaks
H3K4me3	A	2 235
	B	3 623
	C	504
	D	743
	E	1 584
	G	296
	H	1 168
	I	3 910
	J	580
H3K27me3	A	739
	B	707
	C	1 227
	D	1 436
	E	727
	F	1 581
	G	472
	H	762
	I	1 348
	J	918

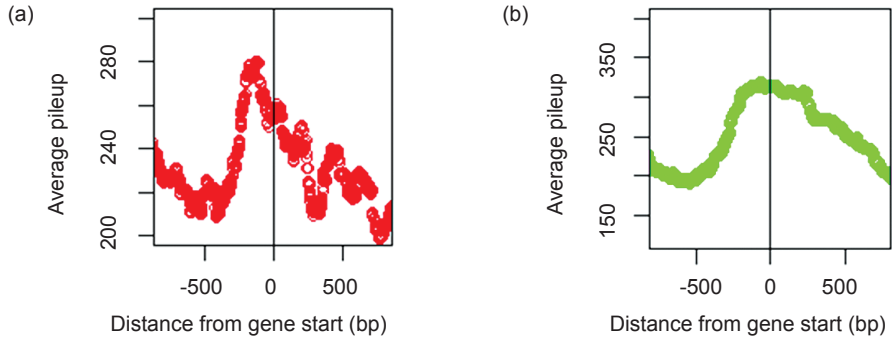

Figure 3. Gene-wide distribution pattern of ChIP-Seq peaks near the transcription start sites. (a) narrow distribution of H3K4me3 profile; (b) broad distribution of H3K27me3 profile. '0' on the x-axis denotes the ATG start codon.

DISCUSSION

In this study, H3K4me3 and H3K27me3 ChIP-Seq libraries were prepared with low amounts of DNA from pooled ChIP reactions on oil palm leaf chromatin. The initial low DNA amounts generated ChIP-Seq data with low numbers of unique mapped reads at low coverage. This was even after pooling the DNA from six to eight ChIP reactions, which yielded between 1 and 10 ng DNA. It thus, appears that the number of ChIP reactions per sample will need to be scaled up significantly. ChIP yields obtained were lower than those obtained for maize, where a pool of three ChIP reactions yielded about 50 ng DNA (Oka *et al.*, 2017). As the purification of immunoprecipitated DNA is a necessary step before library preparation, assessing the efficiency of purification agents could help in maximising DNA recovery without compromising the quality. Among several commercial purification kits and reagents, DNA recovery was higher when phenol-chloroform was used (Zhong *et al.*, 2017).

Nevertheless, using targeted regions in analysing such imperfect datasets has been demonstrated to be a practical approach when a genome-wide interrogation is not feasible. This approach is in line with published ChIP-Seq guidelines when dealing with low-quality data validated based on several quantitative quality metrics (Landt *et al.*, 2012; Nakato and Shirahige, 2017). About 75% of the data could be mapped to a database comprising genes and their upstream and downstream regions, suggesting that these histone marks are enriched mostly at the genic areas of oil palm. Although read mapping to a smaller database does not always increase alignment sensitivity and specificity, it still holds several advantages. In practice, assigning reads to only selected biologically relevant positions could provide a quick estimate when addressing urgent biological problems, a QC step in a pilot study, or in any setting when focusing only on differentially expressed genes is justified. Besides, with large plant genome sizes rich with repeats, the use of a smaller functional database reduces the time for computational analysis and saves space for the storage of processing files. The different ChIP-Seq read coverage among biological replicates contributes to variation in numbers and regions of ChIP enrichment, thus, compromising reproducibility. However, enrichment of H3K4me3 and H3K27me3 marks near TSS is supported by the similar characteristics of these profiles in *Arabidopsis*, peach and potato (de la Fuente *et al.*, 2015; Yang *et al.*, 2018; Zeng *et al.*, 2019), indicating that the ChIP assay worked for oil palm even though sequence coverage was low. Scaling up the immunoprecipitation reactions or improving on the ChIP yield recovery would be required in future ChIP-Seq studies. In *Arabidopsis*, predicted enhancers were characterised and validated using open chromatin signatures, which include H3K27ac and H3K27me3 histone modification patterns and non-coding RNA with GUS-based reporter assays (Zhu *et al.*, 2015). Therefore, histone enrichment profiles could be used to verify predicted TSS locations and improve the annotation of the oil palm genome.

The number of sequencing reads needed to reach a reasonable coverage varies depending on the types of histone binding patterns of the various histone modification types. At least 20 million reads are required for sharp binding patterns, while 60 million reads are suggested for broad binding patterns (Landt *et al.*, 2012; Nakato and Shirahige, 2017). Read coverage is deemed sufficient when the saturation point could be established or when the same histone enrichment sites are repeatedly identified from additional sequencing. A way to improve read coverage is by evaluating the antibody's quality to capture histone-bound regions. The efficiency of the antibody can be tested by conducting a titration of chromatin experiment to a fixed amount of antibody. One can evaluate whether diluting chromatin would improve the precipitation efficiency, thus, assessing the

presence of inhibitory factors within the chromatin (Haring *et al.*, 2007). Monoclonal and polyclonal antibodies, which respectively recognise single and multiple epitopes, affect the degree of enrichment and background noise differently. Testing out several commercial antibodies is also advisable as different brands may exhibit different efficiencies. The number of individual ChIP reactions needs to be increased to achieve the required amount for library construction. However, low amounts of ChIP DNA may provide useful sequencing data if an appropriate sequencing library preparation method explicitly for low DNA input is used. Recently, as low as 0.01 ng DNA, which is ≥100x lower than the starting amount used in this study, can be used for constructing ChIP-sequencing libraries (reviewed by Dahl and Gilfillan, 2018). This is useful for single-cell analysis, whereby the ChIPmentation procedure offers a single-step reaction of chromatin fragmentation and adaptor tagging (Schmidl *et al.*, 2015). The reduction of library preparation steps compared to published ChIP-Seq protocols therefore allows for samples with low cell input, as yield losses throughout the procedure is also reduced. With emerging new technologies, the ChIP-Seq assay is now even feasible at the single-cell level (Clark *et al.*, 2016).

CONCLUSION

This is the first ChIP-Seq report on histone modification patterns for the oil palm *E. guineensis*. Although preliminary, the primary limitation in this study was the low coverage and high duplication of the H3K4me3 and H3K27me3 ChIP-Seq data due to low ChIP recovery. However, the data was still able to provide some preliminary insights on these histone profiles in oil palm through a gene-wide mapping approach, followed by peak calling. The traditional genome-wide mapping approach used for analysing ChIP-Seq data is not suitable for partially assembled genomes combined with the low read yield situation. Restriction to the functionally relevant areas in oil palm genome resulted in H3K4me3 and H3K27me3 profiles consistent with the profiles of these histone modifications in plants such as *Arabidopsis*, peach and potato. This study's findings and recommendations may be useful for other plant species with incomplete genome sequence information to accurately identify histone profiles without requiring intensive computational power.

ACKNOWLEDGEMENT

We are grateful to the Director-General of MPOB for permission to publish this study. We thank members of the Epigenetics Group, Advanced Biotechnology and Breeding Centre, MPOB for their invaluable technical support. We also thank Chan Kuang Lim and Nik Shazana Nik Sanusi from the Bioinformatics Unit, MPOB. Our appreciation also goes to the Clonal Propagation Group, MPOB for the clonal palms used in this study. This study was funded by the MPOB.

REFERENCES

Baulcombe, D C and Dean, C (2014). Epigenetic regulation in plant responses to the environment. *Cold Spring Harb. Perspect. Biol., 6*: 1-19.

Berenguer, E; Bárány, I; Solís, M-T; Pérez-Pérez, Y; Risueño, M C and Testillano, P S (2017). Inhibition of histone H3K9 methylation by BIX-01294 promotes stress-induced microspore totipotency and enhances embryogenesis initiation. *Front. Plant Sci., 8*: 1-19.

Chan, K-L; Tatarinova, T V; Rosli, R; Amiruddin, N; Azizi, N; Halim, M A A; Sanusi, N S N M; Jayanthi, N; Ponomarenko, P; Triska, M; Solovyev, V; Firdaus-Raih, M; Sambanthamurthi, R; Murphy, D and Low, E-T L (2017). Evidence-based gene models for structural and functional annotations of the oil palm genome. *Biol. Direct, 12(1)*: 21. DOI: 10.1186/s13062-017-0191-4.

Clark, S J; Lee, H J; Smallwood, S A; Kelsey, G and Reik, W (2016). Single-cell epigenomics: Powerful new methods for understanding gene regulation and cell identity. *Genome Biol., 17*: 1-10.

Dahl, J A and Gilfillan, G D (2018). How low can you go? Pushing the limits of low-input ChIP-seq. *Brief. Funct. Genomics, 17*: 89-95.

de la Fuente, L; Conesa, A; Lloret, A; Badenes, M L and Ríos, G (2015). Genome-wide changes in histone H3 lysine 27 trimethylation associated with bud dormancy release in peach. *Tree Genet. Genomes, 11*: 45. DOI: 10.1007/s11295-015-0869-7.

Dodt, M; Roehr, J T; Ahmed, R and Dieterich, C (2012). FLEXBAR-flexible barcode and adapter processing for next-generation sequencing platforms. *Biology (Basel), 1*: 895-905.

Engelhorn, J; Blanvillain, R; Kröner, C; Parrinello, H; Rohmer, M; Posé, D; Ott, F; Schmid, M and Carles, C (2017). Dynamics of H3K4me3 chromatin marks prevails over H3K27me3 for gene regulation during flower morphogenesis in *Arabidopsis thaliana. Epigenomes, 1*: 8. DOI: 10.3390/epigenomes1020008.

Gan, E-S; Xu, Y and Ito, T (2015). Dynamics of H3K27me3 methylation and demethylation in plant development. *Plant Signal. Behav., 10(9)*: e1027851.

Haring, M; Offermann, S; Danker, T; Horst, I; Peterhansel, C and Stam, M (2007). Chromatin immunoprecipitation: Optimization, quantitative analysis and data normalization. *Plant Methods, 3*: 11. DOI: 10.1186/1746-4811-3-11.

Kaufmann, K; Muiño, J M; Østerås, M; Farinelli, L; Krajewski, P and Angenent, G C (2010). Chromatin immunoprecipitation (ChIP) of plant transcription factors followed by sequencing (ChIP-SEQ) or hybridization to whole genome arrays (ChIP-CHIP). *Nat. Protoc., 5(3)*: 457-472.

Landt, S G; Marinov, G K; Kundaje, A; Kheradpour, P; Pauli, F; Batzoglou, S; Bernstein, B E; Bickel, P; Brown, J B; Cayting, P; Chen, Y; DeSalvo, G; Epstein, C; Fisher-Aylor, K I; Euskirchen, G; Gerstein, M; Gertz, J; Hartemink, A J; Hoffman, M M; Iyer, V R; Jung, Y L; Karmakar, S; Kellis, M; Kharchenko, P V; Li, Q; Liu, T; Liu, S; Ma, L; Milosavljevic, A; Myers, R M; Park, P J; Pazin, M J; Perry, M D; Raha, D; Reddy, T E; Rozowsky, J; Shoresh, N; Sidow, A; Slattery, M; Stamatoyannopoulos, J A; Tolstorukov, M Y; White, K P; Xi, S; Farnham, P J; Lieb, J D; Wold, B J and Snyder, M (2012). ChIP-seq guidelines and practices of the ENCODE and modENCODE consortia. *Genome Res., 22*: 1813-1831.

Langmead, B and Salzberg, S L (2012). Fast gapped-read alignment with Bowtie2. *Nat. Methods, 9*: 357-359.

Li, H; Handsaker, B; Wysoker, A; Fennell, T; Ruan, J; Homer, N; Marth, G; Abecasis, G and Durbin, R (2009). The sequence alignment/map format and SAMtools. *Bioinformatics, 25*: 2078-2079.

Liu, E T; Pott, S and Huss, M (2010). Q&A: ChIP-seq technologies and the study of gene regulation. *BMC Biol., 8*: 56. DOI: 10.1186/1741-7007-8-56.

Loh, Y-H E; Feng, J; Nestler, E and Shen, L (2017). Bioinformatic analysis for profiling drug-induced chromatin modification landscapes in mouse brain using ChIP-seq data. *Bio Protoc., 7(3)*: e2123. DOI: 10.21769/BioProtoc.2123.

Lu, Y; Zhou, D-X and Zhao, Y (2020). Understanding epigenomics based on the rice model. *Theor. Appl. Genet., 133*: 1345-1363.

Nakato, R and Shirahige, K (2017). Recent advances in ChIP-seq analysis: From quality management to whole-genome annotation. *Brief. Bioinform., 18*: 279-290.

Oka, R; Zicola, J; Weber, B; Anderson, S N; Hodgman, C; Gent, J I; Wesselink, J-J; Springer, N M; Hoefsloot, H C J; Turck, F and Stam, M (2017). Genome-wide mapping of transcriptional enhancer candidates using DNA and chromatin features in maize. *Genome Biol., 18(1)*: 137. DOI: 10.1186/s13059-017-1273-4.

Ong-Abdullah, M; Ordway, J M; Jiang, N; Ooi, S-E; Kok, S-Y; Sarpan, N; Azimi, N; Hashim, A T; Ishak, Z; Rosli, S K; Malike, F A; Bakar, N A A; Marjuni, M; Abdullah, N; Yaakub, Z; Amiruddin, M D; Nookiah, R; Singh, R; Low, E-T L; Chan, K-L; Azizi, N; Smith, S W; Bacher, B; Budiman, M A; Van Brunt, A; Wischmeyer, C; Beil, M; Hogan, M; Lakey, N; Lim, C-C; Arulandoo, X; Wong, C-K; Choo, C-N; Wong, W-C; Kwan, Y-Y; Alwee, S S R S; Sambanthamurthi, R and Martienssen, R A (2015). Loss of Karma transposon methylation underlies the mantled somaclonal variant of oil palm. *Nature, 525*: 533-537.

Ong-Abdullah, M; Ordway, J M; Jiang, N; Ooi, S-E; Mokri, A; Kok, S Y; Sarpan, N; Azimi, N; Hashim, A T; Ishak, Z; Rosli, S K; Nookiah, R; Singh, R; Low, E-T L; Sachdeva, M; Smith, S W; Lakey, N; Martienssen, R A and Sambanthamurthi, R (2016). Tissue culture and epigenetics. *The Planter, 92*: 741-749.

Prakash, K and Fournier, D (2018). Evidence for the implication of the histone code in building the genome structure. *Biosystems, 164*: 49-59.

Ranawaka, B; Tanurdzic, M; Waterhouse, P and Naim, F (2020). An optimised chromatin immunoprecipitation (ChIP) method for starchy leaves of *Nicotiana benthamiana* to study histone modifications of an allotetraploid plant. *Mol. Biol. Rep., 47*: 9499-9509.

Sanusi, N S N M; Rosli, R; Halim, M A A; Chan, K-L; Nagappan, J; Azizi, N; Amiruddin, N; Tatarinova, T V and Low, E-T L (2018). PalmXplore: Oil palm gene database. *Database, 2018*: 1-9.

Sarpan, N; Ong-Abdullah, M and Ooi, S-E (2018). Optimisation of a chromatin immunoprecipitation (ChIP) protocol for histone modification in oil palm. *J. Oil Palm Res., 30*: 242-250.

Schmidl, C; Rendeiro, A F; Sheffield, N C and Bock, C (2015). ChIPmentation: Fast, robust, low-input ChIP-seq for histones and transcription factors. *Nat. Methods, 12*: 963-965.

Shahmuradov, I A; Umarov, R K and Solovyev, V V (2017). TSSPlant: A new tool for prediction of plant Pol II promoters. *Nucleic Acids Res., 45(8)*: e65.

Singh, R; Ong-Abdullah, M; Low, E-T L; Manaf, M A A; Rosli, R; Nookiah, R; Ooi, L C-L; Ooi, S-E; Chan,

K-L; Halim, M A; Azizi, N; Nagappan, N; Bacher, B; Lakey, N; Smith, S W; He, D; Hogan, M; Budiman, M A; Lee, E K; DeSalle, R; Kudrna, D; Goicoechea, J L; Wing, R A; Wilson, R K; Fulton, R S; Ordway, J M, Martienssen, R A and Sambanthamurthi, R (2013). Oil palm genome sequence reveals divergence of interfertile species in old and new worlds. *Nature, 500*: 335-339.

Wollmann, H and Berger, F (2012). Epigenetic reprogramming during plant reproduction and seed development. *Curr. Opin. Plant Biol., 15*: 63-69.

Yang, Z; Qian, S; Scheid, R N; Lu, L; Chen, X; Du, X; Lv, X; Boersma, M D; Scalf, M and Smith, L M (2018). EBS is a bivalent histone reader that regulates floral phase transition in *Arabidopsis. Nat. Genet., 50*: 1247-1253.

Zeng, Z; Zhang, W; Marand, A P; Zhu, B; Buell, C R and Jiang, J (2019). Cold stress induces enhanced chromatin accessibility and bivalent histone modifications H3K4me3 and H3K27me3 of active genes in potato. *Genome Biol., 20*: 1-17.

Zhang, W; Garcia, N; Feng, Y; Zhao, H and Messing, J (2015). Genome-wide histone acetylation correlates with active transcription in maize. *Genomics, 106(4)*: 214-220.

Zhang, X; Bernatavichute, Y V; Cokus, S; Pellegrini, M and Jacobsen, S E (2009). Genome-wide analysis of mono-, di- and trimethylation of histone H3 lysine 4 in *Arabidopsis thaliana. Genome Biol., 10(6)*: R62. DOI: 10.1186/gb-2009-10-6-r62.

Zhang, Y; Liu, T; Meyer, C A; Eeckhoute, J; Johnson, D S; Bernstein, B E; Nussbaum, C; Myers, R M; Brown, M; Li, W and Liu, X S (2008). Model-based analysis of ChIP-Seq (MACS). *Genome Biol., 9(9)*: R137. DOI: 10.1186/gb-2008-9-9-r137.

Zhong, J; Ye, Z; Lenz, S W; Clark, C R; Bharucha, A; Farrugia, G; Robertson, K D; Zhang, Z; Ordog, T and Lee, J-H (2017). Purification of nanogram-range immunoprecipitated DNA in ChIP-seq application. *BMC Genomics, 18(1)*: 985. DOI: 10.1186/s12864-017-4371-5.

Zhu, B; Zhang, W; Zhang, T; Liu, B and Jiang, J (2015). Genome-wide prediction and validation of intergenic enhancers in *Arabidopsis* using open chromatin signatures. *Plant Cell, 27*: 2415-2426.

Zong, W; Zhong, X; You, J and Xiong, L (2013). Genome-wide profiling of histone H3K4-tri-methylation and gene expression in rice under drought stress. *Plant Mol. Biol., 81*: 175-188.

Zulkifli, Y; Norziha, A; Naqiuddin, M H; Fadila, A M; Nor Azwani, A B; Suzana, M; Samsul, K R; Ong-Abdullah, M; Singh, R; Parveez, G K A and Kushairi, A (2017). Designing the oil palm of the future. *J. Oil Palm Res., 29*: 440-455.

Journal of Oil Palm Research Vol. 34 (1) March 2022 p. 46-55
DOI: https://doi.org/10.21894/jopr.2021.0025

CORRELATION BETWEEN NON-RIBOSOMAL PEPTIDE SYNTHETASE (NRPS) PRODUCTION AND VIRULENCE OF *Ganoderma boninense* PER71 ON OIL PALM (*Elaeis guineensis*)

JACKIE CHUA[1]; KWAN YEE MIN[2]; ABRIZAH OTHMAN[1]* and WONG MUI YUN[3]

ABSTRACT

Basal stem rot (BSR) disease caused by the white rot fungus Ganoderma boninense *is the most destructive oil palm disease leading to production losses in fresh fruit bunches (FFB). Non-ribosomal peptide synthetase (NRPS) plays an important role in fungal pathogenicity. These large multi-modular enzymes catalyse the biosynthesis of secondary metabolites (SMs) that act as fungal virulence factors. In this study, the detection of NRPS in* G. boninense *was achieved using polymerase chain reaction (PCR)-based method. Core motifs of adenylation domain of NRPS gene was identified in* G. boninense*. The deduced amino acid sequence showed similarity to the conserved core motifs (A2, A3 and A5) of the adenylation domain. Siderophores were predicted as the potential SMs synthesised by NRPS. Expression analysis of* GbNRPS *in 3-month-old oil palm artificially infected with* G. boninense *has confirmed the upregulation of* GbNRPS *at 1 month after inoculation (MAI) peaking at 4 MAI in susceptible clone but not in tolerant clone. There was a correlation between* GbNRPS *gene expression and disease severity. Susceptible clones showed significantly higher disease severity index (DSI) (62.50%) compared to tolerant clones (28.13%) at 4 MAI. This is the first putative detection of adenylation domain of NRPS (*GbNRPS*) gene and functional analysis of NRPS as a virulence factor in disease development.*

Keywords: adenylation domain, basal stem rot, non-ribosomal peptide synthetase.

Received: 29 September 2020**; Accepted:** 1 March 2021**; Published online:** 31 May 2021.

INTRODUCTION

African oil palm (*Elaeis guineensis* Jacq.) is an oil crop widely cultivated in Southeast Asia for its edible palm oil. Palm oil and palm kernel oil have become important raw materials in food and non-food industries such as pharmaceutical, cosmetics, animal feed and is a promising source of biofuel. Malaysian palm oil industry constituted 27.7% of the global palm oil production, which is equivalent to approximately USD16.14 billion annual export revenue in 2018 (Kushairi *et al.*, 2019).

Basal stem rot (BSR) caused by the soil borne *Ganoderma boninense* which is a basidiomycete white rot fungus is catastrophic to oil palm plantations resulting in a 50%-80% reduction in palm oil production following reduction of standing palms, number and weight of fresh fruit bunches (FFB) (Chong *et al.*, 2017; Corley and Tinker, 2015). The disease kills young palms within 6-24 months after the first appearance of foliar symptoms such as water stress, one-sided canopy mottling, crown flattening and multiple unopened spears followed by the sign

[1] Malaysian Palm Oil Board,
6 Persiaran Institusi, Bandar Baru Bangi,
43000 Kajang, Selangor, Malaysia.

[2] Department of Crop Science,
Faculty of Agriculture and Food Sciences,
Universiti Putra Malaysia Bintulu Sarawak Campus,
97008 Bintulu, Sarawak, Malaysia.

[3] Laboratory of Sustainable Agronomy and Crop Protection,
Institute of Plantation Studies,
Universiti Putra Malaysia,
43400 UPM Serdang, Selangor, Malaysia.

* *Corresponding author e-mail: abi@mpob.gov.my*

of fruiting body at stem base (Paterson, 2007; Rees *et al.*, 2009). The effectiveness of current disease control measures is debatable. These processes include physical (ploughing and fallowing before planting, mechanical soil mounding and surgery removal of basidiocarps), chemical (systemic fungicides) and biological (antagonistic activity of *Trichoderma harzianum* and *Pseudomonas aeruginosa*) (Hushiarian *et al.*, 2013). The incidence of BSR is exacerbated by climate change with an estimated 0.44 million hectares (65.6 million palm trees) in untreated oil palm plantations in 2020 (Abas and Abu Seman, 2012).

In the *G. boninense*-oil palm pathological system, the pathogen establishes as a biotroph in the root system and switches to hemibiotroph as the disease progresses. Necrotrophs and hemibiotrophs employ a wide variety of secondary metabolites (SMs) which are associated with cellular development, pathogenicity and tolerance to various environmental stresses (Pusztahelyi *et al.*, 2015). SMs have a wide variety of chemical structures that are normally produced via biosynthetic pathways such as non-ribosomal peptide synthetases (NRPS) (Gunatilaka and Wijeratne, 2011; Keller *et al.*, 2005). NRP are synthesised by NRPS enzyme complexes and involve a thiotemplate mechanism in which peptide synthesis is independent of ribosome-based translation processes. Instead, proteinogenic and non-proteinogenic amino acids are serially incorporated (Sayari *et al.*, 2019). These enzymes are multi-modular and most NRPS modules consist of three conserved domains: adenylation (A) (identification and substrate activation), thiolation (T) or peptidyl carrier protein (PCP) (covalent binding and transmission) and condensation (C) (formation of peptide bond) which when grouped together are referred to as a single module (Martínez Núñez and López, 2016; Soukup *et al.*, 2016). Each module is responsible for recognition and incorporation of amino acids into the extending peptide backbone depending on the complexity of the peptide. These modules may also occur with other accessory domains such as thioesterase (TE) (release of newly synthesised peptide from enzyme), epimerisation (E) (L to D configuration) and N-methyl transferase (MT) (transfer of methyl group) to further modify the peptide products (Sayari *et al.*, 2019). The final peptide products may be further modified by additional tailoring enzymes which catalyse glycosylation, hydroxylation, acylation or halogenation; thereby resulting in the structural and chemical diversity of NRP (Bushley and Turgeon, 2010). The peptides produced might be of linear type, cyclic or branched. So far, 600 peptides or peptide metabolites have been described from various taxa of bacteria and fungi (Welker and von Döhren, 2006). The size of the peptides produced non-ribosomally ranged from two to 40 amino acids (more in depth information can be obtained from Finking and Marahiel, 2004; Kleinkauf and von Döhren, 1996; Schwarzer *et al.*, 2003; Schwarzer and Marahiel, 2001; Stachelhaus and Marahiel, 1995; von Döhren, 2004). General guidelines of NRPSs lie in the modular structure assembly where the modules are organised in domains: adenylation, thiolation and condensation domains. Examples of enzymatically purified NRPS are HC-toxin synthetase, enniatin synthetase, AM-toxin synthetase and bassianolide synthetase (*Table 1*) (Eisfeld, 2009). One of the most studied functions of NRPS-produced peptide is the role as siderophore in forming Fe^{3+} complex. Two types of siderophores (ferrichrome and coprogen) have been reported in several fungi such as *Aspergillus fumigatus, A. nidulans, Ustilago maydis, Omphalotus olearius, Schizosaccharomyces pombe* and phytopathogenic fungi (*Alternaria brassicicola, Cochliobolus heterostrophus, Fusarium graminearum, Magnaporthe grisea, etc.*) (Philpott, 2006).

Adenylation domain (A-domain) is the most important determinant in NRPS modules as each activity begins with A-domain that loads amino acid substrate onto the carrier protein cofactor. There are around 550 amino acids in A-domain with two purpose which are to select and to activate the related substrate (Eisfeld, 2009). The substrate can be an amino acid, an imino-, a hydroxyl- or a carboxy- acid. The activation will start after that and later on added to the peptide chain as it grows (von Döhren, 2004). The characteristic for A-domains is to recognise and bind the substrates with a set of conserved sequence motifs as shown in *Table 2* (Konz and Marahiel, 1999). These highly conserved motifs are situated mostly around active areas in which the substrates are bound at (Marahiel *et al.*, 1997). *Figure 1* shows the position of the core motifs (A1-A10) in A-domain with their functions and relationship of one another.

To reveal more information on the A-domains, a sequence alignments method was used and the alignments showed an adenylate (AMP) binding motif which is conserved in adenylate forming enzymes superfamily which includes 4-coumerate-CoA ligases, oxidoreductases and acetyl-CoA synthetases (Turgay *et al.*, 1992). There is a homologous structure observed in these family members despite of the low similarity in the sequences. The catalysis by the A-domain is parallel to the initial step done by aminoacyl-tRNA synthetases (Turgay *et al.*, 1992), even though they displayed no sequence or structural similarities (Arnez and Moras, 1997; Weber and Marahiel, 2001).

Siderophores (a class of iron specific chelators) are one of the examples of NRP that are important fungal effectors that supress host immunity. Siderophores' role in fungus (pathogen)-plant interactions has not been clearly established.

TABLE 1. EXAMPLES OF CHARACTERISED NON-RIBOSOMAL PEPTIDE SYNTHETASES (NRPSs), THEIR PRODUCTS AND PROPERTIES

Producer	NRPS/Structure	Product	Properties
Fusarium oxysporum	Enniatin synthetase CATCAMTTC	Cyclo-hexadepsipeptide	Ionophore; inhibitor of acyl-CoA-cholestro lacyltransferase and of phosphodiesterase; potential anticancer compound
Cochlibolus carbonum	HC-toxin synthethase (HTS1) ATEC(ATC)[3]	Cyclo-tetrapeptide	Inhibitor of histone-deacetylases; maize-pathogen
Alternaria alternata	AM-toxin synthetase (ATC)[4]	4-peptidolactone	Phytotoxic
Xylaria sp. BCC1067	Bassianolide synthetase CATCAMTTCR	Cyclooctadepsipeptide	Pathogenic to insects

Source: Eisfeld (2009).

TABLE 2. CORE MOTIFS OF ADENYLATION (A), THIOLATION (T)/PEPTIDYL CARRIER PROTEIN (PCP) AND CONDENSATION (C) WITHIN THE DOMAINS OF NON-RIBOSOMAL PEPTIDE SYNTHETASE (NRPS)

Domain	Core	Consensus protein sequence
Adenylation	A1	L(TS)YxEL
	A2 (core 1)	LKAGxAY(VL)P(LI)D
	A3 (core 2)	LAYxxYTSG(ST)TGxPKG
	A4	FDxS
	A5	NxYGPTE
	A6 (core 3)	GELxIxGxG(VL)ARGYL
	A7 (core 4)	Y(RK)TGDL
	A8 (core 5)	GRxDxQVKIRGxRIELGEIE
	A9	LPxYM(IV)P
	A10	NGK(VL)DR
Thiolation or peptidyl carrier protein	T (core 6)	DxFFxxLGG(HD)S(LI)
Condensation	C1	SxAQxR(LM)(WY)Xl
	C2	RHExLRTxF
	C3 (His)	MHHxISDG(WV)S
	C4	YxD(FY)AVW
	C5	(IV)GxFVNT(QL)(~)Xr
	C6	(HN)QD(YV)PFE
	C7	RDxSRNPL

Source: Konz and Marahiel (1999).

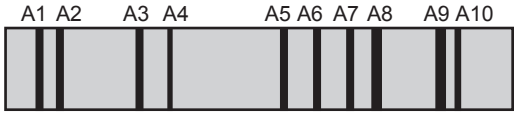

A3 interaction with pyrophosphate leaving group
A4 interaction with amino group
A7 interaction via hydrogen bonds with oxygen atoms of nucleoside ribose moiety
A8 essential for adenylation
A10 binds to substrate and ribose oxygens

Source: Eisfeld (2009).

Figure 1. Position and function of conserved motifs of the adenylation domain.

Nonetheless, over the time, investigation on siderophores have shown pathogenicity in several plant-pathogenic fungi and it was hypothesised that they play essential roles in supplying fungal pathogens with iron, which is a limiting factor within host environments (Lee *et al.*, 2005; Oide *et al.*, 2006; Schrettl *et al.*, 2007). Siderophores are reported to be essential for pathogenicity of most fungal pathogens and associated with the development of disease symptoms (Gerwien *et al.*, 2018).

There were few NRPS genes reported in other basidiomycetes. Synthesis of siderophore was

investigated in the ustilaginomycete *Ustilago maydis* and in the homobasidiomycete *Omphalotus olearius*. Production of ferrichrome and ferrichrome A were found in *U. maydis* (Budde and Leong, 1989). Siderophore synthetases that encode the ferrichrome synthetase is SID2 and the ferrichrome A synthetase is FER3 (Eichhorn *et al.*, 2006; Yuan *et al.*, 2001). A putative ferrichrome A synthetase gene was detected in *O. olearius*. The NRPS gene encoding the ferrichrome A synthetase in this fungus (FSO1) was the first NRPS gene described in a higher basidiomycete. Siderophore synthetase of ferrichome-type from the basidiomycete has high similarity to the siderophore synthetases of ascomycetes. It is interesting to find that there are 48 introns interruption in FSO1 (Welzel *et al.*, 2005). Even though high number of introns is not common in NRPS genes, it is reported that basidiomycete's genes are basically interrupted by a number of introns (Larrondo *et al.*, 2004; Martinez *et al.*, 2004).

Hence, a complete understanding of NRPS as a pathogenicity factor of *G. boninense* may provide insights to the fungal counter defence against innate plant defence system. The goals of this study were to i) identify a putative NRPS gene (A-domain) in *G. boninense*, ii) deduce the possible products of the said gene and iii) correlate between NRPS gene expression and disease severity in oil palm.

MATERIALS AND METHODS

Fungal Strain and Culture Conditions

Ganoderma boninense PER71 culture was obtained from Malaysian Palm Oil Board (MPOB). The culture was maintained on malt extract agar (MEA) and incubated in the dark at 25°C. Mycelial agar discs (5 mm diameter) were obtained from the edge of a 7-day-old culture and inoculated onto malt extract broth (MEB) on a rotary shaker at 150 rpm. Fungal mycelium was harvested at 14 days after inoculation.

Total RNA Extraction

Total RNA was extracted from 100 mg fungal mycelium using Norgen Total RNA Purification Kit (Norgen Biotek Corporation, Canada) according to the manufacturer's instruction. On-column DNase I (Fermentas, Lithuania) digestion was performed at 25°C for 15 min to eliminate traces of genomic deoxyribonucleic acid (DNA). Ribonucleic acid (RNA) concentration was quantified using NanoDrop™ ND-1000 Spectrophotometer and total RNA integrity was determined using 1% agarose gel electrophoresis.

Complimentary DNA (cDNA) Synthesis and Polymerase Chain Reaction (PCR) Amplification

A total of 1 μg DNase-treated RNA was reverse-transcribed using Omniscript Reverse Transcription Kit (Qiagen, German) and oligo (dT) primer at 37°C for 60 min. Degenerate primers were designed from the conserved A-domain of NRPS. Internal transcribed spacer (ITS) was used as an internal control (Utomo *et al.*, 2005). All primer sequences are as listed in *Table 3*. PCR amplification was performed in a total volume of 25 μL consisting 200 ng μL^{-1} cDNA template, 0.5 μM forward and reverse primer each and DreamTaq DNA Polymerase (Fermentas, Lithuania). PCR programs were as follows: initial denaturation at 95°C for 3 min; 40 cycles of 95°C for 30 s, 57°C annealing for 30 s, 72°C extension for 1 min and 7 min of final extension at 72°C. PCR products were purified using the QIAquick Gel Extraction Kit (Qiagen, Germany) according to the instructions from the manufacturer. The purified PCR products were cloned into pDrive cloning vector (Qiagen, Germany) and transformed into the competent Qiagen EZ bacterial cells. The positive recombinant colonies were screened using indicator plates incorporated with 80 μg mL^{-1} X-gal, 50 μM isopropyl-β-d-thiogalactopyranoside (IPTG) and 100 μg mL^{-1} ampicillin. Positive clones were harvested for plasmid purification

TABLE 3. LIST OF PRIMERS USED FOR POLYMERASE CHAIN REACTION (PCR) AMPLIFICATION

Primer	Primer sequence (5′-3′)	Protein sequence (adenylation domain)
A3-4F	CACCACCGGCAAGCCNAARGGNGT	TTGKPKGV (A3)
A8-1R	CCNCKDATYTTNACYTG	QVKIRG (A8)
ITS1	AGCTCGTTCGTTTGACGA	
ITS1	AGCTCGTTCGTTTGACGA	
ITS3	CGATCAATAAAAGACCGA	
GADPH-F	ACTGCTACTCAGAAGACTGTTGATG	
GADPH-R	TGCTGCTAGGAATGATGTTAAAGCT	

using the QIAprep Spin Miniprep Plasmid Kit (Qiagen, Germany). Inserts were verified using *Eco*RI restriction enzyme digestion (Fermentas, Lithuania) and were analysed using 1% agarose gel electrophoresis. DNA fragments were then sequenced and the obtained DNA sequences were analysed using homology-based searches for A-domain in Basic Local Alignment Search Tool (BLAST).

Chrome Azurol S (CAS) Assay

Fungal siderophore producing ability was tested according to a modified chrome azurol S (CAS) assay outlined by Milagres *et al.* (1999). All glassware was treated with 6 M hydrogen chloride (HCl) and rinsed with distilled water to remove all traces of iron. Briefly, 60.5 mg CAS was dissolved in 50 mL distilled water and mixed with 10 mL iron (III) solution (1 mM $FeCl_3.6H_20$ in 10 mM HCl). The mixture was added to 40 mL of hexadecyltrimethylammonium bromide (CTAB) while stirring. CTAB solution was prepared by dissolving 72.9 mg CTAB in 40 mL distilled water. The resulting dark blue solution was kept at 50°C. Agar solution was prepared by dissolving 30.24 g piperazine-N,N'-bis(2-ethanesulphonic acid) (PIPES) and 15 g agar in 750 mL distilled water and, the final pH of the solution was raised to 6.7 using sodium hydroxide (NaOH). CAS agar was prepared by adding the dye solution to the agar solution and autoclaved at 121°C for 15 min. Petri dishes (9 cm diameter) containing potato dextrose agar (PDA) was cut into half in a sterile condition, one of which was replaced by CAS agar. Fungal agar discs were inoculated far from the borderline between the two media. The plates were incubated at 26 ± 2°C in the dark for two weeks. Colour of the CAS agar changed from blue to orange when siderophore was produced. Siderophore production was determined by measuring the distance of the orange zone in the CAS agar. All CAS reactions were performed in triplicates.

Plant Materials and Treatments

Three-month-old susceptible clone PK5407 and tolerant clone PK5505 oil palm seedlings (45 seedlings per clone) were obtained from MPOB Kluang Research Station, Johor, Malaysia. Thirty-six seedlings of each clone were inoculated with one-month-old *G. boninense*- colonised rubber wood block (RWB) (12 cm x 6 cm x 6 cm) using direct sitting technique (Sariah *et al.*, 1994). RWBs were used as carrier medium to provide nutrients for *G. boninense* under host-free condition. Nine seedlings of each clone were used as control. The seedlings were arranged in a completely randomised design (CRD) in the green house and maintained for six months.

Disease Assessment

Disease severity of the inoculated seedlings was assessed at 0, 1, 2, 4, 6 months after inoculation (MAI) according to external disease symptoms and rated based on 0-4 disease severity value. Disease severity index (DSI) was calculated using the Equation: Σ (A x B) x 100 / Σ (n x 4), of which:

A = disease class (0, 1, 2, 3 or 4)
B = number of plants showing that disease class per treatment
n = total number of plants per treatment
(Nur Ain Izzati and Faridah, 2008)

Gene Expression by Reverse Transcription (RT-PCR)

Nine seedlings each were harvested from control, susceptible and tolerant progenies at 0, 1, 2, 4 and 6 MAI, respectively. Root samples were collected, snapped frozen in liquid nitrogen and were stored at -80°C until extraction. Prescott and Martin (1987) method was employed to extract total RNA with the addition of aurintricarboxylic acid in RNA extraction buffer and also using the Norgen Total RNA Purification Kit (Norgen Biotek Corporation, Canada). RNA was analysed on 1% agarose gel to determine its quality. All the extracted RNA root samples of control and infected plants from both progenies were reverse-transcribed using the Omniscript® Reverse Transcription Kit (Qiagen, Germany). The RNA samples were thawed on ice and 4-6 µL (1 µg) of RNA root samples was added to master mix containing 2 µL 10x buffer RT, 2 µL dNTP (5 mM of each dNTP), 2 µL oligo-dT primers (10 µM), 0.3 µL RNase inhibitor (10 units μL^{-1}), 1 µL Omniscript Reverse Transcriptase and 6.7-8.7 µL RNase-free water in 0.2 mL PCR tube. The mixture was incubated for 1 hr at 37°C on a thermocycler to reverse transcribe the template RNA to cDNA. The cDNA was then diluted with nuclease-free water and standardised to a final concentration of 200 ng μL^{-1} to be used for PCR analysis right away or stored at -20°C for later use. Glyceraldehyde 3-phosphate dehydrogenase (GADPH) primers served as PCR positive control. The GADPH primers were designed with PCR product around 100 bp. Primer pair of A3(4)F / A8(1)R were tested using cDNA of root samples. Total RNA from fungal mycelium was extracted using Norgen Total RNA Purification Kit (Norgen Biotek Corporation, Canada). RNA concentration and quality were examined using NanoDrop™ ND-1000 Spectrophotometer and 1% gel electrophoresis. A total of 1 µg DNase-treated RNA was reverse-transcribed using the Omniscript® Reverse Transcription Kit (Qiagen, German) and dT primer at 37°C for 60 min. The concentration of cDNA was quantified and diluted using nuclease-free water to a final concentration of 200 ng μL^{-1}.

PCR amplification was performed according to the condition as mentioned in the previous section. GADPH was used as internal control. All PCR reactions were performed in triplicates.

RESULTS AND DISCUSSION

Detection and Molecular Characterisation of NRPS cDNA

Total RNA extracted from the root samples showed two distinct rRNA bands (28S and 18S). The $A_{260/280}$ and $A_{260/230}$ ratios ranged from 1.89-1.97 and 1.9-2.10, respectively indicating that the RNA samples were of good purity with minimal protein and organic compound contamination. PCR amplification products of 835 bp were obtained. BLAST analysis against NRPS sequences indicated sequence similarity to the A-domain core motifs of NRPS gene. The sequence was identified to contain the putative A2 (LKAGxAYL(VL)P(LI)D, A3 (TSG(TS)TGxPKxV) and A5 (NxYGPxE) motifs of the A-domain. Thus, the sequence was designated as *GbNRPS*. The low sequence similarity of the A-domain motif in *G. boninense* could suggest its novelty.

Siderophore Production in *G. boninense*

The formation of orange-coloured zone on CAS agar indicated the production of siderophores by *G. boninense* (*Figure 2*). Fungal mycelia grew rapidly on PDA agar but did not grow at all on CAS agar. Siderophores were produced and diffused through the CAS agar to cause colour change. Colour change on CAS agar was first observed at seven days after inoculation (DAI) when fungal mycelia started to cover the PDA. CAS reaction rate was calculated at 2 mm per day by measuring radial diameter of the orange-coloured zone. The colour change reaction was the result of iron removal from CAS dye by the siderophores secreted by *G. boninense*. Siderophores are iron-binding compounds produced by various organisms including pathogenic fungi to acquire iron, an important cofactor for iron-dependent enzymes required for various cellular processes (Sayari *et al.*, 2019). In addition, the preclusion of iron from the host plant is an important strategy to weaken the defense mechanism due to nutritional deficiencies (Haas, 2014).

Disease Severity Index (DSI)

Destructive sampling was carried out 1 MAI to examine the external and internal disease symptoms for each clone. DSI was determined based on the disease symptoms observed. The earliest disease symptoms were first observed in both susceptible and tolerant progenies at 4 MAI. Artificial infection of oil palm using direct sitting technique caused successful disease incidence (DI) in both susceptible and tolerant clones. Infection was confirmed by visual observation of white mycelia on root tissues. Uninoculated seedlings showed no sign of BSR foliar symptom, healthy stem and no fungal mycelia on root tissues. At 4 MAI, the tolerant clones showed lower DSI (28.13%) compared to the susceptible clone (62.50%). The disease symptoms observed in both clones followed the typical BSR disease progression patterns in oil palm. The infected

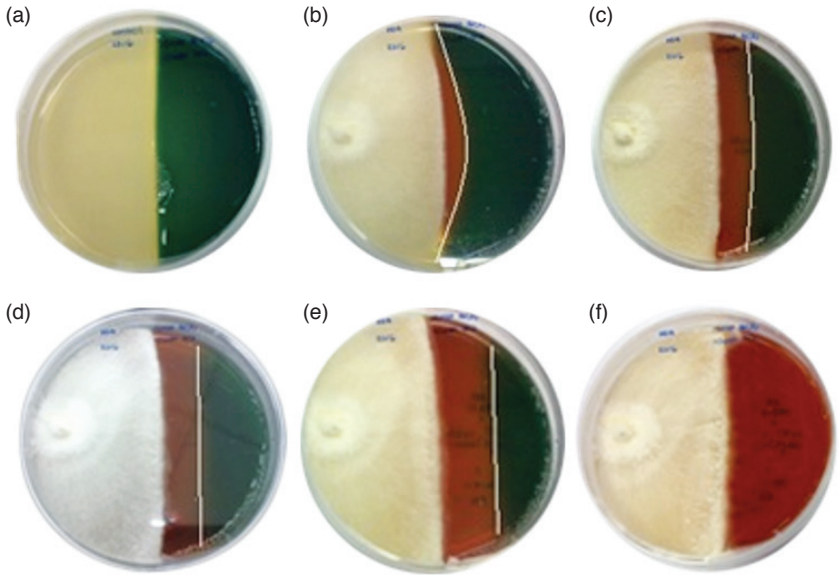

Figure 2. Development of orange-coloured zone on blue chrome azurol S (CAS) agar inoculated with G. boninense. *(a) Uninoculated control, (b) seven days after inoculation (DAI), (c) 10 DAI, (d) 11 DAI, (e) 12 DAI, and (f) 14 DAI.*

seedlings were observed with progressive chlorosis and necrosis from the older to the younger leaves. Fungal mycelia were observed on root tissues and followed by progressive stem necrosis and the formation of basidioma at basal stem. At 6 MAI, DSI of tolerant and susceptible clones were increased to 31.25% and 71.88%, respectively. The symptoms of leaf chlorosis and desiccation in infected palms were caused by restricted water and nutrient uptake due to damaged stem and root tissues (Hushiarian *et al.*, 2013). The differential responses of the tolerant and susceptible clones to *G. boninense* reflect the distinct molecular regulation of defense related genes between both clones. The higher expression of defense related genes such as chitinases, isoflavone reductase, metallothionine-like protein and serine protease inhibitor in the root tissues of the tolerant clone likely contributed to its higher tolerance to *G. boninense* infection (Riza *et al.*, 2016).

NRPS Expression in Relation to DSI

The expression of NRPS gene potentially involved in the invasion of *G. boninense* was examined at 1, 2, 4 and 6 MAI in both tolerant and susceptible clones. The expression levels of the housekeeping gene GAPDH were consistent in all tested samples. NRPS gene was detected at 1 MAI in both tolerant and susceptible clones despite the lack of observable disease symptoms. At 1 MAI, the PCR band intensity of NRPS gene was higher in the susceptible clones compared to the tolerant clones. The expression of NRPS gene has progressively upregulated from 1 to 4 MAI and sustained to 6 MAI in the susceptible clones, whereas in the tolerant clone the expression level has upregulated from 1 to 2 MAI and sustained to 6 MAI (*Figure 3*). NRPS gene expression shows a potential correlation with the higher DSI observed in the susceptible clones compared to the tolerant clones. The induced expression of the NRPS gene in both tolerant and susceptible clones indicates that it might play an important role in the infection process. NRPS is identified as a virulent factor for several pathogenic fungi as it plays an essential role in the biosynthesis of SMs such as siderophores and cyclic peptides with phytotoxic activities (Pusztahelyi *et al.*, 2015). The siderophore-mediated iron acquisition is also required for the synthesis of iron-dependent antioxidants (superoxide dismutase and catalase) in fungal pathogens in response to hydrogen peroxide stresses induced by the host plant defense mechanism (Chung, 2012; Lee *et al.*, 2005; O'Hanlon *et al.*, 2012). The increased expression of NRPS gene in the susceptible clones might suggest its involvement in fungal survival and cell proliferation in the host plant. Gene silencing studies are recommended to verify the function of the NRPS gene in *G. boninense*.

CONCLUSION

A partial cDNA encoding adenylation core motifs of NRPS gene was successfully isolated from *G. boninense*. *GbNRPS* shared a similarity to other fungal NRPS A-domain. Siderophores are mostly produced via NRPS pathway. From this study, *G. boninense* was found to produce siderophore *in vitro* on CAS agar. However, the virulence factor is yet to be determined. There was a correlation between the expression of *GbNRPS* gene and disease severity during *Ganoderma*-oil palm interaction. These findings may contribute to the development of appropriate strategies for BSR disease management. Further studies are recommended to determine the modular structure and other domains of NRPS in *G. boninense*, the role of NRPS to the fungus and during plant-pathogen interaction.

ACKNOWLEDGEMENT

This project was funded and supported by MPOB (Universiti Putra Malaysia-MPOB, KPPK fund)

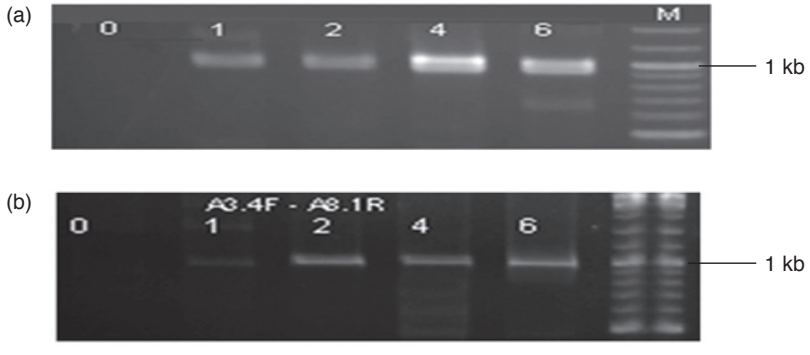

Figure 3. GbNRPS *expression analysis in susceptible and tolerant oil palm clones at 1, 2, 4 and 6 months after inoculation (MAI). (a) root samples of susceptible clones, (b) root samples of tolerant clones, Lane M: GeneRuler DNA Ladder Mix (Fermentas, Lithuania).*

and was part of the MPOB project. We also thank the members and the laboratory staffs of Institute Tropical Agriculture (ITA) for their technical support and assistance.

REFERENCES

Abas, R and Abu Seman, I (2012). Economic impacts of *Ganoderma* incidence on Malaysian oil palm plantation - A case study in Johor. *Oil Palm Industry Economic J., 12(1)*: 24-30.

Arnez, J G and Moras, D (1997). Structural and functional considerations of the amino-acylation reaction. *Trends Biochem. Sci., 22*: 203-206.

Budde, A D and Leong, S A (1989). Characterization of siderophores from *Ustilago maydis*. *Mycopathologia, 108*: 125-133.

Bushley, K E and Turgeon, B G (2010). Phylogenomics reveals subfamilies of fungal nonribosomal peptide synthetases and their evolutionary relationships. *BMC Evol. Biol., 10*: 26. DOI: 10.1186/1471-2148-10-26.

Chong, K P; Dayou, J and Alexander, A (2017). Pathogenic nature of *Ganoderma boninense* and basal stem rot disease. *Detection and Control of* Ganoderma boninense *in Oil Palm Crop*. Springer, Cham. p. 5-12.

Chung, K R (2012). Stress response and pathogenicity of the necrotrophic fungal pathogen *Alternaria alternata*. *Scientifica, 2012*: 635431. DOI: 10.6064/2012/635431.

Corley, R H V and Tinker, P B (2015). *The Oil Palm*. 5th edition. Chichester, United Kingdom. Wiley Blackwell.

Eichhorn, H; Lessing, F; Winterberg, B; Schirawski, J; Kamper, J; Muller, P and Kahmann, R (2006). A ferroxidation/permeation iron uptake system is required for virulence in *Ustilago maydis*. *Plant Cell., 18*: 3332-3345.

Eisfeld, K (2009). Non-ribosomal peptite synthetases of fungi. *Physiology and Genetic* (Anke, T and Weber, D eds.). Springer, Berlin, Heidelberg. *The Mycota (A Comprehensive Treatise on Fungi as Experimental Systems for Basic and Applied Research), 15*: 305-330.

Finking, R and Marahiel, M A (2004). Biosynthesis of nonribosomal peptides. *Annu. Rev. Microbiol., 58*: 453-488.

Gerwien, F; Skrahina, V; Kasper, L; Hube, B and Brunke, S (2018). Metals in fungal virulence. *FEMS Microbiol. Rev., 42(1)*: fux050. DOI: 10.1093/femsre/fux050.

Gunatilaka, A A L and Wijeratne, E M K (2011). Natural products from bacteria and fungi. *Encyclopedia of Life Support Systems (EOLSS)*. p. 1-7.

Haas, H (2014). Fungal siderophore metabolism with a focus on *Aspergillus fumigatus*. *Nat. Prod. Rep., 31(10)*: 1266-1276. DOI: 10.1039/c4np00071d.

Hushiarian, R; Yusof, N A and Dutse, S W (2013). Detection and control of *Ganoderma boninense*: Strategies and perspectives. *SpringerPlus, 2*: 555. DOI: 10.1186/2193-1801-2-555.

Keller, N P; Turner, G and Bennett, J W (2005). Fungal secondary metabolism – from biochemistry to genomics. *Nat. Rev. Microbiol., 3*: 937-947.

Kleinkauf, H and von Döhren, H (1996). A nonribosomal system of peptide biosynthesis. *Eur. J. Biochem., 236*: 335-351.

Konz, D and Marahiel, M A (1999). How do peptide synthases generate structural diversity? *Chem. Biol. 6*: 39-48.

Kushairi, A; Meilina Ong-Abdullah; Balu Nambiappan; Hishamuddin, E; Vijaya, S; Izuddin, Z B; Razmah, G; Sundram, S and Parveez, G K A (2019). Oil palm economic performance in Malaysia and R&D progress in 2018. *J. Oil Palm Res., 31(2)*: 165-193.

Larrondo, L F; Gonzalez, B; Cullen, D and Vicuna, R (2004). Characterization of a multicopper oxidase gene cluster in *Phanerochaete chrysosporium* and evidence of altered splicing of the MCO transcripts. *Microbiology, 150*: 2775-2783.

Lee, B N; Kroken, S; Chou, D Y; Robbertse, B; Yoder, O C and Turgeon, B G (2005). Functional analysis of all nonribosomal peptide synthetases in *Cochliobolus heterostrophus* reveals a factor, NPS6, involved in virulence and resistance to oxidative stress. *Eukaryot. Cell, 4*: 545-555. DOI: 10.1128/EC.4.3.545-555.2005.

Marahiel, M A; Stachelhaus, T and Mootz, H D (1997). Modular peptide synthetases involved in nonribosomal peptide synthesis. *Chem. Rev., 97*: 2651-2267.

Martinez, D; Larrondo, L F; Putnam, N; Gelpke, M D; Huang, K; Chapman, J; Helfenbein, K G; Ramaiya, P; Detter, J C; Larimer, F; Coutinho, P M;

Henrissat, B; Berka, R; Cullen, D and Rokhsar, D (2004). Genome sequence of the lignocellulose degrading fungus *Phanerochaete chrysosporium* strain RP78. *Nat. Biotechnol., 22*: 695-700.

Martínez-Núñez, M A and López, V E L (2016). Nonribosomal peptides synthetases and their applications in industry. *Sustain. Chem. Process., 4*: 13. DOI: 10.1186/s40508-016-0057-6.

Milagres, A M F; Machuca, A and Napoleao, D (1999). Detection of siderophores production from several fungi and bacteria by a modification of chrome azurol S (CAS) agar plate assay. *J. Microbiol. Methods, 37*: 1-6. DOI: 10.1016/S0167-7012(99)00028-7.

Nur Ain Izzati, M Z and Faridah, A (2008). Disease suppression in *Ganoderma*-infected oil palm seedlings treated with *Trichoderma harzianum*. *Plant Prot. Sci., 44*: 101-107.

O'Hanlon, K A; Gallagher, L; Schrettl, M; Jöchl, C; Kavanagh, K; Larsen, T O and Doyle, S (2012). Nonribosomal peptide synthetase genes pes1 and pes1 are essential for Fumigaclavine C production in *Aspergillus fumigatus. Appl. Environ. Microbiol., 78(9)*: 3166-3176. DOI: 10.1128/AEM.07249-11.

Oide, S; Moeder, W; Krasnoff, S; Gibson, D; Haas, H; Yoshioka, K and Turgeon, B G (2006). NPS6, encoding a nonribosomal peptide synthetase involved in siderophore-mediated iron metabolism, is a conserved virulence determinant of plant pathogenic ascomycetes. *Plant Cell., 18*: 2836-2853.

Paterson, R R M (2007). *Ganoderma* disease of oil palm - A white rot perspective necessary for integrated control. *Crop Prot., 26(9)*: 1369-1376. DOI: 0.1016/j.cropro.2006.11.009.

Philpott, C C (2006). Iron uptake in fungi: A system for every source. *Biochim. Biophys. Acta, 1763*: 636-645.

Prescott, A and Martin, C (1987). A rapid method for the quantitative assessment of levels of specific mRNAs in plants. *Plant Mol. Biol. Rep., 4*: 219-224.

Pusztahelyi, T; Holb, I J and Pócsi, I (2015). Secondary metabolites in fungus-plant interactions. *Front. Plant Sci., 6*: 573. DOI: 10.3389/fpls.2015.00573.

Rees, R W; Flood, J; Hasan, Y; Potter, U and Cooper, R M (2009). Basal stem rot of oil palm (*Elaeis guineensis*): Mode of root infection and lower stem invasion by *Ganoderma boninense*. *Plant Pathol., 58*: 982-989. DOI: 10.1111/j.1365-3059.2009.02100.x.

Riza, A P; Indra, S and Asmini, B (2016). Differential gene expression in oil palm varieties susceptible and tolerant to *Ganoderma*. *Proc. of the 6th Indonesian Biotechnology Conference*. p. 233-243.

Sariah, M; Hussin, M Z; Miller, R N G and Holderness, M (1994). Pathogenicity of *Ganoderma boninense* tested by inoculation of oil palm seedlings. *Plant Pathol., 43*: 507-510. DOI: 10.1111/j.1365-3059.1994.tb01584.x.

Sayari, M; van der Nest, M A; Steenkamp, E T; Soal, N C; Wilken, P M and Wingfield, B D (2019). Distribution and evolution of nonribosomal peptide synthetase gene clusters in the *Ceratocystidaceae*. *Genes, 10(5)*: 328. DOI: 10.3390/genes10050328.

Schrettl, M; Bignell, E; Kragl, C; Sabiha, Y; Loss, O; Eisendle, M; Wallner, A; Arst, H N Jr; Haynes, K and Haas, H (2007). Distinct roles for intra- and extracellular siderophores during *Aspergillus fumigatus infection. PLoS Pathog., 3*: 1195-1207.

Schwarzer, D and Marahiel, M A (2001). Multimodular biocatalysts for natural product assembly. *Naturwissenschaften, 88*: 93-101.

Schwarzer, D; Finking, R and Marahiel, M A (2003). Nonribosomal peptides: From genes to products. *Nat. Prod. Rep., 20*: 275-287.

Soukup, A A; Keller, N P and Wiemann, P (2016). Enhancing nonribosomal peptide biosynthesis in filamentous fungi. *Methods Mol. Biol., 1401*: 149-160. DOI: 10.1007/978-1-4939-3375-4_10.

Stachelhaus, T and Marahiel, M A (1995). Modular structure of genes encoding multifunctional peptide synthetases required for nonribosomal peptide synthesis. *FEMS Microbiol. Lett., 125*: 3-14.

Turgay, K; Krause, M and Marahiel, M A (1992). Four homologous domains in the primary structure of GrsB are related to domains in a superfamily of adenylate-forming enzymes. *Mol. Microbiol., 6*: 529-546.

Utomo, C; Werner, S; Niepold, F and Deising, H B (2005). Identification of *Ganoderma*, the causal agent of basal stem rot disease in oil palm using a molecular method. *Mycopathologia, 159*: 159-170. DOI: 10.1007/s11046-004-4439-z.

von Döhren, H (2004). Biochemistry and general genetics of nonribosomal peptide synthetases

in fungi. *Adv. Biochem. Eng. Biotechnol., 88*: 217-264.

Weber, T and Marahiel, M A (2001). Exploring the domain structure of modular nonribosomal peptide synthetases. *Structure, 9*: R3-R9.

Welker, M and von Döhren, H (2006). Cyanobacterial peptides – Nature's own combinatorial biosynthesis. *FEMS Microbiol. Rev., 30*: 530-563.

Welzel, K; Eisfeld, K; Antelo, L; Anke, T and Anke, H (2005). Characterization of the ferrichrome A biosynthetic gene cluster in the homobasidiomycete *Omphalotus olearius*. *FEMS Microbiol. Lett., 249*: 157-163.

Yuan, W M; Gentil, G D; Budde, A D and Leong, S A (2001). Characterization of the *Ustilago maydis* sid2 gene, encoding a multidomain peptide synthetase in the ferrichrome biosynthetic gene cluster. *J. Bacteriol., 183*: 4040-4051.

Journal of Oil Palm Research Vol. 34 (1) March 2022 p. 56-67
DOI: https://doi.org/10.21894/jopr.2021.0030

GROWTH AND DEVELOPMENT OF OIL PALM CLONE P164 EXPOSED TO LONG-TERM CARBON DIOXIDE ENRICHMENT IN OPEN TOP CHAMBER

AMANINA, N S[1]*; LINATOC, A C[2]; HANIFF, M H[1] and ROSLAN, M N[1]

ABSTRACT

The carbon dioxide (CO_2) enrichment study on oil palm clone P164 using open top chamber (OTC) technique was conducted to evaluate the effects on oil palm growth, physiology, bunch production and oil quality. The palms were grown in OTC with two CO_2 concentrations; 600 ppm (CO_2-enriched) and ambient 400 ppm (control), and also planted in the field under normal conditions (absolute control). After six years of observation, CO_2-enriched palms showed a higher biomass percentage of 22.6% and 23.7% than the control and absolute control palms, respectively. The increase in biomass was contributed by rachis length and trunk height with a reading of 689.63 ± 7.70 cm and 201.25 ± 10.18 cm, respectively. This positive growth can be attributed to higher photosynthetic rate (A) of 23.51 ± 0.57 μmol m^{-2} s^{-1} and affecting the water use efficiency (WUE) of 5.33 ± 0.10 μmol mol^{-1} CO_2. Enhanced A due to high CO_2 level markedly increased clonal palm growth and biomass. Valuable information of this study may be beneficial for the oil palm industry to develop suitable mitigation strategies in the future.

Keywords: CO_2 enrichment, oil palm growth, oil palm physiology, open top chamber.

Received: 27 December 2020; **Accepted:** 7 April 2021; **Published online:** 5 July 2021.

INTRODUCTION

Carbon dioxide (CO_2) is the main greenhouse gas that has been increasing in the atmosphere due to anthropogenic activities since the industrial revolution. The contributors are burning of fossil fuel (coal, oil and natural gas) for energy in transportation and machinery, open burning as well as deforestation. These activities release more CO_2 to the atmosphere and influence the forest as a natural sink, consequently modifying the natural carbon cycle process (Pidwirny, 2006). Future climate scenario predicts rising in CO_2 level for the next coming decades, contributing to a warmer climate, influencing rainfall patterns, reducing ice and snow cover, raising sea level and increasing sea acidity. Since 1970 to 2004, its annual emission increased by about 80% and it is projected to continue to increase as much as 500-1000 ppm by year 2100 (Intergovernmental Panel on Climate Change, 2007). Over half of the global carbon uptake is by plants as CO_2 serves as substrates for photosynthesis (Bowes, 1991).

Rising CO_2 level markedly affects growth, physiology and chemistry of plant (Ziska, 2008). In plant metabolism, CO_2 is broken down into smaller carbon molecules chemically. Glucose is used for respiration process, releasing energy to power up metabolic activities. Photosynthesis process which assimilates carbon, hydrogen and oxygen into organic molecules produces about 96%

[1] Malaysian Palm Oil Board,
6 Persiaran Institusi, Bandar Baru Bangi,
43000 Kajang, Selangor, Malaysia.

[2] Faculty of Applied Sciences and Technology,
Universiti Tun Hussein Onn Malaysia,
Pagoh Campus, KM 1, Jalan Panchor,
84600 Muar, Johor, Malaysia.

* *Corresponding author e-mail: nuramanina@mpob.gov.my*

of the total dry mass of a plant (Marschner, 1995). Since the main components of photosynthesis process are CO_2, water and light energy, increasing CO_2 availability may affect plant growth and photosynthesis. The direct physiological effects of enriched CO_2 atmospheres for plant species are becoming increasingly well-documented (Curtis and Wang, 1998). The fertilising effect of elevated CO_2 may give impact to crop productivity and agro-ecosystems (Goudriaan and Unsworth, 1990).

Oil palm (*Elaeis guineensis* Jacq.) is a perennial crop and classified as a C_3 plant (Corley and Tinker, 2003). It is grown expansively in the tropical regions such as Indonesia, Malaysia, Thailand, West Africa and South America. As the perennial crop, it starts yielding fresh fruit bunches (FFB) three years after planting (YAP) to produce oil palm products mainly involved in the food, oleochemical, and biofuel industries. Oil palm has the highest yield amongst oleaginous crops as it can produce three to 10 times more oil than other oil crops planted on a hectare of land (Barcelos *et al.*, 2015). Its production increased worldwide by over 300% between 1985 and 2008 and had overtaken soybean as the major source of vegetable oil in 2006 (Denis, 2017). *Tenera* palm, which is a cross between *Dura* and *Pisifera* varieties, has become the highest yielding variety (Bakuomé *et al.*, 2016). Oil palm cultivation in Malaysia started in 1919 during socio-economic development program with only 3000 ha to a whopping 5.8 million hectares by 2017 (Kushairi *et al.*, 2018). This most efficient oil-bearing crop is the most important commodity in Malaysia as the second largest producer and exporter in the world (Choo, 2012).

Oil palm can use high CO_2 level better than C_4 plants. More than 90% of terrestrial plants are C_3 plants and elevated CO_2 greatly affect their photosynthesis and growth (Makino and Mae, 1999). A study has proven that oil palm seedlings can increase photosynthetic rate (A) and water use efficiency (WUE) by one and five-fold under high CO_2 condition (Ibrahim *et al.*, 2010). CO_2 is a limiting factor of photosynthesis; hence the impact of elevated CO_2 would depend on its photosynthetic acclimation. This acclimation is a change in photosynthetic efficiency of leaves (Ghildiyal and Sharma-Natu, 2000). Photosynthesis acclimation to long-term exposure to elevated CO_2 reduces carbon reduction cycle key enzymes and increases nutrient use efficiency (Drake *et al.*, 1997).

However, CO_2 enrichment studies on tropical plants particularly the technology and techniques are less characterised (Hawa, 2004). Hence, it is important to recognise how increasing CO_2 will impact on crop productivity and food supply in tropical regions especially in Asia. Rising atmospheric CO_2 concentration could have far-reaching implications on oil palm growth, bunch production and oil quality in the future. Information on the effects of elevated CO_2 to oil palm performance and yield is still insufficient and worth exploring.

MATERIALS AND METHODS

The study was conducted at the Biosphere Project facility, Malaysian Palm Oil Board (MPOB) Research Station in Kluang, Johor, Malaysia (103°22′17.62″E 1°57′23.79″N) with an elevation of 75 m above sea level. Twelve-month old oil palms (*Elaeis guineensis* Jacq.) clone P164 were acclimatised for six months before high CO_2 application in four units of open top chambers (OTCs). This clone was obtained from the explants of *Tenera*, high yielding hybrids resulting from crosses between *Dura* and *Pisifera* varieties. Clone P164 had 30.6% oil to bunch ratio (O/B) and 8.71 t of crude palm oil (CPO) ha^{-1} yr^{-1} compared to clone P162 batch (Tarmizi, 2009). The OTC was 9 m in diameter and 10 m in height, suitable for oil palm growth in a normal field condition with triangular (9 m x 9 m x 9 m) planting method. Each OTC consisted of a cylindrical concrete structure with an aluminium frame for a transparent multi-wall polycarbonate sheet, which was 6 mm thick and had direct solar transmission of 76% (Sabic Innovative Plastics, USA) and a truncated top at 45° angle.

All palms were grown in the OTCs at high concentration of CO_2 (600 ppm) and ambient CO_2 level (control) at 400 ppm, and planted in the field under normal conditions (absolute control) with four replicates for each treatment. CO_2 gas (99.8% purity) was injected at 10 litres per min twice per day at 0900 and 1040 (during active photosynthesis period), with each session lasting for 10 min. The injected CO_2 was then mixed with the available air using blower fans located at the base of the OTC. Blower fans were simultaneously used at low speed (<0.5 ms^{-1}) to disperse the CO_2 evenly throughout the chamber and to help remove any leaf boundary layer on the leaf surface that would hinder CO_2 diffusion into the leaf mesophyll (Aldrich and Bartok, 1994).

Oil palm petiole width and thickness; the number, length and width of leaflets; and the rachis length of frond 17 were measured and recorded every six months to determine palm growth and biomass production. Leaves and trunk dry weight, and leaf area of oil palm were estimated using Hardon *et al.* (1969) and Corley *et al.* (1971) formulae. The photosynthetic activity, relative leaf stomatal conductance, instantaneous WUE and transpiration rate (E) measurement of frond 17 leaves were recorded every six months consistent with the palm growth measurements. An infrared gas analyser LI6400 Portable Photosynthesis System (LI-COR,

USA) was used to measure physiological attributes with optimum cuvette conditions at 1000 μmol m^{-2} s^{-1} photosynthetically photon flux density (PPFD), 600 ppm CO_2 for CO_2-enriched palms and 400 ppm CO_2 for control and absolute control palms, 60% relative humidity and 30°C temperature (Ibrahim *et al.*, 2010). This measurement was conducted between 0800 to 1100 hr when photosynthetic activity was active.

Relative leaf chlorophyll reading estimation was measured with a portable Soil Plant Analysis Development (SPAD)-502 (Konica-Minolta Sensing, Japan). The SPAD meter determined the relative amount of chlorophyll present in leaves. Stomatal density was examined from leaf epidermis impressions and observed under a light microscope (Leica DM750, Leica Microsystem, Germany) at 400X magnification. The number of stomata per mm square was recorded.

A flower census was conducted to determine the sex ratio for stress status and foreseen bunch production in the oil palm CO_2 enrichment study. The data was recorded every two months based on the oil palm phylotaxy. Assisted pollination was conducted at 3 YAP to introduce outside weevils to the anthesising female inflorescences (ready to be fertilised) in the OTC. Anthesising male inflorescences with fresh pollens were obtained from palms in normal field plot and directly placed next to the anthesising female.

The harvested fruit bunches (two cycles per month) were analysed based on the number of bunch production per palm and total bunch weight per palm. Several bunch quality components such as bunch weight, fruit to bunch weight ratio (F/B) and O/B were analysed using Nigerian Institute for Oil Palm Research (NIFOR) bunch analysis method (Blaak *et al.*, 1963). P164 oil palms were fertilised using compound MPOB F4 fertiliser (All Cosmos Industries Sdn. Bhd., Malaysia) at 9 kg $palm^{-1}$ yr^{-1} with three applications per year. The F4 fertiliser is a biochemical fertiliser consisting of plant-based organic matters and effective microorganisms with nutrient analysis of $N:P_2O_5:K_2O:MgO:B_2O_3$ at 9:6:18:2:0.5 (Tarmizi, 2009). Water was applied using six units of micro sprinkler installed at 1 m distance from the oil palm base (within the fertilisation zone). Water was sprayed from the sprinkler head at an average of 800 mL min^{-1}. Each palm received about 48 L of water daily, with four applications at 0800, 1000, 1400 and 1600 hr and each session lasted for 15 min. Analysis of variance (ANOVA) and multiple comparison were conducted using IBM SPSS Statistics 23 (2014). The test was run using Tukey Honest Significant Difference (HSD) with the least significant difference of 0.05. Averaged data was pooled and shown on yearly basis and error bar represents standard error of mean in that particular data sets.

RESULTS AND DISCUSSION

After a long exposure to high CO_2 condition, P164 palm clones showed 22.7% and 23.7% significantly higher standing biomass than the controls and absolute controls, respectively. The aboveground standing woody biomass of black poplar (*Populus nigra*) significantly increased up to 27% under elevated CO_2 (Liberloo *et al.*, 2006). The total biomass accumulation of Sitka spruce (*Picea sitchensis*) seedlings increased by 37% in high CO_2 condition and high nitrogen treatment (Murray *et al.*, 2000).

The CO_2-enriched palms showed the longest rachis with 689.63 cm and the highest trunk with 201.50 cm. These values may contribute to a higher biomass. Li *et al.* (2007) reported that tomato (*Solanum lycopersicum*) plant biomass, stem height and thickness were 67%, 22% and 24% higher, respectively when cultivated at high CO_2 level. The stem diameter of Scots pine (*Pinus sylvestris*) enhanced significantly by 60% in elevated CO_2 treatments (Jach and Ceulemans, 1999). However, there was a reduction in the number of leaflets and total leaf area per palm that resulted in low leaf area index (LAI). A decrease in specific leaf area (SLA) of several species of herbs, shrubs and trees from 184% to 100% were due to CO_2 enrichment and also an artefact from the prolonged exposure (Peñuelas and Matamala, 1990). Ainsworth and Long (2005) reported that the SLA decreased by 6% depending on the plant functional group and species when exposed to high CO_2 concentrations.

Under elevated CO_2 levels (800 and 1200 μmol mol^{-1}), the highest oil palm seedling biomass increment was shown from week 12-15 when the total plant biomass had increased by 1.6-fold from week 12 (Ibrahim *et al.*, 2010). The oil palm seedlings have developed sufficient sink strength to accommodate the elevated CO_2 concentrations, thus, increasing the total biomass accumulation (Jeffrey and Richard 1999). The vegetative measurements of CO_2-enriched, control and absolute control palms at 6 YAP are shown in *Table 1*. The standing biomass, rachis length and trunk height annual patterns of all treatments are illustrated in *Figures 1a-c*, respectively.

At 6 YAP, the A of CO_2-enriched palm recorded the highest value with 23.51 μmol CO_2 m^{-2} s^{-1} compared to control and absolute control palms (*Figure 2*). Idso and Kimball (1992) investigated that the net photosynthesis of sour orange tree (*Citrus aurantium*) increased linearly with CO_2 by more than 200%. The photosynthesis of several C_3 grasses, legumes, forbs and woody perennials increased when exposed to elevated CO_2 (Kimball *et al.*, 2002). Under elevated CO_2 concentration, photosynthesis is enhanced mainly due to an increase in ribulose-1,5-bisphosphate (RuBP) carboxylase/oxygenase (Rubisco) activity. Carboxylation of RuBP is catalysed by Rubisco, which is required for the

TABLE 1. VEGETATIVE MEASUREMENT OF CO_2-ENRICHED, CONTROL AND ABSOLUTE CONTROL PALMS AT 6 YAP

Treatment	RL (cm)	TH (cm)	TD (cm)	F17 TLA	LAI	SB (kg)
CO_2-enriched	689.63a	201.25a	64.50a	7.40a	3.62b	195.41a
Control	581.81b	130.38b	65.75a	8.15a	3.83b	159.26b
Absolute control	549.27c	101.19c	64.00a	7.75a	4.43a	158.06c

Note: RL - rachis length; TH - trunk height; TD - trunk diameter; F17 TLA - frond 17 true leaf area; LAI - leaf area index; SB - standing biomass; YAP - year after planting. Distinct letters in the row indicate significant differences according to Tukey's HSD test at $p \leq 0.05$.

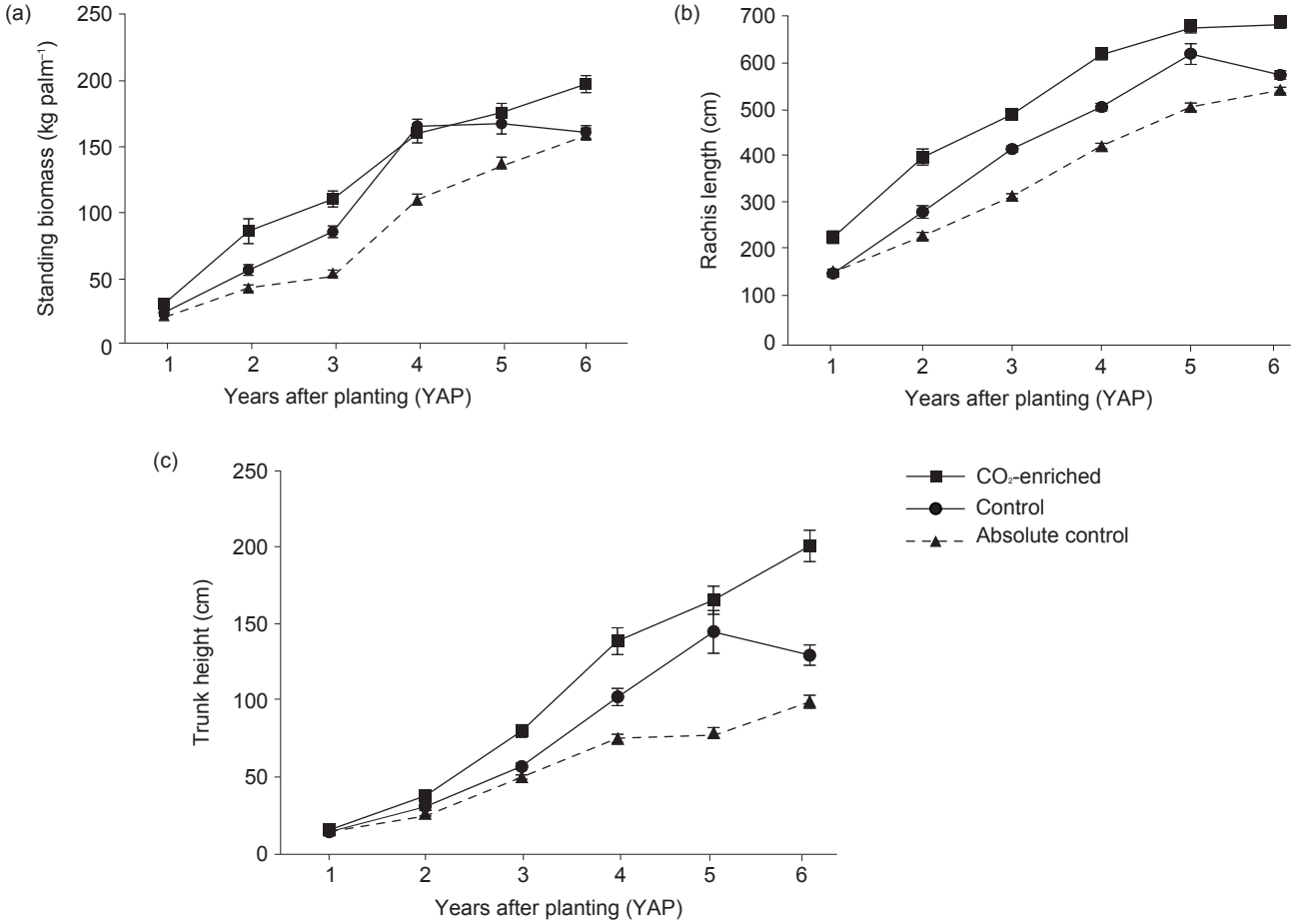

Note: Annual data presented is an averaged value of 6-month intervals data. Error bar represents standard error of mean.

Figure 1. Standing biomass (a) rachis length, (b) trunk height, (c) of CO_2-enriched, control and absolute control palms during 6 YAP.

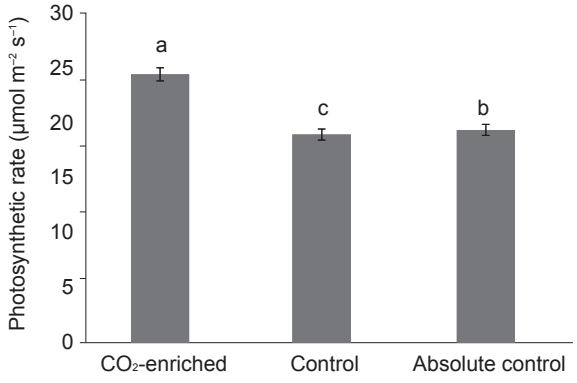

Note: Mean values with different letters differ significantly by Tukey's HSD test at $p \leq 0.05$. Error bar represents standard error of mean.

Figure 2. Photosynthetic rate (A) of CO_2-enriched, control and absolute control palms at 6 YAP.

TABLE 2. LEAF STOMATA DENSITY AT FROND 17 OF CO_2-ENRICHED, CONTROL AND ABSOLUTE CONTROL PALMS AT 6 YAP

Treatment	F17 (pores/mm^2)
CO_2-enriched	102.50 ± 3.78a
Control	106.67 ± 3.83a
Absolute control	103.42 ± 3.04a

Note: Distinct letters in the row indicate significant differences according to ANOVA at $p \leq 0.05$.

fixation of CO_2 but also utilises O_2 as a substrate to oxygenate RuBP in photorespiration process (Makino and Mae, 1999). Plant exposed to long-term CO_2 experiences a photosynthetic down-regulation in both Free-Air Carbon Dioxide Enrichment (FACE) studies (Ainsworth and Long, 2005) and chamber experiments (Warren *et al.*, 2014). This condition is known as photosynthetic acclimation. Ainsworth *et al.* (2003) found that white clover grown under elevated CO_2 (600 ppm) for eight years retained a 37% increase in photosynthesis after acclimation was observed. These findings suggest that the final growth response to the rising CO_2 is generally determined by plant acclimatisation magnitude (Thompson *et al.*, 2017).

Enhanced A value influences an increase in instantaneous WUE value of 5.33 μmol mol^{-1} CO_2 (*Figure 3*). WUE of wheat (*Triticum aestivum*) was enhanced in enriched CO_2 concentrations, leading to higher WUE with more N supply (Li *et al.*, 2003). Increased WUE occurred by partial closure of stomata when exposed to high CO_2 levels (Eamus, 1991). Plants exposed to high CO_2 have also been found to maintain higher total water potentials; and to have greater root-to-shoot ratios, increased biomass and higher resistance to drought than those grown at ambient CO_2. Elevated CO_2 alters plant structure (tracheid anatomy or leaf specific conductivity) and may be related to susceptibility to xylem cavitation or environmental conditions in which embolism is expected to occur (Tyree and Alexander, 1993).

Upon enrichment of CO_2, oil palm showed a decreased stomatal conductance (g_s) and E (*Figures 4* and *5*). Forest species showed a significant

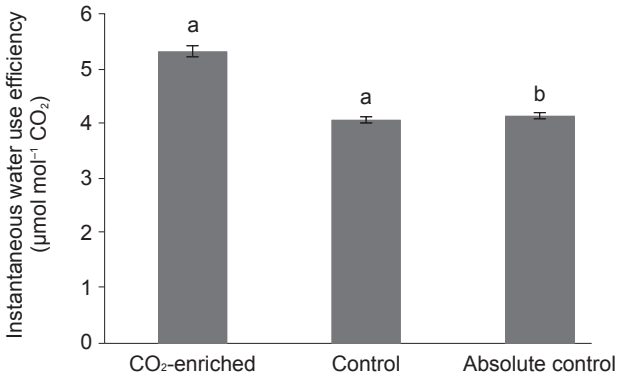

Note: Mean values with different letters differ significantly by Tukey's HSD test at $p \leq 0.05$. Error bar represents standard error of mean.

Figure 3. Instantaneous water use efficiency of CO_2-enriched, control and absolute control palms at 6 YAP.

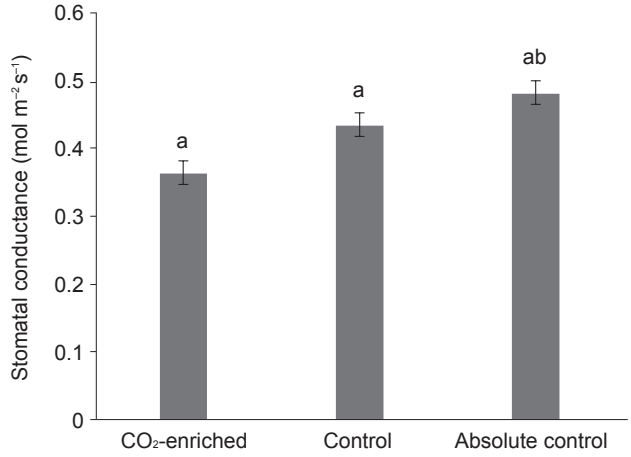

Note: Mean values with different letters differ significantly by Tukey's HSD test at $p \leq 0.05$. Error bar represents standard error of mean.

Figure 4. Stomatal conductance of CO_2-enriched, control and absolute control palms at 6 YAP.

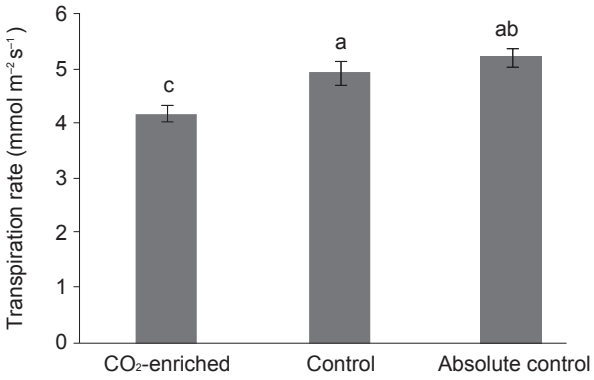

Note: Mean values with different letters differ significantly by Tukey's HSD test at $p \leq 0.05$. Error bar represents standard error of mean.

Figure 5. Transpiration rate of CO_2-enriched, control and absolute control palms at 6 YAP.

decrease of g_s (21%) when exposed to elevated CO_2 concentration across all studies (Medlyn *et al.*, 2001). The g_s of C_3 grass (Poaceae) decreased on average by 20% in elevated CO_2 concentration using a FACE system (Ainsworth and Long, 2005). Reduced g_s under high CO_2 conditions influenced WUE for plant growth although CO_2 fixation may be limited (Xu *et al.*, 2016). Most forest plants when exposed to increasing CO_2 levels possibly reduced g_s (due to stomatal closure), which will decrease E by 37%-44% (Kirschbaum and McMilan, 2018).

Absolute control palms showed the highest SPAD readings during 6 YAP (*Figure 6*), indicating that the absolute control palms grown in ambient CO_2 had higher relative leaf chlorophyll content compared to the CO_2-enriched palms. According to Idso *et al.* (1996), sour orange tree (*Citrus aurantium*) showed higher leaf chlorophyll content in ambient CO_2 concentration than CO_2-enriched trees throughout the four years of measurement. Chlorophyll content reduction was also observed in other plants subjected to CO_2 enrichment. Leaf chlorophyll content of Bintje potato (*Solanum tuberosum*) was reduced by 5% when grown in OTC with double ambient CO_2 concentration (Bindi *et al.*, 2002). This occurrence may be due to the disruption of chloroplast by starch accumulation (Wulff and Strain, 1981) or chlorophyll loss by the decreasing uptake of N as the E decreases due to the g_s reduction under elevated CO_2 (Conroy and Hocking, 1993).

Leaf abaxial stomatal density of clone P164 leaf at frond 17 showed no significant differences between all treatments (*Table 2* and *Figure 7*). High CO_2 concentration did not affect stomatal density of poplar trees clones (*Poplar trichocarpa*) and there was no change in the ratio of adaxial and abaxial stomata between treatments (Radoglou and Jarvis, 1990). Stomatal density of ruderal species, shrub and trees was not affected by long-term exposure to elevated CO_2 level. Stomata number and distribution were not affected at the plant community level even after generations of rising CO_2 exposure (Bettarini *et al.*, 1998). This result was contrary to the hypothesis made by Paoletti and Gellini (1993): long-term CO_2

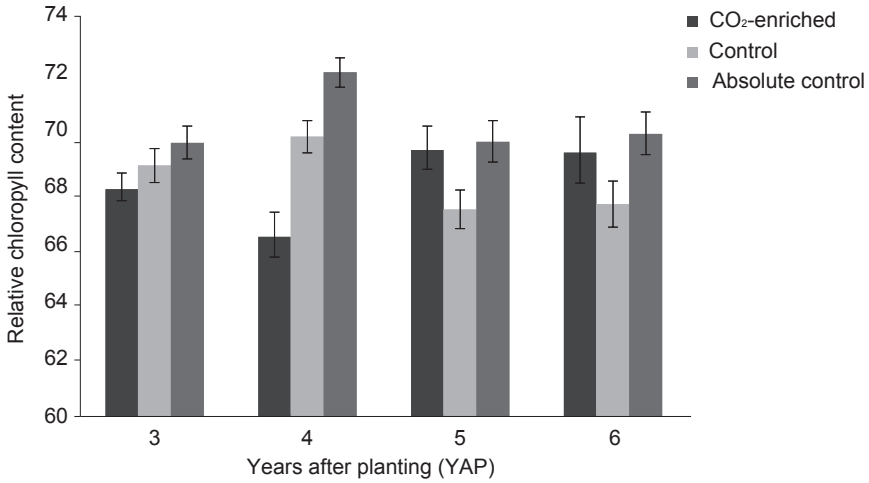

Note: Annual data presented is an averaged value of 6-month intervals data. Error bar represents standard error of mean.

Figure 6. Relative leaf chlorophyll content of CO_2-enriched, control and absolute control palms during 6 YAP.

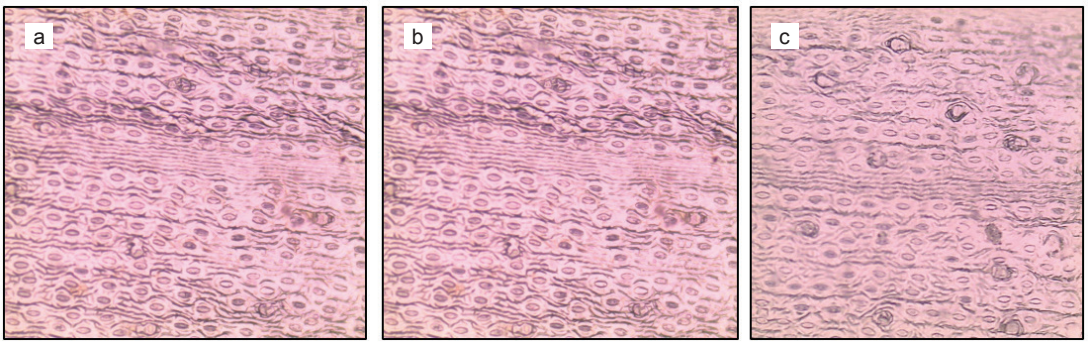

Figure 7. Oil palm clone P164 abaxial leaf stomata (a) CO_2-enriched, (b) control, and (c) absolute control at 6 YAP. The photos were taken at 400X magnification.

exposure may cause stomatal number adaptive modifications.

Sex ratio of CO_2-enriched, control and absolute control palms from 2 to 6 YAP were not significantly different as shown in *Table 3*. The CO_2-enriched palm depicted the highest bunch number at 3 YAP with 19 bunches, followed by the control that gave the greatest bunch number at 4 YAP (22 bunches) and the absolute control showed the highest bunch number at 5 and 6 YAP with 17 bunches (*Figure 8*). The control palm had the highest total bunch weight for three consecutive years (3, 4 and 5 YAP) with 81.85 kg, 196.13 kg and 208.68 kg, respectively. At 6 YAP, the absolute control palm had the highest total bunch weight of 209.18 kg (*Figure 9*). However, there were no significant differences of bunch number and total bunch weight between all treatments.

Control palms showed the highest bunch weight and O/B meanwhile absolute control palms showed the highest F/B over five-year period (*Figures 10a-c*). The CO_2-enriched palms grown in OTC had the lowest bunch weight due to inefficient pollination. Assisted pollination was conducted to introduce outside weevils to the anthesising female inflorescences in the OTC. The OTC structure prohibited the emergence of *Elaeidobius kamerunicus* weevils to pollinate the female inflorescences naturally. After the introduction of *E. kamerunicus* in the oil palm industry, fruit set had increased significantly but fluctuated between seasons (Dhileepan, 1994). According to Haniff and Roslan (2002), poor fruit set and bunch failure were caused by inefficient pollination. *Figure 11* illustrates the comparison of fruit formation and fruit size of clone P164 (CO_2-enriched and control) and DxP palm bunches.

CONCLUSION

After long exposure to high CO_2 concentration, P164 palm clones showed significantly longer rachis and higher trunk, contributing to a significant enhancement of standing biomass. The number of leaflets was reduced, resulting in lower LAI. There was no significant difference in trunk diameter and frond 17 true leaf area (TLA) between CO_2-enriched, ambient CO_2 (control) and normal field (absolute control) palms.

The A of CO_2-enriched palm increased significantly at 6 YAP. Enhanced A value influenced a greater value of instantaneous WUE and reduced g_s and E. Absolute control palms had the highest SPAD

TABLE 3. AN AVERAGE OF FEMALE AND TOTAL INFLORESCENCE AND SEX RATIO OF CO_2-ENRICHED, CONTROL AND ABSOLUTE CONTROL PALMS POOLED FROM 2 TO 6 YAP

YAP	No. of female inflorescence			No. of male inflorescence			Sex ratio* (%)		
	Treatment			Treatment			Treatment		
	CO_2-enriched	Control	Abs. control	CO_2-enriched	Control	Abs. control	CO_2-enriched	Control	Abs. control
2	69	69	50	19	11	10	79.6a	86.2a	84.3a
3	239	204	163	44	42	39	82.8a	84.2a	78.1a
4	371	332	282	56	102	80	87.0a	76.5a	77.9a
5	472	450	396	94	115	108	83.5a	79.6a	78.4a
6	573	536	496	135	228	147	80.9a	71.2a	77.1a

Note: Distinct letters in the row indicate significant differences according to ANOVA at $p \leq 0.05$.
*Sex ratio is defined as the ratio of female inflorescence to total inflorescences of palms in a year.

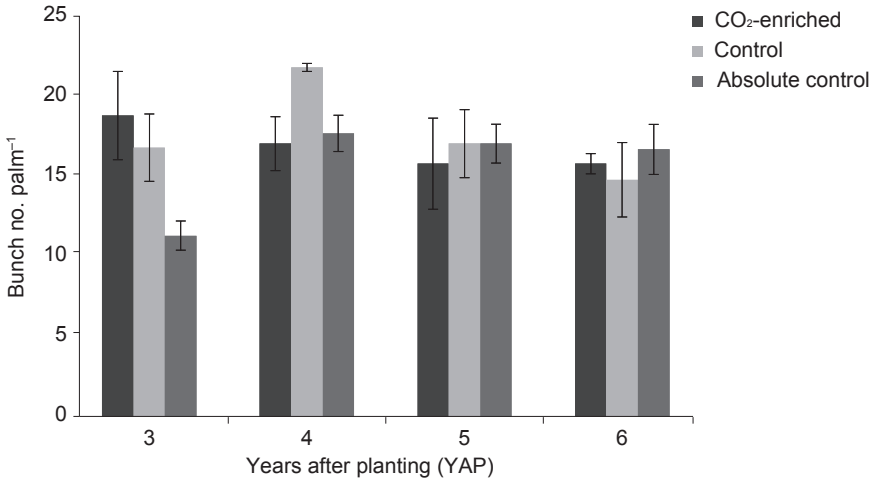

Note: Error bar represents standard error of mean.

Figure 8. Bunch number produced by CO_2-enriched, control and absolute control palms pooled since three to 6 YAP.

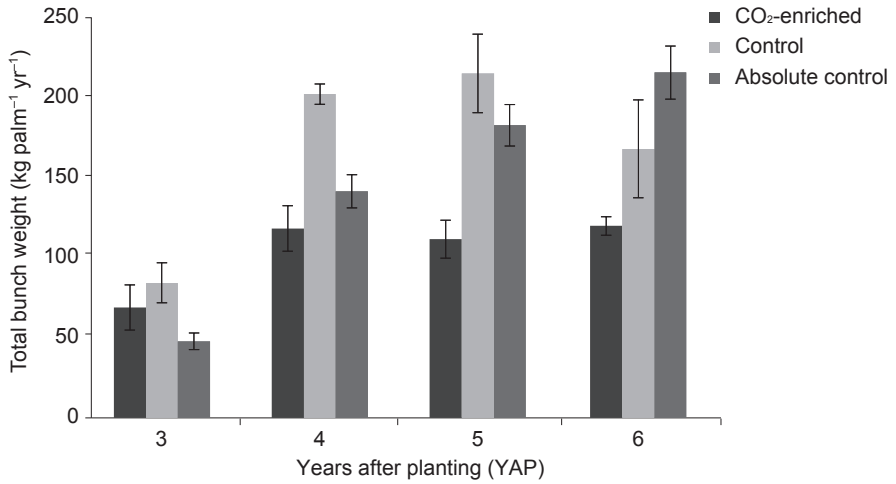

Note: Error bar represents standard error of mean.

Figure 9. Total bunch weight of CO_2-enriched, control and absolute control palms collected since three to 6 YAP.

reading, showing that absolute control palms grown in ambient CO_2 had higher relative leaf chlorophyll content than the CO_2-enriched palms. Reduced chlorophyll content in elevated CO_2 condition may be caused by a disruption of chloroplast by starch accumulation. However, leaf stomatal density of frond 17 did not differ between all treatments.

Female inflorescence of CO_2-enriched palms was the highest during dry period at 3 YAP. As a result, the CO_2-enriched palm produced the highest number of FFB in that particular year. The control palm had the highest total bunch weight for three consecutive years (3, 4 and 5 YAP). Nonetheless, there were no significant differences in bunch number and total bunch weight between all treatments. The CO_2-enriched palms grown in OTC showed the lowest bunch weight due to inefficient pollination. Oil palm weevils (*Elaeidobius kamerunicus*) were unable to enter the OTC and naturally pollinate the anthesising female inflorescences. Therefore, assisted pollination was conducted by taking anthesising male inflorescences to the OTCs to allow the pollination by weevils.

The OTC technology has a potential to study the effects of elevated CO_2 and other atmospheric gases on individual plant, but it is not appropriate for large vegetation study. However, there were some limitations, such as the absence of oil palm weevils and artefacts occurrence particularly reduced light quantity. It is suggested that CO_2 enrichment study on oil palm could be conducted by using FACE technique. This technique is a better way of estimating how palm growth will change in the future. The information on the actual responses of oil palm to rising atmospheric CO_2 is important for the industry to develop suitable mitigation strategies.

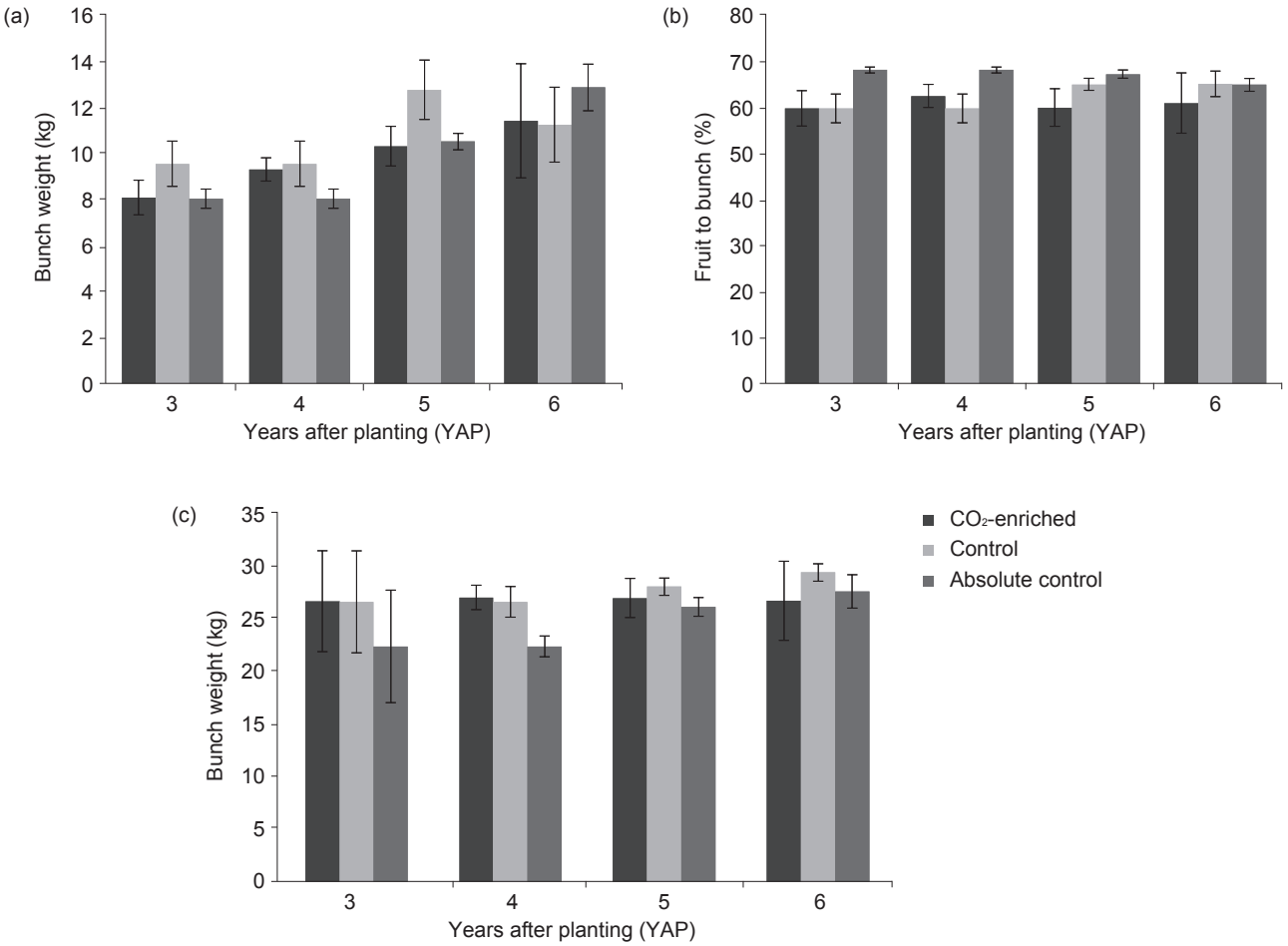

Note: Error bar represents standard error of mean.

Figure 10. (a) Bunch weight, (b) fruit to bunch ratio, and (c) oil to bunch ratio of harvested bunches from CO_2-enriched, control and absolute control palms from 3 to 6 YAP.

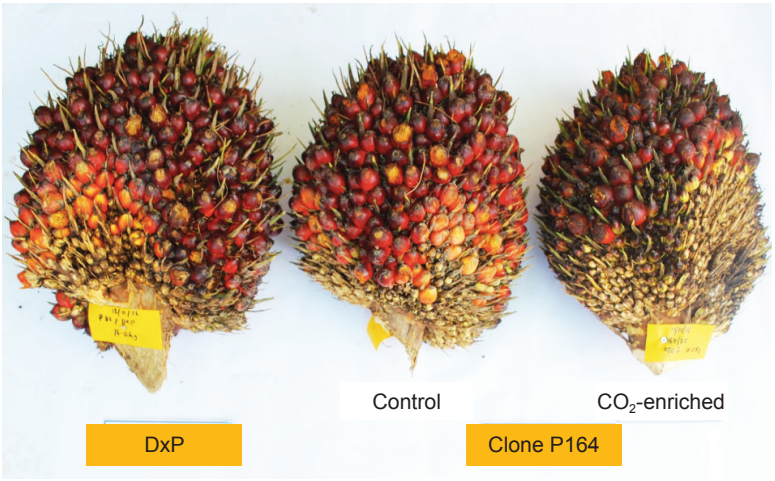

Figure 11. The comparison of fruit formation and fruit size of clone P164 (CO_2-enriched and control) and commercial DxP palm bunches at 6 YAP.

ACKNOWLEDGEMENT

The authors would like to thank the Director-General of MPOB for permission to publish this article and the staff of Crop Physiology Group for their assistance.

REFERENCES

Ainsworth, E A; Rogers, A; Blum, H; Nösberger, J and Long, S P (2003). Variation in acclimation of photosynthesis in Trifolium repens after eight years

of exposure to free-air CO_2 enrichment (FACE). *J. Exp. Bot.*, *54*: 2769-2774.

Ainsworth, E A and Long, S P (2005). What have we learned from 15 years of free-air CO_2 enrichment (FACE)? A meta-analytic review of the responses of photosynthesis, canopy properties and plant production to rising CO_2. *New Phytol., 165*: 351-372.

Aldrich, R A and Bartok, J W (1994). Greenhouse engineering. *Carbon Dioxide Enrichment* (Sailus, M; Chris, N and Sanders, M eds.). University of Connecticut Publication, Ithaca, New York. p. 118-120.

Bakoumē, C; Ngando Ebonguē, G; Ajambang, W; Ataga, C D; Okoye, M N; Enabeme, L O; Konan, J N; Allou, D; Diabate, S; Konan, E and Etta, C E (2016). Oil palm breeding and seed production in Africa. *Proc. of the International Seminar on Oil Palm Breeding and Seed Production and Field Visits*. Kisaran, Indonesia. p. 39-62.

Barcelos, E; de Almeida Rios, S; Cunha, R N V; Lopes, R; Motoike, S Y; Babiychuk, E; Skirycz, A and Kushnir, S (2015). Oil palm natural diversity and the potential for yield improvement. *Front. Plant Sci., 6*: 1-16.

Bettarini, I; Vaccari, F P and Miglietta, F (1998). Elevated CO_2 concentrations and stomatal density: Observations from 17 plants species growing in a CO_2 spring in Central Italy. *Glob. Chang. Biol., 4*: 17-22.

Bindi, M; Hacour, A; Vendermeiren, K; Craigon, J; Ojanperä, K; Selldén, G; Högy, P; Finnan, J and Fibbi, L (2002). Chlorophyll concentration of potatoes grown under elevated carbon dioxide and/or ozone concentrations. *Eur. J. Agron., 17*: 319-335.

Blaak, G; Sparnaaij, L D and Mendez, T (1963). Breeding and inheritance in the oil palm (*Elaeis guineensis* Jacq.). Part II. Methods of bunch quality analysis. *J. West Afr. Inst. Oil Palm Res., 4*: 146-155.

Bowes, G (1991). Growth at elevated CO_2: Photosynthetic responses mediated through Rubisco. *Plant Cell Environ., 14(8)*: 795-806.

Choo, Y M (2012). Malaysia: Economic transformation advances oil palm industry. *Amer. Oil Chem. Soc., 23(8)*: 536-542.

Conroy, J P and Hocking, P (1993). Nitrogen nutrition of C_3 plants at elevated carbon dioxide concentration. *Plant Physiol., 89*: 570-576.

Corley, R H V and Tinker, P B (2003). The classification and morphology of oil palm. *The Oil Palm*. 4th edition. Blackwell Science, Oxford, United Kingdom.

Corley, R H V; Hardon, J J and Tan, G Y (1971). Analysis of growth of the oil palm (*Elaeis guineensis* Jacq.). I. Estimation of growth parameters and application in breeding. *Euphytica, 20*: 307-315.

Curtis, P S and Wang, X (1998). A meta-analysis of elevated CO_2 effects on woody plant mass, form and physiology. *Oecologia, 113*: 299-313.

Denis, J M (2017). Oil palm: Future prospects for yield and quality improvements. *Lipid Technol., 21(11)*: 257-260.

Dhileepan, K (1994). Variation in populations of the introduced pollinating weevil (*Elaeidobius kamerunicus*) (Coleoptera: Curculionidae) and its impacts on fruitset of oil palm (*Elaeis guineensis*) in India. *Bull. Entomol. Res., 84(4)*: 477-485.

Drake, B G; Gonzàlez-Meler, M A and Long, S P (1997). More efficient plants: A consequence of rising atmospheric CO_2? *Annu. Rev. Plant Physiol. Plant Mol. Biol., 48*: 609-639.

Eamus, D (1991). The interaction of rising CO_2 and temperatures with water use efficiency. *Plant, Cell Environ., 14*: 843-852.

Ghildiyal, M C and Sharma-Natu, P (2000). Photosynthetic acclimation to rising atmospheric carbon dioxide concentration. *Indian J. Exp. Biol., 38(10)*: 961-966.

Goudriaan, J and Unsworth, M H (1990). Implication of increasing carbon dioxide and climate change for agricultural productivity and water resources. *Impact of Carbon Dioxide, Trace Gases and Climate Change on Global Agriculture* (Kimball, B A; Rosenberg, N J and Allen L H eds.). *American Society of Agronomy, ASA Special Publications, 53*: 111-130.

Haniff, M H and Roslan, M N (2002). Fruit set and oil palm bunch components. *J. Oil Palm Res., 14(2)*: 24-33.

Hardon, J J; Williams, C N and Watson, I (1969). Leaf area and yield in the oil palm in Malaya. *Exp. Agric., 5(1)*: 25-32.

Hawa, Z E J (2004). Response of *Brassica chinensis* var. chinensis under CO_2-enriched controlled environment production system in the tropics. *Transactions of Malaysian Society of Plant Physiology Vol. 13*.

Ibrahim, M H; Hawa, Z E J; Harun, M H and Yusop, M R (2010). Changes in growth and photosynthetic patterns of oil palm (*Elaeis guineensis* Jacq.) seedlings exposed to short-term CO_2 enrichment in a closed top chamber. *Acta Physiol. Plant., 32(2)*: 305-313.

Idso, S B and Kimball, B A (1992). Effects of atmospheric CO_2 enrichment on photosynthesis, respiration, and growth of sour orange trees. *Plant Physiol., 99(1)*: 341-343.

Idso, S B; Kimball, B A and Hendrix, D L (1996). Effects of atmospheric CO_2 enrichment on chlorophyll and nitrogen concentrations of sour orange tree leaves. *Environ. Exp. Bot., 36(3)*: 323-331.

Intergovernmental Panel on Climate Change (IPCC) (2007). Climate change 2007: The physical science basis. *Contribution of Working Group I to The Forth Assessment Report of the IPCC* (Solomon, S; Qin, D; Manning, M; Chen, Z; Marquis, M; Averyt, K B; Tignor, M and Miller, H L eds.). Cambridge University Press. United Kingdom. 996 pp.

Jach, M E and Ceulemans, R (1999). Effects of elevated atmospheric CO_2 on phenology, growth and crown structure of Scots pine (*Pines sylvestris*) seedlings after two years of exposure in the field. *The Physiol., 19*: 289-300.

Jeffrey, D H and Richard, B T (1999). Effects of carbon dioxide enrichment on the photosynthetic light response of sun and shade leaves of canopy sweetgum trees (*Liquidambar styraciflua*) in a forest ecosystem. *Tree Physiol., 19*: 779-786.

Kimball, B A; Zhu, J; Chong, L; Kobayaki, K and Bindi, M (2002). Responses of agricultural crops of free-air CO_2 enrichment. *J. Appl. Ecol., 13(10)*: 1323-1338.

Kirschbaum, M U F and McMilan, A M S (2018). Warming and elevated CO_2 have opposing influences on transpiration. Which is more important? *Curr. Forestry Rep., 4(2)*: 51-71.

Kushairi, A; Loh, S K; Azman, I; Elina, H; Meilina, O A; Zanal Bidin, M N I; Razmah, G; Sundram, S and Parveez, G K A (2018). Oil palm economic performance in Malaysia and R&D progress in 2017. *J. Oil Palm Res., 30(2)*: 163-195.

Li, F; Kang, S; Zhang, J and Cohen, S (2003). Effects of atmospheric CO_2 enrichment, water status and applied nitrogen on water and nitrogen-use efficiencies of wheat. *Plant Soil, 254(2)*: 279-289.

Li, J; Zhou, J M and Duan, Z Q (2007). Effects of elevated CO_2 concentration on growth and water usage of tomato seedlings under different ammonium-nitrate ratios. *J. Environ. Sci. (China), 19(9)*: 1100-1107.

Liberloo, M; Calfapietra, C; Lukac, M; Godbold, D; Luo, Z B; Polle, A; Hoosbeek, M R; Kull, O; Marek, M; Raines, C; Rubino, M; Taylor, G; Scarascia-Mugnozza, G and Ceulemans, R (2006). Woody biomass production during the second rotation of a bio-energy *Populus* plantation increases in a future high CO_2 world. *Glob. Change Biol., 12(6)*: 1094-1106.

Makino, A and Mae, T (1999). Photosynthesis and plant growth at elevated levels of CO_2. *Plant Cell Physiol., 40(10)*: 999-1006.

Marschner, H (1995). Nutritional physiology. *Mineral Nutrition of Higher Plants.* 2nd edition. Academic Press London, United Kingdom. p. 131-183.

Medlyn, B E; Barton, C V M; Broadmeadow, M S J; Ceulemans, R; De Angelis, P; Forstreuter, M; Freeman, M; Jackson, S B; Kellömaki, S; Laitat, E; Rey, A; Roberntz, P; Sigurdsson, B D; Strassemeyer, J; Wang, K; Curtis, P S and Jarvis, P G (2001). Stomatal conductance of forest species after long-term exposure to elevated CO_2 concentration: A synthesis. *New Phytol., 149(2)*: 247-264.

Murray, M B; Smith, R I; Friend, A and Jarvis, P G (2000). Effects of elevated (CO_2) and varying nutrient application rates on physiology and biomass accumulation of Sitka spruce (*Picea sitchensis*). *Tree Physiol., 20(7)*: 421-434.

Paoletti, E and Gellini, R (1993). Stomatal density variation in beech and holm oak leaves collected over the last 200 years. *Acta Oecologia, 14*: 173-178.

Peńuelas, J and Matamala, R (1990). Changes in N and S leaf content, stomatal density and specific leaf area of 14 plant species during the last three centuries of CO_2 increase. *J. Exp. Bot., 41(9)*: 1119-1124.

Pidwirny, M (2006). Introduction to the atmosphere. *Fundamentals of Physical Geography 2nd Edition* (Sack, D; Petersen, J F and Gabler, R E eds.). http://www.physicalgeography.net/fundamentals/8b.html, accessed on 20 September 2011.

Radoglou, K M and Jarvis, P G (1990). Effects of CO_2 enrichment on four Poplar clones. II. Leaf surface properties. *Ann. Bot., 65(6)*: 627-632.

Tarmizi, M A (2009). *Pembajaan sawit. Perusahaan Sawit di Malaysia. Edisi Ketiga* (Esnan, A G and Idris, O eds.). MPOB, Bangi. p. 149-163.

Thompson, M; Gamage, D; Hirotsu, N; Martin, A and Seneweera, S (2017). Effects of elevated carbon dioxide on photosynthesis and carbon partitioning: A perspective on root sugar sensing and hormonal crosstalk. *Front. Physiol., 8*: 578-589.

Tyree, M T and Alexander, J D (1993). Plant water relations and the effects of elevated CO_2: A review and suggestions for future research. *Vegetatio, 104*: 47-62.

Warren, J M; Jensen, A M; Medlyn, B E; Norby, R J and Tissue, D T (2014). Carbon dioxide stimulation of photosynthesis in *Liquidambar styraciflua* is not sustained during a 12-year field experiment. *AoB Plants, 7*: 1-13.

Wulff, R D and Strain, B R (1981). Effects of CO_2 enrichment on growth and photosynthesis in *Desmodium paniculatum*. *Can. J. Bot., 60(7)*: 1084-1091.

Xu, Z; Jiang, Y; Jia, B and Zhou, G (2016). Elevated CO_2 response of stomata and its dependence on environmental factors. *Front. Plant Sci., 7*: 657-670.

Ziska, L H (2008). Rising atmospheric carbon dioxide and plant biology: The overlooked paradigm. *DNA Cell Biol., 27(4)*: 165-172.

Journal of Oil Palm Research Vol. 34 (1) March 2022 p. 68-78
DOI: https://doi.org/10.21894/jopr.2021.0031

ASSOCIATION OF SEED COLOUR WITH GERMINATION, PHYSICAL AND PHYSIOLOGICAL GROWTH OF OIL PALM (*Elaeis guineensis*) SEEDLINGS

M G NORSAZWAN[1]; U R SINNIAH[1]*; A B PUTEH[1]; P NAMASIVAYAM[2]; D R APPLETON[3]; M MOHAIMI[4] and I A AMINUDDIN[4]

ABSTRACT

In commercial Dura *x* Pisifera *(DxP) seed production, white-coloured seeds are perceived as abnormal despite lack of scientific evidence to support this. This study evaluates different seed colour (black, semi-white and white) during germination and nursery evaluation. Four replications of 10 seeds were used for the evaluation of seed characteristic. Seed germination was conducted using four replications of 100 seeds by subjecting the seeds to 60 days of heat-treatment followed by germination at 30°C. Thirty pre-germinated DxP seeds per replication were then transferred into the nursery for morphological, physiological and growth assessment at three months interval until 12 months after sowing. Germination test shows all seed types indicated similar germination percentage (more than 78%) and speed (13-15 days of mean germination time). Nursery assessment shows black seed indicated higher overall biomass within the first three months, however, no differences in growth were observed from six until 12 months after sowing. Physiological evaluation including net photosynthesis (5.3-18.13 µmol CO_2 m^{-2} s^{-1}), stomatal conductance and transpiration rate were similar among the seedlings produced by seeds differing in colour. Hence, seed colour does not implicate abnormality and should not be discarded for the purpose of seed production.*

Keywords: DxP seeds, nursery management, seed colour.

Received: 27 October 2020**; Accepted:** 23 March 2021**; Published online:** 5 July 2021.

INTRODUCTION

Oil palm (*Elaeis guineensis* Jacq.) is known as the highest yielding oilseed in the world. On average, 4.0 t of oil are produced per hectare of land every year, far exceeding the yield of other sources of oilseed such as soybean, sunflower and rapeseed (Malaysian Palm Oil Council, 2018). According to the USDA (2020), total world vegetable oil consumption in 2018/2019 was 204.83 million tonnes with 74.62 million tonnes (36.4%) being palm oil, followed by soybean (27.8%), rapeseed (13.5%) and sunflower seed (9.3%). It was estimated that oilseed consumption will exceed 240 million tonnes in 2050, based on current requirement along with population growth forecast (Corley, 2009). The increasing demand is a challenge for the oil palm industry to be more efficient particularly in ensuring higher fresh fruit bunch (FFB) yield. The main method of oil palm propagation is through seeds, using the *Dura* x *Pisifera* (DxP) hybrid seeds. It was reported that the reduction

[1] Department of Crop Science, Faculty of Agriculture, Universiti Putra Malaysia, 43400 Serdang, Selangor, Malaysia.

[2] Department of Cell and Molecular Biology, Faculty of Biotechnology and Biomolecular Science, Universiti Putra Malaysia, 43400 Serdang, Selangor, Malaysia.

[3] Sime Darby Technology Centre Sdn. Bhd., First Floor, Block B, UPM-MTDC Technology Centre III Malaysia, Lebuh Silikon, Putra Square, 43400 Serdang, Selangor, Malaysia.

[4] Sime Darby Research Sdn. Bhd., Jalan Klang Banting, Kelanang, 42700 Banting, Selangor, Malaysia.

* *Corresponding author e-mail: umarani@upm.edu.my*

of DxP seeds in Malaysia had declined from 88 million seeds in 2008 (Kushairi *et al.*, 2010) to less than 60 million seeds per year in 2019 (Malaysian Palm Oil Board, 2020), despite the increasing forecasted demand of planting materials for 2050 (Corley, 2009). Therefore, continuous supply of pre-germinated seeds is needed for replanting and land expansion. Currently, the production of DxP pre-germinated seeds is based on a standard guideline described in Malaysian Standard MS 157: 2005 Oil Palm Seeds for Commercial Planting - Specification (Department of Standards Malaysia, 2005).

In commercial DxP seed production, white coloured seeds are often perceived as being abnormal and not favoured by the potential buyers thus, it is mainly discarded during seed production (Sime Darby Seeds and Agricultural Services, 2020). This situation leads to high monetary loss to the seed producers considering the current price of DxP seed, at RM2.35 to RM3.80 per seed. Germination parameters (final germination percentage, speed of germination and uniformity) are the focus for seed producers as it translates to saleable seeds. As for the seed buyers, the primary concern is more on the seedling performance in the nursery and after field planting. To date, despite the practice of removing the semi-white and white seeds, there is no scientific studies conducted to conclusively determine the performance of white seeds as compared with the black coloured seeds in terms of its germination, as well as seedling growth and development. Therefore, the emphasis on this study will extend beyond oil palm seed germination evaluation, by assessing the seedling performance at nursery stage prior to field planting. Various studies have shown the association between seed coat colour with both germination and seedling performance, *e.g.,* seed colour was shown to correlate with other morphological traits such as seed coat thickness; thus, a specific colour would influence imbibition rate and germination capacity (Khan *et al.*, 1997; Powell *et al.*, 1986; Xu *et al.*, 2016; Zhang *et al.*, 2013). Seeds with higher germination percentage and vigour will allow earlier seedling establishment thus, enabling competitive advantage of the developing seedlings (Mohamed-Yasseen *et al.*, 1994; Powell *et al.*, 1986). Nevertheless, the capacity to germinate may not be the sole indicator of a high-quality seed. The plant resource allocation strategies have to be assessed, such as the root and shoot biomass, along with the physiological performance in the field (Padilla and Pugnaire, 2007). In commercial oil palm nursery, specific morphological characteristics of the seedlings were generally screened through standard culling practices to remove abnormal seedlings. Abnormal seedlings such as juvenile and erect seedlings have been reported to cause 88% and 92% yield reduction within the first two years of field planting (Corley and Tinker, 2015). Despite the use of black coloured seed, the expected losses due to culling was up to 20% during the standard 12 months nursery period (Corley and Tinker, 2015; Turner and Gillbanks, 2003). In addition, seedling photosynthetic capability which encompasses the net photosynthesis and relevant parameters including transpiration rate and stomatal conductance level can be evaluated as a measure of physiological performance prior to the field planting (Ibrahim *et al.*, 2010). Therefore, the objective of this study is to evaluate morphological and physiological performance of oil palm DxP seeds varying in colour from germination through one year of nursery stage.

MATERIALS AND METHODS

Seed Collection and Pre-treatment

Freshly harvested DxP seeds from controlled pollination of CALIX 600 *Dura* mother palm sources were collected from Field PT100, Sime Darby Research, Banting, Selangor, Malaysia (2°48'16.2"N 101°27'21.2"E): at 20 weeks after pollination. After mechanical removal of the mesocarp, the seed were treated with 0.05% Benomyl 50% wettable powder (WP) (95% a.i) solution for 5 min to prevent fungal infection. The seed were then air dried at ambient temperature (27.0ºC-28.5ºC) inside plastic containers to check for damage or mesocarp remnants.

Seed Colour Distribution within Bunch and Seed Characteristics

The distribution of seeds varying in colour was assessed according to different sections within the harvested bunch. The oil palm bunch was initially divided into three equidistance sections from the stalk, and recorded as proximal, middle and distal. Each of the sections were further divided into base and apex region of the spikelet. The number of black (endocarp surface is black or dark brown with <10% white), semi-white (10%-90% endocarp surface is white) and white (endocarp surface is white, with <10% black) seeds (*Figure 1*) on each position was recorded.

The seeds were then evaluated for physical characteristics. This include seed weight (g), shell thickness (mm), seed length and width (mm), operculum diameter (mm) and seed moisture content. The moisture content was also determined gravimetrically as a percentage of fresh weight basis. Seed samples were dried using low constant temperature oven method (103 ± 2ºC for 17 hr), following procedures described by International Seed Testing Association (2016).

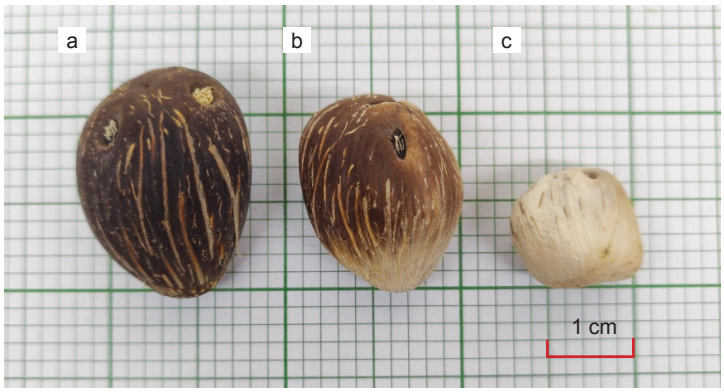

Figure 1. (a) Black, (b) semi-white, and (c) white coloured DxP seeds.

Seed Germination

Germination test. All the samples were subjected to heat treatment of 40 ± 2°C for 60 days. The treated seeds were than imbibed in water for 10 days before commencing germination test. Imbibed DxP seeds were separated into plastic bags containing four replicates of 100 seeds inside germination room. Germinated seeds were monitored daily by recording the number of seeds showing emergence of radicle protrusion from the fibre plug according to Sime Darby Research standard evaluation procedures. Final germination percentage (FGP), percentage of normal, abnormal, and diseased seeds, and mean germination time (MGT) were recorded.

Experimental design. The experimental design for seed germination was Randomised Complete Block Design (RCBD). The treatments (black, semi-white and white seeds) were blocked four times by using four different oil palm fruit bunch.

Nursery Evaluation

Study site and nursery preparation. The nursery assessment was conducted at Sime Darby Research pre and main nurseries in Banting, Selangor, Malaysia (2°48'08.5 N 101°27'26.9 E). At the pre-nursery stage, 6×9 inch polyethylene bags containing media (3:1 topsoil to sand) were prepared and kept under shade netting 50% shade level throughout the three months. Each of the polybag was moistened with approximately 50 mL of water by using automated mist-sprayer sprinkler system (10 min spraying time, two times per day). After three months, the seedlings were transferred into 15 × 18 inch polyethylene polybag at the main nursery site for the next nine months. Triangular spacing of 0.75 m were used to minimise light competition along with ease of access for fertiliser, weeding and pest control application. Prior to the transplanting, each of the polybag were filled with media (3:1 topsoil to sand) and planting holes were made using specialised core-borer. Each of the polybag were supplied with 500 mL of water, twice per day. Nitrogen, phosphorus and potassium (NPK) 15:15:15 compound fertiliser was applied at two weeks interval with increasing rate from 5 g (week 16 to 20), 10 g (week 22 to 26) and 20 g (week 28 to 48). Insecticide application was also applied by alternating cypermethrin (0.02% a.i) and dimethoate (38% a.i) application at every two weeks interval.

Experimental design. For both pre- and main nursery evaluation, the seedlings were arranged in RCBD, where the seedlings were blocked according to sunlight direction in the field. Four replicates of 30 pre-germinated seeds from (black, semi-white, white) were sown into prepared polybags. Data was collected at 3, 6, 9 and 12 weeks after sowing. The data collection was divided into destructive (seedling growth) and non-destructive (seedling physiology) sampling methods.

Seedling growth. Four replications of three seedlings were sampled at every data collection period. Seedling height (cm) was measured using a measuring tape. The height was taken from the base of the stem (or bole) until the end of the third fully opened leaves. Total leaf area (cm^2) was determined by using benchtop Li-COR Area Meter model LI-3100 (LI-COR, Inc., Lincoln, Nebraska, USA) at Plant Physiology Laboratory, Universiti Putra Malaysia. Both shoot and root were dried separately using oven at 70°C for at least 76 hr until no change in mass was observed. The dry biomass was measured using analytical balance model B303-S (Mettler Toledo, Columbus, Ohio, USA).

Seedling physiology. Li-COR LI-6400XT Portable Photosynthesis System (LI-COR, Inc., Lincoln, Nebraska, USA) was used for physiological parameters. This include net photosynthesis (μmol CO^2 m^{-2} s^{-1}), transpiration rate (mmol H_2O m^{-2} s^{-1}), stomatal conductance mol (H_2O m^{-2} s^{-1}) and intercellular carbon dioxide (CO_2) concentration (μmol CO_2 mol^{-1}). Data collection was conducted

between 8.00 am and 11.00 am to minimise error due to stomatal closure in the afternoon. Five data point readings were taken on the mid-section of a fully expanded leaf number three, with a total of four seedlings per treatment.

Statistical Analysis

Analysis of variance (ANOVA) was performed using Microsoft Excel and Statistical Analysis Software, SAS 9.4 (SAS Institute, Cary, North Carolina). Significant levels of $p \leq 0.05$ and $p \leq 0.01$ were applied for Least Significant Difference (LSD) test throughout this study.

RESULTS

Seed Colour Distribution within a Bunch

The ANOVA showed there was a significant effect of seed position within spikelet on percentage of black, semi-white and white seeds. Seeds that developed closer to the stalk (the base part of the spikelet), irrespective of any position within the bunch (either proximal, middle or distal) had higher percentages of white seeds in comparison to the respective apex section of the spikelet. In this study, the CALIX 600 bunches recorded an average of 2150 seeds within a bunch. At the distal section of the bunch, seeds located on the apex of the spikelet recorded 2091, 23 and 34 seeds that were categorised as black, semi-white and white, respectively. In contrast, the base region of the spikelet had 24% (539 seeds) and 15.2% (361 seeds) more semi-white and white seeds. Both, middle and proximal sections of the bunch indicated similar pattern as the distal (*Table 1*).

Seed Characteristics

The ANOVA showed that there were significant relationships of seed colour on all seed characteristics, except for seed width. White seed had significantly lower seed weight, seed length, operculum diameter and shell thickness in comparison with black, and occasionally semi-white seeds (*Table 2*). White seeds were more rounded in shape (due to higher width relative to the length), in comparison with black seeds. Semi-white generally exhibited similar physical characteristics as a black seed, except with lower seed length. In terms of seed moisture content, white seeds recorded highest percentage of moisture content (23.6%), followed by semi-white (19.4%) and black seeds (16.8%).

Seed Germination

No significant relationship of seed colour was recorded on all germination parameters; final germination percentage (FGP), percentage of abnormal and diseased seeds, and mean germination time (MGT). Similar FGP was recorded for black (83.5%), semi-white seeds (82%) and white (79%), as shown in *Table 3*. Majority of the germinated seeds were classified as normal, with the mean value ranging from 78% to 82.5%. Diseased and abnormal seeds were less than 2% in all treatments. All the seeds germinated within 13-15 days of MGT. Based on all other physical characteristics presented above, seeds at 20 WAP had variations in terms of the sizes, weight, along with other morphological features. However, similar level of maturity was shown based on the germination capacity.

TABLE 1. NUMBER OF BLACK, SEMI-WHITE AND WHITE SEEDS AT DIFFERENT SECTIONS OF THE OIL PALM BUNCH

Position within bunch	Position within spikelet	Black	Semi-white	White
Distal	Apex	2 091a	23b	34b
	Base	1 249b	539a	361a
Middle	Apex	1 818a	238ab	92b
	Base	1 337b	395a	417a
Proximal	Apex	2 072a	36b	40b
	Base	1 563b	311a	275a
Source of variation	**df**	**Mean square (MS)**		
Block	3	2 413.98ns	2 741.40ns	2 073.71ns
Seed position	5	574 884.92**	158 447.75**	130 512.44**
Error	15	8 053.43	7 055.74	3 814.85

Note: PB - Proximal-Base; PA - Proximal-Apex; MB - Middle-Base; MA - Middle-Apex; DB - Distal-Base; DA - Distal-Apex. Different letters indicate significant differences based on LSD test at 5% probability level; *,**, and ns indicate significant differences at 0.05%, 0.01% and not significant, respectively.

TABLE 2. DIFFERENCES IN SEED WEIGHT, SEED SIZE, OPERCULUM DIAMETER, SHELL THICKNESS AND MOISTURE CONTENT OF BLACK, SEMI-WHITE AND WHITE SEEDS

Seed colour		Seed weight (g)	Seed length (mm)	Seed width (mm)	Operculum diameter (mm)	Shell thickness (mm)	Seed moisture content (%)
Black		3.66a	23.98a	16.32a	3.45a	3.06a	16.80b
Semi-white		3.00ab	16.62b	17.25a	3.43a	2.91a	19.40b
White		2.80b	14.95b	17.74a	3.07b	2.44b	23.60a
Source of variation	**df**	**Mean square (MS)**					
Blocks	3	2.32ns	15.07ns	4.91ns	1.01ns	0.11ns	1.54ns
Seed colour	2	10.29**	171.21**	19.28ns	1.91*	4.17**	69.22**
Error	114	1.09	12.54	9.53	0.36	0.39	0.64

Note: Different letters indicate significant differences based on LSD test at 5% probability level; *,**, and ns indicate significant differences at 0.05%, 0.01% and not significant, respectively.

TABLE 3. FINAL GERMINATION PERCENTAGE (FGP), PERCENTAGES OF NORMAL, ABNORMAL, AND DISEASED GERMINATED SEEDS, AND MEAN GERMINATION TIME (MGT) FOR BLACK, SEMI-WHITE AND WHITE SEEDS

Seed colour		FGP (%)	Normal (%)	Abnormal (%)	Diseased (%)	MGT (days)
Black		83.50a	82.50a	0.50a	0.50a	14.90a
Semi-white		82.00a	80.50a	1.00a	0.50a	13.42a
White		79.00a	78.00a	0.25a	0.75a	13.97a
Source of variation	**df**	**Mean square (MS)**				
Block	3	168.33ns	172.89ns	0.53ns	0.33ns	6.50ns
Seed colour	2	21.00ns	20.33ns	0.58ns	0.00ns	2.26ns
Error	6	81.00	101.22	1.03	1.33	3.37

Note: Different letters indicate significant differences based on LSD test at 5% probability level; *,**, and ns indicate significant differences at 0.05%, 0.01% and not significant, respectively.

Seedling Growth

The ANOVA showed no significant relationship of seed colour on seedling height, total leaf area and seedling biomass. On the other hand, data collection time recorded a significant effect on all the parameters evaluated.

Seedling height. At the end of the pre-nursery stage (three months after sowing), the plant height ranged from 31.3 cm (white seed) to 33.4 cm (black seed). There were 49.0 cm average increment in height upon seedling transplant into the main nursery at six months after sowing, for all seed colours. At nine and 12 months after sowing, no differences were generally recorded as all the seedlings attained 82.0-90.0 cm and more than 140.0 cm height, respectively (*Table 4*).

Total leaf area. At the end of the pre-nursery stage, seedling from the black seeds recorded 276.8 cm^2, followed by semi-white (238.2 cm^2) and white seed (230 cm^2). The value then increased more than 4-folds at six months, ranging between 888.9 to 996.8 cm^2. At 9 and 12 months after sowing, significant increment was observed, where the total leaf area recorded was between 2000 cm^2 (nine months) to 4700 cm^2 (12 months after sowing).

Seedling biomass. In terms of shoot dry weight, the initial dry weights at three months after sowing recorded were 3.11 g (black seeds), 2.34 g (semi-white seeds) and 2.33 g (white seeds). The root dry weights were generally lower, ranged from 0.87 g to 1.50 g for all the treatments. At 12 months after sowing, more than 280 g of shoot and 260 g of root dry weights were recorded. *Figure 2* shows the seedlings sampled at 12 months after sowing.

Seedling Physiology

The ANOVA showed that time (months after sowing) had a significant effect on all physiological parameters. On the other hand, seed colour showed

TABLE 4. SEEDLING HEIGHT, TOTAL LEAF AREA, SHOOT DRY WEIGHT AND ROOT DRY WEIGHTS AT 3, 6, 9 AND 12 MONTHS AFTER SOWING

Months after sowing	Seed colour	Seedling height (cm)	Total leaf area (cm^2)	Shoot dry weight (g)	Root dry weight (g)
3 months	Black	33.42e	276.79e	3.11c	1.45c
	Semi-white	32.17e	238.16e	2.34c	1.06c
	White	31.34e	230.04e	2.33c	0.87c
6 months	Black	49.25d	904.16d	12.34c	14.30c
	Semi-white	49.00d	888.98d	13.10c	13.51c
	White	48.84d	996.78d	15.05c	16.34c
9 months	Black	82.59c	2 107.20c	50.32b	41.95b
	Semi-white	90.84b	2 003.90c	54.72b	47.08b
	White	89.75b	2 162.40c	63.51b	56.49b
12 months	Black	142.09a	4 368.70b	413.42a	281.50a
	Semi-white	140.75a	4 652.40a	371.33a	260.42a
	White	148.25a	4 671.90a	381.00a	299.75a
Source of variation	**df**		**Mean square (MS)**		
Block	3	73.360ns	490 860.4*	703.84ns	181.60ns
Seed colour (SC)	2	33.53ns	128 230.50ns	642.81ns	1 588.47ns
Time (T)	3	95 031.88**	129 486 248.50**	662 563.95**	630 497.02**
SC × T	6	74.06ns	114 406.80ns	1 424.38ns	707.57ns
Error	129	55.15	93 522.90	1 452.43	572.30

Note: Different letters indicate significant differences based on LSD test at 5% probability level; *,**, and ns indicate significant differences at 0.05%, 0.01% and not significant, respectively.

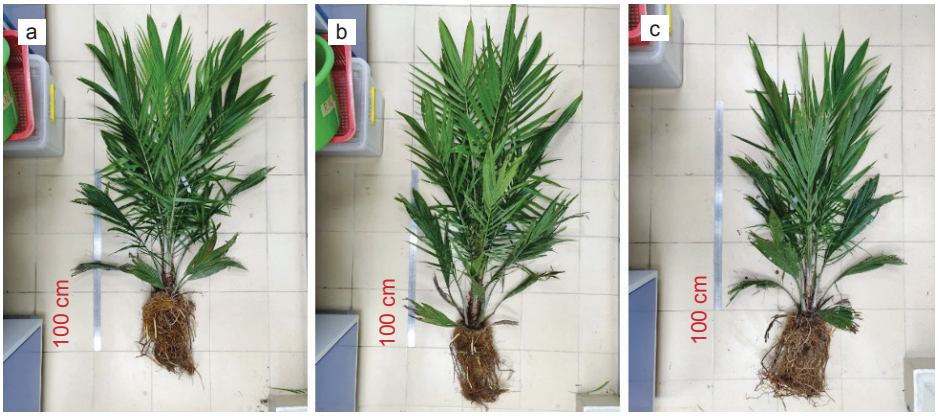

Figure 2. Oil palm seedlings from (a) black, (b) semi-white, and (c) white seeds at 12 months after sowing.

no significant relationship. Net photosynthesis of black, semi-white and white seedlings ranged from 5.3 to 8.8 µmol CO_2 m^{-2} s^{-1} at three months after sowing. After three months in the main nursery, the value significantly increased with semi-white seed recorded highest net photosynthesis of 18.9 µmol CO_2 m^{-2} s^{-1}, followed by white seed (16.87 µmol CO_2 m^{-2} s^{-1}) and black seed (14.16 µmol CO_2 m^{-2} s^{-1}). From 9 to 12 months after sowing, the value fluctuates within 12.87-18.13 µmol CO_2 m^{-2} s^{-1} range (*Table 5*).

Other physiological parameters including stomatal conductance, intercellular concentration, and transpiration rate indicated some variation among different seed types and at different stages of nursery.

DISCUSSION

Germination test conducted clearly showed 79%-84% FGP and 13-15 days mean germination time were attained, with no significant differences among the seed colours. Previous studies on other crops have shown association of seed colour with seed germinability. In most cases, the lighter coloured seeds were linked with being immature, with lower

TABLE 5. NET PHOTOSYNTHESIS, STOMATAL CONDUCTANCE, INTERCELLULAR CONCENTRATION, AND TRANSPIRATION RATE FOR BLACK, SEMI-WHITE AND WHITE SEEDS

Months after sowing	Seed type	Net photosynthesis ($\mu mol\ CO_2\ m^{-2}\ s^{-1}$)	Stomatal conductance ($mol\ H_2O\ m^{-2}\ s^{-1}$)	Intercellular concentration ($\mu mol\ CO_2\ m^{-2}\ s^{-1}$)	Transpiration rate ($mmol\ H_2O\ m^{-2}\ s^{-1}$)
3	Black	8.86e	0.13cd	260.52abcd	1.06cd
	Semi-white	5.25e	0.08d	227.65bcd	0.73d
	White	5.37e	0.10d	249.54bcd	0.84cd
6	Black	14.16cd	0.15abcd	223.44cd	2.00bcd
	Semi-white	18.96a	0.24ab	213.16d	2.95ab
	White	16.86abc	0.25a	237.05d	2.94ab
9	Black	12.87d	0.14bcd	213.05a	2.43ab
	Semi-white	13.87cd	0.20abc	245.70bcd	3.06ab
	White	13.56cd	0.22abc	248.00bcd	3.40a
12	Black	17.02abc	0.15abcd	304.50abc	3.20ab
	Semi-white	18.12ab	0.22abc	309.89ab	2.87ab
	White	14.97bcd	0.16abcd	333.13a	2.10abc
Source of variation	**df**		**Mean square (MS)**		
Block	3	20.55ns	0.01ns	2 687.69ns	4.13ns
Seed colour (SC)	2	7.49ns	0.01ns	1 018.33ns	0.21ns
Time (T)	3	276.98*	0.03*	2 4071.73*	11.03*
SC × T	6	14.56ns	0.01ns	1 069.56ns	1.12ns
Error	33	6.35	0.01	2 884.50	0.55

Note: Different letters indicate significant differences based on LSD test at 5% probability level; *,**, and ns indicate significant differences at 0.05%, 0.01% and not significant, respectively.

germination percentage and vigour (Mavi, 2010; Zhang *et al*., 2013). This could be the reason on the consumer preference towards darker coloured oil palm seeds, and why seed producers discarded the white seeds. The association between colour and germinability is linked to seed water permeability. Powell *et al*. (1986) suggested that lighter coloured seeds such as white seeds imbibed water more rapidly due to higher seed coat disintegration with the cotyledons which in turn increases germination. Similarly, it was reported that dark coloured seed coat of *Panicum miliaceum* species were thicker, imbibed less water, thus, germinated slower (Khan *et al*., 1997). In contrast, dark seeds of *Brassica napus* showed significantly higher germination percentage and speed (Zhang *et al*., 2013). From the seed moisture content evaluation, oil palm white seeds showed nearly 7% higher moisture level as compared to the black seed. Seed moisture content is one of the most important aspect of development, and it is known that underdeveloped seeds generally have higher moisture level with lower capacity to germinate (Lima *et al*., 2012). For example, Mavi (2010) reported that light-yellow watermelon seed was found to have lower moisture content, with 40% lower emergence percentage as compared to dark brown coloured seed. Similarly, Xu *et al*. (2016) suggested that white seed of *Zostera marina* L. were underdeveloped with smaller seed sizes and 11% higher moisture in comparison with the black seed. However, in oil palm seed, despite the prominent difference in moisture; seed capacity to germinate was not affected. Thus, in this scenario, the difference may be due to higher endocarp moisture retention of the white seed, which could possibly be linked to the endocarp composition and was not a measure of seed maturity.

According to the nursery evaluation, oil palm seedlings showed similar growth pattern among different seed colours. In general, there was 4 to 6-fold increase in terms of overall biomass production at every three months data collection interval. Most studies conducted previously, associated seed colour with other characteristics, mainly the water permeability. Higher water permeability enables faster germination and earlier seedling establishment which allows for competitive advantage for a vigorous initial seedling growth (Mohamed-Yasseen *et al*., 1994; Powell *et al*., 1986; Stringam *et al*., 1974) reported that there was a correlation between colour, seed coat thickness and seedling growth in *Brassica rapa*. Velijevic *et al*. (2017) also revealed that bright coloured *Trifolium pratense* seeds showed higher seedling vigour and growth in comparison with darker coloured seeds. The effect of seed colour

was even linked to yield components such as oil production. Bagheri *et al.* (2013) reported that genotypes with reddish-brown seed coat of *Brassica rapa* had higher oil content in comparison to the yellow-seeded genotypes. Similar finding from Zhang *et al.* (2013) reported that darker *Brassica napus* seeds resulted in higher seedling emergence percentage, vigour, shoot and root length, as well as the seed oil content. Interestingly, within the first three months of the nursery evaluation (end of pre-nursery), black seed did show higher growth (such as mean root/ shoot dry weight and total leaf area as shown in *Table 4*), if we analyse the data based on single data collection point (instead of using a pooled LSD-value). Based on the seed characteristics evaluation (*Table 2*), it was evident that black seeds were generally larger in size and weight, as compared to white seeds. Studies have shown previously that seed size plays an important role in early seedling establishment. Larger seed size can be associated with larger endosperm reserve. Finch-Savage and Bassel (2016) suggested that differences in lipid reserve mobilisation rate may contribute to the early seedling establishment after germination commencement. In the case of oil palm seedling, the larger size of black seed may attribute to the more vigorous growth within the first three months, as the seedling utilised more endosperm reserve during initial establishment. It is known that the main role of endosperm is as a primary means of nutrient supply as well as the regulator of embryonic growth during seed development and germination, along with other diverse functions (Copeland and McDonald, 2001; Yan *et al.*, 2014). However, with further seedling growth, and the utilisation of available nutrients from the soil, no differences were observed.

There was limited literature that associate seed colour with the physiological performance on developing seedlings. Most of the evaluation were conducted until germination stage and early seedling vigour assessment as discussed above. However, the performance can still be assessed according to the main physiological component of seedling growth particularly the leaf photosynthetic capacity, along with other contributing factors including chlorophyll contents, stomatal conductance, transpiration rate as well as the intercellular CO_2 concentration. The leaf which serves as main vegetative plant part to capture light was considered as highly plastic, making it the most evaluated components in determining plant physiological function as well as stress indicator (Dickison, 2000). In this study, the net photosynthesis values were similar among different seed colours but varies with time of data collection. Initially, the values were between 5.3 to 8.8 μmol CO_2 m^{-2} s^{-1} (three months) and then increased up to 18.13 μmol CO_2 m^{-2} s^{-1} towards the end of the evaluation period. Ibrahim *et al.* (2010) reported that net photosynthesis of seven months old oil palm seedlings exposed to normal 400 ppm atmospheric CO_2 level were between 15 to 20 μmol CO_2 m^{-2} s^{-1}. On the other hand, lower net photosynthesis ranging from 4 to 9 μmol CO_2 m^{-2} s^{-1} was shown by 12 months old sago palm (Azhar *et al.*, 2018) and young macaw palm seedlings (Dias *et al.*, 2018). By comparing these values from Ibrahim *et al.* (2010) and Azhar *et al.* (2018), it is evident that all the seed colour produces seedlings that have normal photosynthetic capacity at both pre-nursery and main nursery stages. The increasing net photosynthesis value from three months to the remaining nine months of nursery evaluation indicates higher energy requirement of the growing seedlings (Bravdo, 1971). These differences in photosynthesis also explained the variation observed throughout the 12 months evaluation period for other physiological parameters (transpiration rate, stomatal conductance, and intercellular CO_2 concentration) which are known to influence the overall plant photosynthetic capacity. In juvenile oil palm seedlings, the frond leaflets are the main site of gas exchange such as CO_2, water vapour and oxygen as well as photosynthesis. The gas exchange is primarily regulated by the stomata on both the abaxial and adaxial of the leaf surfaces. During periods with high photosynthetic activities, the oxygen concentration will increase which in turn decreases the intercellular CO_2 concentration. This will affect the concentration gradients of these gasses, thus, influence the diffusion rates (Haniff, 2006).

In this study, it was found that white seed occurrence is more prominent in the base section of the spikelet within the bunch. This could be due to less pigmentation from lower sunlight exposure for seed that were located at the base region of the spikelet. For the same reason, slower rate of desiccation was observed for white seeds since as it is well protected underneath seeds located at the apex of the spikelets. Therefore, based on these findings, seed colour in oil palm could be associated with the natural pigmentation during developmental process. In the case of rapeseed, water uptake and tolerance to excessive water was linked to seed coat colour and melanin pigmentation. It was shown that black and red seed have higher melanin pigment as compared to yellow and lighter coloured seeds (Zhang *et al.*, 2006; 2008). The seed morphological features were highly influenced by environmental stimuli which leads to changes in seed composition (Lacey, 1998; Senda *et al.*, 2004). Therefore, it is possible that oil palm seed colour will change from white to black with maturity and upon exposure to environmental stimuli. The possibility of genetic influence towards seed colour was previously shown in sweet clover (*Melilotus alba* Desr), where it was found that green

and brown colour pigmentation on the seed coat were controlled by Y/y and C/c alleles, respectively (Gorz *et al.*, 1975). Similarly, Vandenberg and Slinkard (1990) reported both grey and tan ground colours in lentils were controlled by two dominant genes in an independent locus. In oil palm seeds, the genetic effect was reported only for exocarp colour, where *virescens* (VIR) gene was known to be responsible for the VIR trait (Singh *et al.*, 2014). In this study, there was no evident on genetic influence towards seed colour, since only similar commercial variety of DxP CALIX 600 was evaluated. However, it is possible that different progenies used by seed producers could also affect the seed colour during development process. In general, based on the germination data along with nursery evaluation, it is evident that the quality of white seeds in terms of germination and seedling characteristics are equal to the black seeds. Therefore, white seeds no longer need to be discarded in commercial DxP seed production. Nevertheless, a follow up research on the performance of the plants in the field may benefit this long-term crop in relation to yield and oil content. The main challenge to seed producers would be to spread awareness to buyers and consumers regarding this matter.

CONCLUSION

This is the first study conducted on the performance of commercial oil palm DxP seeds based on seed colour in terms of ability to germinate and subsequent seedling performance at the nursery stages. The results show that seed colour differs in oil palm bunch due to spatial developmental process, which causes white and less pigmented seed at the base region of the spikelet. It was found that all seed types recorded 79%-84% normal germination within 13-15 days. In terms of seedling performance, black seeds show higher overall biomass and other growth parameters only for the first three months. However, at 6, 9 and 12 months, all the seed colours showed similar morphological development. The physiological evaluation also indicated that oil palm seed produces physiologically similar and normal seedlings, regardless of the colour. Overall, oil palm seed colour is not linked to germination capacity and seedling performance prior to field planting.

ACKNOWLEDGEMENT

Highest appreciation to Sime Darby Research Sdn. Bhd., for providing us with the materials, facilities and technical assistance throughout this study. We also thank the Ministry of Higher Education Malaysia and Universiti Putra Malaysia for the financial support through SLAB scholarship and Junior Academic Scheme during this study period.

REFERENCES

Azhar, A; Makihara, D; Naito, H and Ehara, H (2018). Photosynthesis of sago palm (*Metroxylon sagu* Rottb.) seedling at different air temperatures. *Agriculture, 8*: 1-10. DOI: 10.3390/agriculture8010004.

Bagheri, H; Pino-del-Carpio, D; Hanhart, C; Bonnema, G; Keurentjes, J and Aarts, M G M (2013). Identification of seed-related QTL in *Brassica rapa. Span. J. Agric. Res., 11(4)*: 1085-1093. DOI: 10.5424/sjar/2013114-4160.

Bravdo, B (1971). Carbon dioxide compensation points of leaves and stems and their relation to net photosynthesis. *Plant Physiol., 48(5)*: 607-612.

Copeland, L and McDonald, M (2001). Seed dormancy. *Principles of Seed Science and Technology.* 4th edition. Springer Science and Business Media, New York. Cltter. p. 140-164. DOI: 10.1007/978-1-4615-1619-4.

Corley, R H V and Tinker, P B (2015). *The Oil Palm*. 5th edition. Wiley Blackwell Science. Oxford, United Kingdom.

Corley, R H V (2009). How much palm oil do we need? *Environ. Sci. Policy, 12*: 134-139. DOI: 10.1016/j.envsci.2008.10.011.

Department of Standards Malaysia (2005). Oil palm seeds for commercial planting - specification (Third Revision), Malaysian Standard MS 157: 2005. Standards and Industrial Research Institute of Malaysia Berhad, Selangor.

Dias, A N; Siqueira-Silva, A I; Souza, J P; Kuki, K N and Pereira, E G (2018). Acclimation responses of macaw palm seedlings to contrasting light environments. *Sci. Rep., 8*: 15300. DOI: 10.1038/s41598-018-33553-1.

Dickison, W C (2000). *Integrative Plant Anatomy*. Academic Press, San Diego.

Finch-Savage, W E and Bassel, G W (2016). Seed vigour and crop establishment: Extending performance beyond adaptation. *J. Exp. Bot., 67*: 567-591. DOI: 10.1093/jxb/erv490.

Gorz, H J; Specht, J E and Haskins, F A (1975). Inheritance of seed and seedling colour in sweet clover. *Crop Sci., 15*: 235-238. DOI: 10.2135/cropsci1975.0011183X001500020028x.

Haniff, M H (2006). Gas exchange of excised oil palm (*Elaeis guineensis*) fronds. *Asian J. Plant Sci., 5(1)*: 9-13. DOI: 10.3923/ajps.2006.9.13.

Ibrahim, M H; Jaafar, H Z E; Harun, M H and Yusop, M R (2010). Changes in growth and photosynthetic patterns of oil palm (*Elaeis guineensis* Jacq.) seedlings exposed to short-term CO_2 enrichment in a closed top chamber. *Acta Physiol. Plant., 32(2)*: 305-313.

International Seed Testing Association (2016). International Rules for Seed Testing. Bassersdorf, CH-Switzerland.

Khan, M; Cavers, P B; Kane, M and Thompson, K (1997). Role of the pigmented seed coat of proso millet (*Panicum miliaceum* L.) in imbibition, germination and seed persistence. *Seed Sci. Res., 7(1)*: 21-26.

Kushairi, A; Tarmizi, A H; Zamzuri, I; Ong-Abdullah, M; Samsul Kamal, R; Ooi, S E and Rajanaidu, N (2010). Production, performance and advances in oil palm tissue culture. International Seminar on Advances in Oil Palm Tissue Culture. International Society for Oil Palm Breeders (ISOPB). 29 May 2010. Yogyakarta, Indonesia.

Lacey, E P (1998). What is an adaptive environmentally induced parental effect? *Maternal Effects as Adaptations* (Mousseau, T A and Fox, C W eds.). Oxford University Press, Oxford, United Kingdom. p. 54-66.

Lima, C B; Bruno, R L A; Silva, K R G; Pacheco, M V; Alves, E U and Andrade, A P (2012). Physiological maturity of fruits and seeds of *Poincianella pyramidalis (Tul.)* L.P. Queiroz. *Rev. Bras. Sementes, 34(2)*: 231-240. DOI: 10.1590/S0101-31222012000200007.

Malaysian Palm Oil Board (2020). Demand of germinated seed. http://bepi.mpob.gov.my/index.php/en/, accessed on 20 March 2020.

Malaysian Palm Oil Council (2018). Malaysian Palm Oil Council Official website. http://www.mpoc.org.my, accessed on 14 August 2018.

Mavi, K (2010). The relationship between seed coat colour and seed quality in watermelon Crimson sweet. *Hort. Sci., 37(2)*: 62-69.

Mohamed-Yasseen, Y; Barringer, S A; Splittstoesser, W E and Costanza, S (1994). The role of seed coats in seed viability. *Bot. Rev., 60*: 426-439.

Padilla, F M and Pugnaire, F I (2007). Rooting depth and soil moisture control Mediterranean woody seedling survival during drought. *Funct. Ecol., 21*: 489-495.

Powell, A A; Oliveira, M A and Matthews, S (1986). The role of imbibition damage in determining the vigour of white and coloured seed lots of dwarf French beans (*Phaseolus vulgaris*). *J. Exp. Bot., 37(5)*: 716-722.

Sime Darby Seeds and Agricultural Services (2020). DxP Seed Production Protocol, Standard Operation Procedures. Sime Darby Research, Malaysia.

Senda, M; Masuta, C; Ohnishi, S; Goto, K; Kasai, A; Sano, T; Hong, J S and MacFarlane, S (2004). Patterning of virus-infected *Glycine max* seed coat is associated with suppression of endogenous silencing of chalcone synthase genes. *Plant Cell, 16(4)*: 807-818.

Singh, R; Low, E T; Ooi, L C; Ong-Abdullah, M; Nookiah, R; Ting, N C; Marjuni, M; Chan, P L; Ithnin, M; Manaf, M A; Nagappan, J; Chan, K L; Rosli, R; Halim, M A; Azizi, N; Budiman, M A; Lakey, N; Bacher, B; Van-Brunt, A; Wang, C; Hogan, M; He, D; MacDonald, J D; Smith, S W; Ordway, J M; Martienssen, R A and Sambanthamurthi, R (2014). The oil palm *virescens* gene controls fruit colour and encodes a R2R3-MYB. *Nat. Commun., 5*: 4106. DOI: 10.1038/ncomms5106.

Stringam, G R; Mcgregor, D and Pawlowski, S H (1974). Chemical and morphological characteristics associated with seed coat colour in rapeseed. *Proc. of the 4th International Rapeseed Congress*. Giessen, Germany. p. 99-108.

Turner, P D and Gillbanks, R A (2003). *Oil palm cultivation and management*. The Incorporared Society of Planters, Kuala Lumpur.

USDA (2020). *Oilseeds: World Markets and Trades. Foreign Agricultural Service*. United States Department of Agriculture. https://apps.fas.usda.gov/psdonline/circulars/oilseeds.pdf.

Vandenberg, A and Slinkard, A E (1990). Genetics of seed coat color and pattern in lentil. *J. Hered., 81 (6)*: 484-488.

Velijevic, N; Štrbanović, R; Poštić, D; Stanisavljevic, R and Djukanovic, L (2017). Effects of seed coat colour on the seed quality and initial seedling growth of red clover cultivars (*Trifolium pratense*). *J. Process. Energy Agric., 21*: 174-177. DOI: 10.5937/JPEA1703174V.

Xu, S; Zhou, Y; Wang, P; Wang, F; Zhang, X and Gu, R (2016). Salinity and temperature significantly influence seed germination, seedling establishment and seedling growth of eelgrass *Zostera marina* L. *PeerJ, 4*: e2697. DOI: 10.7717/peerj.2697.

Yan, D; Duermeyer, L; Leoveanu, C and Nambara, E (2014). The functions of the endosperm during seed germination. *Plant Cell Physiol., 55(9)*: 1521-1533. DOI: 10.1093/pcp/pcu089.

Zhang, X K; Chen, J; Chen, L; Wang, H Z and Li, J N (2008). Imbibition behaviour and flooding tolerance of rapeseed seed (*Brassica napus* L.) with different testa color. *Genet. Resour. Crop Evol., 55*: 1175-1184.

Zhang, X K; Yang, G T; Chen, L; Yin, J M; Tang, Z and Li, J N (2006). Physiological differences between yellow-seeded and black seeded rapeseed (*Brassica napus* L.) with different testa characteristics during artificial ageing. *Seed Sci. Technol., 34(2)*: 373-381.

Zhang, J; Ying, C; Liyan, Z; Yilin, W; Jing, L; Guijun, Y and Liyong, H (2013). Seed coat color determines seed germination, seedling growth and seed composition of canola (*Brassica napus*). *Int. J. Agric. Biol., 15(3)*: 535-540.

Journal of Oil Palm Research Vol. 34 (1) March 2022 p. 79-91
DOI: https://doi.org/10.21894/jopr.2021.0016

THE EFFECTS OF RECYCLING PALM PRESSED-FIBRE OIL ON CRUDE PALM OIL QUALITY

HASLIYANTI, A[1]*; RUSNANI, A M[1]; WAN HASAMUDIN, W H[1]; NG, M H[1]; NOR FAIZAH, J[1] and ROHAYA, M H[1]

ABSTRACT

Palm pressed-fibre oil (PPFO) is known as a phytonutrients rich oil. PPFO was practically recycled back to the crude palm oil (CPO) processing line to increase oil extraction rates. This study evaluated the effect of blending CPO with PPFO at different PPFO dosage from 5%-25% (w/w) on blended oil quality. Free fatty acid (FFA) of blended oils increased from 3.42%-3.91%, while deterioration of bleachability index (DOBI) and iodine value (IV) decreased from 2.76 to 2.33 and 51.96 ± 0.37 to 50.21 ± 0.03, respectively. Minor components amount in blended oils were found to increase with carotenoids (539-654 ppm), squalene (475-1201 ppm), sterols (433-808 ppm), phospholipids (34.67-63.84 ppm) and vitamin E (1185-1626 ppm). The oxidative stability of blended oils was improved (14.31-16.76 hr) but chlorine, iron and copper content were found to increase from 3.85-7.49 ppm, 13.58-17.63 ppm and 0.19-0.38 ppm, respectively. Although blending PPFO would deteriorate some quality properties of CPO, nonetheless, PPFO is rich with phytonutrients, therefore signifying its potential applications in pharmaceuticals and food industry.

Keywords: blending PPFO, chloride, crude palm oil, heavy metals, oil quality, palm pressed-fibre oil.

Received: 23 December 2020; **Accepted:** 17 February 2021; **Published online:** 26 April 2021.

INTRODUCTION

The rapid increase in palm oil production over the last few decades has made it as one of the most important oils in the world. Malaysia contributes to almost 30% of global palm oil production and 36% of the world exporters in 2019 (Workman, 2020). Parveez *et al.* (2020) reported that oil palm planted areas in Malaysia increased to 5.90 million hectares and fresh fruit bunches (FFB) yield of 17.19 t ha^{-1} in 2019. This would contribute to a generation of massive amount of solid wastes, in the form of lignocellulosic residues from replanting activities and oil mill processing, stemming from oil palm trunk (OPT), oil palm frond (OPF), empty fruit bunches (EFB), palm pressed mesocarp fibre (PPMF), palm kernel cake (PKC), palm kernel shell (PKS) and decanter cake. Solid wastes produced were 20%-28% EFB, 11%-12% PPMF and 5%-8% PKS (Awalludin *et al.*, 2015; Onoja *et al.*, 2019; Sarmidi *et al.*, 2009; Yusoff, 2006).

PPMF is a by-product produced after crude palm oil (CPO) is extracted from the digested oil palm fruits mash, using a screw press. PPMF contains a substantial amount of residual oil (5%-8%) that is usually burnt along with the PPMF in the boiler, in order to supply energy to the mill. Several techniques to recover the residual oils from PPMF have been reported, such as, solvent extraction, enzymatic treatment, supercritical carbon dioxide (SC-CO2) and remnant oil recovery (ROR) system (Lau *et al.*, 2006; Noorshamsiana *et al.*, 2017; Nur Sulihatimarsyila *et al.*, 2019; Vijaya *et al.*, 2013). The residual oil extracted from this technique is known as palm pressed-fibre oil (PPFO). The commercial extraction technique of PPFO from PPMF is solvent extraction using hexane (Nur Sulihatimarsyila *et al.*, 2019). According to a survey done by Malaysian Palm Oil Board (MPOB), the system has been commercially installed in 12 palm oil mills in Malaysia (Ummi Kalsum and Rohaya, 2019).

[1] Malaysian Palm Oil Board,
6 Persiaran Institusi, Bandar Baru Bangi,
43000 Kajang, Selangor, Malaysia.

* *Corresponding author e-mail: hasliyanti@mpob.gov.my*

Non-polar solvent, namely hexane is utilised for extraction. This technique has been used in various vegetable oil extractions, such as rapeseed and soybean (Kumar *et al.*, 2017). Many studies reported that PPFO is rich with carotenoids, vitamin E (tocopherol and tocotrienols) (Choo *et al.*, 1996; Goh *et al.*, 1985; Lau *et al.*, 2017; Ng and Choo, 2011; Noorshamsiana *et al.*, 2017; Nur Sulihatimarsyila *et al.*, 2019; Rusnani *et al.*, 2012), squalene and sterols (Choo *et al.*, 1996; Goh *et al.*, 1985; Lau *et al.*, 2007; Ng and Choo, 2011; Phoon *et al.*, 2018). Since PPFO is rich in natural phytonutrients, almost all previous studies had suggested that PPFO has a wide range of applications in pharmaceuticals, supplementation and cosmetics (Lau *et al.*, 2017; Nur Sulihatimarsyila *et al.*, 2019). PPFO was also found to contain high amounts of water-soluble compounds, such as phospholipids (217-1063 ppm) and phenolics with outstanding antioxidant activities (Lau *et al.*, 2007; Ummi Kalsum and Rohaya, 2019; Valeria *et al.*, 2017). Apart from the normal fatty acid composition (FAC) content, PPFO has high diaclyglycerol (DAG) and triacylglycerol (TAG) (67.04% ± 0.05) with acceptable amount of monoaclyglycerol (MAG)/ free fatty acid (FFA) (13.02% ± 0.02) compositions. Nonetheless, PPFO also contains substantial amount of lauric acid (5.89%-9.09%) due to broken kernels in the mesocarp fibre, thus, making it suitable for the food applications and industry (Lau *et al.*, 2006; Neoh *et al.*, 2011).

However, studies also showed that PPFO is low in quality compared to CPO. Ummi and Rohaya (2019) reported on the deterioration of bleachability index (DOBI) of the PPFO, which ranges from 1.15-2.17 while the FFA ranges from 5.09%-10.6% as shown in *Table 1*. Also, PPFO has a high content of chlorine (207.62-379.58 ppm) which will lead to formation of carcinogenic compounds such as 3-monochloropropane-1,2-diols (3-MCPD) esters (*Table 1*) (Ramli *et al.*, 2015; Ummi Kalsum and Rohaya, 2019). Therefore, PPFO can only be sold at a lower price as compared to CPO because PPFO has not been classified into any oil classification set by MPOB. Since it is chemically extracted, it is therefore forbidden to blend PPFO into the CPO processing line (Ummi Kalsum and Rohaya, 2019). Since PPFO is not under any of the palm oil categories, it is automatically classified as sludge oil, which is the lowest quality of palm oil grade, in terms of price. As a result, palm oil millers tend to blend PPFO into CPO to increase its oil extraction rate. Apparently, the practice of blending PPFO into CPO has been increasing in recent years, as indicated by the increment of phosphorous content and FFA in CPO (Ummi Kalsum and Rohaya, 2019). According to the Code of Good Milling Practice of Palm Oil Mills (GMP), residual oils cannot be recycled or blended with CPO, mainly due to quality deterioration. Nevertheless, the blending effect of PPFO on CPO quality is not extensively studied and reported. Therefore, this study is aimed to examine the quality of PPFO from commercial solvent extraction plant as well as to evaluate the characteristics of blended oil when different dosage of PPFO is used to blend with CPO.

MATERIALS AND METHODS

Materials

CPO and solvent extracted PPFO were collected from eight palm oil mills and eight solvent extraction plants located in central, southern and northern region of Peninsular Malaysia. The samples were freshly collected and kept in the chiller at 4°C prior to the blending study. The PPFO samples collected from eight solvent extractions were used to determine the initial quality properties of PPFO. While, PPFO and CPO samples collected from Sitiawan, Perak and Labu Palm Oil Mill, Negeri Sembilan, Malaysia respectively, were used to evaluate the effect of blending CPO with PPFO at different dosages from 0%-25% (w/w) at 60°C and 300 rpm for 20 min on residual hexane concentration, FFA, DOBI, oxidative stability, iodine value (IV), trace elements, chloride content, phytonutrients content, FAC and acylglycerols compositions. All solvents, chemicals and reference standards (analytical grades) used in this study were purchased from Merck, JT Baker and Sigma, Germany.

Analysis of Quality Properties

The PPFO, CPO and blended oils samples were analysed according to MPOB Test Method (MPOB, 2005) to quantify the FFA, DOBI, carotene content, IV and phosphorus content.

Hexane Residual Analysis using Headspace Chromatography

Headspace analyses was performed by using GC-FID (6890N; Agilent Technologies, Santa Clara, CA, USA) and the headspace-sampler (HS-20; Shimadzu), which was used as preprocessing device (Jeong *et al.*, 2017; Kumar and Gow, 1994). Gas flow for analysis was 1.0 mL min^{-1}, and the detector and injection temperatures were regulated at 100°C and 50°C, respectively. The column used was 30 m × 0.3 mm × 0.2 µm coated with methylpolysiloxane. The analysis was implemented in a 100:1 split mode by applying helium as carrier gas. Residual solvent content was expressed in mg kg^{-1} (ppm) of the sample.

Heavy Metals Concentration Analysis using Flame Atomic Adsorption Spectroscopy (FAAS)

The metals content such as iron (Fe) and copper (Cu) was determined using Atomic Adsorption Spectrophotometer (AA-7000F, Shimadzu, Japan). Samples of 2 g each were weighed in 250 mL round bottom flask, later added with 5 mL of nitric acid (HNO_3), 5 mL sulphuric acid (H_2SO_4) and 2 mL hydrogen peroxide (H_2O_2). The mixture was then heated using water bath at 100°C until a clear solution was obtained. The solution was then filtered and made up to 50 mL using ultrapure water and transferred to a plastic bottle for metal analysis by atomic adsorption spectroscopy (AAS).

Total Chlorine Content Analysis

The amount of chloride in CPO, PPFO and blended oils was measured using a Total Chlorine Analyser (TCA) NSX-2100H (Mitsubishi Chemical Analytech, Kanagawa, Japan). Samples were prepared according to American Society for Testing and Materials (ASTM) D4929-04 method (ASTM, 2004). The operation principle of TCA was combustion and microoulometry. In the presence of oxygen and argon as a carrier gas, 0.065 g of oil aliquot was combusted in the TCA at temperatures between 800°C-1000°C. The hydrogen chloride released as a result of the combustion was then titrated with silver ion emitted from the titration cell. Chlorine content is quantified based on the intensity of electrical current released in the microcoulometer throughout the titration stage (Azmil *et al.*, 2019).

Oxidative Stability Analysis

The oil stability was determined using Rancimat Analyser (743 Metrohm, Switzerland). Oil samples of 3.0 ± 0.1 g each were weighed in a glass vessel. The temperature of heating block was set to 120°C, while the gas flow was set to 20 L hr^{-1} (Farhoosh, 2007).

Fatty Acid Compositions (FAC) Analysis

FAC were determined using gas chromatography flame ionisation (GC-FID) (Agilent Technologies). The samples were analysed according to American Oil Chemists' Society (AOCS) Official Method Ce 2-66 (AOCS 1997).

Triacylglycerols (TAG) Analysis by Ultra-high-Performance Liquid Chromatography (U-HPLC)

TAG analysis was performed by U-HPLC (ACQUITY UPLC H-Class System, Waters Corp., Milford, Massachusetts, USA) according to the AOCS Official Methods Ce 5c-89 and Ce 5c-93 (AOCS 1997). Individual samples were solubilised in acetone to form a 5% w/v solution. The solution was then filtered through a 0.2 µm syringe filter. Exactly 1 µL of the solution was then injected through an ACQUITY UPLC® BEH C18 column (Waters Corp., Milford, Massachusetts, USA) with particle size of 1.7 µm, i.d. 2.1 mm × 150 mm length, and maintained at 30°C. The flowrate was fixed at 0.25 mL min^{-1}. TAG were detected using refractive index detector set at 35°C with full scale setup at 100 µRIU for 20-30 min of total run times.

TABLE 1. INITIAL QUALITY OF CRUDE PALM OIL (CPO) AND SOLVENT EXTRACTED PALM PRESSED-FIBRE OIL (PPFO) FROM DIFFERENT COMMERCIAL PLANTS

	CPO (this study)	PPFO commercial I (this study)	PPFO commercial II (Ummi Kalsum and Rohaya, 2019)	PPFO commercial III (Nur Sulihatimarsyila *et al.*, 2019)	MS 814:2007 specification (Farah Khuwailah *et al.*, 2019)
FFA (%)	3.1 – 4.5	5.38 – 8.26	5.09 – 10.6	5.30 ± 0.19	<5%
DOBI value	2.43 – 2.83	1.62 – 2.02	1.15 – 2.17	2.02 ± 0.18	>2.3
Oxidative stability (hr)	14 – 17	18 – 25	-	-	-
Iodine value (ppm)	49.11 – 51.22	51.96 – 53.22	-	-	52 ± 0.66
Phosphorus content (ppm)	16 – 27	214 – 247	217 – 1 063	633 ± 83	<10
Chloride content (ppm)	1.95 – 10.89	23.41 – 127.23	207.62 – 379.58	-	-
Carotene content (ppm)	537 – 572	1 258 – 1 750	1 025 – 1 913	1 467 ± 35	500 – 600
Vitamin E (ppm)	771 – 1 108	1 686 – 2 600	1 574 – 2 999	1 527 ± 73	-
Hexane concentrations (ppm)	N/A	111 – 4 046	-	-	-

Note: The solvent extracted PPFO was collected from: (I) eight, (II) nine, (III) one, solvent extraction plants in Peninsular Malaysia.
Results are mean values and ± standard deviation (n=3) of oil samples.
FFA – free fatty acid; DOBI - deterioration of bleachability index; N/A - not applicable.

Vitamin E

The vitamin E (tocopherols and tocotrienols) content was determined using HPLC and fluorescence detector (Agilent Technologies), with C18 column (150 mm x 4.6 mm i.d.). Mobile phase was acetonitrile/methanol (50:50 v/v) with 1.0 mL min^{-1} flow.

Squalene and Sterols

CPO, PPFO and blended samples were pre-treated using saponification method prior to analyses of sterols and squalene following the MPOB Test Method (MPOB, 2005). Samples weighing 5.0 g each were mixed with 2.5 g 10% (w/v) potassium hydroxide (KOH) in an ethanolic solution. The mixture was refluxed for 1 hr at temperatures between 70°C-80°C. Hexane was used to extract the unsaponifiable matters from the saponified mixture. Hexane was then removed from the mixture using rotary evaporator and the extracts were then washed using distilled water until a neutral pH was obtained. The remaining moisture was removed using sodium sulphate (Na_2SO_4). The samples were then dissolved in 100% *n*-hexane to an appropriate concentration. The diluted samples were analysed using gas chromatography (GC) Autosystem XL, Perkin Elmer with FID. The samples were separated in the capillary column purchased from Supelco SAC™ -5 (Sigma) (30 mm x 0.25 mm i.d.) bonded with a 0.25 µm film of 5% phenyls/95% dimethylpolysiloxane in the presence of helium gas as mobile phase (Nor Faizah *et al.*, 2020).

RESULTS AND DISCUSSION

Effect on Residual Hexane Concentration

Figure 1 shows the typical flow process of the solvent extraction system that has been commercially used in Malaysia. A non-polar solvent, hexane, is utilised for extraction. This solvent has been used in various vegetable oil extractions, such as rapeseed and soybean (Kumar *et al.*, 2017). Hexane is one of the most widely used solvents in edible oil extractions due to its excellent performance in oil recovery, high solubilising ability and evaporation at narrow boiling temperature (63°C-69°C) (Kumar *et al.*, 2017). Solvent extraction for PPFO production uses high temperatures between 80°C-140°C. The solvent, evaporated through desolventisation of PPF in the desolventiser-toaster (*Figure 1*) and from miscella in the distillation column was carried over into atmospheric condenser to be converted into liquid and later deposited back into the solvent tank (Serrato, 1981). However, there is still excess solvent that would probably be trapped in the miscella which contains oil, gums, waxes and water. Hexane would likely be eliminated further during the refining stage since it is a compulsory process before the oil can be used as a food product. The final product could still contain traces amount of hexane. Several studies revealed that hexane is the most toxic of the alkanes group. If ingested, it causes nausea, vertigo, bronchial and intestinal irritation and affects the central nervous system. A study showed that there was no effect on human if exposed at concentration of up to 2000 ppm. However, it would cause dizziness, slight nausea, headache, and eye and throat irritations if exposed at 5000 ppm concentration (Clough, 2014). Therefore, it is desirable for the trace hexane in edible oil to be as low as possible.

Maximum residual level (MRL) of hexane has been established by various organisations and countries. European Union (EU) regulates the limit of hexane residues at 1 ppm (maximum) (Yousefi and Hosseini, 2017), while in Korea, the maximum level is 5 ppm (Oh *et al.*, 2005). Static headspace analyses using GC-FID and gas chromatography mass spectrometric detector (GC-MSD) were developed to detect residual hexane in food and edible oil products (Jeong *et al.*, 2017; Oh *et al.*, 2005; Othman *et al.*, 2019; Yousefi and Hosseini, 2017). *Table 1* shows the residual hexane concentrations in PPFO collected from eight solvent extraction plants in Malaysia. The hexane's concentration in PPFO ranged from 111-4046 ppm. Results showed that the hexane level in blended oils increased with the increment in PPFO dosage (from 5%-25% w/w of CPO), ranging from 3 ± 0.04 ppm to 18 ± 0.2 ppm, respectively (*Figure 2*). These results indicated that hexane level in blended oils depended on the initial concentration of residual hexane in PPFO.

Effect on Free Fatty Acid (FFA)

The FFA content in palm oil indicates the deterioration level of oil, which then determines the value of the oil (Japir *et al.*, 2017; Saad *et al.*, 2007). *Table 1* depicts the respective quality of CPO and PPFO from this study compared to other researchers' findings. Results showed that PPFO has higher FFA values compared to CPO. The FFA values of PPFO and CPO were 5.38%-8.26% and 3.1%-4.5%, respectively. The maximum level of FFA value in CPO is below 5%, as specified by Palm Oil Refiners Association Malaysia (PORAM) in Malaysian Standard MS814:2007 (Farah Khuwailah *et al.*, 2019). Ummi Kalsum and Rohaya (2019) reported that FFA values of PPFO produced from nine solvent extraction plants in their survey were in the range of 5.1%-10.6% (*Table 1*), higher than those of CPO. PPFO's inferior quality could be contributed by longer storage and exposure of PPMF to atmospheric conditions prior to extraction (Neoh *et al.*, 2011; Nur

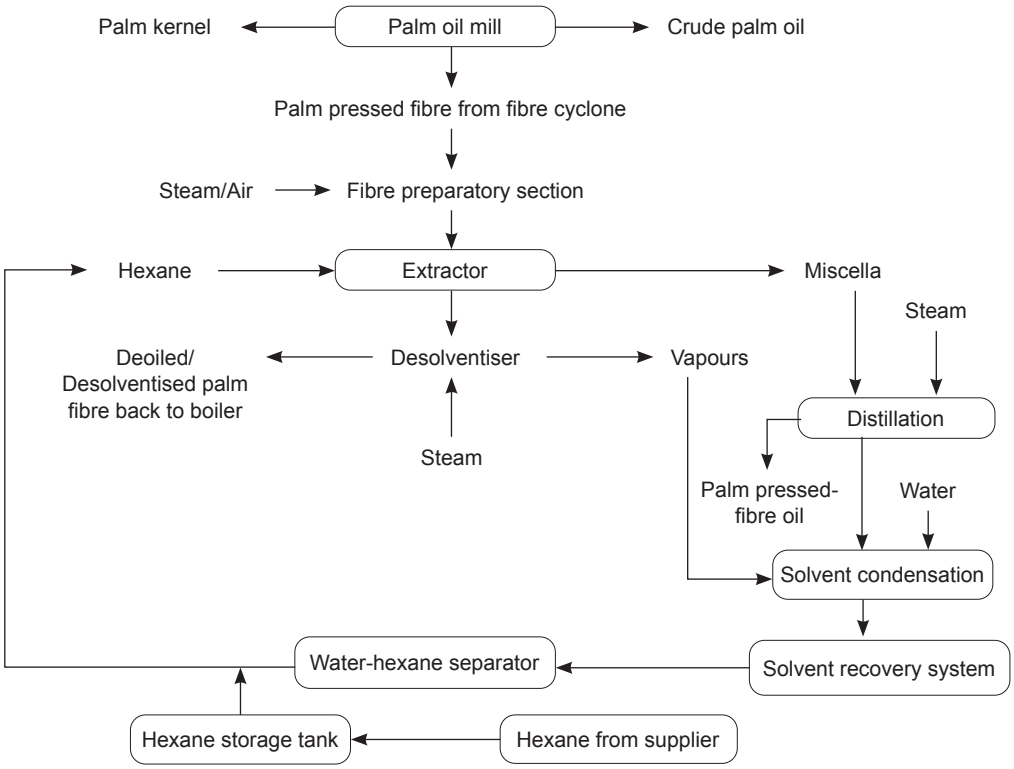

Figure 1. Process flow of solvent extraction plant.

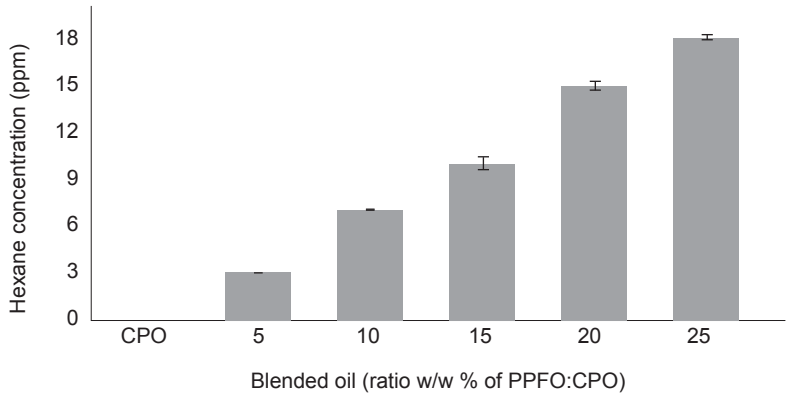

Figure 2. Hexane concentration of crude palm oil (CPO) blended with different dosage of palm pressed-fibre oil (PPFO). Results are mean values (n=3) by triplicate blending oil samples. Error bars represent the standard deviations of mean values.

Sulihatimarsyila *et al.*, 2019; Rusnani *et al.*, 2012). High extraction temperature also led to hydrolysis of the residual oil and thus, increased the FFA values (Bahadi *et al.*, 2016; Che Man, *et al.*, 1999; Japir *et al.*, 2017; Rusnani *et al.*, 2012). *Table 1* exhibited that PPFO and CPO have various initial FFA values and theroretically correlated with the effects of physical blending on the quality properties. As a result, blending of PPFO with CPO gradually increased FFA values from 3.42 ± 0.04% to 3.91 ± 0.06% with the increased in PPFO from 0%-25% (w/w of CPO) as shown in *Figure 3*. This result indicates that FFA value would increase by 2% for every 5% (w/w) PPFO dosage into CPO.

Effect on Deterioration of Bleachability Index (DOBI)

The DOBI indicates the oxidation rate of the product and the ease of refining for the oil. High DOBI value implies that the fruit is fresh, ripe and free of contaminants. Results showed that DOBI values for PPFO were relatively lower than CPO, from 1.62 to 2.02 and 2.43 to 2.83, respectively (*Table 1*). The result was in agreement with other studies conducted by Ummi Kalsum and Rohaya (2019) and Nur Sulihatimarsyila *et al.* (2019). DOBI value is one of the main indicators to show the deterioration of the oil. Good quality oil

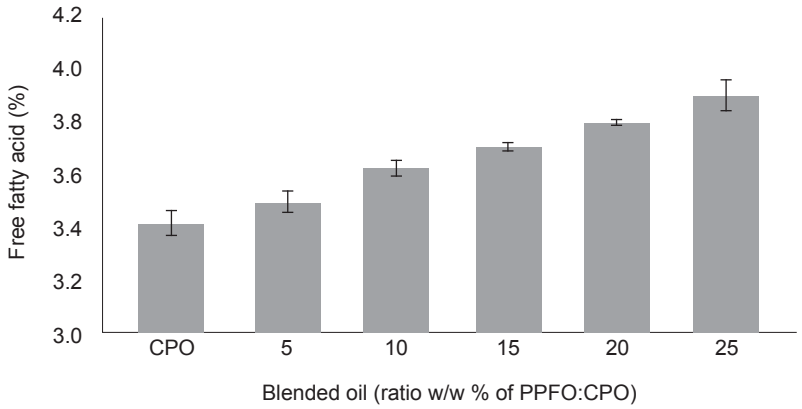

Figure 3. Free fatty acid (FFA) value of crude palm oil (CPO) blended with different dosage of palm pressed-fibre oil (PPFO). Results are mean values (n=3) by triplicate blending oil samples. Error bars represent the standard deviations of mean values.

has a DOBI value of more than 2.3 as specified in MS 814:2007 (Farah Khuwailah *et al.*, 2019). Overheating and oxidation of palm pressed fibre during processing could have contributed to low DOBI value (Rusnani *et al.*, 2012; Tan *et al.*, 2017). Other factors contributing to low DOBI values are prolonged storage before processing and contamination by other materials contained in the pressed fibre. Ummi Kalsum and Rohaya (2019) suggested that the variation in DOBI values among the mills could be attributed to differences in operating parameters and mill practices for solvent extraction. Blending results showed that the DOBI values decreased from 2.76 ± 0.04 to 2.33 ± 0.03 with the increment of PPFO dosage (from 0%-25% w/w) into CPO as shown in *Figure 4*. These results showed that the decrease in DOBI values is proportional to the addition of PPFO into CPO. This blending result indicates that blending more than 25% (w/w) PPFO into CPO will lower DOBI values to less than 2.3, lower than the specification of PORAM in MS 814:2007 (Farah Khuwailah *et al.*, 2019).

Effect on Phosphorus Content

The phosphatides content in good quality CPO normally ranged between 10-20 ppm. Elemental analysis of phosphorus (P) indicated the presence of phospholipids in oil. Previous study showed that good quality CPO containing lower phosphorus content (below than 20 ppm) would exhibit very low level of trace metals, such as iron and copper. Ai (1990) reported that the ideal amount of phosphorus content for good quality CPO is 15 ppm. High acidity CPO which showed high phosphorus content, exceeding 30 ppm, would affect the oil stability which imparts undesirable level of impurities and gums trace metals such as iron and copper. Studies also showed that high amount of phospholipids would destroy the vitamin A in CPO (Goh *et al.*, 1984; Lau *et al.*, 2006; Rakmi *et al.*, 1983). It is thus, desirable to have low phospholipids levels in the blended oils for better oxidative stability and easier bleaching process. However, results from this study showed that PPFO contain significant

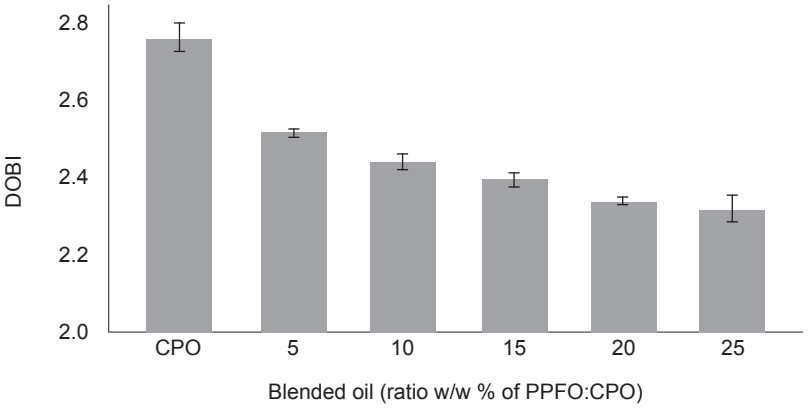

Figure 4. Deterioration of bleachability index (DOBI) of crude palm oil (CPO) blended with different dosage of palm pressed-fibre oil (PPFO). Results are mean values (n=3) by triplicate blending oil samples. Error bars represent the standard deviations of mean values.

amount of phosphorus (214-247 ppm), while CPO has lower phosphorus content (16-27 ppm) (*Table 1*). Ummi Kalsum and Rohaya (2019) also reported phosphorus content of up to 1063 pm in PPFO sample in one of the palm oil mills surveyed by MPOB (*Table 1*). As reported by Goh *et al.* (1982), oil from solvent extracted ripe fruits mesocarp fibre contains high amount of phospholipids (1000-2000 ppm) compared to commercial CPO (20-80 ppm). Results from this study showed that phosphorus content in blended oil increased gradually from 34.67 ± 3.48 ppm to 63.84 ± 4.02 ppm as the ratio of PPFO increased from 0%-25% (w/w of CPO) (*Table 2*). This shows that high PPFO dosage will increase the phosphorus level in CPO, which in turn, will complicate the CPO refining process. Consequently, high amount of bleaching earth is required, which subsequently incur high cost for refining processes (Lau *et al.*, 2013; Ummi Kalsum and Rohaya, 2019). In addition, the initial phosphorus content in CPO and PPFO is crucial to ensure blending CPO with PPFO would not affect the downstream processing. This blending result suggested that phosphorus content will increase by 15% for every 5% (w/w) of PPFO blended into CPO.

Effect on Chlorine Content

Chloride ion was identified as one of the main precursor of 3-MCPD esters formation in refined palm oil (Freudenstein *et al.*, 2013; Ramli *et al.*, 2015). 3-MCPD esters is generally formed when acylglycerols in oil reacted with high temperature (260°C) in the presence of chloride ion during deodourisation in refining process (Parveez *et al.*, 2019; Ramli *et al.*, 2015). In a random survey led by MPOB, the total chlorine content in CPO from eight palm oil mills in 2018 and 2019 ranged from 1.95-10.89 ppm (Ramli *et al.*, 2015; Ummi Kalsum and Rohaya, 2019). Several years later, Ummi Kalsum and Rohaya (2019) reported that PPFO contains 23.41-127.23 ppm of chlorine as depicted in *Table 1*. Theroretically, physical blending of CPO with PPFO would result in increment of chlorine contents in the blended oil. The concentration of chlorine in the blended oils increased, with the increased in PPFO dosage (from 0%-25% w/w of CPO) with the results being in the range from 3.85-7.49 ppm. Consequently, this resulted in the increment of 3-MCPD esters formation in blended oil and in refined palm oil when heated at higher temperature (Ramli *et al.*, 2015). Study conducted by Ummi and Rohaya (2019) is an evident that blending CPO with PPFO would increase 3-MCPD esters from 0.2-15 ppm when PPFO was added up to 10% (w/w) into CPO. In fact, in October 2018, the European commission suggested two maximum levels of 3-MCPD esters in refined vegetable oil, which are 1.25 ppm for oils and fats (coconut, maize, rapeseed, sunflower, soybean and palm kernel) and 2.5 ppm for other vegetables oil, fish oil and also mixture of oils and fats (Parveez *et al.*, 2019; Ummi Kalsum and Rohaya, 2019).

Effect on Heavy Metal Content

Rakmi *et al.* (1983) reported that heavy metals such as iron and copper are active prooxidants that would accelerate the oxidation process in CPO. Heavy metals would also catalyse the decomposition of hydroproxides to free radicals and hastened the oxidation process. Flider and Orthoefer (1981) reported that similar reaction was observed in other oils such as soybean oil where its quality deteriorated when iron and copper's concentrations were greater than 30 ppb and 5 ppb, respectively. Ames *et al.* (1960) also reported that high amount of iron content in CPO would complicate the bleaching process in refinery, while copper would increase the colour of refined palm oil from 2.0 to 4.8 Red Lovibond. Previous studies showed that maximum level of iron and copper in

TABLE 2. TRACE ELEMENTS CONTENT IN CRUDE PALM OIL (CPO), PALM PRESSED-FIBRE OIL (PPFO) AND BLENDED OILS (BO)

Samples	Trace elements concentration (ppm)			
	Iron (Fe)	Copper (Cu)	Phosphorus (P)	Chloride (Cl)
PPFO	45.09 ± 0.03	0.66 ± 0.02	228.05 ± 0.04	23.41 ± 0.03
CPO	13.58 ± 0.02	0.19 ± 0.03	34.67 ± 0.01	3.85 ± 0.02
BO5%PPFO	14.63 ± 0.02	0.22 ± 0.01	44.23 ± 0.03	5.13 ± 0.04
BO10%PPFO	15.45 ± 0.03	0.27 ± 0.02	45.72 ± 0.02	5.82 ± 0.03
BO15%PPFO	17.26 ± 0.04	0.30 ± 0.03	52.91 ± 0.02	6.49 ± 0.02
BO20%PPFO	15.96 ± 0.03	0.35 ± 0.02	57.31 ± 0.03	6.66 ± 0.03
BO25%PPFO	17.63 ± 0.02	0.38 ± 0.01	63.84 ± 0.02	7.49 ± 0.02

Note: Results are mean values (n=3) by triplicate blending oil samples.

refined palm oil to be exported to Australia were 500 ppb and 10 ppb, respectively (Berger, 1982; Rakmi *et al.*, 1983). The concentrations of heavy metals in PPFO, namely iron (45.09 ppm) and copper (0.66 ppm) were higher compared to CPO (*Table 2*). Blending CPO with PPFO would result in the increment of heavy metals concentrations in the blended oil. The concentration of iron and copper in the blended oils had increased, with the increase in PPFO dosage (from 0%-25% w/w of CPO) in the range from 13.58-17.63 ppm and 0.19-0.38 ppm, respectively. This result showed that high initial amount of heavy metals content in PPFO would effect the blended oils and increase by 5% for every 5% (w/w) PPFO dosage blended into CPO.

Effect on Iodine Value (IV)

IV is another important parameter that indicates the oil oxidative stability and for determining oil identities (Ayyildiz *et al.*, 2015; Talpur *et al.*, 2010). Determination of IV involved measuring the degree of unsaturation or double bonds in fats and oils. Higher IV indicates greater degree of unsaturation, hence, lower oxidative stability (Soek *et al.*, 2019). *Table 1* shows that the IV of CPO was higher than PPFO with the values ranges from 51.96-53.22 and 49.11-51.22, respectively. The decrease in IV in PPFO can be attributed to the destruction of double bonds by oxidation or polymerisation. Comparing with CPO, the IV in blended oils decreased from 51.96 ± 0.37 to 50.21 ± 0.03 with the increased in PPFO dosage from 0% to 25% w/w of CPO (*Figure 5*). This indicated that there is an increase in saturated fatty acids (SFA) when CPO is blended with PPFO as this oil contained high SFA compositions (*Table 4*). This result is in agreement with findings by Soek *et al.* (2019) which indicated that IV in PPFO is lower than CPO, implying a higher saturation level in PPFO as compared to CPO.

Effect on Oil Oxidative Stability

Oxidative stability is a significant parameter in evaluating the shelf life of oils and fats. FAC and minor components such as tocols, FFA and IV could affect the oil oxidative stability (Ayyildiz *et al.*, 2015; Bozan and Temelli, 2008; Cao *et al.*, 2014). Oxidative stability is interrelated with the compositions of fatty acids, in which when more unsaturated fatty acids (UFA) are present in the edible oil, the oxidation reaction will occur faster (Liu and White, 1992; Magdalena *et al.*, 2018; Ramli *et al.*, 2017). CPO contains slightly higher UFA (51.96%) compared to PPFO (49.11%) (*Table 4*). UFA in palm oil comprises of C18:3 (linolenic acid), C18:2 (linoleic acid) and C18:1 (oleic acid). Previous studies have found that linolenic acid was the first to be oxidised, followed by linoleic acid and oleic acid (Liu and White, 1992; Magdalena *et al.*, 2018). CPO showed lower oxidative stability with shorter induction time (14-17 hr) in Rancimat test compared to PPFO (18-25 hr) (*Table 1*). As a result, blending PPFO with CPO stabilised the CPO, whereby the oxidative values of the blended oils varied from 14.31 ± 1.50 hr to 16.76 ± 0.74 hr. The oxidative stability of the blended oils of up to 25% (w/w) PPFO was comparable to CPO as depicted in *Figure 6*. PPFO contains of high amount of carotenes that consist of antioxidants properties. This would contribute to the increased stability of the blended oils.

Effect on Phytonutrients Content

Table 3 shows the phytonutrients content in CPO, PPFO and blended oils. PPFO that was commercially produced by solvent extraction at the palm oil mill contained higher amount of carotenes (1258-1750 ppm) compared to CPO (537-572 ppm) (*Table 1*). These results are in agreement

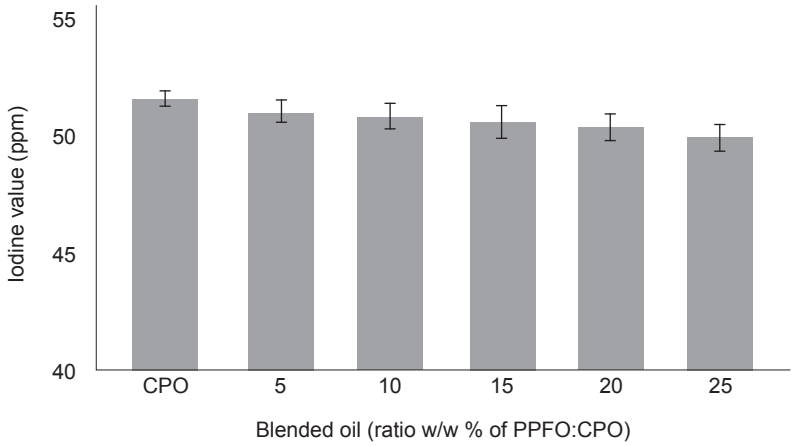

Figure 5. Iodine value (IV) of crude palm oil (CPO) blended with different dosage of palm pressed-fibre oil (PPFO). Results are mean values (n=3) by triplicate blending oil samples. Error bars represent the standard deviations of mean values.

TABLE 3. PHYTONUTRIENTS CONTENT IN CRUDE PALM OIL (CPO) PALM PRESSED-FIBRE OIL (PPFO) AND BLENDED OILS (BO)

Phytonutrients	CPO	PPFO	Blended oil (% w/w PPFO: CPO)				
			BO5%PPFO	BO10%PPFO	BO15%PPFO	BO20%PPFO	BO25%PPFO
Carotene (ppm)	539 ± 14	1 481 ± 27	554 ± 5	608 ± 68	609 ± 22	623 ± 14	654 ± 8
Sterol (ppm)	433 ± 8	1 529 ± 1	444 ± 25	497 ± 15	540 ± 33	629 ± 21	808 ± 17
Squalene (ppm)	475 ± 7	1 721 ± 10	780 ± 8	881 ± 5	962 ± 4	1 048 ± 7	1 201 ± 9
Vitamin E (ppm)	1 185 ± 64	1 609 ± 71	1 489 ± 9	1 494 ± 10	1 591 ± 22	1 607 ± 89	1 626 ± 92
Composition of tocopherol and tocotrienol (%)							
• α-tocopherol	5	24	5	5	6	6	7
• α, β, γ, δ-tocotrienols	95	76	95	95	94	94	93

Note: Results are mean values (n=3) by triplicate blending oil samples.

TABLE 4. COMPARISON OF FATTY ACID COMPOSITIONS AND ACYLGLYCERIDES OF CRUDE PALM OIL (CPO), PALM PRESSED-FIBRE OIL (PPFO) AND BLENDED OILS

	CPO	PPFO	Blended oil (% w/w PPFO: CPO)					MS 814:2007
			BO5%PPFO	BO10%PPFO	BO15%PPFO	BO20%PPFO	BO25%PPFO	
Fatty acid compositions (%)								
Saturated fatty acids (SFA)								
C12:0	0.19 ± 0.02	1.33 ± 0.05	0.24 ± 0.01	0.28 ± 0.01	0.34 ± 0.01	0.39 ± 0.02	0.42 ± 0.03	0.1 – 0.4
C14:0	1.00 ± 0.02	1.34 ± 0.01	1.00 ± 0.02	1.02 ± 0.00	1.03 ± 0.02	1.05 ± 0.01	1.07 ± 0.01	1.0 – 1.4
C16:0	45.69 ± 0.09	41.22 ± 0.02	45.56 ± 0.21	45.16 ± 0.14	44.82 ± 0.04	44.63 ± 0.05	44.44 ± 0.02	40.9 – 47.5
C18:0	3.97 ± 0.08	4.09 ± 0.06	4.18 ± 0.17	4.10 ± 0.03	4.07 ± 0.03	4.09 ± 0.03	4.13 ± 0.04	3.8 – 4.8
Unsaturated fatty acids (UFA)								
C18:1	41.96 ± 0.01	39.24 ± 0.08	39.30 ± 0.27	39.55 ± 0.08	39.57 ± 0.09	39.69 ± 0.08	39.77 ± 0.01	36.4 – 41.2
C18:2	10.00 ± 0.08	9.87 ± 0.02	9.70 ± 0.10	9.87 ± 0.07	9.92 ± 0.04	9.89 ± 0.03	9.90 ± 0.02	9.2 – 11.6
Acylglycerides (%)								
MAG/FFA	5.06 ± 0.01	11.44 ± 0.01	5.38 ± 0.01	5.61 ± 0.03	5.84 ± 0.02	6.05 ± 0.05	6.28 ± 0.00	N/A
DAG	5.58 ± 0.03	9.51 ± 0.06	5.74 ± 0.08	5.88 ± 0.02	6.03 ± 0.02	6.30 ± 0.02	6.32 ± 0.03	N/A
TAG	89.36 ± 0.07	79.05 ± 0.04	88.89 ± 0.03	88.52 ± 0.02	88.13 ± 0.02	87.74 ± 0.06	87.44 ± 0.02	N/A

Note: MAG - monoacylglycerols; DAG - diacylglycerols; TAG - triaclyglycerols; FFA - free fatty acid; BO - blended oil; N/A - not available. Results are mean values (n=3) by triplicate blending oil samples.

with findings by Ummi Kalsum and Rohaya (2019), who reported carotenes content in PPFO can be up to 1913 ppm. The carotenes content in blended oils increased from 539 ± 14 ppm to 654 ± 8 ppm with the increment in PPFO dosage (from 0%-25% w/w of CPO). Vitamin E (tocopherols and tocotrienols) in palm oil comprises of four major isomers: α-tocopherol, α-tocotrienol, γ-tocotrienol and δ-tocotrienol. Vitamin E is well-known for its antioxidant and nutritional values (Lau *et al.*, 2007; 2008; Neoh *et al.*, 2011; Ng and Choo, 2011; Nur Sulihatimarsyila *et al.*, 2019; Rusnani *et al.*, 2012). *Table 3* shows that PPFO has higher amount of vitamin E (1609 ± 71 ppm) compared to CPO (1185 ± 64 ppm). The α-tocopherol content in PPFO was higher (24% of total tocols) than CPO (5% of total tocols) (*Table 3*). These results are consistent with data obtained from previous findings (Choo *et al.*, 1996; Goh *et al.*, 1985; Ng and Choo, 2011; Rusnani *et al.*, 2012). Results also showed that the composition of tocotrienols in PPFO, which comprised of α-tocotrienol, γ-tocotrienol and δ-tocotrienol, was lower (76% of total tocols than CPO (95% of total tocols). However, blending CPO with PPFO affected the tocotrienols and tocopherol compositions in blended oils (*Table 5*). Compositions of tocopherol in blended oils increased from 5%-7% of total tocols while tocotrienols composition decreased from 95%-93% of total tocols with the increment in PPFO dosage from 0%-25% (w/w), respectively. PPFO is also rich in sterols and squalene (*Table 3*). The concentration of sterols in PPFO (1529 ± 1 ppm) was higher than CPO (433 ± 8 ppm). Squalene content in PPFO (1721 ± 10 ppm) was higher than CPO

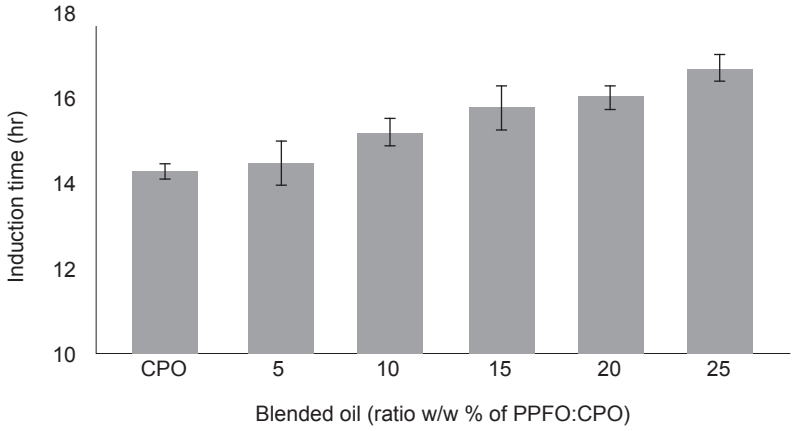

Figure 6. Oxidative stability of crude palm oil (CPO) blended with different dosage of palm pressed-fibre oil (PPFO). Results are mean values (n=3) by triplicate blending oil samples. Error bars represent the standard deviations of mean values.

(475 ± 7 ppm). Blending of CPO with PPFO from 0%-25% (w/w) dosage increased the concentrations of sterols and squalene in the blended oils, from 433 ± 8 ppm to 808 ± 17 ppm and 475 ± 7 ppm to 1201 ± 9 ppm, respectively.

Effect on Fatty Acid Compositions (FAC) and Acylglycerides

PPMF from the palm oil mill consists of a mixture of palm mesocarp fibre, shell, crushed kernel and debris. Hence, the oil recovered from this mixture has the characteristics of all these products (Lau *et al.*, 2006; Rusnani *et al.*, 2012). The nutritional status of palm oil is determined by the types of fatty acids contained in palm oil, which consists approximately 50% SFA with 45% palmitic acid (C16:0), 5% stearic acid (C18:0), and trace amount of myristic acid (C14:0) and lauric acid (C12:0) (Sambanthamurthi *et al.*, 2000). The UFA consist of approximately 40% oleic acid (C18:1), and 10% polyunsaturated linoleic acid (C18:2) and linolenic acid (C18:3) (Noh *et al.*, 2002; Sambanthamurthi *et al.*, 2000). *Table 4* shows the comparison of FAC in PPFO and CPO. The FAC of PPFO is quite similar to CPO with palmitic (41.22 ± 0.02%) and oleic acids (39.24 ± 0.08%) being the major fatty acids. However, composition of lauric acid in PPFO was significantly higher than CPO (1.33 ± 0.05%). Presence of lauric acid in PPFO had attributed towards contamination of kernel oil as the pressed fibre comprised of mixture of broken nuts and kernels, discharged together with mesocarp fibre after mechanical pressing (Neoh *et al.*, 2011; Rusnani *et al.*, 2012). According to Siew and Berger (1981), lauric acid is present in palm kernel oil with a composition of 48%, which discriminates palm kernel oil from CPO. FAC of the blended oils samples were comparable to those of CPO and remained in the range specified by PORAM in MS 814:2007 (*Table 4*). However, composition of palmitic acid decreased slightly from 45.69 ± 0.09% to 44.44 ± 0.02% with the 0%-25% (w/w) PPFO dosage in CPO. Nevertheless, the compositions of lauric, myristic and oleic acids in blended oils increased gradually with the increase in PPFO dosages in CPO, at 0.19 ± 0.02% to 0.42 ± 0.03%, 1.00 ± 0.02% to 1.07 ± 0.01% and 39.24 ± 0.08% to 39.77 ± 0.01%, respectively. CPO constitutes mainly 90%-98% TAG, 2%-6% DAG, 2%-5% MAG/FFA and minor composition of phytonutrients (Neoh *et al.*, 2011). Results indicated that PPFO has higher DAG, 9.51 ± 0.06%, compared to CPO (5.58 ± 0.03%). On the other hand, the TAG content in PPFO (79.05 ± 0.04%) was lower than CPO (89.36 ± 0.07%) (*Table 4*). It was found that the compositions of DAG in blended oils with PPFO dosage from 0%-25% increased slightly, ranging from 5.58 ± 0.03% to 6.32 ± 0.03%, whilst TAG decreased from 89.36 ± 0.07% to 87.44 ± 0.02%.

CONCLUSION

This study has shown that blending CPO with PPFO would deteriorate the original CPO quality, by lowering DOBI and IV and increase levels of phosphorus, FFA, hexane and trace metals, even at low dosage of PPFO. Results indicated that PPFO produced from the commercial solvent extraction plant shows various initial properties. Blending results depicted that physical blending properties would be dependent on initial properties of PPFO and CPO. Furthermore, this blending analysis shows an increment in chloride content, which is one of the main precursors of 3-MCPD esters formation. Thus, it is not recommended to blend PPFO into CPO, as the blended oil deteriorate CPO quality. Nevertheless, PPFO has better quality than CPO in terms of phytonutrient contents, signifying its potential in other applications. Instead of blending PPFO with CPO, it is suggested for PPFO to be classified as valuable oil and sold as pharma-

industrial grade oil since it is rich in phytonutrient and it is suitable for other applications such as pharmaceutical industry and biodiesel.

ACKNOWLEDGEMENT

The authors would like to thank the Director-General specifically and management of MPOB generally for the support in conducting this research.

REFERENCES

Ai, T Y (1990). Analytical techniques in palm and palm kernel oil specifications. 10th Palm Oil Familiarisation Programme (POFP). Bangi.

Ames, G R; Raymond, W D and Ward, J B (1960). The bleachability of Nigerian palm oil. *J. Sci. Food Agric., 2*: 194-202.

AOCS (1997). Quantitative separation of monoglycerides, diglycerides, and triglycerides by silica gel column chromatography. Official Methods and Recommended Practices of the AOCS. AOCS Press, Champaign, Recommended Practice Cd 11c-93.

ASTM (2004). Standard Test Methods for Determination of Organic Chloride Content in Crude Oil (ASTM D4929-04). ASTM International. West Conshohocken, PA, USA.

Awalludin, M F; Sulaiman, O; Hashim, R and Nadhari, W N A W (2015). An overview of the oil palm industry in Malaysia and its waste utilization through thermochemical conversion, specifically via liquefaction. *Renew. Sust. Energ. Rev., 50*: 1469-1484. DOI: 10.1016/j.rser.2015.05.085.

Ayyildiz, H F; Topfaka, M; Kara, H and Sherazi, S T H (2015). Evaluation of fatty acid composition, tocols profile and oxidative stability of some fully refined edible oils. *Int. J. Food Prop., 18(9)*: 2064-2076.

Azmil Haizam, A T; Raznim Arni, A R; Abdul Niefaizal, A H and Ainie, K (2019). Effect of anti-clouding agent on the fate of 3-Monochloropropane-1,2-diol esters and glycidyl esters in palm olein during repeated frying. *Molecules, 24*: 23-32. DOI: 10.3390/molecules24122332.

Bahadi, M A; Japir, A W; Nadia, S and Jumat, S (2016). Free fatty acids separation from Malaysian high free fatty acid crude palm oil using molecular distillation. *Malays. J. Anal. Sci., 20(5)*: 1042-1051.

Berger, K G (1982). Refined palm oil quality as received. *PORIM Bulletin, 4*: 57-67.

Bozan, B and Temelli, F (2008). Chemical composition and oxidative stability of flax, safflower and poppy seed. *Bioresour. Technol., 99*: 6354-6359.

Cao, J; Lia, H; Xia, X; Zou, X G; Li, J; Zhu, X M and Deng, Z Y (2014). Effect of fatty acid and tocopherol on oxidative stability of vegetable oils with limited air. *Int. J. Food Prop., 18*: 808-820. DOI: 10.1080/10942912.2013.864674.

Che Man, Y B; Moh, M H and Van De Voort, F R (1999). Determination of free fatty acids in crude palm oil and refined-bleached-deodorized palm olein using Fourier transform infrared spectroscopy. *J. Amer. Oil Chem. Soc., 76(4)*: 485-490. DOI: 10.1007/s11746-999-0029-z.

Choo, Y M; Yap, S C; Ooi, C K; Ma, A N; Goh, S H and Ong, A S H (1996). Recovered oil from palm-pressed fibre: A good source of natural carotenoids, vitamin E and sterols. *J. Amer. Oil Chem. Soc., 73*: 599-602. DOI: 10.1007/BF02518114.

Clough, S R (2014). Hexane. *Encyclopedia of Toxicology. Elsevier, 2*: 900-904. DOI: 10.1016/b978-0-12-386454-3.00397-3.

Farah Khuwailah, A B; Yeoh, C B and Najwa, S (2019). Revision of Malaysian Standard for Palm Oil- Specification MS 814:2017 (Second revision) Amendment 1:2018 - What's new? *Palm Oil Developments, 71*: 18-32.

Farhoosh, R (2007). The effect of operational parameters of the Rancimat method on the determination of the oxidative stability measures and shelf-life prediction of soybean oil. *J. Amer. Oil Chem. Soc., 84*: 205-209. DOI: 10.1007/s11746-006-1030-4.

Flider, F J and Orthoefer, F T (1981). Metals in soybean oil. *J. Amer. Oil Chem. Soc., 58(3)*: 270-272.

Freudenstein, A; Weking, J and Matthäus, B (2013). Influence of precursors on the formation of 3-MCPD and glycidyl esters in a model oil under simulated deodorization. *Eur. J. Lipid Sci. Technol., 115(3)*: 286-294.

Goh, S H; Khor, H T and Gee, P T (1982). Phospholipids of palm oil (*Elaeis guineensis*). *J. Amer. Oil Chem. Soc., 59*: 296-299.

Goh, S H; Tong, S L and Gee, P T (1984). Inorganic phosphate in crude palm oil: Quantitative analysis and correlations with oil quality parameters. *J. Amer. Oil Chem. Soc., 61*: 1601-1604.

Goh, S H; Choo, Y M and Ong, S H (1985). Minor constituents of palm oil. *J. Amer. Oil Chem. Soc., 62*: 237-240. DOI: 10.1007/BF02541384.

Japir, A A W; Salimon, J; Derawi, D; Bahadi, M; Al-Shuja'a, S and Yusop, M R (2017). Physicochemical characteristics of high free fatty acid crude palm oil. *OCL, 24(5)*. DOI: 10.1051/ocl/2017033.

Jeong, E J; Lee, S H; Kim, B T; Lee, G; Yun, S S; Lim, H S and Kim, Y S (2017). An analysis method for determining residual hexane in health functional food products using static headspace gas chromatography. *Food Sci. Biotechnol., 26(2)*: 363-368. DOI: 10.1007/s10068-017-0049-7.

Kumar, N and Gow, J G (1994). Residual solvent analysis by headspace gas chromatography. *J. Chromatogr. A, 667*: 235-440.

Kumar, S P J; Prasad, S R; Banerjee, R; Agarwal, D K; Kulkarni, K S and Ramesh, K V (2017). Green solvents and technologies for oil extraction from oil seeds. *Chem. Cent. J., 11(1)*: 1-7. DOI: 10.1186/s13065-017-0238-8.

Lau, H L N; Choo, Y M; Ma, A N and Chuah, C H (2006). Quality of residual oil from palm-pressed mesocarp fibre (*Elaeis guineensis*) using supercritical CO_2 with and without ethanol. *J. Amer. Oil Chem. Soc., 83(10)*: 893-898. DOI: 10.1007/s11746-006-5043-9.

Lau, H L N; Choo, Y M; Ma, A N and Chuah, C H (2007). Extraction and identification of water-soluble compounds in palm-pressed fibre by SC-CO_2 and GC-MS. *J. Amer. Environ. Sci., 3*: 54-59.

Lau, H L N; Choo, Y M; Ma, A N and Chuah, C H (2008). Selective extraction of palm carotene and vitamin E from fresh palm-pressed mesocarp fibre (*Elaeis guineensis*) using supercritical CO_2. *J. Food Eng., 84(2)*: 289-296. DOI: 10.1016/j.jfoodeng.2007.05.018.

Lau, H L N; Nur Sulihatimarsyila, A W and Choo, Y M (2013). Novel refining technology of palm pressed fibre oil. *MPOB Information Series No. 536*.

Lau, H L N; Nur Sulihatimarsyila, A W and Nabilah, K M (2017). Recovery and refining of palm-pressed mesocarp fiber oil. *Proc. MPOB Int. Palm Oil Congress 2017*. p. 206-216.

Liu, H R and White, P J (1992). Oxidative stability of soybean oils with altered fatty acid. *J. Amer. Oil Chem. Soc., 69*: 528-532.

Magdalena, M; Florowska, A; Dluzewska, E; Wroniak, M; Katarzyna, M L and Zbikowska, A (2018). Oxidative stability of selected edible oils. *Molecules, 23*: 1746.

Neoh, B K; Thang, Y M; Zain, M Z M and Junaidi, A (2011). Palm pressed fibre oil: A new opportunity for premium hardstock? *Int. Food Res. J., 18*: 769-773.

Ng, M H and Choo, Y M (2011). Phytonutrients in palm: Occurrence and properties. *Palm Oil: Nutrition, Uses and Impacts* (Palmetti, M L ed.). Nova Science Publishers. p. 47-71.

Noh, A; Rajanaidu, N; Kushairi, A; Rafii, M R; Mohd Din, A and Saleh, G (2002). Variability in fatty acid composition, iodine value and carotene content in the MPOB oil palm germplasm collection from Angola. *J. Oil Palm Res., 14*: 18-23.

Noorshamsiana, A W; Astimar, A A; Iberahim, N I; Nor Faizah, J; Anis, M; Hamid, F A and Kamarudin, H (2017). The quality of oil extracted from palm pressed fibre using aqueous enzymatic treatment. *J. Oil Palm Res., 29(4)*: 588-593. DOI: 10.21894/jopr.2017.0004.

Nor Faizah, J; Noorshamsiana, A W; Wan Hasamudin, W H; Kamarudin, H; Nahrul Hayawin, Z and Mohamad Faizal, I (2020). Extraction and purification of phytosterols mixture from palm fatty acid distillate (PFAD) using multistage extraction processes. *J. Oil Palm Res., 33(1)*: 93-102.

Nur Sulihatimarsyila, A W; Lau, H L N; Nabilah, K M and Nur Azreena, I (2019). Refining process for production of refined palm-pressed fibre oil. *Ind. Crop. Prod., 129*: 488-494. DOI: 10.1016/j.indcrop.2018.12.034.

Oh, C H; Kwon, Y K; Jang, Y M; Lee, D L and Park, J (2005). Headspace analysis for residual hexane in vegetable oil. *Food Sci. Biotechnol., 14(4)*: 456-460.

Onoja, E; Chandren, S; Abdul Razak, F I; Mahat, N A and Wahab, R A (2019). Oil palm (*Elaeis guineensis*) biomass in Malaysia: The present and future prospects. *Waste Biomass Valor., 10*: 2099-2117. DOI: 0.1007/s12649-018-0258-1.

Othman, A; Goggin, K A; Tahir, N I; Brodrick, E; Singh, R; Sambanthamurthi, R; Parveez, G K A; Davies, A N; Murad, A J; Muhammad, N H; Ramli, U S and Murphy, D J (2019). Use of headspace-gas chromatography-ion mobility spectrometry to detect volatile fingerprints of palm fibre oil and sludge palm oil in samples of crude palm oil. *BMC Res. Notes, 12*: 229. DOI: 10.1186/s13104-019-4263-7.

Parveez, G K A; Azmil Haizam, A T; Hasliyanti, A and Ahmad Kushairi, D (2019). Palm oil sterilisation technologies and their implications on oil loss, quality and food safety. *International Planters Conference*. 15-17 July 2019. p. 97-108.

Parveez, G K A; Hishamudin, E; Loh, S K; Meilina, O A; Salleh, K M; Bidin, M N I Z; Sundram, S; Hasan, Z A A H and Idris, Z (2020). Oil palm economic performance in Malaysia and R&D progress in 2019. *J. Oil Palm Res., 32(2)*: 159-190.

Phoon, K Y; Ng, H S; Rabitah, Z; Yim, H S and Mokhtar, M N (2018). Enrichment of minor components from crude palm oil and palm-pressed mesocarp fibre oil via sequential adsorption-desorption strategy. *J. Ind. Crops Prod., 113*: 187-195.

Rakmi, A R; Kalm, M and Wan Nor, W M (1983). Reduction of palm oil heavy metal content in the refining process. *PORIM Bulletin, 9*: 16-21.

Ramli, N A S; Mohd Noor, M A; Musa, H and Ghazali, R (2017). Stability evaluation of quality parameters for palm oil products at low temperature storage. *J. Sci. Food Agric., 98(9)*: 3351-3362.

Ramli, M R; Siew, W L; Ibrahim, N A; Kuntom, A and Abd. Razak, R A (2015). Other factors to consider in the formation of chloropropandiol fatty esters in oil processes. *Food Addit. Contam.: Part A: Chem. Anal. Control Expo. Risk Assess., 32(6)*: 817-824.

Rusnani, A M; Mohammad, A W and Choo, Y M (2012). Properties of residual palm pressed fibre oil. *J. Oil Palm Res., 24*: 1310-1317.

Saad, B; Ling, C W; Jab, M S; Lim, B P; Mohamad Ali, A S; Wai, W T and Saleh, M I (2007). Determination of free fatty acids in palm oil samples using non-aqueous flow injection titrimetric method. *Food Chem., 102(4)*: 1407-1414. DOI: 10.1016/j.foodchem.2006.05.051.

Sambanthamurthi, R; Sundram, K and Tan, Y (2000). Chemistry and biochemistry of palm oil. *Prog. Lipid Res., 39*: 507-558.

Sarmidi, M R; Enshasy, H A E and Hamid, M A (2009). Oil palm: The rich mine for pharma, food, feed and fuel industries. *American-Eurasian J. Agric. Environ. Sci., 5(6)*: 767-776.

Serrato, A G (1981). Extraction of oil from soybeans. *J. Amer. Oil Chem. Soc., 58*: 157-159.

Siew, W L and Berger, K G (1981). Malaysian palm kernel oil chemical and physical characteristics. *PORIM Technology, 6*. PORIM, Bangi.

Soek, S T; Harrison, L N L and Siau, H M (2019). Palm-pressed mesocarp fibre oil as an alternative carrier oil in emulsion. *J. Oleo Sci., 68(8)*: 803-808.

Talpur, M Y; Sherazi, S T H; Mahesar, S A and Bhutto, A A (2010). A simplified UV spectrometric method for determination of peroxide value in thermally oxidized canola oil. *Talanta, 80*: 1823-1826.

Tan, C H; Ariffin, A A; Ghazali, H M; Tan, C P; Kuntom, A and Choo, A C (2017). Changes in oxidation indices and minor components of low free fatty acid and freshly extracted crude palm oils under two different storage conditions. *J. Food Sci. Technol., 54(7)*: 1757-1764. DOI: 10.1007/s13197-017-2569-9.

Ummi Kalsum, H M N and Rohaya, M H (2019). Pressed fibre oil: Quality and implication. *Palm Oil Engineering Bulletin, 131*: 16-21.

Valeria, D P; Felipe, C L; Raquel, G V; Rafael, M; Roger, W; Ayres, P L; Denis, M G F; Maria, A; Apostolis, K; Marcio, A A M and Marcelo, B R (2017). Ultrasound-assisted extraction of bioactive compounds from palm pressed fibre with high antioxidant and photoprotective activities. *J. Ultrason. Sonochem., 36*: 362-366.

Vijaya, S; Ravi Menon, N; Helmi, S and Choo, Y M (2013). The development of a residual oil recovery system to increase the revenue of a palm oil mill. *J. Oil Palm Res., 25*: 116-122.

Workman, D (2020). Palm oil imports by country. http://www.worldstopexports.com/palm-oil-imports-by-country/, accessed on 21 July 2020.

Yusoff, S (2006). Renewable energy from palm oil-Innovation on effective utilization of waste. *J. Clean. Prod., 14(1)*: 87-93. DOI: 10.1016/j.jclepro.2004.07.005.

Yousefi, M and Hosseini, H (2017). Evaluation of hexane content in edible vegetable oils consumed in Iran. *J. Exp. Clin. Toxicol., 1*: 27-30. DOI: 10.14302/issn.2641-7669.ject-17-1790.

Journal of Oil Palm Research Vol. 34 (1) March 2022 p. 92-103
DOI: https://doi.org/10.21894/jopr.2021.0022

NUTRIENT ENHANCEMENT OF PALM KERNEL CAKE VIA SOLID STATE FERMENTATION BY LOCALLY ISOLATED *Rhizopus oryzae* ME01

MOHD FIRDAUS, O[1]*; ROHAYA, M H[1]; MISKANDAR, M S[1] and ASTIMAR, A A[1]

ABSTRACT

Palm kernel cake (PKC) is abundantly generated in palm kernel crushing plant throughout the year. Its use as monogastric animal food source is very limited due to its high fibre and moderate protein content. Therefore, this study is aimed to enhance PKC nutritional value, particularly the protein content through solid state fermentation (SSF), using a locally isolated fungus. Fungal identification was performed using partial 18S ribosomal ribonucleic acid (rRNA) nucleotide sequence. A fungus containing 600 base pairs was sequenced and aligned with GenBank database and named Rhizopus oryzae *ME01. SSF was carried out using palm kernel expeller (PKE) which is mechanical pressed and PKC which is solvent extracted, as a single carbon source with minimum mineral addition. Results showed that SSF successfully increased crude protein and ash content of fermented PKC and PKE, respectively. Interestingly, this study also found that the size of PKC's particle had impacted protein content of fermented palm kernel cake (fPKC) during SSF. PKC which has a smaller and uniform size than PKE, gave higher crude protein increment than fermented palm kernel expeller (fPKE). However, the protein content of fPKE had increased by 7.64% more than fPKC which was only 3.45%. Thus, fPKE appeared to enhance PKE's nutrient value, especially for monogastric animal feed applications.*

Keywords: fungus identification, nutrient enhancement, palm kernel cake, solid state fermentation.

Received: 6 November 2020**; Accepted:** 17 February 2021**; Published online:** 19 May 2021.

INTRODUCTION

Raw material for feed formulation in livestock industry, particularly for non-ruminant, such as poultry, depends entirely on the imported raw materials, which resulted in high overall feed cost. The main imported raw materials for non-ruminant feed, such as maize and soybean meal, require approximately RM2.5 billion per year, with maize accounting for more than 50% (Wan Zahari and Wong, 2009). Majority of the livestock gross domestic product (GDP) is contributed mainly by the poultry sub-sector at 62.9%, while the ruminant sub-sector only contributed 12.1% (Shanmugavelu, 2014). It is therefore crucial to reduce the dependency on imported raw materials by using local raw materials in feed formulation for non-ruminants. Palm kernel cake (PKC) appears to be an alternative protein source in livestock feed formulation to stabilise the feed price.

In 2019, Malaysia produced 19.86 million tonnes of crude palm oil (CPO) and 2.59 million tonnes of PKC after 2.29 million tonnes of crude palm kernel oil (CPKO) was extracted (Parveez *et al.*, 2020; Malaysian Palm Oil Board, 2020). Currently, there are two technologies to process palm kernel in the mills, which are solvent extraction and mechanical press. The product produced via solvent extraction is called PKC while mechanical produces palm kernel expeller (PKE). Due to PKC's high fibre and moderate protein content (Sundu

[1] Malaysian Palm Oil Board,
6 Persiaran Institusi, Bandar Baru Bangi,
43000 Kajang, Selangor, Malaysia.

* *Corresponding author e-mail: fidos@mpob.gov.my*

and Dingle, 2003), it had not been widely applied for monogastric animal feed particularly, poultry. Moreover, protein quality and presence of non-digestible polysaccharide components such as non-starch polysaccharide (NSP) in PKC also hindered its maximum utilisation by monogastric animals. Protein quality is closely related to amino acid components bioavailability and animal digestive ability (Bryan and Classen, 2020). Protein quality is also determined by the ability of amino acids to be absorbed by the body which is also known as amino acid digestibility (Alshelmani *et al*., 2017a).

PKC was rarely used in monogastric livestock formulations although it contains up to 18% protein due to the presence of anti-nutritional components besides its high content of mannan (Oluwafemi, 2008). Nevertheless, the potential of PKC can be enhanced through fermentation that serves as an alternative protein source for animal nutrition. Its nutritional quality can be enhanced by the microorganism's biomass and NSP content can be reduced to enable its utilisation as raw material in poultry feed (Alshelmani *et al*., 2014; 2016; 2017b). Mohd Firdaus (2014) and Noraini *et al*. (2009) had proved that fermented PKC can be given to broiler chicks up to 30% in the feed formulation without adverse effects. Sathitkowitchai *et al.* (2018) contended that the application of enzyme for β-mannan degradation in PKC will release the sugar and other digestible sugars that can be absorbed and metabolised by monogastric animals (Zamani *et al*., 2017). Therefore, the solid state fermentation (SSF) method using microorganism is preferred as a treatment for substrates containing high NSP content prior to feed application. The SSF method is also an economically viable method in fermentation biotechnology and its use in the livestock industry which has high operating costs is guaranted an alternative technology (Lateef *et al*., 2008; Rodríguez-Jasso *et al*., 2013). The use of microorganisms in this method is capable of hydrolysing NSP such as lignin, hemicellulose and cellulose, as well as ensuring optimum fermentation factors. This can also assist in lowering the NSP content and increasing substrate utilisation ratio in animal feed, thereby improving animal digestion.

The application of SSF using local isolated fungus could enhance the nutritional content of PKC and indirectly enhanced the application of PKC as livestock feed by dissolving its NSP components. The use of new strains in this study also brings novelty and new scientific findings if it can improve the nutrition value of PKC. This article is intended to identify locally isolated fungus strains that infect the palm kernel naturally using the 18S ribosomal ribonucleic acid (rRNA) method. In addition, the effect of SSF on nutrient content of PKE and PKC after fermentation was also studied.

MATERIALS AND METHOD

Chemicals

All chemicals used were of analytical grades. Fungal growth media, namely potato dextrose agar (PDA) and potato dextrose broth (PDB), were obtained from Oxoid, England. The chemicals used for fungus identification (Tris-HCl, Tris-bes and ethidium bromide) were supplied by Sigma Chemical Company, USA. Ammonium sulphate [$(NH_4)_2SO_4$] and potassium dihydrogen phosphate (KH_2PO_4) for fungus fermentation were obtained from BDH AnalaR, USA. The proximate analysis was carried out using sodium hydroxide, ethylenediaminetetraacetic acid (EDTA), sodium borate deacetylate, sodium lauryl sulphate, triethlene glycol, disodium hydrogen phosphate, sulphuric acid, hydrochloric acid, petroleum ether and acetone provided by Hamburg Chemical, Germany and BDH AnalaR, USA.

Enzyme, Kit, DNA Rulers and Vectors

The restriction enzymes were supplied by Vivantis, Malaysia and the DNA 1 kb ruler was supplied by Promega, USA. The polymerase chain reaction (PCR) components namely PCR buffer (10X), magnesium chloride ($MgCl_2$) (25 mM), deoxynucleoside triphosphate (dNTP) (10 mM), Taq deoxyribonucleic acid (DNA) polymerase, pfu DNA polymerase were supplied by Invitrogen, Brazil and Promega, USA. Promoter DNA (oligo primer) was supplied by First BASE (Malaysia). Vector pGEM®T Easy, ligase buffer and T4 DNA ligase were obtained from Promega, USA. The isopropyl β-D-1-thiogalactopyranoside (IPTG) was supplied by Bio Basic Inc., Canada, while X-gal was sourced from 5 Prime, USA. Universal promoters for the T7, SP6 and M13R sequencing processes were obtained from Promega, USA. Fungal DNA extraction was conducted using the DNeasy Plant Mini Kit (Qiagen). For PCR product purification, the Megaquick-spin PCR Kit and Agarose Gel DNA Extraction System obtained from Intron, USA were used. Meanwhile, the plasmid purification was conducted using the Wizard Plus Minipreps DNA Purification System Kit from Promega, USA. ABI PRISM® Big Dye® Terminator v3.1 Cycle Sequencing provided by Applied Biosystems, USA was used for sequencing.

Fungus Culture

The naturally infected palm kernel samples were taken and cultured on PDA media. New subculture validation test was conducted in triplicates to ensure fungal independence and purity. The locally isolated strain was incubated

for seven days on PDA at 30ºC. After that, it was stored in a refrigerator at 4ºC until further use. New subcultures were created every four weeks on the PDA to maintain the purity of the fungal species.

Identification of Fungus Strain

Isolation and extraction of fungal genomic DNA. The fungal culture fermented in PDB medium for seven days at 30ºC and 180 rpm agitation was harvested for genomic extraction of fungal DNA using the DNeasy Plant Mini Kit (Qiagen).

Determination of DNA concentration and quality. Two methods were used to determine the concentration of DNA in this study. The first method was conducted by using the spectrophotometer (Biophotometer, Eppendorf, Germany). One µL DNA was mixed with 49 µL distilled water and the absorption values at 230, 260 and 280 nm were measured, respectively. Distilled water (dH_2O) was used as evaporator. The second method was conducted by directly comparing the intensity level of the DNA band of interest with the known mass ruler band after both samples and rulers were fractionated in the same gel.

Agarose gel electrophoresis of DNA samples. Agarose gel electrophoresis was run at 50-100 V to obtain the desired band separation. The resulting electrophoresis was subsequently absorbed on an ultraviolet (UV) transiluminator and the resulting band images were taken using the AlphaImager™ 2200 gel documentation system (Alpha Innotech, USA). Prior to that, DNA samples were fractionated using 1.0% (w/v) agarose gel. The agarose gel was dissolved in TAE 1X buffer through microwave heating. After the gel was cooled to 50ºC, 1 µL ethidium bromide (10 mg mL^{-1}) was added to the agarose solution before being poured into the gel mold. A total of 20 µL of DNA sample was mixed with a 6X load buffer before being filled into frozen gel wells. DNA rulers included in other gel wells served as rulers for DNA samples. The use of DNA rulers depended on the analysis, needs and size of the expected results (Sambrook and Russel, 2001). Common rulers used are DNA 1 kb, 100 bp, DNA mass ruler and λ HindIII.

PCR 18S rRNA amplification. Specific oligo primers were used to generate 18S rRNA fragments through PCR amplification chain reactions. They were known as internal transcibed spacer (ITS), for example ITS1-F: 5′-CTTGGTCATTTTAGAGGAAGT-3′ and ITS4-R: 5′-TCCTCCGCTTATTGATATGCC-3′ (Kim *et al.*, 2008). The ITS was synthesised by First BASE Laboratories Sdn. Bhd., Malaysia upon designed by Primer-design program software. The PCR reactions were performed using a GeneAmp Thermal Cycler (Model 2400, USA). *Table 1* summarises the PCR components. The programmed temperature cycles were as follows: A cycle of DNA denaturation at 94ºC for 5 min; 25 cycles for denaturation at 94ºC for 1 min, followed by annealing at 65ºC for 1 min and elongation at 72ºC for 1 min. Then, the PCR reaction was terminated with a final elongation process at 72ºC for 7 min. The resulting PCR products were subsequently analysed by 1% agarose gel electrophoresis. If the presence of the expected single band is found the PCR product is then cut for further action.

TABLE 1. THE POLYMERASE CHAIN REACTION (PCR) COMPONENTS USED TO AMPLIFY 18s rRNA

Component	Volume (µL)
PCR buffer (10X)	2.0
Magnesium chloride ($MgCl_2$) (25 mM)	1.0
Deoxynucleoside triphosphate (dNTP) (4 mM)	1.0
Forward primer (12.5 pmol)	1.0
Reverse primer (12.5 pmol)	1.0
DNA genome (250 ng μL^{-1})	3.0
Taq DNA polymerase (5 U μL^{-1})	0.5
Sterile distilled water	10.5
Final volume	20.0

Extraction and purification of DNA from agarosa gel. The PCR products were extracted and purified from agarose gel after the desired band was found. The commercial Megaquick-spin PCR Kit and Agarose Gel DNA Extraction System were used for this purpose.

Sequence analyses. The sequencing process was performed using the protocol of the ABI PRISM® BIG DYE® Terminator Cycle Sequencing Ready Reaction (PE Biosystems, USA). The components of the sequencing reaction were 200-500 ng DNA template, 3.2 pmol of appropriate promoters, 1 µL Big Dye terminator v.3.1, 0.5 µL of 10X sequence buffer and sterile distilled water were added into the PCR tube until the final volume was equal to 10 µL. The promoters used were universal T7 (5 'TAATACGACTCACTATAGGG 3'), SP6 (5 'GATTTAGGTGACACTATAG 3') and M13R (5 'CAGGAAACAGCTATGACC 3'). The tubes were then centrifuged prior to cyclic reaction using TPersonal Thermal Cycler, Biometra, Germany or PTC-100 Thermal Cycler, MJ Research, USA at 25 cycles at 96ºC for 30 s, 50ºC for 15 s and 60ºC for 4 min. An automated DNA sequencing was then performed on that sample.

The data obtained was displayed on a chromatogram and analysed using Chromaslite201 software. The sequences obtained were compared with nucleotide sequences and amino acids in the National Center for Biotechnology Information

(NCBI) database using BLAST software (Altschul *et al.*, 1990). Through BLAST, the percentage homology of nucleotides and amino acids to sequences from other organisms was determined. Domain analysis was performed using InterProScan software. The sequences then were used to generate phylogenetic tree by using the software (Phylogeny,fr) and the analysis was performed by the software through an automated programme from multiple alignment of the sequence to the construction of phylogenetic tree (Radha and Ashok, 2020).

Solid State Fermentation (SSF)

Preparation of culture media. PKE sample was obtained from Federal Land Development Authority (FELDA) Pasir Gudang, Johor, Malaysia, while PKC sample was produced in-house using a 5 L scale Soxhlet apparatus (Osman *et al.*, 2009). A total of 20 g of untreated PKE and PKC samples were mixed directly with 1% (w/w) $(NH_4)_2SO_4$ and 0.3% (w/w) KH_2PO_4. The mixture was mixed and autoclaved at 121°C for 15 min. The method used was modified from Iluyemi *et al.* (2006). Only two types of minerals were used in this study since PKC already contains several minerals such as magnesium (Mg), iron (Fe), sodium (Na), calcium (Ca), zink (Zn) and copper (Cu) (Osman *et al.*, 2009).

Seed culture production. A total of 1 cm^3 of *R. oryzae* ME01 fungal mycelium aged five days was cut from the PDA and cultured in a 500-mL conical flask containing 250 mL PDB to form pellets. The seed culture was carried out for five days at 30°C with 180 rpm agitation.

Solid state culture. Sterilised culture media was mixed aseptically with seed culture at a ratio of 1:1 (volume: medium) to give an initial moisture of 50%. Fermentation was performed for 10 days according to the study by Swe *et al.* (2003) whereby maximum protein was produced by *Aspergillus niger* on Day 8. To study the effect of fermentation on changes in nutrient content, 20 g samples were harvested from the bioreactor daily, where the growth of fungal biomass was measured.

Bioreactor systems. *Figure 1* shows the schematic diagram of the SSF bioreactor system used in this study. This bioreactor system consisted of an air pump, a water temperature probe, a water heater, an air filter and a bioreactor.

Chemical Composition Analysis

Approximate analysis of fermented PKE and PKC were determined according to the standard method described in Association of Official Agricultural Chemists (AOAC) (AOAC, 1998; Gul and Safdar, 2009). Analysis of total moisture content was carried out using AND Machine MX50 (USA) using 5 g of ground samples. Crude protein was determined according to the Kjeldahl method and each sample was calculated by multiplying the nitrogen content by a factor of 6.25. The fat content of the samples was determined using hexane in soxhlet extraction method (Soxtherm machine). The samples were incinerated for 4 hr at 600°C. The percentage of carbohydrate content and the energy value was determined according to Galla *et al.* (2012), using the following Equation (1) and (2):

$$\% \text{ Carbohydrate} = 100 - (\text{sum of moisture, ash, crude protein, crude fibre and crude fat contents}) \quad (1)$$

$$\% \text{ Energy (kcal/100 g)} = 9 \times \% \text{ fat} + 4 (\% \text{ protein} + \% \text{ carbohydrate}) \quad (2)$$

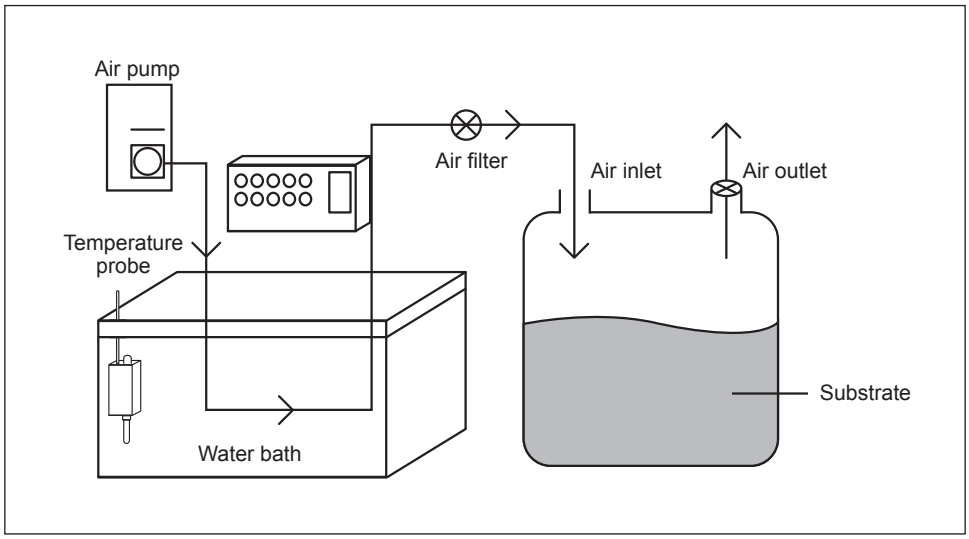

Figure 1. Bioreactor system designed for solid state fermentation of palm kernel cake.

Statistical Analysis

Data were analysed using the general linear models procedure of the Statistical Analysis System (SAS). Differences among treatments were by the least significant difference at $p<0.05$.

RESULTS AND DISCUSSION

Identification of Fungus Strain

The quality and quantity of locally isolated fungal obtained after DNA extraction needs to be determined to ensure high levels of DNA purity and to produce accurate results in strain identification. Thus, spectrophotometric measurements were taken and agarose gel electrophoresis analysis was performed. *Table 2* shows the average spectrophotometer measurements indicating the concentration and purity of the fungal DNA. According to Sambrook and Russell (2001), the measurement of $A_{260/280}$ and $A_{260/230}$ referred to protein and carbohydrate contamination.

Based on *Table 2*, the measurements of $A_{260/280}$ and $A_{260/230}$ samples were 1.86 and 0.41, respectively. This result signified that the $A_{260/280}$ sample was free of protein contamination as the value was more than 1.80 but with low carbohydrate contamination. To examine the DNA quality, agarose gel electrophoresis analysis was performed. Single strand of DNA produced (*Figure 2a*) proved that the DNA sample was not degraded and has a satisfactory concentration for further study. PCR amplification of fungal DNA samples was promoted by internal transcribed spacers (ITS) 1 and ITS 4. It was found that good primers combination and annealing temperature above 53°C as suggested by Cappa and Cocconcelli (2001), produced good results and specific amplitude (*Figure 2b*), as well as reducing products from non-specific reactions.

TABLE 2. CONCENTRATION AND PURITY OF DNA FROM LOCALLY ISOLATED FUNGUS

Fungus	DNA concentration (ng µL^{-1})	Spectrophotometer measurement	
		$A_{260/280}$	$A_{260/230}$
Unknown	5.03 ± 0.57	1.857 ± 0.22	0.407 ± 0.03

Nucleotide sequence analysis was performed using 18S rRNA to determine the unknown strain. 18S rRNA is a small nuclear subunit of ribosomes that evolves very slowly and is therefore suitable to be used to identify and to locate organisms (Dresler-Nurmi *et al.*, 1999). After replication by 18S rRNA, a comparison of sequence data (*Figure 3*) with the European Molecular Biology Laboratory (EMBL) data from GenBank via BLAST was able to identify the unknown strain as *Rhizopus oryzae* as it has a homology sequence and highest score of 100% E value with some *R. oryzae* strain.

To strengthen the finding, DNA of the unknown strain was aligned with the *R. oryzae* strain TY.GF1 sequence (GenBank accession number: JN003654.1) and the *R. oryzae* strain CS1217 sequence (GenBank accession number: GU126375.1). This multiple alignment was performed to seek the relationships and associations between the genus Rhizopus and to look for the distinct differences between the base pairs. The JN and GU sequences were chosen because they had the closest homology and highest score to the unknown strain. According to Schabereiter-Gurtner *et al.* (2001), sequence comparison analysis revealed similarity of the strain studied with the reference strain. Phylogenetic analysis was performed to determine the relationship of strains studied with genus and other fungal strains.

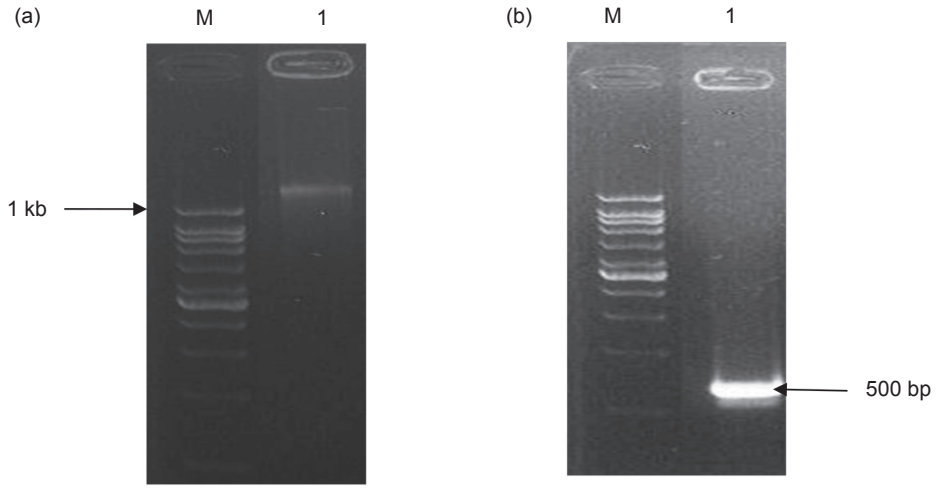

Figure 2. Electrophoresis of agarose gel (1.8% w/v) on extracted DNA; (a) the DNA genome has a single non-degradable band and its size was larger than 1 kb, and (b) the polymerase chain reaction (PCR) 18S rRNA product resulting from DNA amplification where the resulting single band was larger than 500 base pairs (bp) with high concentration.

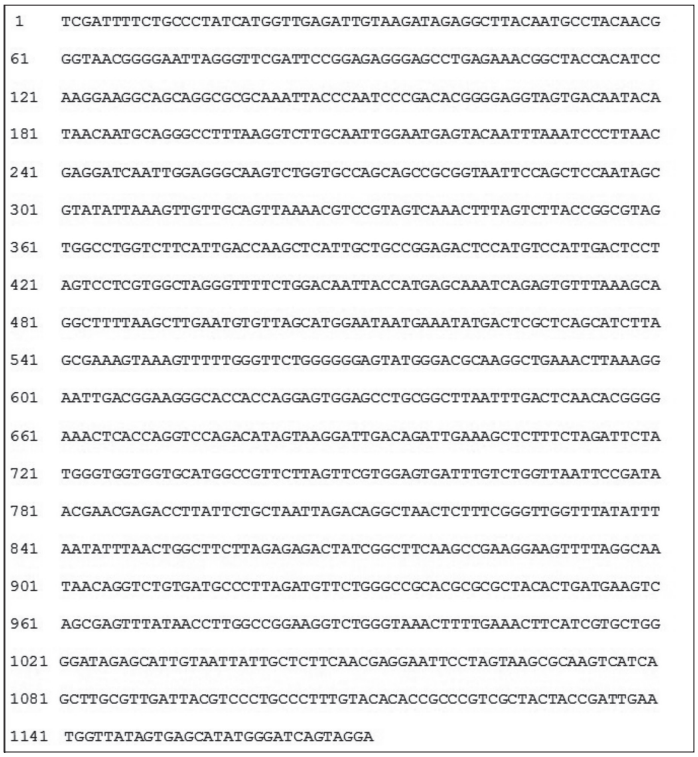

Figure 3. Complete nucleotide sequence of fungal strain A containing 1171 base pairs. Through nucleotide searches using BLAST, the organism has the highest sequence homology and score with Rhizopus oryzae *(99% E value).*

Figure 4 shows the phylogenetic analysis of the 18S rRNA amplitude of a localised isolated fungal strain with its neighbours. The tree was based on a final alignment of 1171 base pairs of the strain. According to Lee *et al.* (2000), the dendrogram generated by genetic distance data separating strains has been clearly studied into specific genera. Similarly, this study classified the unknown strain into *R. oryzae* under Rhizopus genera through phylogenetic analysis.

Chemical Compositions of Fermented PKE and Fermented PKC

Ether Extract Content (EEC). *Figure 5a* shows the effect of SSF by *R. oryzae* ME01 on EEC in fermented PKE (fPKE) and fermented PKC (fPKC). There was a significant decrease (p<0.05) of EEC from Day 1 to Day 10 of fermentation against PKE compared to control, and the lowest EEC was recorded on Day 7, at 1.29% (w/w). Although fermentation of PKC also showed a decrease of EEC up to 0.01% (w/w) on Day 7 at 1.27% (w/w); the decrease was not significantly different (p>0.05) than that of control.

The decrease in EEC showed that the *R. oryzae* ME01 assimilated oils in PKE and PKC for its metabolite use. In another study, Alshelmani *et al*. (2016) contended that EEC digestibility had increased in broilers fed with the fermented PKC. The ability of *R. oryzae* ME01 to lower EEC has opened up new opportunities in extracting the oil through the use of enzymes besides the commonly used mechanical and chemical extraction methods. Extraction of oil from hazelnut containing 10%-12% (w/w) of oil by pectinase and cellulase enzyme achieved 98% oil extraction by producing a product containing only 1.5% (w/w) oil (Zúñiga *et al.*, 2003).

The presence of high EEC in PKE at 3.44% (w/w) compared to PKC (1.27% w/w) was a major determinant of successful nutritional improvement in SSF studies and it was found that products with high EEC were able to increase crude protein content (CPC), ash content and crude fibre content (CFC) compared to PKC through SSF. This is in line with the study of Gao *et al.* (2013) which found that SSF on soybeans by *A. niger* was able to increase CPC and CFC as a result of the use of soybean oil by the fungus.

Ash content. The ash content increased daily from Day 1 for both fermented products (*Figure 5b*). Fermentation that occurred had altered mineral composition in fermented products or in rumen animals (Pino and Heinrichs, 2016). For fPKE, the highest ash content was recorded on Day 10 at 7.81% (w/w), whereas from Day 1 to Day 4, the increase of ash content was not significantly different (p>0.05) from the control (PKE Day 0) at (3.94% w/w). The same condition occurred in fPKC where the increase of ash content from Day 1 to Day 4 did not differ from Day 0 but from Day 5, the increase of ash content was significantly different (p<0.05) from that of control PKC (3.52%

w/w). Day 9 recorded the highest ash content at 6.47% (w/w). The increase in ash content was due to an increase in fungal biomass and this result could be an indirect method to determine fungal growth (Koutinas *et al.,* 2003). It also showed that the mineral contents in fermented products were increased due to fungal biomass. The increment of mineral would decrease inorganic mineral supplementation in the animal feed.

Crude fibre content (CFC). *Figure 5c* shows the effect of SSF by *R. oryzae* ME01 on CFC in fPKE and fPKC. There was an increase in CFC from Day 1 to Day 10 of SSF on PKE and the increase was significantly different (p<0.05) from that of control PKE. SSF on PKC from Day 1 to Day 10 also showed an increase but no significant difference (p>0.05) with PKC without fermentation. Therefore, it was found that fermentation of PKE affected the CFC compared to the PKC and this was due to a very low EEC at 1.27% (w/w) in the PKC which caused deficiency of the fungus to use the oil. This is evident in the study by Gao *et al.* (2013) in which oil and starch became the contributing factor in increasing the CFC and CPC. The increase of CFC in the fermented PKE and PKC was contributed indirectly by fungal biomass and this finding showed that *R. orzyae* was not a good candidate to break down anti-nutritional properties in PKE and PKC. In addition, PKC indeed contained high fibre content for livestock (Agunbiade *et al*., 1999; Perez *et al*., 2000).

Carbohydrate content. The lowest carbohydrate content was recorded on Day 10 of fermentation on PKE at 55.39% (w/w) (*Figure 5d*). The decrease in carbohydrate content of fPKE was found to be significantly different (p<0.05) from that of PKE without fermentation (63.36% w/w), starting on Day 4. For fPKC, the decrease in carbohydrate content was significantly different (p<0.05) from the control PKC from Day 5 of fermentation while Day 9 recorded the lowest carbohydrate content at 60.06% (w/w). However, carbohydrate content on Day 9 was not significantly different (p>0.05) from Day 5 of fermented PKC. According to Gao *et al.* (2013), the reduction of starch through its use by microorganisms is a major cause for the increase in CPC.

Energy content. It was found that the energy content decreased from Day 1 to Day 10 for fPKE and fPKC and the decrease was significantly different (p<0.05) from Day 0 (*Figure 6a*). The lowest energy content was recorded on Day 10 of fermentation (306.54 kcal/100 g) for fPKE while for fPKC, it was on Day 9 (325.17 kcal/100 g).

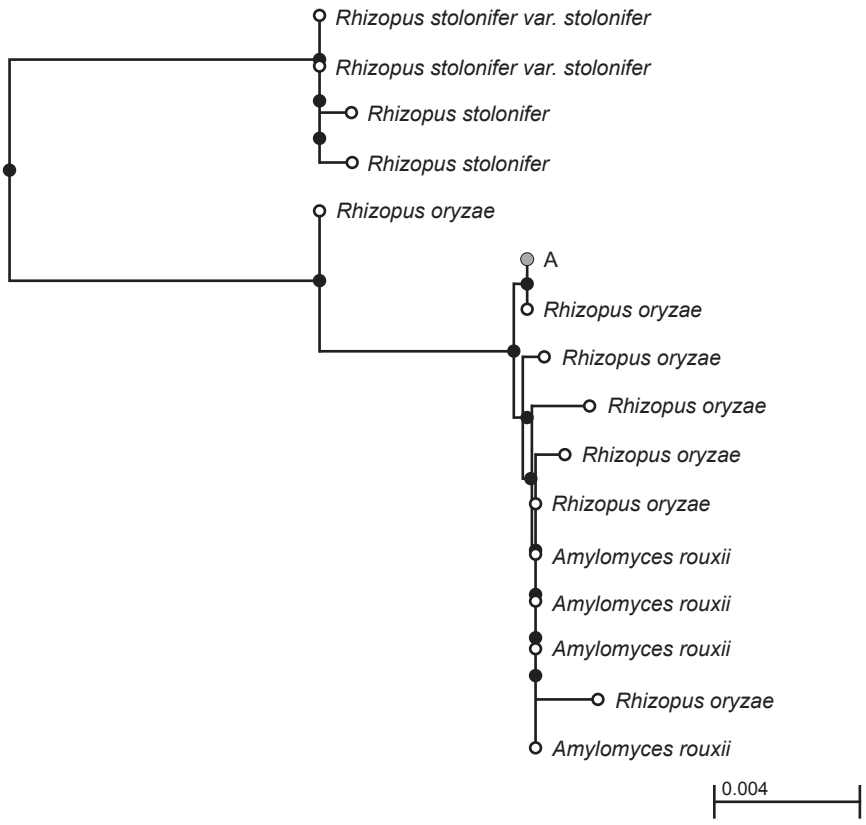

Figure 4. Phylogenetic analysis showed the relationship between amplitude A and its neighbours (the phylogenetic tree was based on the final alignment of the 1171 bp strain.) neighbour-joining phylogenetic tree showed maximum likelihood model showing the relationship based on 18S rRNA gene sequence alignments. The length at the branching points are the percentages of occurrence in hundreds bootstrapped trees.

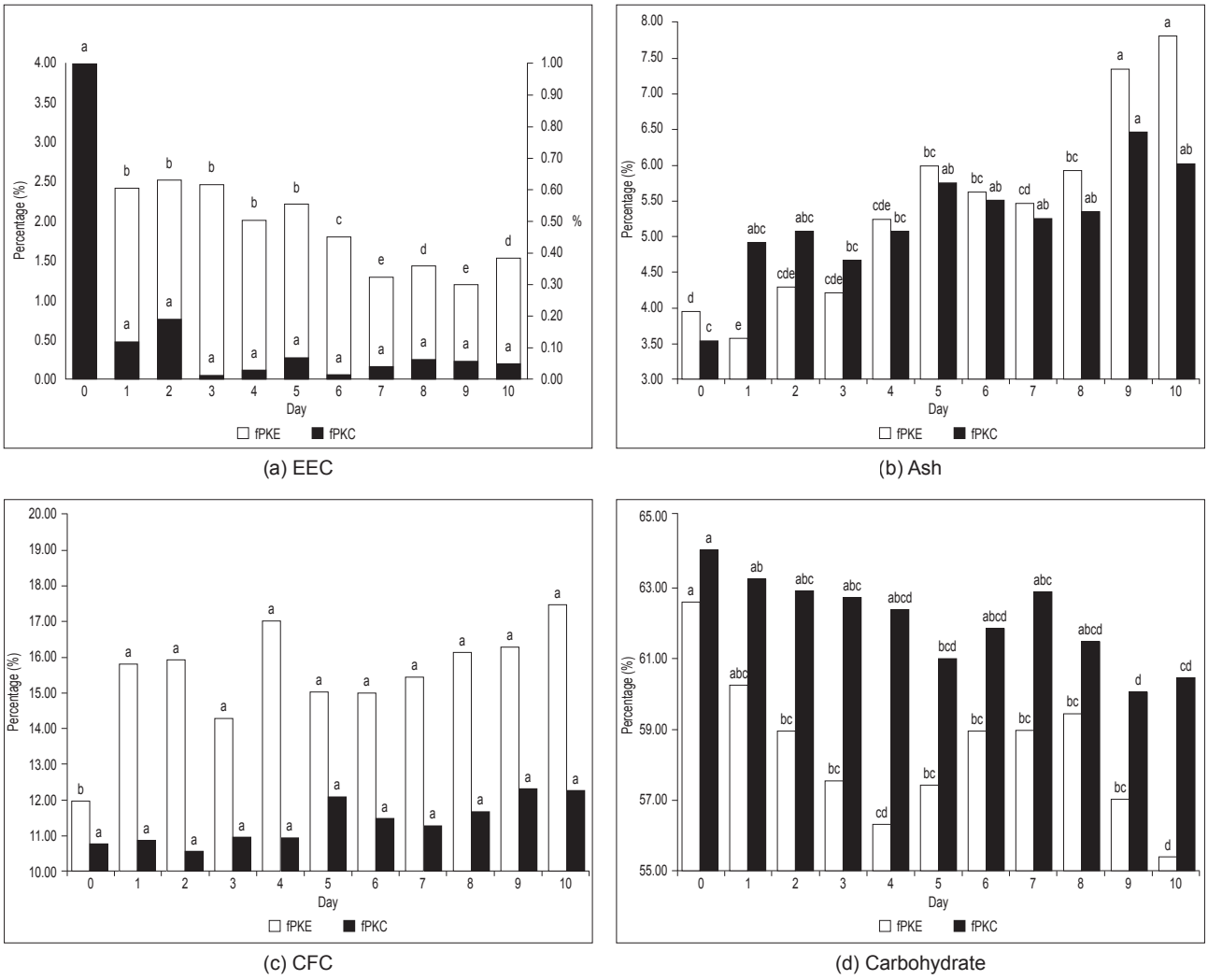

Note: [a,b,c,d,e] Min with different superscript is significantly different (p<0.05).

Figure 5. Effect of solid state fermentation by Rhizopus oryzae *ME01 on (a) ether extract content (EEC), (b) ash, (c) crude fibre content (CFC), and (d) carbohydrate.*

The determination for energy is due to three factors namely EEC, CPC and carbohydrates (Galla *et al.*, 2012). It was found that the decrease in energy content in this study was directly proportional to the decrease in EEC and carbohydrate content in fPKE and fPKC. Energy in fermented products was found to be depleted daily due to the metabolism of *R. oryzae* ME01 which utilised nutrients in PKE and PKC particularly, EEC and carbohydrates, for the production of its biomass. The depletion of energy in fermented products could affect the energy requirement of animal but it can be balanced by addition of other raw materials such as corn or palm oil in the animal feed.

Crude protein content (CPC). *Figure 6b* shows the effect of SSF by *R. oryzae* ME01 on the CPC in fPKE and fPKC. For fPKE, Day 4 and Day 5 of SSF recorded the highest CPC at 19.44% (w/w) and protein gain (PG) at 19.32% (w/w), respectively. These increases were significantly different (p<0.05) from other days as well as Day 0 (non-fermented PKE). Meanwhile, the CPC in fermented PKC from Day 1 to Day 10 was not significantly different (p>0.05) from the control except Day 4 which showed highest protein increase of 21.59% (w/w). In a study by Swe *et al.* (2003) on PKC, it was found that protein increase was significant on Day 8, from 16.8% to 29.6% of SSF yield by *A. niger*.

One factor contributing to the difference in CPC between fPKE and fPKC in this study was the size of the PKC as substrates. PKC has uniform size and light colour appearance due to solvent extraction process. The size of PKC was as small as 0.2 mm, while PKE has a non-uniform size and larger than 0.2 mm. According to Schmidt and Furlong (2012), smaller substrate sizes will result in higher CPC than large-sized substrates. However, large sized substrates will have larger surface area and thus, increases the *R. oryzae* biomass.

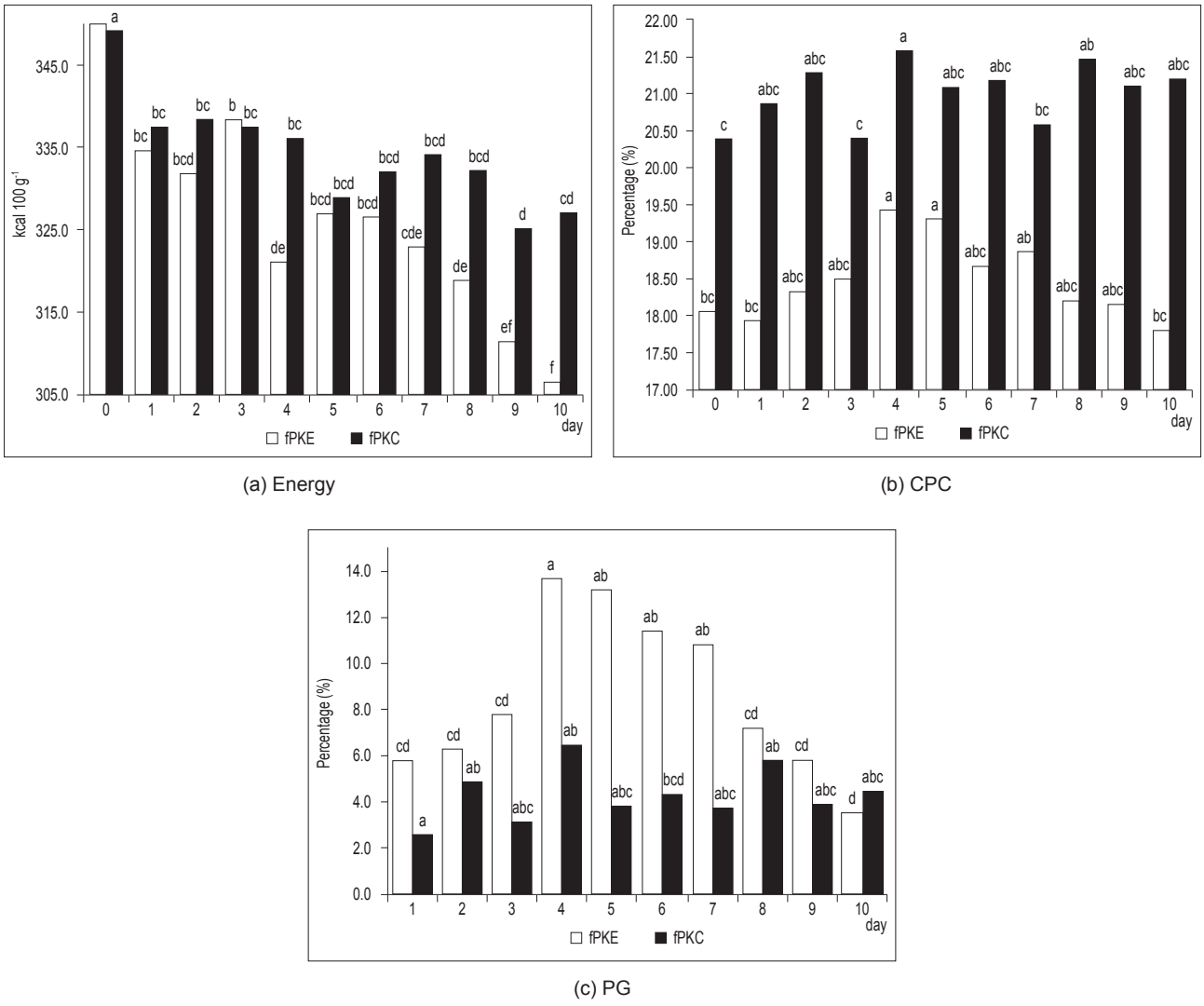

Note: [a,b,c,d,e,f] Min with different superscript is significantly different (p<0.05).

Figure 6. Effect of solid state fermentation by R. oryzae *ME01 on (a) energy, (b) crude protein content (CPC), and (c) protein gain (PG).*

Figure 6c shows the effect of SSF by *R. oryzae* ME01 on PG in fPKE and fPKC. On Day 4 and 5, fPKE indicated the highest PG at 13.63% (w/w) and 12.82% (w/w), respectively. For fPKC, Day 4 recorded the highest PG at 6.46% (w/w). The relationship between CPC and PG was proportional. The highest CPC led to highest PG. Although fPKC recorded higher CPC than fPKE, the PG of fPKE exceeded that of fPKC by two folds. The increase in CPC could be due to the use of fungi and starch (Gao *et al.*, 2013). Since PKE contained higher EEC than PKC, the increase in CPC of fPKE was higher than that of control PKE at 7.64% (w/w), whereas changes in fPKC by 3.45% (w/w) did not differ from PKC and was even lower than fPKE (*Table 3*).

Results summarised in *Table 3* showed significant changes for carbohydrate content, EEC and ash content with a decrease in carbohydrate and EEC content by 11.52% and 55% (w/w), respectively in fPKE. The reduction of carbohydrate is a good indicator so that more fermented PKE and PKC could be added in animal diet due to lesser non-soluble starch in the animal feed but the decrease of fat has to be balanced by adding other fat sources such as palm oil. There was an increase in protein and ash content by 7.6% (w/w) and 200% (w/w), respectively, in fermented PKE by *R. oryzae* ME01. This suggested that the action of fungus which involved the hydrolysis of various enzymes including the action of lipolytic enzymes on lipids in PKE caused a change in nutrient composition in fPKE. Similar trends occurred for carbohydrate content, EEC, protein and ash content in fPKC which verified this fungal activity. It was found that there was a decrease in carbohydrate content by 2.32% (w/w) and EEC content by 100%. The protein and ash content increased by 3.45% (w/w) and 18.35% (w/w), respectively. Small changes in fPKC compared to fPKE are likely driven by differences in fat content as suggested by Gao *et al.* (2013).

TABLE 3. CHANGES IN PKC's NUTRITION CONTENT AFTER FERMENTATION

Nutrition type	PKE	fPKE	% Change	PKC	fPKC	% Change
Crude protein content (CPC) (%w/w)	17.25	19.44	+7.64	20.31	21.59	+3.45
Crude fibre content (CFC) (%w/w)	11.97	16.99	+41.94	10.77	12.35	+14.67
Carbohydrate content (%w/w)	63.36	55.39	-11.52	64.05	59.92	-2.32
Ether extract content (EEC) (%w/w)	3.44	1.29	-55	1.27	0.01	-100
Ash content (%w/w)	3.94	7.81	+200	3.52	6.47	+18.35
Energy content (kcal/100 g)	353.25	306.54	-13.22	335.51	325.17	-3.08

Note: PKC - palm kernel cake; fPKC - fermented palm kernel cake; PKE - palm kernel expeller; fPKE - fermented palm kernel expeller.

CONCLUSION

In conclusion, the enhancement in nutritional value for PKC particularly protein content through SSF using a locally isolated fungus was successfully conducted. The changes in fermented PKC nutrients showed that the ash and protein content increased by 18.26% and 3.45%, respectively. After 10 days fermentation, carbohydrate and fat content decreased significantly by 2.32% and 98%, respectively. The increase of ash and protein content for fermented PKE was significant ($p<0.05$) where ash and protein content increased by 200% and 7.64%, respectively, while carbohydrate (11.52%) and fat content (55%) decreased after 10 days of SSF. Thus, PKE showed better performance for fermentation by *R. oryzae* ME01.

ACKNOWLEDGEMENT

The authors would like to thank the Director-General of MPOB for permission to publish this article. Thanks also to the lecturers and staffs of the Faculty of Science and Technology, Universiti Kebangsaan Malaysia (UKM) for their technical assistance and permission using the facilities.

REFERENCES

Alshelmani, M I; Loh, T C; Foo, H L; Lau, W H and Sazili, A Q (2014). Biodegradation of palm kernel cake by cellulolytic and hemicellulolytic bacterial cultures through solid state fermentation. *Sci. World J., 2014*: 8.

Alshelmani, M I; Loh, T C; Foo, H L; Sazili, A Q and Lau, W H (2016). Effect of feeding different levels of palm kernel cake fermented by *Paenibacillus polymyxa* ATCC 842 on nutrient digestibility, intestinal morphology and gut microflora in broiler chickens. *Anim. Feed Sci. Technol*., *216*: 216-224.

Alshelmani, M I; Loh, T C; Foo, H L; Sazili, A Q and Lau, W H (2017a). Effect of solid state fermentation on nutrient content and ileal amino acids digestibility of palm kernel cake in broiler chickens. *Indian J. Anim. Sci*., *87(9)*: 1135-1140.

Alshelmani, M I; Loh, T C; Foo, H L; Sazili, A Q and Lau, W H (2017b). Effect of feeding different levels of palm kernel cake fermented by *Paenibacillus polymyxa* ATCC 842 on broiler growth performance, blood biochemistry, carcass characteristics, and meat quality. *Anim. Prod. Sci*., *57(5)*: 839-848.

Agunbiade, J A; Wiseman, J and Cole, D J A (1999). Energy and nutrient use of palm kernels, palm kernel meal and palm kernel oil in diets for growing pigs. *Anim. Feed Sci. Technol., 80*: 165-181.

Altschul, S F; Gish, W; Miller, W; Myers, E W and Lipman, D J (1990). Basic local alignment search tool. *J. Mol. Biol., 215*: 403-410.

AOAC (1998). Approved methods of analysis 16th edition. Association of Official Analytical Chemists, Washington, DC, USA.

Bryan, D S L and Classen, H L (2020). *In vitro* methods of assessing protein quality for poultry. *Animals, 10*: 551.

Cappa, F and Cocconcelli, P S (2001). Identification of fungi from dairy products by means of 18S rRNA analysis. *Int. J. Food Microbiol*., *69*: 157-160.

Dresler-Nurmi, A; Kaijalainen, S; Lindstrom, K and Hatakka, A (1999). Grouping of lignin degrading corticoid fungi based on RFLP analysis of 18S rDNA and ITS regions. *Mycology Resource, 103(8)*: 990-996.

Galla, N R; Pamidighantam, P R and Akula, S (2012). Chemical, amino acid and fatty acid composition of *Sterculia urens* L. seed. *Food Hydrocoll., 28(2)*: 320-324.

Gao, Y L; Wang, C S; Zhu, Q H and Qian, G Y (2013). Optimization of solid-state fermentation with *Lactobacillus brevis* and *Aspergillus oryzae* for trypsin

inhibitor degradation in soybean meal. *J. Integr. Agric.*, *12(5)*: 869-876.

Gul, S and Safdar, M (2009). Proximate composition and mineral analysis of cinnamon. *Pak. J. Nutr.*, *8(9)*: 1456-1460.

Iluyemi, F B; Hanafi, M M; Radziah, O and Kamarudin, M S (2006). Fungal solid state culture of palm kernel cake. *Bioresour. Technol., 97(3)*: 477-482.

Kim, Y J; Yong, Z; Kyung-Taek, O; Van-Nam, N and Ro-Dong, P (2008). Enzymatic deacetylation of chitin by extracellular chitin deacetylase from a newly screened *Mortierella* sp. DY-52. *J. Microbiol. Biotechnol., 18(4)*: 759-766.

Koutinas, A; Wang, R and Webb, C (2003). Estimation of fungal growth in complex, heterogeneous culture. *Biochem. Eng. J., 14(2)*: 93-100.

Lateef, A; Oloke, J K; Gueguim Kana, E B; Oyeniyi, S O; Onifade, O R and Oyeleye, A O (2008). Improving the quality of agro-wastes by solid-state fermentation: Enhanced antioxidant activities and nutritional qualities. *World J. Microbiol. Biotechnol., 24(10)*: 2369-2374.

Lee, J C; Cole, M and Linacre, A (2000). Identification of members of the genera *Panaeolus* and *Psilocybe* by a DNA test. A preliminary test for hallucinogenic fungi. *Forensic Sci. Int., 112(2-3)*: 123-133.

Malaysian Palm Oil Board (MPOB) (2020). Production of crude palm kernel oil and palm kernel cake. http://bepi.mpob.gov.my/index.php/en/production/production-2018/production-of-crude-palm-kernel-oil-2018.html, accessed on 10 October 2020.

Mohd Firdaus, O (2014). *Penghasilan Dedak Isirung Sawit (PKE dan PKC) Terfermentasi Melalui Sistem Fermentasi Keadaan Pepejal oleh Kulat Pencilan Tempatan Rhizopus oryzae ME01*. Masters thesis, Universiti Kebangsaan Malaysia.

Noraini, S; Sarah, R; Mohd Fazli, F A; Rosnizah, I and Norham, I (2009). Response of young broiler chickens fed increasing levels of fermented palm kernel expeller (fPKE). *Prosiding Seminar Kebangsaan Kedua Agro-Environment 2009*. Malaysian Agriculture Research and Development Institute (MARDI). Johor Bahru, Johor.

Oluwafemi, R (2008). Palm kernel cake utilization in monogastric animal feeding - Implications for sustainable livestock development. *J. Vet. Med., 6(2)*: 1-5. https://print.ispub.com/api/0/ispub-article/5211.

Osman, A; Jumardi, R; Farah Nurshahida, M S; Raznim Arni, A R and Mardhati, M (2009). MPOB-Q-PKM™. *MPOB Information Series No. 440.*

Parveez, G K A; Elina, H; Soh, K H; Meilina, O B; Kamalrudin, M S; Mohd, N I Z B; Shamala, S; Zafarizal, A Z H and Zainab, I (2020). Oil palm economic performance in Malaysia and R&D progress in 2019. *J. Oil Palm Res., 32(2)*: 159-190.

Perez, J F; Gernat, A G and Murillo, J G (2000). The effect of different levels of palm kernel meal in layer diets. *Poult. Sci. J., 79*: 77-79.

Pino, F and Heinrichs, A J (2016). Effect of trace minerals and starch on digestibility and rumen fermentation in diets for dairy heifers. *J. Dairy Sci.*, 99: 2797-2810.

Radha, S and Ashok, K D (2020). Isolation and characterization of a new endophytic actinobacterium *Streptomyces californicus* strain ADR1 as a promising source of anti-bacterial, anti-biofilm and antioxidant metabolites. *Microorganisms, 8*: 929 pp.

Rodríguez-Jasso, R M; Mussatto, S I; Sepúlveda, L; Agrasar, A T; Pastrana, L and Aguilar, C N (2013). Fungal fucoidanase production by solid-state fermentation in a rotating drum bioreactor using algal biomass as substrate. *Food Bioprod. Process, 91*: 597-594.

Sambrook, J and Russel, D W (2001). *Molecular Cloning: A Laboratory Manual*. 3rd edition. Cold Spring Harbor Laboratory. Cold Spring Harbor, NY, USA.

SAS (2003). Statistical Analysis System. Version 9.1. SAS Institute Inc., Cary, NC, USA.

Sathitkowitchai, W; Nitisinprasert, S and Keawsompong, S (2018). Improving palm kernel cake nutrition using enzymatic hydrolysis optimized by Taguchi method. *3 Biotech., 8*: 407.

Schabereiter-Gurtner, C; Piñar, G; Lubitz, W and Rölleke, S (2001). Analysis of fungal communities on historical church window glass by denaturing gradient gel electrophoresis and phylogenetic 18S rDNA sequence analysis. *J. Microbiol. Methods, 47*: 345-354.

Schmidt, C G and Furlong, E B (2012). Effect of particle size and ammonium sulfate concentration on rice bran fermentation with fungus *Rhizopus oryzae*. *Bioresour. Technol., 123*: 36-41.

Shanmugavelu, S (2014). *Decision Support System in Livestock Production*. Research Inaugural Lecture. Malaysian Agricultural Research and Development Institute (MARDI), Serdang, Malaysia.

Sundu, B and Dingle, J (2003). Use of enzymes to improve the nutritional value of palm kernel meal and copra meal. *Proc. Queensland Poult. Sci. Symp. Univ. Sydney, New South Wales, Australia*. p. 1-15.

Swe, K H; Alimon, A R; Abdullah, N and Mohd Jaafar, D (2003). Protein enrichment of palm kernel cake by solid state fermentation using *Aspergillus niger*. *Mal. J. Anim. Sci., 8(1)*: 71-76.

Wan Zahari, M and Wong, H K (2009). Research and development on animal feed in Malaysia. *WARTAZOA, 19(4)*: 172-179.

Zamani, H U; Loh, T C; Foo, H L; Samsudin, A A and Alshelmani, M I (2017). Effects of feeding palm kernel cake with crude enzyme supplementation on growth performance and meat quality of broiler chicken. *Int. J. Microbiol. Biotechnol., 2(1)*: 22-28.

Zúñiga, M; Soto, C; Mora, A; Chamy, R and Lema, J (2003). Enzymic pre-treatment of *Guevina avellana mol* oil extraction by pressing. *Process Biochem., 39(1)*: 51-57.

Journal of Oil Palm Research Vol. 34 (1) March 2022 p. 104-115
DOI: https://doi.org/10.21894/jopr.2021.0023

EFFECT OF BIOFUEL ON LIGHT-DUTY VEHICLES ENGINE PERFORMANCE AND LUBE OIL DEGRADATION

M ROPANDI[1]; Z NAHRUL HAYAWIN[1]; A A ASTIMAR[1]; A W NOORSHAMSIANA[1]; R RIDZUAN[1]* and I ZAWAWI[1]

ABSTRACT

Biofuel is a renewable, biodegradable and non-toxic fuel that is an alternative to fossil fuel. However, the long-term effect of biodiesel on internal combustion engine operation is not extensively studied. Thus, this study examined the effect of B5 biofuel (blend of 5% refined, bleached and deodourised palm olein oil (RBDPOo) and 95% automotive diesel oil (ADO) on engine performance and lube oil degradation of light-duty vehicles, i.e. *Mercedes Benz (M), Mitsubishi Storm (MS) and Toyota Hilux (TH), up to 80 000 km mileage. ADO was also used for each vehicle brand for comparison. The engine power and torque were examined using chassis dynamometer. Analysis on wear metal content of lube oil was conducted to indicate engine deterioration level. Results showed insignificant deterioration on engine performance of M and MS vehicles using ADO and B5 but B5 vehicles showed lower torque reduction than ADO vehicles. For lube oil analysis, the properties and wear metal contents in B5 vehicles were within acceptable limit as suggested by the International Council on Combustion Engines (CIMAC). Results of this study concluded that the B5 biofuel can be potentially used for selected vehicle brands without engine modifications and normal service intervals can be applied for B5 vehicles.*

Keywords: biofuel, diesel engine, engine performance, lube oil degradation, palm olein oil.

Received: 20 November 2020; **Accepted:** 1 March 2021; **Published online:** 19 May 2021.

INTRODUCTION

Driven by the spiraling cost of fossil fuel, energy security and global warming, alternative energy has become a worldwide priority. Some nations have implemented new renewable energy policies, regulatory controls and regulations to replace fossil fuel with renewable fuel (Lapuerta *et al*., 2011; Mofijur *et al*., 2015). The increasing demand for energy, particularly diesel fuel in industrial and transportation sectors, plays an important role for the development of a country (Varuvel *et al*., 2012). However, the combustion of the automotive diesel oil (ADO) emits greenhouse gases (Radhakrishnan *et al*., 2017), which cause global warming. As a consequence, biofuel is increasingly popular as an alternative fuel to reduce fossil fuel dependency as they are renewable, environmental-friendly, biodegradable and capable of mitigating climate change by expressive carbon dioxide (CO_2) cycle during combustion process (Puppan, 2002). Biofuels are liquid or gaseous fuels that are commercially derived from renewable sources such as vegetable oil and cellulosic biomass (Demirbas, 2007a).

Vegetable oils are a wonderful bio-based resource, can be used as an alternative fuel of conventional compression ignition (CI) engines (Demirbas, 2007b; Huang *et al*., 2012). Among the vegetable oils olive; palm, soybean, peanut and sunflower oils are mentionable. One challenge that is required to overcome is the higher viscosity of the vegetable oils over the petroleum-based

[1] Malaysian Palm Oil Board,
6 Persiaran Institusi, Bandar Baru Bangi,
43000 Kajang, Selangor, Malaysia.

* *Corresponding author e-mail: ridz@mpob.gov.my*

diesel. Sometimes transesterification may help to reduce the viscosity of the vegetable oil-based fuels (Shereena and Thangaraj, 2009). Different parameters such as fatty acid content, reaction temperature and methyl esters have direct influence on the performance of the fuel. Study showed on the direct injected vegetable oils and their esters as an efficient fuel for four stroke, single cylinder diesel engine performance and exhaust emissions (Altin *et al.*, 2001). It also revealed that a higher viscosity, thickening in cold condition and drying with time have some negative impact on atomisation, flow and heavy particulate emissions. In a different study, waste cooking oil was used at different percentages (10%, 20% and 30%) in volume to produce biodiesel blends using transesterification process (Abed *et al.*, 2018). Results showed a comparatively lower thermal efficiency of the biodiesel blends was noticed over the diesel fuel. In addition, a higher specific fuel consumption and higher exhaust gas temperature were noticed for the case of biodiesel blends. In addition to vegetable oils, biodiesel, dimethyl ether and Fishcher-Tropsch diesel are also considered as a potential replacement of traditional petroleum-based fuels (Kaur *et al.*, 2017).

Palm oil has huge potential for biofuel application. Malaysia is the world's second largest exporter of palm oil products with more than 87% worldwide export (Masjuki *et al.*, 2013; Parveez *et al.*, 2020). Apart from its environmental benefits and renewability, biofuels from palm oil are economically competitive compared to fossil fuel (Chin *et al.*, 2019). Owing to this, a mandatory biodiesel blend for transportation sector has been implemented in 2011 in Malaysia as carbon reduction commitment for sustainable development (Lim and Lee, 2012). Therefore, since 1 January 2010, every petrol station in Malaysia started selling B5 biodiesel (5% methyl ester blended with 95% ADO) according to the Malaysian governmental regulation (Lim and Teong, 2010).

However, there are some issues pertaining to vehicle engines due to the use of this biofuel. The emission and combustion characteristics of the biofuel caused deterioration in the performance of the engines (Ahmad *et al.*, 2011; Behçet, 2011). For improvement, modifications on engines in various aspects are needed when using biofuel (Gumus *et al.*, 2012; Hossain and Davies, 2012). However, previous studies on biofuel focused mainly on laboratory testing of the engine dynamometer and may not reflect the actual vehicle performance (Franco *et al.*, 2013; Pelkmans and Debal, 2006). Hence, the objective of this study was to examine the performance of unmodified engine of light-duty vehicles using B5 biofuel in up to 80 000 km mileage. A blend of 5% refined, bleached and deodourised palm olein oil (RBDPOo) and 95% ADO, designated as B5 biofuel, was used for the investigation. In addition, the lubricity performance in terms of used lube oil degradation was also tested and compared with fresh lube oil. Results of this study will be useful in understanding biofuel combustion and emission behaviour as well as providing scientific basis for vehicular emission control.

MATERIALS AND METHOD

Materials

The RBDPOo and ADO used for biofuel production were purchased from a commercial local supplier. The ADO was used as control for comparison study with B5. Both ADO and B5 biofuel were stored at 0°C before use.

Experimental

RBDPOo and ADO were melted and homogenised at 70°C for 30 min to destroy any crystal. Binary biofuels were prepared using RBDPOo and ADO in volumetric percentage (v/v) at a mixing ratio of 5%, by adding 50 mL RBDPOo into 950 mL of ADO in sample bottles. The sample bottle was then vigorously shaken for about 10 min and kept idle for about 5 min prior to density measurement using portable submersible density meter (Brand: Lemis VDM-250). To prepare 13 000 L biofuel, skid tank was used by pumping RBDPOo and ADO at a mixing ratio of 5% and thoroughly mixed using a circulation pump until homogenised. The preparation of B5 biofuel was considered to be complete when the densities at the top, middle and bottom of the skid tank were constant and did not vary beyond 0.006 specific gravity, similar to that of ADO (control).

A total of 12 units light-duty diesel vehicles were used in this study, comprising of four units of Mitsubishi Storm (MS), four units of Toyota Hilux (TH) and four units of Mercedes Benz (M). For each brand, two vehicles were fueled by B5, while the other two were fueled by ADO as control. The vehicles selection was based on engine technology, such as common rail direct injection and distributor pump. *Table 1* shows the general specifications for the vehicles. The selected route was a two-way journey from Klang Valley up to southern part of Perak, covering almost 800 km per day. Selected routes included 70% highways and 30% urban and suburban roads to simulate normal driving conditions in Malaysia. Each vehicle was driven simultaneously using the same route but different fuel to minimise variables, particularly traffic conditions which may affect the outcome. Field trials were conducted for a total of 80 000 km mileage to make it parallel with the standard engine warranty offered for new vehicles in Malaysia.

TABLE 1. GENERAL SPECIFICATIONS OF DIFFERENT LIGHT-DUTY VEHICLES

Maker	Mitsubishi Storm	Toyota Hilux	Mercedes Benz
Model	Storm IDI Intercooled	Hilux double cab	E270 CDI
Engine capacity (cc)	2 477	2 494	2 685
Fuel injection system (FIE)	Distributor pump	Common rail (Denso)	Common rail (BOSCH)
Maximum power (hp)	113 bhp @ 4 000 rpm	101 bhp @ 3 600 rpm	175 bhp @ 4 200 rpm
Maximum torque (Nm)	240 Nm @ 2 000 rpm	260 Nm @ 2 400 rpm	400 Nm @ 1 800 rpm

Characterisations. Physical and chemical analyses were carried out for RBDPOo, ADO and B5. The vehicle performance in terms of power and torque for each fuel was conducted on Mustang chassis dynamometer MD 600 as baseline prior to field trials. Chassis dynamometer functions as simulator for a wide range of engine application, similar to the actual behaviour when operated on the road (Amir *et al*., 2013). Vehicles used for the field trials followed the normal service interval of 5000 km, whereby about 250 mL used lube oil was taken and sent for analysis in accordance to the ASTM D1585 standard method (ASTM, 2015). After achieving cumulative mileage of 80 000 km, the performance of the vehicles was re-analysed using chassis dynamometer at 1500-5000 rpm of third and fourth gears. The experiment was conducted in duplicates for each vehicle.

RESULTS AND DISCUSSION

Physical and Chemical Properties of Fuel

Fuel properties play important roles in CI engines, engine performance, fuel consumption, vehicle emissions and engine durability. *Table 2* shows the chemical and physical properties of RBDPOo, ADO and B5 and their comparisons with the Malaysian Diesel Standard (MS123:1993). The properties of fuels provide a basic knowledge of the fuel performance and potential drawback when they are used in diesel engines. The density of RBDPOo, B5 and ADO are 0.9152, 0.8595 and 0.8565 kg L^{-1}, respectively. The values are close to each other, therefore, the impact of fuel performance and combustion were minimum. B5 showed relatively higher density compared to ADO, which caused the fuel injection system to deliver higher fuel volume, thus, increasing the fuel consumption in B5 light-duty vehicles (Valente *et al*., 2011). The viscosity of B5 biofuel was 5.066 mm^2 s^{-1}, higher than that of ADO, but it still within the requirement according to the Malaysian Diesel Standard MS123:1993 (1.5-5.8 mm^2 s^{-1}). Fuel viscosity plays an important role on engine performance. Biodiesel is more viscous than fossil diesel as it has large triacylglycerol molecules and higher molecular weight (Williamson and Badr, 1998). Fuel with high viscosity will result in high pumping resistance for fuel deliver, causing the pump to fail prematurely. This also results in poor fuel atomisation by injector leading to poor combustion which will directly affect the engine

TABLE 2. PROPERTIES OF RBDPOo, ADO AND B5 IN COMPARISON WITH THE MALAYSIAN DIESEL STANDARD (MS123:1993)

Properties	Test Method	RBDPOo	ADO	B5	MS123:1993	
					Min.	Max.
Density at 15°C (kg L^{-1})	D 4052	0.9152	0.8565	0.8595	-	-
Cetane number	D 6890	53.6	50.6	51.5	45.0	-
Sulphur content (ppm)	D 4294	-	3060	2890	-	5 000
Lubricity (μm)	IP450	119	306	234	-	-
Gross calorific value (GCV) (MJ kg^{-1})	-	39.740	45.258	45.165	-	-
Flash point (°C)	-	284	83	86	60	-
Water content (ppm)	-	124.5	54.1	137.1	-	-
Cloud point (°C)	-	13	13	13	-	18
Pour point (°C)	-	9	3	3	-	15
Viscosity at 40°C (mm^2 s^{-1})	-	34.8	4.5	5.1	1.5	5.8
Cold filter plugging point (°C)	-	-	9	10	-	-
Ash content (mass%)	-	0.001	0.001	0.001	-	0.010
Carbon residue on 10% distillation residue (wt%)	-	4.76	0.02	0.30	-	0.20

Note: RBDPOo - refined, bleached and deodourised palm olein; ADO - automation diesel oil.

performance and exhaust emission (Valente *et al.*, 2011).

Cetane number is a measure of fuel readiness for autoignition in the combustion chamber after injection (Blin *et al.*, 2013; Jeffrey *et al.*, 2015; Lawlor and Olabi, 2015). Fuel with high cetane number has the benefits of easy cold starting, short ignition delay and low engine noise (Jeffrey *et al.*, 2015; Li *et al.*, 2013). On the contrary, fuel with low cetane number results in combustion deterioration and high emission of hydrocarbons and particulate in the exhaust gas (Jayed *et al.*, 2011). B5 has higher cetane number (51.5) than ADO (50.6), exceeding the minimum value stipulated by the Malaysian Diesel Standard (MS123:1993). In addition, pour point, cloud point and cold filter plugging point (CFPP) are associated with fuel flowability in the fuel system. The cloud point, pour point and CFPP for B5 were 13ºC, 3ºC and 10ºC, respectively, which were lower than the year-wide ambient temperature in Malaysia (33ºC-37ºC). The flash point of fuels determines the flammability of the fuels and is an essential criterion for fuel transportation and storage (Masjuki and Kalam, 2013). The flashpoint of B5 was 86ºC, which is slightly higher than ADO (83ºC) and complied with the minimum standard requirement (MS123:1993). Hence, B5 is safe where transportation and storage are concerned.

Other important fuel parameters are carbon residue, ash content and gross calorific value (GCV). Carbon residue indicates the tendency of fuel to deposit on the injector and combustion chamber, which invariably affects the engine performance as well as the emission (Jeffrey *et al.*, 2015). The carbon residue (10% residue) of B5 was higher than standard (MS 123:1993). However, the ash content of B5 and ADO was similar and thus, it was expected that the wear and tear of the engine moving parts would also be similar. In fuel selection, GCV or energy content is a vital criterion as it reflects combustion efficiency and fuel consumption. This study found that B5 biofuel indicated slightly lower GCV value (45.165 MJ kg^{-1}) than ADO (45.258 MJ kg^{-1}), suggesting higher fuel consumption for B5 compared to ADO in vehicles. It can be inferred that the fuel consumption is high for fuel with high density and low energy content (McCarthy *et al.*, 2011; Munack, 2007).

Vehicle Power Performance

The vehicle performance was carried out using a chassis dynamometer at the start (0 km) and at the end of field trials (80 000 km). Comparisons of maximum power output for both fuels on all vehicles at the start and the end of field trials are shown in *Figure 1*. However, some of the vehicle performances for certain mileage are not depicted in the figure due to accident, major breakdown and theft. The vehicle major breakdown was not due to fuel-related problems. At the start of field trials, ADO and B5 fueled TH had an average power output of 69.75 and 59.6 hp, respectively. The vehicles fueled by ADO had higher power output which could be attributed to high GCV and lower viscosity, thereby leading to better engine combustion. Owing to lower GCV, the vehicles fueled by B5, namely TH3 and TH4, showed slight decrease in their performance, 8.54% and 7.56%, respectively, at the start and the end of field trials. Saiful Islam *et al.* (2014) deduced that biodiesel with low energy content caused low engine power output. Other reasons which reduced vehicle power could be wear and tear of vehicle parts and carbon deposited in combustion chamber and injectors.

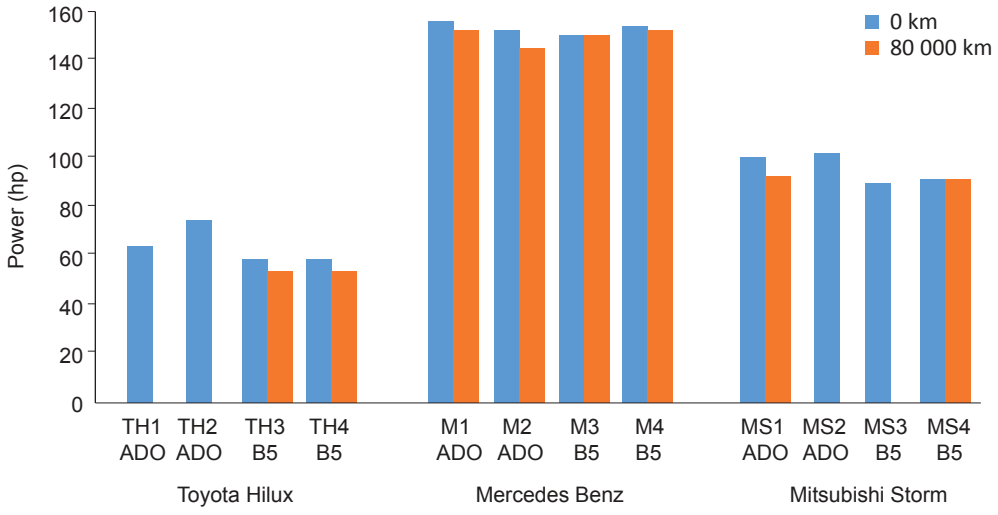

Figure 1. Maximum power output of field trial vehicles measured at 0 km and 80 000 km.

Birgel *et al.* (2008) claimed that the overall system performance may be adversely affected due to the formation of deposits within the holes of the injector nozzle or on the exterior injector tip. Similarly, Husnawan *et al.* (2009) also agreed that the deposits formed in combustion chamber not only affect the engine performance but also its drivability. No comparison can be made on ADO due to a major breakdown of TH1 at 63 000 km, while TH2 was stolen before reaching 80 000 km.

Mercedes Benz (M) which employed common rail fuel injection, showed average maximum power outputs of 116.3 kW (155.9 hp) and 114.7 kW (153.8 hp), for ADO and B5, respectively. B5 has lower power output by 1.3% and this may be related to the GCV of B5 (45.165 MJ kg^{-1}), which was lower by 0.21% compared to ADO. The reductions of power output at the start and end of the trials for B5 were in the range of 0.19%-1.16%, and 1.47%-4.97% for ADO. According to McCarthy *et al.* (2011), low reduction in power output for B5 is probably due to higher oxygen content in biofuel, thus, improving fuel combustion in the engine. A complete combustion can be achieved by diesel engine fueled by biodiesel due to the presence of oxygen in the biodiesel's molecule.

The distributor pump for diesel injection (MS that used old technology) showed an average maximum power of 103.5 and 91.9 hp for ADO and B5, respectively, at the start of the field trials. Decrease in power output (11.16%) on B5 was recorded for vehicles fueled by ADO. After undergoing 80 000 km field trials, the maximum power output of the vehicles fueled by B5 and ADO decreased by 0.54 and 8.44%, respectively. Lower reduction of power output for B5 was recorded compared to ADO. This could be due to high oxygen content in B5 biofuel, thereby resulting in better combustion, as occurred in M vehicles (Lahane and Subramaniam, 2015; Zulqarnaine *et al.*, 2020). Less carbon was deposited in the injectors in the long run, rendering marginal decline in the engine performance. Generally, ADO showed slightly better performance compared to B5 regardless of the engine technologies used. Although common rail diesel injection system is more sensitive and less tolerant to fuel quality, the system employs high injection pressure at low combustion temperature for better engine performance and fuel efficiency while lowering pollutant emission (Jeffrey *et al.*, 2015).

Vehicle Torque Performance

Figure 2 shows the maximum torque produced from vehicles measured at 0 and 80 000 km. Vehicles fueled by B5 showed lower torque compared to vehicles fueled by ADO at 0 km. TH and MS vehicles showed a decrease in performance by 13.6% and 12.33% at maximum torque when fueled by B5, while M vehicles showed only a marginal performance decrease of 0.5% using B5 at 0 km. By comparing the torque at 0 and 80 000 km, TH vehicles showed an average reduction of 1.8% and 3.8% for vehicles fueled by B5. M vehicles showed a reduction of 1.8% and 8.51% for ADO and torque reductions were 1.7% and 2.1% for B5, which were less than ADO. Meanwhile, for ADO of MS vehicles, lower torque reduction (1.15%) was obtained compared to B5 (4.49%). The injection characteristics are greatly affected by the viscosities of the fuel (Sugozu *et al.*, 2011). The reduced torque performance is also due to the lower heating value of the fuel used. In addition, the torque performance is influenced by energy content (GCV), similar to power. Fuel with lower energy content exhibited lower torque performance as reported by McCarthy *et al.* (2011).

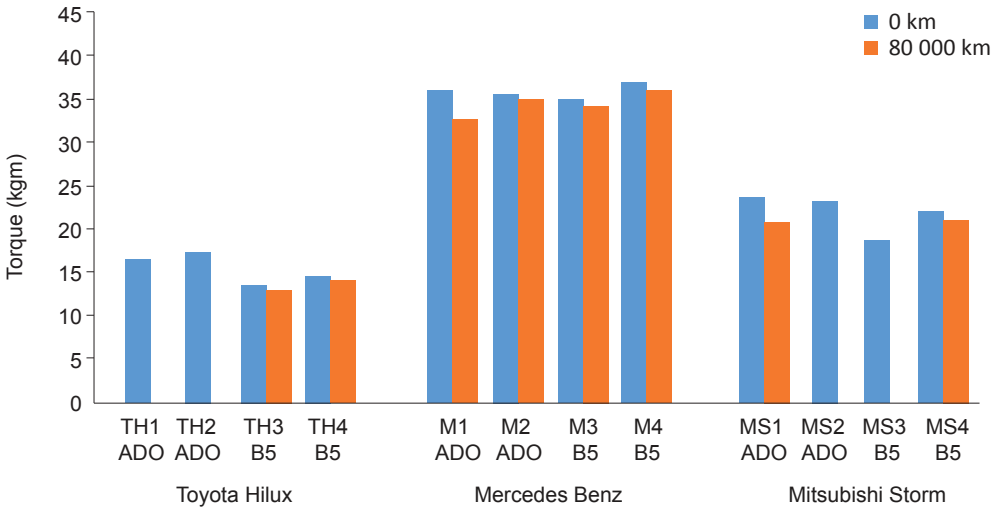

Figure 2. Maximum torque of field trials vehicles measured at start and end of field trials.

Lube Oil Analysis

Lubricant oil for engine serves several purposes including friction and wear reduction, protection of engine parts from corrosion and oxidation and transfer of heat from core engine components (Nagy *et al.*, 2019). It has been reported that biodiesel tends to accumulate in engine crankcase affecting lubricant oil quality compared to diesel owing to its higher viscosity (He *et al.*, 2011; Uy *et al.*, 2011). Thus, by analysing the used lube oil of vehicles fueled by B5 and ADO, the engine conditions could be evaluated. In this study, the analysis of used lube oil was carried out during routine services at 5000 km interval for MS and TH vehicles and 10 000 km interval for M vehicles as recommended by the service center. The effect of fuel used on the performance of lubricant oil in terms of degradation and wear of metal was performed by an accredited external laboratory according to standard method. This can be used to indicate the level of engine deterioration (Vališ *et al.*, 2015). All the analysis of lube oils throughout the routine services up to 80 000 km showed that the properties of used lube oils were still within acceptable limits for all parameters measured. Thus, normal service intervals were appropriate for vehicles fueled by B5. The typical warning limit for metal wear as well as additive deterioration in used lube oil was set by the lube oil laboratory based on their history on engine type, engine technology, type of fuel used, type of lube oil used, service interval, engine operating conditions and top up amount.

In a previous study, the impact of diesel fuel blended with biodiesel from palm oil and jatropha oil were assessed for the evaluation of engine lube oil performance by long duration testing (Gulzar *et al.*, 2016). The blending ratio of biodiesel and diesel fuel was 1:4. A single-cylinder CI engine was chosen for the testing. It was noticed that the acidity and viscosity of used blended fuels were increased and decreased, respectively. On the other hand, a slight increase in wear losses and friction were also noticed. In another study, 20% biodiesel and ultra low sulphur diesel blend were used for the comparative analysis in the assessment of lubricating properties (He *et al.*, 2011). Light duty vehicles and 4000 miles of operation were considered for the testing. Analysis showed a little difference in wear scar, viscosity, total base number, total acid number and soot.

Viscosity. *Figure 3* shows the viscosity of used lube oils of TH vehicle fueled by B5 and ADO. Typical warning limit for used lube oil viscosity is either 45% increase or 25% decrease (viscosity at 40°C) in comparison with fresh lube oil viscosity. Vehicles fueled by ADO were THB0-1 and THB0-2, while THB5-1 and THB5-2 vehicles were fueled by B5. The viscosity of fresh lube oil for THB0-1 was 52.56 $mm^2 s^{-1}$, while the upper and lower limits were 70.96 and 39.43 $mm^2 s^{-1}$, respectively. The viscosity for THB0-1 showed a decreasing trend due to dilution, which gave rise to lowest viscosity (23.22 $mm^2 s^{-1}$) at vehicle mileage of 60 000 km. After inspection, the vehicles were found to have mechanical problems and unable to continue the trials after 63 000 km. For THB0-2, the upper and lower limit viscosities were 170.51 and 94.72 $mm^2 s^{-1}$. For the first 15 000 km, the viscosity of used lube oil was found to be lower (121.8 $mm^2 s^{-1}$) than fresh lube oil (126.3 $mm^2 s^{-1}$). This may be due to contamination that stemmed from fuel dilution which decreased the lubricant viscosity, which in turn, may accelerate wear process as reported by Newell (1999). In addition, Wakiru *et al.* (2017) postulated that viscosity of fuel and the types of engine could increase or reduce the lubricant viscosity. For automotive application, lubricant viscosity tends to decrease due to dilution when the viscosity of fuel used is lower than that of lubricant.

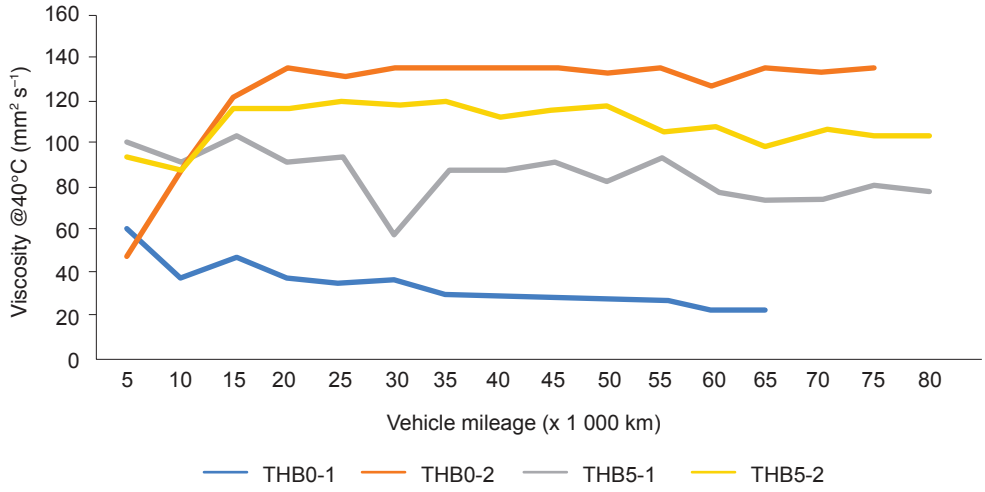

Figure 3. Viscosity of used lube oil at 40°C for Toyota Hilux fueled by automation diesel oil (ADO) and B5.

Subsequently, the viscosity of the used lube oil was almost consistent with an average of 134.06 $mm^2 s^{-1}$. Used lube oil viscosity of THB5-1 a showed slight decreasing trend with average viscosity of 87.6 $mm^2 s^{-1}$, which is still within acceptable limits (76.95 $mm^2 s^{-1}$ to 138.5 $mm^2 s^{-1}$). On the other hand, the upper and lower viscosity limits for THB5-2 were 160.24 and 89.02 $mm^2 s^{-1}$, respectively. The average viscosity of used lube oil was 112.12 $mm^2 s^{-1}$ and it is within acceptable limit.

Total base number. Total base number (TBN) in used lube oil is a measurement of reserved alkalinity in lubricating oil to neutralise acidic materials originated from combustion products condensed in engine parts (CIMAC, 2011). The acidic materials are corrosive to the engine components. Typical minimum level for TBN in used lube oil is 2. Based on *Figure 4*, the TBN for all used lube oils were within limit, indicating that normal service intervals were sufficient to provide required protection to the engine (Marie *et al.*, 2020).

Insoluble pentanes content. Pentanes insoluble is a measure of lube oil degradation due to insoluble contaminants either from fuel combustion and fuel degradation or from oil degradation. Fresh lube oil normally has a value of less than 0.10% by weight and the warning limit for used lube oil is 1.5%. All the TH vehicles tested fueled by ADO or B5 showed pentanes insoluble to be less than 1.5%. The values for THB0-1 ranged from 0.1%-0.24% and for THB0-2 the values were in the range of 0.1%-0.38%. The values for THB5-1 and THB5-2 were in the range of 0.1%-0.75% and 0.1%-1.25%, respectively. This indicated that more insoluble contaminants are present in the used lube oil for the vehicles fueled by B5 (Emma, 2010). The amount of insoluble may increase due to fuel contamination, lube oil degradation and incomplete fuel combustion (CIMAC, 2011).

Wear metal. Wear metal analysis is pivotal for maintenance evaluation. Wear metals measured for used lube oil in this study were chromium (Cr), copper (Cu), aluminum (Al), iron (Fe) and lead (Pb). Iron and lead are two main indicators of potential engine failure mostly analysed for used lube oil (Vališ *et al.*, 2015). *Figures 5* to *7* show the wear metal contents for aluminum, iron and copper in used lube oils at 80 000 km vehicle service. The wear metals of used lube oils of the tested vehicles were within acceptable limit according to CIMAC (2011). The Cr and Pb contents measured in used lube oil throughout the field trials were 1 ppm or less. Their typical warning limits were 40 ppm and 100 ppm, respectively. The origin of Cr was mainly from wear resistant of alloy steel used to fabricate piston ring, roller bearing and crankshaft. The source of lead could be detected from the crankshaft bearing or from the additive used in the lube oil itself (Yunus *et al.*, 2013). The typical warning limit for Al content is 40 ppm and the sources of Al metal were mostly piston, blower and oil pump bushing (Yunus *et al.*, 2013).

All the tested vehicles showed Al content of 5 ppm and below, except for THB0-2. Slightly high Al content was obtained for THB0-2 for the first 20 000 km, which may indicate running condition or mechanical problem. However, after servicing the vehicles at least for four times, the Al content in the used lube oils was below 5 ppm. Cu is the main component for copper bushing, particularly used for valve train bushing, camshaft bushing, bearing overlay and connecting rod bearing (Yunus *et al.*, 2013). The typical warning limit for Cu in used lube oil is 40 ppm and all the vehicles tested had Cu content of less than 10 ppm in used lube oils regardless of the type of fuel used. However, THB0-2 showed a slight increase in Cu content (18 ppm) for 20 000 km service interval. The Fe content in used lube oil mostly originates from piston ring, cylinder liner, valve train

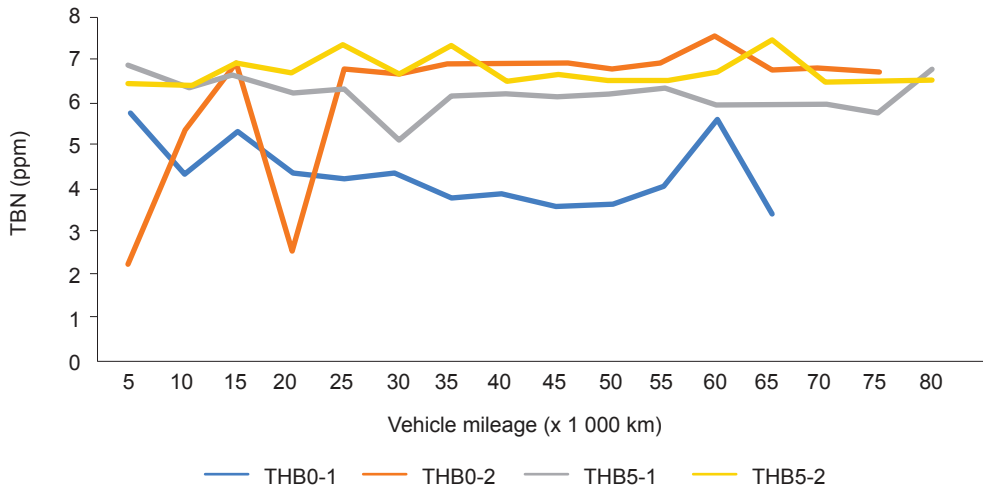

Figure 4. The total base number (TBN) of used lube oil for Toyota Hilux fueled by automation diesel oil (ADO) and B5.

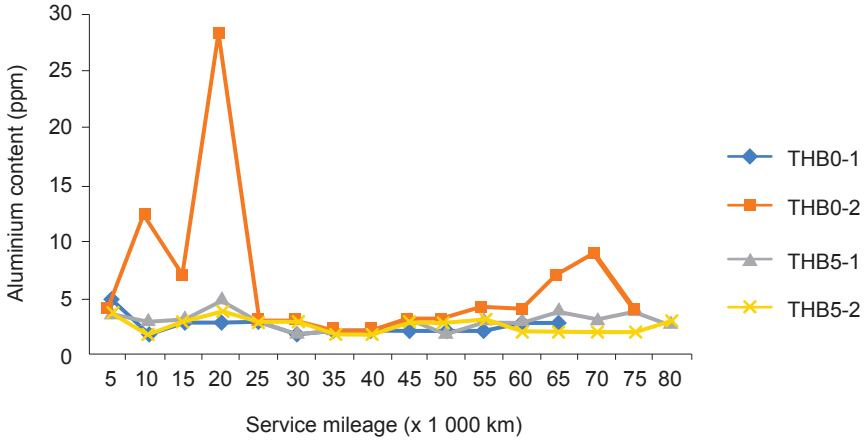

Figure 5. Aluminium (Al) content in used lube oils throughout field trials.

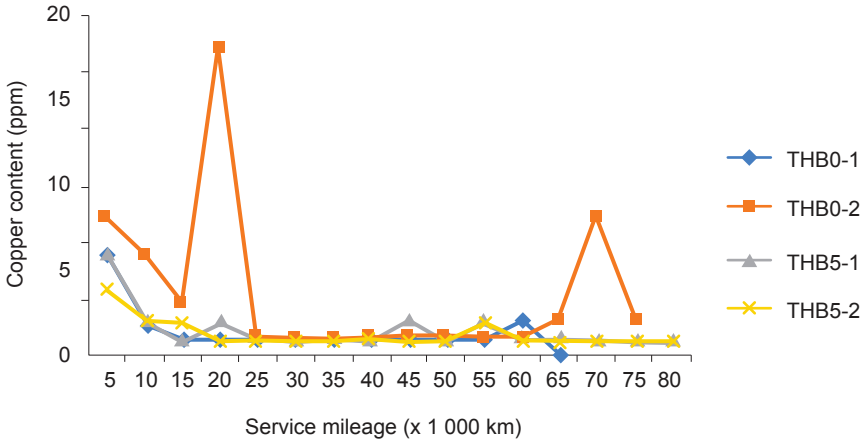

Figure 6. Copper (Cu) content in used lube oils throughout field trials.

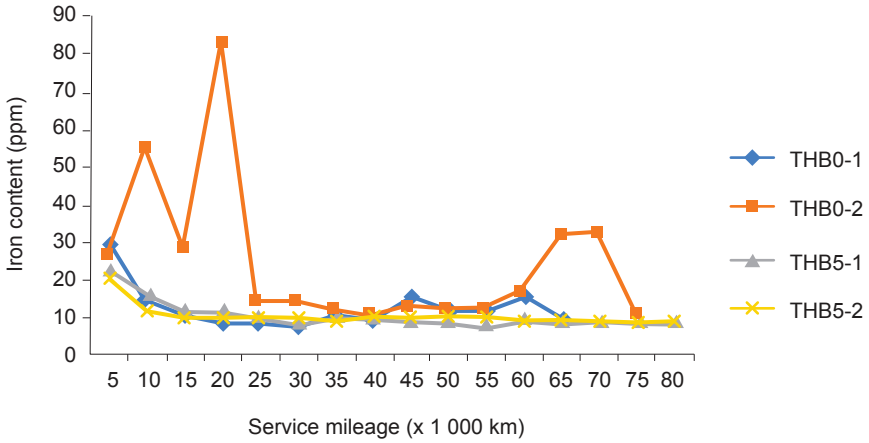

Figure 7. Iron (Fe) content in used lube oils throughout field trials.

and camshaft since Fe is the main engine component (Yunus *et al.*, 2013). The typical warning limit for Fe in used lube oil is 100 ppm. Thus, Fe content in lube oil in all the vehicles tested, regardless of fuel and injection technology used, were less than 30 ppm, except for THB0-2, which exhibited slightly higher Fe content of 30 ppm at second, fourth, 13th and 14th lube oil service intervals. However, the reported values were still lower than 100 ppm.

Silicon content. Silicon is one of the main micro constituents which may expedite the wear and tear of engine parts as well as contaminate the lube oil (Sendilvelan and Anandanatarajan, 2017).

Silicon could enter the engine from air filter, engine breathing systems and seal joint materials (Sendilvelan and Anandanatarajan, 2017). *Figure 8* shows the silicon content in used lube oils of the vehicles tested. It was found that silicon contents of fresh lube oil for THB0-1, THB0-2 and THB5-1 shared the same results, which were at 22 ppm, while THB5-2 recorded 18 ppm. The limit for silicon (Si) content is 20 ppm.

CONCLUSION

In this study, blending of 5% RBDPOo with 95% ADO was performed to produce B5 biofuel, which demonstrated great potential as alternative renewable fuel for diesel vehicles application. Results from field trials on different types of diesel injection systems showed insignificant deterioration on the engine performance as well as on service intervals. The engine power output of B5 was lower than ADO for TH and M vehicles but different scenarios were observed for MS vehicles. All the vehicles fueled by B5 showed lower torque reduction for M and MS vehicles compared to those fueled by ADO. The analysis of used lube oils showed that all the parameters studied including wear metal content of the engine oil were within acceptable limits. Thus, normal service intervals were appropriate for vehicles fueled by B5 (after 80 000 km mileage). There was no fuel-related problem reported on those vehicles tested. Therefore, it can be inferred that B5 biofuel can be used in diesel vehicles, particularly vehicles and machineries in oil palm plantations as part of strategies to reduce and mitigate the use of fossil fuel consumption and global warming, respectively. Sustainability of palm oil in global market could also be enhanced. Nevertheless, it is suggested that this study be extended for exhaust emission, long term fuel storage stability, maximum blending ratio and shelf life to support the results of the use of biofuel blend in compressed ignition engine, either mobile or stationary.

ACKNOWLEDGEMENT

The authors would like to thank the Director-General of MPOB for the financial support to conduct this study. The authors also thank all MPOB officers and staff in Engineering and Processing Division as well as Mechanisation and Engineering Unit for providing assistance throughout the field trials.

REFERENCES

Abed, K A; Morsi, A K; Sayed, M M; El-Shaib, A A and El Gad, M S (2018). Effect of waste cooking-oil biodiesel on performance and exhaust emissions of a diesel engine. *Egypt. J. Pet., 27*: 985-989.

Althin, R; Cetinkaya, S and Yucesu, H S (2001). The potential of using vegetable oil fuels as fuel for diesel engines. *Energy Convers. Manag., 42*: 529-538.

ASTM (2015). Standard test methods for fatty acids content of pine chemicals, including rosin, tall oil and related products. ASTM D1585-15. ASTM International, West Conshohocken, Pennsylvania, USA.

Ahmad, A; Ghufran, R and Wahid, Z A (2011). Bioenergy from anaerobic degradation of lipids in palm oil mill effluent. *Rev. Environ. Sci. Biotechnol., 10(4)*: 353-376.

Amir, K; Shahrul, A O; Md Norrizam, M J; Norrizal, M; Siti Mariam, B and Manshoor, B (2013). Performance and emissions characteristics of diesel engine fuelled by biodiesel derived from palm oil. *Appl. Mech. Mater., 315*: 517-522.

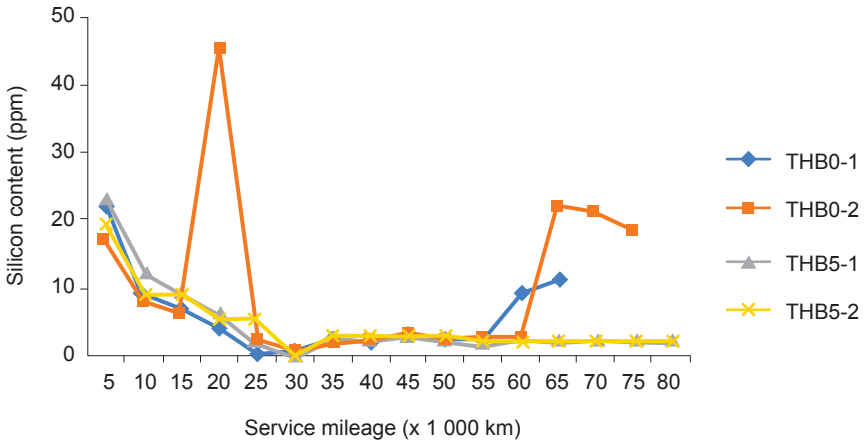

Figure 8. Silicon content in used lube oils throughout field trials.

Behçet, R (2011). Performance and emission study of waste anchovy fish biodiesel in a diesel engine. *Fuel Process. Technol., 92(6)*: 1187-1194.

Birgel, A; Ladommatos, N; Aleiferis, P and Zülch, S (2008). Deposit formation in the holes of diesel injector nozzles: A critical review. SAE Tech. Paper 2008-01-2383.

Blin, J; Brunschwig, C; Chapuis, A; Changotade, O; Sidibe, S S; Noumi, E S and Girard, P (2013). Characteristics of vegetable oils for use as fuel in stationary diesel engines - Towards specifications for a standard in West Africa. *Renew. Sust. Energ. Rev., 22*: 580-597.

Chin, H-C; Choong, W-W; Alwi, S R W and Mohammed, A H (2019). A PLS-MGA analysis of farming characteristics on the intentions of smallholder oil palm planters to collect palm residues for biofuel production. *Biomass Bioenergy, 120*: 404-416.

CIMAC (2011). Used engine oil analysis – User interpretation guide. https://www.cimac.com/cms/upload/Publication_Press/Recommendations/Recommendation_30.pdf, accessed on 1 July 2020.

Demirbas, A (2007a). Progress and recent trends in biofuels. *Prog. Energ. Combust. Sci., 33*: 1-18.

Demirbas, A (2007b). Alternatives to petroleum diesel fuel energy sources. *Energy Sources B: Econ. Plan. Policy, 2(4)*: 343-351. DOI: 10.1080/15567240600629518.

Emma, M (2010). Monitoring of lubricant degradation with ruler amd mpc. Masters thesis, Linkoping University.

Franco, V; Kousoulidou, M; Muntean, M; Ntziachristos, L; Hausberger, S and Dilara, P (2013). Road vehicle emission factors development - A review. *Atmos. Environ., 70*: 84-97.

Gumus, M; Sayin, C and Canakci, M (2012). The impact of fuel injection pressure on the exhaust emissions of a direct injection diesel engine fuelled with biodiesel – diesel fuel blends. *Fuel, 95*: 486-494.

Gulzar, M; Masjuki, H H; Varman, M; Kalam, M A; Zulkifli, N W M; Mufti, R A; Liaquat, A M; Rehan, Z and Arslan, A (2016). Effects of biodiesel blends on lubricating oil degradation and piston assembly energy losses. *Energy, 111*: 713-721.

He, X; Williams, A; Christensen, E; Burton, J and McCormick, R (2011). Biodiesel impact on engine lubricant dilution during active regeneration of aftertreatment systems. *SAE Int. J. Fuels Lubr. 4*: 158-178.

Hossain, A K and Davies, P A (2012). Performance, emission and combustion characteristics of an indirect injection (IDI) multi-cylinder compression ignition (CI) engine operating on neat Jatropha and karanj oils preheated by jacket water. *Biomass Bioenergy, 46*: 332-342.

Huang, D; Zhou, H and Lin, L (2012). Biodiesel: An alternative to conventional fuel, international conference on future energy, environment and materials. *Energy Procedia, 16*: 1874-1885.

Husnawan, M; Masjuki, H H; Mahlia, T M I and Saifullah, M G (2009). Thermal analysis of cylinder head carbon deposits from single cylinder diesel engine fueled by palm oil-diesel fuel emulsions. *Appl. Energy, 86*: 2107-2113.

Sugozu, I; Eryilmaz, T; Örs, I and Solmaz, Ö (2011). Biodiesel production from animal fat–palm oil blend and performance analysis of its effects on a single cylinder diesel engine. *EEST A Energy Sci. Res., 28(1)*: 505-514.

Jayed, M H; Masjuki, H H; Kalam, M A; Mahlia, T M I; Husnawan, M and Liaquat, A M (2011). Prospects of dedicated biodiesel engine vehicles in Malaysia and Indonesia. *Renew. Sust. Energ. Rev., 15(1)*: 220-235.

Jeffrey, M; Bergthorson, A N and Thomson, M J (2015). A review of the combustion and emissions properties of advanced transportation biofuels and their impact on existing and future engines. *Renew. Sust. Energy Rev., 42*: 1393-1417.

Kaur, H; Vipasha, V; Kumar, T and Isha (2017). Biodiesel produced from waste cooking oil the best alternative for fossil fuels. A review. *Int. J. Medical Sci. Innov. Res. (IJMSIR), 2*: 136-142.

Lahane, S and Subramaniam, K A (2015). Effect of different percentages of biodiesel-diesel blends on injection, spray, combustion, performance and emission characteristics of a diesel engine. *Fuel, 139*: 537-545.

Lapuerta, M; Villajos, M; Agudelo, J R and Boehman, A L (2011). Key properties and blending strategies of hydrotreated vegetable oil as biofuel for diesel engines. *Fuel Process. Technol., 92(12)*: 2406-2411.

Lawlor, V and Olabi, A G (2015). Review of scientific research regarding PPO, tallow and RVO as diesel engine fuel. *Fuel, 145*: 25-38.

Li, H; Biller, P; Hadavi, S A; Andrews, G E; Przybyla, G and Lea-Langton, A (2013). Assessing combustion and emission performance of direct use of SVO in a diesel engine by oxygen enrichment of intake air method. *Biomass Bioenergy, 51*: 43-52.

Lim, S and Teong, L (2010). Recent trends, opportunities and challenges of biodiesel in Malaysia: An overview. *Renew. Sust. Energy Rev., 14*: 938-954.

Lim, S and Lee, K (2012). Implementation of biofuels in Malaysian transportation sector towards sustainable development: A case study of international cooperation between Malaysia and Japan. *Renew. Sust. Energy Rev., 16*: 1790-1800.

Malaysian Standard (1993). Diesel Fuel-Specification, MS123:1993.

Marie, S; Branislav, S; Petr, V and Ivana, H (2020), FTIR spectrometry with PLS regression for rapid TBN determination of worn mineral engine oils. *Energies, 13*: 6438.

Masjuki, H H and Kalam, M A (2013). An overview of biofuel as a renewable energy source: Development and challenges. *Procedia Eng., 56*: 39-53.

Masjuki, H H; Kalam, M A; Mofijur, M and Shahabuddin, M (2013). Biofuel: Policy, standardization and recommendation for sustainable future energy supply. *Energy Procedia, 42*: 577-586.

McCarthy, P; Rasul, M G and Moazzem, S (2011). Comparison of the performance and emissions of different biodiesel blends against petroleum diesel. *Int. J. Low-Carbon Technol., 6*: 255-260.

Mofijur, M; Masjuki, H H; Kalam, M A; Ashrafur Rahman, S M and Mahmudul, H M (2015). Energy scenario and biofuel policies and targets in ASEAN countries. *Renew. Sust. Energy Rev., 46*: 51-61.

Munack, A (2006). Biodiesel - A Comprehensive Handbook (Mittelbach, M and Remschmidt, C eds.). *Biotechnology Journal, 1*. p. 102.

Nagy, A L; Knaup, J and Zsoldos, I (2019). Investigation of used engine oil lubricating performance through oil analysis and friction and wear measurements. *Acta Tech. Jaurinensis, 12(3)*: 237-251.

Newell, G E (1999). Oil analysis cost-effective machine condition monitoring technique. *Ind. Lubr. Tribol., 51*: 119-124. DOI: 10.1108/00368799910268066.

Parveez, G K A; Elina, H; Soh, K H; Meilina, O B; Kamalrudin, M S; Mohd, N I Z B S; Shamala, S; Zafarizal, A Z H and Zainab, I (2020). Oil palm economic performance in Malaysia and R&D progress in 2019. *J. Oil Palm Res., 32(2)*: 159-190.

Pelkmans, L and Debal, P (2006). Comparison of on-road emissions with emissions measured on chassis dynamometer test cycles. *Transp. Res. D: Transp. Environ., 11*: 233-241.

Puppan, D (2002). Environmental evaluation of biofuels. *Period Polytech. Ser. Soc. Man. Sci., 10*: 95-116.

Radhakrishnan, S; Devarajan, Y; Mahalingam, A and Nagappan, B (2017). Emissions analysis on diesel engine fueled with palm oil biodiesel and pentanol blends. *J. Oil Palm Res., 29(3)*: 380-386.

Saiful Islam, M; Ahmed, A S; Islam, A; Abdul Aziz, S; Xian, L C and Mridha, M (2014). Study on emission and performance of diesel engine using Castor biodiesel. *J. Chem., 2014*: 8. DOI: 10.1155/2014/451526.

Sendilvelan, S and Anandanatarajan, R (2017). Controlling silicon and soot content in the crank case oil to improve performance of diesel engine. *J. Chem. Pharm. Sci., 10(1)*: 185-188.

Shereena, K M and Thangaraj, T (2009). Biodiesel: An alternative fuel produced from vegetable oils by transesterification. *Electron. J. Biol., 5(3)*: 67-74.

Uy, D; Zdrodowski, R J; O'neill, A E; Simko, S J; Gangopadhyay, A K; Morcos, M; Lauterwasser, F and Parsons, G (2011). Comparison of the effects of biodiesel and mineral diesel fuel dilution on aged engine oil properties. *Tribol. Trans., 54*: 749-763.

Valente, O S; Pasa, V M D; Belchior, C R P and Sodré, J R (2011). Physical-chemical properties of waste cooking oil biodiesel and castor oil biodiesel blends. *Fuel, 90*: 1700-1702.

Vališ, D; Zak, L and Pokora, O (2015). Failure prediction of diesel engine based on occurrence of selected wear particles in oil. *Eng. Fail. Anal., 56*: 501-511.

Varuvel, E G; Mrad, N; Tazerout, M and Aloui, F (2012). Experimental analysis of biofuel as an alternative fuel for diesel engines. *Appl. Energy, 94*: 224-231.

Wakiru, J; Pintelon, L; Chemweno, P and Muchiri, P (2017). Analysis of lubrication oil contamination by fuel dilution with application of cluster analysis. XVII International Scientific Conference on Industrial Systems. 4-6 October 2017. Novi Sad, Serbia.

Williamson, A M and Badr, O (1998). Assessing the viability of using rape methyl ester (RME) as an alternative to mineral diesel fuel for powering road vehicles in the United Kingdom. *Appl. Energy, 59(2-3)*: 187-214.

Yunus, S; Amirul, A R; Syazuan, A L; Nik Rosli A; Mohammad Ali, A and Abdul Hakim, A (2013). Comparative study of used and unused engine oil (Perodua Genuine and Castrol Magnatec Oil) based on property analysis basis. *Procedia Eng., 68*: 326-330.

Zulqarnain; Mohd Hizami, M Y; Muhammad, A; Norwahyu, J and Ahmad Zuhairi, A (2020). The challenges of a biodiesel implementation program in Malaysia. *Proceses, 8*: 1244.

Journal of Oil Palm Research Vol. 34 (1) March 2022 p. 116-128
DOI: https://doi.org/10.21894/jopr.2021.0027

THE COLD FLOW PROPERTIES OF PALM BIODIESEL FOR DIESEL BLENDS MANDATE IN MALAYSIA'S HIGHLANDS

NURSYAIRAH JALIL[1,2]; HARRISON LIK NANG LAU[1]* and RIFQI IRZUAN ABDUL JALAL[2]

ABSTRACT

Greenhouse gas emission from burnt fossil fuels in transportation leads to global warming. Therefore, biodiesel which is believed to help in reducing carbon dioxide (CO_2) emission has been widely used as renewable energy that will replace diesel fuel. Biodiesel of 7% in diesel or B7 has been accepted worldwide to be the automotive fuel. In the last decade, most countries that implemented biodiesel program have gradually increased its biodiesel blending ratio above 7% for economic and environmental reasons. Malaysia has also announced the implementation of B20 starting January 2020. However, the biodiesel mandate in Malaysia's highlands was maintained at B7 because of the concern on low temperature vehicle operability. This study focuses on the cold flow properties of the blended diesel fuels and the quality of the palm biodiesel for the national biodiesel program. The monoglycerides and the water content in the biodiesel were evaluated in relation to cold temperature fuel performance. Cloud point (CP) and cold filter plugging point (CFPP) of B7 diesel sold at highlands were found below the lowest ambient temperature recorded at highlands for the past 10 years. Both CP and CFPP of Euro 5 diesel were lower than Euro 2M diesel. A 41-months survey of the monoglycerides and the water contents in the palm biodiesel indicated that the palm biodiesel used in Malaysia's biodiesel mandate meets both the EN14214:2019 and the Malaysian Standard MS2008:2014 specifications. CP and CFPP of the blended fuels increase with the increase of biodiesel blending ratio. Based on the study, it is anticipated that B20 could be introduced at Malaysia's highlands without any problem.

Keywords: biodiesel, CFPP, CP, monoglyceride content, palm biodiesel, water content.

Received: 21 December 2020**; Accepted:** 11 March 2021**; Published online:** 15 June 2021.

INTRODUCTION

The search of environmental-friendly and renewable energy sources to meet the worldwide energy demand has become immensely important to address global warming and climate change issues. The development of liquid biofuels has been seen to be favourable as a substitute to fossil fuels. Biodiesel or mono-alkyl esters of long-chain fatty acid derived from vegetable oils or animal fats, has been used as the diesel replacement without much technical studies or being supported by its suitability studies (Bari and Hossain, 2019; Graboski and McCormick, 1998; Javed and Anurag, 2014). Biodiesel has rapidly emerged as one of the fastest growing alternative fuels in the world attributed by its clean emissions profile, ease of use for transport and many other benefits (Abed *et al.*, 2019; Ali *et al.*, 2016; Ayhan, 2007). The first internal combustion engine developed by Rudolf Diesel in 1900 was also based on food crops (biodiesel) (Ziolkowska, 2018). When crude oil was discovered a few years later, vegetable oil-based biofuel became irrelevant but resurfaced

[1] Malaysian Palm Oil Board,
6 Persiaran Institusi, Bandar Baru Bangi,
43000 Kajang, Selangor, Malaysia.

[2] Universiti Kuala Lumpur Malaysia France Institute (UniKL MFI)
Section 14, Jalan Damai, Seksyen 14,
43650 Bandar Baru Bangi, Selangor, Malaysia.

* *Corresponding author e-mail: harrison@mpob.gov.my*

later due to oil crisis in the 1970's. Based on data by Organization or Economic Co-operation and Development (OECD) and Food and Agriculture Organization (FAO) (2020), the global biodiesel production from 2016-2018 stood at 43.1 billion litres with projected growth of 0.1% to reach 44 billion litres by 2028. The main driver for the increase of biodiesel usage is due to the government's mandate of some countries like Indonesia and Malaysia.

The research of renewable biofuel from palm oil in Malaysia was inspired in 1982. The biofuel was produced by converting palm oil into biodiesel (B100) or palm methyl ester (PME) via transesterification process (Choo *et al*., 1997). Choo *et al*. (2005) reported that PME had been thoroughly examined, tested and proven as a superior diesel substitute and gained worldwide acceptance. There are 19 operational biodiesel plants in Malaysia with a total production capacity of 2.2 million tonnes per year (Parveez *et al*., 2020).

Biodiesel can be produced from various feedstock such as palm, rapeseed, soybean, used cooking oil, tallow and others. Among all other oils, oil palm has the highest oil yield per cultivated area among all vegetable oils (Murphy, 2014). Thus, it is the most promising raw material for biodiesel production (Khairul and Manabu, 2018). Palm oil producing countries like Indonesia, Malaysia dan Thailand are aggressively implementing biodiesel program to encourage the use of renewable resources *i.e.,* palm oil domestically while reducing dependency on petroleum imports. Both Malaysia and Indonesia contributed to 85% of the global palm oil supply (Kushairi *et al*., 2019).

Biodiesel has been mandated in Malaysia since 2010 starting with blending of 5% PME (B5) and gradually increased to 20% (B20) in January 2020. The implementation of B30 program in Malaysia is expected by 2025 (Ministry of International Trade and Industry, 2020). On the other hand, Indonesia had implemented B20 program in January 2016 and recently increased the mandate to B30 starting January 2020 (Agus *et al*., 2019; Ministry of Energy and Mineral Resources, 2014). The increase in domestic consumption of palm oil through biodiesel program could help to absorb the surplus palm oil in the market as a result of the European Union's proposal to phase out palm oil-based biofuels by 2030 [Commission Delegated Regulation (2019) EU 2019/807]. There are two grades of diesel available at retail stations in Malaysia which are B10 (blends of 10% v/v palm biodiesel with 90% v/v diesel petroleum) with Euro 2M diesel (E2B10) and B7 (blends of 7% v/v palm biodiesel with 93% diesel petroleum) with Euro 5 diesel (E5B7). E5B7 is an optional diesel fuel sold at selected stations across all states throughout the country. B20 with Euro 2M diesel (E2B20) has been implemented at certain locality to replace E2B10 beginning January 2020. Due to the concern on low temperature vehicle operation at cold places, the retail stations at highlands have been exempted from selling E2B10 but only supply B7 with Euro 5 diesel (E5B7) and Euro 2M diesel (E2B7).

In terms of technical performance, biodiesel has its limitation of low temperature flow characteristics which may lead to clogging of fuel filters and/or choking of the injectors (Dwivedi *et al*., 2013). Researchers have found that high viscosity biodiesel at low temperature condition affects the engine performance, fuel consumption, emissions, and the engine components' function (Chen *et al*., 2016; Hossain *et al*., 2017). Concerning low temperature condition at cold places with potential temperature dropping below 15°C, three Malaysian highlands namely Cameron Highlands and Genting Highlands, in Pahang, and Kundasang, in Sabah, Malaysia have been exempted from selling B10 and continued to supply B7. Based on 10 years ambient temperature data recorded at Cameron Highlands by Meteorology Malaysia seismic station, there were trend of low temperature spikes from January to March each year with the temperature recorded between 11°C-13°C as shown in *Figure 1*. The lowest temperatures recorded at Cameron Highlands was 10.9°C in December 2007. There has not been any problem reported on using B7 diesel at Cameron Highlands since 2015 with the lowest ambient temperature ranging from 12°C-17°C. Since there is no meteorological station at Genting Highlands and Kundasang, no temperature data can be obtained.

The cold flow properties describe the behaviour of fuels under the influence of cold temperature and measured in terms of Cloud Point (CP), Cold Filter Plugging Point (CFPP) and Pour Point (PP). CP refers to the minimum temperature at which the first crystal is formed while PP is the lowest temperature below which a liquid loses its flow characteristics. The Malaysian diesel fuel standard (MS123) has specified the CP to be lower than 19°C (Department of Standard Malaysia, 2018; 2020). CFPP is often used to determine the low-temperature operability of a fuel that can be used to forecast the lowest temperature at which the fuel will flow freely through fuel filters in a diesel engine system (Hamon *et al*., 1994; Zöldy, 2019).

The quality of the blending stock is important to ensure a problem-free biodiesel program. In Malaysia, the final diesel fuel blends shall meet the Malaysian Standard for Diesel Fuel (MS 123-4:2020) which allows up to 20% of palm in biodiesel (Department of Standards Malaysia, 2020). It is equally important that the specifications of palm biodiesel must comply with MS 2008:2014 for biodiesel used in any blending purposes (Department of Standards Malaysia, 2014). The MS 2008:2014 is equivalent to European Biodiesel

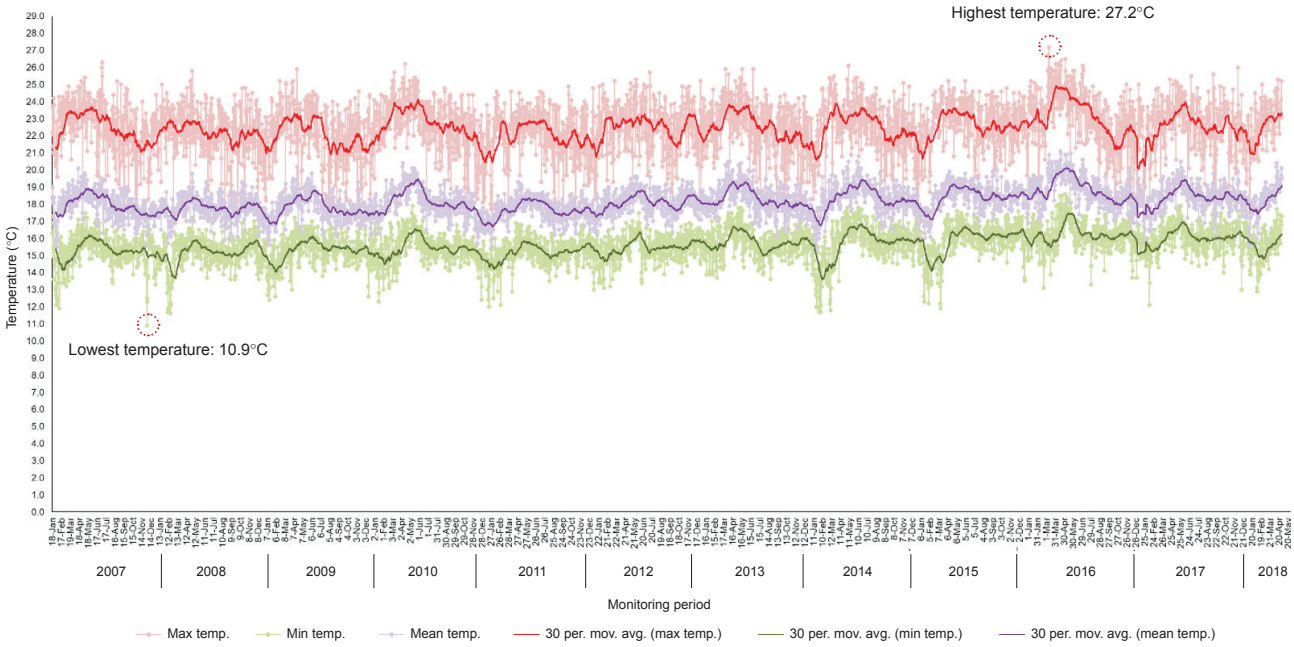

Figure 1. Average ambient temperature at Cameron Highlands from January 2007 to May 2018.

Standard (EN 14214) with tightened parameter on oxidative stability of 10 hr minimum induction period (European Standard, 2008).

The monoglycerides content and the water content in biodiesel are associated with the fuel precipitation and storage issue while using biodiesel. The monoglycerides content is crucial especially when the biodiesel blended fuel is used at low temperature condition that may lead to fuel filter plugging (Van Gerpen *et al.*, 1997). The presence of excessive water in fuels may cause damage to the fuel-injection system as well as corrosion in storage tanks. The hygroscopic nature of biodiesel could lead to an increase of the soluble water content during transportation and storage (Ferella *et al.*, 2010; Oliveira *et al.*, 2008). This stringent fuel specifications must be strictly followed to avoid any negative effects of using biodiesel in the internal combustion engine system.

This article discussed the cold flow properties of biodiesel blended fuels and quality of palm biodiesel supplied for national biodiesel program with special focus on monoglycerides and water contents. The CP, CFPP and PP of cold flow properties for B10, B20 and B30 were also investigated.

MATERIALS AND METHOD

The study was divided into three parts. First, samplings of B7 diesel were carried out at all three Malaysia's highlands (Cameron Highlands, Genting Highlands and Kundasang), then B7 diesel samples were analysed for cold flow properties. Second, collection of data for monoglyceride content and water content of palm biodiesel (PME) supplied for national biodiesel program was done by reviewing the quality of PME in terms of these two parameters. Finally, poor quality of B7 diesel with high CFPP and CP, and PME containing high monoglyceride content were selected for higher biodiesel blending and further assessed for CP and CFPP of the blending.

Sampling of B7 Diesel

Sampling of B7 diesel fuels from retail stations was carried out in order to understand the behaviour of cold flow properties of B7 diesel fuel in three highlands. B7 diesel namely Euro 2M (500 ppm max. sulphur) and Euro 5 (10 ppm max. sulphur) were collected from 12 retail stations at all three Malaysia's highlands. *Table 1* summarises the sample collected from all three highlands. Three rounds of sampling were carried out at all retail stations in the highlands; two retail stations at Genting Highlands, five stations at Cameron Highlands and five stations at Ranau and Kundasang, Sabah, respectively. A total of 43 B7 samples were collected of which 15 samples obtained were from 14-19 May 2018 for

TABLE 1. SAMPLES COLLECTED FROM HIGHLANDS

Highland	Euro 2M (500 ppm max. of sulphur)	Euro 5 (10 ppm max. of sulphur)
Cameron Highlands	C1, C2, C4, C6 and C8	C3, C5 and C7
Genting Highlands	G1 and G2	-
Kundasang/Ranau	K1, K2, K3, K4 and K5	-

sampling 1, 14 samples collected from 16-18 July 2018 for sampling 2 and from 10-13 September 2018 for sampling 3, respectively. Sample from one of retail stations located at Cameron Highland (C8) was unable to be collected during samplings 2 and 3 due to the inability of the station to provide the biofuel.

All samples were analysed based on its cold flow properties such as CP, CFPP and PP according to the ASTM D2500, ASTM D97 (ASTM International 2011; 2017) and EN 116 (European Standard, 2015), respectively. Each analysis was carried out in triplicate with the mean results reported.

Data Collection of Palm Biodiesel

Two important parameters *i.e.*, monoglycerides content and water content of palm biodiesel were monitored to ensure the quality of the final blended fuels was at its desirable quality prior to blending. Data of these two parameters was collected from their respective Certificate of Assurance (CoA) and analysed to get an overview of the quality of biodiesel supplied for national biodiesel program in Malaysia. Data collection was done for a period of 41 months from January 2016 to May 2019 from 12 biodiesel producers involved in the supply chain of the national biodiesel program. A total of 4373 certificates were collected from PME delivery tankers from petroleum depots. The analyses on monoglycerides content and water content were carried out by each producer according to the EN14105 (European Standard, 2011) and ISO 12937 (ISO, 2000), respectively.

Preparation of B10, B20 and B30 Blended Fuels

Based on the analyses for cold flow properties of B7 diesel fuels and monoglycerides content of palm biodiesel properties, further evaluation was conducted to study the behaviour of cold flow properties of high palm biodiesel blends at relevant temperature reflecting Malaysia's cold condition. B7 diesel with high CFPP was bought from a retail station at Genting Highlands. The palm biodiesel with monoglycerides content of 0.61% (m/m) was obtained from one of the biodiesel producers. The blends of B10, B20, B30 were prepared by measuring a fixed volume of diesel and biodiesel, homogenised and stored in glass bottles at room temperature. The blended fuels were analysed for CP, CPFF and PP according to the methods described above.

RESULTS AND DISCUSSION

A total of 43 B7 samples were collected from 12 retail stations at Cameron Highlands, Genting Highlands and Kundasang. Out of which, 34 samples were E2B7 with the remaining, of E5B7. The biodiesel content for both E2B7 and E5B7 were validated and it was in the range of 6.68% v/v to 7.51% v/v as shown in *Figure 2*. The average biodiesel content was determined to be 7.09% v/v as compared to the maximum limit of 7.5% v/v. The measurement of biodiesel content is very much depending on the purity of biodiesel and standard diesel used for equipment calibration. Based on the results, the range of biodiesel

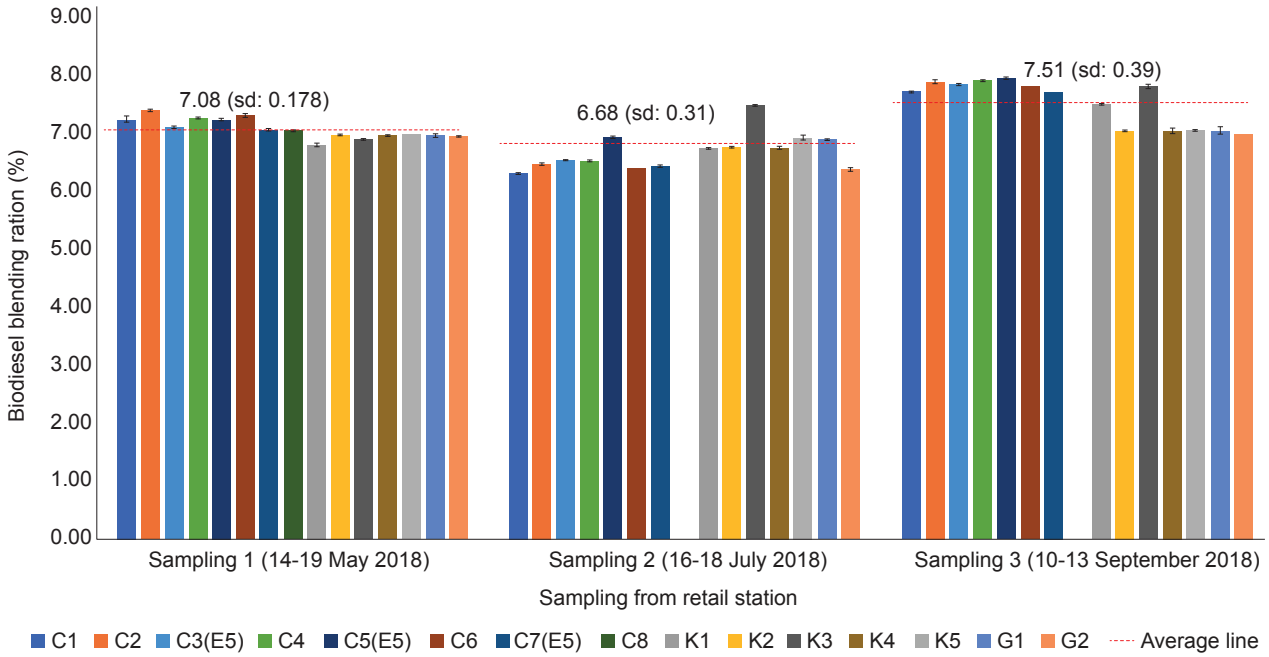

Note: C - Cameron Highlands; K - Kundasang/Ranau; G - Genting Highlands.

Figure 2. Biodiesel content in diesel sold at highland retail stations.

blending ratio is within 6.5%-7.5% v/v which falls within the acceptable range.

The samples were grouped based on the company and location, in which there are four brands representing petroleum companies in three highlands. *Figure 3* shows the CP of B7 samples collected from retail stations at highlands with the highest value of 9°C as compared to the maximum limit of 19°C as stipulated in MS 123:2018/2020. All CP of E5B7 was lower than E2B7 except for sample K5 which was below 0°C.

There was noticeable fluctuation of CFPP for all diesel fuel samples collected from retail stations at highlands as shown in *Figure 4*. In general, the CFPP of E5B7 samples was found ranging from -2°C to -7°C as compared to E2B7 from 1°C-10°C.

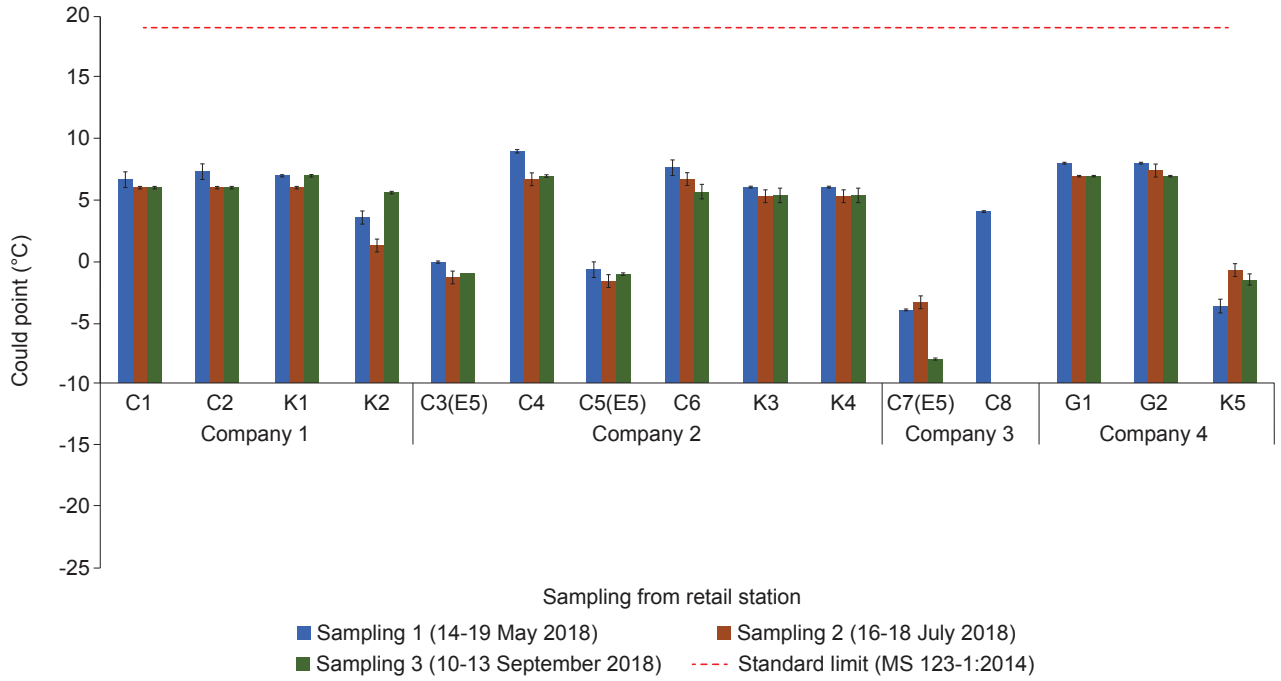

Note: C - Cameron Highlands; K - Kundasang/Ranau; G - Genting Highlands.

Figure 3. Cloud point of E5B7 and E2B7 from retail station at highlands.

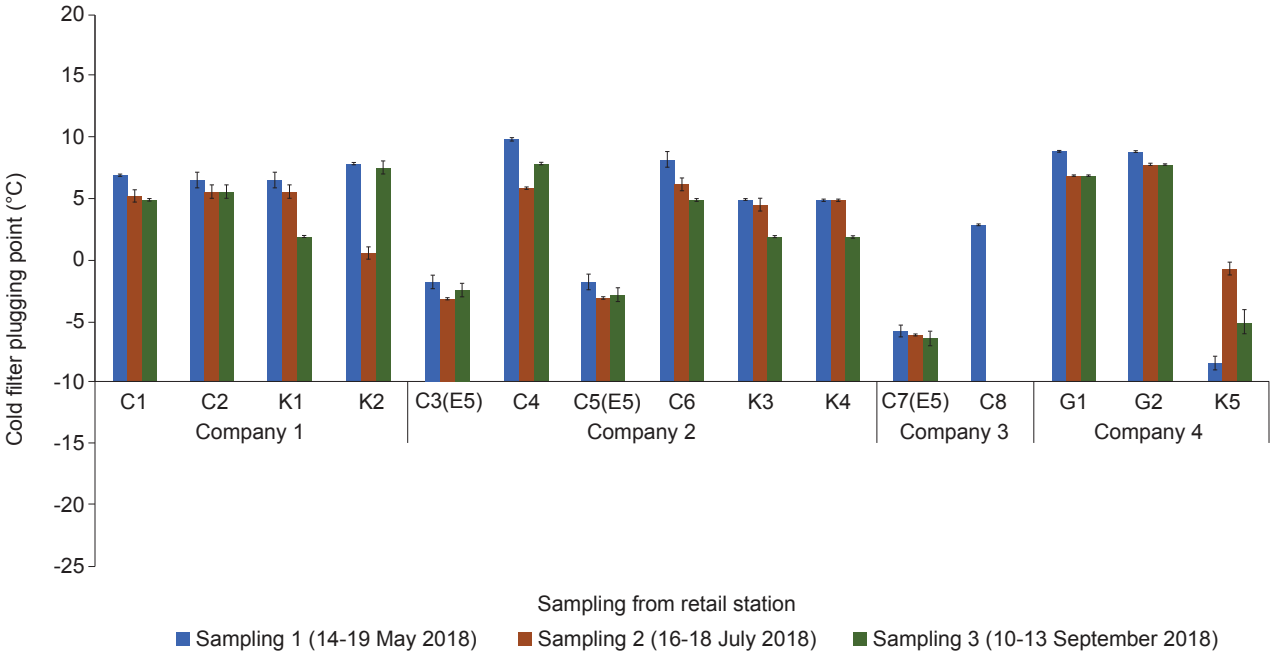

Note: C - Cameron Highlands; K - Kundasang/Ranau; G - Genting Highlands.

Figure 4. Cold filter plugging point of E5B7 and E2B7 from retail station at highlands.

The samples from station C4 has the highest CFPP recorded at 10°C with similar trend observed for G1 and G2. *Figure 5* shows 32 samples of the diesel fuel having PP ≤0°C where the lowest PP was -19°C from sample C7 (E5). A similar trend with CP can be seen for PP in which all E5B7 samples were below -5°C, lower than E2B7 except for K5. The wide range in variation of CP, CFPP and PP could be contributed by different sources of diesel supply of individual petroleum companies. There are four brands of retail stations at the highlands. Blending of biodiesel in diesel takes place at petroleum terminals via in-line blending facilities. The quality of diesel as main blending component is important to ensure a good cold flow property of blended fuel is achieved. In addition, the content of saturated fatty acids in biodiesel plays an important role in determining the CFPP and CP of the blended fuel (Knothe, 2005). The cold flow property of a normal grade PME varies between a narrowed range of 12°C-15°C depending on its fatty acid composition. Based on the study, it is proven that the B7 fuels sold at retail stations at highlands has met the CP specification as stipulated in MS 123. Further investigation of CFPP revealed that all B7 fuels has CFPP that can withstand the coldest temperature ever experienced in Cameron Highlands.

As the tests of CP and CFPP were conducted in a laboratory atmosphere, it may not be accurately representing the actual vehicle running condition in the open environment. It is anticipated that with the latest common rail diesel technology, the return fuel to the diesel tank will raise the fuel temperature above ambient temperature (unpublished data: Lau *et al.*, MPOB, 2020). Thus, the concern on fuel precipitation could only be verified through on-the-road field test in actual environment.

Apart from investigating the cold flow properties of blended fuel sold at highlands, the assessment on the quality of palm biodiesel supplied for the national biodiesel program was needed to ensure the blended fuel meets the standard requirement. Monoglycerides content in palm biodiesel (B100) is a crucial parameter to be monitored prior to blending with diesel. It is reported that the major cause of precipitate formation at low temperatures in palm biodiesel blended fuel is attributed to monoglycerides content (Tang *et al.*, 2008). *Figure 6* shows the monoglycerides content of palm biodiesel produced in Malaysia from January 2016 to May 2019. The yearly average of monoglycerides content of palm biodiesel was between 0.456% m/m to 0.505% m/m which meets the requirement of less than 0.7% m/m as stipulated in the MS 2008:2014. Monoglycerides content was widespread from 0.1% m/m to 0.69% m/m from the second half of 2017 until the first half of 2019 compared to those of narrower range prior to this, ranging from 0.2% m/m to 0.6% m/m. Statistically, changes of monoglycerides content is significant within collection period with $p>0.05$.

Figure 7 shows the monoglycerides content of biodiesel by producer. The amount of biodiesel supplied by producer from January to June 2019 was within 100-6700 t month^{-1} based on demand by the petroleum depots (unpublished data: Noraida

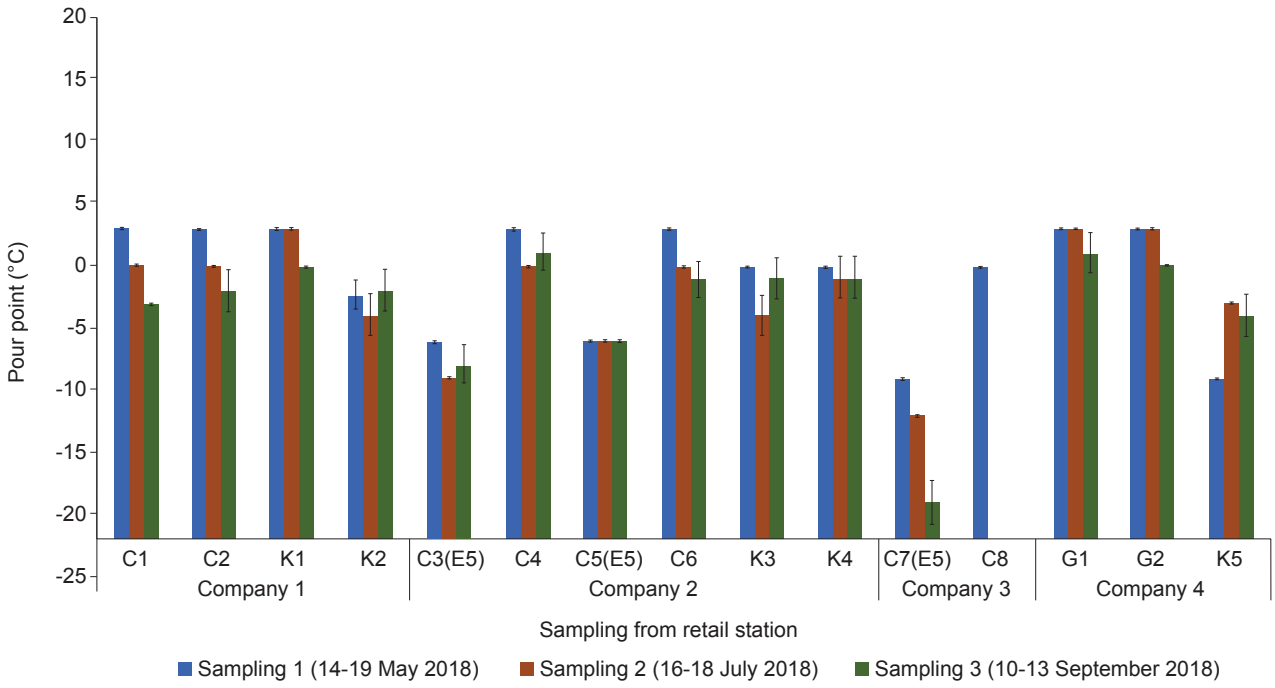

Note: C - Cameron Highlands; K - Kundasang/Ranau; G - Genting Highlands.

Figure 5. Pour point of E5B7 and E2B7 from retail station at highlands.

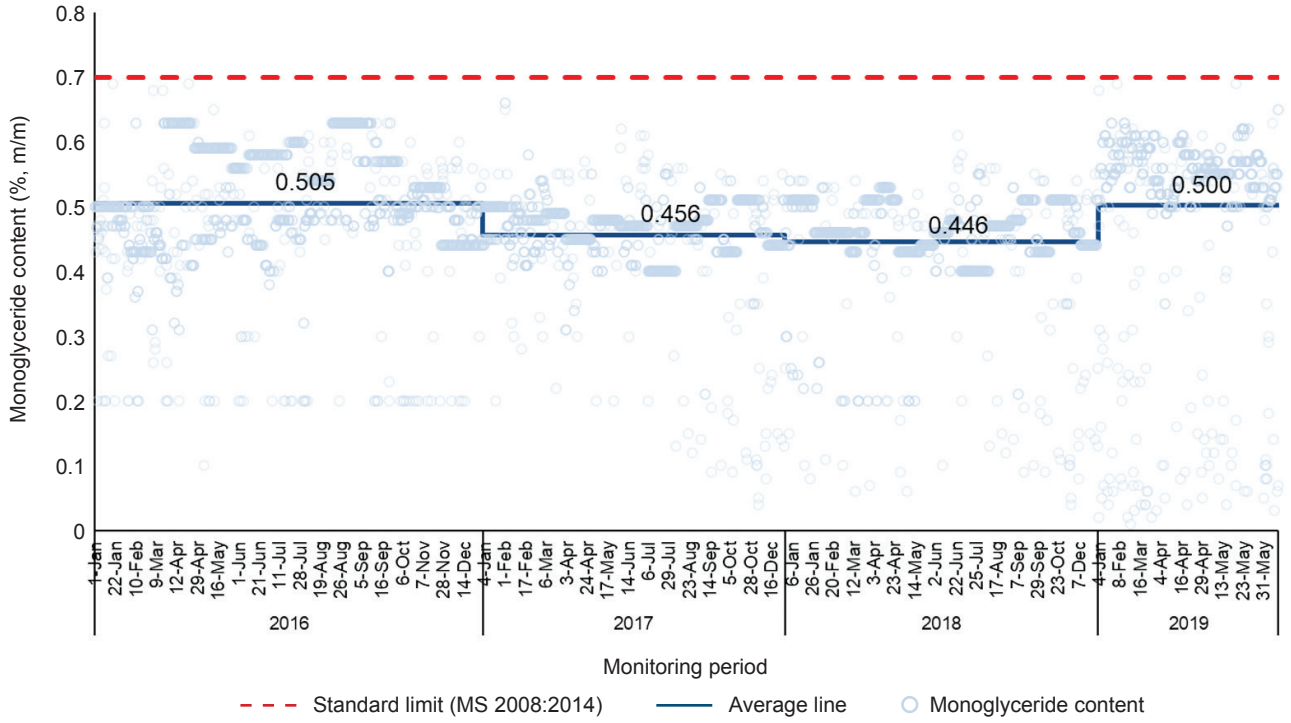

Figure 6. Monoglycerides content of palm biodiesel supplied to petroleum depots from January 2016 to May 2019.

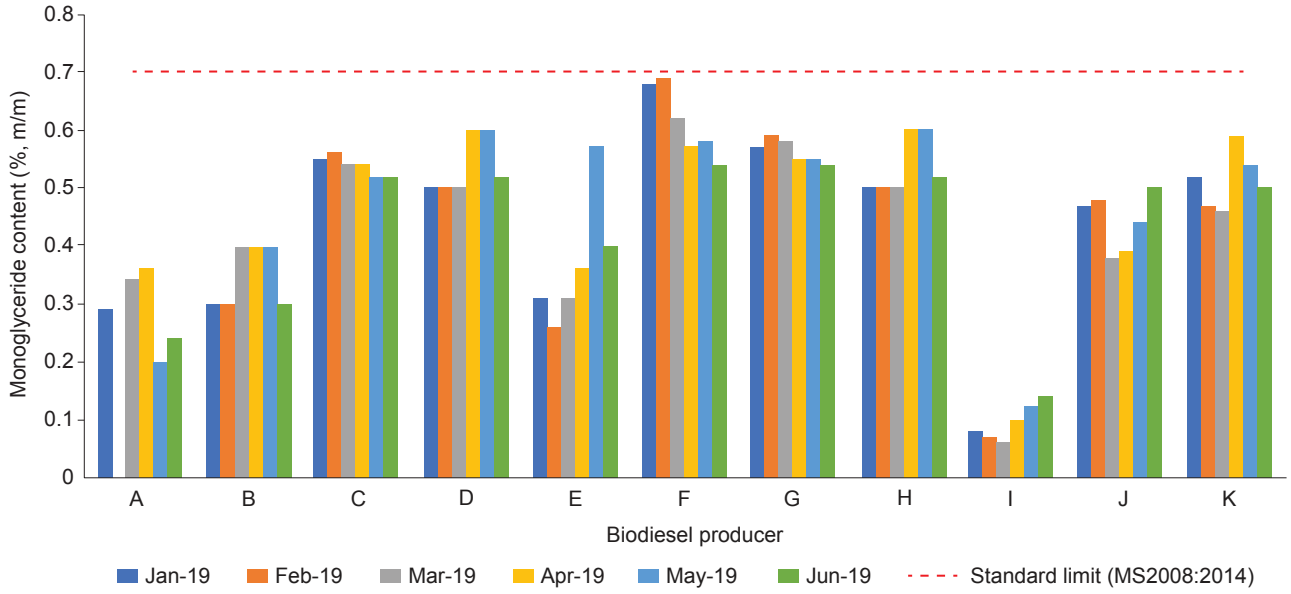

Figure 7. Monoglycerides content of palm biodiesel by different producer from January to June 2019.

et al., MPOB, 2021). In actual practice, biodiesel from different producers is commingled in the same storage tank at blending terminals. This means that the biodiesel with high monoglycerides content will be diluted with those of low monoglycerides content. Biodiesel with very low monoglycerides content of less than 0.1% can be achieved by incorporating additional distillation process of biodiesel which allows production of high-quality product without diglycerides and triglycerides, and only containing traces of monoglycerides. The unreacted neutral oils left in the biodiesel such as mono-, di-, and triglycerides, might have high melting points and very low solubilities (Poalo *et al.*, 2013). Owing to this, their presence especially the monoglycerides could form solid residues when exposed to cold temperature. As such, the properties of biodiesel will be affected at low temperature (Aisyah *et al.*, 2018; Imam *et al.*, 2019). Monoglycerides content in pure palm biodiesel needs to be investigated for the use of B30.

Besides monoglycerides content, precipitate formation was also found to be influenced by water content in biodiesel (Plata *et al.*, 2015). Biodiesel is known to have high affinity of absorbing moisture *i.e.,* 6.5 to nine times and retaining water than petroleum diesel (He *et al.*, 2007; Patricia *et al.*, 2012). High moisture in biodiesel could possibility be attributed by inadequate drying during processing and absorption of atmospheric moisture during storage. Water content of biodiesel is correlated with surrounding temperature. Water precipitation and condensation might occur when the moisture level in biodiesel falls beyond its saturation point leading to accumulation of water that settles at the bottom of storage tank. High water content in biodiesel or diesel is also associated with microbial growth which may result in fuel filter plugging, and corrosion of fuel tank and fuel delivery system (Van Gerpen, 2005). As illustrated in *Figure 8*, the water content of palm biodiesel supplied for blending purposes ranging between 200-350 mg kg^{-1}, *i.e.,* below the maximum limit of <500 mg kg^{-1} as required under MS 2008:2014. The average water content in biodiesel for 2016, 2017, 2018 and 2019 were below 300 mg kg^{-1} or 240, 243, 242 and 282 mg kg^{-1} respectively. As the storage of biodiesel at blending depots is typically less than seven days, the moisture content in biodiesel has maintained below the specified limit before it is blended into diesel.

To evaluate on the worst-case scenario, the B10, B20 and B30 fuels were prepared by blending E2B7 diesel with high CFPP of 8°C and PME that contains the highest average monoglycerides content of 0.61% m/m. The properties of E2B7 diesel and PME are summarised in *Tables 2* and *3*, respectively.

The CFPP and CP of blended fuels (B10, B20 and B30) will increase with the increase of biodiesel blending ratio as shown in *Figure 9*. The same observation was reported in most previous literatures *e.g.,* José *et al.* (2019); Kassem and Camur (2017); Verma *et al.* (2016). The viscosity of blended fuel was also directly proportional to biodiesel blending ratio in which the increasing trend of viscosity can be observed from B7 to B30. The higher the biodiesel concentration, the more viscous the resulted fuel would be (Alptekin and Canakci, 2008; Kiran *et al.*, 2018; Samuel *et al.*, 2019). CP of all blended fuels (B7, B10, B20 and B30) were well below the limit of 19°C as in the MS 123:2018/2020. As shown in *Figure 9*, B7 and B10 should be safe to be used in the highlands as its CP and CFPP were below the lowest recorded temperature of 10.9°C. For B20, both CP and CFPP are close to the lowest temperature in the highlands. With the increase of 30% v/v palm biodiesel in diesel, the CP of 10°C was approaching the lowest temperature of 10.9°C while the CFPP has increased significantly above the lowest temperature in the highlands. This might indicate the use of B30 could contribute to the vehicle's cold operability problems. Interestingly, CFPP of B100 does not change much compared to B30 but the CP increased from 10°C (B30) to 16°C. To consider actual fluctuation of temperature in the highlands, both CFPP and CP of B20 were below 10°C which suited the minimum temperature range of 12°C-17°C at Cameron Highlands (*Figure 1*). Based on the results, B20 could be used at Malaysia's highlands as its CFPP and CP are below the minimum temperature at highlands over the last 10 years. However, as the lowest temperature had once reached 10.9°C, the

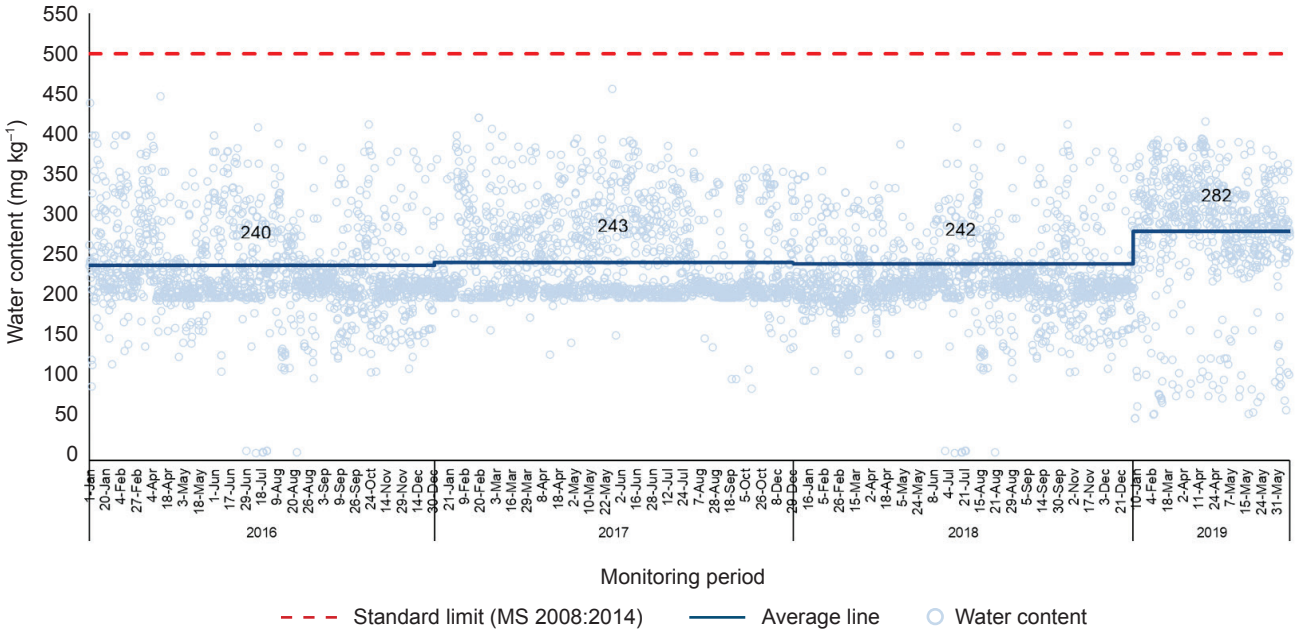

Figure 8. The water content of palm biodiesel supplied to petroleum depots from January 2016 to May 2019.

TABLE 2. PROPERTIES OF E2B7 DIESEL

Parameter	Unit	Method	Specification	Result
Ester content	%	EN 14103	-	6.98
CFPP	°C	EN 116	-	8
CP	°C	ASTM D2500	19.0 max	7.7
PP	°C	ASTM D97	-	1
Viscosity	$mm^2 s^{-1}$	ASTM D445	1.5-5.8	3.086
Density at 15°C	$g cm^{-1}$	ASTM D4052	0.81-0.87	0.8376
Flash point	°C	ASTM D93	60 min	68.5

Note: CFPP - cold filter plugging point; CP - cloud point; PP - pour point.

TABLE 3. PROPERTIES OF PALM BIODIESEL

Parameter	Unit	Method	Specification	Result
Ester content	% m m^{-1}	EN 14103	96.5 min	98.05
Density @ 15°C	kg m^{-3}	EN ISO 12185	860-900	874.2
Flash point	°C	EN ISO 2719	120 min	178
Water content	mg kg^{-1}	EN ISO 12937	400 max	365
Acid value	mg KOH g^{-1}	EN 14104	0.50 max	0.4
Iodine value	g iodine 100 g^{-1}	EN 14111	110 max	50.3
Total contamination	mg kg^{-1}	EN 12662	24 max	21
Oxidation stability, 110°C	hr	EN 15751	8.0 min	20.8
Cloud point	°C	ASTM D2500	-	15
Cold filter plugging point, CFPP	°C	EN 116	15 max	13
Breakdown of MG:		GC		
MG-C16:0				0.3
MG-C18:0				0.03
MG-C18:1, C18:2, C18:3				0.25

Note: CFPP - cold filter plugging point; MG-C - monoglyceride content.

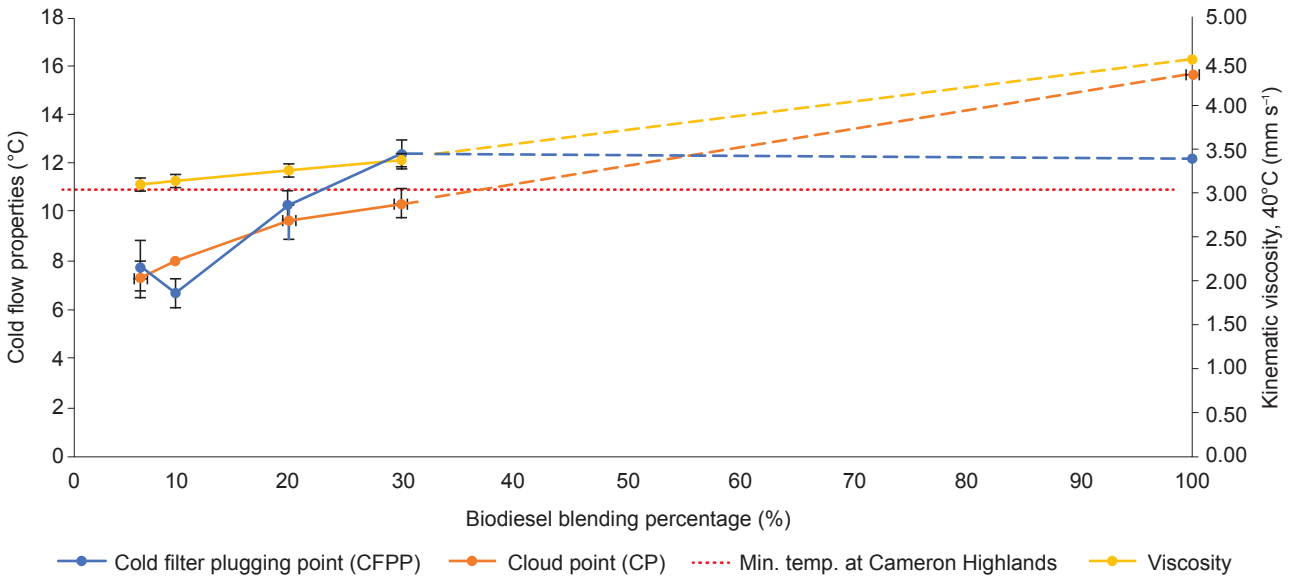

Figure 9. Cold flow properties and kinematic viscosity of blended fuel.

use of B20 needs to be approached with caution as precipitation might happen and could lead to potential filter plugging incident; that to be further confirmed by vehicle testing. For any increase of biodiesel blending in diesel at low temperature conditions, the specifications of CP and CFPP of the blended fuel shall be set on par with the minimum ambient temperatures. This is to ensure no low operability issues of long running vehicles in the highlands.

Table 4 shows the standard specification of cold flow properties of the blended diesel fuel for some countries. The cold flow properties of a particular fuel are of concern for temperate countries as compared to tropical countries like Malaysia, as the extreme temperature changes will impact the fuel properties. Some of the countries have specified the CFPP and CP in the standard according to the specific climatic environments like EN590. Hence, the existing diesel standard, MS123 is significant to be improved, which is to include CFPP to cater the use of the high biodiesel blends in the highlands, in addition to CP with maximum limit of 19°C. This is to ensure that the cold operability issues of the diesel vehicles using the high biodiesel blend have been taken into account under the standard for future national biodiesel implementation plan.

CONCLUSION

Periodical monitoring of the critical parameters in diesel fuel and biodiesel are essential to ensure the best quality of blended fuels to be delivered and used without any problems across the nation. Concerning the cold operability issues using the biodiesel blends, cold flow properties *i.e.*, CP and CFPP of B7 diesel fuel was investigated to understand the behaviour of these parameters in the B7 diesel fuel sold in the highlands. The B7 diesel fuel samples collected from retail stations at the highlands have been validated to contain 6.5% v/v to 7.5% v/v of palm biodiesel and have been used for this study. All the samples showed the CP of B7 were within

TABLE 4. STANDARD SPECIFICATION OF DIESEL/ BIODIESEL BLENDS FOR COLD FLOW PROPERTIES OF SOME OF THE COUNTRIES

Country	Malaysia	Indonesia	Europe (CEN)		America		German	Japan	Brazil
Standard	MS 123-1:2018/2020	CN 48: SK 978/2013 CN 51 or above: SK 3675/2006	EN 590:2013 *Temperate climatic zones*	*Arctic climatic zones*	ASTM D975	ASTM D7467 (B6 - B20)	DIN 51605	JIS K 2204	ANP 42/2009
CP, max	19°C ASTM D2500	18°C D97	-	-10°C (Class 0) -16°C (Class 1) -22°C (Class 2) -28°C (Class 3) -34°C (Class 4) EN 23015:1994	Only guidance provided D2500	Only guidance provided D2500	-	-	-
CFPP, max	-	-	5°C (Class A) 0°C (Class B) -5°C (Class C) -1°C (Class D) -15°C (Class E) -20°C (Class F) EN 116:199	-20°C (Class 0) -26°C (Class 1) -32°C (Class 2) -38°C (Class 3) -44°C (Class 4) EN 116:1997	Only guidance provided D4539/ D6371	Only guidance provided D4539/ D6371		Depends on regions and month	0°C-12°C Depends on regions and month ASTM D6371
PP, max	-	-	-	-	-	-	-		-

Note: CFPP - cold filter plugging point; CP - cloud point; PP - pour point.

the maximum limit of 19°C as stipulated in MS 123:2018/2020 with the highest value of 9°C. The CFPP of E5B7 was found lower compared to E2B7 with the highest CFPP recorded at 10°C. Besides B7's cold flow properties, the monoglycerides and water contents of palm biodiesel supplied for the Malaysia biodiesel program have also been analysed, as these parameters contribute to the formation of precipitates at low temperatures. Both monoglycerides and water contents were found to meet the stringent requirements as stipulated under MS 2008:2014 for the period of 42 months.

Conceiving the worst-case scenario on the behaviour of cold flow properties, CP and CFPP of high palm biodiesel blend fuels was assessed to predict its usability in cold areas such as highlands. Based on the evaluation, the blending percentage of biodiesel in diesel had correlated with the CFPP and CP of the blended fuel. The CFPP and CP had increased with the increase of biodiesel content in diesel. The CP and CFPP of B7, B10 and B20 were below the lowest temperature of 10.9°C in the highlands while CFPP of B30 was 12°C, above the lowest temperature. This indicates that biodiesel up to 20% v/v can be used in the highlands, whereas the use of B30 may cause some problems to vehicles.

With the strong correlation between biodiesel percentage and CFPP, this parameter is considered as a better indicator for blended fuel as compared to CP of diesel fuel at cold climate usage. Thus, the specification of CFPP could be introduced with a maximum limit of 10°C to allow the use of B20 in the existing MS123 diesel standard, as this parameter is also included in the EU standards.

From the assessment of cold flow properties, biodiesel blends up to B20 are predicted to be suitable for the diesel vehicles operating at Malaysia's highlands as its CFPP was below the lowest recorded temperature of highlands. This can be confirmed through engine testing in future studies.

ACKNOWLEDGEMENT

We would like to extend our appreciation to the Director-General of MPOB for permission to publish this article. Thanks are also due to the participating petroleum companies and biodiesel producers for their cooperation.

REFERENCES

Abed, K A; Gad, M S; El Morsic, A K; Sayedd, M M and Abu Elyazeede, S (2019). Effect of biodiesel fuels on diesel engine emissions. *Egyp. J. Pet., 28*: 183-188.

Aisyah, L; Wibowo, C S; Bethari, S A; Ufidian, D and Anggarani, R (2018). Monoglyceride contents in biodiesel from various plants oil and the effect to low temperature properties. *IOP Conf. Ser.: Mater. Sci. Eng., 316*: 012023. DOI: 10.1088/1757-899X/316/1/012023.

Agus, S; Anindhita, I R A F; La, O M A W and Adiarso (2019). Indonesia Energy Outlook 2019 - The Impact of Increased Utilisation of New and Renewable Energy on the National Economy. *Badan Pengkajian dan Penerapan Teknologi* (BPPT). Jakarta, Indonesia. p. 60.

Alptekin, E and Canakci, M (2008). Determination of the density and the viscosities of biodiesel-diesel fuel blends. *Renew. Energy, 33(12)*: 2623-2630.

Ali, O M; Mamat, R; Abdullah, N R and Abdullah, A A (2016). Analysis of blended fuel properties and engine performance with palm biodiesel-diesel blended fuel. *Renew. Energy, 86*: 59-67.

ASTM International (2011). ASTM D2500-11. Standard Test Method for Cloud Point of Petroleum Products. ASTM International, West Conshohocken.

ASTM International (2017). ASTM D97. Standard Test Method for Pour Point of Petroleum Products. ASTM International, West Conshohocken.

ASTM International (2017). D2500-17. Standard Test Method for Cloud Point of Petroleum Products and Liquid Fuels. ASTM International, West Conshohocken.

Ayhan, D (2007). Importance of biodiesel as transportation fuel. *Energy Policy, 35*: 4661-4670.

Bari, S and Hossain, S N (2019). Performance and emission analysis of a diesel engine running on palm oil diesel (POD). *Energy Procedia, 160*: 92-99.

Chen, H; Guo, Q; Zhao, X and Xu, M (2016). Influence of fuel temperature on combustion and emission. *J. Energy Inst., 89*: 231-239.

Choo, Y M; Ma, A N; Chan, K W and Yusof, B (2005). Palm diesel: An option for greenhouse gas mitigation in the energy sector. *J. Oil Palm Res., 17*: 47-52.

Choo, Y M; Ma, A N and Ong, A S H (1997). Biofuel. *Lipids: Industrial Applications and Technology* (Gunstone, F D and Padley, F B eds.). Marcel Dekker Inc., New York. p. 771-785.

Commission Delegated Regulation (2019). Commission Delegated Regulation (EU) 2019/807 (2019). http://data.europa.eu/eli/reg_del/2019/807/oj, accessed on 4 November 2020.

Department of Standards Malaysia (2014). MS 2008:2014, Automotive Fuels – Palm Methyl Ester (PME) for Diesel Engines – Requirement and Test Methods (First revision). Department of Standards Malaysia, Ministry of Science, Technology and Innovation, Cyberjaya.

Department of Standards Malaysia (2018). MS 123-1:2018, Malaysian Standard – Diesel – Specification – Part 1: Euro 2M (Fifth revision). Department of Standards Malaysia, Ministry of Science, Technology and Innovation, Cyberjaya.

Department of Standards Malaysia (2020). MS 123-4:2020, Malaysian Standard – High PME Diesel Fuel – Specification – Euro 2M. Department of Standards Malaysia, Ministry of Science, Technology and Innovation, Cyberjaya.

Dwivedi, G; Jain, S and Sharma, M P (2013). Diesel engine performance and emission analysis using biodiesel from various oil sources – Review. *J. Mater. Environ. Sci., 4*: 434-447.

European Standard (2008). EN 14214:2008 (E). Automotive Fuels - Fatty Acid Methyl Ester (FAME) for Diesel Engines - Requirement and Test Methods. European Standards, Brussels, Belgium.

European Standard (2011). EN14105 Fat and Oil Derivatives - Fatty Acid Methyl Esters (FAME) - Determination of Free and Total Glycerol and Mono-, Di-, Triglyceride Contents. European Standard, Brussels, Belgium.

European Standard (2015). EN 116 Diesel and domestic heating fuels – Determination of cold filter plugging points. European Standards, Brussels, Belgium.

Ferella, F; Di Celso, G M; De Michelis, I; Stanisci, V and Veglio, F (2010). Optimization of the transesterification reaction in biodiesel production. *Fuel, 89*: 36-42.

Fregolente, P B L; Fregolente, L V and Maciel, M R W (2012). Water content in biodiesel, diesel and biodiesel-diesel blends. *J. Chem. Eng., 57(6)*: 1817-1821.

GraboskI, M S and Mccormick, R L (1998). Combustion of fat and vegetable oil derived fuels in diesel engines. *Prog. Energy Combust. Sci., 24*: 125-164.

Hamon, D; Damin, B and China, P (1994). New Diesel Low Temperature Operability Test - Agelfi Filtration Test. SAE Technical Paper 940081.

He, B B; Thompson, J C; Routt, D W and Van Gerpen, J H (2007). Moisture absorption in biodiesel and its petro-diesel blends. *Appl. Eng. Agric., 23(1)*: 71-76.

Hossain, A K; Smith, D I and Davies, P A (2017). Effects of engine cooling water temperature on performance and emission characteristics of a compression ignition engine operated with biofuel blend. *J. Sustain. Dev. Energy, Water Environ. Syst., 5*: 46-57.

ISO (2000). ISO 12937. Petroleum products – Determination of water – Coulometric Karl Fisher titration method. Geneva, Switzerland.

Javed, A and Anurag, S (2014). Biodiesel as an alternative fuel for diesel engine - An overview. *Int. J. Appl. Eng. Res., 9(10)*: 1159-1168.

Kassem, Y and Camur, H (2017). A laboratory study of the effects of wide range temperature the properties of biodiesel produced from various waste vegetable oils. *Waste Biomass Valor., 8*: 1995-2007.

Knothe, G (2005). Dependence of biodiesel fuel properties on the structure of fatty acid alkyl esters. *Fuel Process. Technol., 86*: 1059-1070.

Kiran, R B; Rahul, T S, Kundla, S and Vardhan, G V (2018). Effects of blending on the properties of diesel and palm biodiesel. *IOP Conf. Se.: Mater. Sci. Eng., 330*: 012092. DOI: 10.1088/1757-899X/330/1/012092.

Ministry of Energy and Mineral Resources (2014). MEMR Regulation No. 20/2014' Mandatory biofuel. Ministry of Energy and Mineral Resources (MEMR), Jakarta, Indonesia.

Ministry of International Trade and Industry (2020). National Automotive Policy (NAP 2020). Ministry of International Trade and Industry, Malaysia. p. 57.

Murphy, D J (2014). The future of oil palm as a major global crop: Opportunities and challenges. *J. Oil Palm Res., 26(1)*: 1-24.

Oliveira, M B; Varanda, F R; Marrucho, I M; Queimada, A J and Coutinho, A P (2008). Prediction of water solubility in biodiesel with the CPA equation of state. *Ind. Eng. Chem. Res., 47*: 4278-4285.

OECD/FAO (2020). *OECD-FAO Agricultural Outlook 2020-2029*. https://www.oecd-ilibrary.org/agriculture-and-food/oecd-fao-agricultural-outlook_19991142, accessed on 27 October 2020.

Parveez, G K A; Elina, H; Loh, S K; Meilina, O; Kamalrudin, M; Mohd, N I Z B; Shamala, S; Zafarizal, A A H and Zainab, I (2020). Oil palm economic performance in Malaysia and R&D progress in 2019. *J. Oil Palm Res., 32(2)*: 159-190.

Paryanto, I; Prakoso, T; Suyono, E A and Gozan, M (2019). Determination of the upper limit of monoglyceride content in biodiesel for B30 implementation based on the measurement of the precipitate in a biodiesel-petrodiesel fuel blend (BXX). *Fuel, 258*: 116104. DOI: 10.1016/j.fuel.2019.116104.

Plata, V; Gauthier-Maradei, P and Kafarov, V (2015). Influence of minor components on precipitate formation and filterability of palm oil biodiesel. *Fuel, 144*: 130-136.

Rodriguez-Fernãndez,J; Harnandez, J J; Calle-Asensio, A; Ramos, Ã and Barba, J (2019). Selection of blends of diesel fuel and advanced biofuels based on their physical and thermochemical properties. *Energies, 12*: 2034. DOI: 10.3390/en12112034.

Samuel, O D; Oreko, B U; Oyejide, J O; Idi, S; Ojo, S I and Fayomi, O S I (2019). Experimental and empirical study of diesel and biodiesel produced from blend of fresh vegetable and waste vegetable oil on density, viscosity, sulphur content and acid value. *J. Phy.: Conf. Ser., 1378*: 042024. DOI: 10.1088/1742-6596/1378/4/042024.

Tang, H; Salley, S O and Simon Ng, K Y (2008). Fuel properties and precipitate formation at low temperature in soy-, cottonseed-, and poultry fat-based biodiesel blends. *Fuel, 87*: 3006-3017.

Verma, P; Sharma, M P and Dwivedi, G (2016). Evaluation and enhancement of cold flow properties of palm oil and its biodiesel. *Energy Rep., 2*: 8-13.

Van Gerpen, J (2005). Biodiesel processing and production. *Fuel Process. Technol., 86(10)*: 1097-1107.

Van Gerpen, J H; Hammond, E G; Yu, L and Monyem, A (1997). Determining the influence of contaminants on biodiesel properties. SAE Technical Paper No. 971685.

Zahan, K A and Kano, M (2018). Biodiesel production from palm oil. Its by-products, and mill effluent: A review. *Energies, 11(8)*: 2132. DOI: 10.3390/en11082132.

Ziolkowska, J R (2018). Introduction to biofuel and potentials of nanotechnology. *Green Nanotechnology for Biofuel Production* (Srivastava, N; Srivastava, M; Pandey, H; Mishra, P K and Ramteke, P W eds.). *Biofuel and Biorefinery Technologies*. Springer, Basel. p. 1-15.

Zöldy, M (2019). Investigation of correlation between diesel fuel cold operability and standardized cold flow properties. *Period. Polytech. Transp. Eng., 49(2)*: 120-125. DOI: 10.3311/PPtr.14148.

Journal of Oil Palm Research Vol. 34 (1) March 2022 p. 129-138
DOI: https://doi.org/10.21894/jopr.2021.0029

ASSESSMENT OF *TRANS* FATTY ACID LEVELS IN REFINED PALM-BASED OILS AND COMMERCIAL VEGETABLE OILS IN THE MALAYSIAN MARKET

HISHAMUDDIN, E[1]*; ABD RAZAK, R A[1]; YEOH, C B[1]* and AHMAD TARMIZI, A H[1]

ABSTRACT

Trans *fats consumption is a major concern worldwide due to the deleterious effects associated with increased risks of coronary heart disease. The* trans *fatty acid (TFA) content of 104 refinery and commercial vegetable oils in the Malaysian market were analysed by gas chromatography. TFA levels in 29 samples of refined, bleached and deodourised palm oil, palm olein, palm stearin and palm kernel olein from palm oil refineries ranged from 0.12 ± 0.00 to 0.84 ± 0.01 g/100 g. Commercially packaged vegetable oils namely palm olein, sunflower, corn, coconut, rice bran, peanut, olive and sesame oils contained less than 1 g TFA/100 g while higher TFA levels ranging from 1 to 3 g/100 g were detected in canola oil, soybean oil and canola-based oil blend samples. Amongst the premium oils, cold pressed unrefined almond and walnut oils were found to contain TFA levels exceeding 2 g/100 g while other oils in this category contained TFA less than 1 g/100 g. All retail palm-based vegetable oils and palm-based vegetable fat shortenings except for three samples conformed to the conditions for nutrition claims of low TFA of 1.5 g/100 g and 0.75 g/100 mL in both solids and liquids, respectively, as regulated in the Malaysian Food Act 1983.*

Keywords: palm oil, *trans* fatty acids, vegetable oils.

Received: 14 October 2020**; Accepted:** 8 March 2021**; Published online:** 21 June 2021.

INTRODUCTION

Trans fatty acids (TFA) are defined as unsaturated fatty acids possessing at least one double bond in the *trans* configuration. TFA are derived primarily from two sources; (1) ruminant *trans* fats which occur naturally in dairy products and meat from ruminant animals; and (2) industrial *trans* fats which are produced from the partial hydrogenation of vegetable oils (Mozaffarian *et al.*, 2006). Industrial *trans* fats or more commonly known as partially hydrogenated vegetable oils (PHO) are found in a myriad of bakery, frozen and fast food products, margarines and shortenings, packaged snacks and biscuits. In the past, food manufacturers preferred using industrial *trans* fats as an ingredient in their food formulations as the partial hydrogenation process increases the solidity and reduces rancidity of the oil. This resulted in improved stability and shelf-life of food products containing industrial *trans* fats (Nishida and Uauy, 2009).

In the last three decades, there has been a growing body of convincing scientific evidence on the health-damaging effects of TFA. Worldwide consumption of *trans* fats has been strongly associated with an elevated risk of coronary heart disease (CHD) and death from CHD, systemic inflammation, diabetes and cancer (De Souza *et al.*, 2015; Islam *et al.*, 2019; Mozaffarian *et al.*, 2009). Both industrial and ruminant TFAs have been shown to equally raise low-density lipoprotein (LDL) and lower high-density lipoprotein (HDL) cholesterols,

[1] Malaysian Palm Oil Board,
6 Persiaran Institusi, Bandar Baru Bangi,
43000 Kajang, Selangor, Malaysia.

* *Corresponding author e-mail: elina@mpob.gov.my*

although controlled human studies on the latter are rather limited (Brouwer *et al.*, 2010; World Health Organization and Brouwer, 2016). Recognising the growing epidemic of cardiovascular diseases worldwide, the World Health Organization (WHO) in 2003 recommended limiting the daily intake of TFA to less than 1% of total energy intake (Nishida *et al.*, 2004).

Since then, countries such as Denmark, USA and Canada initiated the reduction and elimination of *trans* fats in food through legislative initiatives involving the implementation of regulations setting maximum limits of *trans* fat or mandated labelling of *trans* fats which was subsequently instigated in more than 30 countries (Hendry *et al.*, 2015; Zuchowska-Grzywacz and Kowalska, 2019). The United States Food and Drug Administration (USFDA) revoked the Generally Recognised as Safe (GRAS) status of PHO and banned PHO usage in human food effective June 2018 (USFDA, 2015). The European Parliament adopted a resolution the following year to limit PHO in foods and to establish legal limits for TFAs in food by 2018 (EP, 2016). Starting from 1 April 2021, the European Commission will impose a maximum limit of 2 g TFA per 100 g fat in food products intended for the final consumer and food intended for supply to retail, which excludes those naturally occurring *trans* fat in animal fat (European Commission, 2019).

With the implementation of these government legislations and mandated regulations, worldwide TFA consumption has seen a tremendous decline in the past two decades with an average global *trans* fat intake lower than the 2003 WHO recommendation of a daily TFA intake limit of 1% total energy (Craig-Schimdt and Rong, 2009; Li *et al.*, 2019; Wanders *et al.*, 2017). The WHO in 2018 launched the REPLACE action package which serves to support governments to eliminate industrially produced TFA from the global food supply by 2023 and replacement of TFA with healthier oils and fats through six strategic actions, namely Review, Promote, Legislate, Assess, Create and Enforce (Ghebreyesus and Frieden, 2018). As of 2018, mandatory TFA limits are in effect in 34 countries and passed in 24 additional countries (World Health Organization, 2019). Amongst the Southeast Asian countries, Thailand and Singapore have banned PHO in their food supply while Indonesia has implemented a national policy commitment to eliminate TFA from their food products (Non-Communicable Diseases Alliance, 2019). In Malaysia, mandatory declaration of TFA and/or the setting of maximum limits of TFA in the food supply are still not in place; however, conditions for nutrient contents for use in nutrition claims are stipulated in the Malaysian Food Act 1983. For food claiming to be low in TFA, the maximum allowable limits are 1.5 g/100 g and 0.75 g/100 mL in both solids and liquids, respectively, while a product claiming to be TFA-free must contain no more than 0.1% TFA in both solids and liquids (Legal Research Board, 2015).

Palm oil products have long been regarded as excellent *trans*-fat replacement ingredients as they do not require hydrogenation due to the inherent saturated fatty acid components which provide structure to solid fats (Parveez *et al.*, 2020). To date, there are very few studies which have examined TFA levels in commercial food products available in the Malaysian market. One of the earliest studies by Tang (2002) investigated the TFA levels of various palm-based and non-palm-based vegetable oils from local manufacturers and retailers in Malaysia. The author found that the TFA content of palm-based products ranged between 0.25% and 0.67% while those of non-palm-based cooking oils were present at a higher range of 0.45% to 3.85%. Many authors have reported that the major sources of industrial TFA in the Malaysian diet are semi-solid fats and cooking oils, fast foods, bakery products, breakfast cereals, snacks, dairy products and fried foods (Akmar *et al.*, 2013; Azimah *et al.*, 2013; Nurshahbani and Azrina, 2014). The TFA contents of biscuits in the Malaysian market have also been reported in two separate studies by Neo *et al.* (2007); Norhayati *et al.* (2011). These studies reported that locally-made Malaysian biscuits possessed low TFA levels below 1% as a result of using palm oil in the ingredients whereas imported biscuits were found to contain higher levels of TFA between 0.03 and 3.09 g/100 g of total fatty acids. Karupaiah *et al.* (2014) examined the TFA content of 158 Malaysian supermarket food samples comprising fats and oils, dairy products, snacks, soups, confectionery, meat and meat products. Five products within the chocolate, ghee and butter products contained high TFA contents exceeding the 1.5 g/kg solids level indicated in the Malaysian Food Standard for a TFA nutrient label claiming a product as low *trans*.

Realising the need for an updated assessment of TFA levels in commercial cooking oils and fats, the aims of this study were to analyse the current levels of TFA in vegetable oils in the Malaysian market and to investigate the relationship between the levels of TFA and the contents of different fatty acid groups within the oils. It is hoped that this study would establish the present levels of TFA from retail cooking oils and fats which could contribute to the current TFA intake in the Malaysian population. This would provide authorities with an indication on TFA levels in vegetable oil products as a result of changes in refining and processing practices and further support the implementation of a national commitment for the elimination of TFA from food products on the Malaysian market.

MATERIALS AND METHODS

Materials

A total of 104 samples of vegetable oils were sampled in this study. The oils included refined, bleached and deodourised (RBD) palm-based oils and fats obtained from palm oil refineries throughout Malaysia and commercial vegetable oils and fats bought from major supermarkets as well as small sundry shops in the state of Selangor, Malaysia. The samples were collected between 2017 and 2019, and analysed within the same year. All samples were stored at 4°C and thoroughly homogenised prior to fatty acid composition analysis.

Fatty Acid Composition Analysis

The fatty acid composition was analysed according to the American Oil Chemists' Society (AOCS) Official Method Ce 1f-96 (AOCS, 2009). Methyl esters of fatty acids were analysed using an Agilent 6890 Series gas chromatography (GC) system (J&W Scientific, Folsom, USA) equipped with a flame ionisation detector (FID) (Agilent Technologies, Wilmington, USA) on a fused silica capillary column (BPX-70, 60 m length × 0.25 mm i.d., film thickness 0.25 µm, SGE Inc., Austin, TX). The column temperature was set at 192°C while injector (with split ratio 100:1) and detector temperatures were both set at 250°C. Helium (purity 99.999%) flowrate was set at 0.8 mL min^{-1}. FAME were identified based on the retention times of FAME mix standards, namely Grain FAME Mix (Supelco, Bellefonte, USA), rapeseed oil reference mixture (AOCS, Urbana, USA), linoleic acid methyl ester isomer mix (Supelco, Bellefonte, USA) and comparisons with earlier literature. Analyses were carried out in duplicate and reported as mean ± standard deviation (SD). All oil samples analysed in this study were categorised as refined oils and fats, hence the TFA content using the abovementioned procedure was defined as the sum of C18:1*t*, C18:2*t* and C18:3*t* components relative to the total fatty acids present in the oil sample. Results are reported in g per 100 g fat.

Statistical Analysis

One-way analysis of variance (ANOVA) was performed to evaluate significant differences between results using Tukey's test at a confidence level of 95% ($p<0.05$). Pearson's correlation coefficient was used to determine the relationship between TFA and selected fatty acid parameters, *i.e.*, saturated fatty acids (SFA), monounsaturated fatty acids (MUFA) and polyunsaturated fatty acids (PUFA). All statistical analyses were conducted using Minitab software (Minitab 16, Minitab Inc., State College, USA).

RESULTS AND DISCUSSION

Distribution of *Trans* Fatty Acids Content in RBD Palm-based Oils and Fats from Malaysian Refineries

The compositions of TFA, TFA isomers, SFA, MUFA and PUFA groups for RBD palm-based samples from Malaysian refineries are presented in *Table 1*. TFA was detected in all RBD palm-based samples with TFA concentrations varying from 0.12 ± 0.00 g/100 g to 0.84 ± 0.01 g/100 g. These results agree with Tang (2002) who demonstrated that small amounts of TFA present in refined palm oils are a result of thermal isomerisation due to the relatively high temperatures of up to 260°C employed during deodourisation. There was a significant difference between the TFA levels in RBD palm olein and RBD palm kernel olein. Higher TFA levels in RBD palm olein samples compared to that of RBD palm kernel olein can be attributed to higher deodourisation temperatures used during palm oil refining and higher content of PUFA in RBD palm olein compared to RBD palm kernel olein. This is supported by

TABLE 1. COMPOSITION OF TFA, TFA ISOMERS AND FATTY ACID GROUPS OF RBD PALM OIL AND PALM KERNEL OIL PRODUCTS FROM MALAYSIAN PALM OIL REFINERIES

RBD palm oil fractions	SFA (g/100 g)	MUFA (g/100 g)	PUFA (g/100 g)	C18:1*t* (g/100 g)	C18:2*t* (g/100 g)	C18:3*t* (g/100 g)	TFA (g/100 g)	Average TFA (g/100 g)
Palm oil (*n*=18)	50.38 ± 0.62	39.27 ± 1.19	9.99 ± 0.61	0.05 ± 0.01	0.34 ± 0.13	0.09 ± 0.03	0.24 – 0.67	0.48 ± 0.16
Palm olein (*n*=7)	44.62 ± 1.33	43.94 ± 0.92	10.99 ± 0.58	0.07 ± 0.02	0.45 ± 0.14	0.11 ± 0.02	0.39 – 0.84	0.62 ± 0.15
Palm stearin (*n*=3)	67.67 ± 0.22	25.92 ± 0.26	6.09 ± 0.06	0.06 ± 0.03	0.22 ± 0.01	0.06 ± 0.01	0.32 – 0.38	0.34 ± 0.03
Palm kernel olein (*n*=1)	74.08	22.09	3.75	0.04	0.08	ND	-	0.12

Note: Values expressed as mean ± standard deviation. The number of products (*n*) is descripted within parentheses.
SFA - saturated fatty acid; MUFA - monounsaturated fatty acid; PUFA - polyunsaturated fatty acids; TFA - *trans* fatty acids; ND - not detected.

a previous study by Tasan *et al.* (2011) which showed that PUFA such as linoleic acid (C18:2) and linolenic acid (C18:3) are more prone to geometrical isomerisation during deodourisation. Furthermore, the considerably lower TFA observed in palm kernel fractions can also be ascribed to the milder deodourisation temperatures of 240°C and below used during palm kernel oil refining (Tang, 2002).

The average TFA content of RBD palm-based samples in the present study were found to be slightly higher compared to the average TFA for similar sample groups in the study by Tang (2002). The author reported average TFA levels for RBD palm oil, RBD palm olein, RBD palm stearin and RBD palm kernel olein at 0.32 ± 0.16%, 0.30 ± 0.17%, 0.26 ± 0.13% and 0.03 ± 0.03%, respectively. The higher TFA values observed in this study suggest that there may be differences in refining practices employed by the Malaysian palm oil industry within the last two decades, in particular during the deodourisation step. Wolff (1993) previously showed that TFA formation strongly depends on heating time and deodourisation temperature, thus, prolonged deodourisation time at higher temperatures may increase TFA content of refined oils. Thus, it is possible that the use of higher deodourisation temperatures in the past few decades may have contributed to the rise in TFA levels in the current RBD palm-based samples in this study. All RBD palm-based samples in this study conformed to the condition for nutrition claims of low TFA levels in the Malaysian Food Act 1983 of 0.75 g per 100 mL liquid. Only one RBD palm olein sample with TFA level of 0.84 ± 0.01 g/100 g was found to exceed this limit.

Distribution of *Trans* Fatty Acids Content in Commercial Cooking Oils and Fats from Malaysian Supermarkets and Sundry Shops

Table 2 summarises the composition of TFA, TFA isomers and fatty acid groups of selected commercial cooking oils purchased in their final packaging form from supermarkets and sundry shops in Malaysia. The commercial cooking oil samples were grouped into different oil types, namely palm olein, canola oil, sunflower oil, soybean oil, corn oil, coconut oil, sesame oil, olive oil, peanut oil, rice bran oil, palm-based oil blend, canola-based oil blend, vegetable shortenings and premium oils. The premium oils category comprised of various cold pressed oils, specifically avocado oil, apricot kernel oil, almond oil, organic flaxseed (linseed) oil, unrefined pumpkin oil and safflower oil. The category also included macadamia oil, walnut oil, grapeseed oil, black seed oil and black seed and olive oil blend. TFA was detected in all the commercial cooking oil samples analysed in this study with the exception of cold pressed virgin coconut oil.

TABLE 2. COMPOSITION OF TFA, TFA ISOMERS AND FATTY ACID GROUPS OF COMMERCIAL VEGETABLE OILS IN MALAYSIA

Category	SFA (g/100 g)	MUFA (g/100 g)	PUFA (g/100 g)	C18:1*t* (g/100 g)	C18:2*t* (g/100 g)	C18:3*t* (g/100 g)	TFA Range (g/100 g)	TFA (g/100 g)
Palm olein (*n*=14)	43.65 ± 1.79	44.31 ± 1.28	11.79 ± 0.75	0.04 ± 0.01	0.26 ± 0.18	0.07 ± 0.04	0.04 – 0.86	0.37 ± 0.22
Canola oil (*n*=4)	7.51 ± 0.71	61.48 ± 3.57	30.79 ± 2.92	0.04 ± 0.01	0.28 ± 0.17	1.62 ± 0.54	1.43 – 2.96	1.94 ± 0.70
Sunflower oil (*n*=4)	9.18 ± 2.41	56.43 ± 33.53	34.24 ± 31.08	0.03 ± 0.02	0.16 ± 0.15	0.06 ± 0.03	0.10 – 0.47	0.24 ± 0.16
Soybean oil (*n*=2)	15.90 ± 0.25	24.49 ± 1.29	59.33 ± 1.34	0.08 ± 0.01	0.49 ± 0.23	1.06 ± 0.52	1.10 – 2.15	1.63 ± 0.74
Corn oil (*n*=4)	14.51 ± 0.37	32.04 ± 2.08	53.15 ± 2.31	0.05 ± 0.03	0.45 ± 0.23	0.14 ± 0.06	0.25 – 0.97	0.64 ± 0.30
Coconut oil (*n*=3)	92.23 ± 2.17	6.24 ± 1.40	1.52 ± 0.75	0.04 ± 0.01	0.03 ± 0.01	0.05 ± 0.01	0.00 – 0.14	0.06 ± 0.07
Sesame oil (*n*=5)	16.10 ± 0.58	41.68 ± 1.30	41.59 ± 1.55	0.18 ± 0.12	0.27 ± 0.15	0.33 ± 0.00	0.10 – 0.76	0.52 ± 0.27
Olive oil (*n*=8)	15.62 ± 0.95	74.49 ± 2.96	9.66 ± 2.21	0.07 ± 0.07	0.07 ± 0.04	0.07 ± 0.04	0.04 – 0.45	0.19 ± 0.14
Palm-based oil blend (*n*=6)	36.69 ± 6.35	41.45 ± 3.42	21.54 ± 9.63	0.05 ± 0.02	0.43 ± 0.25	0.20 ± 0.18	0.32 – 1.04	0.67 ± 0.33
Canola-based oil blend (*n*=6)	10.53 ± 3.71	54.21 ± 8.46	34.99 ± 7.97	0.03 ± 0.02	0.23 ± 0.19	1.13 ± 0.32	1.00 – 2.06	1.38 ± 0.39
Premium oils (*n*=11)	12.22 ± 3.78	45.72 ± 26.13	41.66 ± 27.81	0.04 ± 0.03	0.37 ± 0.62	0.37 ± 0.76	0.01 – 2.64	0.64 ± 0.93
Vegetable fat shortenings (*n*=5)	51.62 ± 13.79	31.42 ± 6.34	16.70 ± 19.28	0.06 ± 0.02	0.40 ± 0.20	0.26 ± 0.36	0.34 – 1.37	0.71 ± 0.44
Peanut oil (*n*=1)	16.69	61.65	21.42	0.04	0.19	0.09	0.32	0.32
Rice bran oil (*n*=1)	23.88	41.89	34.17	0.13	0.18	0.07	0.39	0.39

Note: Values are expressed as mean ± standard deviation. The number of products (*n*) is descripted within parentheses.
SFA - saturated fatty acid; MUFA - monounsaturated fatty acid; PUFA - polyunsaturated fatty acids; TFA - *trans* fatty acids.

Among the 75 commercial cooking oils analysed, the highest TFA levels were found in canola oil, followed by soybean oil and canola-based oil blends. This can be attributed to significantly higher contents of C18:3*t* in these three oil categories compared to all other oils. High TFA contents in soybean and canola oils are primarily caused by the geometrical isomerisation of their inherently high PUFA contents during deodourisation at temperatures above 200°C (Ceriani and Meirelles, 2007; Wolff, 1992). Higher concentrations of α-linolenic acid are present in canola oils and their bonds are more labile compared to that of linoleic acid, resulting in higher isomerisation degrees of α-linolenic acid (Kemény *et al.*, 2001). Hénon *et al.* (1999) reported that linolenic acid isomerisation in canola oil increases greatly beyond deodourisation temperatures of 220°C-230°C. Similar TFA levels were observed in US canola oils (TFA range 0.73-4.16 g/100 g) as reported by O'Keefe *et al.* (1994). The TFA of soybean oil in this study were comparable to values reported earlier by Tang (2002) (TFA range 1.63-3.83 g/100 g), Martin *et al.* (2008) for Brazilian soybean oils (TFA range 0.83-2.58 g/100 g) and Hou *et al.* (2012) for soybean oil from China (TFA range 0.23-3.11 g/100 g). However, the values were lower than those observed by Wolff (1993) for soybean oil from Great Britain (TFA range 1.73-2.52 g/100 g) and those by Akmar *et al.* (2013); Azimah *et al.* (2013), both reporting a mean TFA of 5.79 g/100 g for one soybean oil sample in Malaysia. This could be due to the wide variation in processing conditions by refiners which give rise to varying TFA levels in different soybean oil brands in Malaysia.

Commercial vegetable oils which showed TFA below 0.5 g/100 g include rice bran oil, palm olein, peanut oil, sunflower oil and coconut oil in descending order. The lowest TFA level amongst all commercial oils analysed was detected in coconut oil. The coconut oils in this study contained a significantly higher content of SFA (more than 90%) and relatively low amount of PUFA (less than 3%) compared to all other commercial oils. This was expected since coconut oil is well-known for its high saturated fatty acid content, comprising mainly medium-chain SFA such as lauric acid and myristic acid which give the oil higher thermal resistance. As a consequence, coconut oil requires deodourisation at lower temperatures between 240°C-250°C (Withana-Gamage *et al.*, 2005). The coconut oil category in this study included one cold pressed virgin coconut oil sample where TFA was not detected. This can be explained through the nature by which virgin coconut oil is obtained from fresh, mature kernel of the coconut by mechanical or natural means, with or without the application of heat and which does not result in the alteration of the nature of the oil (Phillipines National Standard, 2007). The TFA in coconut oils in our study agreed with those reported by Dayrit *et al.* (2011) for coconut oils from Phillipines and Marina *et al.* (2009) for Malaysian and Indonesian coconut oils.

Palm olein, rice bran and peanut oils contained similar TFA levels, however, the SFA content in palm olein was higher compared to the latter two. There were no significant differences between the MUFA and PUFA levels among the three oil categories with palm olein containing much lower PUFA levels compared to the other two oils. The major TFA isomer contributing to total TFA in all three oil types was C18:2*t*. As there was only one sample each for rice bran and peanut oils, there was insufficient data to draw a conclusion from these oils. However, results from this study were similar to that of Huang *et al.* (2016) who reported TFA levels ranging from 0.10-1.62 g/100 g and 0.1-1.63 g/100 g for palm oils and peanut oils in China, respectively.

A substantial reduction in the mean TFA was observed in sunflower oils to below 0.3 g/100 g in this study in comparison to the TFA levels for sunflower oils in Malaysia reported by Tang (2002) which exceeded 1%, and that of French sunflower oils (mean 0.5 g/100 g) in the study by Vingering *et al.* (2010). It is worth noting that the sunflower oil samples analysed in this study included conventional as well as high oleic sunflower oils which contained approximately 27% and 85% MUFA on average, respectively. The major TFA isomer in sunflower oil samples were those of C18:2*t*. The TFA observed in sunflower oils in this study could be attributed to the various sunflower oil species and possibly different refining methods used for the oils. High oleic sunflower oil predominantly contains oleic acid which is less prone to isomerisation compared to PUFA (Martinčič *et al.*, 2008). Tasan and Demirci (2003) demonstrated that physically refined sunflower oils contained a higher level of TFA (2.56 $\pm$ 0.25 g/100 g) compared to chemically refined sunflower oils (0.76 $\pm$ 0.27 g/100 g) due to the high temperature applied in the last stage of physical refining. The C18:3*t* range in sunflower oil samples was observed to be significantly lower compared to that of canola and soybean oils and equivalent to that of palm olein. Optimisation of processing conditions during the deacidification step of physical refining of sunflower oil, through the application of lower deodourisation temperatures and shorter heating times could minimise the degree of isomerisation of PUFA in sunflower oils (Ceriani *et al.*, 2008) and this may explain the reduced TFA levels of sunflower oils in this study.

A very low TFA level averaging at 0.19 g/100 g was found for the olive oil category and this could be due to the significantly higher MUFA content (more than 70%) compared to other commercial oils. The olive oils in this study included extra virgin olive oil, virgin + refined olive oil and olive pomace oil based on the labels provided on the packaging. Virgin olive

oils are obtained from the fruit of the olive tree solely by mechanical or other physical means, particularly thermal conditions that do not lead to alterations in the oil and have not undergone any treatment other than washing, decanting, centrifuging and filtration (Codex Alimentarius, 2015). On the other hand, olive pomace oil is obtained by treating olive pomace with solvents other than halogenated solvents or by other physical treatments, to the exclusion of oils obtained by re-esterification processes and of any mixture with oils of other kinds. The production of olive pomace oil also involves a drying step using hot drying gases normally within a temperature range of between 400°C and 800°C (Sánchez Moral and Ruiz Méndez, 2006). Amongst the olive oils sampled, extra virgin olive oils (n=3) contained the lowest levels of TFA (less than 0.1 g/100 g), while virgin olive oils (n=3) showed TFA levels less than 0.3 g/100 g. The highest level of TFA was observed in olive pomace oil (n=1) at 0.45 g/100 g oil. The varying TFA levels within the different types of olive oils are indicative of the different extraction processes and whether the oils had undergone any thermal treatment. TFA levels of all olive oils in this study were lower than that reported by Azimah *et al.* (2013) and Akmar *et al.* (2013) at 0.79 g/100 g and fell within the TFA ranges specified in the Codex Standard for Olive Oils and Olive Pomace Oils (Codex Alimentarius, 2015).

From the 14 commercial vegetable oil categories, five oil categories were found to contain TFA levels between 0.5-1.0 g/100 g. These included vegetable fat shortenings, palm-based oil blends, corn oil, premium oils and sesame oil in descending order. There were no significant differences (p<0.05) between the TFA levels of these oil categories, however, vegetable shortenings contained a significantly higher SFA content followed by palm-based blended cooking oils. This can be explained by the presence of palm-based solid fraction with 50%-60% SFA content as one of the solid fat ingredients used in four out of five of the vegetable shortenings samples (individual results not shown). Only one vegetable shortening sample contained fully hydrogenated palm oil and soybean oil as indicated in its ingredients list with over 50% PUFA. This consequently gave the highest TFA level of 1.37 g/100 g within this oil category. It is important to note that this study only considered shortenings derived from vegetable oils and fats in order to avoid the naturally occurring ruminant TFA that are usually present in dairy products.

TFA levels above 2 g/100 g were found in two out of the 13 premium oil samples (individual results not shown in *Table 2*), specifically cold pressed unrefined almond oil (2.18 g/100 g) and walnut oil (2.64 g/100 g). As the almond oil was cold pressed and unrefined, one would expect a significantly low TFA value for the almond oil as TFA levels below 0.3 g/100 g was detected in all the other cold pressed oils, *i.e.*, avocado, apricot, flaxseed, pumpkin seed and safflower oils. A possible explanation for the presence of TFA in cold pressed oils can be a result from mixing oils that have been deodourised under different conditions in the same tank or may be due to their storage in unswept tanks (Wolff, 1993).

The TFA of walnut oil in our study was higher than those reported by Wolff (1993) (range 0.84-1.83 g/100 g) for German and French walnut oils and Vingering *et al.* (2010) (range 0.9-1.7 g/100 g oil) for French walnut oil. The walnut oil sample in this study contained about 73% PUFA and the TFA value was mainly contributed by C18:3*t*. TFA was present at an average of less than 1 g/100 g in all other oils in the premium cooking oil category. The large variation in TFA values between commercial oil samples in this study may be influenced by the differences in oil species, processing conditions prior to packaging as well as any additional ingredients such as anti-oxidants or anti-clouding agents used in the oils (Azimah *et al.*, 2013). The nutrient conditions for claiming low TFA is met in all retail cooking oils and fats with the exception of soybean oils, canola oils, canola-based blended oils and one sample of palm olein blend, walnut oil, cold pressed unrefined almond oil and vegetable shortening containing soybean oil.

Relationship of TFA with Different Fatty Acid Groups

In this study, Pearson correlation analysis was carried out to determine the relationship between TFA with fatty acid groups SFA, MUFA, PUFA, as well as selected PUFA, namely C18:1, C18:2 and C18:3. The strength of the relationship between variables tested is expressed as Pearson correlation coefficient (r). Correlation between variables were defined as follows: very weak (0.0<r<0.3), weak (0.3<r<0.5), moderate (0.5<r<0.7), strong (0.7<r<0.9) and very strong (r>0.9) (Zady, 2000). The relationships were considered significant if p-value <0.05.

TABLE 3. PEARSON CORRELATIONS BETWEEN TFA AND DIFFERENT FATTY ACID GROUPS AND UNSATURATED FATTY ACIDS IN RBD PALM-BASED PRODUCTS FROM MALAYSIAN PALM OIL REFINERIES

Parameters	r	p-value
SFA	-0.549	0.002
MUFA	0.511	0.005
PUFA	0.587	0.001
C18:1	0.509	0.005
C18:2	0.581	0.001
C18:3	-0.117	0.546

Note: TFA - *trans* fatty acids.

Table 3 tabulates results from the Pearson correlation analyses between the levels of TFA and SFA, MUFA, PUFA, C18:1, C18:2 and C18:3 for all samples of RBD palm-based oils from Malaysian palm oil refineries. MUFA and PUFA showed significant moderate positive correlations with TFA (r=0.511 and r=0.587, respectively) while SFA displayed a significant moderate inverse correlation (r=-0.549), all showing p-value <0.05. The levels of C18:1 and C18:2 fatty acids both exhibited moderate positive correlations with TFA (r=0.509 and r=0.581, respectively) and the correlations were significant (p-value <0.05). On the other hand, C18:3 showed a very weak inverse correlation (r=-0.117) with TFA and the correlation was insignificant. It is worth noting that the levels of C18:3 present in the RBD palm-based samples were very low, ranging on average between 0.00 to 0.17 g/100 g total fat.

There were large variations in the TFA content found in the palm-based samples from Malaysian refineries produced by different manufacturers, presumably using dissimilar processing conditions. According to Gibon (2012), palm oils which undergo physical refining are more prone to form TFA compared to the chemical route due to the more severe thermal treatments applied during physical refining. Chemical refining involves the application of milder temperatures of between 220°C and 240°C compared to physical refining and Gibon *et al.* (2007) reported that a typical mean value of 0.6 g/100 g TFA was found in commercial palm oil products refined at 260°C-275°C with short residence times of 45-90 min. TFA formation can significantly accelerate if higher temperatures and longer residence times are employed. This was further demonstrated by Siew and Mohammad (1989) for palm olein and palm mid fraction which showed TFA values as high as 2.1 g/100 g and 1.5 g/100 g, respectively, when processed at 280°C.

In the case of commercial cooking oils, Pearson correlation coefficients between TFA and different fatty acid groups as well C18:1, C18:2 and C18:3 for all commercial vegetable oil samples are shown in *Table 4*. SFA yielded a weak negative correlation with TFA (r=-0.329) while PUFA, C18:2 and C18:3 displayed weak positive correlations (r=0.405; r=0.321; r=0.240, respectively) with TFA, and all these correlations were significant (p<0.05). This indicates that commercial vegetable oils with higher SFA tend to have lower TFA content and *vice versa* for oils containing higher PUFA concentration. These observations are in agreement with the study by Akmar *et al.* (2013) on the TFA content of selected foods in Malaysia. The authors concluded that high TFA prevailed in oils with low SFA content. Furthermore, it was observed that the TFA in all commercial vegetable oil samples were not associated with MUFA (r=-0.079) and C18:1 (r=-0.074). It is important to note that the majority of commercial vegetable oil samples in this study consisted primarily of refined oils. This observation appears to be consistent with Djikstra (2008) who reported that the main fatty acid to isomerise during hydrogenation is the monounsaturated oleic acid (C18:1). Previous studies have also shown that *trans* MUFA are generally produced by hydrogenation of vegetable oils or biohydrogenation in ruminants, whereas *trans* PUFA are formed as a result of deodourisation of oils or during frying treatments (Chen *et al.*, 2014; Stender *et al.*, 2008). These results suggest that the TFA present in commercial vegetable oils in this study were mainly associated with the levels of PUFA (C18:2 and C18:3) and not MUFA (C18:1).

TABLE 4. PEARSON CORRELATIONS BETWEEN TFA AND DIFFERENT FATTY ACID GROUPS AND UNSATURATED FATTY ACIDS IN COMMERCIAL VEGETABLE OIL SAMPLES

Parameters	*r*	*p*-value
SFA	-0.329	0.004
MUFA	-0.079	0.501
PUFA	0.405	0.000
C18:1	-0.074	0.529
C18:2	0.321	0.005
C18:3	0.240	0.039

Note: TFA - *trans* fatty acids.

CONCLUSION

The majority of palm-based cooking oils in Malaysia contained TFA below 1 g/100 g and were found to conform to the conditions for nutrition claims of low TFA in solid and liquid products, respectively, as regulated in the Malaysian Food Act 1983. All soybean, canola and canola-based blended oils as well as walnut and cold-pressed almond oils sampled contained TFA levels exceeding 1 g/100 g. In general, PUFA exhibited significant moderate positive correlations with TFA while SFA showed significant moderate inverse correlations with TFA in all oil categories. These findings indicate that the TFA in the oil samples were mostly generated through refining at high deodourisation temperatures and not through partial hydrogenation. Thus, it is imperative that vegetable oil manufacturers reassess the thermal conditions employed during processing in order to minimise the isomerisation of linoleic and linolenic acids. An overview of the overall TFA levels in various vegetable oils in Malaysia is crucial for manufacturers to evaluate current refining practices to meet the recommended TFA levels by WHO. Results evidently show that palm-based

oils and fats continue to be excellent alternative sources to PHO in the global quest to eliminate *trans* fat consumption by 2023. In addition, the findings provide further data in support of the national health authority for the implementation of a national commitment to eliminate TFA from food products on the Malaysian market.

ACKNOWLEDGEMENT

The authors wish to thank the Director-General of the MPOB for permission to publish this article. Technical assistance from the Innovative Products Group is gratefully acknowledged. The authors would like to extend their sincere appreciation to MPOB for funding this research.

REFERENCES

Akmar, Z D; Norhaizan, M E; Azimah, R; Azrina, A and Chan, Y M (2013). The *trans* fatty acids content of selected foods in Malaysia. *Malays. J. Nutr., 19*: 87-98.

AOCS Official Method Ce 1f-96 (2009). Cis and *trans* fatty acids in oils and fats by capillary GC. *AOCS Official Methods and Recommended Practices of the AOCS*. 7th edition. The American Oil Chemists' Society, Urbana, USA.

Azimah, A; Azrina, A; Norhaizan, M E; Sokhini, M A and Daud, A Z (2013). Industrially produced *trans* fatty acids: Major potential sources in Malaysian diet. *Int. Food Res. J., 20*: 1157-1164.

Brouwer, I A; Wanders, A J and Katan, M B (2010). Effect of animal and industrial *trans* fatty acids on HDL and LDL cholesterol levels in humans – A quantitative review. *PLoS ONE, 5*: e9434. DOI: 10.1371/journal.pone.0009434.

Ceriani, R and Meirelles, A J (2007). Formation of *trans* PUFA during deodorization of canola oil: A study through computational simulation. *Chem. Eng. Process, 46*: 375-385. DOI: 10.1016/j.cep.2006.05.023.

Ceriani, R; Costa, A M and Meirelles, A J A (2008). Optimization of the physical refining of sunflower oil concerning the final contents of *trans*-fatty acids. *Ind. Eng. Chem. Res., 47*: 681-692.

Chen, Y; Yang, Y; Nie, S; Yang, X; Wang, Y; Yang, M; Chang, L and Xie, M (2014). The analysis of *trans* fatty acid profiles in deep frying palm oil and chicken fillets with an improved gas chromatography method. *Food Control, 44*: 191-197. DOI: 10.1016/j.foodcont.2014.04.010.

Codex Alimentarius (2015). Codex Standard for Olive Oils and Olive-pomace Oils (CODEX-STAN 33-1981). http://www.fao.org/fao-who-codexalimentarius/sh-proxy/en/?lnk=1&url=https%253A%252F%252Fworkspace.fao.org%252Fsites%252Fcodex%252FStandards%252FCXS%2B33-1981%252FCXS_033e.pdf, accessed on 15 May 2020.

Craig-Schmidt, M C and Rong, Y (2009). Evolution of worldwide consumption of *trans* fatty acids. *Trans Fatty Acids in Human Nutrition* (Destaillats F; Sébédio, J-L; Dionisi, F; Chardigny, J-M eds.). 2nd edition. Woodhead Publishing, Cambridge. p. 329-380. DOI: 10.1533/9780857097873.329.

Dayrit, F M; Dimzon, I K D; Valde, M F; Santos, J E R; Garrovillas, M J M and Villarino, B J (2011). Quality characteristics of virgin coconut oil: Comparisons with refined coconut oil. *Pure Appl. Chem., 83*: 1789-1799. DOI: 10.1351/PAC-CON-11- 04-01.

De Souza, R J; Mente, A; Maroleanu, A; Cozma, A I; Ha, V; Kishibe, T; Uleryk, E; Budylowski, P; Schünemann, H; Beyene, J and Anand, S S (2015). Intake of saturated and *trans* unsaturated fatty acids and risk of all cause mortality, cardiovascular disease, and type 2 diabetes: Systematic review and meta-analysis of observational studies. *BMJ, 351*: h3978. DOI: 10.1136/bmj.h3978.

Dijkstra, A J (2008). Controlling physical and chemical properties of fat blends through their triglyceride compositions. *Trans Fatty Acids* (Dijkstra, A J; Hamilton, R J; Hamm, W eds.). Blackwell Publishing, Oxford. p. 132-146.

European Commission (2019). Commission regulation (EU) 2019/649 of 24 April 2019 amending Annex III to Regulation (EC) No 1925/2006 of the European Parliament and of the Council as regards *trans* fat, other than *trans* fat naturally occurring in fat of animal origin, OJ L110/17.

European Parliament (EP) (2016). European Parliament resolution of 26 October 2016 on *trans* fats (TFAs) (2016/2637(RSP)).

Ghebreyesus, T A and Frieden, T R (2018). REPLACE: A roadmap to make the world *trans* fat free by 2023. *Lancet, 391*: 1978-1980. DOI: 10.1016/S0140-6736(18)31083-3.

Gibon, V; De Greyt, W and Kellens, M (2007). Palm oil refining. *Eur. J. Lipid Sci. Technol., 109*: 315-335. DOI: 10.1002/ejlt.200600307.

Gibon, V (2012). Palm oil and palm kernel oil refining and fractionation technology. *Palm Oil*

(Lai, O-M; Tan, C-P; Akoh, C C eds.). AOCS Press, Champaign. p. 329-375. DOI: 10.1016/B978-0-9818936-9-3.50015-0.

Hendry, V L; Almíron-Roig, E; Monsivais, P; Jebb, S A; Benjamin Neelon, S E; Griffin, S J and Ogilvie, D B (2015). Impact of regulatory interventions to reduce intake of artificial *trans*-fatty acids: A systematic review. *Am. J. Public Health, 105*: e32-e42. DOI: 10.2105/AJPH.2014.302372.

Hénon, G; Kemény, Z; Recseg, K; Zwobada, F and Kovari, K (1999). Deodorization of vegetable oils. Part I: Modelling the geometrical isomerization of polyunsaturated fatty acids. *J. Amer. Oil Chem. Soc., 76*: 73-81. DOI: 10.1007/s11746-999-0050-2.

Hou, J C; Wang, F; Wang, Y T; Xu J and Zhang, C W (2012). Assessment of *trans* fatty acids in edible oils in China. *Food Control, 25*: 211-215. DOI: 10.1016/j.foodcont.2011.10.044.

Huang, X; Nie, S; Yang, M; Xie, J; Li, C and Xie, M (2016). Are Chinese edible oils safe? A survey of *trans* fatty acid contents in Chinese edible oils. *Food Sci. Biotechnol., 25*: 631-636. DOI: 10.1007/10068-016-0088-5.

Islam, M A; Amin, M N; Siddiqui, S A; Hossain, M P; Sultana, F and Kabir, M R (2019). *Trans* fatty acids and lipid profile: A serious risk factor to cardiovascular disease, cancer and diabetes. *Diabetes Metab. Syndr., 13*: 1643-1647. DOI: 10.1016/j.dsx.2019.03.033.

Karupaiah, T; Tan, H K; Ong, W W; Tan, C H and Sundram, K (2014). *Trans* fatty acid content in Malaysian supermarket foods: A field-to-laboratory approach in assessing food risk. *Food Addit. Contam. Part A Chem. Anal., 31*: 1375-1384. DOI: 10.1080/19440049.2014.929183.

Kemény, Z S; Recseg, K; Henon, G; Kővári, K and Zwobada, F (2001). Deodorization of vegetable oils: prediction of *trans* polyunsaturated fatty acid content. *J. Amer. Oil Chem. Soc., 78*: 973-979. DOI: 10.1007/s11746-001-0374-0.

Legal Research Board (2015). *Food Act 1983 (Act 281); & Food Regulations 1985: as at 20 February 2015*. International Law Book Services, Kuala Lumpur. http://www.agc.gov.my/agcportal/uploads/files/Publications/LOM/EN/Act%20281%20-%20Food%20Act%201983.pdf.

Li, C; Cobb, L K; Vesper, H W and Asma, S (2019). Global surveillance of *trans*-fatty acids. *Prev. Chronic Dis., 16*. DOI: 10.5888/pcd16.190121.

Marina, A M; Che Man, Y B; Nazimah, S A H and Amin, I (2009). Chemical properties of virgin coconut oil. *J. Amer. Oil Chem. Soc., 86*: 301-307. DOI: 10.1007/s11746-009-1351-1.

Martin, C A; Visentainer, J V; Oliveira, A N D; Oliveira, C C D; Matsushita, M and Souza, N E D (2008). Fatty acid contents of Brazilian soybean oils with emphasis on *trans* fatty acids. *J. Braz. Chem. Soc., 19*: 117-122. DOI: 10.1590/S0103-50532008000100017.

Martinčič, V; Golob, J; de Greyt, W; Verhé, R; Knez, S; Van Hoed, V; Žilnik L F; Potočnik, K; Hraš, A R and Ayala, J V (2008). Optimization of industrial-scale deodorization of high-oleic sunflower oil via response surface methodology. *Eur. J. Lipid Sci. Technol., 110*: 245-253. DOI: 10.1002/ejlt.200700194.

Mozaffarian, D; Katan, M B; Ascherio, A; Stampfer, M J and Willett, W C (2006). *Trans* fatty acids and cardiovascular disease. *N. Engl. J. Med., 354*: 1601-1613. DOI: 10.1056/nejmra054035.

Mozaffarian, D; Aro, A and Willett, W C (2009). Health effects of *trans*-fatty acids: Experimental and observational evidence. *Eur. J. Clin. Nutr., 63*: S5-S21. DOI: 10.1038/sj.ejcn.1602973.

Neo, Y P; Tan, C H and Ariffin, A (2007). Fatty acid composition of five Malaysian biscuits (cream crackers) with special reference to *trans*-fatty acids. *ASEAN Food J., 14*: 197-204.

Nishida, C; Uauy, R; Kumanyika, S and Shetty, P (2004). The joint WHO/FAO expert consultation on diet, nutrition and the prevention of chronic diseases: Process, product and policy implications. *Public Health Nutr., 7*: 245-250. DOI: 10.1079/PHN2003592.

Nishida, C and Uauy, R (2009). WHO scientific update on health consequences of *trans* fatty acids: Introduction. *Eur. J. Clin. Nutr., 63*: S1-S4. DOI: 10.1038/ejcn.2009.13.

Non-Communicable Diseases (NCD) Alliance (2019). *Trans* fat free by 2023: Case studies in *trans*-fat elimination, https://ncdalliance.org/resources/TransFatFree2023Report, accessed on 15 May 2020.

Norhayati, M; Azrina, A; Norhaizan, M E and Muhammad Rizal, R (2011). *Trans* fatty acids content of biscuits commercially available in Malaysian market and comparison with other countries. *Int. Food Res. J., 18*: 1097-1103.

Nurshahbani, S S and Azrina, A (2014). *Trans* fatty acids in selected bakery products and its potential dietary exposure. *Int. Food Res. J., 21*: 2175-2181.

O'Keefe, S; Gaskins-Wright, S; Wiley, V and Chen, I (1994). Levels of *trans* geometrical isomers of essential fatty acids in some unhydrogenated US vegetable oils. *J. Food Lipids, 1*: 165-176. DOI: 10.1111/j.1745-4522.1994.tb00244.x.

Parveez, A G K; Hishamuddin, E; Loh, S K; Ong-Abdullah, M; Mohamed Salleh, K; Zanal Bidin, M N I; Sundram, S; Azizul Hasan, Z A and Idris, Z (2020). Oil palm economic performance in Malaysia and R&D progress in 2019. *J. Oil Palm Res., 32*: 159-190. DOI: 10.21894/jopr.2020.0032.

Philippine National Standard (2007). Virgin Coconut Oil (VCO) (PNS/BAFPS 22:2007/ ICS 67.200.10. http://spsissuances.da.gov.ph/index.php/da-philippine-national-standards/1087-pns-bafs-22-2007-vco-revised, accessed on 14 May 2020.

Sánchez Moral, P and Ruiz Méndez, M (2006). Production of pomace olive oil. *Grasas Y Aceites, 57*: 47-55. DOI: 10.3989/gya.2006.v57.i1.21.

Siew, W L and Mohammad, Y (1989). Effects of refining on chemical and physical properties of palm oil products. *J. Amer. Oil Chem. Soc., 66*: 1116-1119. DOI: 10.1007/bf02670096.

Stender, S; Astrup, A and Dyerberg, J (2008). Ruminant and industrially produced *trans* fatty acids: Health aspects. *Food Nutr. Res., 52*: 1651. DOI: 10.3402%2Ffnr.v52i0.1651.

Tang, T S (2002). Fatty acid composition of edible oils in the Malaysian market, with special reference to the *trans*-fatty acids. *J. Oil Palm Res., 14*: 1-8.

Tasan, M and Demirci, M (2003). *Trans* FA in sunflower oil at different steps of refining. *J. Amer. Oil Chem. Soc., 80*: 825-828. DOI: 10.1007/S11746-003-0779-9.

Tasan, M; Gecgel, U and Demirci, M (2011). Comparison of geometrical isomerization of unsaturated fatty acids in selected commercially refined oils. *Grasas y Aceites, 62*: 284-289. DOI: 10.3989/gya.102310.

United States Food and Drug Administration (USFDA) (2015). Final determination regarding partially hydrogenated oils. *Fed. Regist, 80*: 116.

Vingering, N; Oseredczuk, M; du Chaffaut, L; Ireland, J and Ledoux, M (2010). Fatty acid composition of commercial vegetable oils from the French market analysed using a long highly polar column. *OCL, 17*: 185-192. DOI: 10.1051/ocl.2010.0309.

Wanders, A; Zock, P and Brouwer, I (2017). *Trans* fat intake and its dietary sources in general populations worldwide: A systematic review. *Nutrients, 9*: 840. DOI: 10.3390/nu9080840.

Withana-Gamage, T S; Perera, S P and Wanasundara, U N (2005). Coconut Oil. *Bailey's Industrial Oil and Fat Products* (Shahidi, F ed.). John Wiley and Sons, Ltd., Hoboken, NJ. DOI: 10.1002/047167849X.bio054.pub2.

Wolff, R L (1992). *Trans*-polyunsaturated fatty acids in French edible rapeseed and soybean oils. *J. Amer. Oil Chem. Soc., 69*: 106-110. DOI: 10.1007/BF02540558.

Wolff, R L (1993). Further studies on artificial geometrical isomers of α-linolenic acid in edible linolenic acid-containing oils. *J. Amer. Oil Chem. Soc., 70*: 219-224. DOI: 10.1007/BF02545298.

World Health Organization and Brouwer, Ingeborg A (2016). Effect of *trans*-fatty acid intake on blood lipids and lipoproteins: A systematic review and meta-regression analysis. World Health Organization. https://apps.who.int/iris/handle/10665/246109, accessed on 14 May 2020.

World Health Organization (2019). Countdown to 2023: WHO report on global *trans* fat elimination 2019. World Health Organization, 1-40. https://www.who.int/docs/default-source/documents/replace-transfats/report-on-tfa-elimination-2019.pdf?sfvrsn=c9378613_4, accessed on 14 May 2020.

Zady, M F (2000). Correlation and simple least squares regression. http://www.westgard.com/lesson44.htm, accessed on 14 May 2020.

Zuchowska-Grzywacz, M and Kowalska, M (2019). *Trans* fatty acids in food–current legal regulations as protections for consumers and food manufacturers. *Acta Aliment., 48*: 105-114. DOI: 10.1556/066.2019.48.1.12.

Journal of Oil Palm Research Vol. 34 (1) March 2022 p. 139-151
DOI: https://doi.org/10.21894/jopr.2021.0028

INHIBITION OF CHOLINESTERASES BY WATER-SOLUBLE PALM FRUIT EXTRACT

SOON-SEN LEOW[1]*; SYED FAIRUS[1] and RAVIGADEVI SAMBANTHAMURTHI[2]

ABSTRACT

Cholinesterase (ChE) inhibitors are used for the symptomatic treatment of Alzheimer's disease and other neurological pathologies. There is interest in developing new ChE inhibitors from natural plant compounds. Water-Soluble Palm Fruit Extract (WSPFE) recovered from the aqueous oil palm vegetation liquor is rich in phenolic acids and has potential neuroprotective effects. Here, we investigated the effects of WSPFE samples on acetylcholinesterase (AChE) and butyrylcholinesterase (BChE). WSPFE ethyl acetate fraction (EAF) inhibited these enzymes the most (AChE IC_{50}: 0.218 ± 0.029 µg mL^{-1}; BChE IC_{50}: 222.860 ± 5.777 µg mL^{-1}) and had the highest AChE selectivity index (SI) value (1022.294) compared to whole samples and seven individual fractions but these effects were weaker than those of the AChE selective agent donepezil hydrochloride (DH) (AChE IC_{50}: 0.013 ± 0.001 µg mL^{-1}; BChE IC_{50}: 19.820 ± 1.415 µg mL^{-1}; AChE SI: 1524.615). Fractions containing p-*hydroxybenzoic acid and protocatechuic acid had the lowest AChE SI values (7.584 and 9.367 respectively) and may thus, function as dual ChE inhibitors. Binary mixtures of DH and WSPFE EAF might have more potent inhibitory effects against these enzymes, as well as higher BChE/AChE selectivity. Further studies to investigate the ChE inhibition potential of these WSPFE samples are warranted.*

Keywords: cholinesterases, neurodegenerative diseases, oil palm phenolics.

Received: 18 November 2020; **Accepted:** 11 March 2021; **Published online:** 17 June 2021.

INTRODUCTION

Neurodegeneration negatively affects mental and physical functioning in elderly people suffering from neurodegenerative diseases, such as Alzheimer's disease, Parkinson's disease, multiple sclerosis and amyotrophic lateral sclerosis. The global population suffering from Alzheimer's disease, which is the main cause of dementia, was established to be around 45 million in 2015, and this number is expected to double by 2030 and triple by 2050 (Scheltens *et al.*, 2016). The cholinergic system appears to be the earliest and most affected molecular mechanism that describes Alzheimer's disease pathophysiology (Craig *et al.*, 2011). In the cholinergic hypothesis, damage to brain nerve cells by senile plaques leads to decreases in choline transferase activities and losses in cognitive functions (Davies and Maloney, 1976). At the heart of the cholinergic system are the cholinesterase (ChE) enzymes. ChEs are enzymes splitting esters of choline (Pohanka, 2011). There are two types of ChEs, namely acetylcholinesterase (AChE) and butyrylcholinesterase (BChE).

AChE (EC 3.1.1.7), also known as true ChE, catalyses the hydrolysis of acetylcholine (ACh) into choline and acetic acid, a reaction necessary to return a cholinergic neuron to its resting state after activation. AChE is localised in the synaptic gaps of the central and peripheral nervous systems. This membrane-bound enzyme is projected into the synapse and terminates nervous impulses by catalysing ACh hydrolysis. AChE is

[1] Malaysian Palm Oil Board,
6 Persiaran Institusi, Bandar Baru Bangi,
43000 Kajang, Selangor, Malaysia.

[2] Academy of Sciences Malaysia,
Level 20, West Wing, MATRADE Tower,
Jalan Sultan Hj. Ahmad Shah,
off Jalan Tuanku Abdul Halim,
50480 Kuala Lumpur, Malaysia.

* *Corresponding author e-mail: ssleow@mpob.gov.my*

known to participate in vicious cycles resulting in the aggregation of beta-amyloid plaques and neurofibrillary tangles found in Alzheimer's disease (Garcia-Ayllon *et al.*, 2011). Strategies that increase ACh levels through the use of AChE inhibitors demonstrate symptomatic efficacy in Alzheimer's disease (Nordberg *et al.*, 2013). In addition to dementia, AChE inhibitors are also clinically used to counteract other neurological pathologies, such as myasthenia gravis (Colovic *et al.*, 2013). They are also used in pain management by decreasing the nociception pain response and generating analgesic actions (Eldufani and Blaise, 2019), as well as in postanaesthesia by recovering neuromuscular blockade induced by certain anaesthetics (Srivastava and Hunter, 2009).

On the other hand, BChE (EC 3.1.1.8), also known as pseudo ChE or plasma ChE, catalyses the hydrolysis of the neurotransmitter butyrylcholine (BCh) into choline and butyric acid. BChE can also hydrolyse ACh and compensate for AChE when its levels are depleted. BChE accounts for up to 90% total serum ChE, while its activity is 20-fold lower than AChE in hydrolysing ACh (Arbel *et al.*, 2014). Many studies have highlighted that BChE plays a more important role in Alzheimer's disease and selective inhibitors of BChE could be promising drug candidates (Greig *et al.*, 2005; Nordberg *et al.*, 2013).

The most commonly prescribed ChE inhibitors are donepezil, rivastigmine and galantamine. Among these inhibitors however, donepezil is the only ChE inhibitor approved for the treatment of all stages of Alzheimer's disease (Allgaier and Allgaier, 2014; Schneider *et al.*, 2014). Natural plant resources possessing ChE inhibitory activities may potentially improve dementia and other neurodegenerative symptoms (Tundis *et al.*, 2016). Galantamine and rivastigmine are plant-derived alkaloids (Balkrishna *et al.*, 2019). There is also interest in developing new ChE inhibitors from among plant non-alkaloid compounds, such as polyphenols (Jabir *et al.*, 2018; Khan *et al.*, 2018). As such, various plant extracts have been shown to have AChE and/or BChE inhibitory activities, including those from Africa (Adewusi and Steenkamp, 2011), China (Kaufmann *et al.*, 2016), Europe (Ferreira *et al.*, 2006; Wszelaki *et al.*, 2010), India (Kadiyala *et al.*, 2014; Mathew and Subramanian, 2014; Sheeja Malar *et al.*, 2017), Middle East (Orhan *et al.*, 2004; 2008), South America (Nino *et al.*, 2006) and Southeast Asia (Kumaran *et al.*, 2019; Nuria *et al.*, 2020; Tappayuthpijarn *et al.*, 2012).

The oil palm (*Elaeis guineensis*) is a high oil-producing tropical plant. There continues to be increasing evidence showing the potential health benefits of nutraceuticals and phytonutrients derived from the oil palm (Kushairi *et al.*, 2019). The water-soluble part of the oil palm fruit is rich in phenolic acids, including three caffeoylshikimic acid isomers, *p*-hydroxybenzoic acid, protocatechuic acid (Sambanthamurthi *et al.*, 2011) and an indoleacetic acid derivative (Sambanthamurthi *et al.*, 2014), as well as shikimic acid (Sambandan *et al.*, 2011). Termed Water-Soluble Palm Fruit Extract (WSPFE), palm fruit bioactives (PFB), palm fruit juice (PFJ) or oil palm phenolics (OPP), these compounds could be recovered from the aqueous vegetation liquor during the palm oil milling process (Sambanthamurthi *et al.*, 2011). WSPFE has been shown to have potential neuroprotective effects, such as reducing neuroinflammatory factors *in vitro* (Weinberg *et al.*, 2018a), inhibiting beta-amyloid peptide aggregation *in vitro* (Weinberg *et al.*, 2018b), up-regulating genes involved in brain development and activity *in vivo* (Leow *et al.*, 2013) and increasing brain tyrosine hydroxylase levels *in vivo* (Weinberg *et al.*, 2019). As such, we hypothesised that WSPFE might also have possible ChE inhibition effects in the present study.

MATERIALS AND METHODS

Preparation of WSPFE Samples

Liquid WSPFE was obtained from the Malaysian Palm Oil Board (MPOB) Phenolic Antioxidant Pilot Plant in Labu, Negeri Sembilan, Malaysia (Sambanthamurthi *et al.*, 2008). Spray dried (SD) WSPFE was obtained through the spray drying process carried out on liquid WSPFE at Biotropics Malaysia Berhad, Shah Alam, Selangor, Malaysia. Freeze dried (FD) WSPFE was obtained by freeze drying liquid WSPFE at MPOB. WSPFE ethyl acetate fraction (EAF) was obtained by fractionating liquid WSPFE with ethyl acetate, followed by rotary evaporation and freeze drying. The remaining water partition was also collected, followed by rotary evaporation and freeze drying to obtain WSPFE water fraction (WF).

The different WSPFE fractions (F1–F7) were prepared by subjecting WSPFE EAF to preparative HPLC using a Waters Preparative AutoPurification High Performance Liquid Chromatography (HPLC) System (Waters Corporation, Milford, MA, USA). Separation was achieved by using a reverse phase Waters Atlantis C18 5 μm column (Waters Corporation, Milford, MA, USA). A binary gradient system was used as the mobile phase, with phase A comprising distilled water containing 0.02% (v/v) trifluoroacetic acid and phase B comprising 70%:30% (v/v) methanol-acetonitrile. A flow rate of 20 mL min^{-1} and a pressure limit of 2.76×10^4 kPa were used. The gradient elution with a total run time of 55 min was as follows: Started from 100% (v/v) phase A and 0% (v/v) phase B, increased to 32.5% (v/v) phase B over 40 min, then increased to 62.5%

(v/v) phase B over 6 min and finally decreased to 0% (v/v) phase B over 9 min. Seven fractions (F1-F7) as characterised by ultraviolet/visible (UV/VIS) detection at 280 nm UV wavelength were collected based on their retention time.

The total phenolic content of these samples at 5000 μg mL^{-1} was determined in terms of μg mg^{-1} gallic acid equivalent (GAE) by using the Folin-Ciocalteu reagent (Merck, Germany) and an absorbance reading at 765 nm using the U-2800 spectrophotometer (Hitachi, Japan) (Gao *et al.*, 2000). These prepared samples were stored at -20°C until use.

AChE Assays

AChE assays were carried out using the commercial AChE Assay Kit (Fluorometric-Red) (ab138873) (Abcam PLC, Cambridge, United Kingdom), according to manufacturer's instructions. The kit uses AbRed Indicator to quantify the choline produced from the hydrolysis of ACh by AChE through choline oxidase-mediated enzyme coupling reactions. The fluorescence intensity of AbRed Indicator is used to measure the amount of choline formed, which is proportional to the AChE activity and was measured at Ex/Em = 540/590 nm in a kinetic mode of 1-min intervals for 30 min using the Infinite M200 Microplate Reader (Tecan, Switzerland). WSPFE samples were tested at varying concentrations between 0 to 500 μg mL^{-1} to determine the half maximal inhibitory concentration (IC_{50}) values of the samples on AChE. Negative control wells containing the substrate and enzyme without inhibitor samples, positive control wells containing the substrate, enzyme and the positive control inhibitor donepezil hydrochloride (DH) (ab120763) (Abcam PLC, Cambridge, United Kingdom) (Augustin *et al.*, 2020; Sheeja Malar *et al.*, 2017; Suganthy and Devi, 2016), as well as colour control samples which functioned as blanks for the corresponding samples were also prepared in these experiments.

BChE Assays

BChE assays were carried out using the commercial BChE Assay Kit (Colourimetric) (ab241010) (Abcam PLC, Cambridge, United Kingdom), according to manufacturer's instructions. The kit is based on the ability of BChE to hydrolyse a substrate and produce thiocholine. Thiocholine reacts with 5, 5′-dithiobis (2-nitrobenzoic acid) and generates a yellow chromophore that can be quantified at 412 nm. This was measured in a kinetic mode of 1-min intervals for 30 min using the Infinite M200 Microplate Reader (Tecan, Switzerland). WSPFE samples were tested at varying concentrations between 0 to 500 μg mL^{-1} to determine the IC_{50} values of the samples on BChE. Negative control wells containing the substrate and enzyme without inhibitor samples, positive control wells containing the substrate, enzyme and the positive control inhibitor DH (ab120763) (Abcam PLC, Cambridge, United Kingdom), as well as colour control samples which functioned as blanks for the corresponding samples were also prepared in these experiments.

Synergistic Assays Using Binary Mixtures of DH and WSPFE EAF

To determine the potential synergistic effects of DH and WSPFE EAF on the inhibition of AChE and BChE, binary-mixture experiments were performed using the assays described in the previous section. Two sets of experiments were performed, *i.e.*, set A to identify the effects of adding DH on the IC_{50} value of WSPFE EAF, and *vice versa* in set B. For set A, fixed concentrations of DH used were 0.01 μg mL^{-1} and 20 μg mL^{-1} for AChE and BChE enzymatic assays respectively, chosen on the basis of the respective IC_{50} values. WSPFE EAF in varying concentrations between 0 to 500 μg mL^{-1} were used. For set B, fixed concentrations of WSPFE EAF used were 0.2 μg mL^{-1} and 200 μg mL^{-1} for AChE and BChE enzymatic assays respectively, also chosen on the basis of the respective IC_{50} values. DH in varying concentrations between 0 to 500 μg mL^{-1} were used.

Statistical Analyses

Statistical analyses were performed using SPSS Statistics (IBM Corporation, Armonk, New York, USA). Analysis of variance (ANOVA), repeated measures or one-way where appropriate, with Tukey's HSD (honestly significant difference) post-hoc test were performed and differences with p values of less than 0.05 were considered statistically significant. Pearson's correlation analysis was performed to correlate the total phenolic content and ChE inhibition in the WSPFE samples. IC_{50} values were calculated using the Quest Graph™ IC_{50} Calculator (AAT Bioquest, Inc., Sunnyvale, CA, USA) (AAT Bioquest, 2019). AChE Selectivity Index (SI) values were calculated in Microsoft Excel (Microsoft Corporation, Redmond, WA, USA) using the formula: AChE SI = IC_{50} of BChE/IC_{50} of AChE (Zhao *et al.*, 2013).

RESULTS AND DISCUSSION

Cholinergic nerves are a major portion of the central, as well as peripheral parasympathetic and sympathetic nervous systems (Craig *et al.*, 2011). The main pathogenic feature connected with the progression of Alzheimer's disease is the weakening

of the brain cholinergic system. ChE inhibitors are recognised as one of the choices in treating Alzheimer's disease, approved as a therapeutic strategy to reduce symptoms and prevent its progression (Hussein *et al*., 2018).

The neuroprotective effects attributed to plant phenolic compounds could be mediated by their AChE inhibitory activities, in addition to other mechanisms of action, such as antioxidant, anti-inflammatory and anti-amyloid production activities, as well as interactions with brain cell signalling (Nwidu *et al*., 2017; Szwajgier *et al*., 2017; 2018). Among plant phenolic compounds, the pharmacokinetic properties of phenolic acids make them suitable drugs for Alzheimer's disease, owing to their simplicity and structural similarity to popular ChE inhibitors (Szwajgier *et al*., 2018). They are not degraded in the gastrointestinal tract prior to absorption (Rechner *et al*., 2002), easily released from foods in the gastrointestinal tract by bacterial esterases and directly absorbed (Rondini *et al*., 2002), as well as being transformed only to a limited extent (Couteau *et al*., 2001).

The majority of phenolic compounds present in WSPFE are phenolic acids. In the present study, seven preparative liquid chromatographic fractions (F1-F7) of WSPFE were prepared based on information obtained from previous literature on WSPFE (*Figure 1*). F1 contained shikimic acid (Sambandan *et al*., 2011), F3 contained protocatechuic acid (Sambanthamurthi *et al*., 2011), F4 contained *p*-hydroxybenzoic acid (Sambanthamurthi *et al*., 2011), F5 contained an indoleacetic acid derivative (Sambanthamurthi *et al*., 2014), while F6 contained three caffeoylshikimic acid isomers (Sambanthamurthi *et al*., 2011). The components of F2 and F7 are still unknown.

Total phenolic content analysis of these samples at 5000 μg mL^{-1} (*Figure 2*) showed that SD WSPFE had a higher total phenolic content compared to FD WSPFE ($p<0.05$). This was similar to a previous study in which higher chokeberry polyphenol levels were present after drying at high temperatures, compared to after freeze drying (Horszwald *et al*., 2013). SD papaya products also retained higher levels of flavonoids and phenolic compounds compared to

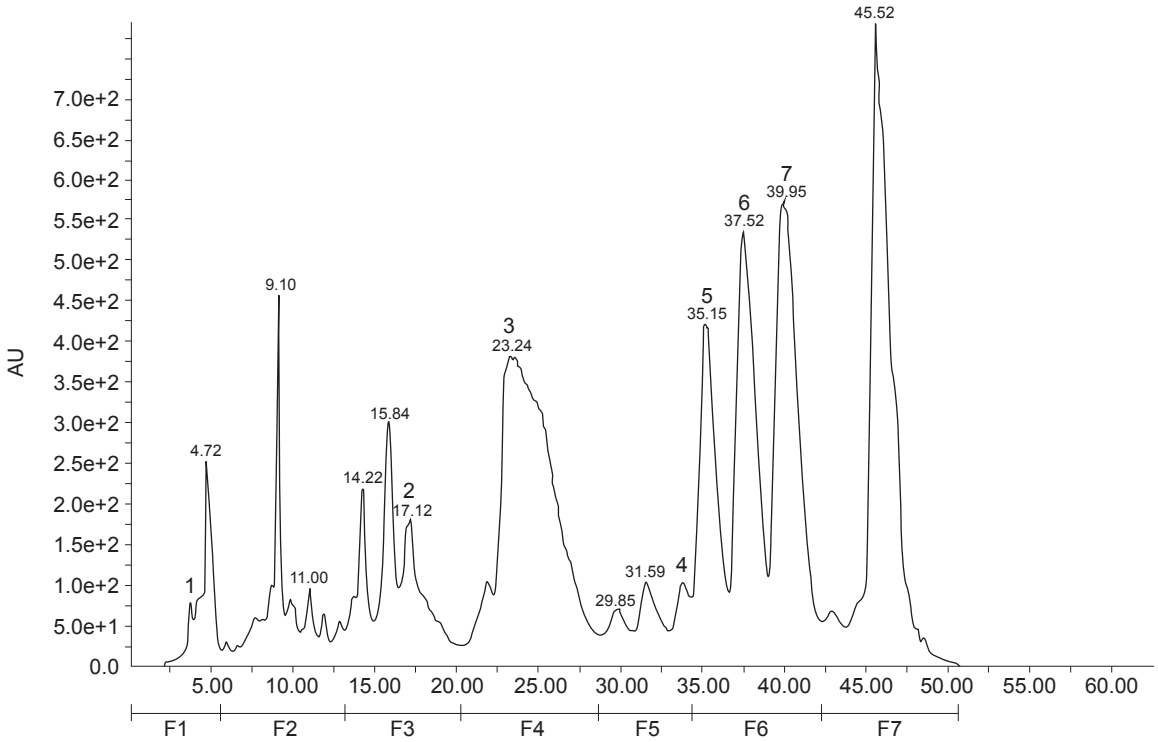

Note: The different Water-Soluble Palm Fruit Extract (WSPFE) fractions (F1–F7) were prepared using a Waters Preparative AutoPurification High Performance Liquid Chromatography (HPLC) System (Waters Corporation, Milford, MA, USA). Stationary phase: Reverse phase Waters Atlantis C18 5 μm column (Waters Corporation, Milford, MA, USA). Mobile phase: Binary gradient system, with phase A comprising distilled water containing 0.02% (v/v) trifluoroacetic acid and phase B comprising 70%:30% (v/v) methanol-acetonitrile. Flow rate: 20 mL min^{-1}. Pressure limit: 2.76×10^4 kPa. Total run time: 55 min. Gradient elution: Started from 100% (v/v) phase A and 0% (v/v) phase B, increased to 32.5% (v/v) phase B over 40 min, then increased to 62.5% (v/v) phase B over 6 min and finally decreased to 0% (v/v) phase B over 9 min. Detection: Ultraviolet/visible (UV/VIS) at 280 nm UV wavelength. Peaks: 1: Shikimic acid; 2: Protocatechuic acid; 3: *p*-hydroxybenzoic acid; 4: Indoleacetic acid derivative; 5: 5-O-caffeoylshikimic acid; 6: 3-O-caffeoylshikimic acid; 7: 4-O-caffeoylshikimic acid.

Figure 1. Preparative liquid chromatogram of WSPFE fractions viewed at 280 nm ultraviolet wavelength.

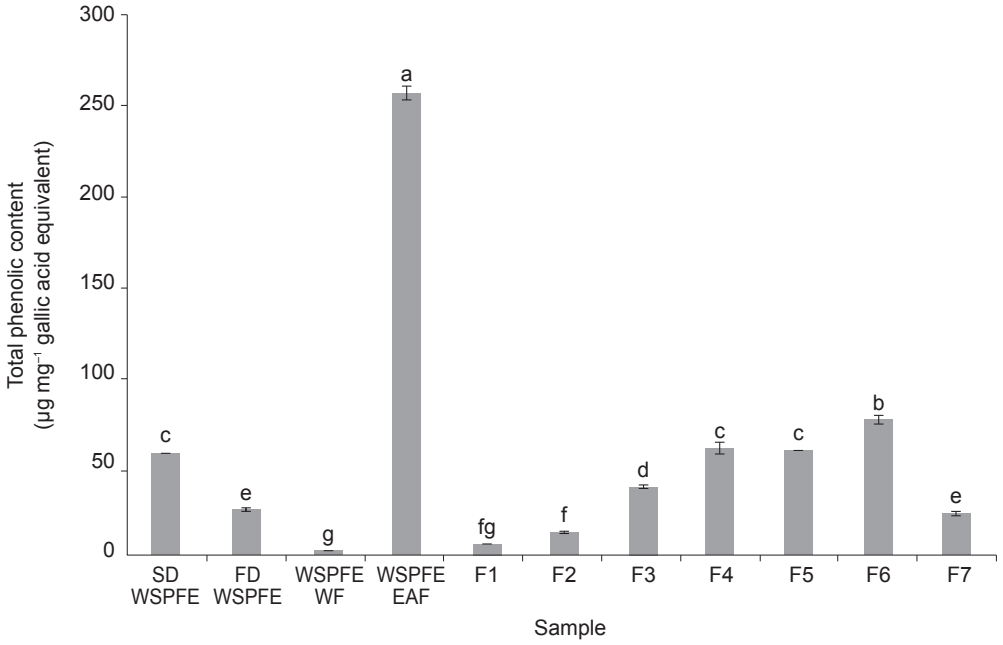

Note: Values are means ± standard error of the mean (SEM) from triplicate determinations. Means with different letters are significantly different (p<0.05) by one-way analysis of variance (ANOVA) with Tukey's honestly significant difference (HSD) *post-hoc* test. WSPFE - Water-Soluble Palm Fruit Extract; EAF - ethyl acetate fraction; WF - water fraction; SD - spray dried; FD - freeze dried.

Figure 2. Total phenolic content of WSPFE samples at 5000 µg mL^{-1}.

FD products (Gomes *et al.*, 2018). Drying is a major food processing operation to increase shelf life. The choice of drying method influences product quality, as it is related to the retention of bioactive compounds and antioxidant activities (Abascal *et al.*, 2005). Freeze drying is a technique based on water removal by sublimation under low pressure and is used to obtain various industrial products (Santo *et al.*, 2013). It makes a product lightweight, prevents yeast and bacteria survival, as well as retains its taste, shape and appearance when water is reintroduced. However, freeze drying equipment is expensive, while the process is very time-consuming and labour-intensive. Conversely, spray drying removes moisture from products by rapid evaporation on spray droplet under high temperature exposure. Spray drying produces a dry powder from a liquid or slurry by rapidly drying with a hot gas in a single processing step. Spray drying is suitable for heat-sensitive materials, despite the high temperatures of the drying gas, owing to the cooling effect of the evaporating solvent which keeps the droplet temperature relatively low (Haggag and Faheem, 2015). The heat and mass transfer occurs in the air with vapour films surrounding the product droplets, which form protective envelopes to keep product particles from approaching the dryer outlet temperature. Spray drying also has high performance due to low residence time of a few seconds (Verma and Singh, 2015).

In the present study, fractionation of liquid WSPFE with ethyl acetate resulted in WSPFE EAF which had the highest total phenolic content among all of the WSPFE samples, with the remaining components in WSPFE WF having the least. WSPFE EAF had a total phenolic content of around 25%. The total phenolic content of the WSPFE fractions increased from F1 to F6, but dipped down in F7, *i.e.*, the total phenolic content of the WSPFE fractions followed the ascending order of F1 < F2 < F7 < F3 < F5 < F4 < F6. Initial comparison of whole WSPFE, *i.e.*, SD WSPFE and FD WSPFE, showed that SD WSPFE had higher AChE and BChE inhibition activities compared to FD WSPFE, while WSPFE EAF had higher AChE and BChE inhibition activities compared to WSPFE WF (*Figure 3*). Although these results appeared to reflect the total phenolic content of the samples, in which samples with higher total phenolic content had higher AChE and BChE inhibition activities, there was weak positive correlation between the total phenolic content of all the WSPFE samples with AChE (R^2=0.527, p>0.05) and BChE (R^2=0.411, p>0.05) inhibition potential, which was in line with previous studies (Elufioye *et al.*, 2019; Zengin *et al.*, 2020). As the fractions used in the present study were not pure compounds, unidentified non-phenolic inhibitors might justify the activities observed. In addition, these findings might be due to the complex nature of these fractions and interactions between phytochemicals present in them.

Further AChE and BChE assays were then carried out using WSPFE samples of varying concentrations between 0 to 500 µg mL^{-1}, alongside

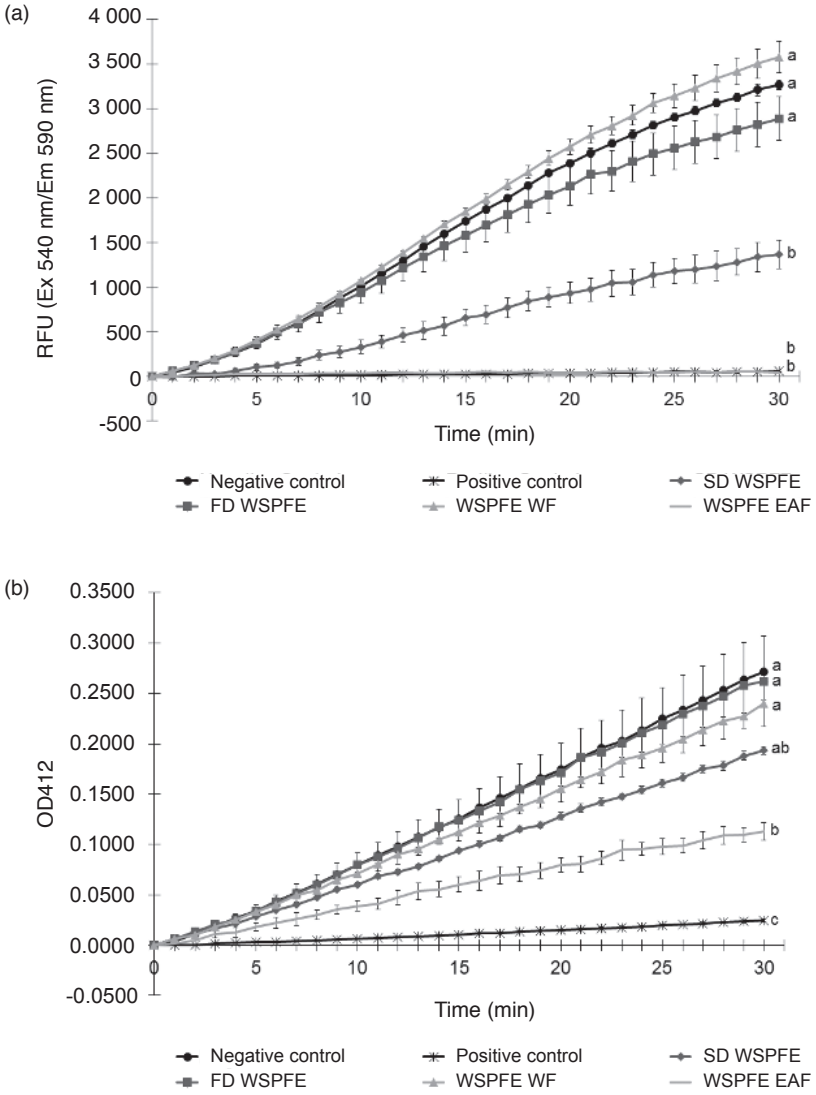

Note: Values are means ± standard error of the mean (SEM) from triplicate determinations. Means with different letters are significantly different (p<0.05) by repeated measures analysis of variance (ANOVA) with Tukey's honestly significant difference (HSD) *post-hoc* test. AChE - acetylcholinesterase; BChE - butyrylcholinesterase; WSPFE - Water-Soluble Palm Fruit Extract; EAF - ethyl acetate fraction; WF - water fraction; SD - spray dried; FD - freeze dried.

Figure 3. Effects of WSPFE samples on (a) AChE at 100 μg mL^{-1}, and (b) BChE at 400 μg mL^{-1}.

the positive control DH, in order to obtain the IC_{50} values on the respective enzymes (*Table 1*). Based on the IC_{50} values determined, the inhibitory effects of WSPFE samples on AChE followed the ascending order of SD WSPFE < F4 < F2 < F3 < F5 < F1 < F6 < F7 < WSPFE EAF. The IC_{50} values of FD WSPFE and WSPFE WF were not achieved as they were higher than the highest concentration tested (500 μg mL^{-1}). For BChE, the inhibitory effects of WSPFE samples on this enzyme were not strong, since the IC_{50} values of several samples, *i.e.*, SD WSPFE, FD WSPFE, WSPFE WF, F2, F6 and F7 were not achieved as they were higher than the highest concentration tested (500 μg mL^{-1}). On the other hand, among the WSPFE samples of which their IC_{50} values were determined, their inhibitory effects on BChE followed the ascending order of F4 < F1 < F5 < F3 < WSPFE EAF. Hence, in both assays, WSPFE EAF showed the highest inhibitory activities (AChE IC_{50}: 0.218 ± 0.029 μg mL^{-1}; BChE IC_{50}: 222.860 ± 5.777 μg mL^{-1}). However, the positive control DH still had lower IC_{50} values (AChE IC_{50}: 0.013 ± 0.001 μg mL^{-1}, BChE IC_{50}: 19.820 ± 1.415 μg mL^{-1}) and hence higher inhibitory potency when compared to WSPFE EAF.

AChE selectivity index (SI) is defined as IC_{50} BChE/IC_{50} AChE ratio, with a higher IC_{50} BChE/IC_{50} AChE ratio indicating a higher selectivity towards AChE rather than BChE. All of the WSPFE samples tested in the present study were found to be more AChE selective. AChE SI values calculated based on IC_{50} values which could be determined indicated that the AChE selectivity of the WSPFE samples followed the ascending order of F4 < F3 < F5 < F1 < WSPFE EAF. The AChE SI value of

WSPFE EAF was 1022.294. This was lower than that of the AChE selective positive control DH, which had the highest AChE SI value of 1524.615. Two of the fractions, F4 and F3, which contained *p*-hydroxybenzoic acid and protocatechuic acid, respectively, had the lowest AChE SI values (7.584 and 9.367, respectively), indicating that these fractions were less AChE selective compared to the other WSPFE samples tested and may thus, function better as dual ChE inhibitors. The samples F5 and F1 which contained an indoleacetic acid derivative and shikimic acid, respectively, had AChE SI values of 27.879 and 38.897, respectively. F6 which contained three caffeoylshikimic acid isomers showed mainly AChE inhibitory properties.

Protocatechuic acid and *p*-hydroxybenzoic acid in particular have been shown to have potential neuroprotective properties (Winter *et al.*, 2017). The amount of *p*-hydroxybenzoic acid present in plant extracts has been shown to be significantly correlated only with BChE inhibition (Kobus-Cisowska *et al.*, 2019a; 2019b). On the other hand, the amount of protocatechuic acid present in plant extracts was significantly correlated with both AChE and BChE inhibition (Kobus-Cisowska *et al.*, 2019b). In the present study however, we found that both fractions containing protocatechuic acid and *p*-hydroxybenzoic acid respectively demonstrated dual ChE inhibitory properties. This discrepancy might be because fractions and not pure compounds were used in the present study. Indoleacetic acid derivatives have been shown to have inhibitory activities against both AChE (Dileep *et al.*, 2013) and BChE (Bodur and Cokugras, 2005) as well. Shikimic acid and caffeoylshikimic acids have not been shown to have ChE inhibitory activities as pure compounds, but plant extracts containing caffeoylshikimic acids and other shikimic acid derivatives possessing these properties have been documented in the literature (Kim *et al.*, 2018; Song *et al.*, 2020).

The possibility to isolate pure lead compounds from crude plant extracts or to administer these as nutraceuticals or cheap alternatives to drugs makes plants a versatile source of natural ChE inhibitors. However, plants produce a variety of secondary metabolites representing a complex mixture of compounds from several chemical classes. The action modes of most plant metabolites cannot be attributed to one single lead chemical compound, but to their pleiotropic effects (Wink, 2015). Hence, synergies within and between chemical groups of different compounds in plant extracts may take place and should thus, be considered (Kaufmann *et al.*, 2016). In the present study, WSPFE EAF which contained all the seven WSPFE fractions had the strongest inhibitory effects on AChE and BChE. This suggests that the seven WSPFE fractions when given together have synergistic inhibitory effects against these enzymes and would work better in attenuating these enzymes compared to giving individual WSPFE fractions.

In order to identify whether WSPFE EAF has potential synergistic effects in inhibiting AChE or BChE when used in combination with DH, we tested binary mixtures of these two compounds in the respective assays (*Table 1*). We found that adding DH to WSPFE EAF (AChE IC_{50}: 0.218 ± 0.029 μg mL^{-1}; BChE IC_{50}: 222.860 ±5.777 μg mL^{-1}) resulted in lower IC_{50} values of WSPFE EAF for both enzymes (AChE IC_{50}: 0.041 ± 0.013 μg mL^{-1}; BChE IC_{50}: 40.127 ± 8.063 μg mL^{-1}), but only the differences for BChE were statistically significant ($p<0.05$). However, the AChE SI values were almost similar (WSPFE EAF: 1022.294; DH + WSPFE EAF doses: 978.707), indicating that BChE/AChE selectivity was maintained. Adding WSPFE EAF to DH (AChE IC_{50}: 0.013 ± 0.001 μg mL^{-1}; BChE IC_{50}: 19.820 ± 1.415 μg mL^{-1}) also resulted in lower IC_{50} values of DH for both enzymes (AChE IC_{50}: 0.008103 ± 0.000174 μg mL^{-1}; BChE IC_{50}: 1.643 ± 0.403 μg mL^{-1}), but these differences were not statistically significant ($p>0.05$). Nevertheless, the AChE SI value was 7.5-fold lower (DH: 1524.615; WSPFE EAF + DH doses: 202.764), indicating that BChE/AChE selectivity was higher.

Hence, although WSPFE EAF by itself had high AChE selectivity, it reduced rather than increased the AChE selectivity of DH. A previous study showed that phenformin with an AChE SI value of 0.052 indicating that it was BChE selective did not alter the AChE SI value of donepezil, whereas a metformin sulphonamide derivative with an AChE SI value of 3.23 increased the AChE SI value of donepezil around 200-fold higher. On the other hand, metformin with an AChE SI value of > 425.53 did not alter the AChE SI value of donepezil either (Markowicz-Piasecka *et al.*, 2018). Many factors may thus, be at work for this apparent discrepancy. The exact mechanism by which synergistic effects could be achieved could only be explained by conducting combination index-isobologram analysis and enzyme kinetic studies (Balkrishna *et al.*, 2019; Huang *et al.*, 2019; Kaufmann *et al.*, 2016). *In silico* molecular docking experiments would also be helpful to identify the molecular mechanistics of AChE and BChE inhibition by the compounds present in WSPFE, as well as the structure-activity relationships of individual compounds with these ChEs (Jang *et al.*, 2018).

A limitation of the present study is that the bioavailability and biotransformation of most of the phenolic compounds in WSPFE and their metabolites are unknown at the moment. This information must be considered and applied, as metabolism is important in defining actual activity. Drugs that cross the blood brain barrier do not have dissociable groups (Tayeb *et al.*, 2012). Increasing

TABLE 1. THE IC_{50} AND SELECTIVITY INDEX (SI) VALUES OF WSPFE SAMPLES AS WELL AS BINARY MIXTURES OF WSPFE EAF AND DH AGAINST AChE AND BChE

Sample	IC_{50} (μg mL^{-1})		AChE SI
	AChE	BChE	
SD WSPFE	110.177 ± 7.141[a]	>500	*
FD WSPFE	>500	>500	*
WSPFE WF	>500	>500	*
WSPFE EAF	0.218 ± 0.029[d]	222.860 ± 5.777[d]	1 022.294
F1	9.903 ± 1.751[cd]	385.193 ± 11.966[ab]	38.897
F2	37.093 ± 7.439[b]	>500	*
F3	33.530 ± 3.131[bc]	314.087 ± 10.251[c]	9.367
F4	53.393 ± 11.972[b]	404.913 ± 12.793[a]	7.584
F5	12.197 ± 2.038[cd]	340.043 ± 24.633[bc]	27.879
F6	3.327 ± 0.052[d]	>500	*
F7	0.645 ± 0.283[d]	>500	*
DH	0.013 ± 0.001[d]	19.820 ± 1.415[e]	1 524.615
DH + WSPFE EAF doses (set A)	0.041 ± 0.013[d]	40.127 ± 8.063[e]	978.707
WSPFE EAF + DH doses (set B)	0.008103 ± 0.000174[d]	1.643 ± 0.403[e]	202.764

Note: The IC_{50} indicates the dose that induced a 50% enzymatic inhibition as compared to negative control (enzyme only) over 30 min. These IC_{50} values were expressed as means ± standard error of the mean (SEM) from triplicate determinations. Means in a column with different letters are significantly different ($p<0.05$) by one-way analysis of variance (ANOVA) with Tukey's honestly significant difference (HSD) *post-hoc* test. >500 indicates IC_{50} was not achieved as it was higher than the highest concentration tested (500 μg mL^{-1}). AChE SI is the AChE selectivity index defined as IC_{50} BChE/ IC_{50} AChE ratio. * indicates AChE SI was not calculated. AChE - acetylcholinesterase; BChE - butyrylcholinesterase; WSPFE - Water-Soluble Palm Fruit Extract; EAF - ethyl acetate fraction; DH - donepezil hydrochloride; WF - water fraction; SD - spray dried; FD - freeze dried.

the availability of ACh at receptors in the brain would result in better neuron to neuron transport. However, the poor ability to cross the blood brain barrier can be an advantage when a compound to regulate the peripheral nervous system is needed (Pohanka, 2014), such as in the treatment of myasthenia gravis (Benatar and Kaminski, 2012) and in post-anaesthesia (Chambers *et al.*, 2010). While direct measurements have not been done to confirm the availability of WSPFE in the brain, a previous study confirmed the increased expression of tyrosine hydroxylase in the brains of Nile rats fed WSPFE (Weinberg *et al.*, 2019). In addition, the bioavailability of two of the components present in WSPFE, *i.e.*, protocatechuic acid and *p*-hydroxybenzoic acid, has been indicated before in the literature. Protocatechuic acid has been found to be the major human plasma metabolite of cyanidin-glucosides following oral consumption of blood orange juice (Vitaglione *et al.*, 2007), while *p*-hydroxybenzoic acid is the major human plasma metabolite of pelargonidin-glucosides following oral consumption of strawberries (Azzini *et al.*, 2010). However, while protocatechuic acid has been found to be present in the brain following oral supplementation in animals (Lin *et al.*, 2011), *p*-hydroxybenzoic acid was not (Margalef *et al.*, 2015). Hence, understanding the bioavailability of WSPFE components in either the central or peripheral nervous system would further help to determine the applications of the ChE inhibition properties of WSPFE samples found in the present study.

CONCLUSION

SD WSPFE had higher AChE and BChE inhibition activities compared to FD WSPFE. WSPFE EAF was found to possess the highest inhibitory activities against these enzymes and the highest AChE selectivity among all the WSPFE samples compared, but these effects were weaker than those of the positive control DH. Fractions containing *p*-hydroxybenzoic acid and protocatechuic acid had the lowest AChE selectivity indices and may thus, function as dual ChE inhibitors. Binary mixtures of DH and WSPFE EAF might have more potent inhibitory effects against these enzymes, as well as higher BChE/AChE selectivity. Further studies, especially *in vivo* ones, to further confirm the *in vitro* results obtained in the present study are warranted.

ACKNOWLEDGEMENT

The authors thank the Director-General of MPOB for permission to publish these results. They also thank the support staff from MPOB who provided technical assistance in various parts of the study, namely Mohamad Daniel Noorazmi for technical assistance in preparing liquid WSPFE, as well as Wan Saridah Wan Omar and Jabariah Md Ali for technical assistance in preparing the FD WSPFE samples and fractions, in addition to carrying out the enzymatic assays. This project was funded by MPOB and the Eleventh Malaysia Plan (RMK-11) PROFENOLIS (2011101805) budget.

REFERENCES

AAT Bioquest (2019). Quest Graph™ IC_{50} calculator. https://www.aatbio.com/tools/ic50-calculator, 19 February 2021.

Abascal, K; Ganora, L and Yarnell, E (2005). The effect of freeze-drying and its implications for botanical medicine: A review. *Phytother. Res., 19(8)*: 655-660.

Adewusi, E A and Steenkamp, V (2011). *In vitro* screening for acetylcholinesterase inhibition and antioxidant activity of medicinal plants from Southern Africa. *Asian Pac. J. Trop. Med., 4(10)*: 829-835.

Allgaier, M and Allgaier, C (2014). An update on drug treatment options of Alzheimer's disease. *Front. Biosci. (Landmark Ed.), 19*: 1345-1354.

Arbel, Y; Shenhar-Tsarfaty, S; Waiskopf, N; Finkelstein, A; Halkin, A; Revivo, M; Berliner, S; Herz, I; Shapira, I; Keren, G; Soreq, H and Banai, S (2014). Decline in serum cholinesterase activities predicts 2-year major adverse cardiac events. *Mol. Med., 20*: 38-45.

Augustin, N; Nuthakki, V K; Abdullaha, M; Hassan, Q P; Gandhi, S G and Bharate, S B (2020). Discovery of helminthosporin, an anthraquinone isolated from *Rumex abyssinicus* Jacq. as a dual cholinesterase inhibitor. *ACS Omega, 5(3)*: 1616-1624.

Azzini, E; Vitaglione, P; Intorre, F; Napolitano, A; Durazzo, A; Foddai, M S; Fumagalli, A; Catasta, G; Rossi, L; Venneria, E; Raguzzini, A; Palomba, L; Fogliano, V and Maiani, G (2010). Bioavailability of strawberry antioxidants in human subjects. *Br. J. Nutr., 104(8)*: 1165-1173.

Balkrishna, A; Pokhrel, S; Tomer, M; Verma, S; Kumar, A; Nain, P; Gupta, A and Varshney, A (2019). Anti-acetylcholinesterase activities of mono-herbal extracts and exhibited synergistic effects of the phytoconstituents: A biochemical and computational study. *Molecules, 24(22):* 4175. DOI: 10.3390/molecules24224175.

Benatar, M and Kaminski, H (2012). Medical and surgical treatment for ocular myasthenia. *Cochrane Database Syst. Rev., 12*: CD005081. DOI: 10.1002/14651858.CD005081.pub3.

Bodur, E and Cokugras, A N (2005). The effects of indole-3-acetic acid on human and horse serum butyrylcholinesterase. *Chem-Biol. Interact., 157-158*: 375-378.

Chambers, D; Paulden, M; Paton, F; Heirs, M; Duffy, S; Craig, D; Hunter, J; Wilson, J; Sculpher, M and Woolacott, N (2010). Sugammadex for the reversal of muscle relaxation in general anaesthesia: A systematic review and economic assessment. *Health Technol. Assess., 14(39)*: 1-211.

Colovic, M B; Krstic, D Z; Lazarevic-Pasti, T D; Bondzic, A M and Vasic, V M (2013). Acetylcholinesterase inhibitors: Pharmacology and toxicology. *Curr. Neuropharmacol., 11(3)*: 315-335.

Couteau, D; Mccartney, A L; Gibson, G R; Williamson, G and Faulds, C B (2001). Isolation and characterization of human colonic bacteria able to hydrolyse chlorogenic acid. *J. Appl. Microbiol., 90(6)*: 873-881.

Craig, L A; Hong, N S and Mcdonald, R J (2011). Revisiting the cholinergic hypothesis in the development of Alzheimer's disease. *Neurosci. Biobehav. Rev., 35(6)*: 1397-1409.

Davies, P and Maloney, A J (1976). Selective loss of central cholinergic neurons in Alzheimer's disease. *Lancet, 2(8000)*: 1403. DOI: 10.1016/s0140-6736(76)91936-x.

Dileep, K V; Remya, C; Tintu, I and Sadasivan, C (2013). Inhibition, ADME and structure based modification of IAA and IBA against acetylcholinesterase: An attempt towards new drug development for Alzheimer's disease. *Front. Life Sci., 7(3-4)*: 164-173.

Eldufani, J and Blaise, G (2019). The role of acetylcholinesterase inhibitors such as neostigmine and rivastigmine on chronic pain and cognitive function in aging: A review of recent clinical applications. *Alzheimers Dement. (N Y), 5*: 175-183.

Elufioye, T O; Chinaka, C G and Oyedeji, A O (2019). Antioxidant and anticholinesterase activities of *Macrosphyra longistyla* (DC) Hiern relevant in the

management of Alzheimer's disease. *Antioxidants (Basel), 8(9)*: 400. DOI: 10.3390/antiox8090400.

Ferreira, A; Proenca, C; Serralheiro, M L and Araujo, M E (2006). The *in vitro* screening for acetylcholinesterase inhibition and antioxidant activity of medicinal plants from Portugal. *J. Ethnopharmacol., 108(1)*: 31-37.

Gao, X; Ohlander, M; Jeppsson, N; Bjork, L and Trajkovski, V (2000). Changes in antioxidant effects and their relationship to phytonutrients in fruits of sea buckthorn (*Hippophae rhamnoides* L.) during maturation. *J. Agric. Food Chem., 48(5)*: 1485-1490.

Garcia-Ayllon, M S; Small, D H; Avila, J and Saez-Valero, J (2011). Revisiting the role of acetylcholinesterase in Alzheimer's disease: Cross-talk with P-tau and beta-amyloid. *Front. Mol. Neurosci., 4*: 22. DOI: 10.3389/fnmol.2011.00022.

Gomes, W F; Franca, F R M; Denadai, M; Andrade, J K S; Da Silva Oliveira, E M; De Brito, E S; Rodrigues, S and Narain, N (2018). Effect of freeze- and spray-drying on physico-chemical characteristics, phenolic compounds and antioxidant activity of papaya pulp. *J. Food Sci. Technol., 55(6)*: 2095-2102.

Greig, N H; Utsuki, T; Ingram, D K; Wang, Y; Pepeu, G; Scali, C; Yu, Q S; Mamczarz, J; Holloway, H W; Giordano, T; Chen, D; Furukawa, K; Sambamurti, K; Brossi, A and Lahiri, D K (2005). Selective butyrylcholinesterase inhibition elevates brain acetylcholine, augments learning and lowers Alzheimer beta-amyloid peptide in rodent. *Proc. Natl. Acad. Sci. USA, 102(47)*: 17213-17218.

Haggag, Y A and Faheem, A M (2015). Evaluation of nano spray drying as a method for drying and formulation of therapeutic peptides and proteins. *Front. Pharmacol., 6*: 140. DOI: 10.3389/fphar.2015.00140.

Horszwald, A; Julien, H and Andlauer, W (2013). Characterisation of *Aronia* powders obtained by different drying processes. *Food Chem., 141(3)*: 2858-2863.

Huang, R Y; Pei, L; Liu, Q; Chen, S; Dou, H; Shu, G; Yuan, Z X; Lin, J; Peng, G; Zhang, W and Fu, H (2019). Isobologram analysis: A comprehensive review of methodology and current research. *Front. Pharmacol., 10*: 1222. DOI: 10.3389/fphar.2019.01222.

Hussein, W; Saglik, B N; Levent, S; Korkut, B; Ilgin, S; Ozkay, Y and Kaplancikli, Z A (2018). Synthesis and biological evaluation of new cholinesterase inhibitors for Alzheimer's disease. *Molecules, 23(8)*: 2033. DOI: 10.3390/molecules23082033.

Jabir, N R; Khan, F R and Tabrez, S (2018). Cholinesterase targeting by polyphenols: A therapeutic approach for the treatment of Alzheimer's disease. *CNS Neurosci. Ther., 24(9)*: 753-762.

Jang, C; Yadav, D K; Subedi, L; Venkatesan, R; Venkanna, A; Afzal, S; Lee, E; Yoo, J; Ji, E; Kim, S Y and Kim, M H (2018). Identification of novel acetylcholinesterase inhibitors designed by pharmacophore-based virtual screening, molecular docking and bioassay. *Sci. Rep., 8(1)*: 14921. DOI: 10.1038/s41598-018-33354-6.

Kadiyala, M; Ponnusankar, S and Elango, K (2014). Screening of siddha medicinal plants for its *in vitro* acetylcholinesterase and butyrylcholinesterase inhibitory activity. *Pharmacogn. Mag., 10(Suppl 2)*: S294-S298.

Kaufmann, D; Kaur Dogra, A; Tahrani, A; Herrmann, F and Wink, M (2016). Extracts from traditional Chinese medicinal plants inhibit acetylcholinesterase, a known Alzheimer's disease target. *Molecules, 21(9)*: 1161. DOI: 10.3390/molecules21091161.

Khan, H; Marya; Amin, S; Kamal, M A and Patel, S (2018). Flavonoids as acetylcholinesterase inhibitors: Current therapeutic standing and future prospects. *Biomed. Pharmacother., 101*: 860-870.

Kim, M S; Lee, D Y; Sung, S H and Jeon, W K (2018). Anti-cholinesterase activities of hydrolysable tannins and polyhydroxytriterpenoid derivatives from *Terminalia chebula* Retz. fruit. *Rec. Nat. Prod., 12(3)*: 284-289.

Kobus-Cisowska, J; Szymanowska-Powalowska, D; Szczepaniak, O; Kmiecik, D; Przeor, M; Gramza-Michalowska, A; Cielecka-Piontek, J; Smuga-Kogut, M and Szulc, P (2019a). Composition and *in vitro* effects of cultivars of *Humulus lupulus* L. Hops on cholinesterase activity and microbial growth. *Nutrients, 11(6)*: 1377. DOI: 10.3390/nu11061377.

Kobus-Cisowska, J; Szymanowska, D; Maciejewska, P; Kmiecik , D; Gramza-Michałowska, A; Kulczyński, B and Cielecka-Piontek, J (2019b). *In vitro* screening for acetylcholinesterase and butyrylcholinesterase inhibition and antimicrobial activity of chia seeds (*Salvia hispanica*). *Electron. J. Biotechnol., 37*: 1-10. DOI: 10.1016/j.ejbt.2018.10.002.

Kumaran, K R; Ahad, M A; Rawa, M S A; Wahab, H and Hassan, Z (2019). Potential Malaysian medicinal plants for the treatment of Alzheimer's disease. *Aust. Herb. Insight, 1(4)*: 22-27.

Kushairi, A; Ong-Abdullah, M; Nambiappan, B; Hishamuddin, E; Bidin, M N I Z; Ghazali, R;

Subramaniam, V; Sundram, S and Parveez, G K A (2019). Oil palm economic performance in Malaysia and R&D progress in 2018. *J. Oil Palm Res., 31(2)*: 165-194.

Leow, S S; Sekaran, S D; Tan, Y A; Sundram, K and Sambanthamurthi, R (2013). Oil palm phenolics confer neuroprotective effects involving cognitive and motor functions in mice. *Nutr. Neurosci., 16(5)*: 207-217.

Lin, C Y; Tsai, S J; Huang, C S and Yin, M C (2011). Antiglycative effects of protocatechuic acid in the kidneys of diabetic mice. *J. Agric. Food Chem., 59(9)*: 5117-5124.

Margalef, M; Pons, Z; Iglesias-Carres, L; Bravo, F I; Muguerza, B and Arola-Arnal, A (2015). Lack of tissue accumulation of grape seed flavanols after daily long-term administration in healthy and cafeteria-diet obese rats. *J. Agric. Food Chem., 63(45)*: 9996-10003.

Markowicz-Piasecka, M; Huttunen, K M and Sikora, J (2018). Metformin and its sulphonamide derivative simultaneously potentiate anti-cholinesterase activity of donepezil and inhibit beta-amyloid aggregation. *J. Enzyme Inhib. Med. Chem., 33(1)*: 1309-1322.

Mathew, M and Subramanian, S (2014). *In vitro* screening for anti-cholinesterase and antioxidant activity of methanolic extracts of ayurvedic medicinal plants used for cognitive disorders. *PLoS ONE, 9(1)*: e86804. DOI: 10.1371/journal.pone.0086804.

Nino, J; Hernandez, J A; Correa, Y M and Mosquera, O M (2006). *In vitro* inhibition of acetylcholinesterase by crude plant extracts from Colombian flora. *Mem. Inst. Oswaldo Cruz, 101(7)*: 783-785.

Nordberg, A; Ballard, C; Bullock, R; Darreh-Shori, T and Somogyi, M (2013). A review of butyrylcholinesterase as a therapeutic target in the treatment of Alzheimer's disease. *Prim. Care Companion CNS Disord., 15(2)*: PCC. 12r01412. DOI: 10.4088/PCC.12r01412.

Nuria, M C; Suganda, A G; Sukandar, E Y and Insanu, M (2020). Acetylcholinesterase: Inhibitory activity of some Indonesian vegetables and fraction of selected plants. *J. Appl. Pharm. Sci., 10(1)*: 101-107.

Nwidu, L L; Elmorsy, E; Thornton, J; Wijamunige, B; Wijesekara, A; Tarbox, R; Warren, A and Carter, W G (2017). Anti-acetylcholinesterase activity and antioxidant properties of extracts and fractions of *Carpolobia lutea. Pharm. Biol., 55(1)*: 1875-1883.

Orhan, I; Sener, B; Choudhary, M I and Khalid, A (2004). Acetylcholinesterase and butyrylcholinesterase inhibitory activity of some Turkish medicinal plants. *J. Ethnopharmacol., 91(1)*: 57-60.

Orhan, I; Aslan, S; Kartal, M; Sener, B and Husnu Can Baser, K (2008). Inhibitory effect of Turkish *Rosmarinus officinalis* L. on acetylcholinesterase and butyrylcholinesterase enzymes. *Food Chem., 108(2)*: 663-668.

Pohanka, M (2011). Cholinesterases, a target of pharmacology and toxicology. *Biomed. Pap. Med. Fac. Univ. Palacky Olomouc Czech Repub., 155(3)*: 219-229.

Pohanka, M (2014). Inhibitors of acetylcholinesterase and butyrylcholinesterase meet immunity. *Int. J. Mol. Sci., 15(6)*: 9809-9825.

Rechner, A R; Kuhnle, G; Bremner, P; Hubbard, G P; Moore, K P and Rice-Evans, C A (2002). The metabolic fate of dietary polyphenols in humans. *Free Radic. Biol. Med., 33(2)*: 220-235.

Rondini, L; Peyrat-Maillard, M N; Marsset-Baglieri, A and Berset, C (2002). Sulfated ferulic acid is the main *in vivo* metabolite found after short-term ingestion of free ferulic acid in rats. *J. Agric. Food Chem., 50(10)*: 3037-3041.

Sambandan, T G; Rha, C K; Sambanthamurthi, R; Sinskey, A J; Tan, Y A; Sundram, K and Wahid, M B (2011). Compositions comprising shikimic acid obtained from oil palm-based materials and method of producing thereof. Malaysian Palm Oil Board. *WIPO Patent Application WO 2011/159144*.

Sambanthamurthi, R; Tan, Y A and Sundram, K (2008). Treatment of vegetation liquors derived from oil-bearing fruit. Malaysian Palm Oil Board. *United States Patent US 7387802 B2*.

Sambanthamurthi, R; Tan, Y A; Sundram, K; Abeywardena, M; Sambandan, T G; Rha, C; Sinskey, A J; Subramaniam, K; Leow, S S; Hayes, K C and Wahid, M B (2011). Oil palm vegetation liquor: A new source of phenolic bioactives. *Br. J. Nutr., 106(11)*: 1655-1663.

Sambanthamurthi, R; Tan, Y A; Omar, W S W; Ali, J M; Sambandan, T G; Yang, M F; Rha, C K and Sinskey, A J (2014). Isolation of a novel bioactive compound obtained from oil palm base materials. Malaysian Palm Oil Board. *WIPO Patent Application WO 2014/209100*.

Santo, E F D E; Lima, L K F D; Torres, A P C; Oliveira, G D and Ponsano, E H G (2013). Comparison between

freeze and spray drying to obtain powder *Rubrivivax gelatinosus* biomass. *Food Sci. Technol., 33*: 47-51.

Scheltens, P; Blennow, K; Breteler, M M; De Strooper, B; Frisoni, G B; Salloway, S and Van Der Flier, W M (2016). Alzheimer's disease. *Lancet, 388(10043)*: 505-517.

Schneider, L S; Mangialasche, F; Andreasen, N; Feldman, H; Giacobini, E; Jones, R; Mantua, V; Mecocci, P; Pani, L; Winblad, B and Kivipelto, M (2014). Clinical trials and late-stage drug development for Alzheimer's disease: An appraisal from 1984 to 2014. *J. Intern. Med., 275(3)*: 251-283.

Sheeja Malar, D; Beema Shafreen, R; Karutha Pandian, S and Pandima Devi, K (2017). Cholinesterase inhibitory, anti-amyloidogenic and neuroprotective effect of the medicinal plant *Grewia tiliaefolia* - An *in vitro* and *in silico* study. *Pharm. Biol., 55(1)*: 381-393.

Song, K; Sivanesan, I; Ak, G; Zengin, G; Cziaky, Z; Jeko, J; Rengasamy, K R; Lee, O N and Kim, D H (2020). Screening of bioactive metabolites and biological activities of calli, shoots, and seedlings of *Mertensia maritima* (L.) Gray. *Plants (Basel), 9(11)*: 1551. DOI: 10.3390/plants9111551.

Srivastava, A and Hunter, J M (2009). Reversal of neuromuscular block. *Br. J. Anaesth., 103(1)*: 115-129.

Suganthy, N and Devi, K P (2016). *In vitro* antioxidant and anti-cholinesterase activities of *Rhizophora mucronata*. *Pharm. Biol., 54(1)*: 118-129.

Szwajgier, D; Borowiec, K and Pustelniak, K (2017). The neuroprotective effects of phenolic acids: Molecular mechanism of action. *Nutrients, 9(5)*: 477. DOI: 10.3390/nu9050477.

Szwajgier, D; Baranowska-Wojcik, E and Borowiec, K (2018). Phenolic acids exert anticholinesterase and cognition-improving effects. *Curr. Alzheimer Res., 15(6)*: 531-543.

Tappayuthpijarn, P; Sattaponpan, C; Sakpakdeecharoen, I and Ittharat, A (2012). Cholinesterase inhibitory and antioxidant activities of Thai traditional remedies potentially used for Alzheimer's disease. *Thai J. East Asian Stud., 17(1)*: 18-25.

Tayeb, H O; Yang, H D; Price, B H and Tarazi, F I (2012). Pharmacotherapies for Alzheimer's disease: Beyond cholinesterase inhibitors. *Pharmacol. Ther., 134(1)*: 8-25.

Tundis, R; Bonesi, M; Menichini, F and Loizzo, M R (2016). Recent knowledge on medicinal plants as source of cholinesterase inhibitors for the treatment of dementia. *Mini Rev. Med. Chem., 16(8)*: 605-618.

Verma, A and Singh, S V (2015). Spray drying of fruit and vegetable juices - A review. *Crit. Rev. Food Sci. Nutr., 55(5)*: 701-719.

Vitaglione, P; Donnarumma, G; Napolitano, A; Galvano, F; Gallo, A; Scalfi, L and Fogliano, V (2007). Protocatechuic acid is the major human metabolite of cyanidin-glucosides. *J. Nutr., 137(9)*: 2043-2048.

Weinberg, R P; Koledova, V V; Schneider, K; Sambandan, T G; Grayson, A; Zeidman, G; Artamonova, A; Sambanthamurthi, R; Fairus, S; Sinskey, A J and Rha, C (2018a). Palm fruit bioactives modulate human astrocyte activity *in vitro* altering the cytokine secretome reducing levels of TNFalpha, RANTES and IP-10. *Sci. Rep., 8(1)*: 16423. DOI: 10.1038/s41598-018-34763-3.

Weinberg, R P; Koledova, V V; Shin, H; Park, J H; Tan, Y A; Sinskey, A J; Sambanthamurthi, R and Rha, C (2018b). Oil palm phenolics inhibit the *in vitro* aggregation of beta-amyloid peptide into oligomeric complexes. *Int. J. Alzheimers Dis., 2018*: 7608038. DOI: 10.1155/2018/7608038.

Weinberg, R P; Koledova, V V; Subramaniam, A; Schneider, K; Artamonova, A; Sambanthamurthi, R; Hayes, K C; Sinskey, A J and Rha, C (2019). Palm fruit bioactives augment expression of tyrosine hydroxylase in the nile grass rat basal ganglia and alter the colonic microbiome. *Sci. Rep., 9(1)*: 18625. DOI: 10.1038/s41598-019-54461-y.

Wink, M (2015). Modes of action of herbal medicines and plant secondary metabolites. *Medicines (Basel), 2(3)*: 251-286.

Winter, A N; Brenner, M C; Punessen, N; Snodgrass, M; Byars, C; Arora, Y and Linseman, D A (2017). Comparison of the neuroprotective and anti-inflammatory effects of the anthocyanin metabolites, protocatechuic acid and 4-hydroxybenzoic acid. *Oxid. Med. Cell Longev., 2017*: 6297080. DOI: 10.1155/2017/6297080.

Wszelaki, N; Kuciun, A and Kiss, A K (2010). Screening of traditional European herbal medicines for acetylcholinesterase and butyrylcholinesterase inhibitory activity. *Acta Pharm., 60(1)*: 119-128.

Zengin, G; Sinan, K I; Mahomoodally, M F; Angeloni, S; Mustafa, A M; Vittori, S; Maggi, F and Caprioli, G (2020). Chemical composition, antioxidant and enzyme inhibitory properties of different extracts obtained from spent coffee ground and coffee silverskin. *Foods, 9(6)*: 713. DOI: 10.3390/foods9060713.

Zhao, T; Ding, K M; Zhang, L; Cheng, X M; Wang, C H and Wang, Z T (2013). Acetylcholinesterase and butryrylcholinesterase inhibitory activities of β-carboline and quinoline alkaloids derivatives from the plants of genus *Peganum*. *J. Chem., 2013*: 717232. DOI: 10.1155/2013/717232.

Journal of Oil Palm Research Vol. 34 (1) March 2022 p. 152-166
DOI: https://doi.org/10.21894/jopr.2021.0032

SYNTHESIS AND PHYSICOCHEMICAL PROPERTIES OF NEW ESTOLIDE ESTERS AS POTENTIAL BIOLUBRICANT BASE OIL

SENG SOI HOONG[1]*; MOHD ZAN ARNIZA[1]; NEK MAT DIN NIK SITI MARIAM[1]; ABU HASSAN NOOR ARMYLISAS[1]; SOOK WAH TANG[1]; TUAN NOOR MAZNEE TUAN ISMAIL[1] and SHOOT KIAN YEONG[1]

ABSTRACT

In this study, plant oil-derived oleic acid was modified chemically to generate estolide esters that displayed low pour points and good oxidation stability. Specifically, oleic acid was reacted with hydrogen peroxide (H_2O_2) to yield estolide with hydroxyl groups, which were then end-capped with various organic acids of different chain lengths and structures, while the carboxylic acid group of estolide was esterified with 2-ethylhexanol (2EH). Analysis results revealed that products end-capped with lauric acid (C12) and 2-ethylhexanoic acid, respectively recorded the best pour point at -36°C, while other products made with shorter or longer chain length organic acids showed higher pour points. Additionally, product end-capped with longer chain length organic acid exhibited better anti-wear properties and lower kinematic viscosity than product made with shorter chain length organic acid. Furthermore, the oxidation stability of products end-capped with linear organic acid were higher than those end-capped with branched organic acids and the oxidation onset temperature (OOT) of products were between 193°C-200°C, which is an improvement in comparison with starting material. Physicochemical properties evaluation revealed that most of the prepared estolides esters have lubricant properties comparable to commercial product, which suggested that they are suitable to be used as base oil for lubricants.

Keywords: epoxidation, esterification, estolide, fatty acids, lubricant.

Received: 25 February 2021; **Accepted:** 23 May 2021; **Published online:** 21 July 2021.

INTRODUCTION

Most of lubricants that we use today are made with non-renewable petrochemicals, which have poor biodegradability and consequently are harmful to the environment. These undesirable traits of petrochemical-based lubricants make them a great threat to the environment because of their disposal and inadvertent release to the environment (Luther, 2007; Nowak *et al*., 2019). As a countermeasure to this problem, some countries have implemented regulations that favour the use of biolubricants such as the 2002 Farm Bill (Farm Security and Rural Investment Act) (Erhan *et al*., 2006), California Senate Bill 916 introduced in 2014 (Abi-Akar, 2017) and a Belgium law that imposes the use of biolubricants in all operations conducted near non-navigable waters (Salimon *et al*., 2010).

Additionally, the German government had supported the use of biolubricants by implementation of 'Market Introduction Program' for biolubricants from year 2001 to 2008, in which financial grants, and technical advices were given to companies that adopted biolubricants (Theissen, 2010). Furthermore, current global consumers and lubricant industry players are shifting towards environment friendly lubricants by adopting biolubricants (Cecilia *et al*., 2020; Reeves *et al*., 2017). All these 'green' demand and initiatives have contributed to steadily increasing production of biolubricants as much as 10% annually (Chan *et al*., 2018). Based on current development trend for lubricant market, the future of biolubricant is very promising.

[1] Malaysian Palm Oil Board,
6 Persiaran Institusi, Bandar Baru Bangi,
43000 Kajang, Selangor, Malaysia.

* *Corresponding author e-mail: sengsoi@mpob.gov.my*

Biolubricants have been made from plant oils and animal fats such as palm oil, soybean oil, rapeseed oil and tallow, which are sustainable and renewable resources. Plant oil-based biolubricants are known to be environmental-friendly because of their excellent biodegradability as compared to petrochemical-based lubricants (Battersby *et al*., 1992; Borugadda and Dalai, 2018; Parveez *et al*., 2020). Additionally, they also offer other beneficial properties such as low volatility, high flash point and high viscosity indices (Sammaiah *et al*., 2016; Santos *et al*., 2004). Furthermore, the polar ester group of plant oil-based biolubricant contributes to good boundary lubrication because of its attraction towards metal surface (Salimon *et al*., 2010) and better solubility for polar contaminant as well as polar additives (Erhan *et al*., 2006).

Nonetheless, plant oil-based biolubricant is not without drawbacks due to its triglycerides molecular structure. One of the main drawbacks is poor oxidation stability mainly because of the alkene group of unsaturated fatty acids that is susceptible to oxidation through free radical mechanism. Consequently, the viscosity of plant oil-based biolubricant will increase over time and form insoluble deposits that shorten the service lifespan of the biolubricant (Nowicki *et al*., 2019; Soni and Agarwal, 2014). Another major weakness of plant oil-based biolubricant is the high melting point attribute of plant oil that translates to high pour point for corresponding biolubricant, which limits its usage in cold climate applications. As such, the plant oil-based biolubricants have high tendency to solidify in winter climate that make them unfavourable to consumer (Kassfeldt and Goran, 1997; Kim *et al*., 2019).

The disadvantages of plant oil-based biolubricant can be resolved by chemical modification of the alkene group of plant oil or its derivatives such as fatty acids and methyl esters. One of the main methods to modify alkene group of unsaturated plant oil derivatives is through epoxidation of alkene with hydrogen peroxide (H_2O_2) and formic acid to generate epoxidised plant oil derivatives (Armylisas *et al*., 2017; Chen *et al*., 2019; Hoong *et al*., 2008). The purified epoxidised plant oil derivatives were then subjected to epoxide-ring opening reaction with various nucleophiles such as fatty acids (Salih *et al*., 2011), alcohols (Salimon *et al*., 2011) and water (Adhvaryu *et al*., 2005; Lv *et al*., 2017) to yield modified plant oil derivatives. Subsequent reactions conducted to convert all functional groups of modified plant oil derivatives to ester functionality, significantly lower the pour point and improved the oxidation stability of plant oil-based biolubricants. Nevertheless, the main drawback of this method is the multi-steps process including purification steps required to produce biolubricants with commercially acceptable properties, which contribute to high production cost that may not be economically attractive to consumer.

Alternatively, the properties of plant oil-based lubricants can be improved through a simpler method known as transesterification, in which plant oils can be reacted with various polyhydric alcohols to generate polyol esters that exhibited improved lubricant properties. For example, Heikel *et al*. (2017) reported a two-steps synthesis of trimethylolpropane (TMP) esters from palm oil and jatropha oil. Both plant oils were first converted to methyl esters through transesterification with methanol and subsequently the methyl esters were further transesterified with TMP to yield TMP esters that exhibited improved cold flow properties in comparison with starting materials. Additionally, the prepared TMP esters also showed better viscosity indices and improved flash points. However, the prepared TMP esters still contain alkene groups that are prone to oxidation degradation, which could reduce the service life of the lubricants. Hence, it is beneficial to make biolubricants with minimal amount of alkene group and simultaneously display good cold flow properties.

Another renowned approach to improve the lubricant properties of plant oil-based lubricant is through formation of estolide from unsaturated fatty acids that generally show good cold flow properties with minimal alkene group in resultant biolubricants (Chen *et al*., 2020). Estolide is formed when the carboxylic acid group of a fatty acid reacts with the alkene group of another unsaturated fatty acid to form an ester linkage between the two fatty acids, in which the reaction requires the use of strong acids such as perchloric acid as the catalyst (Cermak and Isbell, 2001). Further reaction of the estolide with a branched alcohol afforded estolide ester that achieved desirable low pour point (Cermak and Isbell, 2003a; 2003b; Cermak *et al*., 2015). Nonetheless, the disadvantage of this approach is the need to use corrosive and hazardous perchloric acid that is known to form explosive mixture, which poses significant threats to human and the environment (Everett and Graf, 1971). Therefore, an alternative method to make estolide without the use of perchloric acid would be a way forward.

An alternative method to make estolide is through esterification of hydroxy fatty acid such as ricinoleic acid with other fatty acids (Salih *et al*., 2013) or diacids (Sammaiah *et al*., 2016). Similarly, the prepared estolide esters originated from hydroxy fatty acids displayed excellent cold flow properties and good thermal oxidation stability. Nonetheless, the main drawback of this approach is that the prepared estolides still contain significant amount of alkene groups that require further chemical modification in order to improve the oxidation stability of the prepared estolides, which will incur

higher production cost that may hinder commercial acceptance (Cermak *et al*., 2006; Greco-Duarte *et al*., 2019). Additionally, global production of hydroxy fatty acids is substantially less than commodity fatty acid and the cost of hydroxy fatty acid is significantly higher than commodity fatty acid such as oleic acid (Mubofu, 2016), which makes hydroxy fatty acid less attractive to be used as raw material for estolide-based biolubricant.

After taking into consideration the advantages and weaknesses of disclosed methods for chemical modification of plant oils and fatty esters, we have reported a direct one-pot method to synthesis polyhydroxy estolide (PE) from oleic acid (Hoong *et al*., 2017). The reported method did not require the use of purified epoxidised methyl esters or hydroxy fatty acids as starting material, which simplify the process to produce estolides. The process also did not use hazardous perchloric acid as catalyst, instead it used only H_2O_2 as the reactant. Additionally, the prepared PE had minimal alkene group that imparted good oxidation stability to lubricant made from it. Nevertheless, the prepared PE has multiple hydroxyl groups that need to be converted to ester group in order to further enhance its oxidation stability and low temperature properties.

A thorough search of relevant literature revealed that no previous study has investigated the structure-properties relationship between organic acids employed to end-cap the hydroxyl groups of PE and the physicochemical properties of the resultant estolide esters. Therefore, the objective of this study is to prepare various organic acids end-capped PE and their respective 2-ethylhexyl estolide esters. Another objective is to examine the structure-properties relationship between the end-capping organic acids and the physicochemical properties of the prepared estolide esters. The findings of this study will help to establish the aptness of estolide esters made from organic acids end-capped PE as lubricant base oil.

MATERIALS AND METHODS

Materials

Oleic acid (75%, PALMAC 750) was kindly provided by IOI Oleochemical Industries Bhd. (Pulau Pinang, Malaysia). H_2O_2 (50% in H_2O), acetic anhydride (99%), isovaleric acid (bC5) (98%), hexanoic acid (C6) (98%), octanoic acid (C8) (99%), lauric acid (C12) (98%), stearic acid (C18) (95%), 2-ethylhexanoic acid (bC8) (99%) and 2-ethylhexanol (2EH) (99%) were purchased from Sigma Aldrich (St. Louis, MO, USA). Pentaerythritol tetraoleate was obtained from commercial sources. All chemicals were used as received without further purification.

Characterisation and Procedures

Fourier-transform infrared spectroscopy (FTIR) spectra of products were recorded neat on a Perkin-Elmer FTIR Spectrum 100 with 16 scans per sample at 4 cm^{-1} resolution in the range of 650-4000 cm^{-1}.

Proton (^1H) and carbon (^{13}C) nuclear magnetic resonance (NMR) spectroscopy were recorded using JOEL JNM-ECZ600R at 600 MHz and 150 MHz, respectively. Sample (10 mg mL^{-1}) was prepared with deuterated chloroform.

Gel permeation chromatography (GPC) was carried out using Polymer Laboratories PL-GPC 50 Plus integrated GPC system furnished with differential refractive index (DRI)/viscometer detectors. Sample (2 mg mL^{-1}) was dissolved in tetrahydrofuran (THF) and was analysed through a set of Phenogel columns with molecular weight in the range of 10^2–10^6 Da. Sample was eluted in THF at a flow rate of 1 mL min^{-1}. The GPC was calibrated using polystyrene standards with range from 162 to $1x10^5$ Da.

Wet chemistry analysis was conducted in accordance with American Oil Chemists' Society (AOCS) methods: Acid value (AV) Te 2a-64; Hydroxyl value (OHV) Cd 13-60; Iodine value (IV) Cd 1d-92; Oxirane oxygen content (OOC) Cd 9-57.

Kinematic viscosity measurement was carried out according to ASTM D445 in calibrated Ubbellohde tubes submerged in a Normalab NVB Classic viscosity bath. Viscosity index (VI) was calculated in accordance with American Society for Testing and Materials (ASTM) - ASTM D2270-93.

Pour point of sample was recorded using a Normalab CPP Classic test cabinet with integrated cooling system in accordance with ASTM D97.

The oxidation onset temperature (OOT) of sample was determined using DSC Q20P thermal analyser (TA Instruments) in accordance with ASTM E2009.

The anti-wear property of sample was assessed through wear scar diameter (WSD) test in accordance with ASTM 4172 (Four-ball method) by using a TR-30L four-ball equipment (DUCOM Instrument). Steel balls were acquired from SKF Malaysia Sdn. Bhd.

Synthesis of PE from Oleic Acid

Oleic acid (300 g, 1.06 mole) and H_2O_2 (50% in H_2O) (360 g, 5.3 mole) were weighed into a 1 L three-neck round bottom flask equipped with a condenser, thermometer and magnetic stirrer. The mixture was stirred (500 rpm) and heated at 80°C for 24 hr. Then, reaction mixture was poured into a separating funnel and left to separate. Next, the aqueous layer was discharged from the organic layer. Subsequently, ethyl acetate (200 mL) and water (200 mL) were added to the organic layer.

Again, the aqueous layer was discharged from the separating funnel. The organic layer was washed with more water (2 x 200 mL). The organic layer was dried with anhydrous magnesium sulphate ($MgSO_4$) and ethyl acetate was removed to yield a viscous colourless liquid labelled as PE (321 g, 76% yield). v_{max}/cm^{-1} 3440 (OH) 2924, 2854 (C-H) 1733, 1708 (C=O) 1465 (C-H) 1241, 1176 (C-O) 723 (CH_2); ^1H NMR (600 MHz, $CDCl_3$): δ_H=4.80-4.76 (1H, m, HCOC=O), 3.57-3.52 (1H, m, HCO) 3.39-3.34 (2H, m, HCO), 2.29 (4H, t, *J*=7.5 Hz, O=CCH$_2$CH$_2$), 1.62-1.53 (4H, m, O=CCH$_2$CH$_2$), 1.46-1.32 (8H, m, CH$_2$COH), 1.33-1.17 (40H, m, CH$_2$CH$_2$), 0.84 (6H, t, *J*=7.0 Hz, CH$_2$CH$_3$); ^{13}C NMR (150 MHz $CDCl_3$): δ_C=179.0, 174.0 (C=O), 76.3 (HCOC=O), 74.6, 72.5 (HC-O), 34.5 (O=CCH$_2$), 25.1 (O=CCH$_2$CH$_2$), 31.9, 29.4, 24.7, 22.7 (CH$_2$CH$_2$), 14.2 (CH$_2$CH$_3$).

Synthesis of Acetylated Estolide (C2E)

PE (230 g, 0.70 mole of OH, OHV=170 mg KOH g^{-1}), acetic anhydride (60 g, 0.59 mole) and xylene (60 mL) were charged into a 500 mL round bottom flask equipped with a Dean-Stark apparatus and magnetic stirrer. The mixture was stirred (300 rpm) and heated to 150°C for 16 hr. Thereafter, excess acetic anhydride and xylene were distilled from the reaction product at 140°C under vacuum of 20 mbar. The product was left to cool to room temperature and chloroform (200 mL) was added to the product. The diluted product was dried with anhydrous $MgSO_4$ and chloroform was removed to yield a viscous yellowish liquid labelled as C2E (229 g, 97% yield). v_{max}/cm^{-1} 2925, 2855 (C-H) 1736, 1709 (C=O) 1464 (CH_2) 1372 (CH_3) 1235, 1167 (C-O) 723 (CH_2); ^1H NMR (600 MHz, $CDCl_3$): δ_H=4.97-4.92 (2H, m, HCOC=O), 2.3-2.2 (4H, m, O=CCH$_2$), 2.02 (3H, s, O=CCH$_3$), 1.6-1.52 (4H, m, O=CCH$_2$CH$_2$), 1.47-1.41 (4H, m, CH$_2$CHO), 1.32-1.14 (44H, m, CH$_2$CH$_2$), 0.81 (6H, t, *J*=6.9 Hz, CH$_2$CH$_3$); ^{13}C NMR (150 MHz $CDCl_3$): δ_C=179.6, 173.4, 170.7 (C=O), 73.9, 73.5 (HCOC=O), 34.3, 34.1 (O=CCH$_2$), 25.1 (O=CCH$_2$CH$_2$), 31.8, 29.7, 29.4, 29.2, 25.2 24.6, 20.9 (CH$_2$CH$_2$), 22.6 (O=CCH$_3$), 14.1 (CH$_2$CH$_3$).

General Procedure for Synthesis of Organic Acid-capped Estolide (OAE)

Synthesis of isovaleric acid-capped estolide (bC5E) as an example. PE (250 g, 0.76 mole of OH, OHV=170 mg KOH g^{-1}), bC5 (102 g, 1 mole) were charged into a 500 mL round bottom flask equipped with a Dean-Stark apparatus and magnetic stirrer. The mixture was stirred (300 rpm) and heated to 210°C for 8 hr. Thereafter, excess bC5 was removed from the reaction product at 200°C under vacuum of 20 mbar. The product was left to cool to room temperature and chloroform (200 mL) was added to the product. The diluted product was dried with anhydrous $MgSO_4$ and chloroform was removed to yield a viscous yellowish liquid labelled as bC5E (298 g, 95% yield). v_{max}/cm^{-1} 2925, 2855 (C-H) 1735, 1709 (C=O) 1465 (CH_2) 1371 (CH_3) 1240, 1166 (C-O) 723 (CH_2); ^1H NMR (600 MHz, $CDCl_3$): δ_H=4.99-4.91 (2H, m, HCOC=O), 2.31-2.26 (2H, m, O=CCH$_2$), 2.25-2.20 (2H, m, O=CCH$_2$), 2.18-2.11 (2H, m, O=CCH$_2$), 2.08-2.01 (1H, m, (CH$_3$)$_2$CH), 1.62-1.53 (6H, m, O=CCH$_2$CH$_2$), 1.52-1.42 (4H, m, CH$_2$CHO), 1.32-1.16 (44H, m, CH$_2$CH$_2$), 0.93-0.90 (6H, m, CH$_3$CH) 0.83 (6H, t, *J*=6.0 Hz, CH$_2$CH$_3$); ^{13}C NMR (150 MHz $CDCl_3$): δ_C=179.7, 173.5, 172.8 (C=O), 74.1, 73.5 (HCOC=O), 43.6 (O=CCH$_2$), 34.5, 34.0 (O=CCH$_2$), 25.7 (O=CCH$_2$CH$_2$), 31.9, 29.7, 29.4, 29.2, 25.5, 25.1, 24.6 (CH$_2$CH$_2$), 22.7, 22.4 (CHCH$_3$), 14.1 (CH$_2$CH$_3$).

Synthesis of hexanoic acid-capped estolide (C6E). The experiment was conducted according to the general procedure for synthesis of OAE. PE (250 g, 0.76 mole of OH, OHV=170 mg KOH g^{-1}), C6 (116 g, 1 mole), viscous yellowish liquid labelled as C6E (274 g, 97% yield). v_{max}/cm^{-1} 2925, 2855 (C-H) 1735, 1709 (C=O) 1465 (CH_2) 1377 (CH_3) 1242, 1166 (C-O) 756 (CH_2); ^1H NMR (600 MHz, $CDCl_3$): δ_H=5.01-4.91 (2H, m, HCOC=O), 2.34-2.28 (2H, m, O=CCH$_2$), 2.28-2.20 (4H, m, O=CCH$_2$), 1.64-1.55 (6H, m, O=CCH$_2$CH$_2$), 1.51-1.43 (4H, m, CH$_2$CHO), 1.35-1.17 (48H, m, CH$_2$CH$_2$), 0.89-0.83 (9H, m, CH$_3$CH); ^{13}C NMR (150 MHz $CDCl_3$): δ_C=179.8, 173.5 (C=O), 74.0, 73.6 (HCOC=O), 34.4, 34.0 (O=CCH$_2$), 25.5 (O=CCH$_2$CH$_2$), 31.9, 31.4, 29.7, 29.4, 29.2, 25.2, 24.8, 22.7, 22.4 (CH$_2$CH$_2$), 14.1, 13.9 (CH$_2$CH$_3$).

Synthesis of octanoic acid-capped estolide (C8E). The experiment was conducted according to the general procedure for synthesis of OAE. PE (200 g, 0.61 mole of OH, OHV=170 mg KOH g^{-1}), C8 (100 g, 0.69 mole), viscous yellowish liquid labelled as octanoic acid-capped estolide (C8E) (239 g, 98% yield). v_{max}/cm^{-1} 2923, 2854 (C-H) 1735, 1708 (C=O) 1464 (CH_2) 1377 (CH_3) 1162 (C-O) 723 (CH_2); ^1H NMR (600 MHz, $CDCl_3$): δ_H=4.94-4.86 (2H, m, HCOC=O), 2.27-2.20 (2H, m, O=CCH$_2$), 2.20-2.14 (4H, m, O=CCH$_2$), 1.58-1.47 (6H, m, O=CCH$_2$CH$_2$), 1.45-1.36 (4H, m, CH$_2$CHO), 1.29-1.09 (52H, m, CH$_2$CH$_2$), 0.81-0.74 (9H, m, CH$_3$CH); ^{13}C NMR (150 MHz $CDCl_3$): δ_C=179.4, 173.3 (C=O), 73.8, 73.5 (HCOC=O), 34.4, 33.9 (O=CCH$_2$), 25.1 (O=CCH$_2$CH$_2$), 31.8, 31.6, 29.7, 29.4, 29.2, 25.2, 24.6, 22.7, 22.6 (CH$_2$CH$_2$), 14.1 (CH$_2$CH$_3$).

Synthesis of 2-ethylhexanoic acid-capped estolide (bC8E). The experiment was conducted according to the general procedure for synthesis of OAE. PE (200 g, 0.61 mole of OH, OHV=170 mg KOH g^{-1}), 2-ethylhexanoic acid (100 g, 0.69 mole), viscous yellowish liquid labelled as 2-ethylhexanoic acid-capped estolide (bC8E) (235 g, 97% yield).

v_{max}/cm^{-1} 2925, 2855 (C-H) 1733, 1709 (C=O) 1460 (CH_2) 1377 (CH_3) 1167 (C-O) 724 (CH_2); ^{1}H NMR (600 MHz, $CDCl_3$): δ_H=5.05-4.88 (2H, m, HCOC=O), 2.33-2.29 (2H, m, O=CCH$_2$), 2.28-2.17 (4H, m, O=CCH$_2$), 1.63-1.53 (8H, m, O=CCH$_2$CH$_2$), 1.53-1.41 (4H, m, CH$_2$CHO), 1.29-1.09 (44H, m, CH$_2$CH$_2$), 0.91-0.82 (12H, m, CH$_3$CH); ^{13}C NMR (150 MHz $CDCl_3$): δ_C=179.7, 175.9, 173.5 (C=O), 74.0, 73.5 (HCOC=O), 44.7 (HCC=O), 34.5, 34.1 (O=CCH$_2$), 25.6, 25.1 (O=CCH$_2$CH$_2$), 31.9, 31.7, 29.7, 29.5, 29.2, 25.0, 24.6, 22.7, 22.6 (CH$_2$CH$_2$), 14.1, 11.9 (CH$_2$CH$_3$).

Synthesis of lauric acid-capped estolide (C12E). The experiment was conducted according to the general procedure for synthesis of OAE. PE (200 g, 0.61 mole of OH, OHV=170 mg KOH g^{-1}), C12 (120 g, 0.6 mole), viscous yellowish liquid labelled as lauric acid-C12E (247 g, 96% yield). v_{max}/cm^{-1} 2923, 2854 (C-H) 1737, 1709 (C=O) 1465 (CH_2) 1377 (CH_3) 1235, 1166 (C-O), 723 (CH_2); ^{1}H NMR (600 MHz, $CDCl_3$): δ_H=5.01-4.92 (2H, m, HCOC=O), 2.32-2.29 (2H, m, O=CCH$_2$), 2.28-2.21 (4H, m, O=CCH$_2$), 1.63-1.54 (6H, m, O=CCH$_2$CH$_2$), 1.52-1.43 (4H, m, CH$_2$CHO), 1.33-1.16 (54H, m, CH$_2$CH$_2$), 0.86-0.82 (9H, m, CH$_3$CH); ^{13}C NMR (150 MHz $CDCl_3$): δ_C=180.0, 173.5 (C=O), 74.0, 73.6 (HCOC=O), 34.5, 34.1 (O=CCH$_2$), 24.7 (O=CCH$_2$CH$_2$), 31.9, 29.6, 29.4, 29.2, 25.6, 25.0, 22.7 (CH$_2$CH$_2$), 14.1 (CH$_2$CH$_3$).

Synthesis of stearic acid-capped estolide (C18E). The experiment was conducted according to the general procedure for synthesis of OAE. PE (200 g, 0.61 mole of OH, OHV=170 mg KOH g^{-1}), C18 (100 g, 0.35 mole), viscous yellowish liquid labelled as stearic acid-capped estolide (C18E) (285 g, 98% yield). v_{max}/cm^{-1} 2917, 2850 (C-H) 1736, 1707 (C=O) 1464 (CH_2) 1371 (CH_3) 1234, 1166 (C-O) 721 (CH_2); ^{1}H NMR (600 MHz, $CDCl_3$): δ_H=5.02-4.95 (2H, m, HCOC=O), 2.35-2.31 (2H, m, O=CCH$_2$), 2.31-2.23 (4H, m, O=CCH$_2$), 1.65-1.57 (6H, m, O=CCH$_2$CH$_2$), 1.53-1.45 (4H, m, CH$_2$CHO), 1.36-1.21 (66H, m, CH$_2$CH$_2$), 0.87 (9H, t, CH$_3$CH); ^{13}C NMR (150 MHz $CDCl_3$): δ_C=180.1, 173.6 (C=O), 74.1, 73.7 (HCOC=O), 34.5, 34.1 (O=CCH$_2$), 25.2 (O=CCH$_2$CH$_2$), 32.0, 29.8, 29.5, 29.3, 25.6, 24.8, 22.8 (CH$_2$CH$_2$), 14.2 (CH$_2$CH$_3$).

General Procedure for Synthesis of 2-ethylhexyl Ester of OAE

Synthesis of 2-ethylhexyl ester of octanoic acid-capped estolide (2EH-C8E). Octanoic acid-capped estolide (C8E) (182 g, 0.32 mole of CO_2H, AV = 100 mg KOH g^{-1}) and 2EH (102 g, 0.78 mole) were weighed into a reaction flask connected to a Dean-Stark apparatus. The mixture was stirred (300 rpm) and heated at 210°C for 8 hr. Thereafter, the excess 2EH was removed through distillation at 210°C under 10 mbar vacuum. The product was diluted with 200 mL chloroform and dried with anhydrous $MgSO_4$. Then, solvent was removed to yield a yellowish liquid known as 2-ethylhexyl ester of octanoic acid-capped estolide (2EH-C8E) (215 g, 98% yield). v_{max}/cm^{-1} 2924, 2855 (C-H) 1735 (C=O) 1463 (CH_2) 1378 (CH_3) 1244, 1165 (C-O) 723 (CH_2); ^{1}H NMR (600 MHz, $CDCl_3$): δ_H= 4.97-4.87 (2H, m, HCOC=O), 3.95-3.88 (2H, m, H$_2$COC=O), 2.29-2.16 (6H, m, O=CCH$_2$), 1.59-1.51 (6H, m, O=CCH$_2$CH$_2$), 1.51-1.46 (1H, m, CHCHO), 1.46-1.40 (4H, m, CH$_2$CHO), 1.33-1.10 (60H, m, CH$_2$CH$_2$), 0.85-0.76 (15H, m, CH$_3$CH); ^{13}C NMR (150 MHz $CDCl_3$): δ_C=173.9, 173.2 (C=O), 73.9, 73.5 (HCOC=O), 66.5 (H$_2$COC=O) 38.8 (HCCH$_2$O) 34.4, 34.3 (O=CCH$_2$), 25.5 (O=CCH$_2$CH$_2$), 31.8, 31.7, 30.4, 29.7, 29.4, 29.3, 28.9, 25.0, 23.8, 22.9, 22.7 (CH$_2$CH$_2$), 14.1, 10.9 (CH$_2$CH$_3$).

Synthesis of 2-ethylhexyl ester of acetic acid-capped estolide (2EH-C2E). The experiment was conducted according to the general procedure for synthesis of 2-ethylhexyl ester of OAE. Acetic acid-capped estolide (C2E) (195 g, 0.27 mole of CO_2H, AV=80 mg KOH g^{-1}) and 2EH (75 g, 0.57 mole). A yellowish liquid known as 2-ethylhexyl ester of acetic acid-capped estolide (2EH-C2E) (224 g, 98% yield). v_{max}/cm^{-1} 2925, 2855 (C-H) 1735 (C=O) 1463 (CH_2) 1373 (CH_3) 1234, 1169 (C-O) 724 (CH_2); ^{1}H NMR (600 MHz, $CDCl_3$): δ_H=4.95-4.87 (2H, m, HCOC=O), 3.93-3.85 (2H, m, H$_2$COC=O), 2.26-2.15 (4H, m, O=CCH$_2$), 1.97 (3H, s, O=CCH$_3$) 1.56-1.49 (4H, m, O=CCH$_2$CH$_2$), 1.49-1.44 (1H, m, CHCHO), 1.43-1.37 (4H, m, CH$_2$CHO), 1.33-1.10 (52H, m, CH$_2$CH$_2$), 0.84-0.73 (12H, m, CH$_3$CH); ^{13}C NMR (150 MHz $CDCl_3$): δ_C=173.9, 173.2, 170.4 (C=O), 73.8, 73.4 (HCOC=O), 66.5 (H$_2$COC=O) 38.7 (HCCH$_2$O) 34.3 (O=CCH$_2$), 25.4 (O=CCH$_2$CH$_2$), 31.8, 30.4, 29.6, 29.3, 28.9, 25.0, 23.8, 22.9, 22.6 (CH$_2$CH$_2$), 20.9 (H$_3$CC=O) 14.1 (CH$_2$CH$_3$).

Synthesis of 2-ethylhexyl ester of isovaleric acid-capped estolide (2EH-bC5E). The experiment was conducted according to the general procedure for synthesis of 2-ethylhexyl ester of OAE. bC5E (200 g, 0.31 mole of CO_2H, AV=86 mg KOH g^{-1}) and 2EH (120 g, 0.92 mole). A yellowish liquid known as 2EH-bC5E (224 g, 96% yield). v_{max}/cm^{-1} 2925, 2855 (C-H) 1735 (C=O) 1464 (CH_2) 1370 (CH_3) 1245, 1167 (C-O) 724 (CH_2); ^{1}H NMR (600 MHz, $CDCl_3$): δ_H=4.99-4.90 (2H, m, HCOC=O), 3.97-3.90 (2H, m, H$_2$COC=O), 2.29-2.20 (4H, m, O=CCH$_2$), 2.19-2.11 (2H, m, O=CCH$_2$), 2.10-2.01 (1H, m, (CH$_3$)$_2$CH), 1.61-1.54 (4H, m, O=CCH$_2$CH$_2$), 1.53-1.49 (1H, m, CHCHO), 1.49-1.42 (4H, m, CH$_2$CHO), 1.37-1.15 (52H, m, CH$_2$CH$_2$), 0.94-0.89 (6H, m, HCCH$_3$), 0.88-0.80 (12H, m, CH$_3$CH); ^{13}C NMR (150 MHz $CDCl_3$): δ_C=173.9, 173.3, 172.6 (C=O), 74.0, 73.8 (HCOC=O), 66.6 (H$_2$COC=O) 43.6 (O=CCH$_2$), 38.8 (HCCH$_2$O), 34.5, 34.4 (O=CCH$_2$), 25.7

($O=CCH_2\underline{C}H_2$), 31.8, 30.5, 29.7, 29.4, 29.2, 28.9, 25.0, 23.8, 23.0 ($CH_2\underline{C}H_2$), 22.7, 22.4 ($CH\underline{C}H_3$), 14.1, 11.0 ($CH_2\underline{C}H_3$).

Synthesis of 2-ethylhexyl ester of hexanoic acid-capped estolide (2EH-C6E). The experiment was conducted according to the general procedure for synthesis of 2-ethylhexyl ester of OAE. C6E (200 g, 0.32 mole of CO_2H, AV=90 mg KOH g^{-1}) and 2EH (100 g, 0.77 mole). A yellowish liquid known as 2-ethylhexyl ester of hexanoic acid-capped estolide (2EH-C6E) (232 g, 98% yield). v_{max}/cm^{-1} 2925, 2856 (C-H) 1734 (C=O) 1463 (CH_2) 1378 (CH_3) 1242, 1168 (C-O) 725 (CH_2); ^1H NMR (600 MHz, $CDCl_3$): δ_H=4.99-4.90 (2H, m, $\underline{H}COC=O$), 3.98-3.91 (2H, m, $\underline{H}_2COC=O$), 2.32-2.21 (6H, m, $O=C\underline{C}H_2$), 1.63-1.55 (6H, m, $O=CCH_2\underline{C}H_2$), 1.55-1.49 (1H, m, $C\underline{H}CHO$), 1.49-1.43 (4H, m, $C\underline{H}_2CHO$), 1.37-1.17 (56H, m, $CH_2\underline{C}H_2$), 0.89-0.82 (15H, m, $C\underline{H}_3CH$); ^{13}C NMR (150 MHz $CDCl_3$): δ_C= 174.0, 173.4 (C=O), 73.9, 73.5 ($H\underline{C}OC=O$), 66.7 ($H_2\underline{C}OC=O$) 38.8 ($H\underline{C}CH_2O$) 34.5 ($O=C\underline{C}H_2$), 25.5 ($O=CCH_2\underline{C}H_2$), 31.8, 31.4, 30.5, 29.7, 29.4, 29.2, 28.9, 25.2, 25.0, 24.8, 23.8, 23.0, 22.7 ($CH_2\underline{C}H_2$), 14.1, 11.0 ($CH_2\underline{C}H_3$).

Synthesis of 2-ethylhexyl ester of 2-ethylhexanoic acid-capped estolide (2EH-bC8E). The experiment was conducted according to the general procedure for synthesis of 2-ethylhexyl ester of OAE. 2-ethylhexanoic acid-capped estolide (bC8E) (188 g, 0.26 mole of CO_2H, AV=79 mg KOH g^{-1}) and 2EH (70 g, 0.54 mole). A yellowish liquid known as 2-ethylhexyl ester of 2-ethylhexanoic acid-capped estolide (2EH-bC8E) (210 g, 97% yield). v_{max}/cm^{-1} 2925, 2856 (C-H) 1734 (C=O) 1464 (CH_2) 1378 (CH_3) 1238, 1167 (C-O) 724 (CH_2); ^1H NMR (600 MHz, $CDCl_3$): δ_H=5.04-4.86 (2H, m, $\underline{H}COC=O$), 3.97-3.90 (2H, m, $\underline{H}_2COC=O$), 2.30-2.17 (6H, m, $O=C\underline{C}H_2$), 1.63-1.53 (8H, m, $O=CCH_2\underline{C}H_2$), 1.52-1.49 (1H, m, $C\underline{H}CHO$), 1.48-1.42 (4H, m, $C\underline{H}_2CHO$), 1.35-1.12 (56H, m, $CH_2\underline{C}H_2$), 0.89-0.79 (18H, m, $C\underline{H}_3CH$); ^{13}C NMR (150 MHz $CDCl_3$): δ_C=175.8, 173.9 (C=O), 74.2, 73.9 ($H\underline{C}OC=O$), 66.2 ($H_2\underline{C}OC=O$) 47.7($H\underline{C}C=O$), 38.8 ($H\underline{C}CH_2O$) 34.4 ($O=C\underline{C}H_2$), 25.5 ($O=CCH_2\underline{C}H_2$), 31.9, 30.5, 29.7, 29.4, 29.2, 28.9, 25.0, 23.8, 23.0, 22.7 ($CH_2\underline{C}H_2$), 14.1, 11.8, 11.0 ($CH_2\underline{C}H_3$).

Synthesis of 2-ethylhexyl ester of lauric acid-capped estolide (2EH-C12E). The experiment was conducted according to the general procedure for synthesis of 2-ethylhexyl ester of OAE. Lauric acid-capped estolide (C12E) (200 g, 0.37 mole of CO_2H, AV=103 mg KOH g^{-1}) and 2EH (96 g, 0.74 mole). A yellowish liquid known as 2-ethylhexyl ester of lauric acid-capped estolide (2EH-C12E) (235 g, 97% yield). v_{max}/cm^{-1} 2924, 2855 (C-H) 1736 (C=O) 1464 (CH_2) 1378 (CH_3) 1236, 1169 (C-O) 724 (CH_2); ^1H NMR (600 MHz, $CDCl_3$): δ_H=4.98-4.91 (2H, m, $\underline{H}COC=O$), 3.96-3.89 (2H, m, $\underline{H}_2COC=O$), 2.30-2.18 (6H, m, $O=C\underline{C}H_2$), 1.63-1.53 (6H, m, $O=CCH_2\underline{C}H_2$), 1.52-1.47 (1H, m, $C\underline{H}CHO$), 1.47-1.41 (4H, m, $C\underline{H}_2CHO$), 1.35-1.11 (66H, m, $CH_2\underline{C}H_2$), 0.88-0.78 (15H, m, $C\underline{H}_3CH$); ^{13}C NMR (150 MHz $CDCl_3$): δ_C= 174.0, 173.3 (C=O), 73.9, 73.5 ($H\underline{C}OC=O$), 66.6 ($H_2\underline{C}OC=O$) 38.8 ($H\underline{C}CH_2O$) 34.5, 34.3 ($O=C\underline{C}H_2$), 25.5 ($O=CCH_2\underline{C}H_2$), 31.9, 31.7, 30.5, 29.6, 29.4, 29.2, 28.9, 25.1, 23.8, 23.0, 22.7 ($CH_2\underline{C}H_2$), 14.1, 11.0 ($CH_2\underline{C}H_3$).

Synthesis of 2-ethylhexyl ester of stearic acid-capped estolide (2EH-C18E). The experiment was conducted according to the general procedure for synthesis of 2-ethylhexyl ester of OAE. Stearic acid-capped estolide (C18E) (200 g, 0.35 mole of CO_2H, AV=99 mg KOH g^{-1}) and 2EH (92 g, 0.71 mole). A yellowish liquid known as 2-ethylhexyl ester of stearic acid-capped estolide (2EH-C18E) (232 g, 97% yield). v_{max}/cm^{-1} 2923, 2854 (C-H) 1736 (C=O) 1464 (CH_2) 1378 (CH_3) 1242, 1169 (C-O) 723 (CH_2); ^1H NMR (600 MHz, $CDCl_3$): δ_H=5.03-4.91 (2H, m, $\underline{H}COC=O$), 3.99-3.91 (2H, m, $\underline{H}_2COC=O$), 2.32-2.21 (6H, m, $O=C\underline{C}H_2$), 1.61-1.56 (6H, m, $O=CCH_2\underline{C}H_2$), 1.56-1.51 (1H, m, $C\underline{H}CHO$), 1.49-1.44 (4H, m, $C\underline{H}_2CHO$), 1.35-1.18 (80H, m, $CH_2\underline{C}H_2$), 0.89-0.81 (15H, m, $C\underline{H}_3CH$); ^{13}C NMR (150 MHz $CDCl_3$): δ_C=174.0, 173.4 (C=O), 74.0, 73.6 ($H\underline{C}OC=O$), 66.6 ($H_2\underline{C}OC=O$) 38.8 ($H\underline{C}CH_2O$) 34.5, 34.4 ($O=C\underline{C}H_2$), 25.5 ($O=CCH_2\underline{C}H_2$), 31.9, 31.8, 30.5, 29.7, 29.4, 28.9, 25.1, 23.9, 23.0, 22.7 ($CH_2\underline{C}H_2$), 14.1, 11.0 ($CH_2\underline{C}H_3$).

RESULTS AND DISCUSSION

One-pot Synthesis of Polyhydroxy Estolide from Oleic Acid

Estolide with multiple hydroxyl groups was prepared from oleic acid in accordance with a one-pot method that we have reported earlier (Hoong *et al*., 2017) but with reaction time shortened to 24 hr instead of 72 hr. *Figure 1* illustrates the one-pot reaction between oleic acid and H_2O_2 that yielded PE. Generally, oleic acid was reacted with only H_2O_2 at 80°C for about 24 hr and *Figure 2* illustrates the experimental setup for the reaction. Oleic acid was converted to peroxy acid by H_2O_2, which subsequently converted oleic acid to epoxidised oleic acid. Thereafter, the epoxidised oleic acid was ring-opened by another oleic acid, which yielded estolide with hydroxyl groups. OOC analysis conducted on PE showed a value of 0.05%, which indicated that almost all the epoxide groups generated during the reaction were transformed to other functionalities.

Additionally, IV analysis performed on PE revealed that the product had IV of 3 g I_2 100 g^{-1} sample, which indicated that almost all the alkene

groups of oleic acid were transformed to either ester or hydroxyl groups. The newly formed hydroxyl groups of PE were detected through OHV analysis that recorded a value of 170 mg KOH g^{-1}. Moreover, ^{1}H NMR analysis confirmed the formation of hydroxyl and ester groups of PE because similar ^{1}H NMR spectrum of PE was observed in literature (Hoong *et al*., 2017). Furthermore, GPC analysis (*Figure 3*) showed that the prepared PE consisted of 72% estolide and 28% of 9,10-dihydroxystearic acid, which is the monomer of PE. The average molecular weight of PE was about 700 Da.

Synthesis of OAE

According to literature (Salih *et al*., 2013), base oil that contain hydroxyl group is more susceptible to oxidation degradation than those without hydroxyl group. Consequently, the hydroxyl groups of the prepared PE were end-capped with organic acids to enhance the oxidation stability of the base oil. Various organic acids were employed to end-capped the hydroxyl groups of PE that included linear and branched organic acids as shown in *Figure 4*.

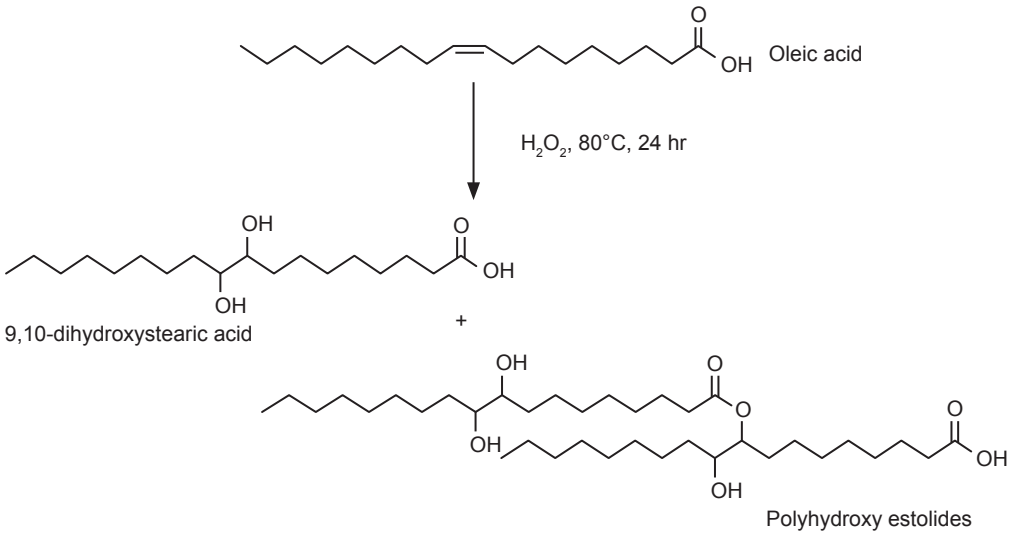

Figure 1. One-pot reaction between oleic acid and hydrogen peroxide (H_2O_2) that yielded polyhydroxy estolide.

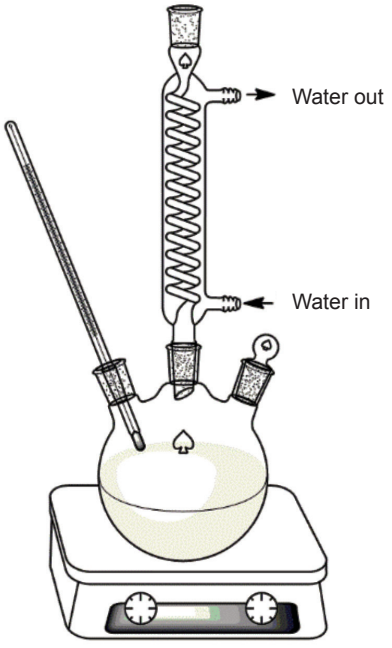

Figure 2. Experimental setup for synthesis of polyhydroxy estolide from oleic acid.

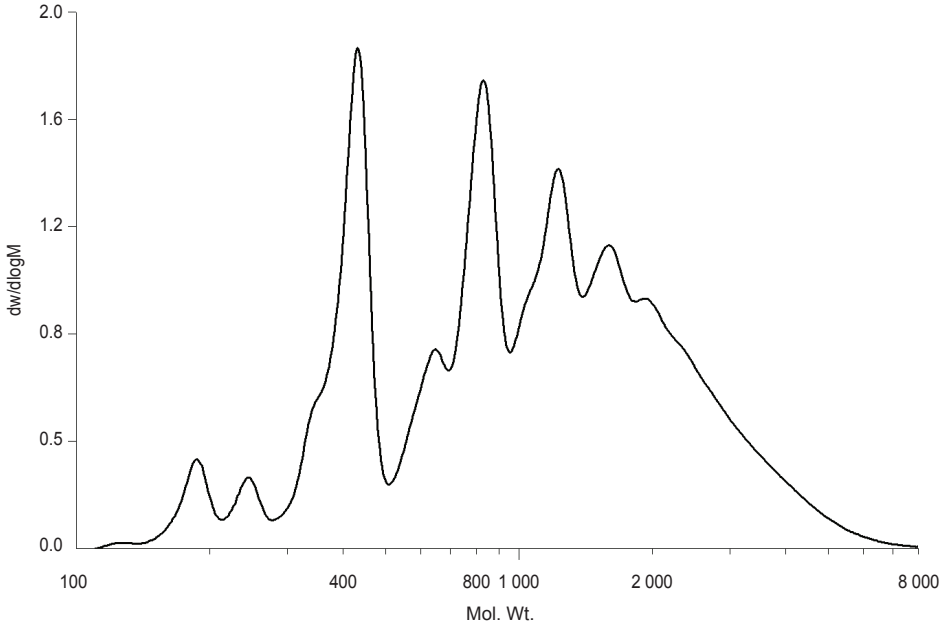

Figure 3. The gel permeation chromatography (GPC) of polyhydroxy estolide.

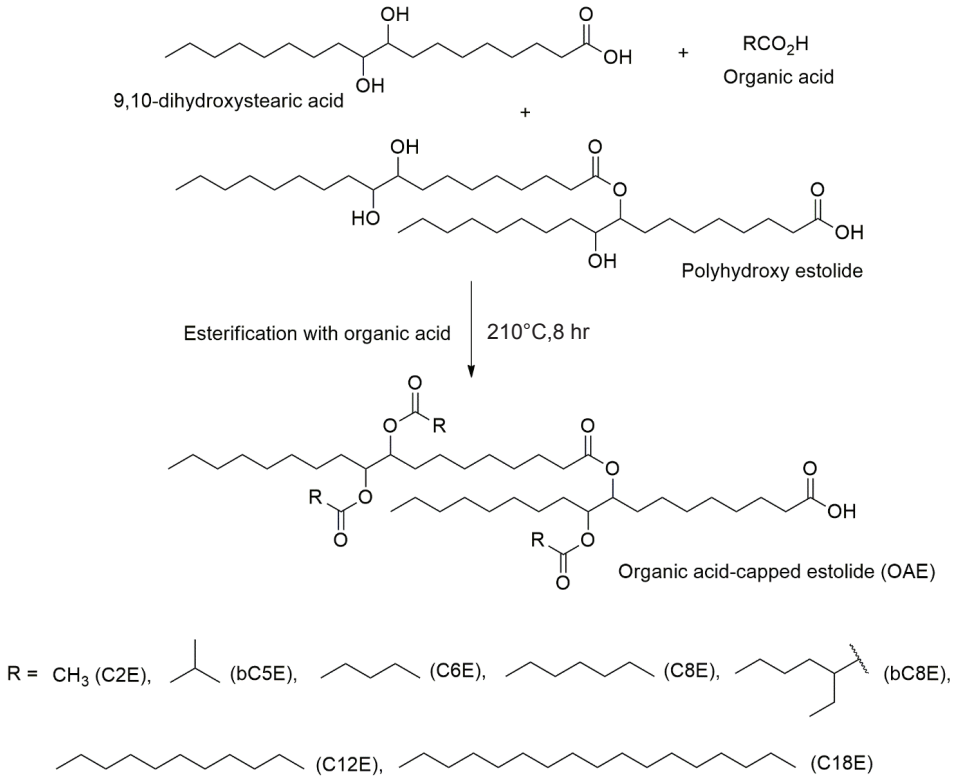

Figure 4. Esterification of polyhydroxy estolide with various organic acids.

The hydrocarbon chain length of linear organic acid used to end-capped PE was varied from short to long chain length. This exercise was meant to evaluate the effect of hydrocarbon chain length of organic acid on the physicochemical properties of resultant lubricant base oil. Selected linear organic acids were acetic acid (C2), C6, C8, C12 and C18. Literature reported that base oils made of branched molecule showed lower pour point in comparison with linear molecule (Liu *et al.*, 2019). Therefore, branched organic acids were included in this study to evaluate the effect of branched moiety on the properties of base oil. Branched organic acids selected for this study are bC5 and bC8.

The esterification between PE and organic acids that generate OAE was conducted without catalyst at temperature between 150°C-210°C, depending on the boiling point of the organic acid and *Figure 5* illustrates the experimental setup for the reaction. For esterification with acetic anhydride, the reaction was carried out at 150°C with xylene as the solvent to remove water from the reaction system. While for esterification with the rest of organic acids, reaction temperature was set at 210°C to accelerate the reaction. For most of the reaction, an excess amount of organic acid in regard to hydroxyl groups of PE was used in the reaction, in order to end-cap all the hydroxyl groups to form ester groups. The targeted OHV of the OAE should be less than 10 mg KOH g^{-1} and all the prepared OAE achieved OHV less than the targeted value, which indicated that almost all the hydroxyl groups were end-capped with organic acid. For reaction conducted with lauric and stearic acids, the amount of organic acid employed was 50% w/w of PE because excess lauric and stearic acids were difficult to be removed from the product through vacuum distillation.

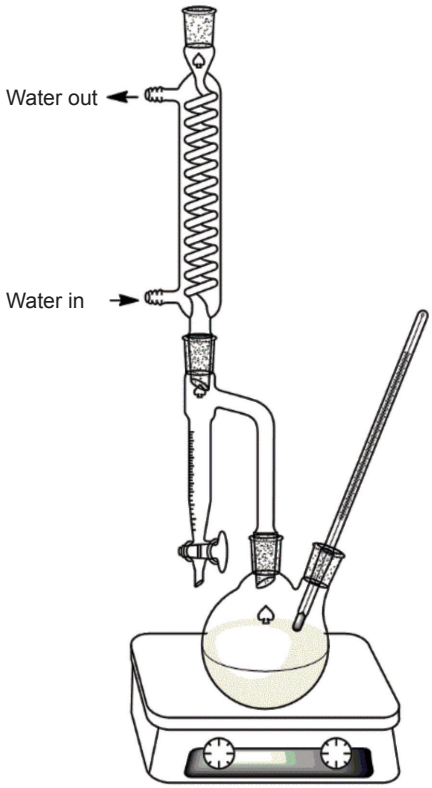

Figure 5. Experimental setup for esterification of between PE and organic acids.

^{1}H NMR analysis of product supported the results of OHV analysis that almost all the hydroxyl groups of PE were end-capped by organic acid to form ester groups. For example, ^{1}H NMR spectrum of hexanoic end-capped estolide (*Figure 6a*) showed a new peak at 4.97 ppm, which correlated to a methine proton attached to an ester group that was formed when hexanoic acid end-capped the hydroxyl group of PE. Additionally, two peaks at 3.57-3.33 ppm in the ^{1}H NMR spectrum of PE (*Figure 6b*) that correlated to methine protons attached to hydroxyl groups of PE were not observed in the ^{1}H NMR spectra of OAE, which clearly suggested that almost all the hydroxyl groups were converted to ester groups.

Synthesis of 2-ethylhexyl Ester of Organic Acid-capped Estolides

The synthesised OAE have carboxylic acid groups that are weak acid and may cause corrosion problem to metallic surfaces they intend to protect especially at high operating temperature (Owuna *et al.*, 2020). Therefore, carboxylic group of OAE need to be transformed to ester group in order to impart better qualities to the lubricant base oil. The conversion of carboxylic acid group of OAE to ester group was conducted through esterification with an alcohol. The alcohol selected for the esterification reaction was 2EH because literature reported (Moser *et al.*, 2007) that branched alcohols such as 2EH imparted lower pour points to lubricant made with them as compared to linear alcohols.

The esterification between OAE and 2EH was carried out without catalyst at 210°C for about 8 hr as shown in *Figure 7*. The experimental setup as shown in *Figure 5* was used for the esterification reaction. The 2EH was used in excess relatively to carboxylic acid group of OAE with the aim of converting all the carboxylic acid groups to esters and to push the reaction forward. The reaction was followed by monitoring the AV of reaction mixture and the targeted AV of product should be less than 2 mg KOH g^{-1} to ensure that the resultant base oil has good lubricant properties. AV analysis performed on all the prepared 2-ethylhexyl ester of organic acid-capped estolides (2EH-OAE) showed AV less than 2 mg KOH g^{-1}, which indicated that the reaction was successful.

The result of AV analysis was supported by FTIR analysis conducted on 2EH-OAE. As an example, the FTIR spectrum of 2-ethylhexyl ester of octanoic acid-capped estolide (2EH-C8E) (*Figure 8*) showed a narrow band at 1735 cm^{-1} that indicated the presence of ester group in the product, while no band associated with carboxylic acid group at 1710 cm^{-1} was observed, which suggested that all the carboxylic acid groups were transformed to ester groups. Additionally, ^{13}C NMR analysis on products also did not detect peak associated with carboxylic acid group at 179 ppm but instead it detected peak at 174 ppm, which indicated the presence of ester group.

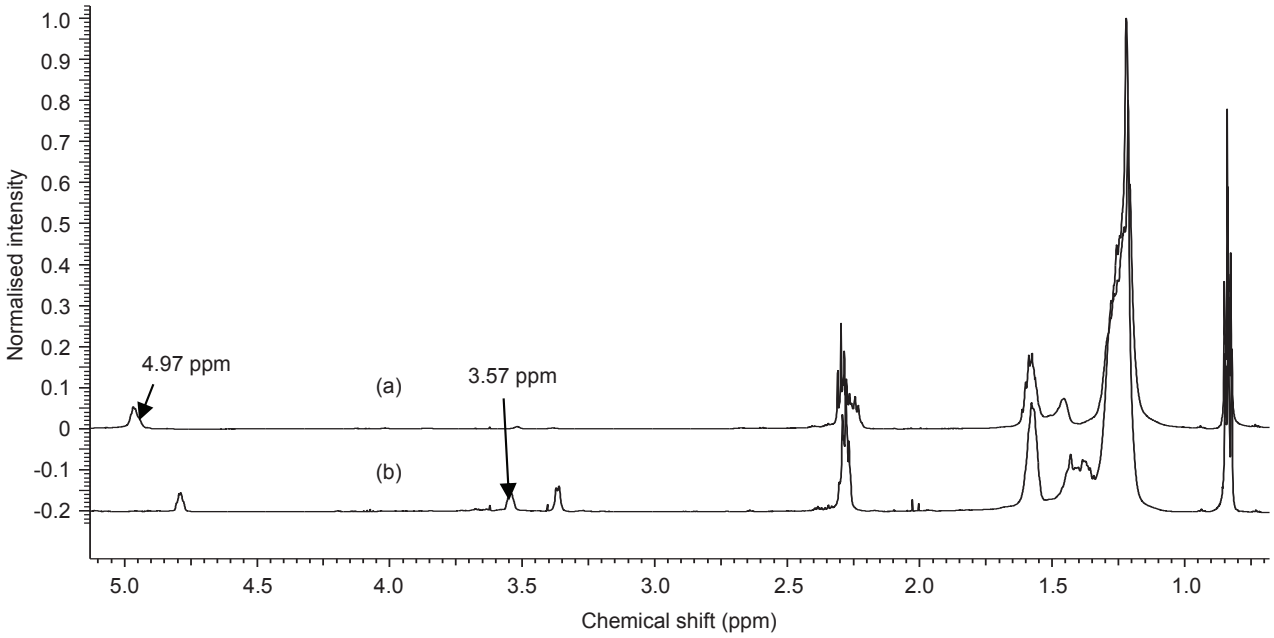

Figure 6. [1]H NMR spectrum of (a) hexanoic acid-capped estolide, and (b) polyhydroxy estolide (PE).

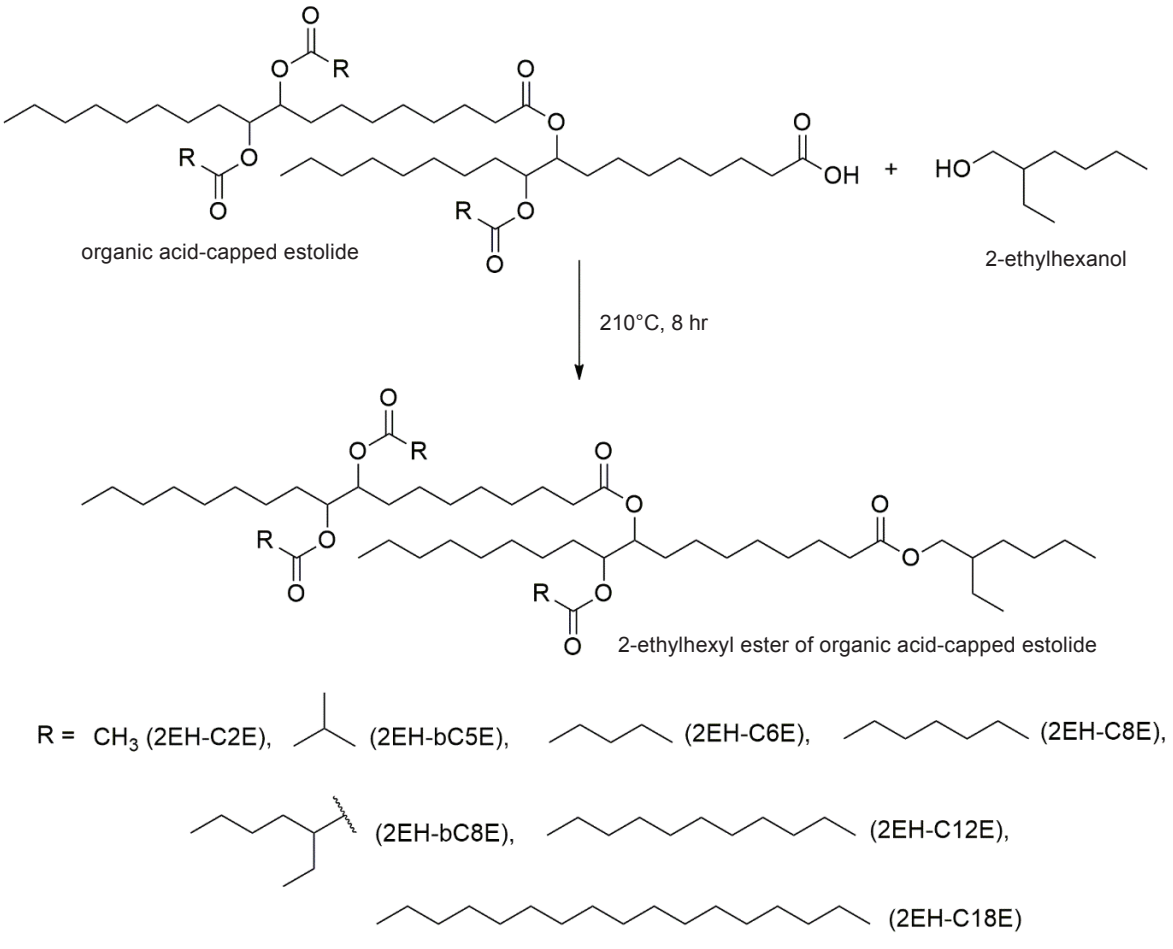

Figure 7. Esterification of organic acid-capped estolide with 2-ethylhexanol (2EH).

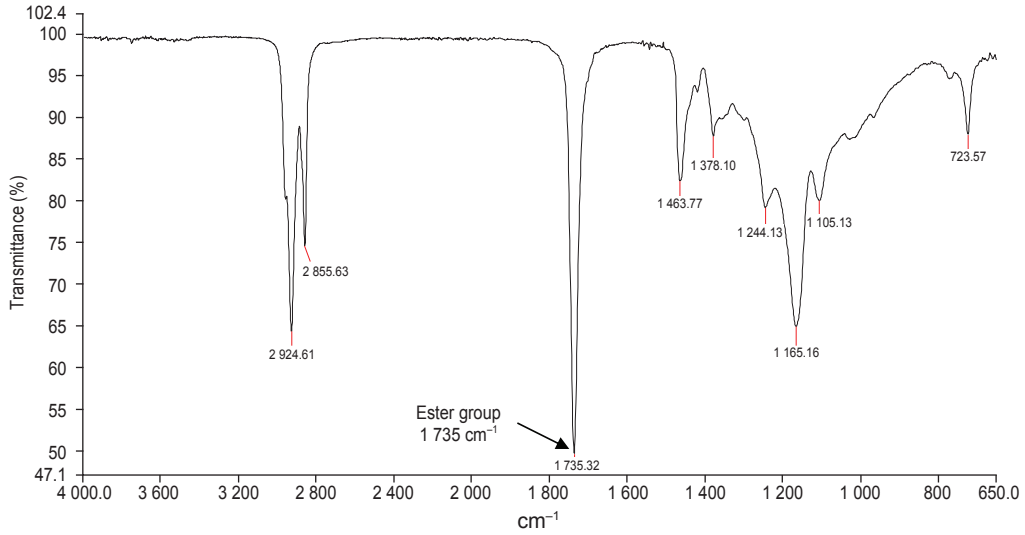

Figure 8. FTIR spectrum of 2-ethylhexyl ester of octanoic end-capped estolide (2EH-C8E).

Evaluation of 2-ethylhexyl Ester of Organic Acid-capped Estolides as Lubricant Base Oil

The synthesised 2EH-OAE were evaluated as lubricant base oil in accordance with typical specifications of commercial lubricant base oil which included kinematic viscosity, pour point, oxidation stability and wear prevention. For the evaluation, a commercial product was included in the study, which served as a benchmark for commercially acceptable lubricant properties. The commercial product was a biolubricant base oil consisted of pentaerythritol tetraoleate, prepared from esterification between pentaerythritol and oleic acid. The results of the physicochemical evaluation of all prepared 2EH-OAEs are shown in *Table 1*.

One of the main purposes of chemical modification performed on plant oils is to improve the pour point of plant oil-based lubricants to a level comparable to synthetic lubricants that they can be used in arctic condition. As a result of chemical alteration performed on oleic acid, majority of the synthesised 2EH-OAE products showed improved low temperature properties with pour points that were lower than most of commoditised plant oils such as soybean oil and canola oil. For example, 2EH-C2E recorded a pour point of -21°C, which was lower than the pour point of canola oil at -18°C (Asadauskas and Erhan, 1999).

Referring to pour points of 2EH-OAE in *Table 1*, we noticed there was a strong correlation between the chain length of organic acid employed to end-cap the hydroxyl group of PE and the pour point of the resultant 2EH-OAE. For example, when organic acid with longer chain length such as C8 was used to make 2EH-C8E, the product showed a pour point of -33°C, which was lower than pour point of 2EH-C2E (-21°C) that was made with C2. This observation suggested that the longer chain length of C8 contributed to the lower pour point. Thus, as anticipated, 2EH-C12E displayed even lower pour point of -36°C as it was made with longer chain organic acid namely C12 in comparison with C8.

TABLE 1. PHYSICOCHEMICAL PROPERTIES OF 2-ETHYLHEXYL ESTER OF ORGANIC ACID-CAPPED ESTOLIDES

Product	KV		VI	PP (°C)	OOT (°C)	WSD (mm)
	40°C, cSt	100°C, cSt				
2EH-C2E	295	40	189	-21	200	0.715
2EH-bC5E	269	35	177	-24	196	0.757
2EH-C6E	285	37	180	-24	198	0.692
2EH-C8E	274	35	175	-33	198	0.663
2EH-bC8E	222	28	163	-36	193	0.734
2EH-C12E	129	20	177	-36	197	0.631
2EH-C18E	124	19	173	-6	196	0.612
C1	63	12	190	-21	150	0.648

Note: KV - kinematic viscosity; VI - viscosity index; PP - pour point; OOT - oxidation onset temperature; WSD - four-ball wear scar diameter.
C1 = commercial biolubricant (pentaerythritol tetraoleate).

The reason for this outcome was due to the ability of C12 to fully cover the alkyl chain of PE beyond the hydroxyl group that it end-capped and thus, disrupted the intermolecular stacking of estolide molecules, which inhibited crystal formation, and consequently contributed to the low pour point of the product. Conversely, when shorter chain organic acid such as C2 was used to end-cap the hydroxyl group of PE as in 2EH-C2E, the short chain length of C2 was not able to cover the entire alkyl chain length of PE and this allowed alkyl stacking interaction to occur, which eventually resulted in crystal formation and higher pour point value of 2EH-C2E at -21°C.

This observation is contrarily to general knowledge on ester-based lubricants, which dictates that longer alkyl chain length will impart higher pour point to ester-based lubricant because longer chain length has higher efficiency to pack and form wax-like material than shorter chain length (Stepina and Vesely, 1992). The observed divergence from the norm occurred because the molecular structure of prepared 2EH-OAE is a branched ester unlike mostly linear ester-based lubricant, and the end-capping of hydroxyl group of PE with an organic acid of proper chain length, further disrupted crystal formation that resulted in lower pour point. Similar observation was reported in literature (Isbell, 2011).

Nonetheless, when C18 was used to end-cap hydroxyl groups of PE, the resultant product 2EH-C18E exhibited the highest pour point (-6°C) among prepared products. This was due to the long alkyl chain of C18 that exceeded the length of alkyl chain beyond the hydroxyl group of PE that it end-capped and the extra length of C18 encouraged intermolecular stacking and crystal formation, which led to higher pour point of the product.

The use of branched organic acids had significant effect on the pour point of products made with them, in which products made with branched acids recorded lower pour points than their linear counterpart. This observation was made evidence when comparing pour point of 2EH-bC8E with 2EH-C8E. The branched structure of bC8 has higher efficacy to obstruct stacking of molecules and avert crystal formation, which resulted in lower pour point than linear C8 (Isbell, 2011). Overall, all the prepared 2EH-OAE exhibited pour points lower or equivalent to commercial product except for 2EH-C18E, which suggested that most of the 2EH-OAE are good candidates for lubricant base oil.

Another objective of chemical modification conducted on plant oil derivatives is to improve the oxidation stability of plant oil-based lubricants, which is considered inferior in comparison with mineral oil-based lubricants. The oxidation stability of base oil can be evaluated by measuring the OOT of base oil by using pressure differential scanning calorimetry (PDSC) method. Referring to *Table 1*, the PDSC analysis results showed that the prepared 2EH-OAE had OOT values between 193°C-200°C, which were remarkably higher than OOT value of the commercial sample. This indicated that the chemical modification performed on the alkene group of oleic acid was able to substantially improve the oxidation stability of resultant base oils, in comparison with commercial samples that contain alkene groups. The observation suggested that conversion of alkene group to ester group can enhance the oxidation stability of base oil made from plant oil derivatives that contain unsaturation sites. Furthermore, the OOT results showed that products made with branched organic acid such as 2EH-bC8E registered a lower OOT value (193°C) than product made with linear organic acid (2EH-C8E, 198°C), which indicated that products made with linear organic acids were more stable oxidatively.

One of the important attributes of lubricant is its ability to reduce friction and prevent wear on surfaces, which contributes to longer lifespan of machineries. The anti-wear properties of lubricants can be measured by a four-ball method in accordance with ASTM 4172 and usually test result is reported as WSD, in which lubricant with better anti-wear properties would exhibit smaller WSD. As shown in *Table 1*, product 2EH-C18E exhibited the smallest WSD among all prepared 2EH-OAE, which suggested that it had the best anti-wear properties. The good anti-wear attribute of 2EH-C18E was most likely contributed by the long chain linear C18 employed to end-cap the hydroxyl group of PE as similar observation was reported by Salih *et al.* (2011).

Thus, for products that were made with shorter chain linear organic acids such as 2EH-C12E and 2EH-C8E, the WSD recorded for these products were slightly larger (0.631–0.663 mm) than 2EH-C18E, which reflected the negative effect of shorter chain organic acids on the anti-wear properties. For product made with even shorter chain fatty acid namely 2EH-C6E, the WSD was even larger (0.692 mm). Eventually, the product 2EH-C2E prepared with the shortest chain length organic acid (C2) exhibited the largest WSD among 2EH-OAE made with linear organic acids.

In comparison to products made with linear organic acids, the WSD for products made with branched organic acids were even larger, which suggested that they provided less wear prevention than products made with linear organic acids. This observation was made evidence when comparing WSD of 2EH-bC8E with 2EH-C8E, in which 2EH-bC8E showed larger WSD due to its branched moiety as reported in literature (Sharma and Erhan, 2013). Nevertheless, three products namely 2EH-C8E, 2EH-C12E and 2EH-C18E exhibited anti-wear properties similar or better than the commercial product used as benchmark.

Viscosity is a crucial physical property of base oil for lubricant. In the context of lubrication, viscosity of lubricant is commonly measured by kinematic viscosity and can be classified according to ISO VG system, which uses the kinematic viscosity of a fluid at 40°C as the reference point for classification. Referring to *Table 1*, the viscosity of 2EH-OAE was inversely proportionate to the chain length of organic acid employed in their syntheses. For example, product 2EH-C2E, which was made with the shortest chain length organic acid showed the highest kinematic viscosity of 295 cSt, while product made with the longest chain length organic acid (2EH-C18E) exhibited the lowest viscosity of 124 cSt. Additionally, product made with branched acid exhibited slightly lower viscosity when compared with its linear counterpart and this was made evidence when comparing product 2EH-bC8E to 2EH-C8E. Similar observation on the effect of alkyl chain length on the viscosity of OAE was reported by Isbell (2011).

The prepared 2EH-OAE can be divided into two groups based on their kinematic viscosity at 40°C. The first group consisted of product 2EH-C12E and 2EH-C18E, which recorded kinematic viscosity between 124-129 cSt and can be classified as ISO VG 150 base oil. The second group consisted of the rest of the 2EH-OAE that were made with C2 to C8 organic acids, which displayed kinematic viscosity between 200-300 cSt at 40°C. Product 2EH-bC8E can be classified as ISO VG 220 base oil while the rest of products can be classified as ISO VG 320 base oil. All the prepared products with viscosity between ISO VG 150 and ISO VG 320 can be used as lubricant for gears and bearings, which require base oil with relatively high viscosity (Pirro *et al.*, 2016).

VI is an indication of a lubricant change in viscosity relative to temperature change. It is a classification to describe the viscosity-temperature relationship of lubricant. Lubricant with higher VI indicates that the viscosity of the lubricant is less affected by temperature fluctuations. Generally, any base oil with VI more than 100 is considered to have good viscosity-temperature consistency profile (Tanveer and Prasad, 2006). As shown in *Table 1*, all the prepared products exhibited VI between163-189 and this result suggested that all the prepared 2EH-OAE have excellent VI quality.

CONCLUSION

The present study has shown that estolides esters can be made from oleic acid through chemical modification performed on alkene group of oleic with H_2O_2 that generated PE. Subsequently, the hydroxyl groups of PE were end-capped by various organic acids in order to evaluate the effect of organic acid moiety on the lubricant properties of resultant base oil. Afterward, the carboxylic acid group of OAE was converted to ester group with 2EH to further enhanced its lubricant properties.

Generally, the chemical modifications conducted on oleic acid that eventually generated estolides esters, not only significantly improved the low temperature properties of estolide esters but also remarkably enhanced the oxidation stability of estolide esters in comparison with the starting material and a commercial product. These results highlighted that the two major drawbacks associated with plant oil-based lubricants namely high pour point and poor oxidation stability can be resolved by converting oleic acid to estolide esters.

In particular, the chain length of organic acid that end-capped the hydroxyl group of PE strongly affected the properties of base oil. Products made with linear lauric acid (2EH-C12E) and branched 2-ethylhexanoic acid (2EH-bC8E), respectively exhibited the best pour point (-36°C), while products made with shorter or longer chain length organic acids showed higher pour points. Furthermore, products made with longer chain organic acid recorded better anti-wear properties and lower kinematic viscosity than products made with shorter chain length organic acid. Additionally, the oxidation stability of products made with linear organic acid were higher than those made with branched organic acids.

Most of the 2EH-OAE prepared in this study have physicochemical properties that comply with standard specifications of hydraulic oil, gear oil and stern tube lubricants, which indicated that most of the prepared 2EH-OAE are suitable to be used as base oil for lubricants.

ACKNOWLEDGEMENT

We would like to thank the Director-General of MPOB for permission to publish this article. We are grateful to Ahmad Lutfi Md Yusof, Zuraidah Kamarudin, Sapiah Hashim, Selasiah Abdullah, Mohd Taib Samsudin, Norizan Ali and Makmor Abd. Wahab for all the analyses conducted. We would like to express our gratitude to IOI Acidchem Sdn. Bhd. for providing free sample of oleic acid (PALMAC 750).

REFERENCES

Abi-Akar, H (2017). Performance and technical requirements of low-environment impact lubricants. *Environmentally Friendly and Biobased Lubricants* (Sharma, B K and Biresaw, G eds.). 1st edition. CRC Press, Boca Raton, USA. p. 102-103.

Adhvaryu, A; Liu, Z and Erhan, S Z (2005). Synthesis of novel alkoxylated triacylglycerols and their lubricant base oil properties. *Ind. Crops Prod.*, *21*: 113-119.

Armylisas, A H N; Hazirah, M F S; Yeong, S K and Hazimah, A H (2017). Modification of olefinic double bonds of unsaturated fatty acids and other vegetable oil derivatives via epoxidation: A review. *Grasas Y Aceites*, *68*: e174.

Asadauskas, S and Erhan, S Z (1999). Depression of pour points of vegetable oils by blending with diluents used for biodegradable lubricants. *J. Amer. Oil Chem. Soc., 76*: 313-316.

Battersby, N S; Pack, S E and Watkinson, R J (1992). A correlation between the biodegradability of oil products in the CEC L-33-T-82 and modified Sturm tests. *Chemosphere*, *24*: 1989-2000.

Borugadda, V B and Dalai, A K (2018). *In-situ* synthesis and characterization of biodegradable estolides via epoxidation from canola biodiesel. *Lubricants*, *6*: 94.

Cecilia, J A; Plata, D B; Saboya, R M A; Luna, F M T; Cavalcante, C L and Castellon, E R (2020). An overview of the biolubricant production process: Challenges and future perspectives. *Processes*, *8*: 257.

Cermak, S C and Isbell, T A (2001). Synthesis of estolides from oleic and saturated fatty acids. *J. Amer. Oil Chem. Soc.*, *78*: 557-565.

Cermak, S C and Isbell, T A (2003a). Synthesis and physical properties of estolide-based functional fluids. *Ind. Crops Prod.*, *18*: 183-196.

Cermak, S C and Isbell, T A (2003b). Improved oxidative stability of estolide esters. *Ind. Crops Prod.*, *18*: 223-230.

Cermak, S C; Brandon, K B and Isbell, T A (2006). Synthesis and physical properties of estolides from lesquerella and castor fatty acid esters. *Ind. Crops Prod.*, *23*: 54-64.

Cermak, S C; Bredsguard, J W; Roth, K L; Thompson, T; Feken, K A; Isbell, T and Murray, R E (2015). Synthesis and physical properties of new coco-oleic estolide branched esters. *Ind. Crops Prod.*, *74*: 171-177.

Chan, C H; Tang, S W; Mohd, N K; Lim, W H and Yeong, S K (2018). Tribological behavior of biolubricant base stocks and additives. *Renew. Sust. Energ. Rev.*, *93*: 145-157.

Chen, J M; Beaufort, M L; Gyurik, L; Dorresteijn, J; Otte, M and Gebbink, R J M K (2019). Highly efficient epoxidation of vegetable oils catalyzed by a manganese complex with hydrogen peroxide and acetic acid. *Green Chem.*, *21*: 2436-2447.

Chen, Y Z; Biresaw, G; Cermak, S C; Isbell, T A; Ngo, H L; Chen, L and Durham, A L (2020). Fatty acid estolides: A review. *J. Amer. Oil Chem. Soc.*, *97*: 231-241.

Erhan, S Z; Sharma, B K and Perez, J M (2006). Oxidation and low temperature stability of vegetable oil-based lubricants. *Ind. Crops Prod.*, *24*: 292-299.

Everett, K and Graf, F A J (1971). Handling perchloric acid and perchlorates. *CRC Handbook of Laboratory Safety* (Steere, N V ed.). CRC Press, Boca Raton, USA. p. 265.

Greco-Duarte, J; Collaco, A C A; Costa, A M M; Silva, L O; Da Silva, J A C; Torres, A G; Fernandez-Lafuente, R and Freire, D M G (2019). Understanding the degree of estolide enzymatic polymerization and the effects on its lubricant properties. *Fuel*, *245*: 286-293.

Heikal, E K; Elmelawy, M S; Khalil, S A and Elbasuny, N M (2017). Manufacturing of environment friendly biolubricants from vegetable oils. *Egypt. J. Pet.*, *26*: 53-59.

Hoong, S S; Norhisham, M S; Maznee, T N T I; Kosheela, D P P; Nurul, A H; Hazimah, A B; Ooi, T L and Salmiah, A (2008). Preparation of a low viscosity and light coloured fatty acid-based polyol. *J. Oil Palm Res.* (*Special Issue-October 2008*) *20*: 44-52.

Hoong, S S; Yeong, S K and Hazimah, A B (2017). Non-catalytic one-pot synthesis of polyhydroxy estolides from oleic acid. *J. Oil Palm Res.*, *29*: 88-96.

Isbell, T (2011). Chemistry and physical properties of estolides. *Grasas Y Aceites*, *62*: 8-20.

Kassfeldt, E and Goran, D (1997). Environmentally adapted hydraulic oils. *Wear*, *207*: 41-45.

Kim, H J; Choi, N K; Kim, Y H; Kim, H R; Lee, J S and Kim, I H (2019). Immobilized lipase-catalyzed esterification for synthesis of trimethylolpropane triester as a biolubricant. *Renew. Energy*, *130*: 489-494.

Liu, S B; Saha, B and Vlachos, D G (2019). Catalytic production of renewable lubricant base oils from bio-based 2-alkylfurans and enals. *Green Chem.*, *21*: 3606-3614.

Luther, R (2007). Lubricants in the environment. *Lubricants and Lubrication* (Mang, T and Dresel, W eds.). Wiley-VCH, Weinheim, Germany. p. 120-123.

Lv, N N; He, W; Fang, Z; Sun, Q; Qiu, C H and Guo, K (2017). Epoxidation of methyl oleate and subsequent ring-opening catalyzed by lipase from *Candida* sp. 99-125. *Eur. J. Lipid Sci. Technol.*, *120*: 1700257.

Moser, B R; Sharma, B K; Doll, K M and Erhan, S Z (2007). Diesters from oleic acid: Synthesis, low temperature properties and oxidation stability. *J. Amer. Oil Chem. Soc.*, *84*: 675-680.

Mubofu, E B (2016). Castor oil as a potential renewable resource for the production of functional materials. *Sustain. Chem. Process.*, *4*: 11.

Nowak, P; Kucharska, K and Kaminski, M (2019). Ecological and health effects of lubricant oils emitted into the environment. *Int. J. Environ. Res. Public Health*, *16*: 3002.

Nowicki, J; Drabik, J; Woszczynski, P; Gebura, K; Nowakowska-Bogdan, E and Kozdrach, R (2019). Tribological characterization of plant oil derived fatty acid esters of higher polyols: Comparative experimental study. *Lubr. Sci.*, *31*: 61-72.

Owuna, F J; Dabai, M U; Sokoto, M A; Dangoggo, S M; Bagudo, B U; Birnin-Yauri, U A; Hassan, L G; Sada, I; Abubakar, A L and Jibrin, M S (2020). Chemical modification of vegetable oils for the production of biolubricant using trimethylolpropane: A review. *Egypt. J. Pet.*, *29*: 75-82.

Parveez, G K A; Hishamuddin, E; Loh, S K; Ong-Abdullah, M; Salleh, K M; Bidin, M N I Z; Sundram, S; Hasan, Z A A and Idris, Z (2020). Oil palm economic performance in Malaysia and R&D progress in 2019. *J. Oil Palm Res.*, *32*: 159-190.

Pirro, D M; Webster, M and Daschner, E (2016). *Lubrication Fundamentals.* CRC Press, Boca Raton, USA. p. 197.

Reeves, C J; Siddaiah, A and Menezes, P L (2017). A review on the science and technology of natural and synthetic biolubricants. *J. Bio Tribo Corros.*, *3*: 11.

Sammaiah, A; Padmaja, K V and Prasad, R B N (2016). Synthesis and physical properties of novel estolides from dicarboxylic acids and methyl ricinoleate. *Eur. J. Lipid Sci. Technol.*, *118*: 486-494.

Salih, N; Salimon, J and Yousif, E (2011). The physicochemical and tribological properties of oleic acid based triesters biolubricants. *Ind. Crops Prod.*, *34*: 1089-1096.

Salih, N; Salimon, J; Yousif, E and Abdullah, B M (2013). Biolubricant basestocks from chemically modified plant oils: Ricinoleic acid based-tetraesters. *Chem. Cent. J.*, *7*: 128.

Salimon, J; Salih, N and Yousif, E (2010). Biolubricants: Raw materials, chemical modifications and environmental benefits. *Eur. J. Lipid Sci. Technol.*, *112*: 519-530.

Salimon, J; Salih, N and Yousif, E (2011). Synthesis, characterization and physicochemical properties of oleic acid ether derivatives as biolubricant basestocks. *J. Oleo Sci.*, *60*: 613-618.

Santos, J C; Santos, I M; Conceico, M M; Porto, S L; Trindade, M F; Souza, A G; Prasad, S; Fernandes, J and Araujo, A S (2004). Thermoanalytical, kinetic and rheological parameters of commercial edible plant oils. *J. Therm. Anal. Calorim.*, *75*: 419-428.

Sharma, B K and Erhan, S Z (2013). Modified vegetable oil for environmentally friendly lubricant applications. *Synthetics, Mineral Oils and Bio-based Lubricants* (Rudnick, L R ed.). CRC Press, Boca Raton, USA. p. 400.

Soni, S and Agarwal, M (2014). Lubricants from renewable energy sources – A review. *Green Chem. Lett. Rev.*, *7*: 359-382.

Stepina, V and Vesely, V (1992). *Lubricants and Special Fluids*. Elsevier, Amsterdam, Netherlands. p. 167.

Tanveer, S and Prasad, R (2006). Enhancement of viscosity index of mineral base oils. *Indian J. Chem. Technol.*, *13*: 398-403.

Theissen, H (2010). The German market introduction program for biobased lubricants. *Tribol. Online*, *5*: 225-229.

Journal of Oil Palm Research Vol. 34 (1) March 2022 p. 167-176
DOI: https://doi.org/10.21894/jopr.2021.0034

PHYSICOCHEMICAL PROPERTIES OF PALM OLEIN-BASED POLYOLS PREPARED USING HOMOGENEOUS AND HETEROGENEOUS CATALYSTS

NORHAYATI MOHD NOOR[1]*; TUAN NOOR MAZNEE TUAN ISMAIL[1]; MOHD AZMIL MOHD NOOR[1]; KOSHEELA DEVI POO PALAM[1]; MOHD NORHISHAM SATTAR[1]; NURUL 'AIN HANZAH[1]; SRIHANUM ADNAN[1] and YEONG SHOOT KIAN[1]

ABSTRACT

Research and development of palm-based polyols have been intensively carried out to improve their features and characteristics appropriate for their required applications. The physicochemical properties of palm olein-based polyols prepared using homogeneous ($BF_3.Et_2O$) and heterogeneous (K10 montmorillonite) catalysts in the ring-opening reaction of epoxidised palm olein (EPOo) were compared. Mono alcohols, i.e.*, methanol and isobutanol were selected as ring opening reagents. The formation of palm olein-based polyols was confirmed by the oxirane oxygen content (OOC), Fourier transformed infrared (FTIR) spectra and hydroxyl value (OHV) determinations. Based on the observation, the molecular weight (MW) of reagent used in the epoxide ring-opening reaction affected the viscosity of the obtained palm olein-based polyols. High oligomerisation was detected in palm olein-based polyol prepared using a homogeneous catalyst. The composition of hydroxyl monomer, dimer, trimer and tetramer in palm olein-based polyols were obtained from Gel Permeation Chromatography (GPC). Palm olein-based polyols prepared using heterogeneous catalyst exhibited the highest mono composition compared to other palm olein-based polyols. Heterogeneous catalyst provided palm olein-based polyols with low viscosity, less oligomerisation and functionality close to theoretical as compared to homogeneous catalyst. This finding can be used as a guideline in the synthesis of polyols with desired properties for targeted applications.*

Keywords: homogeneous and heterogeneous catalysts, palm olein-based polyol, ring-opening reaction.

Received: 1 March 2021; **Accepted:** 31 May 2021; **Published online:** 25 August 2021.

INTRODUCTION

A growing worldwide research effort is driven by concern about renewable resources and the environment. Malaysia's oleochemical industry is mostly derived from vegetable oil, *i.e.*, palm oil and palm kernel oil, as the major feedstocks (Parveez *et al.*, 2020). Vegetable oil-based intermediates and products are continuously being developed for valuable polymeric materials as they are known to be cheap in price, abundant supply, environmental-friendly and provide excellent properties (Flora, 2014; Lin *et al.*, 2008; Narine *et al.*, 2007a). The productions of polyols from vegetable oil have been the subject of many studies. Several studies have reported their methods for the preparation of vegetable oil-based polyol such as hydroformylation, transesterification and ozonolysis (Abraham, 2012; Arniza *et al.*, 2015; Narine *et al.*, 2007b). The most widely practiced

[1] Malaysian Palm Oil Board,
6 Persiaran Institusi, Bandar Baru Bangi,
43000 Kajang, Selangor, Malaysia.

* *Corresponding author e-mail: norhayati.mohdnoor@mpob.gov.my*

methods are epoxidation followed by a ring-opening reaction which has been identified as the safest route and most economical (Armylisas *et al.*, 2017; Chasar *et al.*, 2005; Hazimah *et al.*, 2011; Silverajah *et al.*, 2012; Siti Munira *et al.*, 2013; Tuan Ismail *et al.*, 2018a).

Alcohols were reported as the best ring-opening reagent for synthesis of polyols where secondary and primary hydroxyl groups were created when using mono alcohols and diols, respectively (Li *et al.*, 2015; Tuan Ismail *et al.*, 2018a; 2018b). In the study by Tuan Ismail *et al.* (2018a), the effect of various nucleophiles (ring-opening reagents) on oligomeric composition and properties of polyols derived from epoxidised palm olein (EPOo) was investigated. The polyols were synthesised using homogeneous catalyst, *i.e.*, $BF_3.Et_2O$ and the mole ratio of EPOo to nucleophiles was 1:1. Lower degree of oligomerisation was observed in polyols prepared with mono alcohol compared to polyols made with diols. In this study, the oxirane ring of EPOo was opened by mono alcohols such as methanol and isobutanol to form palm olein-based polyols with secondary hydroxyls similar to report by Tuan Ismail *et al.* (2018a). Methanol and isobutanol were selected as ring-opening reagents because of their promising characteristics. Methanol is the cheapest and simplest alcohol, which leads to an easier reaction, while isobutanol contains a branch in β-position, which forms steric hindrance in the reaction and enables the formation of the compound with desired properties.

A catalyst is a substance that increases the rate of a chemical reaction without being consumed and not permanently involved in the reaction process (Clark, 2013; Farnetti *et al.*, 2009; Johannes and David, 2012; Piet, 2004). The catalyst is added into the reaction mixture to reduce the activation energy and thus, increases the reaction rate. Acids or alkalies can be used to catalyse the ring-opening reaction. In the presence of alkaline catalysts, for example sodium methylate and caustic soda, they will react with water and reduction of catalytic activity occurs. The most important factor that influences the success of ring-opening reaction catalysed by alkali is that the oil must contain a total of zero free fatty acids (Seigfried *et al.*, 2002).

Acidic catalysts in the form of homogeneous and heterogeneous catalysts were used in the study. Both catalysts possess some advantages and disadvantages (*Table 1*). A homogeneous catalyst is a class of catalysis in which the catalyst occupies the same phase as the reactants that allow a great interaction with the reaction mixture by affecting their bond polarisation. The degree of collisions between catalyst and reactants is high because the catalyst is uniformly dispersed in the reaction mixtures. The difficulty of homogeneous catalyst recovery from the reaction medium becomes one of their major drawbacks. Meanwhile, heterogeneous catalyst occupies a different phase from the reactants. In order to speed up the reaction, the reactant molecules must collide with proper orientation. A heterogeneous catalyst will align molecules in the right way, so it is easier for them to combine and react. The main advantage of heterogeneous catalyst over the homogeneous catalyst is that it makes the separation and re-utilisation of heterogeneous catalyst cheaper and easier. The availability of surface area of the catalyst is one of the limitations of a heterogeneous catalyst. Once the surface of the catalyst is saturated with reactant molecules, the reaction cannot continue until products leave the surface, and some space opens up again for a new reactant molecule to attach (Anonymous, 2019; Farnetti *et al.*, 2009).

The common homogeneous catalysts that have been used in the ring-opening reaction of epoxidised oils to produce polyols are formic acid, sulphuric acid, phosphoric acid, pentamethyldiethylenetriamine, acid-blocked version of 70% bis(dimethylaminoethyl)ether, 30% dipropylene glycol (DABCO® BL 17), ρ-toluenesulfonic acid monohydrate, heat-activated catalyst based on 1,8-diaza-bicyclo (5,4,0) undecene-7 and boron trifluoride diethyl etherate (BF3.Et2O) (Flora, 2014; Hazimah *et al.*, 2011; Lozada *et al.*, 2009; Siti Munira *et al.*, 2013; Tuan Ismail *et al.*, 2018a). Lewis acid in $BF_3.Et_2O$ also has been reported to play a role in organic synthesis such as in accomplishing esterification of acids, hydroxylation of the double bond, cleavage of epoxides and many other cyclisation reactions (Banerjee *et al.*, 2019). $BF_3.Et_2O$ was practically used in the ring-opening reaction of EPOo with alcohols to produce palm-based polyols as reported by Hazimah *et al.* (2011) and Tuan Ismail *et al.* (2018a) in their previous studies. Heterogeneous catalysts such as metal salts of carboxylic acids, acid resins copolymer styrene + 20% divinylbenzene (Amberlyst 15), copolymer styrene + 8% divinylbenzene (Amberlite IR-120), copolymer styrene + 2% divinylbenzene (Dowex 50X2) and copolymer of tetrafluoroethene + perfluoro-2-(fluorosulfonylethoxy) propylvinyl ether entrapped on silica (SAC13) and various types of clays (Nafion-H, K10 montmorillonite, Retrol F, Y zeolite, H-Y zeolite and KSF/O) were also being used in the ring-opening reaction of epoxidised oils (Chasar *et al.*, 2005; Fási *et al.*, 2004; Norhayati *et al.*, 2013; 2016; 2018; Rios *et al.*, 2003; 2005).

Based on many literatures that reports on the ring-opening reaction of epoxidised oil in the presence of various types of catalysts, $BF_3.Et_2O$ and K10 montmorillonite catalysts, which represent homogeneous and heterogeneous catalysts, respectively, were used in the study.

There are limited reports in the literature on the production of palm-based polyols using homogeneous and heterogeneous catalysts and comparison of their properties. This article will highlight the physicochemical properties of palm olein-based polyols obtained using homogeneous and heterogeneous catalysts in the epoxide ring-opening reactions.

TABLE 1. ADVANTAGES AND DISADVANTAGES OF HOMOGENEOUS AND HETEROGENEOUS CATALYSTS

Item	Homogeneous	Heterogeneous
Active centers	All atoms	Only surface atoms
Selectivity	High	Low
Structure	Defined	Undefined
Applicability	Limited	Wide
Catalyst separation	Expensive/tedious	Cheap/easy
Cost of catalyst losses	High	Low

Source: Ali *et al.* (2010).

MATERIALS AND METHODS

Materials

The EPOo was obtained from Malaysian Palm Oil Board (MPOB) polyol pilot plant with the moisture content of 0.04%-0.05%, iodine value (IV) of 0.8-1.0 g I_2 100 g^{-1}, oxirane oxygen content (OOC) of 2.9%-3.2%, acid value (AV) of 0.4-0.6 mg KOH g^{-1} and viscosity of 120-140 mPa.s at 25°C. The EPOo was produced by reacting refined, bleached and deodourised (RBD) palm olein with mixture of formic acid and hydrogen peroxide. Acetone and isobutanol (analytical reagent grade) were purchased from Fisher Scientific, United Kingdom. Methanol (analytical reagent grade) was purchased from Systerm, Malaysia. Boron trifluoride diethyl etherate, $BF_3.Et_2O$ (50% purity) was obtained from Merck, Germany. K10 montmorillonite was obtained from Fluka-Chemica, Germany. Sodium carbonate (Na_2CO_3) and sodium chloride (NaCl) (analytical reagent grade) were purchased from Mallinckrodt Chemicals, USA and Systerm, Malaysia, respectively. Distilled water was used to prepare NaCl and Na_2CO_3 solutions. All materials were used without further modification.

Methods

Syntheses of palm olein-based polyols in the presence of homogeneous catalyst. Reactions were carried out using a 2 L water-jacketed glass reactor equipped with a mechanical stirrer (a flat anchor propeller), thermocouple, dropping funnel and circulating water bath. A calculated amount of EPOo was placed in the glass reactor and preheated to 60°C under continuous stirring. A freshly prepared mixture of $BF_3.Et_2O$ and isobutanol were added dropwise into the preheated EPOo. The mole ratio of EPOo to isobutanol was 1:10 and 1.0% $BF_3.Et_2O$ catalyst was used in the study. The reaction mixture was withdrawn for OOC analysis in every 30 min interval until the final OOC was less than 0.1%.

The obtained polyol was washed and neutralised at 60°C-65°C with 1% NaCl solution, followed by 0.5% Na_2CO_3 solution. The washing process was repeated a few times until the pH of the polyol was in the range of 6 to 8 (initial pH of polyol was 2). The pH of polyol was measured using pH paper (MColorpHast™). The final washing process was carried out with 1% NaCl solution in order to remove the residual carbonate in the polyol. The pH of the final polyol product was 7. The washed and neutralised polyol was dried under a vacuum of 9 mbar at 90°C-100°C until the moisture content of the obtained polyol was less than 0.05%.

The method described above was applied for the synthesis of EPOo with methanol at 40°C-60°C. The reaction set-up was equipped with a condenser and a chiller to prevent the evaporation of methanol during the reaction. The obtained polyols were designated as PI-HO and PM-HO for polyols prepared with isobutanol and methanol, respectively. The yields of the both polyols were >80 wt% based on the mass of initial EPOo.

Syntheses of palm olein-based polyols in the presence of heterogeneous catalyst. Reactions were carried out using a 500 mL three-necked reaction flask equipped with a mechanical stirrer (a flat anchor propeller) and a thermometer. A calculated amount of K10 montmorillonite catalyst was pre-mixed with isobutanol at 60°C for 10-15 min before the addition of EPOo. The mole ratio of EPOo to isobutanol was 1:10 and 10% of K10 montmorillonite catalyst was used in the reaction following the optimum reaction parameter reported by Norhayati *et al.* (2013). The excess of isobutanol will ease the pre-mixing process between K10 montmorillonite catalyst and isobutanol. It will also avoid the formation of thick slurry of the mixture. Therefore, the activation of the K10 montmorillonite catalyst can occur effectively. The reaction was performed under continuous stirring. The OOC of the reaction mixture was monitored every 30 min and the reaction was stopped when the OOC reached below 0.1%. The obtained reaction mixture was cooled down to room temperature (23°C).

Acetone was added into the reaction mixture to ease the separation of the K10 montmorillonite

catalyst from the reaction mixture. The catalyst can be separated easily from the less viscous reaction mixture by using vacuum filtration (Whatman filter paper No. 5). The used K10 montmorillonite catalyst can be recycled and reused in the alcoholysis of EPOo to produce palm olein-based polyol (Norhayati *et al.*, 2018). The obtained filtrate underwent distillation process to remove the excess alcohol and acetone from the reaction product. The set-up for the distillation process consisted of a 1000 mL three-necked round bottom flask containing the filtrate. The flask was placed in an oil bath, equipped with a condenser and a vacuum pump. A stirring process was carried out by using a magnetic stirrer. Within 5-6 hr at 115°C and 70-80 mbar of vacuum pressure, the excess alcohol and acetone were successfully removed from the reaction product. The reaction product was dried under vacuum (9 mbar) at 115°C until the moisture content of the reaction product was less than 0.05%. The yield of the final polyol was >90 wt% based on the mass of initial EPOo.

The method was also applied for the synthesis of EPOo with methanol at various reaction temperatures, *i.e.*, 40°C, 50°C and 60°C. The reaction set-up was equipped with a condenser to prevent the loss of methanol during the reaction. The ring-opening reaction of EPOo and methanol was only observed at 60°C with a slow reduction of OOC as monitored up to 23 hr of reaction time. No reaction was observed at 40°C and 50°C. The obtained polyols were labeled as PI-HE and PM-HE for polyols prepared with isobutanol and methanol, respectively. Idealised reaction scheme for the ring-opening reaction of EPOo with alcohols in the presence of homogeneous and heterogeneous catalysts is shown in *Figure 1*.

Characterisation of Palm Olein-based Polyols

The Fourier transformed infrared (FTIR) spectra of palm olein-based polyols were recorded using Perkin Elmer FTIR Spectrum 100 equipped with Universal ATR Attachment in the 650-4000 cm^{-1} wavenumber range. The OOC of the reaction mixture and palm olein-based polyol was determined following the AOCS Official Method Cd 9-57 (AOCS, 2007). The hydroxyl value (OHV) and AV were determined according to the AOCS Official Method Cd 13-60 (pyridine-acetic anhydride titration method) and AOCS Official Method TE 2a-64, respectively. The IV was analysed according to AOCS Official Method Cd 1d-92 (cyclohexane-acetic acid titration method). The viscosity of the palm olein-based polyol was measured using a Brookfield Digital Rheometer, Model DV-III+.

The molecular weight (MW) and molecular weight distribution (MWD) of the palm olein-based polyols were measured using a PL-GPC 50 Plus (an integrated Gel Permeation Chromatography (GPC) system by Polymer Laboratories Ltd, United Kingdom). The system was equipped with a differential refractive index (DRI) detector. A set of four Phenogel columns (5 μm particle size and porosities of 50, 100, 1000 and 10 000 Å) from Phenomenex (Torrance, CA, USA), covering a MW range of 10^2 - 10^6 Dalton, was used for separation. Tetrahydrofuran (THF) was used as the eluent at a flow rate of 1 mL min^{-1}. Palm olein-based polyol was dissolved in THF with a concentration of 2 mg mL^{-1}. The solution was left for 1 hr prior to the GPC analysis. The detectors and columns were thermostated at 30°C. The MWDs were obtained based on a calibration curve generated from polyether polyols standards (Mohd Noor *et al.*, 2016).

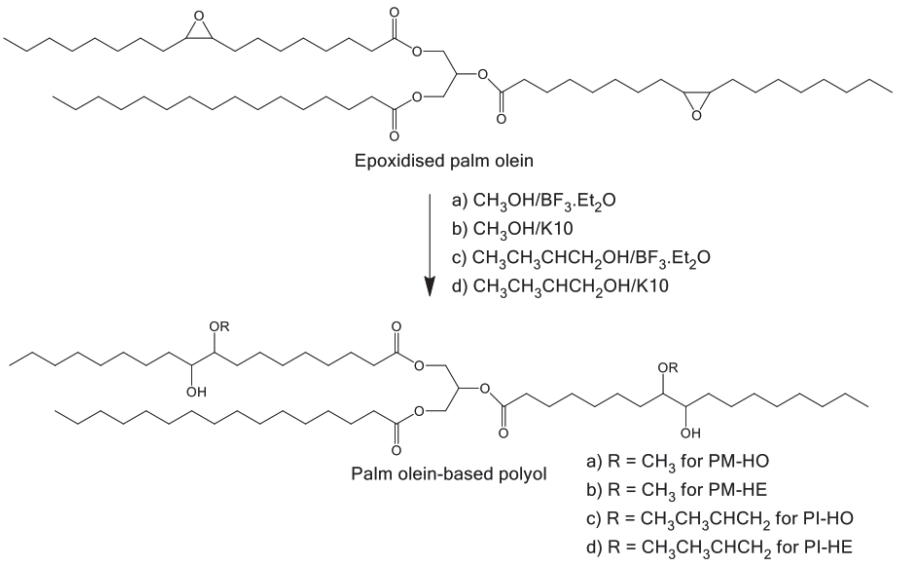

Figure 1. Idealised reaction scheme for the ring-opening reaction of EPOo with a, and b, methanol, c, and d, isobutanol, in the presence of $BF_3.Et_2O$ and K10 montmorillonite catalysts to produce palm olein-based polyols.

RESULTS AND DISCUSSION

Reaction Profile for Syntheses of Palm Olein-based Polyols

Reaction profile such as reaction time, reaction temperature and OOC conversion in syntheses of palm olein-based polyols are shown in *Table 2*. Generally, homogeneous catalyst was more active and selective compared to the heterogeneous catalyst as observed in the ring-opening reaction of EPOo with both alcohols. In the presence of homogeneous catalyst, the reaction was faster and gave high OOC conversion, and it was opposite with the heterogeneous catalyst. This situation occurred when every single catalytic entity in homogeneous catalyst acted as a single active site and accomplished the reaction as required. Interestingly, a different situation occurred when isobutanol was used as a reactant in the reaction involving heterogeneous catalyst. A branch in β-position in isobutanol had created steric hindrance in alcoholysis reaction and this helped heterogeneous catalyst to promote the reaction effectively (Rios *et al.*, 2003; 2005).

All the palm olein-based polyols either prepared using homogeneous or heterogeneous catalysts showed high conversion of OOC, *i.e.*, ≥90%. Both catalysts had played their roles in the ring-opening reaction of epoxide groups.

Properties of Palm Olein-based Polyols

The structural characteristic and the presence of functional groups in the palm olein-based polyols were identified through FTIR analysis. The disappearance of the epoxide group stretching band observed at a wavenumber of 824 and 842 cm^{-1}, confirmed the ring-opening of the EPOo as determined via OOC analysis (*Table 2*). Besides, the emergence of broad stretching band at 3450-3500 cm^{-1} for OH group was observed for all the palm olein-based polyols. Ester carbonyl stretching vibration, C-O ester stretching vibrations and ether stretching vibrations were observed at 1743 cm^{-1}, 1125-1250 cm^{-1} and 1092-1098 cm^{-1}, respectively. All these characteristics peaks confirmed the formation of palm olein-based polyol (Norhayati *et al.*, 2018; Tuan Ismail *et al.*, 2018a).

Other properties of the palm olein-based polyols are shown in *Table 3*. The epoxide ring-opening of EPOo via alcoholysis reaction is a slow reaction that requires addition of a catalyst to accelerate the rate of the reaction. Both of the catalysts used showed a high catalytic reactivity that promoted the ring-opening reaction and yielded a maximum OOC reduction for all the polyols except for PM-HE polyol, as shown in *Table 3*. The free fatty acid content in the palm olein-based polyols was low as measured by AV analysis. The AVs of palm olein-based polyols prepared using homogeneous catalyst were lower than AVs of palm olein-based polyols prepared using heterogeneous catalyst. It might be caused by the features of the catalysts themselves, where a single active site in the homogeneous catalyst is more selective towards the desired product as compared to multiple active sites in the heterogeneous catalyst (Farnetti *et al.*, 2009).

The theoretical OHV calculated from idealised structure of palm olein-based polyol prepared from EPOo and isobutanol in the presence of

TABLE 2. REACTION PROFILE FOR SYNTHESES OF PALM OLEIN-BASED POLYOLS

Types of catalyst		Alcohol	Sample designation	Reaction time	Reaction temperature (°C)	OOC conversion (%)
Homogeneous	$BF_3.Et_2O$	Methanol	PM-HO	1 hr	40-60	99
		Isobutanol	PI-HO	1 hr	60-70	98
Heterogeneous	K10	Methanol	PM-HE	23 hr	60	90
	montmorillonite	Isobutanol	PI-HE	2 hr	60	99

TABLE 3. PROPERTIES OF PALM OLEIN-BASED POLYOLS

Sample designations	Properties				
	Oxirane oxygen content (%)	Acid value (mg KOH g^{-1})	Hydroxyl value (mg KOH g^{-1})	Viscosity at 25°C (mPa.s)	Iodine value (g I_2 100 g^{-1})
PI-HO	0.04	1.5	102.6	4 533.0	7.1
PI-HE	0.03	1.0	88.6	679.5	16.0
PM-HO	0.03	0.9	95.5	780.0	4.7
PM-HE	0.32	1.4	99.0	447.5	5.8

K10 montmorillonite catalyst is 108.1 mg KOH g^{-1} (Norhayati *et al.*, 2018). All the palm olein-based polyols prepared showed their OHVs, ranging from 88.6-102.6 mg KOH g^{-1}, and some of them were incomparable to the theoretical OHV, where OHV of the polyols depend to the OOC in the EPOo. All the palm olein-based polyols are expected to have a lower degree of oligomerisation in the alcoholysis process due to an excess amount of alcohol used as reactant. Besides, the OHV of PM-HO polyol, was slightly higher, *i.e.*, 95.5 mg KOH g^{-1}, than palm olein-based polyol prepared using a similar method, *i.e.*, 83.4 mg KOH g^{-1}, in the presence of $BF_3.Et_2O$ but with a different molar ratio of EPOo to methanol of 1:1 as reported by Tuan Ismail *et al.* (2018a).

All palm olein-based polyols prepared with methanol and isobutanol exhibited significantly higher viscosities than EPOo. The viscosity of palm olein-based polyols increased with the increase of MW of reagents used in the epoxide ring-opening reaction. Palm olein-based polyols prepared using heterogeneous catalyst exhibited lower viscosity compared to the palm olein-based polyols prepared using homogeneous catalyst. PM-HE polyol exhibited the lowest viscosity. It can be ascribed to the significantly lower degree of oligomerisation of this polyol in comparison to other palm olein-based polyols. This indicates that substantial side reaction such as polymerisation and crosslinking can be minimised by using heterogeneous catalyst (Chasar *et al.*, 2005).

The presence of the unsaturated fatty chain in the palm olein-based polyol was measured by IV analysis. The IVs of all palm olein-based polyols were observed to be higher than IV of EPOo. The intramolecular elimination reaction of alkane group may occur during the distillation or drying processes of polyol at high temperature thus contributed to the increase of IV (Daley and Daley, 2005). EPOo ring-opened with methanol and isobutanol led to the formation of palm olein-based polyols with secondary hydroxyl groups (2° OH) (*Figure 1*). The sterically hindered 2° OH made it less susceptible for intermolecular epoxide ring-opening reaction.

Molecular Weights and Oligomerisation of Palm Olein-based Polyols

Number average molecular weight (M_n) values determined via GPC analysis were higher in all palm olein-based polyols than the calculated MW based on the ideal structure of palm olein-based polyols. This indicated that some oligomerisations formed during the alcoholysis process except PM-HE polyol (*Table 4*). It was further confirmed with different peaks observed in the GPC chromatogram. In general, the MW of the prepared polyols increased with an increased of MW of reactant used in the preparation of polyols. However, a similar trend was not observed for palm olein-based polyols prepared using homogeneous catalyst. It could be caused by side reaction, which had affected their MW (Chasar *et al.*, 2005).

Excess amount of alcohol present in the reaction is important to prevent polymerisation and formation of polyols having higher MW due to the reaction between the polyol molecules (Petrovic *et al.*, 2002). Palm olein-based polyols prepared using homogeneous and heterogeneous catalysts had a relatively narrow polydispersity index (PDI), *i.e.*, 1.28-1.45, regardless of the type of reactant used in the ring-opening reaction, demonstrating that the alcoholysis of epoxide ring with an excess amount of reactant led to least formation of oligomerisation. The highest PDI of 1.45 was obtained for PI-HO polyol.

The average equivalent weights and average functionalities of all palm olein-based polyols are tabulated in *Table 5*. The average functionalities were calculated from the average equivalent weights of palm olein-based polyols (from measured OHV) and molecular weight (M_n and M_w) obtained from GPC analysis. Palm olein-based polyols prepared using heterogeneous catalyst exhibited functionalities in the range of 1.67-2.28, which are approximately close to 2. Formation of two hydroxyl groups are expected (*Figure 1*) in one molecule of triglyceride (TAG) with two alkene groups. Functionalities of palm olein-based polyols prepared using homogeneous catalyst were in the range of 2.26-3.42 (*Table 5*) which were related to high degree of oligomerisation during ring-opening reaction (*Table 4*).

The OH functional oligomers that existed in EPOo were identified. OH-functional monomer and diglyceride (DAG) were observed at 32.8 min (91.1%) and 33.8 min (8.0%) of retention times and peak areas (in parenthesis), respectively (*Table 6*). Similar observations were reported by Mohd Noor *et al.* (2016), where mono-triglyceride and DAGs in EPOo were observed at 32.8 min (92.6%) and 33.7 min (7.4%) of retention times and peak areas (in parenthesis), respectively. All palm olein-based polyols prepared in this study showed comparable retention times of all peaks.

The overlaid GPC chromatograms of all palm olein-based polyols are shown in *Figure 2*. All the palm olein-based polyols exhibited a multimodal pattern in their GPC chromatograms, which indicated the formation of oligomers (Mohd Noor *et al.*, 2016; Tuan Ismail *et al.*, 2018a). A slightly lower degree of oligomerisation was observed for palm olein-based polyols prepared using heterogeneous catalyst in comparison to the palm olein-based polyols prepared using homogeneous catalyst. The highest mono composition was found in polyols prepared using heterogeneous catalyst, *i.e.*, 77.1% and 71.8% for PM-HE and PI-HE polyols, respectively

TABLE 4. MOLECULAR WEIGHT OF PALM OLEIN-BASED POLYOLS MEASURED BY GPC ANALYSIS

Sample designations	GPC			Theoretical molecular weight[a] (g mol^{-1})
	M_w (g mol^{-1})	M_n (g mol^{-1})	PDI	
PI-HO	1 795	1 237	1.45	1 024
PI-HE	1 443	1 122	1.28	1 024
PM-HO	2 008	1 528	1.31	940
PM-HE	1 219	944	1.29	940

Note: M_w - weight average molecular weight; M_n - number average molecular weight; PDI - polydispersity index; [a]Theoretical molecular weight were calculated based on the molar mass of the ideal structure of palm olein-based polyol (deeming complete conversion of epoxide group to hydroxyls in triglyceride of RBD palm olein without the formation of oligomers).

TABLE 5. CALCULATED EQUIVALENT WEIGHTS AND FUNCTIONALITIES OF PALM OLEIN-BASED POLYOLS

Sample designations	Calculated equivalent weight[a]	Calculated functionality[b]	
		MW = M_n	MW = M_w
PI-HO	546.8	2.26	3.28
PI-HE	633.2	1.77	2.28
PM-HO	587.4	2.60	3.42
PM-HE	566.7	1.67	2.15

Note: [a] Equivalent weight was calculated based on the method reported by Tuan Ismail *et al.* (2018) and Ionescu (2005).
[b] Functionality was calculated based on the method reported by Tuan Ismail *et al.* (2018) and Furniss *et al.* (1989).

TABLE 6. THE M_n, PEAK AREA AND RETENTION TIME OF THE DIFFERENT PEAKS IN GPC CHROMATOGRAMS OF EPOo AND PALM OLEIN-BASED POLYOLS

Sample designations	Sample designations				
	EPOo	PI-HO	PI-HE	PM-HO	PM-HE
Peak 1: (Tetra- and higher TAG)	-	4 596 (7.1) (29.2)	3 401 (3.0) (28.9)	4 839 (9.6) (29.0)	-
Peak 2: (Tri-TAG)	-	3 239 (7.4) (29.6)	-	3 243 (10.0) (29.6)	3 198 (1.2) (29.9)
Peak 3: (Di-TAG)	2 135 (0.9) (30.8)	2 288 (20.7) (30.6)	2 245 (14.6) (30.6)	2 220 (22.1) (30.6)	2 178 (10.4) (30.7)
Peak 4: (Mono-TAG)	1 062 (91.1) (32.8)	1 226 (59.8) (32.5)	1 243 (71.8) (32.4)	1 195 (53.3) (32.5)	1 161 (77.1) (32.6)
Peak 5: (DAG)	757 (8.0) (33.8)	855 (5.0) (33.7)	868 (10.6) (33.5)	834 (5.0) (33.7)	807 (11.3) (33.6)

Note: M_n (g mol^{-1}), peak area (%) (in parenthesis) and retention time (min) (in parentheses) of assigned OH functional palm olein oligomers.

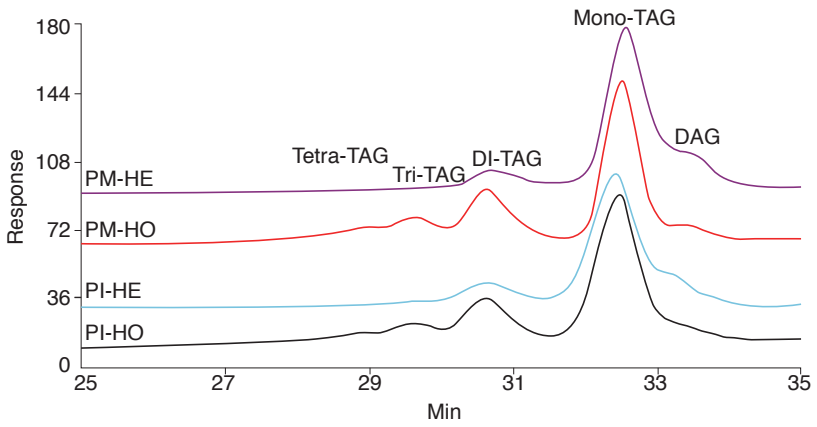

Figure 2. Overlaid of GPC chromatograms of palm olein-based polyols.

(*Table 6*). Based on GPC chromatogram, PM-HE polyol had the lowest degree of oligomerisation, where 77.1% of the total area was assigned to the OH-functional monomer, 10.4% to the dimer and 1.2% to the trimer of TAG.

The reduction of peak area of DAG was observed in palm olein-based polyols prepared using homogeneous catalyst compared to the DAG peak area measured in EPOo, *i.e.*, 8.0%. This phenomenon might be caused by oligomerisation of EPOo with DAG present in EPOo itself (Mohd Noor *et al.*, 2016). However, the increase of DAG composition in PM-HE and PI-HE polyols were detected. Limitation of heterogeneous catalyst in reactivity and selectivity possibly led to the formation of DAG, where glycerolysis of TAG might occur during the epoxide ring-opening reaction. During the glycerolysis process, an acyl moiety from TAG molecule was removed and DAG was formed. This process happened in the presence of homogeneous or heterogeneous catalysts at high temperature (Satriana *et al.*, 2016).

CONCLUSION

The physicochemical properties of palm olein-based polyols prepared using homogeneous ($BF_3.Et_2O$) and heterogeneous (K10 montmorillonite) catalysts were evaluated. Both catalysts were selected to be used in ring-opening reactions of EPOo based on their performance as reported in previous literatures. The ring-opening reaction of EPOo with methanol and isobutanol had led to faster reaction time in the presence of homogeneous catalyst with high reduction of OOC. The special feature in isobutanol has established steric hindrance in the reaction, which allowed the heterogeneous catalyst to play a role in the reaction efficiently. All the palm olein-based polyols exhibited low OHV than their theoretical OHV. The OHV of the palm olein-based polyols were dependent on their OOC in the EPOo itself. The viscosities of palm olein-based polyols prepared using heterogeneous catalyst were low as compared to palm olein-based polyols prepared using homogeneous catalyst. Increase in the MW of the reagent used in the epoxide ring-opening reaction had also increased the viscosity of palm olein-based polyol.

The obtained M_n of palm olein-based polyols prepared using homogeneous catalyst was much higher than the calculated MW based on ideal structure of palm olein-based polyol. While, palm olein-based polyols prepared using heterogeneous catalyst contain M_n values close to the theoretical MW. It clearly indicated that the degree of oligomerisation was higher in palm olein-based polyols prepared using homogeneous catalyst than heterogeneous catalyst as evidenced in GPC chromatograms that exhibited a prominent multimodal pattern. The excess of alcohols used in the reaction had minimised the polymerisation reaction and oligomerisation of the product, as shown in palm olein-based polyols prepared using both catalysts. The results from our study can serve as a reference in the production of the polyol with desired properties. The relationship between different degree of oligomerisation in polyol and polyurethane's mechanical properties could be useful for exploring target application of polyols in polyurethanes.

ACKNOWLEDGEMENT

The authors would like to thank the Director-General of MPOB for permission to publish this article. Special thanks to Zulhilmy Sulaiman, Norhidayah Ahmad Yusoff and Zailan Abu Bakar of the Advanced Oleochemical Technology Division, MPOB for their technical support. This study was funded by MPOB.

REFERENCES

Abraham, T W (2012). Chapter II: Advances in the use of BiOH® polyols in polyurethane. *Biobased Monomers, Polymers and Materials* (Smith, P B and Gross, R A eds.). ACS Symposium Series: American Chemical Society, Washington, DC. p. 165-181.

Ali, Z F; Pamela, P; Charles, L L and Charles, A E (2010). Combining the benefits of homogeneous and heterogeneous catalysis with tunable solvents and nearcritical water. *Molecules, 15(11)*: 8400-8424.

Anonymous (2019). Heterogeneous catalysis. https://courses.lumenlearning.com/boundless-chemistry/chapter/catalysts/, accessed on 24 October 2019.

AOCS (2007). Section C: Sampling and analysis of commercial fats and oils (reapproved 1997). *Official Methods and Recommended Practices of the AOCS*. 5th edition. AOCS, IL, USA.

Armylisas, S K; Hazirah, M F S; Yeong, S K and Hazimah, A H (2017). Modification of olefinic double bonds of unsaturated fatty acids and other vegetable oil derivatives via epoxidation: A review. *Grasas Y Aceites, 68(1)*: e174.

Arniza, M Z; Hoong, S S; Idris, Z; Yeong, S K; Hassan, H A; Din, A K and Choo, Y M (2015). Synthesis of transesterified palm olein-based polyol and rigid polyurethane from this polyol. *J. Amer. Oil Chem. Soc., 92*: 243-255.

Banerjee, A K; Maldonado, A; Arrieche, A D; Bedoya, L; Vera, W J; Cabrera, E V and Poon, P S (2019). Boron trifluoride etherate in organic synthesis. *MOJ Biorg. Org. Chem., 3(1)*: 1-9.

Clark, J (2013). Types of catalysis. https://www.chemguide.co.uk/physical/catalysis/introduction.html, accessed on 24 October 2109. p. 1-7.

Chasar, D W; Hills, S and Hughes, M J (2005). Method of making oleochemical oil-based polyols. *US Patent 6, 891, 053 B2*.

Daley, R F and Daley, S J (2005). Elimination reaction. *Organic Chemistry*. www.ochem4free.com, accessed on 7 February 2017.

Farnetti, E; Di Monte, R and Kašpar, J (2009). Homogeneous and heterogeneous catalysis. *Inorganic and Bio-Inorganic Chemistry*, Vol. 2, Oxford, United Kingdom: Eolss Publishers Co. Ltd. p. 50-86.

Fási, A; Pálinkó, I; Gömöry, A and Kiricsi, I (2004). Ring opening, dimerization and oligomerisation reactions of methyloxirane on solid acid and base catalysts. *J. Mol. Catal. A Chem., 2008*: 307-311.

Flora, E F (2014). The selection reaction of homogeneous catalyst in soy-epoxide hydroxylation. *J. Phys.: Conf. Ser., 495*: 012013.

Furniss, B S; Hannaford, A J; Smith, P W G and Tatchell, A R (1989). *Vogel's Textbook of Practical Organic Chemistry*. 5th edition. Longman Scientific and Technical. Longman Group UK Ltd. London, England. p. 487.

Hazimah, A H; Tuan Noor Maznee, T I; Mohd Norhisham, S; Hoong, S S; Ooi, T L; Salmiah, A; Kosheela Devi, P P and Cheong, M Y (2011). Process to produce polyols. *US Patent 7, 932, 409 B2*.

Ionescu, M (2005). *Chemistry and Technology of Polyols for Polyurethanes*. Rapra Technol Ltd. Shawbury, England. p. 32-41.

Johannes, G D V and David, S J (2012). Homogeneous and heterogenous catalysis in industry. *Catal. Sci. Technol., 2*: 2009.

Li, Y; Luo, X and Hu, S (2015). Polyols and polyurethanes from vegetable oils and their derivatives. *In: Bio-based polyols and polyurethanes. SpringerBriefs in Molecular Science*. Springer, Cham. p. 15-43.

Lin, B; Yang, L; Dai, H and Yi, A (2008). Kinetic studies on oxirane cleavage of epoxidized soybean oil by methanol and characterization of polyols. *J. Amer. Oil Chem. Soc., 85(2)*: 113-117.

Lozada, Z; Suppes, G J; Tu, Y C and Hsieh, F H (2009). Soy-based polyols from oxirane opening by alcoholysis reaction. *J. Appl. Polym. Sci., 113(4)*: 2552-2560.

Mohd Noor, M A; Sendijarevic, V; Hoong, S S; Sendijarevic, I; Tuan Ismail, T N M; Hanzah, N A H; Mohd Noor, N; Kosheela Devi, P P; Ghazali, R and Abu Hassan, H (2016). Molecular weight determination of palm olein polyols by gel permeation chromatography using polyether polyols calibration. *J. Amer. Oil Chem. Soc., 93*: 721-730.

Narine, S S; Kong, X; Bouzili, L and Sporns, P (2007a). Physical properties of polyurethanes produced from polyols from seed oils: I. Elastomers. *J. Amer. Oil Chem. Soc., 84*: 55-63.

Narine, S S; Yue, J and Kong, X (2007b). Production of polyols from canola oil and their chemical identification and physical properties. *J. Amer. Oil Chem. Soc., 84*: 173-179.

Norhayati, M N; Tuan Ismail, T N M; Yeong, S K and Hazimah, A H (2013). Synthesis of palm-based polyol: Effect of K10 montmorillonite catalyst. *J. Oil Palm Res., 25(1)*: 92-99.

Norhayati, M N; Tuan Ismail, T N M; Hoong, S S; Nurul 'Ain, H; Srihanum, A; Kosheela Devi, P P; Mohd Norhisham, S; Yeong, S K and Hazimah, A H (2016). Reproducibiltiy of palm-based polyols production. *J. Oil Palm Res., 28(281)*: 114-120.

Norhayati, M N; Hoong, S S; Tuan Ismail, T N M; Nurul 'Ain, H; Yeong, S K and Zainab, I (2018). Performance of recycled K10 montmorillonite catalyst in the alcoholysis of epoxidised palm olein. *J. Oil Palm Res., 30(2)*: 326-337.

Parveez, G K A; Hishamuddin, E; Loh, S K; Ong-Abdullah, M; Salleh, K M; Zanal Bidin, M N I; Sundram, S; Azizul Hasan, Z A and Idris, Z (2020). Oil palm economic performance in Malaysia and R&D progress in 2019. *J. Oil Palm Res., 32(2)*: 159-190.

Petrovic, Z; Javni, I; Guo, A and Zhang, W (2002). Method of making natural oil-based polyols and polyurethane thereform. *US patent 6433121 B1*.

Piet, W N M V L (2004). *Homogeneous catalysis, Understanding the Art*. Dordrecht, Kluwer Academic Publishers. The Netherland. p. 1-10.

Rios, L A; Weckes, P P; Schuter, H; Hausmann, H and Hölderich, W F (2003). Modification and characterization of aluminosilicates used for nucleophilic addition of alcohols to epoxidized oils. *Appl. Catal. A- Gen., 253*: 487-497.

Rios, L A; Weckes, P P; Schuter, H and Hölderich, W F (2005). Resin catalyzed alcoholysis of epoxidized fatty esters: Effect of the alcohol and the resin stuctures. *Appl. Catal. A- Gen., 284*: 155-161.

Satriana Arpi, N; Lubis, Y M; Adisaluman; Supardan, M D and Mustapha, W A W (2016). Diacylgylcerol-enriched oil production using chemical glycerolysis. *Eur. J. Lipid Sci. Technol, 118*: 1880-1890.

Seigfried, K F P; Ruth, G; Hans-Peter, N and Hölderich, W F (2002). Alcoholysis of triacyglycerols by heterogeneous catalysis. *Eur. J. Lipid. Sci. Technol., 104*: 324-330.

Silverajah, V S G; Ibrahim, N A; Zainuddin, N; Wan Yunus, W M Z and Abu Hassan, H (2012). Mechanical, thermal and morphology properties of poly(lactic acid)/epoxidized palm olein blend. *Molecules, 17(10)*: 11729-11747.

Siti Munira, Y; Mohd, A F and Rahmah, M (2013). Synthesis and characterization of palm oil based polyol. *Adv. Mat. Res., 812*: 275-280.

Tuan Ismail, T N M; Mohd Noor, M A; Hoong, S S; Poo Palam, K D; Yeong, S K and Idris, Z (2018a). Oligomeric composition of palm olein-based polyols: The effect of nucleophiles. *Eur. J. Lipid Sci. Technol., 120(4)*: 1700354.

Tuan Ismail, T N M; Ibrahim, N A; Mohd Noor, M A; Hoong, S S; Poo Palam, K D; Yeong, S K; Idris, Z; Schiffman, C M; Sendijarevic, I; Abd Malek, E; Zainuddin, N and Sendijarevic, V (2018b). Oligomeric composition of polyols from fatty acid methyl ester: The effect of ring-opening reactants of epoxide groups. *J. Amer. Oil Chem. Soc., 95*: 509-523.

Journal of Oil Palm Research Vol. 34 (1) March 2022 p. 177-183
DOI: https://doi.org/10.21894/jopr.2020.0108

SENSORY EVALUATION OF FILLETS FROM TILAPIA (*Oreochromis niloticus*) FED DIETS CONTAINING OIL PALM LIPIDS

WAN NOORAIDA, W M[1]*; ABIDAH, M N[1]; NUR ATIKAH, I[1]; MOOKIAH, S[1]
MUHAMMAD AMIRUL, F[1] and RAFIDAH, A H[1]

ABSTRACT

This study aimed to investigate the effects of feeding tilapia (Oreochromis niloticus) *with a diet containing oil palm lipids on the sensory evaluation of tilapia fillet in relation to commercial and control feeds. Six tilapia fish grower diets were formulated with the inclusion of emulsified palm fatty acid distillate (Malaysian Palm Oil Board-High Energy, MPOB-HIE) and crude palm oil (CPO) at 5%, 8% and 10%. The negative control diet was made using similar raw materials, but without the inclusion of any lipid, while the commercial diet was used as a positive control. Thirty panellists were recruited from the staff of the Malaysian Palm Oil Board and students, without any specific priority in selection. Each panellist was required to evaluate steamed fish fillet samples on six attributes, namely colour, texture (firmness and sliminess), aroma, taste and overall quality using a nine-point hedonic scale of a quantitative descriptive analysis method. There were no significant differences (*p>*0.05) in all sensory attributes among fillets of tilapia fed with different dietary treatments. The results of this study suggest that the incorporation of CPO and MPOB-HIE in tilapia feed formulation did not impart any negative effects on the sensory properties of the tilapia fillets.*

Keywords: crude palm oil, sensory evaluation, tilapia fillet.

Received: 2 June 2020**; Accepted:** 29 September 2020**; Published online:** 9 December 2020.

INTRODUCTION

Aquaculture is one of the major sectors in Malaysia that contributes to the economy of the nation and to the income of local fishers. In 2017, the total fishery production of the country amounted to 1.7 million tonnes, with 1.5 and 0.2 million tonnes of both fisheries and aquaculture productions, respectively (FAO, 2019). The overall demand for fish in Malaysia is projected to increase to around 1.93 million tonnes by 2020 (Yusoff, 2015). The rise in demand for fish is attributed to the increasing population and preferences for fish consumption. Fish is one of the nutritious foods that contain high-quality proteins, vitamins and minerals. The availability of local fish, derived from 65% of coastal fisheries and the remaining from deep-sea fishing, has contributed to positive food security and will increase foreign exchange earnings through the production of value-added fish and fishery products for international trade (Yusoff, 2015).

Tilapia (*Oreochromis niloticus*), also known as Nile tilapia, is a lean fish species found in warm waters with good commercial potential (Bolivar *et al*., 2004). Tilapia is the second most farmed fish in the world and its production has quadrupled over the last decade due to the ease of aquaculture, marketability and stable market prices (Wang and Lu, 2016). Tilapia and value-added tilapia products are also classified as food fish and cash crops in developing countries, particularly in Asia (Abdel-Fattah, 2019). Tilapia has been a popular freshwater species reared by farmers in Malaysia due to its high demand and affordability. The production of tilapia culture began with a land-

[1] Malaysian Palm Oil Board,
6 Persiaran Institusi, Bandar Baru Bangi,
43000 Kajang, Selangor, Malaysia.

* *Corresponding author e-mail: wannooraida@mpob.gov.my*

based system followed by floating net cages and, recently, by polar-circle high-density polyethylene cages to increase productivity. Tilapia aquaculture must follow sustainable practices for continued production and improved sustainability (Wang and Lu, 2016). Local tilapia production reached 35 400 t in 2015, priced at RM248 million (Metro News, 2016). The Malaysian Department of Fisheries has set a tilapia development target of 130 000 t by 2020 to meet the national demand. Traditionally, tilapia has been exported to other countries in a variety of product forms, such as frozen fillets (*Figure 1*) and whole fish (Conte *et al*., 2014), but lately frozen fillets, which have been offered in various sizes and packaging styles, have become more common and convenient and more favoured by consumers.

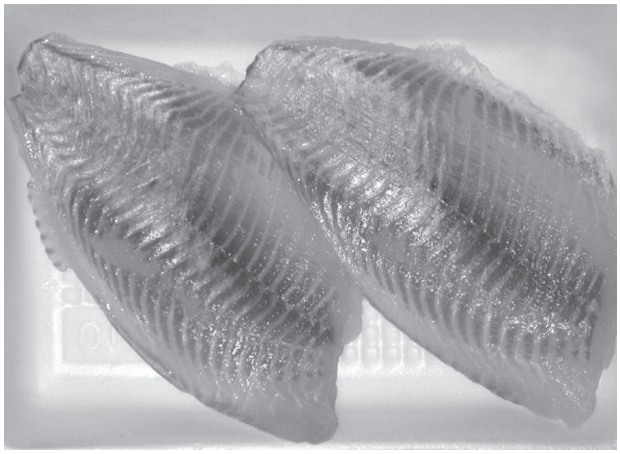

Source: Ng and Bahurmiz (2010).

Figure 1. Frozen tilapia fish fillets offered in the market.

Feed plays an important role in influencing the performance of cultivated fish (*e.g*., tilapia, carp, catfish and trout) and is influenced by factors such as behaviour of fish, stocking density, feed quality, daily ration size, feeding frequency and water temperature (Firew *et al*., 2019). About 70% of the total cost of fish production is from fish feeds, which is the highest cost in fish farming operations (Paul *et al*., 2018). Fish oil is commonly used in the processing of fish feed as a source of energy, but supplies are very limited. Since the price of fish oil is too expensive, replacing the energy source with vegetable oils can be an alternative to the conventional fish oil as well as reducing the dependency on imported corn grain in the fish feed industry due to stable prices and abundant supply (Babalola and Apata, 2012).

Being the world's most-produced vegetable oil, crude palm oil (CPO) could potentially be an alternative to fish oil in aquafeeds (Ng, 2006). CPO is rich in carotenes (provitamin A) and vitamin E consisting of tocopherols and tocotrienol homologues (Nesaretnam and Muhammad 1993). Carotenes and vitamin E have strong antioxidant properties (Loganathan *et al*., 2009). CPO also contains a high proportion of essential fatty acid (EFA), *i.e*., linoleic acid. Palm fatty acid distillates (PFAD), which have a subsubstantial quantity of nutritious micronutrients, such as vitamin E, is a by-product obtained during CPO refining (Bonnie and Yusof, 2009). The Malaysian Palm Oil Board-High Energy (MPOB-HIE) is a specialty feed ingredient formulated using PFAD and a food grade emulsifier (Wan Nooraida and Abidah, 2020). The role of the emulsifier is to improve the digestion of lipids by the animals (Osman *et al*., 2009).

Oil palm lipids, especially CPO and PFAD, have an enormous potential to be used in fish diets and a bright future in the aquaculture sector based on their nutritional values and economic price. Both CPO and PFAD also have a positive impact on improving the quality of fish flesh (Ng, 2004). A study conducted by Ng and Bahurmiz (2010) found that tilapia fillets fed with oil-based palm diets exhibit higher oxidative stability during frozen storage than tilapia fillets fed with fish oil-based diets. Improving oxidative stability, in turn, can help to extend the shelf-life of tilapia fillets.

Supplementation of natural antioxidants (carotenoids and vitamin E) rich in oil palm lipids in the fish feed formulation can add value to the final products as these antioxidants could be deposited in fish fillets. The antioxidants could improve the oxidative stability of tilapia fillets. Tilapia fillets fed diet supplemented with other vegetable oils containing a significant amount of omega-6 polyunsaturated fatty acids (PUFA) that are easily oxidised, making the final products easily rancid. Ng *et al*. (2004) observed an accumulation of the natural palm vitamin E in the tilapia fillets by feeding tilapia fish with diets supplemented with a palm-based tocotrienol-rich fraction (TRF). The presence of the palm TRF in the tilapia fillet provides strong oxidative stability to the tilapia fillets (Ng *et al*., 2006). Moreover, the low concentration of PUFA in oil palm lipids also helps to reduce the effects of oxidation (Ng *et al*., 2013). Thus, the combination of these two factors decreased the incidence of rancidity in fish fillets. In addition, freshness, taste and long-term storage properties of the fish fillet are relatively increased when fed the oil palm lipid sources.

Freshness is an important quality parameter in fish and fish products and is of great concern in the fish sector and fish inspection service (Martinsdottir, 2002; Martinsdottir *et al*., 2000). Sensory is the most relevant tool for evaluating freshness in fisheries. Sensory assessment is characterised as a scientific approach to stimulating, quantifying, assessing and interpreting food and material-related reactions of people through vision, smell, taste, touch and hearing (Huss, 1995). Sensory evaluation needs

to be carried out to determine the acceptability of food products by the customer, leading to effective product adjustment and efficient market launch. The goal of this study was therefore to investigate the effect of feeding tilapia fish with diet containing oil palm lipids (MPOB-HIE and CPO) on the sensory evaluation of tilapia fish fillets in comparison to commercial and control feeds.

MATERIALS AND METHODS

Materials

Mixed-sex tilapia fingerlings (*Oreochromis niloticus*) were purchased from Aqasia Aquatic, Seremban, Negeri Sembilan, Malaysia and transported alive to the Feed Research Group, MPOB Keratong Research Station, Pahang, Malaysia. Raw materials for floating tilapia fish feed production (fishmeal, soybean meal, corn, broken rice, wheat pollard and feed additives) were purchased from local suppliers. PFAD and CPO were obtained from Felda Vegetable Oil Product (FVOP), Gebeng, Pahang. Starter and grower floating tilapia fish feeds were produced using an extruder machine at Shuzam Feedmill, Seremban 2, Negeri Sembilan. The commercial feed, Cargill® was purchased from a local supplier in Segamat, Johor, Malaysia.

Feeding Trial

Feed formulations of tilapia starter and grower diets are shown in *Tables 1* and *2*, respectively. Control feed (CNT) was made using similar raw materials with treatment feeds, but without any oil palm lipids inclusion as negative control while commercial feed (COM) was used as positive control. The proximate composition of starter and grower feeds are presented in *Tables 3* and *4*, respectively. All treatments, CNT and COM feeds met the recommended starter and grower feed requirements for tilapia fish (Malaysia Standard, 2013). A total of 600 tilapia fingerlings with an initial mean weight of about 23.0 g were randomly allocated to the eight treatments with three replications per treatment (n=25). All tilapia fish were fed with the commercial feed diet for the first two weeks during the adaptation period and continued with the experimental feed diets for the subsequent 22 weeks. Starter feeds were fed to the tilapia fish from Week 2 to Week 12 followed by grower feeds from Week 13 to Week 24. Six fish per replication were randomly selected for sensory evaluation at Week 24.

TABLE 1. TILAPIA STARTER FEED FORMULATION

Ingredients	MPOB-HIE			CPO			CNT
	5%	8%	10%	5%	8%	10%	
Fishmeal	10.00	7.00	5.00	10.00	7.00	5.00	7.00
Soybean meal	46.50	51.00	54.00	46.50	51.00	54.00	46.00
Corn	18.80	14.30	11.30	18.00	13.50	10.50	20.00
Broken rice	15.00	15.00	15.00	15.80	15.80	15.80	22.30
Wheat pollard	0.50	0.50	0.50	0.50	0.50	0.50	0.50
MPOB-HIE	5.00	8.00	10.00	0.00	0.00	0.00	0.00
CPO	0.00	0.00	0.00	5.00	8.00	10.00	0.00
Feed additives*	4.20	4.20	4.20	4.20	4.20	4.20	4.20

Note: CNT - control diet; CPO - diet containing crude palm oil; MPOB-HIE - diet containing emulsified palm fatty acid distillates. *Feed additives consist of dicalcium phosphate, calcium propionate, fish hydrolysate, vitamin and mineral premixes.

TABLE 2. TILAPIA GROWER FEED FORMULATION

Ingredients	MPOB-HIE			CPO			CNT
	5%	8%	10%	5%	8%	10%	
Fishmeal	5.00	5.00	5.00	5.00	5.00	5.00	5.00
Soybean meal	48.00	48.60	49.00	48.00	48.60	49.00	42.90
Corn	17.30	13.70	11.30	17.30	13.70	11.30	20.00
Broken rice	20.00	20.00	20.00	20.00	20.00	20.00	27.40
Wheat pollard	0.50	0.50	0.50	0.50	0.50	0.50	0.50
MPOB-HIE	5.00	8.00	10.00	0.00	0.00	0.00	0.00
CPO	0.00	0.00	0.00	5.00	8.00	10.00	0.00
Feed additives*	4.20	4.20	4.20	4.20	4.20	4.20	4.20

Note: CNT - control diet; CPO - diet containing crude palm oil; MPOB-HIE - diet containing emulsified palm fatty acid distillates. *Feed additives consist of dicalcium phosphate, calcium propionate, fish hydrolysate, vitamin and mineral premixes.

TABLE 3. PROXIMATE COMPOSITION OF TILAPIA STARTER FISH FEED

Proximate analysis (%)	MPOB-HIE			CPO			CNT	COM	Standard specification*
	5%	8%	10%	5%	8%	10%			
Moisture	11.36 ± 0.40	11.24 ± 0.19	8.25 ± 0.34	8.77 ± 0.16	8.27 ± 0.09	8.13 ± 0.22	8.78 ± 0.12	8.58 ± 0.14	Max, 12
Ash	5.93 ± 0.03	5.71 ± 0.02	5.93 ± 0.01	5.81 ± 0.12	5.85 ± 0.06	6.04 ± 0.03	6.21 ± 0.03	7.79 ± 0.04	-
Crude fat	5.17 ± 0.001	7.82 ± 0.001	10.01 ± 0.005	5.17 ± 0.007	8.44 ± 0.002	9.41 ± 0.005	0.86 ± 0.001	3.89 ± 0.003	Min, 5
Crude protein	33.46 ± 0.04	33.66 ± 0.13	33.11 ± 0.17	32.91 ± 0.07	33.10 ± 0.03	33.44 ± 0.06	33.34 ± 0.02	37.07 ± 0.03	Min, 30
Crude fibre	3.92 ± 1.04	3.86 ± 0.22	2.49 ± 0.81	2.58 ± 0.60	3.13 ± 0.22	3.75 ± 0.75	2.17 ± 0.49	1.79 ± 1.31	Max, 8
Energy (cal g^{-1})	4 242 ± 8.9	4 295 ± 7.6	4 241 ± 20.1	4 214 ± 24.9	4 223 ± 6.4	4 186 ± 15.1	4 056 ± 6.5	4 164 ± 64.1	-

Note: CNT - control diet; COM - commercial diet; CPO - diet containing crude palm oil; MPOB-HIE - diet containing emulsified palm fatty acid distillates.

Source: *Malaysian Standard (2013).

TABLE 4. PROXIMATE COMPOSITION OF TILAPIA GROWER FISH FEED

Proximate analysis (%)	MPOB-HIE			CPO			CNT	COM	Standard specification*
	5%	8%	10%	5%	8%	10%			
Moisture	10.88 ± 0.26	14.75 ± 0.16	10.43 ± 0.16	10.61 ± 0.19	10.52 ± 0.27	10.14 ± 0.13	10.59 ± 0.30	6.95 ± 0.29	Max, 12
Ash	5.74 ± 0.01	5.29 ± 0.02	5.85 ± 0.01	5.63 ± 0.02	5.74 ± 0.01	5.81 ± 0.02	6.24 ± 0.01	8.74 ± 0.01	-
Crude fat	5.74 ± 0.009	8.92 ± 0.006	9.66 ± 0.002	5.18 ± 0.002	7.62 ± 0.002	9.22 ± 0.002	0.47 ± 0.003	3.60 ± 0.000	Min, 5
Crude protein	31.25 ± 0.13	30.61 ± 0.16	31.14 ± 0.11	31.03 ± 0.04	31.33 ± 0.23	31.76 ± 0.16	32.20 ± 0.11	31.32 ± 0.12	Min, 25
Crude fibre	3.76 ± 0.17	3.96 ± 0.12	2.83 ± 0.21	3.09 ± 0.14	3.53 ± 0.13	4.23 ± 0.55	3.91 ± 0.20	3.28 ± 0.43	Max, 8
Energy (cal g^{-1})	4 068 ± 38.6	4 210 ± 19.7	4 011 ± 23.6	4 099 ± 6.6	4 223 ± 29.0	3 802 ± 37.5	3 926 ± 37.4	3 239 ± 20.3	-

Note: CNT - control diet; COM - commercial diet; CPO - diet containing crude palm oil; MPOB-HIE - diet containing emulsified palm fatty acid distillates.

Source: *Malaysian Standard (2013).

Sensory Evaluation

Thirty panellists were recruited from the staff of the Malaysian Palm Oil Board (MPOB) and students. The panellists have been introduced to basic knowledge about sensory evaluation and have been screened for the thresholds of four basic tastes - sweet, salty, sour and bitter. Smell test to identify common flavour related to oils and fats was also carried out to determine their smell sensitiveness. The finalists of the panellists were all with a passing mark of more than 75%. During the sensory evaluation, each panellist was asked to evaluate five steamed fish fillet samples at one time using a quantitative descriptive analysis method.

Sensory evaluation was carried out at the Sensory Laboratory, MPOB Bangi, Selangor, Malaysia (*Figure* 2). Tilapia fillets fed 5%, 8% and 10% MPOB-HIE and 5%, 8% and 10% CPO feed diets were compared against fillet from tilapia fed COM and CNT feed diets. The evaluation was based on six attributes, namely colour, texture (firmness and sliminess), aroma, taste and overall quality, using a nine-point hedonic scale. Scale 1 indicates the least preferable score, while nine indicates the highest or most acceptable score. The fish fillets were trimmed from the belly to the tail, cut into 3.8 cm-5.1 cm (1.5-2.0 in) cubes and steamed for 3 min before serving to the panellist. The fish fillet samples were individually blind-coded, labelled in three digits and placed on a clean plate (*Figure 3*).

Figure 2. Sensory evaluation by the panellists at Sensory Laboratory.

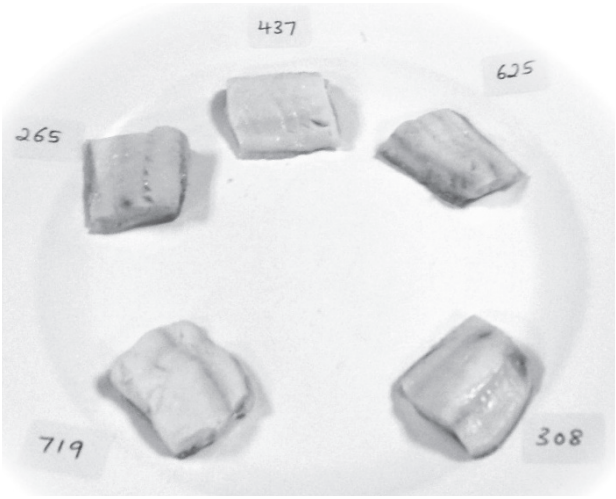

Figure 3. Fish fillet samples with random three digit numbers.

Statistical Analysis

All data collected were subjected to statistical analysis with analysis of variance (ANOVA) and mean differences among treatments were analysed by Duncan's Multiple Range Test using SAS 9.1™ statistical package (SAS Institute Inc. Cary, North Carolina, USA). Differences were considered statistically significant when $p<0.05$.

RESULTS AND DISCUSSION

The sensory evaluation scores for tilapia fillets fed with MPOB-HIE, CPO, COM and CNT diets are as tabulated in *Table 5* and graphically illustrated in *Figure 4*. There were no significant differences ($p>0.05$) in all sensory attributes among tilapia fillets fed with different diets. Tilapia fed MPOB-HIE and CPO were fairly accepted by the panellists and were comparable to tilapia fillets fed CNT and COM diets. These results are consistent with Ng and Bahurmiz (2010) since tilapia with various dietary oil sources (fish oil, CPO, PFAD and refined, bleached and deodourised palm oil) has had little effect on sensory attributes. In addition, Ochang *et al*. (2007) conducted a study on the effect of different levels of dietary palm oil on the organoleptic properties of juvenile Nile tilapia. Similar results with our current research have been documented, with no significant differences in the sensory attributes between treatment diets were observed.

In terms of colour, fillet from tilapia fed 5% MPOB-HIE received numerically highest score (mean = 6.43 ± 1.19) as compared with that of the other treatments. According to Nair *et al*. (2017), fish fillet colour plays an important role in a consumer's purchasing decision and fish fillets

TABLE 5. MEANS OF SENSORY ATTRIBUTES OF MPOB-HIE, CPO, COMMERCIAL AND CONTROL TREATMENTS

Attributes	Treatment								*p*-value
	5% MPOB-HIE	8% MPOB-HIE	10% MPOB-HIE	5% CPO	8% CPO	10% CPO	COM	CNT	
Colour	6.43 ± 1.19	5.60 ± 1.43	5.63 ± 2.24	6.07 ± 1.36	6.07 ± 1.31	5.77 ± 1.70	6.20 ± 1.62	5.72 ± 1.58	0.26
Firmness	5.27 ± 1.68	5.20 ± 1.88	5.10 ± 1.67	5.00 ± 1.68	4.73 ± 1.76	5.07 ± 1.74	5.08 ± 2.01	5.18 ± 1.81	0.97
Sliminess	5.87 ± 1.66	5.70 ± 1.84	5.93 ± 2.05	5.57 ± 2.01	5.33 ± 2.00	5.53 ± 1.68	5.17 ± 1.99	5.62 ± 1.83	0.64
Aroma	5.73 ± 1.62	5.67 ± 1.69	5.53 ± 1.59	5.33 ± 1.52	5.50 ± 1.31	5.70 ± 1.62	5.55 ± 1.71	5.47 ± 1.52	0.98
Taste	6.00 ± 1.62	6.17 ± 1.84	5.70 ± 1.56	5.67 ± 1.65	5.67 ± 1.71	5.80 ± 1.61	5.87 ± 1.69	5.62 ± 1.39	0.85
Overall quality	6.00 ± 1.64	6.07 ± 1.78	5.93 ± 1.70	6.00 ± 1.74	6.00 ± 1.82	5.97 ± 1.47	5.97 ± 1.69	5.77 ± 1.41	0.99

Note: COM - commercial diet; CNT - control diet; CPO - diet containing crude palm oil; MPOB-HIE - diet containing emulsified palm fatty acid distillates.

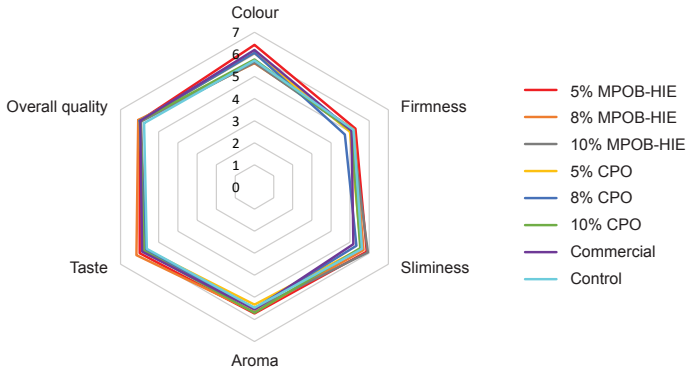

Figure 4. Sensory evaluation of fillets from tilapia fed diet containing emulsified palm fatty acid distillate (MPOB-HIE), crude palm oil (CPO), control and commercial diets.

that deviate from the typical white flesh colour are less marketable. Fillet of tilapia fed 5% MPOB-HIE also showed the most desirable results in terms of firmness and aroma. The firmness of cooked fish is influenced by the type of fish, but the flesh should look intact, be able to pull out and the meat remain chunky while poking with a fork. According to Ng and Bahurmiz (2010), fish fillets fed with the PFAD diet were considered to be substantially softer than fish fillets fed with the CPO diet, which is contrary to our current study. For aroma attributes, all treatment groups had a mean score ranging from 5.33-5.73, which expressed moderate acceptance towards the smell of fish fillet samples. Ng (2006) reported that supplementation of CPO and PFAD, which are rich in vitamin E in the fish diet, could prevent the production of off-odour and could improve freshness and preserve fish fillets over a longer period of time. With regard to sliminess, fillet of tilapia fed 10% MPOB-HIE diet received the most acceptable score compared to other treatment groups. Meanwhile, fillet of tilapia fed 8% MPOB-HIE received the highest or most desirable taste and overall quality ratings. Our results are consistent with those of Drewnowski and Almiron-Roig (2010) that, apart from providing a dietary energy source for daily consumption, the addition of fat to food may also contribute to human preferences in terms of texture, taste and smell.

CONCLUSION

The findings of this study indicated that palm oil lipids, *i.e*., CPO and MPOB-HIE can be successfully used in fish feed formulations to substitute fish oil dietary without adverse effects on sensory evaluation by the panellists. Considering the availability of oil palm lipid sources at affordable prices, as well as the acceptance of sensory attributes of fish fillets, there is a strong opportunity for the oil palm industry to provide alternative dietary lipid in the aqua feed industry.

ACKNOWLEDGEMENT

The authors would like to thank the Director-General of MPOB for permission to publish this article. The authors also thank the staff of Feed Research Group, MPOB Keratong Research Station for their contribution in ensuring the success of this study.

REFERENCES

Abdel-Fattah, M E (2019). *Tilapia Culture.* 2nd edition. Academic Press. 358 pp.

Babalola, T O and Apata, D F (2012). Effects of dietary lipid source on growth, digestibility and tissue fatty acid composition of *Heterobranchus longifilis* fingerlings. *J. Agric. Rural Dev. Trop. Subtrop.*, *113(1)*: 1-11.

Bolivar, R B; Mair, G C and Fitzsimmons, K (2004). New dimensions in farmed tilapia. *Proc. Sixth Int. Symposium Tilapia Aquaculture.* Manila, Philippines. p. 241-248.

Bonnie, T Y P and Yusof, M (2009). Characteristic and properties of fatty acid distillates from palm oil. *Oil Palm Bulletin, 59*: 5-11.

Conte, F; Passantino, A; Long, S and Voslarova, E (2014). Consumers' attitude towards fish meat. *Ital. J. Food Saf., 3(3)*: 178-181.

Drewnowski, A and Almiron-Roig, E (2010). Human perceptions and preferences for fat-rich foods. *Fat Detection: Taste, Texture and Post Ingestive Effects* (Montmayeur, J P and Le Coutre, J eds.). Boca Raton (FL): CRC Press/Taylor and Francis. 646 pp.

FAO (2019). Fishery and aquaculture country profiles. Malaysia. FAO Fisheries and Aquaculture Department (online). http://www.fao.org/fishery, accessed on 10 April 2020. 8 pp.

Firew, A H; Abebe, G and Mulugeta, W (2019). The process of tilapia feed formulation and implementation in pond aquaculture: Low cost and locally available ingredients option for small-scale farmers. *J. Agric. Aquac.*, *1(2)*: 1-14.

Huss, H H (1995). Quality and quality changes in fresh fish. *FAO Fisheries Technical Paper*. 348 pp.

Loganathan, R; Selvaduray, K R; Radhakrishnan, A and Nesaretnam, K (2009). Palm oil: Rich in health promoting phytonutrients. *Palm Oil Developments, 50*: 16-25.

Malaysian Standard (2013). *MS 2538:2013 Formulated Fish Feed – Specification*. Department of Standards Malaysia. 7 pp.

Martinsdottir, E; Sveinsdottir, K and Olafsdottir, G (2000). *Development and Implementation of a Computerized Sensory System (QIM) for Fish Freshness*. Project Report CRAFT FAIR FA-S2-9063. p. 18.

Martinsdóttir, E (2002). Quality management of stored fish. *Safety and Quality Issues in Fish Processing* (Bremmer, H A ed.). Woodhead Publishing Limited, United Kingdom. p. 360-378.

Metro News (2016). Dept. sets high target for tilapia production. https://www.thestar.com.my/metro/community/2016/06/27/dept-sets-high-target-for tilapia-production/, accessed on 10 April 2020.

Nair, M N; Costa-Lima, B R C; Schilling, M W and Suman, S P (2017). Chapter 10 - Proteomics of color in fresh muscle foods. *Proteomics in Food Science*. (Colgrave, M L ed.). Academic Press. p. 163-175. DOI: 10.1016/B978-0-12-804007-2.00010-2.

Nesaretnam, K and Muhammad, B (1993). Nutritional properties of palm oil. *Selected Readings on Palm Oil and its Uses*. PORIM, Bangi. p. 57-67.

Ng, W K (2004). Palm oil as a novel dietary lipid sources in aquaculture feeds. *Palm Oil Developments*, *41*: 14-18.

Ng, W K; Wang, Y and Yuen, K H (2004). Tocotrienols from palm oil are more potent antioxidants than dietary α-tocopherol acetate or α-tocopherol succinate for red hybrid tilapia. *Proc. of the Eleventh International Symposium on Nutrition and Feeding in Fish*. Phuket, Thailand. p. 46.

Ng, W K (2006). Palm oil: Malaysia's gift to the global aquafeed industry. *Asian Aquafeeds*: *Current Developments in the Aquaculture Feed Industry* (Ng, W K and Ng, C K eds.). Malaysian Fisheries Society Occasional Publication No. 13. p. 40-54.

Ng, W K; Wang, Y and Yuen, K H (2006). Vitamin E levels in tilapia diets affect fillet quality. https://www.aquaculturealliance.org/advocate/vitamin-e-levels-in-tilapia-diets-affect-fillet-quality/, accessed on 12 September 2020. 8 pp.

Ng, W K and Bahurmiz, O M (2010). Palm oil replaces fish oil in tilapia feed: Substitution also increases shelf life. *Global Aquaculture Advocate*, *March/April 2010*. p. 69-70.

Ng, W K; Chong, C Y; Wang, Y and Romano, N (2013). Effects of dietary fish and vegetable oils on the growth, tissue fatty acid composition, oxidative stability and vitamin E content of red hybrid tilapia and efficacy of using fish oil finishing diets. *Aquaculture*, *372-375*: 97-110.

Ochang, S N; Fagbenro, O and Adebayo, O T (2007). Influence of dietary palm oil on growth response, carcass composition, haematology and organoleptic properties of juvenile Nile Tilapia, *Orechromis niloticus*. *Pak. J. Nutr.*, *6(5)*: 424-429.

Osman, A; Farah Nurshahida, M S and Jumardi, R (2009). MPOB-HIE as a high energy fat supplement for lactating dairy cows. *MPOB Information Series, 439*: 2 pp.

Paul, A K; Rahman, M M; Rahman, M M and Islam, M S (2018). Effects of commercial feeds on the growth and carcass compositions of monosex tilapia (*Oreochromis niloticus*). *J. Fish. Aquat. Sci., 13*: 1-11.

Wang, M and Lu, M (2016). Tilapia polyculture: A global review. *Aquac. Res., 47(8)*: 2363-2374.

Wan Nooraida, W M and Abidah, M N (2020). Effects of pellet supplemented with different percentages of oil palm lipid sources on broiler performance, carcass trait and feed quality. *J. Oil Palm Res., 32(2)*: 313-325.

Yusoff, A (2015). Status of resource management and aquaculture in Malaysia. *Resource Enhancement and Sustainable Aquaculture Practices in Southeast Asia: Challenges in Responsible Production of Aquatic Species. Proc. of the International Workshop on Resource Enhancement and Sustainable Aquaculture Practices in Southeast Asia* 2014 *(RESA)* (Romana-Eguia, M R R; Parado-Estepa, F D; Salayo, N D and Lebata-Ramos M J H eds.). Aquaculture Dept., Southeast Asian Fisheries Development Centre, Tigbauan, Iloilo, Philippines. p. 53-65.


See You at
PIPOC 2023
MPOB INTERNATIONAL PALM OIL CONGRESS AND EXHIBITION
7-9 NOVEMBER
KUALA LUMPUR CONVENTION CENTRE, KUALA LUMPUR, MALAYSIA

JOURNAL OF OIL PALM RESEARCH

GUIDE FOR AUTHORS

(for more details, kindly surf http://jopr.mpob.gov.my)

Type of Articles

1. **Regular Article**
   Full-length original empirical investigations, consisting of introduction, materials and methods, results and discussion, conclusions. Original work must provide references and an explanation on research findings that contain new and significant findings. Conclusion should be brief and focus on the research output, should not be in point form. These papers should not exceed 6000 words of text (including tables, figures and references) and generally not more than a total of 10 figures and tables. After peer-review, the article word count limit can be extended to a maximum of 8000 words to better address the reviewers' and editors' comments. Any additional figures or tables can be included in the supplementary data. Please note that papers submitted to JOPR will be sent back to authors because of poor figure resolution or exceeding the number of figures permitted.

2. **Short Communication**
   Significant new information to readers of the Journal in a short but complete form. Preferably not exceeding 3000 words (including tables, figures and references), and is intended for rapid publication. They are not intended for publishing preliminary results or to be a reduced version of regular article.

3. **Review Article**
   Critical evaluation of materials about current research that have already been published by organising, integrating, and evaluating previously published materials. Re-analyses as meta-analysis and systemic reviews are encouraged. Review articles provide systemic overview, evaluation and interpretation of research in a given field. They should not exceed 12 000 words (excluding references only) and should contain no more than a total of 20 figures and tables. Any additional figures or tables can be included in the supplementary data. Please note that papers submitted to JOPR will be sent back to authors because of poor figure resolution or exceeding the number of figures permitted. The same information should not be repeated in a figure and a table.

Language

Please write your text in good English (only British English is accepted). We do not accept American English or a mixture of these.

JOPR's Template

JOPR's template, which is a standard format that facilitates the manuscript writing and copyediting process. This template is created to provide a detail and clear house style of JOPR. The template is drafted according to JOPR's house style, but in standard word version format. When writing a paper, authors need to format their papers to fit into the journal's house style. To make this easier, Word templates are available for many of other established journals, ready for them to download and apply to their research paper format. It is crucial for author to write a research paper while considering formatting. Each journal has its own guidelines for formatting; hence, the template defines how an article will look when it is published online or in print.

JOPR's Aims & Scope

This is established to provide a detail and clear aims and scope for author reference. Authors should declare in the cover letter how the research fits the aims and scope of JOPR.

JOPR's House Style

A detail listing of JOPR's house style for authors and a checklist to facilitate the copyediting process and standardise the copyediting process. The JOPR's house style remains the same and is drafted into a detail version for author's reference.

Manuscript Submission

- Manuscripts should be submitted via: https://mc04.manuscriptcentral.com/jopres
- JOPR does not permit dual submission, publication and/or any archive platform (preprint) in violation of journal ethical practices.

For more details and to download the JOPR's House Style and Template, kindly surf http://jopr.mpob.gov.my

Journal of Oil Palm Research ISSN 1511-2780
An international refereed journal on oil palm
Impact Factor: 2.057 (2020)
CiteScore: 3.0 (2020)
SJR: 0.498 (2020)

Contents of the Coming Issue
Journal of Oil Palm Research
Vol. 34 (2) June 2022*

Note: * Subject to change.